Dissertation zur Erlangung des Doktorgrades
der Fakultät für Chemie und Pharmazie
der Ludwig-Maximilians-Universität München

Functional analysis of PIP2 aquaporins in *Arabidopsis thaliana*

Olivier Da Ines

aus

Mâcon, France

2008

Erklärung

Diese Dissertation wurde im Sinne von § 13 Abs. 3 bzw. 4 der Promotionsordnung vom 29. Januar 1998 von PD Dr. Anton R. Schäffner betreut.

Ehrenwörtliche Versicherung

Diese Dissertation wurde selbstständig, ohne unerlaubte Hilfe erarbeitet.

München, am 11.03.2008

Olivier Da Ines

Dissertation eingereicht am   11.03.2008

1. Gutacher   PD Dr. Anton Schäffner

2. Gutachter   Prof. Karl-Peter Hopfner

Mündliche Prüfung am   08.05.2008

ABSTRACT

Plants harbor about 30 genes encoding major intrinsic proteins (*MIP*) which were named aquaporins because of the frequently observed water channel activity and their putative involvement in water relations. Plasma membrane intrinsic proteins (PIP) are subdivided into two groups with five PIP1 and eight PIP2 members in the model plant *Arabidopsis thaliana*. *PIP2* genes are highly homologous to each other, which might indicate a redundant function. However, several lines of evidence argue for gene-specific and non-redundant functions. *PIP2* genes exhibit overlapping, but differential expression patterns when assessed by promoter::GUS transgenic lines. Most *PIP2* genes were expressed in the region of the vascular tissue, however with differential cellular patterns. *PIP2;5* and *PIP2;7* were more uniformly found in leaves. *PIP2;4* was the only root-specific member and preferentially expressed in outer cell layers, whereas *PIP2;6* and *PIP2;8* were mostly found in young leaves with a distinct expression. PCA analyses based on publicly available stress-responsive expression patterns revealed distinct transcriptional responsiveness of *PIP2* genes. No visible phenotypes were observed for *pip2* knock-out lines under normal growth conditions. However, *pip2;3* mutants specifically showed salt-sensitivity, although the duplicated gene PIP2;2 has only eight amino acids different from PIP2;3 that mostly cluster in the region of the extracellular loop C. Transcriptional analysis using a custom-made DNA array focusing on membrane proteins indicated that loss-of-function of distinct *PIP2* genes did not interfere with major transport processes, at least at the transcriptional level. For several mutants of abundantly expressed PIP2 isoforms, root transcriptome analysis was extended to the whole genome using Affymetrix ATH1 GeneChip. Furthermore, *PIP2* co-expression analyses revealed enrichment for different functional categories. Only *PIP2;1* and *PIP2;2* showed significant correlations with other *PIP* genes, however most *PIP2* genes were also correlated to *TIP* isoforms, suggesting an functional relationship of plasma membrane and tonoplast permeabilities. Surprisingly, at the protein level, the loss of PIP2;1 or PIP2;2 specifically provoked a decrease in PIP1 proteins indicating a dependence of PIP1 stability on these PIP2 members.

So far, direct evidence for a participation of single PIP aquaporins in water transport *in planta* is scarce. To study non-invasively the impact of PIP2 on water uptake, the kinetics of water translocation was analyzed by mass spectrometry of water extracted from in *pip2;1* and *pip2;2* mutants grown in D-enriched medium. Retarded deuterium transfer into leaves of the single mutants indicated a direct involvement of both PIP proteins in water relations, whereas surprisingly the corresponding double mutant had compensated this slower uptake.

C O N T E N T S

Contents 5

ABBREVIATIONS

ABA	Abscisic Acid
ABC	ATP-binding cassette
BSA	Bovine Serum Albumin
CTAB	Cetyltrimethylammoniumbromide
d	day
ddH_2O	double distilled water
DEPC	Diethylpyrocarbonate
DMSO	Dimethyl sulfoxide
dNTPs	Deoxynucleotide-5'-triphosphates
DTT	Dithiothreitol
EDTA	Ethylene Diamine Tetra-acetic Acid
GFP	Green Fluorescent Protein
GUS	β-Glucuronidase
GST	Glutathione-S-transferase
kb	Kilo base pair
kDa	KiloDalton
MES	2-(N-Morpholino)-ethanesulfonic acid
MIP	Major Intrinsic Protein
MIPS	Munich information center for protein sequences (Helmholtz Zentrum München)
MS	Murashige and Skoog
NASC	Nottingham *Arabidopsis* Stock Center
NIP	NOD26-like Intrinsic Protein
PCR	Polymerase chain reaction
PIP	Plasma membrane Intrinsic Protein
PM	Plasma membrane
RNA	Ribonucleic Acid
rpm	rotations per minute
RT-PCR	Reverse Transcription-PCR
SD	Standard Deviation
SDS	Sodium Dodecyl Sulfate
SIP	Small and basic Intrinsic Protein
TAE	Tris-Acetate-EDTA
TE	Tris-EDTA
TEMED	N,N,N',N'- Tetramethylethylenediamine
TIP	Tonoplast Intrinsic Protein
T-DNA	Transfer DNA
UTR	untranslated region
v/v	volume per volume
Vol	Volume
w/v	weight per volume
wt	wild-type
X-Gluc	5-Bromo-4-chloro-3-indolyl-β-D-glucuronic acid

FIGURES AND TABLES

FIGURES

TABLES

1 INTRODUCTION

1.1 Water uptake and transport across plant tissues

Water, often regarded as the "solvent of life", is the single most abundant molecules in all cells and organisms and the maintenance of water status in suitable range is fundamental to life. In addition to the use of water in biochemical reactions and as a solvent, plants maintain their cellular turgor via sufficient water uptake. During development a plant can absorb water up to 500 times its fresh weight. However, only 2 to 5% of the water absorbed is retained by tissues for their growth, the remaining water is being lost by the leaves through evapotranspiration (Passioura, 1980). The passage of water through the whole plant is usually starting from the roots, the site of absorption, up to the aerial parts.

Water is first entering the roots due to water potential difference with the source water (e.g. soil, hydroponic medium) which is encompassing osmotic potential, pressure potential as well as gravity. The root is the fundamental organ for uptake and root water uptake in plants is related to processes such as transpiration and stomatal conductance, leaf water relations, leaf growth, and photosynthesis.

In the first place, to move into the roots, water has to flow radially across several cell layers (epidermis, cortex, endodermis and pericycle) to finally reach the vascular tissues constituting the xylem for long-distance transport (Fig. 1).
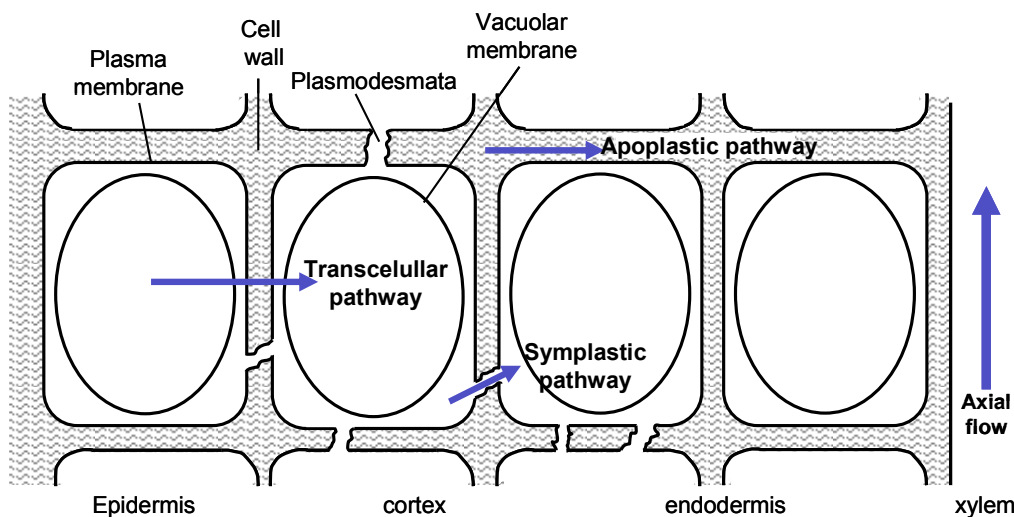
Figure 1. Schematic representation of the three different pathways involved in radial water transport across plant living tissues.

Three paths, for which relative contributions can vary depending upon growth conditions and species, co-exist for water transport across living tissues in plants (Fig. 1). The apoplastic path, i.e. within the extracellular cell wall space, is complemented by a cell-to-cell path,

which can be subdivided into the symplastic path through cytoplasmic continuities called plasmodesmata and the transcellular path across plasma and vacuolar membranes (Steudle, 2001). The latter is supposed to be important in root endodermis due to the presence of the hydrophobic deposits of the Casparian band, which obstruct the apoplastic path (not shown in Fig. 1). The composite transport model (Steudle, 1994; Steudle and Peterson, 1998) proposes that depending on the exact circumstances, the relative contribution of each water movement pathway to flow across the composite structure of tissues and organs in plants varies, which provide a useful mechanism by which the plant can respond to changing environmental conditions.

It is known that in case of low transpiration, for instance at night when stomata are closed, tension (negative hydrostatic pressure) generated by transpiration is considerably lower and therefore the cell to cell path governed by osmotic differences is favored. On the contrary, during transpiration, when stomata are open, water demand by the leaves leads to high tension exerted in the xylem, which will pull water up to aerial parts. Because of the low resistance of water flow exhibited by plant cell walls, water is mainly passing the apoplast in case of high transpiration.

Although the small and non-charged water molecule can cross membranes by simple diffusion, transmembrane path may be enhanced due to the high abundance of proteinaceous water channels (aquaporins, AQP) in biological membranes. Once water has reached the apoplastic region connected into vascular xylem tissue, water will flow axially through these vessels (Fig. 1 and 2). However, in the vascular tissues, apart from the uptake zone, radial exchange of water can also occur between surrounding cells (parenchyma cells) along the route (i.e. in hypocotyl and stem). This radial exchange between cells may also involve aquaporins (Fig. 2).

In the apoplastic xylem vessels, water transport occurs without penetrating lipid bilayer membranes. Xylem vessels are made up of dead cells that have lost their protoplasts and oppose a negligible resistance to water flow and thus, allow the bulk flow of water.

In the aerial organs, water arrives from the xylem vessels and hence it will be distributed in the apoplastic space following the water potential gradient. From there, it can enter mesophyll and epidermal cells of a leaf (Fig. 2). Within that compartment it may also be redistributed. In addition, part of the water may also circulate back to the root from the aerial part via a second long-distance transport system, the phloem (Fig. 2). Xylem tissues take part in the conduction of minerals, while the living, connected tissue of phloem cells is involved in metabolite transport along with water. On the contrary to water flow in xylem tissues, phloem loading

needs membrane transport potentially involving aquaporins. However, depending on the environmental conditions the major part of the water taken up by the roots may be lost by transpiration to the atmosphere. Transpiration is mainly occurring via the stomata, but may not be completely prevented by cuticular waxes on the epidermal surface as well (Riederer, 2006). Importantly, the diffusion through stomata is not unidirectional, but it also allows the diffusion of gases including CO_2 and H_2O into the leaf. Thereby, plants can also absorb water from the atmosphere. The amount of water lost by a plant through transpiration is primarily related to stomata aperture and on the water potential difference between atmosphere and leaf internal spaces, which is also influenced by physiological parameters such as leaf size, size and surface properties of leaf air spaces, and water supply via vascular tissues. The atmosphere's water potential is governed by environmental parameters like humidity, temperature, and wind.

As a summary, water transport across living tissues represents the critical parameter, due to the stronger resistance, for water uptake by root and redistribution to the surrounding cells and in aerial parts. Therefore, the presence of aquaporins in cellular membrane is supposed to play an important role in these processes.

Transpiration
through
stomatal pore

R_{trans} **Atmosphere**

Cuticular transpiration

Epidermal cells

guard cell · guard cell **Stoma**

R_{leaf}

L E A F

Leaf apoplast/
sub-stomatal
cavity

Mesophyll cells

Xylem vessels
supplying water to meso-
phyll & epidermis cells

Companion cell/
adjacent tissue

Phloem R_{phloem}

R_{xyl}

**Root
axial
flow via
xylem
vessels**

cell-to-cell
path

R O O T

O U T S I D E

R_{soil}
$=$
R_{xyl}

Apoplastic path

Parenchyma
cells

Casparian
Band

Radial water transport in root

Figure 2. Schematic representation of whole plant water transport within and between tissues.
Arrows indicate flow of water with different thickness related to putative transport capacity. Stippled arrows refer to apoplastic path, whereas solid arrows relate to paths possibly involving aquaporins. In case of deuterium enriched water (see below, Results 3.7) R is the molar ratio of the heavy (D) and light isotope (H) in the respective compartments. Red: D enriched water. Black arrow indicates low isotopic ambient water.

1.2   Aquaporin water channels

1.2.1   History and discovery of aquaporins

The organization of water within biological compartments is fundamental to life. Water can move through the membrane simply by diffusion through the lipid bilayer. However, the discovery of aquaporins brought the new view that, in addition, a set of proteins exists that enhance water permeability of biological membranes.

Historically, red cells´ membrane has been a key system for the molecular characterization of water channels, because erythrocytes exhibited a 10- to 20-fold increased water permeability that cannot be explained by the facile diffusion of water through lipid bilayer membranes (Dainty and Ginzburg, 1963; Macey, 1984; Finkelstein, 1987; Schäffner, 1998). Several researchers suggested the participation of a proteinaceous agent in water permeability (Macey, 1984; Benga et al., 1986; Wayne and Tazawa, 1990), but none of them could identify the nature of the protein. Eventually, CHIP28, a <u>Ch</u>annel-forming <u>I</u>ntegral <u>P</u>rotein of 28 kDa was first characterized as a contaminant of the rhesus factor (Agre et al., 1987). It had been never considered with respect to water-channel activity, because it was hardly detected on stained gels, although later it turned out to be very abundant in the red cell membranes. The discovery that this protein is also abundantly expressed in renal tubules, which show a high hydraulic permeability as well, lead to the hypothesis that **CHIP28 could be a water channel** (Preston and Agre, 1991). The water channel hypothesis was then confirmed by heterologous expression of this protein in *Xenopus* oocytes, which lead to a high water permeability of the oocyte membrane (Preston et al., 1992). CHIP28 was later renamed AQP1 (aquaporin1). AQP1/CHIP28 showed homology to the Major Intrinsic Protein (MIP) in the membrane of mammalian eye lens fiber cells, which is now, designated AQP0. The gene family was therefore generally named MIP family and is now known to be a large family of related proteins.

Representatives of the family have been found in all kingdoms, and, currently, more than 200 members of the aquaporin family have been found in bacteria, plants, fungi, animals and humans; the physiological and pathological implications are being uncovered. For instance, in vertebrates, combined efforts of several laboratories have led to the molecular identification of 11 to 13 aquaporin homologues clustered in two subsets referred to as aquaporins (AQP0-2, 4-6, 8, 11 and 12) and aquaglyceroporin (AQP 3, 7, 9 and 10) since they are permeated by water and/or glycerol. *Escherichia coli* has one member of each subset, AqpZ and GlpF (Zardoya, 2005). In the model plant *Arabidopsis thaliana*, 35 isoforms have been identified (Johanson et al., 2001; Quigley et al., 2002).

1.2.2 Classification of the plant MIP superfamily of proteins

Due to the fact that most plants are immobile, a rapid response of physiological processes to environmental conditions is essential for their survival. Thus, in comparison to many other organisms, plants might need a more sophisticated tuning of water balance, which might be reflected by the comparably large amount of aquaporin genes in plant genomes. In *Arabidopsis*, 35 isoforms, spread over all 5 chromosomes, have been found (Johanson et al., 2001; Quigley et al., 2002), while 36 and 33 aquaporin isoforms have been identified in maize and rice, respectively (Chaumont et al., 2001; Sakurai et al., 2005). According to sequence homologies the plant MIP family has been classified into four clades, which to some extent correspond to their sub-cellular localizations, the PIPs (Plasma membrane Intrinsic Proteins), the TIPs (Tonoplast Intrinsic Proteins), the NIPs (Nod26-like Intrinsic Proteins) and the SIPs (Small basic Intrinsic Proteins) (Chaumont et al., 2001; Johanson et al., 2001; Quigley et al., 2002) (Fig. 3).

The PIP proteins, the largest plant aquaporin subfamily, are divided into two subgroups, PIP1 and PIP2 (Chaumont et al., 2000; Johanson et al., 2001). *Arabidopsis* harbors five PIP1 and eight PIP2 members. All plant PIP2 proteins examined have been shown to have high water channel activity when tested in heterologous system (e.g. *Xenopus* oocytes), whereas PIP1 proteins often are inactive or have lower activity (Daniels et al., 1994; Kammerloher et al., 1994; Yamada et al., 1995; Weig et al., 1997; Johansson et al., 1998; Biela et al., 1999; Dean et al., 1999; Chaumont et al., 2000; Marin-Olivier et al., 2000; Dixit et al., 2001; Moshelion et al., 2002; Fetter et al., 2004; Temmei et al., 2005).

TIP proteins with 10 members in *Arabidopsis* are expressed in vacuolar membranes and may represent, together with the PIPs, central pathways for transcellular and intracellular water transport (Maurel et al., 2002).

A third clade, NIP, encompasses nine members that are close homologues to soybean Nodulin 26 (Nod26), an abundant major integral protein of symbiosome membrane of nitrogen fixing root organ called nodule. Nod26 has been classified into the MIP superfamily and describes the archetype of the subfamily (Sandal and Marcker, 1988). Consequently, all proteins related to nodulin26-like intrinsic proteins were named NIP.

SIP proteins, the smallest subfamily, comprise three members which were recently identified by database mining and phylogenic analysis (Johanson and Gustavsson, 2002). They are the most divergent aquaporins in plants and show a high level of diversity even within the subfamily. Although their transport specificity and physiological functions remain to be elucidated, SIP1;1 and SIP1;2 were recently characterized as water channels by heterologous

expression in yeast, whereas SIP2;1 showed no water channel activity. In addition, transient expression of *Arabidopsis* SIP proteins fused to GFP demonstrated these proteins to be mostly detected in the endoplasmic reticulum (ER) (Ishikawa et al., 2005).
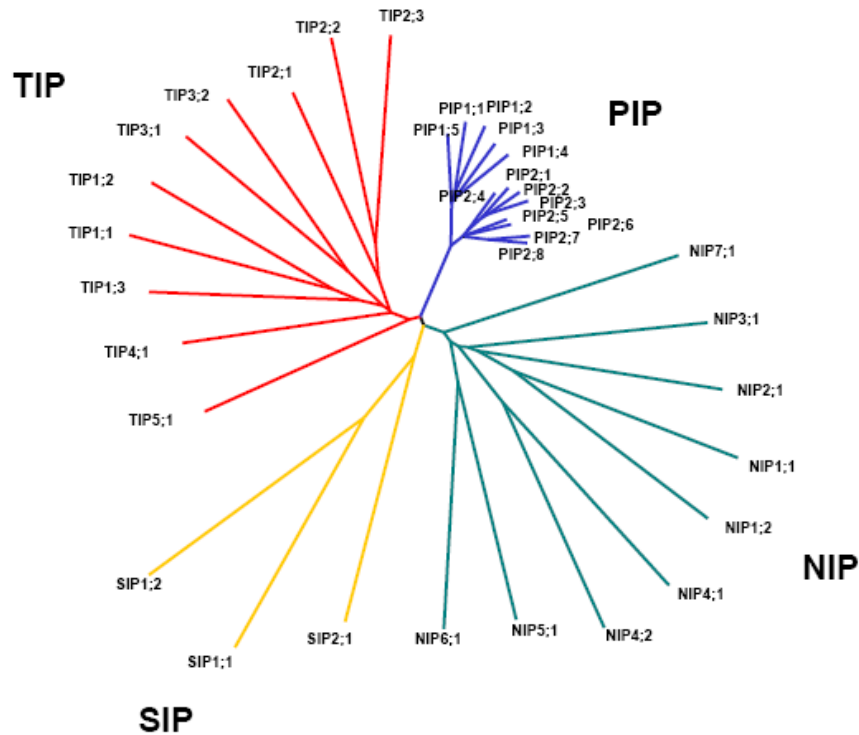
Figure 3. Phylogenetic tree of the 35 MIP proteins in *Arabidopsis thaliana* and their grouping in four subfamilies.

1.2.3 Structural features of aquaporins and transport selectivity

1.2.3.1 Common structural features of aquaporins

Aquaporins are small (23-34 kDa) transmembrane proteins that contain six membrane-spanning helices and 5 loops (loops A to E) with N- and C-termini residing in the cytosol (Jung et al., 1994) (Fig. 4a). Loops A and C are extracellular and loop D is intracellular. Loops B and E fold back into the membrane from the inner (B) and the extracellular (E) sides forming two short half helices penetrating the membrane as a seventh helix. They contain the highly conserved duplicated asparagine-proline-alanine (NPA) signature motif (Fig. 4a). Structural investigations and simulations elucidated that the seventh transmembrane domain is intimately involved in creating an aqueous pathway through the protein (Jung et al., 1994; Murata et al., 2000; Sui et al., 2001). The pore narrows to approximately 3 Å in diameter, which constraints the transport of large uncharged molecules through aquaporin; the pore is just large enough to accommodate a single water molecule.
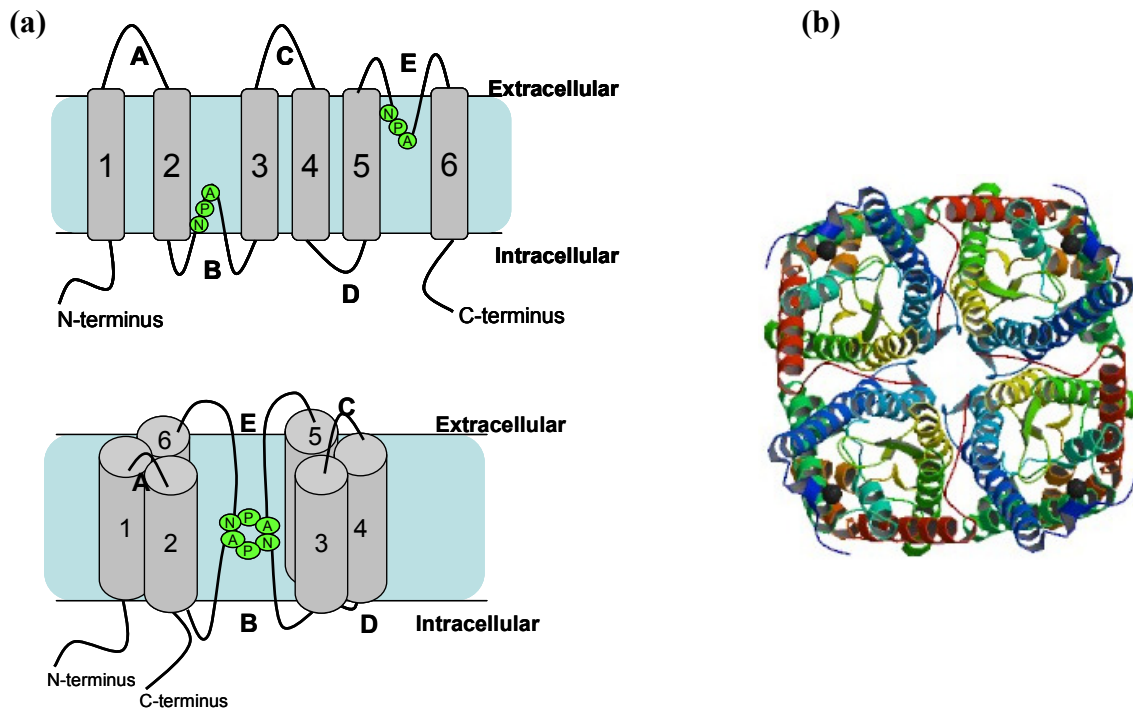
Figure 4. Hourglass model of AQP showing its membrane topology.
(a) Schematic representation of an AQP. Six transmembrane alpha helices (1 to 6) are connected by five loops (A to E). With folding of loop B and E the two helical domains containing the conserved NPA motifs overlap within the lipid bilayer to form a single aqueous pathway. (b) Molecular structure of the closed conformation of spinach *So*PIP2;1 showing the conserved tetrameric structure of aquaporins (Protein Data Bank code 1Z98). Each subunit defines its own pore surrounding a fifth pore in the center of the tetramer.

Three-dimensional structure analyses of archaeal AqpM (Lee et al., 2005), bacterial AqpZ (Ringler et al., 1999; Savage et al., 2003), mammalian AQP0, 1, 2 and 4 (Murata et al., 2000; Sui et al., 2001; Gonen et al., 2004; Schenk et al., 2005; Hiroaki et al., 2006), and recently the spinach *So*PIP2;1 (Kukulski et al., 2005; Törnroth-Horsefield et al., 2006) have shown that AQPs share typical but conserved structural properties. They form tetramers in the membrane with each subunit defining its own pore. The four subunits are arranged in parallel, forming a fifth pore in the center of the tetramer (Fig. 4b). The conductance of ions (K^+, Cs^+, Na^+ and tetramethylammonium) through the central pore of the human AQP1 tetramer had been reported (Saparov et al., 2001; Yool and Weinstein, 2002), but this property could not be reproduced by others.

In plants, aquaporin structure has been observed by cryo-electron microscopy of 2D crystals of bean *Pv*TIP3;1 (Daniels et al., 1999) and spinach SoPIP2;1 (Fotiadis et al., 2001; Kukulski et al., 2005). *So*PIP2;1 is the only plant aquaporin for which an atomic resolution at 2.1 Å based on X-ray crystallography is available (Törnroth-Horsefield et al., 2006).

1.2.3.2 Water transport selectivity

The movement of water through aquaporin is driven by osmotic or pressure gradients, i.e. aquaporins are not pumps or transporters. They form a simple pore that allows a bidirectional flow of water across membranes due to water potential differences. The permeability has been measured to be around 3×10^9 water molecules per subunit per second with a low Arrhenius activation energy (<20 kJ mol^{-1}), which is close to the activation energy for water diffusion. Importantly, the permeability is selective since water (H_2O) passes through the membranes with almost no resistance, while oxonium ions (H_3O^+) are completely excluded from the pores. Furthermore, migration of H^+ via hydrogen bonding is also prevented. The resolution of the bacterial aquaglyceroporin GlpF and of mammalians AQP1 structures by X-ray crystallography has enabled molecular dynamics simulations, which led to the understanding of the mechanism how aquaporins transport water and exclude proton movement (Fu et al., 2000; de Groot and Grubmüller, 2001; Sui et al., 2001). At the narrow center of the pore, the highly conserved Asn76 and Asn192 in the NPA motif of loop B and E are juxtaposed (Fig. 4a). Except the two Asn residues the constraint points are hydrophobic. Therefore, the interaction of the oxygen atom of water molecules from a single file with these Asn residues reorients the two hydrogen atoms when water passes through this constraint. The formation of hydrogen bonds with adjacent water molecules is thus prevented, contributing to the exclusion of proton-permeation through hydrogen bonds. In addition, a second narrower constriction point, named aromatic/Arg (Ar/R) region is formed towards the extracellular part, above the NPA region. In AQP1, the Ar/R region is constituted of aromatic residues Phe58, His182, Cys191 and Arg197. This tetrad, due to steric effects, functions as a selectivity filter, which permits the flux of water, but excludes bigger solutes. In fact, Arg197 residue forms a positive charge acting as a site for electrostatic repulsion of protons. At low pH, His182 on the other wall becomes protonated and forms a partial positive charge. The positive charges of Arg197 and His 182 provide a strong repelling charge against the passage of protons during water permeation (Fujiyoshi et al., 2002). Thus, by combining an aromatic/R-region and the NPA motives aquaporins possess a two-stage filter.

Plant aquaporin water permeability has mostly been shown by heterologous expression in *Xenopus* oocytes or yeast. The vacuolar TIP1;1 (initially named γ-TIP) from *Arabidopsis thaliana* was the first plant MIP member that showed water transport activity when assayed by heterologous expression in *Xenopus* oocytes (Maurel et al., 1993). Later homologues of *Arabidopsis* residing in plasma membrane were characterized (Daniels et al., 1994; Kammerloher et al., 1994; Weig et al., 1997). Since then, MIPs from a broad range of species

tested for water transport activity have been found to be water channels, such as from maize (Barrieu et al., 1998; Chaumont et al., 1998), wheat (Niemietz and Tyerman, 1997), rice (Lian et al., 2004), tomato (Werner et al., 2001), barley (Katsuhara et al., 2002), tobacco (Fray et al., 1994; Maurel et al., 1997), potato (Heymann and Engel, 1999), ice plant (Yamada and Bohnert, 2000), sunflower (Sarda et al., 1997), cauliflower (Reisen et al., 2003), radish (Higuchi et al., 1998; Suga et al., 2001), olive (Secchi et al., 2007) or *Panax ginseng* (Lin et al., 2007).

1.2.3.3 Additional transport specificities

Besides water, additional permeabilities have been shown for various aquaporin isoforms of all subclasses of plant aquaporins. Indeed, it has become evident that some aquaporins do not have strict water permeability and may transport other molecules. Most evidences for AQP permeability come from heterologous expression in *Xenopus* oocyte or yeast, or after reconstitution in proteoliposomes but studies *in planta* are rare (see below). Thus, besides water, some plant aquaporins have also been shown to transport glycerol, urea, formamide (Rivers et al., 1997; Whittembury et al., 1997; Dean et al., 1999; Gerbeau et al., 1999) or other small, uncharged molecules like boric acid (Dordas et al., 2000).

Heterologous expression in yeast of *Arabidopsis* NIPs (*AtNIP1;1*, *AtNIP1;2*) indicated that they formed functional glycerol permeases and exhibited low water conductivity (Weig et al., 1997; Weig and Jakob, 2000; Wallace et al., 2002).

New evidences that aquaporins can transport additional physiologically important molecules have recently been presented. For instance, recent studies suggested participation of TIPs to transport ammonium NH_4^+ and ammonia NH_3 from the cytoplasm into the vacuole. TIPs of *Arabidopsis* (Loque et al., 2005) and wheat (Jahn et al., 2004; Holm et al., 2005) could be identified in yeast complementation assays that conferred permeability to ammonium as well as to methylammonium or to formamide. Expression of *At*TIPs, several mammalian aquaporins (AQP1, 3, 8 and 9) or wheat TIP2;1 in *Xenopus* oocytes showed an increased permeability for NH_4^+/NH_3 (Holm et al., 2005; Loque et al., 2005). Consequently, TIPs could be involved in the detoxification of ammonia from the cytoplasm by an acid-trap mechanism as suggested by Loque et al. (2005). NH_3 was transported into the acidic vacuolar lumen, where it binds a proton to form NH_4^+. However, transgenic *Arabidopsis* plants overexpressing *At*TIP2;1 showed no differences in capacity and rate of ammonium accumulation in root cells compared to wild-type plants. Hence, the physiological consequences of TIP mediated NH_3 transport are still unknown (Loque et al., 2005). A contribution for NH_3 permeation has also

been considered for the NIP soybean Nod26 (Niemietz and Tyerman, 2000; Wallace et al., 2006).

Although it has been previously suggested, the first molecular genetic evidence for the diffusion of hydrogen peroxide through aquaporin has been presented only recently. In this study, among 24 aquaporins from plants and mammals tested, human AQP8 as well as *Arabidopsis* TIP1;1 and TIP1;2 showed hydrogen peroxide permeability (Bienert et al., 2007). Various studies have also demonstrated that essential nutrient may permeate through aquaporin. Thus, evidence for boric acid uptake has been shown for the *Arabidopsis* NIP5;1 (Takano et al., 2006) while heterologous expression of rice Lsi1 in oocytes has shown transport activity for orthosilicic acid (Ma et al., 2006). In rice, the *Lsi1* gene is constitutively expressed in roots and has been shown to belong to the NIP subfamily; its closest homologue in *Arabidopsis* is *AtNIP7;1*.

Eventually, one of the most fascinating proposals for aquaporin permeability is certainly CO_2 transport. Indeed, CO_2 permeability has been suggested for mammalian aquaporins as well as tobacco *NtAQP1* (Cooper and Boron, 1998; Nakhoul et al., 1998; Prasad et al., 1998; Cooper et al., 2002; Uehlein et al., 2003). The PIP1 member NtAQP1 was shown to increase membrane permeability to CO_2 in *Xenopus* oocytes (Uehlein et al., 2003). CO_2 transport mediated by PIP2 aquaporins has been suggested for the barley aquaporin *Hv*PIP2;1 when overexpressed in rice. The level of *Hv*PIP2;1 was found to be strongly related to mesophyll conductance and the results were interpreted in a way that *Hv*PIP2;1 has a role in CO_2 diffusion in rice leaves (Hanba et al., 2004). However in this study molecular characterization in the oocyte system was not provided. Consequently, compelling evidences for aquaporin-mediated CO_2 transport *in planta* are still missing although promising evidence for the *in vivo* involvement of aquaporin NtAQP1 in mesophyll conductance to CO_2 has been provided by indirect measures (Flexas et al., 2006).

Although the name aquaporin appears to be justified in many cases, the idea that the primary function of some MIP proteins may not be restricted to water transport has found support and may involve solute transport or other regulatory functions (Hill et al., 2004). Indeed, the ability of some MIPs homologues to transport a wide range of small neutral molecules has also been inferred from structural studies showing that aquaporin have structural features that may explain their transport specificities. As mentioned above, aquaporin has a two-stage filter that defines, at least partly, its permeability. Thus, comparison of the narrow selectivity filter region (Ar/R region) of all 35 aquaporins of *Arabidopis* showed that they exhibited a conserved overall Ar/R region but could be classified in eight subgroups based on their pore

configuration at the Ar/R region. Arg195 was found to be conserved in all members of aquaporins and positioned at the narrowest segment of channel. It was therefore suggested that although plant aquaporins show a common fold their distinct differences in the pore configuration likely results in divergent transport selectivities (Wallace and Roberts, 2004). For instance, all PIPs exhibited a uniform Ar/R signature characteristic of "true aquaporin", i.e. high water transport aquaporins. In comparison, a much higher diversity in the pore configuration was observed for TIPs and NIPs which are organized into three and two structurally and functionally distinct subgroups with different transport selectivity and potentially distinct regulatory properties, respectively (Wallace and Roberts, 2004; Wallace et al., 2006). In the NIP group II (*NIP5;1*, *NIP6;1*, *NIP7;1*), the Ar/R selectivity filter close to the NPA pore region differs to that of NIP I and the predicted pore has an increased size than NIP I subgroups suggesting a permeability for larger solutes such as urea. This new property is, for unknown reason, linked to a reduced water permeability (Wallace et al., 2006). Finally, akin to their diverging sequences in the aquaporin family, SIPs exhibited a rather unusual pore configuration.

1.2.4 Plant aquaporins expression and localization

A complete understanding of aquaporin functions requires a precise knowledge of their expression pattern in specific tissues, cell types and compartments. Specific tools such as DNA arrays carrying aquaporin gene specific probes or quantitative real-time RT-PCR have been used to monitor the respective abundance of aquaporins in various tissues, organs or stress conditions in *Arabidopsis thaliana* (Jang et al., 2004; Alexandersson et al., 2005; Boursiac et al., 2005), maize (Zhu et al., 2005; Hachez et al., 2006b) or rice (Sakurai et al., 2005).

Whole genome analysis using Affymetrix ATH1 array has also been initiated by the AtGenExpress consortium to study *Arabidopsis* transcriptome in various developmental stages and upon diverse stresses and hormone treatments (Schmid et al., 2005; Kilian et al., 2007). However, analyses of MIP transcripts in *Arabidopsis* by DNA arrays have been somewhat limited by the high homology of aquaporins. E.g. for some genes, probe sets present on the Affymetrix array are not specific and do not discriminate several isoforms (e.g. *PIP2;2* and *PIP2;3* or *PIP2;7* and *PIP2;8*). In addition, divergent results have emerged from such studies. In *Arabidopsis*, strong and low expression have been measured for *PIP2;7* and *PIP2;1*, respectively (Jang et al., 2004) whereas the opposite has been demonstrated in other studies (Alexandersson et al., 2005; Boursiac et al., 2005). However, such studies definitely

showed that in *Arabidopsis*, *PIP1* genes as well as *PIP2;1*, *PIP2;2*, *PIP2;7* are usually abundantly expressed in both roots and aerial parts. In addition, high responsiveness of plant aquaporins to a wide range of environmental cues has been reported. For instance, aquaporin transcripts have been shown to be differentially deregulated by water stress conditions such as osmotic, drought, salt, and cold stress or abscisic acid (ABA) treatments (Kreps et al., 2002; Seki et al., 2002a; Bray, 2004; Jang et al., 2004; Alexandersson et al., 2005; Boursiac et al., 2005; Zhu et al., 2005). In *Arabidopsis*, *PIP2;3* was upregulated in leaves upon salt stress and downregulated by drought stress in both roots and leaves. In contrast, *PIP2;5* was upregulated upon drought and cold stress (Jang et al., 2004; Alexandersson et al., 2005; Boursiac et al., 2005). Similarly, a transcriptome analysis of *Arabidopsis* root transporters revealed differential responses of aquaporins upon cation stresses. Thus, salt stress lead to an initial down-regulation of aquaporins followed by an up-regulation (e.g. *PIP2;1*, *PIP2;3* or *PIP2;7*), while Ca^{2+}-starvation triggered an general down-regulation of aquaporins such as *PIP2;1*, *PIP2;2*, *PIP2;3*, *PIP2;4* and TIPs. K^+-deprivation specifically affected only a small number of aquaporin isoforms such as *PIP1;3*, *PIP2;1* and *PIP2;2* (Maathuis et al., 2003).

Thus, although these studies gave valuable information regarding the presence of aquaporin transcripts in various organs or tissues, there is only very limited knowledge in *Arabidopsis* as well as in other plants regarding the cellular expression profile of individual aquaporins. Recently, cell-specific expression of aquaporin genes in *Arabidopsis thaliana* roots has been determined in a genome-wide analyses based on fluorescence-activated cell sorting and Affymetrix ATH1 microarray analyses (Birnbaum et al., 2003). Cell-specific expression of aquaporin genes has been recently well detailed in primary root tips of maize using in situ RT-PCR (Hachez et al., 2006b). All *ZmPIP* genes except *ZmPIP2;7* showed expression in primary roots with strong expression towards the elongation and mature zones. Immunodetection techniques have also been used in *Arabidopsis* to characterize aquaporin expression in various organs, cell types or compartments, although most antibodies cross-reacted with several members of subclasses of plant aquaporins (Robinson et al., 1996; Frangne et al., 2001; Kobae et al., 2006; Vander Willigen et al., 2006; Hachez et al., 2006b). In tobacco flower, differential expression has been found for PIP1 and PIP2 proteins during anther and stigma development (Bots et al., 2005a; Bots et al., 2005b).

The use of reporter gene systems has proven useful and gave most valuable informations regarding the expression of a few aquaporin genes so far. In *Arabidopsis thaliana*, the *in situ* localization of the β-glucuronidase reporter gene led to the elucidation of the expression of several aquaporin isoforms. Individual aquaporins had been shown to be highly expressed

during cell elongation and frequently in the region of vascular cells (Ludevid et al., 1992; Kaldenhoff et al., 1995; Javot et al., 2003). Thus, expression of *AtTIP1;1* and *AtPIP1;2* has been observed in expanding as well as differentiated cells in both roots and aerial parts (Ludevid et al., 1992; Kaldenhoff et al., 1995), whereas high expression of *AtNIP5;1* has been found in epidermal, cortical, and endodermal cells of root elongation zone but not in aboveground tissues (Takano et al., 2006). High expression of *PIP1;2* and *TIP2;1* has also been observed in vascular tissue and surrounding cells of roots and aboveground tissues in *Arabidopsis thaliana* (Kaldenhoff et al., 1995; Daniels et al., 1996). The presence of these aquaporin may raise water permeability and facilitate water transport from symplast to apoplast in the roots and assist the opposite phenomenon in the aerial parts of plants.

An *AtPIP2;2* promoter β-glucuronidase gene fusion indicated predominant expression in root cortex, endodermis and stele. These expression data together with decrease of root osmotic hydraulic conductivity of *pip2;2* knockout mutants provided the first evidence for the contribution of a single PIP aquaporin, *At*PIP2;2, in root water uptake (Javot et al., 2003). Provided that AQPs function indeed as water channels *in vivo*, these localizations may mean that the corresponding MIP proteins could play a role in regulating bulk flow of water across membranes and/ or in maintaining turgor homeostasis during active solute exchange.

Another crucial issue is the membrane location of aquaporins. The high amino acid sequence identity between close aquaporin homologues (up to 97%) is a big challenge for the discrimination of single aquaporin isoform expression profiles at the protein level. On the other hand, the high abundance of many aquaporins has successfully allowed using biochemical methods for analyzing their expression. High resolution techniques such as mass spectrometry can distinguish between very close aquaporin homologues and, therefore, permit a precise inventory of aquaporins present in well-defined sub-cellular membrane fractions (Santoni et al., 2003; Alexandersson et al., 2004; Marmagne et al., 2004; Nelson et al., 2006). Historically, the assignment of plant MIPs to specific membrane locations has been biochemically proven for several isoforms and was further extended based on sequence homology. However, this is not necessarily true in all cases and recent evidence suggests that MIP proteins may have more than one location or may move depending on physiological states or environmental stresses (Barkla et al., 1999; Kirch et al., 2000; Ma et al., 2004; Vera-Estrella et al., 2004; Boursiac et al., 2005). Utilizing specific antibodies against several MIP members from *Mesembryanthenum crystallinum* (common ice plant), it has been suggested that their distribution might be more complex than previously thought. In fact, immunological

detection of the TIP member MIP-F confirmed that it is exclusively localized to a tonoplast fraction. However, signals for three other putative plasma membrane PIP members (MIP-A, -B, -C) were not clearly defined (Barkla et al., 1999). Proteins might cycle through endomembranes in a manner resembling the mammalian aquaporins to regulate water flux (Marples et al., 1998; Tamarappoo and Verkman, 1998). Microscopic analysis has revealed that plasma membrane localized PIP1 isoforms from *Arabidopsis* are also present in high abundance in plasma membrane invaginations, termed plasmalemmasomes. These might represent transitory structures connecting the plasma membrane and plant endosomes (Robinson et al., 1996).

In *Arabidopsis thaliana*, the use of GFP fusion protein has allowed to locate individual MIP proteins in plasma or vacuolar membrane as well as in intracellular vesicles (Reisen et al., 2003; Ma et al., 2004; Boursiac et al., 2005; Takano et al., 2006). By mean of GFP-fusion protein expressed in transgenic plants, a NIP protein involved in orthosilicic acid transport in rice has been localized on the plasma membrane of the distal side of endodermis and exodermis root cells (Ma et al., 2006). Similarly, TIP1;1-GFP and PIP1;1-GFP or PIP2;1-GFP fusion proteins, localized in the vacuolar and plasma membrane, respectively, where also observed to be relocalized into intracellular spherical structures after exposure to salt (Boursiac et al., 2005).

1.2.5 Regulation of plant aquaporins

Apart from transcriptional regulation (see 1.2.4) aquaporins are regulated by additional mechanisms acting through modifications at their protein structure (for a recent review see Chaumont et al., 2005).

1.2.5.1 Phosphorylation

Several post-translational modifications have been found to regulate aquaporin activity. Phosphorylation of aquaporin seems to be an important mechanism for aquaporin regulation involved in a broad range of processes and that can itself be regulated by external parameters. Phosphorylation of soybean nodulin 26 at serine residue 262 is stimulated in response to water deficit, resulting in enhanced transport activity (Guenther et al., 2003). Furthermore, phosphorylation of a plasma membrane aquaporin in tulip has been shown to accompany opening of petals (Azad et al., 2004). This phosphorylation was temperature-dependent and reduced by low temperature. In contrast, chilling enhanced PIP2 phosphorylation in maize (Aroca et al., 2005). In *Arabidopsis thaliana*, regulation of the seed-specific *At*TIP3;1 by

phosphorylation has also been demonstrated (Maurel et al., 1995; Guenther et al., 2003). A conserved phosphorylation site exists in loop B of all plant PIPs (Johansson et al., 1998; Törnroth-Horsefield et al., 2006) and it has been established that the N- and C- terminal tails can be important domains for water channel regulation. In particular, compared with PIP1 proteins, PIP2 have a shorter N-terminal extension and a longer C-terminal end containing multiple putative phosphorylation sites (Schäffner, 1998; Chaumont et al., 2000; Johansson et al., 2000; Chaumont et al., 2001; Johanson et al., 2001). For instance, it has been shown that the water transport activity of the PIP2 member PM28A in spinach was regulated by phosphorylation at serine residue; upon hyperosmotic treatment a cytoplasmic serine residue was dephosphorylated (Johansson et al., 1998).

Interestingly, recent membrane proteomics studies revealed that the N-terminal tail of PIP2 members can be methylated at adjacent sites. Thus, Lys3 and Glu6 residues of AtPIP2;1 can be dimethylated and monomethylated, respectively (Santoni et al., 2006). Measurements of water transport in plasma membrane vesicles indicated that this novel post-translational modification of aquaporins did not interfere with their intrinsic water permeability. However, it was suggested that methylation may represent a crucial step towards the identification of new regulatory mechanisms of plant membrane proteins (Santoni et al., 2006; Maurel, 2007).

1.2.5.2 Regulation by pH and Ca^{2+}

The plasma membrane water permeability appears also to be influenced by divalent cations and pH (Gerbeau et al., 2002; Alleva et al., 2006). Addition of Ca^{2+} reduced cell hydraulic conductivity of *Arabidopsis* suspension cells and purified plasma membrane vesicles and H^{+} was shown to reversibly decrease water channel activity (Gerbeau et al., 2002). In addition, beneficial effect of inhibition of water transport by calcium during salt stress has been described (Cabanero et al., 2006; del Martinez-Ballesta et al., 2006). However, whether this inhibition results from direct inhibition of aquaporins or through a signaling cascades still remains to be elucidated. Because environmental stresses known to affect water transport trigger calcium signaling cascades, Ca^{2+} has also been linked to aquaporin regulation and aquaporin phosphorylation is largely mediated by calcium-dependent protein kinases (Johnson and Chrispeels, 1992; Johansson et al., 1996; Sjovall-Larsen et al., 2006).

Interestingly, it has been shown that apoxia-inducing flooding of plants leads to inhibition of water uptake. It has been demonstrated that this down-regulation was accompanied by a sustained intra-cellular acidification (Tournaire-Roux et al., 2003). In experiments expressing *Arabidopsis* aquaporins (AtPIP2;1, AtPIP2;2, AtPIP2;3 and AtPIP1;2) in *Xenopus* oocytes a

drop of intra-cellular pH resulted in a decrease of water conductance implicating a closure of aquaporins by protons. In *At*PIP2;2, a histidine (His) residue at position 197 in Loop D was identified to be the major pH-sensing site under physiological conditions (Tournaire-Roux et al. 2003, Chaumont et al. 2005). In a structural model of *At*PIP2;2 with protonated His197, Loop D is folded over the pore and caused the closure of the protein (Tournaire-Roux et al., 2003; Chaumont et al., 2005).

1.2.5.3 Aquaporin interaction and trafficking

Multimerization can regulate the activity and function of membrane proteins (Veenhoff et al., 2002). The importance of aquaporin heteromerization was previously suggested *in planta* by analysis of PIP1 and PIP2 antisense *Arabidopsis* plants. Indeed, the inhibition of water transport in transgenic *Arabidopsis* with down-regulation of both PIP1 and PIP2 members was not more pronounced than in transgenic *Arabidopsis* with reduced expression of only PIP1s or PIP2s. The authors argued that PIP1 and PIP2 form a common water channel unit in the plasma membrane (Martre et al., 2002).

More recently it has been shown that the water transport ability of PIP isoforms can be enhanced by co-expression of PIP1 with PIP2 proteins (Fetter et al., 2004; Temmei et al., 2005). Thus, while *Zm*PIP1;2 alone did not show water transport activity, co-expression of maize *Zm*PIP1;2 and different PIP2 isoforms (*Zm*PIP2;1/ -2;4/ -2;5 and even *At*PIP2;3) in *Xenopus* oocytes resulted in an increase in water permeability compared with individual expression of these PIP isoforms (Fetter et al., 2004). In addition, the authors showed that co-expression of *Zm*PIP1;2-GFP fusion protein with *Zm*PIP2 proteins enhanced the targeting of *Zm*PIP1;2-GFP to the plasma membrane or its stability. Since physical interaction was demonstrated by chromatographic co-purification using His-tagged *Zm*PIP2 and *Zm*PIP1;1-GFP, it was suggested that the enhanced water permeability was the result of heteromerization of PIP1 and PIP2 isoforms, which improves targeting of PIP1 to the plasma membrane (Fetter et al., 2004; Chaumont et al., 2005). Heteromerization was also suggested for *Mimosa pudica* aquaporins *Mp*PIP1;1 and *Mp*PIP2;1 by co-immunoprecipitation of tagged proteins when co-expressed in COS7 cells (Temmei et al., 2005). Moreover, phosphorylation in loop B of *Mp*PIP1 was important for the positive effect on water transport after co-expression (Temmei et al., 2005). Although this phosphorylation was not required for physical interaction, an effect on water transport was only observed upon co-expression of *Mp*PIP1;1 with *Mp*PIP2.

In contrast to these heterologous expression systems, PIP2-PIP1 interaction has now been clearly demonstrated in living maize cells using FRET and fluorescence lifetime imaging

microscopy (Zelazny et al., 2007). When expressed alone, several *Zm*PIP1s fused to the monomeric cyan fluorescent protein (mCFP) were retained in the endoplasmic reticulum, whereas *Zm*PIP2s fused to the monomeric yellow fluorescent protein (mYFP) were found in the plasma membrane (Zelazny et al., 2007). Interestingly, when co-expressed, mYFP::*Zm*PIP2s and mCFP::*Zm*PIP1s interacted resulting in relocalization of mCFP::*Zm*PIP1s to the plasma membrane. Additional evidence for the interaction of *Zm*PIP1 and *Zm*PIP2s in maize roots was provided by co-immunoprecipitation of *Zm*PIP1;2 with *Zm*PIP2;1 using isoform-specific antibodies (Zelazny et al., 2007).

The importance of four amino acid substitution in loop E was demonstrated by their replacement in *Zm*PIP1;1 with those from *Zm*PIP1;2. This replacement conferred to *Zm*PIP1;1 similar properties like *Zm*PIP1;2 upon co-expression in increasing oocytes membrane water permeability (Fetter et al., 2004). Thus, co-expression of *Zm*PIP2;5 and *Zm*PIP1;1 in *Xenopus* oocytes does not lead to an increase of the oocyte membrane water permeability unless the *Zm*PIP1;1 loop E is replaced with that of *Zm*PIP1;2. It was concluded that *Zm*PIP1;1 and *Zm*PIP2;5 do not interact functionally in *Xenopus* oocytes and that loop E plays an important role in *Zm*PIP1/PIP2 interactions (Fetter et al., 2004). However, FRET in living maize cells demonstrated that *Zm*PIP2;5 interacts with *Zm*PIP1;1, enhancing its targeting to the plasma membrane. The authors suggested that *Zm*PIP1;1 and *Zm*PIP2;5 do physically interact, but this heteromerization does not increase the oocyte membrane water permeability because *Zm*PIP1;1 would not be functional (Zelazny et al., 2007). Comparison of the structural models of *Zm*PIP1;1 and *Zm*PIP1;2 suggested that loop E might be important in propagating structural changes (i.e. multimerization) affecting the structure of the channel and, hence, its specificity (Chaumont et al., 2005).

These results suggest that PIP1-PIP2 heteromerization is required for *in planta* PIP1 trafficking to the plasma membrane and to modulate plasma membrane permeability. Accordingly, PIP1 aquaporins might need to be activated in the plant in order to function as water channels.

Additionally, molecular trafficking is an important regulation mechanism of aquaporins. Such regulation of aquaporin has been well described in humans. In kidney collecting duct epithelia, AQP2 containing vesicles were routed to the membrane in response to a hormonal stimulus (Brown, 2003). In plants, the regulation and redistribution of PIP and TIP aquaporins from *Mesembryanthemum crystallinum* has been shown to occur when plants were submitted to hyperosmotic stress or salt stress (Kirch et al., 2000; Vera-Estrella et al., 2004). Hyperosmotic stress induces a delocalization of a TIP protein from *Mesembryanthemum*

crystallinum (*Mc*TIP1;2) from the tonoplast to endosomal compartments. This delocalization could be blocked by inhibitors of vesicle trafficking processes and was linked to aquaporin glycosylation (Vera-Estrella et al., 2004). Similar redistribution was seen in *Arabidopsis* root upon exposure to salt stress (Boursiac et al., 2005). GFP fusions indicated a relocation of *At*TIP1;1 and *At*PIPs into vacuolar substructures called bulbs after 45 min and 2 h, respectively. Eventually, plant death by RNAi inhibition of *AtTIP1;1* has been explained by a function of *At*TIP1;1 in sugar metabolism and vesicle trafficking (Ma et al., 2004).

Thus, trafficking appears to be an essential regulation mechanism for plant aquaporin activity and raises the question of their subcellular localizations. In fact, aquaporin localization may not be restricted to one compartment. For instance, only a preferential accumulation of *At*SIP and *At*NIP2;1 in the endoplasmic reticulum has been reported. Studies have also reported presence of aquaporins in mitochondria in both animals (Amiry-Moghaddam et al., 2005; Calamita et al., 2005) and in *Arabidopsis thaliana* plants (Jones et al., 2006).

1.2.6 Integrated function of plant aquaporins inferred from transgenic plants

Aquaporins are presumed to participate in many different physiological processes (for recent review see Kaldenhoff and Fischer, 2006; Hachez et al., 2006a; Maurel, 2007), including photosynthesis (Uehlein et al., 2003), reproduction (Bots et al., 2005b) and restriction of root water uptake regulation by low pH values (Tournaire-Roux et al., 2003). Studies on the integrated function of aquaporins in plants have been somehow limited by the high genetic diversity of aquaporins in these organisms and other methodological difficulties such as the lack of specific inhibitors. Yet, there is now a substantial body of evidence in different plant species, based on alteration of aquaporin functions by various inhibitors (e.g. mercurials, silver or gold compounds). However, because of the overall toxicity of these inhibitors and their effects on other physiological processes, such studies are unspecific and make any analysis of aquaporin function at the tissue level difficult. In addition, some aquaporin isoforms have been shown to be mercury insensitive such as PIP2;3 in *Arabidopsis thaliana* (Daniels et al., 1994). Nevertheless, several reports may suggest that aquaporins significantly contribute to water transport in plants (Tyerman et al., 1999; Niemietz and Tyerman, 2002). For instance, using mercury, a rapid drop in root elongation rate was shown in maize, suggesting a central role of aquaporins in this process (Hukin et al., 2002).

Modulation of aquaporin genes *in planta* offers more reliability and has become the strategy of choice to elucidate the function of aquaporins. Thus, most of our knowledge on the physiological relevance of aquaporins in plant water relations comes from analyses of

transgenic plants with modified expression of various aquaporins either from overexpression or from gene silencing by antisense or RNAi suppression (Kaldenhoff and Fischer, 2006; Hachez et al., 2006a).

The first evidence for a function of aquaporins in cellular water uptake and whole-plant water transport came from plants expressing antisense *PIP1* RNA reducing both *PIP1;1* and *PIP1;2* transcripts. Mesophyll protoplasts of these plants showed a reduced water permeability (Kaldenhoff et al., 1998). *Arabidopsis* plants expressing antisense *AtPIP1;2/1;1* or *AtPIP2;3* gene alone or together (double antisense) showed a reduction in transcript or protein levels for several PIP1 and/or PIP2 homologues (Kaldenhoff et al., 1998; Martre et al., 2002). The altered *PIP* expression resulted in a reduction of water permeability in isolated protoplasts as well as a decline in the total root hydraulic conductivity. Interestingly, plants developed a larger root system than the controls which was interpreted as a response to compensate for the reduced cell water permeability. Since the leaf hydraulic conductance was not changed with respect to the control, the overall hydraulic conductance of these plants was unaffected.

In tobacco, overexpression of *AtPIP1;2* significantly increased growth rate, transpiration rate, stomatal density and photosynthetic efficiency under favorable growth conditions, but caused faster wilting in drought conditions (Aharon et al., 2003). Reduced expression of several PIP1 homologues in tobacco *NtAQP1* antisense plants resulted in a significant decrease of protoplast membrane water permeability. However, in contrast to *Arabidopsis* PIP antisense lines, *NtAQP1* antisense tobacco did not show any increase in root mass (Siefritz et al., 2002). Instead, tobacco root hydraulic conductivity was reduced, plant water potential was decreased and plant transpiration was diminished. In addition, the diurnal epinastic leaf movement, a process involving high rates of cellular water transport was reduced, pointing to the importance of aquaporin-mediated water transport in this process (Moshelion et al., 2002; Siefritz et al., 2004).

Plants with impaired expression of a PIP1 aquaporin showed differences not only in water transport but also in CO_2-dependent processes such as photosynthesis, or in stomatal and even mesophyll conductance (Siefritz et al., 2002; Uehlein et al., 2003; Flexas et al., 2006). The effect of mercuric compounds on CO_2 conductance in leaves also suggested an involvement of aquaporins in case of an increased gas transport rate (Terashima and Ono, 2002). Although, the physiological significance of CO_2 transport through AQP1 in mammals is a matter of debate, CO_2 permeability in plants as demonstrated for several aquaporins may imply a function in photosynthesis, one of the most important metabolic processes in plants.

Studies on RNAi transgenic *Arabidopsis* plants with reduced *AtTIP1;1* showed a lethal phenotype. Gene expression profiling and metabolite analysis suggested a function in sugar metabolism and vesicle-based metabolite routing through or between pre-vacuolar compartments and the central vacuole (Ma et al., 2004).

Although these transgenic approaches resulted in valuable information about the potential involvement of aquaporins in different processes, they could not resolve the contribution of single aquaporin members. In fact, suppression by antisense or RNAi typically leads to silencing of several isoforms which makes interpretation difficult; a differential suppression of different isoforms could be an explanation for some controversial results. Similarly, interpretations based on overexpression studies have to be taken with care. A recent work demonstrated that *Arabidopsis* and tobacco plants overexpressing PIP1;4 or PIP2;5 exhibited retarded seed germination and seedling growth under drought, whereas germination was facilitated under cold stress (Jang et al., 2007a). In this study, the authors nicely showed that the overexpression of an aquaporin (PIP1;4 or PIP2;5) also affects the expression of endogenous *PIP2* genes and thereby impacts on plant development under various stress conditions. Similar results were provided with other aquaporins and other plants (Jang et al., 2007b). Thus, overexpression does not reflect the function of the modulated protein as there is a strong influence on several endogenous transcripts; consequently, physiological functions of individual aquaporins cannot be deduced from those studies due to unknown effects on the aquaporin complement.

The use of knockout mutant might provide a more specific approach to address the function of a given isoform *in planta*. However, studies using knockout mutants are very limited. To date, in *Arabidopsis*, *pip2;2* T-DNA knockout lines demonstrated the involvement of this aquaporin in root water uptake (Javot et al., 2003). Although *Atpip2;2* knockout mutants did not reveal any visible phenotype, a reduced osmotic hydraulic conductivity of roots has been measured in two *pip2;2* mutants compared with the wild-type by cell pressure probe and root exudation measurements. These data provided evidence for the contribution of *At*PIP2;2 in root water uptake. In addition, the authors indicated that the disruption of *PIP2;2* was not compensated for by enhanced expression of any other *PIP* homolog. Accordingly, the authors claimed the observed phenotype indicated that *At*PIP2;2 and *At*PIP2;3, its closest homologue (showing 97% amino acid identity), have evolved with non-redundant functions. Thus, analysis on aquaporin knockout mutants will surely contribute to a better understanding of the integrated functions of individual aquaporin isoform in plants.

1.3 Goals of the project

To further our molecular understanding of plant water relations the major aim of this work was to provide new insights into individual aquaporin isoforms and the processes and functional contexts in which they are involved. I focused on the *Arabidopsis* PIP2 subfamily with eight members; all have been shown to facilitate the permeation of water or at least to possess the critical amino acids indicating water permeation (see above). Furthermore, PIP2 members exhibit a high amino acid sequence homology. Thus, a central issue of this work was asking whether they might exhibit differential or mostly redundant, overlapping functions.

Several molecular genetic, biochemical and physiological approaches were undertaken to infer their roles in plant physiology:

- Transgenic *PIP2*-promoter-reporter (GUS) lines were examined to comprehensively elucidate the organ and cellular expression patterns of all members.

- A collection of *pip2* knockout mutants was established as an important tool to study and compare the effects of individual loss-of-function, since overexpression and antisense-suppression had turned out to be less specific. To analyze the importance of single *PIP2* genes, the phenotypes of the knockouts were analyzed under different conditions including water stress. Furthermore, the transcriptome levels and PIP protein levels were analyzed for differential alterations provoked by the mutation.

- Public expression data were mined to identify co-expressed genes and stress-responsive transcriptional patterns of *PIP2* genes.

- So far only a few examples could demonstrate that a single aquaporin was involved in plant water relations. Therefore, a method using deuterated water as a tracer and subsequent mass spectrometric analysis was adapted to study non-invasively the impact of PIP2 on water uptake using *pip2* knockout mutants.

Based on these analyses, a differential and mostly non-redundant function for the closely related *PIP2* genes in *Arabidopsis* is proposed and their individual involvement in plant water relation discussed.

2 MATERIALS AND METHODS

2.1 Materials

2.1.1 Plant materials

Insertion lines and wild-type plants used in this study were of *Arabidopsis thaliana* ecotype Col-0 except mutant line FLAG572D12 that was of ecotype Ws (Wassilewskija). Informations about *AtPIP2* insertional mutant candidates were obtained by screening the publicly accessible SIGnal T-DNA Express database of the SALK Institute (http://signal.salk.edu/cgi-bin/tdnaexpress (Alonso et al., 2003). Mutant candidates from various sources were retrieved; i.e. from the SALK, the GABI-Kat (Rosso et al., 2003), the JIC SM (Tissier et al., 1999), the Genoplante FLAGdb/FST (Balzergue et al., 2001) and the SAIL collections (Sessions et al., 2002). The seeds were purchased from the Nottingham *Arabidopsis* Stock Center (NASC) or from the *Arabidopsis* Biological Resource Center (ABRC, Ohio state University, USA, http://www.biosci.ohio-state.edu/pcmb/Facilities/abrc/abrchome.htm). GABI lines and FLAG lines were purchased from GABI-Kat (MPI, Köln, Germany) and the Institut National de la Recherche Agronomique (INRA, Versailles, France), respectively. Insertional mutants used and isolated in this work are listed in Table 1.

Plant transformation with *PIP2* promoter::GUS constructs or *PIP2* promoter::PIP2-ORF-GFP constructs were performed on *Arabidopsis thaliana* Col-0 and C24 or Col-0, respectively. Transgenic plants expressing *PIP2* promoter::GUS fusion protein for *PIP2;1*, *PIP2;2*, *PIP2;3* and *PIP2;4* were established earlier in the lab in C24 background (Franck, 1999). In addition, seeds of transgenic plants expressing a *PIP2;5* promoter::GUS fusion protein were obtained from a colleague (Dr. Ulrich Hammes, Molekulare Pflanzenphysiologie, FAU Erlangen) within the priority program "Dynamics and Regulation of Plant Membrane Transport" (DFG-Schwerpunktprogramm 1108 "Dynamik und Regulation des pflanzlichen Membrantransportes").

Table 1. *AtPIP2* insertional mutants.
Single and double mutants used in this work are listed. Absence (A) or presence (P) of transcripts expression was tested by RT-PCR. Mutants showing loss-of-transcripts are labeled in bold. Nd: Not determined. collections used: AMAZE (ZIGIA project, MPI, Köln, Germany), JIC SM (Tissier et al., 1999), GABI (Rosso et al., 2003), SAIL (Sessions et al., 2002), SALK (Alonso et al., 2003) and FLAG (Balzergue et al., 2001).

AGI code/ Name	Mutant name	Line	Mutant Lab name	Ecotype	Transcript	Reference
			pip2 single mutants			
	pip2;1-1	**6AAS98**	**Amaze**	***pip2;1En***	Col-0	**A** (Affenzeller, 2003)	Affenzeller, 2003
At3g53420 *PIP2;1*	***pip2;1-2***	**SM_3_35928**	**JIC SM**	***pip2;1sm***	Col-0	**A** (RT-PCR/ array)	This work
	pip2;1-3	Salk_040961	SALK	*pip2;1K*	Col-0	No insertion detected	This work
	pip2;1-4	Gabi_158B11	GABI	*pip2;1G1*	Col-0	**P** (RT-PCR)	This work
	pip2;1-5	Gabi_895D12	GABI	*pip2;1G2*	Col-0	**Nd** (Hemizygous)	This work
At2g37170 *PIP2;2*	***pip2;2-3***	**Sail_169A03**	**SAIL**	***pip2;2L***	Col-0	**A** (RT-PCR/ array)	This work
	pip2;2-4	**Gabi_098D07**	**GABI**	***pip2;2G***	Col-0	**A** (RT-PCR/ array)	This work
	pip2;2-5	Sail_80A06	SAIL	*pip2;2L2*	Col-0	**P** (RT-PCR)	This work
At2g37180 *PIP2;3*	***pip2;3-1***	**Salk_117876**	**SALK**	***pip2;3K***	Col-0	**A** (RT-PCR/ array)	This work
	pip2;3-2	**Sail_1215D03**	**SAIL**	***pip2;3L***	Col-0	**A** (RT-PCR/ array)	This work
At5g60660 *PIP2;4*	***pip2;4-1***	**SM_3_20853**	**JIC SM**	***pip2;4sm***	Col-0	**A** (RT-PCR/ array)	This work
	pip2;4-2	Sail_1251G12	SAIL	*pip2;4L1*	Col-0	**P** (RT-PCR/ array)	This work
	pip2;4-3	Sail_535D05	SAIL	*pip2;4L2*	Col-0	**P** (RT-PCR)	This work
At3g54820 *PIP2;5*	***pip2;5-1***	**Sail_452H09**	**SAIL**	***pip2;5L1***	Col-0	**A** (RT-PCR/ array)	This work
	pip2;5-2	**Sail_1179F10**	**SAIL**	***pip2;5L2***	Col-0	**A** (RT-PCR)	This work
	pip2;5-3	**SM_3_30592**	**JIC SM**	***pip2;5sm***	Col-0	**A** (RT-PCR/ array)	This work
	pip2;5-4	Salk_072405	SALK	*pip2;5K*	Col-0	**P** (RT-PCR)	This work
	pip2;5-5	Flag_572D12	FLAG	*pip2;5F*	Ws-4	**P** (RT-PCR)	This work
At2g39010 *PIP2;6*	***pip2;6-1***	**Salk_029718**	**SALK**	***pip2;6K***	Col-0	**A** (RT-PCR/ array)	This work
	pip2;6-2	**Sail_1286G02**	**SAIL**	***pip2;6L***	Col-0	**A** (RT-PCR/ array)	This work
At2g16850 *PIP2;8*	***pip2;8-1***	**Salk_099098**	**SALK**	***pip2;8K***	Col-0	**A** (RT-PCR/ array)	This work
			pip2 double mutants			
PIP2;2/ PIP2;1	***pip2;2-3/*** ***pip2;1-2***	**Sail_169A03** SM_3_35928	**SAIL** JIC SM	*Pip2;2L-* *pip2;1sm*	Col-0 Col-0	**A** (RT-PCR/ array) **A** (RT-PCR/ array)	This work
PIP2;1/ PIP2;4	***pip2;1-2/*** ***pip2;4-1***	**SM_3_35928** SM_3_20853	**JIC SM** JIC SM	*Pip2;1sm -* *pip2;4sm*	Col-0 Col-0	**A** (RT-PCR/ array) **A** (RT-PCR/ array)	This work
			pip1 single mutants			
At3g61430 *PIP1;1*	***pip1;1-1***	**Gabi_437B11**	**GABI**	***pip1;1G***	Col-0	**A** (RT-PCR)	This work
At2g45960 *PIP1;2*	***pip1;2-1***	**Salk_145347**	**SALK**	***pip1;2K1***	Col-0	**A** (RT-PCR)	This work
	pip1;2-2	**Salk_019794**	**SALK**	***pip1;2K2***	Col-0	**A** (RT-PCR)	This work

2.1.2 Vectors and bacteria

The plasmid vectors and *E. coli* bacteria used in this work are listed below. For plant transformation the *Agrobacterium tumefaciens* strain GV3101 (pMP90) was used.

Bacteria:

E. coli DH-5α

E. coli DH-5α (DB3.1) (Gateway, Invitrogen, Karlsruhe, Germany)

E. coli BL-21 (DE3)

Vectors:

pDEST15 (Gateway, Invitrogen, Germany)

pDONR221 (Gateway, Invitrogen, Germany)

pGEM-T easy vector system (Promega, Germany)

pBGWFS7 (containing T-DNA; Gateway, Invitrogen, Germany) (Karimi et al., 2002)

pK7FWG2 (containing T-DNA; Gateway, Invitrogen, Germany) (Karimi et al., 2002)

2.1.3 Antibiotics

Table 2. Antibiotic stock and working solutions. Stock solutions were stored at -20°C.

Antibiotics	Stock solution (mg/ mL)	Working concentration (μg/ mL)
Ampicillin (Roche, Mannheim, Germany)	100 (in water)	100
Gentamicin (Roche, Mannheim, Germany)	50 (in water)	25
Kanamycin (Sigma, Deisenhofen, Germany)	50 (in water)	50
Rifampicin (Sigma, Deisenhofen, Germany)	50 (in methanol)	100
Spectinomycin (Sigma, Deisenhofen, Germany)	100 (in water)	100

2.1.4 Restriction enzymes and Modifying enzymes

The restriction enzymes and their buffers were obtained from MBI Fermentas Life Sciences (St. Leon-Rot, Germany) or New England Biolabs (Frankfurt, Germany). All the modifying enzymes like T4-DNA-ligase, DNase, RNase A and H, T4-DNA-Polymerase, Reverse transcriptase Superscript II, Rnase H, *Taq* DNA Polymerase, *Pfu Turbo*®, alkaline phosphatase, etc. were purchased from Q-Biogene, MBI Fermentas, Stratagene, Roche, Sigma, Gibco-BRL, Amersham Pharmacia, and Promega.

Gateway cloning enzymes were purchased from Invitrogen (Karlsruhe).

2.1.5 Antibodies

Antiserum:

- Rabbit brown antiserum against C-terminus RASGSKSLGSFRSAANV of *At*PIP2;2 (=2;1, 2;3) fused to keyhole limpet hemocyanin (Heidi Sieber & Anton Schäffner).

- Rabbit 5.1 antiserum against N-terminus
MEGKEEDVRVGANKFPERQPIGTSAQSDKDYKEPPPAPFFEP of *At*PIP1;1
expressed as a GST-fusion protein (Heidi Sieber & Anton Schäffner)

<u>Secondary antibody:</u>

Anti Rabbit IgG, Cy™5-Linked (from goat; Amersham Pharmacia, Freiburg)

2.1.6   Isotopically labeled compounds

[α-^{33}P]dATP (>2500 Ci/mmol), Redivue stabilized and regular form (Amersham
Pharmacia, Freiburg)

[γ-^{33}P]ATP (>2500 Ci/mmol), Redivue (Amersham Pharmacia, Freiburg)

D_2O (90%) (Merck)

2.1.7   Oligonucleotides and sequencing

Primers were designed using Primer3 software (http://frodo.wi.mit.edu/cgi-bin/primer3/primer3_www.cgi) and oligonucleotides were obtained either from the Helmholtz
Zentrum München facility or from Thermo Electron (Ulm, Germany). Stock solutions were
prepared at a concentration of 200 µM. All primers used in this work are listed in Annex 1.

2.1.8   Chemicals

All commonly used media chemicals used in this study were of molecular biology grade and
purchased from commercial sources: Amersham Pharmacia (Freiburg), Bio-Rad Lab GmbH
(München), Gibco-BRL (Eggenstein), Merck (Darmstadt), Roche (Mannheim), Roth
(Karlsruhe), Serva (Heidelberg) and Sigma (Deisenhofen).
Detergent Silwet L-77 was purchased from Lehle Seeds (Round Rock, Texas, USA).
Plasmid isolation, agarose gel extraction, PCR purification kits and other purification columns
used in this work were obtained from Qiagen (Hilden) or Amersham Pharmacia (Freiburg).
Special chemicals are detailed in the corresponding methods below.

2.1.9   Medium and solutions

Common media, buffers and solutions were prepared according to recipe and informations
obtained from the laboratory manual Current Protocols in Molecular Biology (Ausubel et al.,
1987 with quarterly updates). Special media and solutions are depicted in the corresponding
methods below.

2.1.10 Apparatus

Table 3. Apparatus and equipment

Name	Company
ABI PRISM 7900HT	Applied Biosystem, Foster City, USA
Bio-Rad Gel Doc 2000	Bio-Rad Lab GmbH, Munich, Germany
Centrifuge rotanta 460R	Hettich, Tuttlingen, Germany
Electroporation Gene Pulser^{TM}	Bio-Rad Lab GmbH, Munich, Germany
Eppendorf centrifuge 5451C	Eppendorf, Hamburg, germany
FLA-3000 image reader	Fuji, Düsseldorf, Germany
Illuminated refrigerated incubator shaker Innova 4340	New Brunswick scientific, Nürtingen, Germany
Light microscope Olympus SZ-40	Olympus optical, Hamburg, Germany
MicroGrid II robot	BioRobotics, Cambridgeshire, England
Microtiterplate centrifuge 4K15C	Sigma GmbH, Osterode, Germany
MultiCycler PTC-200	Biozym, Oldenburg, Germany
Nanodrop ND-1000 spectrophotometer	Kisker-biotech, Steinfurt, Germany
Precision Balance	Sartorius, Göttingen, Germany
Rotary Kilns for Hybridization	Bachofer GmbH, Munich, Germany
Scintillation counter LS 6000SC	Beckman Coulter, Krefeld, Germany
SORVALL RC 5B+ superspeed centrifuge	DuPont Instruments GmbH, Bad Homburg, Germany
Spectrophotometer DU640	Beckman Coulter, Unterschleissheim, Germany
Speed-Vac UNIVAPO 100H	UNIEQUIP, Martinsried, Germany
Stereomicroscope Leica MZ16F with Leica DFC 320 camera	Leica, Munich, Germany
Table centrifuge Mikro 24-48R	Hettich, Tuttlingen, Germany
Thermocycler UNO-Thermoblock	Biometra, Göttingen, Germany
Ultracentrifuge LE-70	Beckman Coulter, Munich, Germany
UV Stratalinker	Stratagene, La Jolla, USA
VacuGene-XL Blotting	Amersham Pharmacia, Freiburg, Germany
Zeiss Axioskop (fluorescence microscope)	Zeiss, Jena, Germany

2.2 Methods

2.2.1 Culture of *Arabidopsis thaliana* plants

2.2.1.1 Growth conditions

Arabidopsis thaliana plants were grown on soil or in vitro in a growth chamber under the following environmental parameters (or otherwise mentioned): 16-h/8-h light/dark cycle, 150-200 $\mu mol.m^{-2}.s^{-1}$ light intensity, 24/20°C day/night temperature and relative humidity ranged from 45 to 60%. In all cases, seeds were vernalized in the dark at 4°C for 2 to 5 days to synchronize germination and further placed in growth chamber.

2.2.1.2 Growth in soil, crossing, seeds harvesting and storage

For growth in soil, seeds were placed onto trays filled with a 3:1 soil: sand mixture, vernalized and then placed in growth chamber. Plant material was collected 5 h after the onset

of light and used either immediately for analyses or frozen in liquid nitrogen and stored until further use at -80°C .

Double *pip2* mutant were obtained by crossing *pip2* single mutant plants together. *Arabidopsis* plants were grown until mature flowers are present and at a stage where they are not open, yet not closed (4 to 6 weeks). An inflorescence is chosen and all the flowers that are too young or too old as well as all other plant parts in the immediate vicinity (flowers, siliques) were removed leaving 2-3 flowers and a free work environment. Using very fine forceps (Dumont No. 5) sepals, petals and stamen of a recipient flower are removed leaving only the pistil. During all the procedure, care has to be taken not to damage recipient pistil and its stigma. Pollen is then obtained from a donor plant by getting fully mature flowers and removing the stamens. These stamens, containing pollen grains, are used to place pollen on the top of the prepared ovaries. This step is repeated at least twice to ensure proper pollination. Each pollinated inflorescence is labeled accordingly and ovaries were let developing and seeds harvested once siliques were dry. Siliques should develop in about 5 days. If several crosses are done in a row, forceps were cleaned by dipping them in 95% ethanol (v/v) followed by rising with distilled water.

For mass harvesting of seeds, it was stopped watering the plants after the first siliques are beginning to turn brown (about two months). The plants were allowed to dry out and seeds from yellow brown siliques were harvested by gently tapping the dried plants onto a sheet of paper. Seeds were then transferred in seed packets and allowed to dry for one more week in a dessicator before being stored at room temperature.

2.2.1.3 Seed sterilization

For in vitro cultures, seeds in an Eppendorf tube were surface-sterilized under a sterile bench with 70% (v/v) ethanol for 1 min followed by soaking in 30% (v/v) commercial bleach solution Klorix (DanKlorix, Colgate-Palmolive GmbH, Germany) for 5 min and then rinsed four times in sterile double-distilled water.

2.2.1.4 *In vitro* culture on solid medium

Standard medium (SM) for in vitro culture was composed of 0.5X Murashige and Skoog Basal medium (Sigma, Germany) supplemented with 1.5% (w/v) sucrose and 0.5% (w/v) Gelrite (Duchefa, The Netherlands), pH 5.7 adjusted with KOH. Medium was autoclaved (20 min, 120°C) and square Petri dishes (120 mm x 120 mm x 17 mm, Greiner bio-one, Germany) were poured with 75 mL SM medium each. Surface-sterilized seeds were sown

onto solidified medium and plates were wrapped with parafilm and placed at 4°C for stratification before being transferred into growth chamber in a vertical orientation.

2.2.1.5 Hydroponic culture

Nutrient solution for hydroponically grown plants was prepared according to Gibeaut et al. (1997; Table 4). Seed holders (1.5 mL Eppendorf tubes) were overfilled with a sterile growth gel. The gel contained 0.65% (w/v) agar (Plant Cell Culture tested, Sigma, Germany) and 0.5X hydroponic nutrient solution dissolved in double distilled water and was autoclaved prior to pouring of the Eppendorf tubes. Once the gel has solidified, 1-2 seeds were placed on the top of the gel in every tube which were then wrapped with saran wrap and vernalized in the dark at 4°C for 2 days to synchronize germination. The tubes were then transferred to a home-made hydroponic rack containing 56 holes and placed over a 15 liters hydroponic container filled with deionized water and placed in the growth chamber. Hydroponic racks and containers were opaque to produce healthy roots and to prevent growth of algae. To maintain high humidity and sterile conditions, the hydroponic containers were covered with a transparent plastic box. Standard growth conditions of the growth chamber were used (Method 2.2.1.1). After about six days, the Eppendorf tubes were cut at the bottom to allow roots to grow through the agar and reach the medium and placed in a new hydroponic box filled with 15 liters of fresh hydroponic medium. After cutting, the bottom of the tubes should be submerged in the nutrient solution. Care was taken to avoid cutting of the root tip of the seedlings. At this stage, the plastic cover was gradually elevated to prevent stress of the young seedlings. At day 10 to 12, the cover can be completely removed and growth conditions were changed to 11.5 h/12.5 h light/ dark cycle. The plants were then allowed to grow for 10 more days (ultimately, three-week-old plants).

Table 4. Hydroponic medium composition (Gibeaut et al., 1997)
To control the pH MES was additionally added.

Macro-elements (200X stock solutions, autoclaved)	250 mM KNO_3 300 mM $Ca(NO_3)_2$ 150 mM $MgSO_4$ 100 mM KH_2PO_4
Micro-elements (1000X stock solutions, autoclaved)	50 mM KCl 50 mM H_3BO_3 10 mM $MnSO_4$ 2 mM $ZnSO_4$ 1.5 mM $CuSO_4$ 0.075 mM $(NH_4)_6Mo_7O_{24}$ 100 mM Na_2SiO_3 72 mM Fe-EDTA
MES is then added (0.5 g/L, w/v) and pH adjusted to 5.7 with KOH	

2.2.1.6 Growth measurements on *in vitro* culture

For growth measurements, surface sterilized and vernalized seeds were allowed to germinate on SM medium (Method 2.2.1.4) and 4-days-old wild-type and mutant seedlings grown on a vertical position were then transferred and placed with roots pointing downward onto new vertical Gelrite plates supplemented (or not) with various solutes; 50 or 100 mM NaCl, KCl or 200 mM Sorbitol. Each plate contained 5 to 6 mutant and wild-type seedlings (3 genotypes, i.e. wild-type and 2 mutants were placed per plate). All experiments were repeated 3 to 5 times. For the kinetics, increases in root length were measured with a ruler every day for 7 days. Means ± standard deviation (SD) of the root length were calculated for each experiment (n = 5 to 6).

Relative root growth was calculated as the percentage of final root length of the mutants over the final root length of the wild-type plants in the same plate. Mean ± standard error (SE) of all experiments (n = 5 to 6 plants per experiment independently repeated 3 to 5 times) were calculated and p-value were determined using an unpaired t-test assuming unequal variance and with 95% confidence ($p < 0.05$).

2.2.1.7 Leaf water loss measurement using detached-rosette assay

For leaf water loss measurements, plants were grown on soil with standard growth conditions for 1 week and then under short day conditions (11.5 h/12.5 h light/ dark cycle). Plants were grown under these conditions for 2 more weeks. The decline of fresh weight of excised rosette leaves from 21 day old plants was determined to compare the speed of loss of water by the leaves from wild-type and *pip2* mutant plants. The whole rosette was detached from the plant, weighed and left at room temperature (25°C, 55% humidity) in a laminar flow bench with

continuous ventilation. Water loss was measured by weighing the plants every one hour for 4 hours. Four separate plants were used for each genotype and experiment was repeated 3 times (n = 3). Decline in fresh weight was expressed in percentage of the initial fresh weight and mean ± SE of the 3 independent experiments were calculated and used for comparison of the different genotypes. P-values were calculated using an unpaired t-test assuming unequal variance and a 95% confidence was chosen ($p < 0.05$).

2.2.1.8 Root bending assay (gravitropism response)

Wild-type and *pip2 Arabidopsis* mutant seeds were germinated on SM medium (Method 2.2.1.4) for 4 days under standard conditions and in a vertical position. Each plate contained 5 to 6 mutant and wild-type seedlings (3 genotypes, i.e. wild-type and 2 mutants were placed per plate). The plates were then turned 90° and the seedlings grew in their new horizontal orientation for 24 h. Plants were photographed every one hour for 8 h and a final photograph was taken at 24 h using a digital camera. Roots that reoriented completely to the new gravity vector resulting in vertical growth were considered to have a bending angle of 90°.

2.2.1.9 Analysis of deuterium (D) translocation in plant

Plant material and growth conditions

Arabidopis wild-type and *pip2* mutant plants were grown hydroponically in a growth chamber (Methods 2.2.1.1 and 2.2.1.5). In order to have controlled and reproducible conditions, 19 days-old plants were transferred into a sun simulator (Helmholtz Zentrum München-Institute for Soil Ecology-Department of Environmental Engineering, Neuherberg, Germany). In the sun simulator, the following conditions were set: 16-h/8-h light/dark cycle, 450 to 500 µmol m^{-2} s^{-1} light intensity, 22°C and 50% relative humidity. Due to the changing conditions plants are stressed when put in the sun simulator. Consequently, before starting the experiment, plants are left in the sun simulator 3 days for accommodation. Fresh hydroponic medium containing 1 mL of a 90% D_2O solution per 15 L hydroponic medium with δD = -75‰ was prepared. A big bottle was used to have enough isotopically identical medium that was further distributed in new hydroponic containers. After placing the new hydroponic containers in the sun simulator, it was left for about 2 h to restore the conditions (i.e. temperature, humidity).

Leaf and water sampling

Hydroponic racks with the plants were transferred in the new containers with deuterated water. Experiment started 5 to 6 hours after the onset of the light. Prior sampling, each plants

was given a name (e.g. A1, A2, A3, etc) in order to harvest and weigh roots of each plants at the end of the experiment. Plants and water were then collected at the corresponding time point to have a 24 hours kinetic study (0, 20 min, 40 min, 60 min, 80 min, 100 min, 2 h, 3 h, 4 h, 5 h, 6 h, 8 h and 24 h). Three plants and water samples (1 mL water per sample) were collected per time point. For plants, the entire rosette was harvested, placed into gas-tight glass vials tightly closed to prevent evaporation and stored at -20°C until the water could be extracted for isotopic analysis. Water samples from the medium without deuterium were also collected as a reference.

Atmospheric water vapor was also collected to measure its deuterium content. Air was continuously drawn from the sun simulator and pumped through a moisture freezing trap immersed in a dry ice-acetone mixture.

Sample preparation and analysis

Water from rosette leaves was extracted by cryogenic vacuum distillation. Rosette leaves were frozen in liquid nitrogen for about 10 min and fixed on a cryogenic distillation device. The system was then evacuated and isolated from the vacuum pump. The rosette leaves were boiled with a heating device and whole leaf water was collected in a tube immersed in liquid nitrogen. To obtain unfractionated water sample, extraction must proceed to completion and was therefore carried out for 2 h. The collection tubes were then stored in the freezer until processed for isotopic analysis. For each sample, rosette dry and fresh weight, water volume (fresh weight − dry weight) and relative water content ((fresh weight − dry weight) / fresh weight × 100) were measured.

The hydrogen isotope ratios (D/H) of water samples were measured twice by standard mass spectrometry (Delta-S, Finnigan MAT, Germany) and were expressed in parts per thousand (‰) as: $\delta D = \left(\dfrac{R_{sample}}{R_{s\,\tan dard}} - 1 \right) \times 1000$ (where R is the respective D/H ratio)

relative to the Vienna-Standard Mean Ocean Water (V-SMOW) (absolute ratio is D/H = 0.00015576).

The δD measurements of water samples have a precision of ± 1‰.

Fitting of the model

For each time point, mean values of measured leaf isotopic content were calculated. Fitting routines were then performed in Excel using equation 12 (see below Results 3.3.4). For each

time point difference between measured and modeled values were calculated. The sum of the squares of these differences was then determined and values for q and f were adjusted to get the lowest sum of the squares as possible. All other parameters (e.g. humidity) were constant and initially entered in the model.

2.2.2 Microbiological methods

2.2.2.1 Preparation of competent cells

A single colony of bacteria was inoculated into 2.5 mL of Rich Broth medium (RB) in a plating tube and cultivated overnight at 37°C with moderate shaking (250 rpm). An aliquot of 2.5 mL of culture was then subcultured in 250 mL RB medium containing 20 mM $MgSO_4$ and grown to an OD_{590} of 0.4 to 0.6.

The suspension was centrifuged at 5000 rpm for 5 min at 4°C. The supernatant was discarded and the bacteria pellet resuspended carefully in 100 mL of ice-cold TFB1 and kept on ice for 5 min. The bacteria suspension was centrifuged at same speed. The new pellet was resuspended gently in 10 mL cold TFB2 and incubated on ice for 15-60 min. One hundred microliters were aliquoted in ice-cold Eppendorf tubes, immediately frozen in liquid nitrogen and stored at -80°C.

To assure the efficiency of transformation the prepared competent cells were tested. Plasmid DNA containing 100, 10, 1 and 0.1 pg were added to100 µL competent *E. coli* competent cells and placed on ice for 30 min. Cells were then incubated in a 42°C water-bath for 30 sec and immediately placed on ice for 2-3 min. After addition of 900 µL SOC medium, samples were incubated at 37°C in a water-bath for 1 hour. Cells were mixed from time to time. After incubation, cells were centrifuged at 4000 g for 5 min. The supernatant was discarded, the pellet re-suspended in about 100 µL SOC medium and plated onto LB medium agar plate containing appropriate antibiotics. The plates were incubated overnight at 37°C.

TFB1

      30 mM KOAc (potassium acetate)

      100 mM RbCl

      10 mM $CaCl_2$

      50 mM $MnCl_2$

      15% glycerol

      pH adjusted to 5.8 with acetic acid

TFB2

    10 mM MOPS

    75 mM $CaCl_2$

    10 mM RbCl

    15% glycerol

    pH adjusted to 5.8 with acetic acid

Both solutions were filtered sterilized using 0.45 µm filter (Millipore, Germany).

2.2.2.2 Transformation of competent cells

A 100 µL aliquot of deep frozen competent cells is thaw on ice for 10 min and mixed with 5-10 µL of template DNA (ligation assay, Plasmid DNA). After incubation for 30 min on ice the mix is exposed to 42°C for 1 min and transferred on ice for 2 to 3 min. In order to allow expression of the antibiotics resistance, 900 µL of LB medium are added and bacteria are incubated for 1h in a 37°C water bath. Bacteria are then plated onto agar plate and incubated overnight at 37°C. The same transformation procedure was used independently of the plasmid (pDONR221, pK7FWG2, pBGWFS7). In case of Gateway-based vectors containing the ccdB gene, *E. coli* DB3.1 strain was used.

2.2.2.3 Transformation of *Agrobacterium tumefaciens*

Plasmids DNA were transferred into *Agrobacterium tumefaciens* by electroporation. A 100 µL aliquot of competent *Agrobacterium tumefaciens* strain GV3101 containing an appropriate helper Ti plasmid (pMP90) was thaw on ice. One µL of plasmid DNA (roughly up to a few 100 ng) is added to the cells and mixed on ice. The mixture is then transferred to a pre-chilled 0.2 cm electroporation cuvette. The electroporation was carried out as recommended for *E. coli* by the electroporator's manufacturer with slight modifications:

    Capacitance: 25 µF

    Voltage: 2.48 kV

    Resistance: 400 Ω

After a pulse, the time constant should be at least larger than 9.1 (optimal is 9.4 to 9.6) to give a relevant number of transformants. A control without plasmid DNA was always done in parallel. Immediately after electroporation, 1 mL of SOC medium is added to the cuvette,

gently resuspended and transferred to a 15 mL culture tube with SOC medium. Cells were then incubated at room temperature for 60-90 min with gentle agitation. The cells were collected by gently centrifuging at 5000 rpm for 2-3 min. A part of supernatant was discarded and the cells resuspended by gently pipetting in the remaining supernatant. Cells (1/2 and 1/4 of total) were spread onto LB agar plate with appropriate antibiotic selection (Rifampicin and Gentamicin for agrobacteria and appropriate antibiotic for T-DNA vector) and incubated at 28-30°C for 2 to 3 days.

2.2.2.4 *Agrobacterium tumefaciens*-mediated plant transformation

Transformed *Agrobacterium tumefaciens* strain GV3101 carrying the construct of interest within its T-DNA were used to transform *Arabidopsis thaliana* plants by the floral dip procedure (Clough and Bent, 1998). *Arabidopsis* plants were grown over long day (16h, 22°C) in pots to flowering stage. Once the primary bolt was formed, it was clipped in order to get multiple secondary bolts per plants. Siliques already formed were also clipped to achieve higher transformation rates by eliminating non-transformed seeds. Agrobacteria were grown overnight at 28°C to stationary phase in sterilized LB medium (1:100 bacteria in 200 mL LB medium). The culture was then centrifuged for 20 min at room temperature at 5500 g and then resuspended in a 5% (w/v) sucrose solution to a final OD_{600} of approximately 0.8. Before dipping, Silwet L-77 was added to the suspension to a final concentration of 0.05% (v/v). The solution was transferred to a beaker, and plant inflorescences were dipped for about 5 seconds into this solution. The same solution (100-200 mL) can be used for 2 to 3 small pots. Care was taken that only above-ground tissues were submerged and not leaves and soil. Dipped plants were then covered with a transparent plastic bag to maintain humidity and kept in a low light location for one day. Plant were then returned to the growth chamber and grown until siliques were brown and dry.

The first generation of seeds (T1) was collected, surface sterilized and grown either on soil and selected on the basis of BASTA resistance or in vitro in MS-agar solid medium (0.5X Murashige and Skoog Basal medium/ 1.5% sucrose/0.8% Agar, pH 5.8 with KOH) supplemented with appropriate selection antibiotics. Transformation rates are theoretically around 1%. After about 15-days of growth, transgenic seeds were able to germinate and produce green leaves in the presence of antibiotics while the non-transgenic seeds were not able to grow with true green leaves. The positive seedlings (transgenic lines) were transferred into soil trays and allowed to grow for the next generation of seeds (T2). At least, three independent transformant lines for each construction were used for further analyses.

2.2.3   Nucleic acid isolation

2.2.3.1 CTAB DNA Minipreparation from plant tissue

A small leaf (or part of inflorescense) was squeezed with small pistil (e.g. flamed blue tip) in an Eppendorf tube and 250 µL extraction buffer were then added. The tube was vortexed briefly and placed in a 65°C water bath for at least 10 min and 200 µL of chloroform-isoamylalcohol (24:1) were added, tube vortexed vigorously and thoroughly and subsequently centrifuged at full speed for 2 min in a table-top centrifuge. The upper aqueous phase was transferred (care was taken not to touch the interface) into a new Eppendorf tube containing 1 µL of 1% LPA. For DNA precipitation, 3 volume of absolute Ethanol p.a were added, mixed and left at -20°C for 20 min or longer. This step was followed by a 15 min centrifugation at 4°C and full speed in a table-top centrifuge. DNA pellet was then washed once with 70% Ethanol p.a., centrifuged at full speed for 10 min at 4°C. Pellet was allowed to dry on the bench or using a Speed-Vac and dissolved in 100 µL TE buffer. One µL was used for subsequent analyses (e.g. PCR).

1X CTAB Buffer for DNA preparation

      1.4 M NaCl

      100 mM Tris-HCl, pH 8.0

      2% (w/v) CTAB

      20 mM EDTA, pH 8.0

      1% (w/v) polyvinylpyrrolidone, Mr 40,000 (Sigma PVP-40 or P-0930)

2.2.3.2 Genomic DNA preparation for Southern blotting using DNeasy Plant Mini Kit

Genomic DNA used for Southern blotting was isolated using DNeasy Plant Mini Kit (Qiagen, Hilden, Germany). Leaf (or root) material was ground and 100 mg powder were weighed and used for DNA extraction according to the manufacturer's protocol. The concentration and purity of DNA was measured using spectrophotometer (Method 2.2.3.6).

2.2.3.3 Plasmid DNA preparation

Plasmid DNA were prepared with the help of Qiaprep® Spin Miniprep Kit (Qiagen, Hilden, Germany), according to the manufacturers protocol. Up to 20 µg of high copy plasmid DNA could be obtained from 1 to 5 mL overnight cultures of bacteria in LB medium.

2.2.3.4 Isolation of total RNA for RT-PCR

An RNA isolation protocol particularly well suitable for samples rich in polyphenolics or polysaccharides was used in this study (Chang et al., 1993). This method is very effective for isolation of total RNA from a wide range of samples and was therefore applied for isolation of whole RNA. About 100 mg of liquid nitrogen frozen or fresh material were ground to the very fine powder with a mortar and pestle under liquid nitrogen, transferred to a 2 mL Eppendorf tube and 500 mL of 65° C pre-warmed extraction buffer (490 µL CTAB-Buffer + 10µL 2-Mercaptoethanol) were then added. Samples were vortexed thoroughly and total RNA was extracted by addition of 500 µL chloroform/isoamylalcohol (24:1) followed by a centrifugation at 10 000 rpm for 5 min. This step was repeated once to increase the purity of the RNA sample. The supernatant was then transferred to an Eppendorf tube and total RNA precipitated overnight at 4° C by addition of 1/4 volume of 10 M Lithium chloride. Samples were then centrifuged at 14 000 rpm for 20 min at 4° C and pellet resuspended in 500 µL of SSTE buffer and incubated at room temperature for 2 h with agitation. After a new extraction with 500 µL chloroform/isoamylalcohol (24:1), the supernatant was transferred to a fresh Eppendorf tube and 1/10 Volume of 3 M Sodium-Acetate (NaOAc, pH 5.2) and 2 volume of absolute ethanol p.a. was added (or 1 volume of isopropanol in case of large volume). After 20 min at -20° C samples were centrifuged at 14 000 rpm for 20 min at 4° C, washed with 75% ethanol p.a. and centrifuged as above. Pellet were then allowed to dry on the bench and resuspended with 500 µL of TM buffer. Any traces of DNA were removed by addition of 1 µL DNase and incubation at 37° C for 15 min. DNAse was then extracted by addition of 500 µL chloroform/isoamylalcohol (24:1); samples were centrifuged and RNA precipitated by addition of 1/10 Volume of 3 M Sodium-Acetate (pH 5.2) and 2 volume of absolute ethanol p.a. and incubation for 30 min at -20° C. After centrifugation and washing by 75% ethanol as mentioned above, pellet was allowed to dry and resuspended in 20 µL DEPC-treated sterile water. Quality and concentration of RNA samples were than assessed by measuring the absorption at 260 nm in a spectrophotometer and integrity was analyzed in a 1% agarose gel electrophoresis (Methods 2.2.3.6 and 2.2.4.4).

CTAB RNA Extraction buffer

      2 % CTAB

      2 % PVP K30

      100 mM Tris/HCl pH 8.0

      25 mM EDTA

2 M NaCl

0,5 g/l Spermidine

SSTE Buffer

1 M NaCl

0,5 % SDS

10 mM Tris/HCl pH 8,0

1 mM EDTA

TM Buffer

40 mM Tris/HCl pH 7.5

6 mM $MgCl_2$

2.2.3.5 Isolation of total RNA using Qiagen RNeasy Plant Mini Kit

For isolation of Total RNA to be used for Affymetrix ATH1 microarray hybridization, RNeasy Plant Mini Kit (Qiagen, Hilden, Germany) was used. 100 mg leaf (or root) powder was weighed and RNA was extracted according to the manufacturer's protocol.

2.2.3.6 Determination of nucleic acids concentration

The concentration of DNA or RNA was determined by measuring the absorption at 260 nm and 280 nm. 10 mM Tris/HCl pH 7.5 was used to zero the spectrophotometer (Nanodrop ND-1000, Kisker-biotech, Germany). The ratio A260/A280 was calculated to estimate the purity of total DNA or RNA with respect to contaminants that absorb in the UV (e.g. proteins absorb at 280 nm). The ratio of isolated DNA (RNA) was about 1.8 (2.0) indicating high quality DNA (RNA). The integrity of RNA was then check in 1% agarose gel electrophoresis (Method 2.2.4.4).

2.2.4   Molecular biology methods

2.2.4.1 PCR (Polymerase Chain Reaction)

The purpose of a PCR is to make a big number of copies of a DNA fragment which can then be subsequently used (e.g. for sequencing or DNA cloning). There are three major steps in a PCR, which are repeated for 30 to 40 cycles. It starts with a denaturation step that occurs at high temperature (95°C) and during which the double strand melts, open to single stranded DNA and all enzymatic reactions stop. It is followed by annealing step at lower temperature

which depends on primer sequence. The primers bind to complementary sequence of the template and the polymerase can attach and starts copying the template. Once there are a few bases built in, the base pairing is so strong between the template and the primer, that it does not break anymore. The final step is the extension step at 72°C (ideal working temperature for the polymerase). The bases (complementary to the template) are coupled to the primer on the 3' side, polymerase adds dNTPs from 5' to 3', reading the template from 3' to 5' side, and bases are added complementary to the template.

PCR mix was prepared as followed:

- Template DNA (e.g. 1 µL from CTAB DNA preparation, 20 ng plasmid DNA)

- 2 µL of 10X reaction buffer

- 0.2 µL 20 mM dNTPs

- 1 µL of 10 µM forward primer

- 1 µL of 10 µM forward primer

- 0.1 µL (5 U/ µL) of Taq polymerase (Q-Biogen)

- Sterile ddH$_2$O to an end volume of 20 µL

PCR was performed in an automated Multicycler PTC-200 (Biozym, Germany) as followed:

- 95°C	2 min	1 cycle
- 95°C	30 sec	
- X°C (annealing)	30 sec	30-40 cycles
- 72°C	1 min/1kb	
- 72°C	5 to 7 min	
- 4°C	∞	

PCR products were then separated and visualized on agarose gel (Method 2.2.4.5).

2.2.4.2 Reverse Transcription Polymerase Chain Reaction (RT-PCR)

To analyze the transcript presence in the *pip2* mutants, total RNA was extracted from *Arabidopsis* tissues (Method 2.2.3.4) and used to synthesize cDNA. One µg total RNA was added to a cocktail containing 1X first-strand-synthesis buffer (Invitrogen, Germany), 1 mM dNTP Mix (MBI fermentas, Germany), 0.01 M DTT, 20 units RNase Inhibitor (MBI Fermentas, Germany), 3.5 µL of 0.05 µg/µL oligo (dT)$_{12-18}$ (Invitrogen, Germany) and DEPC-treated water to a final volume of 20 µL. After a 10 min incubation at room temperature 1 µL Reverse transcriptase Superscript II (diluted 1:3 in 1X first-strand-synthesis buffer, 67 U; Invitrogen, Germany) was added. The cDNA was then synthesized

using the following temperature scheme in PCR machine:

- 42°C 30 min

- 50°C 40 min

- 95°C 5 min

- cool down to 4°C.

As a control for genomic DNA contamination, a reaction without Reverse transcriptase was performed in parallel. A PCR reaction (Method 2.2.4.1) was then performed in a Multicycler PTC-200 (Biozym, Germany) using 1 to 2 µL cDNA and gene specific primers. Polymerized fragments were then separated and visualized on agarose gel (Method 2.2.4.5).

2.2.4.3 Purification of PCR product and DNA gel extraction

After PCR reaction or other enzymatic reactions, DNA fragments were purified from primers, nucleotides, polymerases and salts. The purification was performed with Qiaquick® PCR Purification Kit (Qiagen, Hilden, Germany) following manufacturer's instructions.

To purify or extract target DNA fragment from unspecific fragments from standard or low melting agarose Qiaquick® Gel Extraction Kit (Qiagen, Hilden, Germany) was applied according to the manufacturer's protocol. The method was appropriate for extraction and purification of DNA of 70 bp to 10 kb.

2.2.4.4 Digestion by restriction endonucleases

To check the length of insert in plasmid, the plasmid was cleaved by restriction endonucleases. Restriction endonucleases were chosen depending on the sequence of nucleic acid that insert was flanked. Digest contained about 0.5 µg plasmid DNA, 1X reaction buffer, ca. 5 units of restriction endonuclease(s), ddH$_2$O was added to the volume up to 20 µL. The mixture was incubated at 37°C for about 2-3h. The enzyme(s) was (were) deactivated at 65°C for 10 min. The fragments sizes were checked by agarose gel electrophoresis (Method 2.2.4.5).

2.2.4.5 Separation and visualization of nucleic acids on agarose gel electrophoresis

Nucleic acids were separated on agarose gel (0.5 to 2% in 1X TAE buffer) according to size of nucleic acids. It was added 0.5 µg/mL ethidium bromide (nucleic acids staining) to the agarose gel prior allowing it to polymerize. Nucleic acid samples were mixed with 5X DNA loading buffer. The samples as well as DNA standard marker were then loaded in the gel and

run at 5-10 V/cm for 1 to 2 h. DNA fragments were visualized under UV light and recorded with Bio-Rad Gel Doc 2000 (Bio-Rad, Munich, Germany).

The integrity and size distribution of total RNA was checked by 1% agarose gel electrophoresis and ethidium bromide staining. The respective ribosomal bands appeared as sharp bands on the stained gel.

2.2.4.6 Molecular cloning using the Gateway recombination technology

DNA fragments encoding different PIP2 promoters, PIP2-promoter-Open Reading Frame or PIP2 epitopes were polymerized by PCR using forward and reverse primers containing 29mer attachments allowing recombination according to the Gateway® Technology (Invitrogen, Germany). PCR were performed using the Pfu-Turbo proof-reading polymerase according to the manufacturer's recommendations (Stratagene, Germany). Two recombination reactions constitute the basis of the Gateway® Technology (Fig. 5). PCR fragments were first recombined by mean of the BP recombination in a 5 µL reaction (1/4 the recommended volume) into a vector pDONR221 (Fig. 5a). In this new vector, the integrity of the insert was confirmed by sequencing. This new vector carrying the insert is then used for the second recombination (LR recombination) to transfer the insert into the final destination vector. Destination vectors are binary vector allowing the transfer of the T-DNA into *Agrobacterium tumefaciens* (Method 2.2.2.3) and the subsequent transformation of *Arabidopsis thaliana* plants by the floral dip method (Method 2.2.2.4).

This cloning procedure was used to generate transgenic plants expressing β-glucuronidase (GUS) reporter gene under the control of different PIP2 promoters. *PIP2;1*, *PIP2;2*, *PIP2;3* and *PIP2;4* have been analyzed in the past in our group using such promoter:GUS fusion constructs (Franck, 1999). In addition, seeds of transgenic plants expressing a *PIP2;5* promoter::GUS fusion protein were kindly provided by Dr. Ulrich Hammes (Molekulare Pflanzenphysiologie, FAU Erlangen) (Hammes et al., 2005). Consequently, constructs were generated for *PIP2;6*, *PIP2;7* and *PIP2;8*. The promoter of *PIP2;6*, *PIP2;7* and *PIP2;8* were fused to the GUS gene and transferred into *Arabidopsis* plants. Since constructs previously made were in *Arabidopsis thaliana* ecotype C24 background whereas the *PIP2;5* promoter::GUS line was introduced in *Arabidopsis thaliana* ecotype Col0, the new *PIP2* promoter::GUS constructs were introduced into both Col0 and C24 ecotype.

Promoter regions of *PIP2;6*, *PIP2;7* and *PIP2;8* were isolated by PCR. DNA fragments containing about 2.5 kb of the 5' upstream region of the corresponding *PIP2* coding sequence were amplified using a proof-reading polymerase and forward and reverse primers allowing

recombination according to the Gateway system. The polymerized promoter regions were then inserted into pDONR221 transformation vectors (which allow reporter translational fusion constructs with GFP-GUS under the control of the *PIP2* promoter) by mean of a BP recombination (Fig. 5a). This new vector was then used for the second recombination (LR recombination) to transfer the insert upstream the GFP/GUS sequence within the T-DNA of the destination vector pBGWFS7 (Fig. 5b). The resulting construct was then transferred into *Arabidopsis thaliana* plants.

(a)

(b)
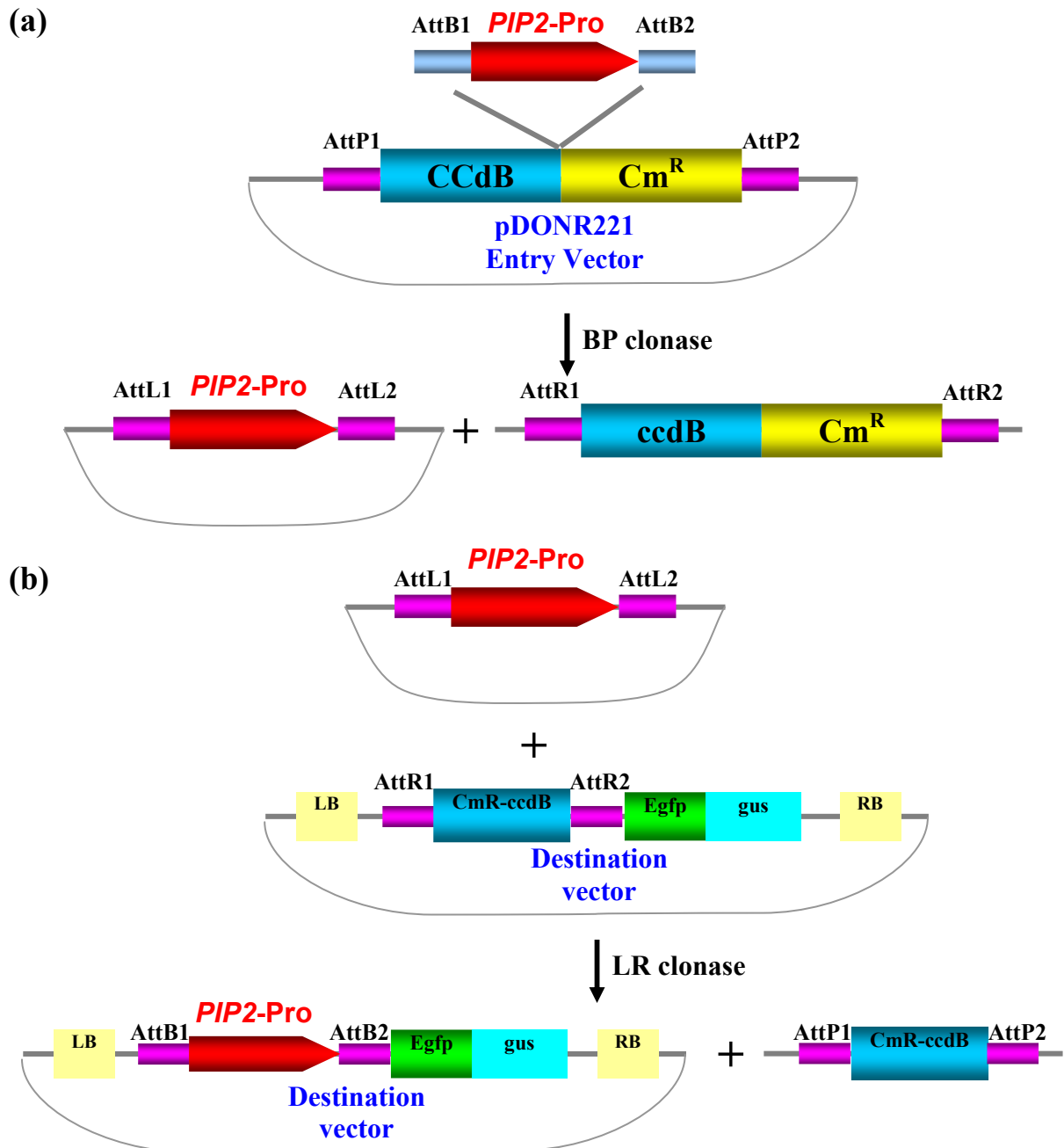
Figure 5. Schematic representation of *PIP2* promoter::GUS constructs using the Gateway technology.
(a) BP recombination into the entry vector pDONR221. (b) LR recombination into the destination vector pBGWFS7. In case of the promoter-ORF-GFP fusion constructs for *PIP2;1* and *PIP2;4*, the destination vector pK7FWG2 was used. LB: T-DNA left border; RB: T-DNA right border.

In case of *PIP2;1* and *PIP2;4* a promoter-ORF-GFP fusion construct has also been introduced into *Arabidopsis* thaliana ecotype Col-0 (as well as in a *pip2;1* knockout mutant for *PIP2;1*). Transgenic plants expressing these fusion proteins were generated in a way similar to that of *PIP2* Promoter::GUS constructs. However, the stop codon of *PIP2;1* (or *PIP2;4*) was modified to allow simultaneous expression of our gene of interest and the GFP. In both *PIP2;1* and *PIP2;4* constructs, the inserts had been verified by sequencing after recombination/cloning into the entry vector pDONR221. The destination vector pK7FWG2 used for *AtPIP2*-promotor-ORF_GFP fusion construct (Karimi et al., 2002) allows translational fusion of ORFs with the coding sequence of GFP under the control of CaMV 35S promoter. However, in the present study, the 35S-promoter was released by digestion of the vector, using the unique, flanking restriction sites SpeI and SacI, and religation. The resulting, derivative vector, pK7FWG2Δ35S, has been checked by restriction analysis and sequencing.

In case of PIP2 epitopes, the insert was transferred into destination vector pDEST15 allowing the expression as a GST fusion protein in *E. coli*.

2.2.4.7 DNA sequencing

Samples (e.g. PCR products, Plasmid DNA) for sequencing were prepared according to manufacturer's instructions and processed either by Medigenomix GmbH (Martinsried, Germany) or AGOWA GmbH (Berlin, Germany).

2.2.4.8 Southern blotting

Genomic DNA to be used for Southern blotting was extracted using DNeasy Plant Mini Kit (Qiagen, Hilden, Germany; Method 2.2.3.2).

Genomic DNA (2 µg) extracted from *Arabidopsis thaliana pip2* mutant was digested in a reaction volume of 300 µL with 30 to 40 U of restriction enzyme by incubation at 37°C for 12 to 16 h (overnight). After phenolization (300 µL roti-Phenol/Chloroform/Isoamylalcohol, 25/24/1, Roth Carl GmbH, Karlsruhe, Germany), DNA in upper phase was transferred to a fresh eppendorf tube containing 1 µL 1% LPA. DNA was then precipitated by 2.5 volume of ethanol p.a. and 1/10 volume of NaOAc 3 M and placed at -80°C for 1 h. After centrifugation at 14 000 rpm, 4°C for 20 min, DNA pellet was washed with 750 µL 75% ethanol p.a., dried and resuspended in 20 µL TE-buffer, pH 8.0 and 5 µL 5X gel loading buffer. Digests of *Arabidopsis thaliana* wild-type col-0 DNA were always included as an internal control.

To quickly check for complete digestion and confirming the amount of DNA, 1/5 of the digests were run on a small 0.7% agarose gel for 1 h. Although not well separated, a characteristic pattern due to repetitive DNA and the organellar DNA content could be visible. The remaining digests were then separated on a 0.7% agarose gel containing 0.5 µg/mL ethidium bromide in 1X TAE buffer. The electrophoretic separation was carried out at around 5 V/cm in a cold room (4°C) overnight (about 20 h). Additional lanes with Lambda DNA/Eco91I (BstEII; MBI Fermentas, Germany) digest were included as a size marker: 1 lane containing about 700 ng which are visible after UV illumination and additional lanes with about 2 ng directly adjacent to the lanes with the genomic DNA sample digests. After the gel has run completely, it was visualized under UV light and photographed with Bio-Rad Gel Doc 2000 (Bio-Rad, Munich, Germany). Unused lanes and extra of the gel were excised as well as the lane containing 700 ng of λ-DNA.

After visualization, a piece of positively charged nylon membrane (Hybond-N$^+$, Amersham, Germany) was cut according to the size of the gel and soaked with 0.4M NaOH. DNA was transferred onto the nylon membrane by alkaline transfer with a vacuum blotting chamber (VacuGene-XL, Pharmacia, Germany) according to manufacturer's protocol. The transfer was carried out for 1h 40 min at 40 cm H$_2$O with 0.4M NaOH. The gel was then removed and the membrane washed and neutralized in 2X SSC buffer. With a positively charged nylon membrane, the transferred DNA is covalently linked to the membrane if an alkaline transfer buffer is used. Therefore DNA immobilization by baking or UV crosslinking was not needed. The membrane was dried, wrapped in plastic wrap and stored at 4°C (-20°C for long storage) until processed.

To block unspecific binding sites on the membrane, it was prehybridized for 4h at 68°C with 1 mL/20 cm² prehybridization buffer (see method 2.2.8 for pre-hybridization solution).

DNA probes were prepared by PCR amplification of a part of the T-DNA left border of Gabi, Sail, Salk and SM insertion lines (For primers see Annex 1). DNA probe were then radioactively labeled with [α-^{33}P]dATP (>2500 Ci/mmol). Labeling was performed using 40 ng DNA probes with Strip-EZ$^®$ DNA kit (Ambion, USA) according to manufacturer's instructions. However, reverse and forward primers were used with their corresponding probe instead of decamers. Lambda DNA/Eco91I was labeled in a similar way using 25 ng DNA and decamers. The labeling reaction was carried out for 1h at 37°C and was stopped by addition of 1 µL 0.5 M EDTA (pH 8.0). The labeled probes were diluted by addition of 75 µL water and purified by spinning through S400-HR MicroSpin column (Amersham, Germany). The incorporation was estimated by measuring radioactivity before (total radioactivity) and

after purification (incorporated radioactivity). If less than 30% were incorporated, a new labeling procedure was done. For hybridization, labeled probes were denatured by boiling at 95°C for 5 min and immediate chilling in ice-water. After about 3 min denatured probes were added to the prehybridization solution (in case of Lambda DNA/Eco91I, only 1/4 of the labeled probe was added to each membrane). Hybridization was carried out at 68°C for about 20 hours. Membranes were then rinsed once with 2X SSC, 0.1% SDS prewarmed to about 68°C. Unspecifically bound probes were then removed by washing once with 2X SSC, 0.1% SDS for 15 min at 68°C followed by two washes with 0.2X SSC, 0.1% SDS at the same conditions. Membranes were then placed over a Whatman paper (prewet in 2X SSC), wrapped into plastic wrap and exposed with DNA side facing a Fuji imaging plate. Exposure was performed for about 24h and hybridization signals were revealed by scanning the membrane using FLA3000 image reader (Fuji, Düsseldorf, Germany).

2.2.5 Isolation and molecular characterization of *pip2* T-DNA insertional mutants

Informations about *AtPIP2* insertional mutant candidates were obtained by screening the publicly accessible SIGnal T-DNA Express database of the SALK institute (http://signal.salk.edu/cgi-bin/tdnaexpress). Mutant candidates from various sources were retrieved; i.e. from the SALK (Alonso et al., 2003), the GABI-Kat (Rosso et al., 2003), the SM (Tissier et al., 1999), the Genoplante FLAGdb/FST (Balzergue et al., 2001) and the SAIL collections (Sessions et al., 2002). The seeds were purchased from the Nottingham *Arabidopsis* Stock Center (NASC) or from the *Arabidopsis* Biological Resource Center (ABRC, Ohio state University, USA, http://www.biosci.ohio-state.edu/pcmb/Facilities/abrc/abrchome.htm). GABI lines and FLAG lines were purchased from GABI-Kat (MPI, Köln, Germany) and the Institut National de la Recherche Agronomique (INRA, Versailles, France), respectively.

Insertional mutant candidate lines were first screened by PCR analysis using a combination of primers specific for the corresponding *PIP2* gene and for the T-DNA left border sequences, respectively. Since the orientation of the insertions were not known, a reverse and forward primer specific for the *PIP2* genes were used in combination with primer specific for the T-DNA left border (see Annex 1 for primers). In addition, to reveal homozygous mutants (i.e. insertion in both alleles) the integrity of the *PIP2* coding sequence was then probed using *PIP2* gene-specific primers flanking the predicted T-DNA insertion sites. In our PCR conditions (Methods 2.2.4.1), the presence between the two gene-specific primers of a T-DNA or transposon insertion should prevent any DNA amplification. Consequently, the gene-

specific primer combination generated a product from the wild-type gene in wild-type and heterozygous plants but not in homozygous plants. To verify PCR products and identify T-DNA insertion sites, all amplified products were sequenced.

Homozygous mutants were further analyzed by RT-PCR to check whether homologous mutations in *pip2* mutants resulted in loss of transcripts (Method 2.2.4.2).

Insertional mutants isolated and characterized in this work are listed in table 1.

2.2.6 Protein methods

2.2.6.1 Preparation of microsomal fractions from *Arabidopsis thaliana* tissues

To avoid protein degradation, every step until resuspension was done in a cold room (4°C). Mortar, pestle as well as centrifuge and ultracentrifuge tubes were pre-cooled at 4°C before use. About 0.5 to 1 g plant material (roots or leaves) were ground to a fine powder and mixed with 8 mL homogenization buffer. The homogenate was filtered through 2 layers of miracloth into pre-chilled centrifuge beaker (SS-34). Mortar was washed with 2 mL homogenization buffer which were filtered as well and added to the homogenate for a final volume of 10 mL. After centrifugation at 8000g for 10 min at 4°C (Sorvall RC 5B+), the supernatant was filtered through a layer of miracloth into Beckman-ultra-clear tubes (for rotor SW 28) and centrifuged at 110 000 g for 40 min at 4°C (Ultracentrifuge LE-70). The supernatant was discarded and 100 µL of resuspension buffer was added to the pellet. The pellet was then incubated on ice for 30 min. The pellet was resuspended using a douncer after addition of 200 µL resuspension buffer. Microsomal fractions were thereafter transferred into a fresh eppendorf tube and stored at -80°C.

Homogenization buffer

     50 mM Hepes-KOH pH 7.5

     5 mM EDTA pH 8.0

     1 mM PMSF (freshly added)

     0.1 mg/mL BHT

     2 mM DTT (freshly added)

     0.1% PVPP (freshly added)

     0.5 M sucrose

Resuspension buffer

     0.33 M sucrose

5 mM K_3PO_4 pH 7.8

4 mM KCl

2 mM DTT

ddH_2O

2.2.6.2 Protein isolation from E. coli

One mL culture of transformed *E. coli* BL21 (DE3) were grown on 100 mL LB medium containing 100 µg/mL ampicillin at 37°C, 250 rpm until OD_{600} = 0.6. For induction of protein synthesis, 0.1 mM IPTG was added in the medium and it was then incubated for 3h, centrifuged at 9000 g for 10 min at 4°C and pellet was then frozen in liquid nitrogen and stored at -80°C until isolation of GST-fusion proteins. Bacterial pellet was resuspended in 2.5 mL homogenization buffer 1 and incubated at room temperature for 15 min with gentle shaking. Cells were lyzed by addition of 3 mL homogenization buffer 2 with 1% Triton X-100 and 15 min incubation at room temperature with shaking. Cell lysate was then centrifuged at 15 000 rpm for 10 min at 4°C and supernatant was collected.

Homogenization buffer 1

25 mL Bugbuster TM HT protein

25 µL 2-Mercaptoethanol

500 µL Lysozym (0.5 mg/ 50 µL in 0.1 M Tris/HCl pH 8.0)

125 µL Complete protease inhibitor cocktail (Roche, Mannheim, Germany)

Homogenization buffer 2

30 mL 1X PBS

30 µL 2-Mercaptoethanol

2.2.6.3 Purification of GST-fusion protein

A 300 µL aliquot of Glutathione Sepharose™ 4B (Amersham, Germany) equilibrated by 1X PBS was added into the supernatant and shaken at room temperature for 30 min, centrifuged at less than 1000 rpm for 5 sec to pellet Glutathione Sepharose™ 4B beads. Supernatant was discarded and pellet transferred to column. After 3 washes with 1X PBS, fusion proteins were eluted by addition of two times 300 µL Glutathione (20 mg/ 3 mL in 0.1 M Tris/HCl pH 8.0).

2.2.6.4 GST-fusion protein activity assay

The following solutions 10 µL of 100 mM 1-Chloro-2,4-Dinitrobenzene (CNDB), 100 µL KH$_2$PO$_4$ pH 6.5, 10 µL 100 mM Glutathione and 880 µL double distilled were mixed in two cuvette labeled by blank and sample. The two cuvettes were mixed and 55 µL of the sample (supernatant or eluate) was added into sample cuvette and mixed. Absorbance at 340 nm was recorded at 1 min interval for 5 min by first blanking the spectrophotometer. The activity of GST (glutathione S-transferase) was calculated as A340 nm/min/mL.

2.2.6.5 Determination of protein concentration using Bradford method

800 µL samples containing 2.5 to 20 µg BSA in 0.1 M Tris/HCl pH 8.0 were mixed with 1X Bradford solution, incubated at room temperature for 15 min and absorbance at 595 nm was measured.

2.2.6.6 ESEN test for determination of protein concentration

The protein content of the microsomal fractions was precisely determined using the Esen test (Esen, 1978). This test is based on the protein coloration by Coomassie brilliant Blue. It measures the protein concentration in their denatured form and do not need any further preparation and can therefore be immediately used for a SDS-polyacrylamide gel electrophoresis. This assay is specific for proteins and virtually free from interference by common laboratory reagents and other nonproteinaceous substances.

The microsomal fractions were prepared by adding, on ice, the following to 90 µL microsomal fractions:

15 µL 1M DTT (final concentration 0.1M)

15 µL 20% SDS

30 µL 5X Laemmli buffer (Laemmli, 1970) (without Bromophenol Blue) + 1.5 µL 2-mercaptoethanol freshly added

Similarly, BSA standard solutions of 0.2 µg/µL, 0.5 µg/µL, 0.75 µg/µL and 1 µg/µL were prepared with similar final concentration of DTT, SDS and Laemmli buffer.

Microsomal fractions as well as standard solutions were then denatured for 20 min at 56°C, centrifuged for 2 min at 15300 rpm and supernatants transferred into a fresh 1.5 mL Eppendorf tube. Proteins were then spotted on a 1 cm x 2 cm Whatman paper; 10 µL of protein solution were spotted in two neighboring spots of 5 µL each and allowed to dry for 5 min. A sample without protein was used as a control. Whatman papers containing the protein were then incubated for 5 min in fixation solution (25% (v/v) Isopropanol and 10% (v/v)

Glacial acetic acid) followed by 15 min incubation in coloration solution (0.1% (w/v) Coomassie brilliant Blue R250 in fixation solution), both under agitation. After destaining with water (boiled in microwave) and drying, the stained spots are cut, placed in a 2 mL Eppendorf tube and the dye-protein complex is eluted in 1.5 mL 0.5% SDS. Samples were incubated 1 h at 56°C (or overnight at room temperature). Protein concentration was determined by measuring the absorbance at 578 nm. The control sample was used as a blank. The protein concentration usually ranged between 0.25 and 0.5 µg/µL.

2.2.6.7 SDS polyacrylamide Gel Electrophoresis (SDS-PAGE)

This gel system uses the method described by Laemmli (1970). The protein sample is denatured and coated with detergent by heating in the presence of SDS and a reducing agent. The SDS coating gives the protein a high net negative charge that is proportional to the length of the polypeptide chain. The sample is separated on a polyacrylamide gel containing SDS by electrophoresis. Since a net negative charge taken by proteins is roughly proportional to their size, the molecular mass of the proteins can be estimated by comparing the mobility of a band with protein standards.

Electrophoretic separation was done using an Amersham biosciences Mighty Small II unit for 8 x 7 cm gels with a thickness of about 0.75 mm. The separating gel consisted of 12% acrylamide and 10% ammonium persulfate and TEMED were added just prior to pouring the gel. The resolving gel mix was poured into assembled plates, leaving sufficient space at the top for the stacking gel to be added later. The top was layered with water saturated butanol and allowed to polymerize at room temperature for about half an hour. Then the 6% stacking gel was poured after removing the butanol and rinsing the surface. The appropriate combs were fixed and the gel allowed to polymerize. At least 1 cm of stacking gel should be present between the bottom of the loading wells and the resolving gel. 1X SDS-PAGE running buffer was poured into the apparatus till the top of the wells.

Microsomal fractions (2 or 5 µg, for PIP1 or PIP2 blot, respectively) were denatured at 56°C for 20 min. Since all loading reagents (Laemmli buffer, SDS and 0.1M DTT) were added during protein determination by ESEN, no further reagents had to be added and samples were simply denatured at 56°C for 20 min. Under these conditions, PIP1 and PIP2 aquaporins run mostly as monomers of 28-30 kDa. The denatured protein samples were then loaded onto the gel as well as a prestained protein standard marker (Broad range, 6-175 kDa, New England Biolabs, also denatured similarly as for the microsomal fractions). Electrophoresis was carried

out initially at 80V until the due front reached the separating gel. Subsequently, electrophoresis was continued at 100V till completion.

SDS-polyacrylamide gel electrophoresis buffers:

4X separate buffer

      1.5 M Tris/HCl pH 8.8

      0.4% (w/v) SDS

4X stock buffer

      5 M Tris/HCl pH 6.8

      0.4% (w/v) SDS

12% separating gel (10 mL)

      ddH$_2$O 3.350 mL

      4X separate buffer pH 8.8 2.5 mL

      30% acrylamide (Rotiphorese) 4.0 mL

      10% Ammonium persulfate 50 µL

      TEMED 5 µL

6% Stacking gel (5 mL)

      ddH$_2$O 2.5 mL

      4X stock buffer pH 6.8 1.25 mL

      30% acrylamide (Rotiphorese) 1.0 mL

      10% Ammonium persulfate 40 µL

      TEMED 20 µL

1X Running buffer

      0.025 M Tris, pH 8.3

      0.192 M glycine

      SDS 0.1%

      ddH$_2$O

5X Laemmli buffer (Laemmli, 1970)

      10% (w/v) SDS

30% (v/v) glycerol

100 mM Tris/HCl pH 6.8

5% (v/v) 2-mercaptoethanol (add fresh)

(Optionally 0.1% bromophenolblue)

<u>Prestained Protein Marker, Broad Range (6-175 kDa)</u>

MBP-β-galactosidase, 175 kDa

MBP-paramyosin, 83 kDa

Glutamic dehydrogenase, 62 kDa

Aldolase, 47.5 kDa

Triosephosphate isomerase, 32.5 kDa

β-Lactoglobulin A, 25 kDa

Lysozyme, 16.5 kDa

Aprotinin, 6.5 kDa

2.2.6.8 Staining of SDS-PAG with Coomassie Brilliant blue

To visualize the proteins on the SDS-PAG, it was stained 2 h to overnight with a Coomassie dye solution (0.05% Coomassie R-250, 50% methanol, 10% acetic acid) and destained in destaining solution (10% methanol, 10% acetic acid). The bands were visualized as blue bands, photographed and documented with Bio-Rad Gel Doc 2000 (Bio-Rad, Munich, Germany).

2.2.6.9 Western blot

Protein transfer onto PVDF membrane was done using a semi-dry transfer unit (Milliblot-Graphite Electroblotter I, Millipore, USA). The transfer unit was rinsed with transfer buffer. The stacking gel was removed and the size of the separating gel was measured. The PVDF membrane and 9 blotter sheets (Whatman-3MM paper) were cut to the same size as the gel. They were pre-wet in transfer buffer. Six sheets of presoaked blotting paper were placed first, then the PVDF membrane, then the gel and finally 3 more buffer saturated blotter paper. At each step care was taken to remove air bubbles with a pipette by rolling over the sandwich. The transfer was carried out for 60 min according to the size of the gel (2.5 mA per cm^2). To check the efficiency of the transfer the gel was stained with Coomassie brilliant blue solution (see above).

After blotting the PVDF membrane could be stained or used for immunological visualization of proteins. The PVDF membrane was immersed in the blocking solution and incubated at room temperature for 3 hours to overnight with gentle shaking. It was then washed once with TTBS for 10 min. After decanting the TTBS, the primary antibody in antibody buffer was added. A 1:1000 dilution was used for rabbit anti-PIP2 antiserum and a 1:3000 dilution was used in the case of rabbit anti-PIP1 antiserum. It was incubated for 2 hr at room temperature (or overnight at 4°C). Unbound antibody was removed by washing twice for 5 min each with TTBS. An anti-rabbit cy5-linked secondary antibody in antibody buffer was added (1:1000) and incubated for 1 hr. The conjugate solution was decanted and the membrane was washed twice for 5 min each with TTBS at room temperature. It was given a final wash with TBS and then ddH$_2$O and membrane was scanned at 635 nm (Cy5 detection) using a FLA3000 image reader (Fuji, Düsseldorf, Germany). For quantification of the immunoblot signal, the intensity of each band was corrected for background and measured using ImageJ software (version 1.37v; http://rsb.info.nih.gov/ij/).

Transfer buffer

      80% 1X running buffer

      20% Methanol

Tris buffered saline (1X TBS)

      10 mM Tris/HCl pH 7.5

      150 mM NaCl

Wash solution (1X TTBS)

      0.05% of Tween 20 in 1X TBS (10μl of Tween 20 + 20mL of TBS).

Blocking solution

      2% Milk powder

      1% BSA (Fraction V, Boehringer Mannheim)

      1X TTBS to 100 mL

Antibody buffer

      0.1% Milk powder

      1X TBS to 100 mL

2.2.7   GUS staining of *Arabidopsis thaliana* plants

In order to study the expression pattern of different PIP2 isoforms *in situ*, the histochemical localization of the bacterial *ß-glucuronidase* gene (*uidA* or *gusA*) commonly referred to as GUS was assessed in transgenic plants expressing this reporter gene under the control of different *PIP2* promoters. The visualization of GUS activity was done using the histochemical GUS-Assay with X-Gluc as substrate (Jefferson et al., 1987). The GUS enzyme catalyses the cleavage of 5-Bromo-4-chloro-3-indolyl-β-D-glucuronic acid (X-Gluc) (a colorless substrate), which undergoes a dimerization leading to a final insoluble blue precipitate known as dichloro-dibromoindigo (ClBr-indigo). The ability of ClBr-indigo to immediately precipitate upon formation was used to trace the location site of GUS activity under the control of different *PIP2* promoters, allowing thereby an analysis of tissue specific localization of gene expression. Treated/untreated plant material was harvested, vacuum-infiltrated with fixation solution and further incubated in fixation solution for 30 min at room temperature. Samples were washed three times with phosphate buffer (Na-phosphate, pH 7.0) and then vacuum-infiltrated with GUS staining solution and incubated in this staining solution overnight at 37 ºC (a minimum volume of the staining solution was used). Samples were thereafter incubated in several changes of 70 % (v/v) ethanol solution at 80 ºC until complete destaining of chlorophyll. The samples were finally submerged and stored in 70% (v/v) ethanol at 4°C. Photographs were taken to show the expression pattern of the *PIP2* genes in plants.

GUS-fixation solution

     0.5% Formaldehyde

     0.05 % Triton X 100

     50 mM Na-phosphate, pH 7.0

GUS-staining solution

     1 mM X-Gluc in DMSO

     1 mM Potassiumhexacyanoferrat (II)

     1 mM Potassiumhexacyanoferrat (III)

     0.1 % Triton X 100

     50 mM Na-phosphate, pH 7.0

2.2.8 Custom-made DNA array harboring transport-related genes

A DNA array harboring gene-specific probes was established with the collaboration of several laboratories within the priority program "Dynamics and Regulation of Plant Membrane Transport" (DFG-Schwerpunktprogramm 1108 "Dynamik und Regulation des pflanzlichen Membrantransportes"). It harbors about 500 known and putative membrane transporter genes (e.g. aquaporins, ABC transporters, and vATPases and cation channels). The complete list of genes represented on the array can be found in supplementary Table 1.

2.2.8.1 Construction of target DNA sequences and array production.

Gene-specific probes were produced by selecting 3'-UTR sequences. Target sequences were then amplified by PCR using specific primer pairs and genomic DNA. PCR products were verified by sequencing and specificity of gene targets was checked by BLAST analyses. After purification, PCR products were cloned into pGEM-T easy vector (Promega, Germany), amplified using flanking vector DNA sequences, concentrated using Multiscreen plates (Millipore, USA), resuspended in water and spotted in duplicate onto Hybond-N$^+$ nylon membranes (Amersham, Germany) using MicroGrid II Robot (400 μm pins, 10 repeats per spot to transfer sufficient amount of DNA; BioRobotics, Cambridge, UK). Eventually, the membranes consisted of 8 rows x 12 columns of 4 x 4 subgrids (Fig. 6).

After spotting the membranes are dried (air) and nucleic acids were UV-cross-linked to the membrane using regular, default program of a Stratalinker (UV-Stratalinker 240, Stratagene, USA). Membranes were denatured with 0.5 M NaOH/ 1.5 M NaCl soaked Whatman paper for 5 min, neutralized with 0.5 M Tris/HCl pH 7.5/ 1.5 M NaCl soaked Whatman paper and washed with 2 SSC several times for pH neutralization.

Before processing with reference hybridization, the membranes are incubated in 0.4 M NaOH at room temperature for 20 min on a shaker to remove non-fixed PCR products, neutralized in 2X SSC, blotted dry on a Whatman filter paper, air dried and stored at 4°C for further use.

2.2.8.2 Hybridization with T7 reference probes

Prior to hybridization with T7 oligonucleotides, the membranes were pre-hybridized at 42°C for 3 hours in 10 mL pre-hybridization solution containing 5X SSC, 5X Denhardt's solution, 0.5% SDS, 100 μg/mL denatured salmon sperm DNA (or Herring sperm). T7 Reference probes mixture were prepared and contained for each membrane 2.5 μL 10 μM T7 oligonucleotide (5′-GACTCACTATAGGGCGAATTG), 1.25 μL 10X polynucleotide kinase buffer A, 1 μL [γ-^{33}P]ATP (2500 Ci/mmol, 10 μCi/μl; Amersham, UK), 1 μL T4

polynucleotide kinase (10 u/µL) and distilled water was added to a total volume of 12.5 µL. The mixture was incubated at 37°C for 30 min and additional distilled water was added to the mixture to a total volume of 50 µL. The non-incorporated nucleotides were removed by purification using MicroSpin G-25 Sephadex columns (Amersham, Germany) following manufacturer´s protocol applying a total volume of 100 µL. One µL T7 reference probe was then added to 10 mL scintillation solution and radioactive incorporation was measured by liquid scintillation counter (Beckman, USA). The calculated total activity of the eluate should be at least 10 to 15.10^6 cpm. Radiolabeled oligonucleotides were then added to the prehybridized filters in prehybridization solution. Hybridization was performed for about 20 h at 42°C. Filters were removed from hybridization solution, rinsed briefly with 2X SSC/0.1% SDS, then washed once in 2X SSC/0.1% SDS at 42°C for 30 min followed rinsing briefly in 0.2X SSC/0.1% SDS and a final wash in 0.2X SSC/0.1% SDS at 42°C for 30 min. The membranes were finally rinsed with 2X SSC, placed onto 2 sheets of 3MM Whatman paper soaked with 2X SSC and carefully wrapped into plastic film to prevent any drying during exposure. The membranes were then exposed to imaging plate (Fuji, Düsseldorf, Germany) for 3 hours and primary data were collected using a Fuji FLA 3000 image reader (Fuji, Düsseldorf, Germany).

Labeled probes were completely removed from filters by two washes with 0.4 M NaOH for 30 min. Membranes were completely neutralized by several washes with 2X SSC (until pH of the washing solution was less than 8), air dried and stored dry at 4°C until further use. Removal of the labeled probes was controlled by testing the radioactivity before and after with a hand-held monitor and by exposure (1 day) of the filters. Usually more than 95% should be removed and filters can be used for subsequent application.
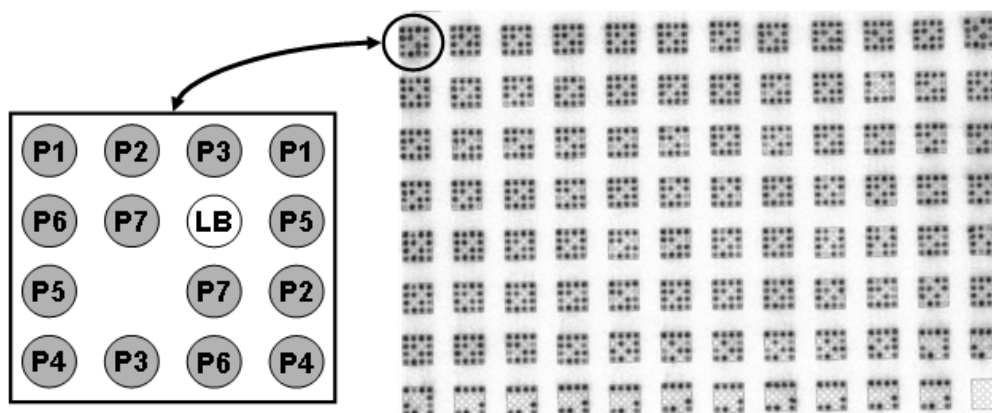
Figure 6. DNA array spotting scheme.
Typical picture from a reference hybridization showing the distribution of probes on the DNA array (right panel) and representation of the spotting scheme on each 4 x 4 subgrid (left panel). Hybridization occurs with radioactive marked T7 oligonucleotide. P1 to P7 represent 7 microtiter plates. LB, Local Background.

2.2.8.3 Isolation of mRNA using Oligo(dT)25 Dynabeads and preparation of complex probes

For transcript analyses, mRNA was isolated from roots of 3-week-old hydroponically grown plants. For each genotypes (wild-type and twelve *pip2* mutants), roots of three independent biological replicates were grown and harvested in parallel and stored at -80°C prior to RNA isolation. To decrease biological variation each replicate represented about 10 individual plants. Isolation of root mRNA was done using Oligo(dT) Dynabeads (Dynal Biotech, Hamburg, Germany).

Beads were prepared by mixing original tube well, but gently. Gentle handling is important throughout the whole procedure to reduce shearing and mechanic forces. Hundred µL aliquots per reaction of the suspension were transferred into 1.5 mL RNase-free Eppendorf vials. Tubes were then placed into magnetic stand for 30 sec liquid removed by pipetting. After taking out the tube from the stand, 200 µL lysis buffer (with DTT) were added, beads resuspended and placed back into magnetic stand. Supernatant was removed and 200 µL Lysis buffer was added. At this stage, buffer is left in the tubes and removed just before addition of the plant lysate to prevent the beads from drying.

About 100 mg frozen root material was ground under liquid nitrogen to a fine powder. Frozen powder was then transferred into pre-cooled 2 mL Eppendorf tube and 1 mL lysis buffer was added and tube was quickly vortexed thoroughly to make sure that powder is "dissolved". It was then centrifuged for 5 min, 15000 rpm, 4°C to remove cell debris. Beads were then separated from the lysis buffer on a magnet and supernatant discarded. Supernatant from the centrifuged samples (without any piece of tissue) was then added to the beads. It was then incubated for 5 min at RT by inverting several times the tubes. Tubes were placed into magnetic stand for approximately 30 sec until solution has cleared and supernatant were removed by pipetting; mRNA is hybridized to oligo(dT) covalently bound to the beads. Beads were washed twice with 800 µL washing buffer/LiDS/0.05% Tween 20. Beads were removed from the washing buffer using a PickPen® 1-M (pjk, Germany) and transferred into a fresh, RNase-free Eppendorf tube. Similarly, two washes using a Pick-Pen in 500 µL Washing buffer/0.05% SDS (but without LiDS) were done. Resuspended beads were divided into two portions which may be frozen in liquid nitrogen and stored at -80°C or used to proceed.

One portion of the beads was then used for cDNA synthesis. Beads were washed two times with 250 µL 1X Superscript buffer (self-made), transferred into fresh Eppendorf tube and resuspended in 100 µL superscript RT-Mix without Reverse Transcriptase Superscript II.

RT-Mix

     20 µL 5X RT buffer

     1 µL 100 mM DTT   (10 µL; 0,1 M)

     25 µL 2 mM dNTPs (2.5 µL from 20 mM dNTP)

     2.6 µL RNase Inhibitor (40 U/µL)

     Add ddH$_2$O to 98 µL

Mix was preincubated at 42°C for 2 min; 2 µL Superscript II (200 U/ µL; Invitrogen, Germany) were added and samples were incubated at 42°C for 1 h and mixed by hand from time to time. Beads were separated on the magnetic stand and supernatant discarded. After two washes with 250 µL RT Buffer/0.05 % Tween to remove protein and nucleotides, mRNA was eluted with 50 µL Elution Buffer (TE, 10 mM Tris-EDTA, pH 8.5) by incubation for 2 min at 95°C and immediate separation of the beads on a magnet. Supernatant (mRNA) is transferred to a fresh Eppendorf tube. Elution step is repeated once and mRNA was stored at - 80°C for further analyses.

Beads were washed twice with 250 µL TE buffer (pH 8.5) and twice with water and [^{33}P]-labeled cDNA probes were synthesized via random primed labeling using Strip-EZ$^®$ DNA kit (Ambion, USA) following manufacturer's instructions with slight modifications. Briefly, water was removed from beads as completely as possible and 14.0 µL ddH$_2$O, 4.0 µL 10X Decamer solution were then added. After denaturing the beads 2 min at 95°C, the following solutions were added:

     8 µL 5X buffer without dATP, dCTP

     4 µL 10X modified dCTP

     7 µL [α-^{33}P]dATP (2500Ci/mmol, 10 µCi/µl; Amersham, UK)

     3 µL Exonuclease-free Klenow (5 u/µL)

Beads were then incubated for 2.5 h at 37°C and mixed every 10 to 15 min. Supernatant containing non-incorporated nucleotides was then removed by magnetic separation and diluted to a total volume of 500 µL. A 2 µL aliquot was added to 10 mL scintillation solution for scintillation counting.

The synthesized, labeled DNA strand is then eluted from the beads with 50 µl elution buffer (10mM TE, pH 8.5) by incubating for 3 min at 95°C and collecting the supernatant containing the labeled DNA in a fresh Eppendorf tube as soon as possible after magnetic separation. This elution step was repeated once and the eluates were combined. The beads may be frozen and stored with TE and reused for new second strand synthesis.

The eluate was then purified by centrifugating over Whatman Anopore filter units (VWR, Germany) at 4000 rpm for 1 min and 2 µL of the eluate were mixed with 10 mL of scintillation solution. After scintillation counting, labeling efficiency was calculated (about 1.10^6 cpm).

2.2.8.4 Hybridization with complex probes and data acquisition

Filters were placed into a bottle with the DNA side facing towards the inside of the bottle with 4 mL pre-hybridization solution per filter (Method 2.2.8.2) and pre-hybridized for at least 4 h at 68°C in a roller oven. Eventually, labeled probe were denatured at 95°C for 3 min, and placed immediately and completely into ice/water. Denatured probe were added to the prehybridized membranes. Hybridization was then carried out in a roller oven at 68°C for 18 to 20 h. Membranes were rinsed with 2X SSC/ 0.1% SDS and washed once in 2X SSC/ 0.1% SDS solution at 65°C for 15 min followed by two washes with 0.2X SSC/ 0.1% SDS at 65°C for 15 min. Similarly as for reference hybridization, membranes were placed onto 2 sheets of Whatman 3MM soaked with 2X SSC (with DNA side up, i.e. facing towards the imaging plate), wrapped into plastic film to prevent drying, exposed to imaging plate for 20 to 48 h and scanned using the Fuji FLA 3000 image reader at resolution of 50 µm. After data acquisition, membranes were stripped using Strip-EZ® DNA kit (Ambion, USA) according to manufacturer's protocol and stored dry at 4°C. The success of the stripping was always checked using a hand-held monitor and by exposing the membranes in the same way as after the complex hybridization. If stripping is efficient, membranes can be re-used several times.

2.2.8.5 Microarray buffers
Lysis buffer with LiDS

       100 mM Tris

       500 mM LiCl

       10 mM Na_2EDTA

       1 % LiDS

       adjust to pH 8.0 with HCl, autoclave

       before use add DTT to 5 mM

Washing buffer with LiDS (RNase free)

       10 mM Tris

       150 mM LiCl

1 mM Na_2EDTA

0.1% LiDS

adjust to pH 8.0 with HCl

Washing buffer without LiDS (RNase-free)

10 mM Tris

150 mM LiCl

1 mM Na_2EDTA

adjust to pH 8.0 with HCl (you may use Tris-HCl pH 8.0)

5X RT buffer self-made (RNase-free)

250 mM Tris

250 mM KCl

50 mM $MgCl_2$

adjust to pH 8.0 with HCl (you may use Tris-HCl pH 8.3)

Prehybridization buffer

5X SSC

5X Denhardts

0.5% SDS

100 µg/mL Sheared salmon sperm/ herring sperm DNA (Promega, Germany)

ddH_2O to final volume

ssDNA was heated at $95^{\circ}C$ for 5 min prior to be added to the rest of the mixture which was pre-warmed to $65^{\circ}C$.

100X Denhardts:

10 g Ficoll

10 g Polyvinylpyrrolidone (PVP-360; MW: 360.000)

10 g BSA (Fraction V, Sigma)

Add ddH_2O to 500 mL

Filter sterilize (0.2 µm) to remove particles and store at $-20°C$.

2.2.8.6 Data evaluation and analysis

The spot detection and quantification of hybridization signals from the phosphorimager data were analyzed using the Array Vision 8.1 software (Inter Focus, Mering, Germany) yielding the raw data of each experiment. Raw data from individual hybridizations were processed and normalized using the Haruspex expression database (http://euklid.mpimp-golm.mpg.de/gxdb/). The local background signal of each 4 x 4 subgrid was subtracted from all related spot intensities. If the signal intensity of the spot was lower than 2 folds of local background (LB), it was replaced by local background value. These values were labeled later as "negative" gene activity values. Furthermore, the LB value was substracted from all signal values which were more than 2 folds the LB value. For normalization, the signal intensities were divided by the mean of the all signal values on the array. The same initial procedures were used for the T7 reference and complex (cDNA) hybridization signals. The ratio of normalized complex value/normalized reference value was calculated thereby taking the amount of DNA spotted into account (as referred from the reference hybridization). As there were two replicates on each array, the average values of these technical replicates were taken as the gene activity.

To compare *pip2* mutants vs. wild-type, the ratio of the corresponding gene activities was obtained by dividing gene activity of mutant sample by the value of wild-type sample. Fold change was calculated by averaging expression ratios for mutant vs. control experiments from two biologically independent experiments. In order to allow division indicating a transcriptional ratio individual hybridization signals that were labeled 'negative' (i.e. not above 2 folds of the local background) were used as positive. Hence, if the gene activity of either the mutant sample or the wild-type sample was "negative", the ratio was included as a positive value. Thus, these values were considered as estimates for the real induction or repression, since one of the values was indicated as below detection limit. However, ratios were labeled n.d. (not detected), if both gene activities of mutant and wild-type samples were labeled "negative" in both biological replicates. If transcription was only detected in one replicate, a mean value was calculated using ratio 1.0 (no change) for the "not detected" replicate, unless the resulting mean value would indicate a larger (lower) than two-fold change. In the latter case, values were not taken into consideration and labeled 'o.o.' (only once). Any results, which showed inconsistent, up- and down-regulated changes in replica experiments, were labeled 'exp' (conflicting experimental results). For further discussions about transcriptional changes of individual genes, only expression ratios smaller than 0.5 or larger than 2.0 were considered.

2.2.9   Genome-wide microarray analyses using Affymetrix ATH1 GeneChip

2.2.9.1 RNA preparation and Affymetrix GeneChip hybridization

Roots and leaves of 21-day-old hydroponically grown plants were used for whole genome microarray experiments. For each genotypes (wild-type and *pip2* mutants) three independent biological replicates were grown and harvested in parallel and stored at -80°C prior to RNA isolation. To decrease biological variation each replicate represented about ten plants.

Total RNA was isolated from 100 mg frozen material using RNeasy plant mini kit according to the manufacturer's protocol (Qiagen, Hilden, Germany). Five μg of RNA of *pip2* mutants and wild-type were then processed according to standard Affymetrix protocol and hybridized to Affymetrix GeneChip *Arabidopsis* ATH1 Genome arrays. Two rounds of hybridizations were done and, each in a different array facility. In fact, biological triplicates of *pip2;1* (s1), *pip2;2* (s2), *pip2;4* (s3) and *pip2;1-pip2;4* (s4) together with their wild type (wt1) were grown, harvested and hybridized in parallel whereas the second round of hybridizations was done using *pip2;2L-pip2;1sm* and wild type (WT) roots and leaves material extracting from plants grown in parallel but at different time than the previous mutants and wild-type. The first round of microarray hybridizations was carried out at the Affymetrix core lab facilities (Munich, Germany) using the Affymetrix One-Cycle Labeling and control (Target) kit according to the manufacturer's instructions. Concerning *pip2;2L-pip2;1sm* double mutants, RNA from roots and leaves tissues were processed and hybridized at the KFP Center of Excellence for Fluorescence Bioanalysis (Regensburg, Germany). RNA quality was controlled using Agilent bioanalyzer.

2.2.9.2 Normalization, statistical processing and data analysis

Due to annotation updates, Affymetrix probe sets were remapped onto actual *Arabidopsis* thaliana annotation and ambiguous probe sets aligning to more than one gene and probes without perfect matches were excluded from the analysis as previously described (Haberer et al., 2006).

CEL files were used for data processing. All probe set summary data were transformed to log-scale (basis 2). Chips raw data were normalized by Loess normalization (LMPN method) based on the local polynomial regression fitting method loess (Cleveland et al., 1992) operating on MA scale (Dudoit et al., 2000). Such polynomial regression method was required since datasets consisted of experiments from various Affymetrix lab facilities. Ignoring this would introduce additional, technical rather than biological bias. Consequently, a wild-type reference data set was generated by averaging and normalizing the expression of

each gene over all 6 wild-type hybridizations leading to more robust estimates of the real expression level. It was first checked whether ATH1 gene chip hybridization of the wild type from these two rounds yielded comparable results. Figure 7 shows that expression signals of the 3 replicates from wild-type of the first and second round were highly correlated. Consequently, this wild-type reference data set produced from the 6 WT replicates was used to calculate fold change ratio between mutants versus wild-type. Nonetheless, multiple testing hypotheses to check for significant differential expression were done for each mutant using his corresponding wild type replicates (See below).

An expression threshold of 6 (log basis 2) was chosen and genes showing expression below this threshold were excluded from further calculations. Similarly, a 0.5/ -0.5 (log basis 2) fold-change mutants versus wild-type cutoff was applied.
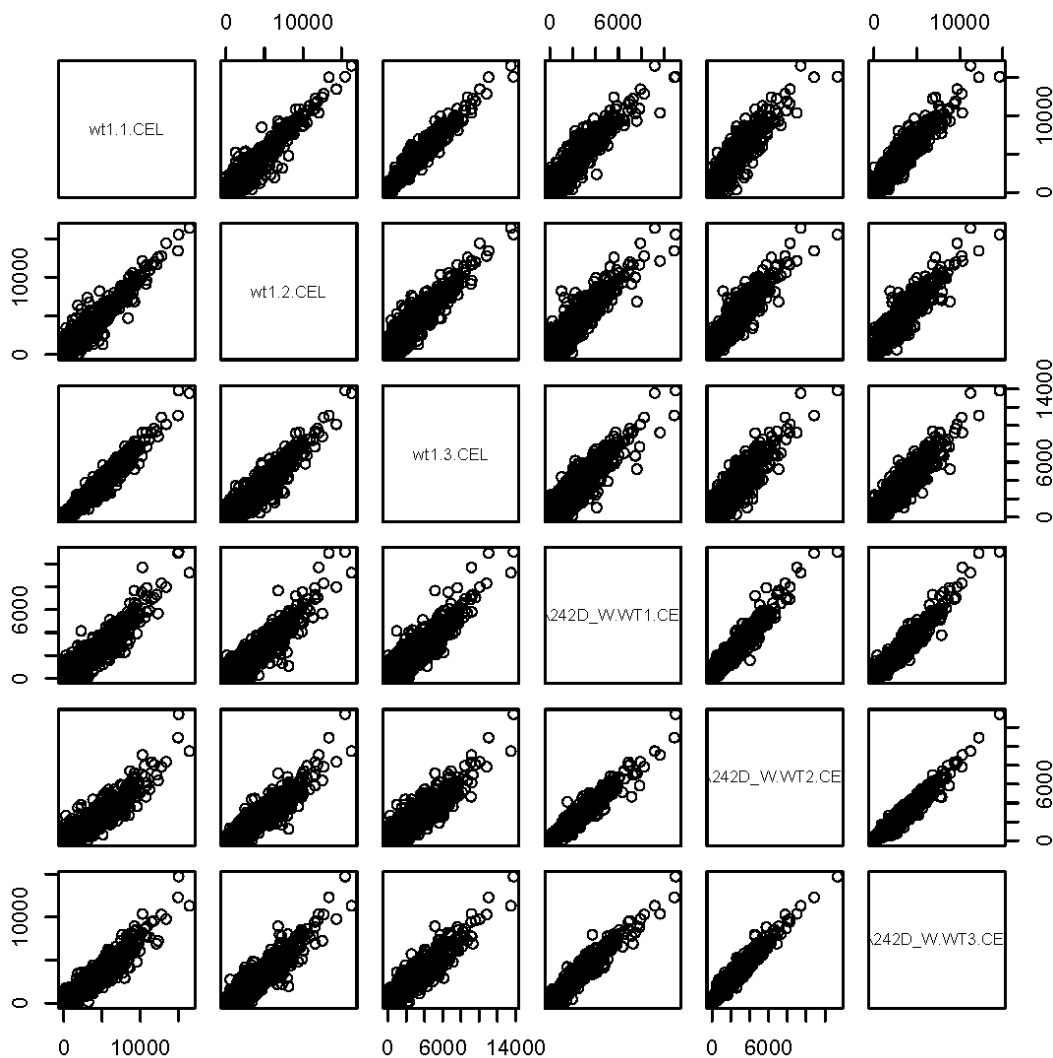
Figure 7. Scatter plot of hybridizations of the different wild type biological replicates obtained from two different Affymetrix laboratory facilities.
Wt1.1, wt1.2 and wt1.3 are the 3 biological replicates for the first facility plotted against each other and against the 3 biological replicates of A_242D_W.WT 1 to 3, which correspond to the wt obtained at the second Affymetrix facility.

After this filtering, the statistical significance for differential gene expression between mutants and wild-type reference was computed by multiple hypothesis testing (Baldi & Long Bayesian regularized t-test, Welch 2-variance t-test) and correction for multiple testing was done using Benjamini-Hochberg FDR (False Discovery Rate)-controlling method (significance level 0.05) (Benjamini and Hochberg, 1995). The top hundred genes passing all these requirements were used for further analyses and assigned to functional categories using MapMan software version 2.0 (Thimm et al., 2004) (see also Method 2.2.10).

2.2.10 Co-expression analyses

To identify genes that exhibit co-regulation with *PIP2* genes, the *Arabidopsis* Co-expression Data Mining Tool (ACT) (Manfield et al., 2006) and the Bio-Array Resource (BAR; Expression Angler tool) (Toufighi et al., 2005) were used. These programs calculate the correlation coefficients for all genes as compared to the query gene. Both web-based tools use publicly available ATH1 Affymetrix Whole Genome GeneChip expression data. The datasets used by ACT come from NASCarrays (322 ATH1 samples) while BAR uses 392 ATH1 samples from NASCarrays as well as data sets from the AtGenExpress Consortium (Tissue, Abiotic Stress, Pathogen or Hormone series) and from the BAR itself. In this study, *PIP2* co-expression analyses were done using a Pearson correlation coefficient cutoff of 0.6. Both the positively (r-value $\geq$ 0.6) and negatively (r-value $\leq$ -0.6) co-expressed genes were retrieved from ACT using all available ATH1 array experiment and from BAR using AtGenExpress Abiotic Stress, Pathogen or Hormone datasets (all experiments involving seeds were excluded from the analysis). Moreover, in the case of AtGenExpress Abiotic Stress subset of arrays, co-expression analyses were done for roots and aerial parts separately. In each case, a list was created containing the co-expressed genes and the correlation coefficient. Co-expressed genes were then assigned to functional categories using MapMan software version 2.0 (Thimm et al., 2004). MapMan categories were slightly modified for those that cover few genes. Merging of categories was done as previously described by Lisso et al. (2005). Statistical analyses were done to determine the significance of over-representation for each category. The probability for the observed frequency of genes assigned to a category with respect to the expected frequency of the category in the whole genome (based on MapMan) was calculated using a two-sided Fisher's exact test.

2.2.11 Principal component analysis (PCA) of *PIP* transcriptional responses to diverse stimuli using publicly available microarray data

Public efforts have been directed to *Arabidopsis* global transcript profiling that monitored the response of the plant under different treatments. Large sets of data have been made publicly available through several databases, e.g. TAIR, NASC, and many web-based tools (e.g. Genevestigator, BAR, ACT) have been developed to assist the interpretation of these large microarray gene expression databases. The Genevestigator Meta-Analyzer tool was used to extract *PIP* transcriptional responses in a broad range of stress conditions to investigate whether *PIP2* genes can be distinguished based on their differential stress responsiveness. Especially useful has been the AtGenExpress consortium which had generated standard Affymetrix microarray data for *Arabidopsis*. Although, data from NASC, TAIR, and several other sources are made available at Genevestigator, only AtGenExpress data were used. In contrast with other sources, the AtGenExpress consortium provided more homogenous and more comparable data since all experiments were done in a similar way and using *Arabidopsis thaliana* Col-0 ecotype. In addition, in many cases, roots and leaves were analyzed separately. Here, the abiotic, biotic and hormone treatment subsets of array generated by the consortium were used. A total of 61 different arrays were exploited. Expression ratios of PIP genes with respect to control experiments were extracted for the 61 arrays using the Genevestigator Meta-Analyzer tool (Version 3). In order to avoid any bias, several atypical treatments were removed (i.e. genotoxic stress (abiotic stress), cycloheximide, MG13 and PNO8 treatments (chemical treatments). Finally, expression ratios of *PIP* genes in 54 conditions were retained (Supplementary table 9 for *PIP* genes expression ratio and list of all stress conditions and treatments). After expression ratios were log-transformed to the basis 2 and raw-centered, data were subjected to a principal component analyses (PCA) to explore the concomitant or differential participation of PIP genes to diverse stimuli. PCA reduces the dimensionality of the multivariate data while only slightly reducing information: a large proportion of the variance will be explained by a smaller number of variables. Stress or treatments with great variances contribute more significantly to the differentiation of PIP transcriptional responses. The angular distance was used to extract from the PCA a subset of stimuli that contributed most significantly to the differentiation or association. The radius was arbitrarily set to $r > 3$ resulting in a selection of 8 out of 54 conditions.

2.2.12 Microscopy

Stereomicroscopy, light and fluorescence microscopy were used to visualize and photograph *Arabidopsis pip2* mutants, *PIP2* promoter::GUS transgenic plants as well as wild-type plants. For this purpose, a Leica MZ16F microscope with Leica DFC 320 camera was used and light and fluorescence microscopy were carried out with a Zeiss Axioskop.

GFP, Propidium iodide (PI, sigma, P-4170), FM$^®$4-64 (*N*-(3-triethylammoniumpropyl)-4-(6-(4-(diethylamino)-phenyl)hexatrienyl)pyridinium dibromide (Molecular Probes, Germany) and DAPI fluorescence were visualized using Confocal Laser Scanning microscope (LSM 510 Axiovert 100 M; Carl Zeiss, Jena).

For staining, 1 week-old seedlings grown on vertically orientated plates were immerged in 0.1 mg/mL PI (in water) for 30 min, washed three times with double-distilled water and observed thereafter.

Regarding FM4-64, seedlings were incubated in a 10 µM FM4-64 solution for 10 min, briefly rinsed with water and immediately observed. Observation should be quick since FM4-64 dye is internalized.

The LSM 510 was equipped with an argon laser emitting at 488 nm and helium-neon lasers emitting at 514, 543 and 633 nm, among others. GFP was excited with Argon laser at 488 nm and detected with a 505-530 bandpass; Others fluorescence were detected with the following wavelength for excitation and detection: 543 nm (or 488 nm) and 578-642 (565-615) bandpass for Propidium Iodide, 514 nm and 620-670 nm for FM4-64, and 364 / 454 nm and 488 nm for DAPI. C-Apochromat 10x/0.45, Plan-Neofluar 10×/0.3, C-Apochromat 20x/0.45w or Plan-Neofluar 20×/0.5Ph2 water immersion objectives were used for both observation and image recording. Systematically, monochrome images were taken sequentially at each wavelength. Artificial colors were assigned to the images taken for each excitation wavelength: green for 488 nm, red for 543 nm, and blue for 633 nm. Images were further processed using the AIM software, version 3.0 (Carl Zeiss, Jena).

2.2.12 Internet addresses

GABI-KAT (Insertion lines)	http://www.mpiz-koeln.mpg.de/GABI-Kat/
Genevestigator	https://www.genevestigator.ethz.ch/
Haruspex	http://euklid.mpimd-golm.mpg.de/gxdb/
Image J for image analysis	http://rsb.info.nih.gov/ij/
MapMan software	http://gabi.rzpd.de/projects/MapMan/
MIPS *Arabidopsis Thaliana* DataBase	http://mips.gsf.de/proj/thal/
NCBI (BLAST analyses)	http://www.ncbi.nlm.nih.gov/
Primer3	http://www-genome.wi.mit.edu/cgi-bin/primer/primer3_www.cgi

SIGnAL T-DNA Express (Insertion lines) http://signal.salk.edu/cgi-bin/tdnaexpress
The *Arabidopsis* Information Resource (TAIR) http://www.arabidopsis.org/
The Bio-Array Resource (BAR) http://bar.utoronto.ca/
The *Arabidopsis* Co-expression Tool (ACT) http://www.arabidopsis.leeds.ac.uk/act/
SWISS-MODEL http://swissmodel.expasy.org/

3 RESULTS

3.1 *PIP2* expression in *Arabidopsis* plants

3.1.1 Analysis of *PIP2* promoter::GUS expression profiles in *Arabidopsis* plants

Plants are sessile organisms and have therefore to adapt to their challenging environment. Many processes in plant development are dependent on massive water flow into and out of the cells such as water uptake by roots, elongation growth, phloem transport or even photosynthesis. These necessary water movements into and within the cells/tissues and the fine regulation required for plant growth may suggest a putative involvement of aquaporins. Identifying the cellular expression pattern constitutes a major piece of information in elucidating the function of a gene. Thus, functional analysis of *PIP2* genes function requires a precise knowledge of the specific expression profile of these genes. To gain a comprehensive insight into the *Arabidopsis PIP2* expression patterns *in planta*, the histochemical localization of the bacterial β-glucuronidase gene (*uidA* or *gusA*) commonly referred to as GUS was investigated in transgenic plants expressing this reporter gene under the control of different *PIP2* promoters.

DNA fragments corresponding to about 2.5 kb 5' upstream regions including the start codon of the *PIP2* genes were fused to the GUS sequence within the T-DNA of the destination vector pBGWFS7 (Fig. 5b). The resulting construct was then transferred into *Arabidopsis thaliana* plants (Methods 2.2.2.4 and 2.2.4.6). GUS expression was confirmed on T1 transgenic plants (self-fertilization of the primary transformants) and more precise analyses were done on T2 and T3 generations. Different growth stages and organs were analyzed on 3 to 5 lines for each *PIP2* promoter::GUS constructs. All lines of a particular *PIP2* promoter::GUS fusion showed about the same expression profile although the expression level varied depending upon the lines. Similarly, *Arabidopsis thaliana* transformant plants ecotype Col-0 or C24 exhibited similar expression pattern except for *PIP2;7* where slight differences could be observed between the two different ecotypes as explained below.

Differential expression profile of *PIP2* promoter::GUS fusions in *Arabidopsis*

Most *PIP2* genes exhibited a wide-spread expression in roots, leaves and flowers, but their expression pattern was different (Fig. 8). *PIP2;1*, *PIP2;2* and *PIP2;7* exhibited high GUS activity in roots as well as in leaves, while *PIP2;3* and *PIP2;5* showed a relatively lower GUS activity in both organs. In contrast, *PIP2;4* was strictly root-specific and strongly expressed in lateral roots and younger roots but not in hypocotyl, while *PIP2;6* was predominantly detected in young leaves and the main root. *PIP2;8* exhibited a special pattern in roots and

leaves; significant expression was observed in the basal part of young leaves and at the base of emerging lateral roots (Fig. 8 and 9).
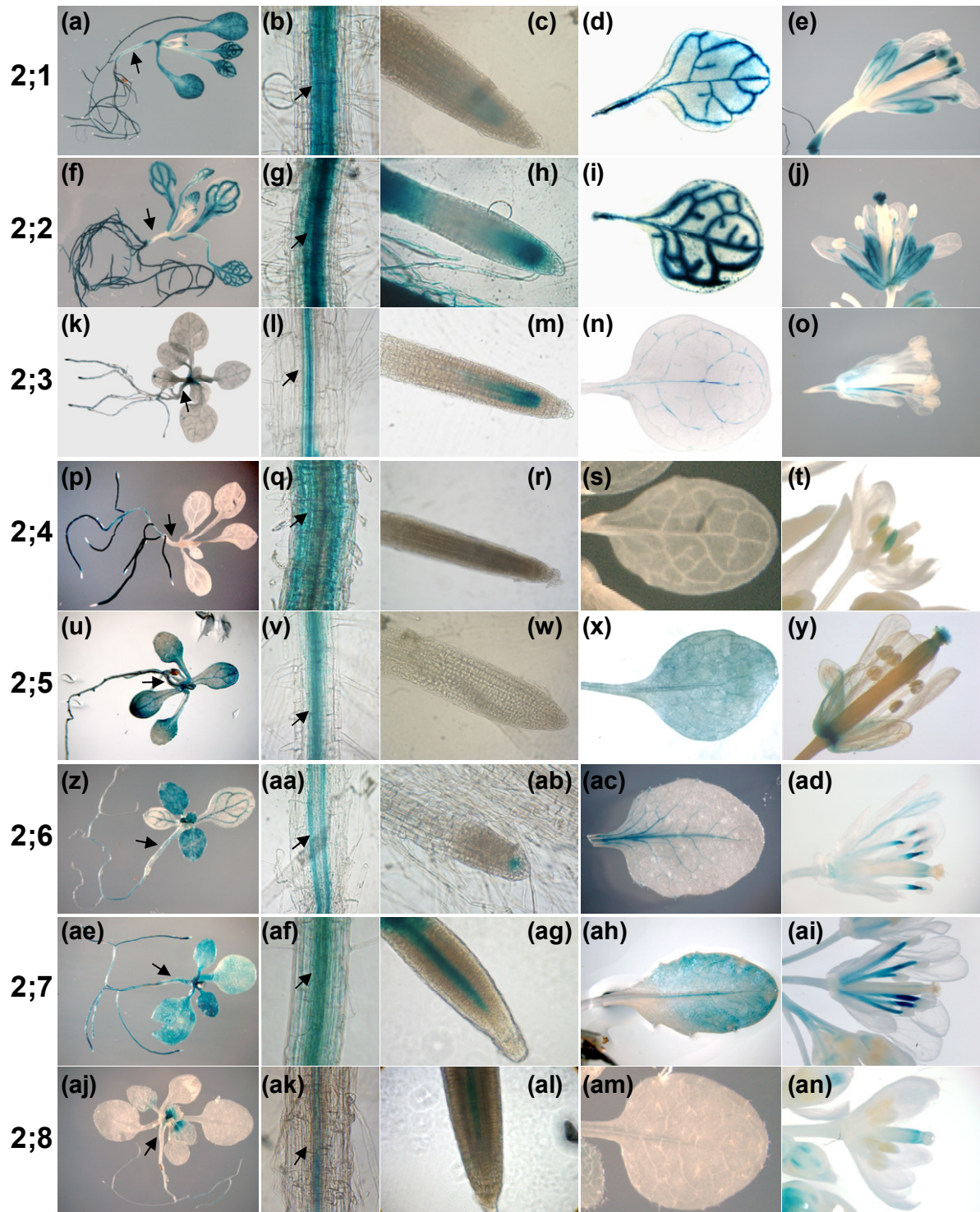
Figure 8. Histochemical localization of PIP2::GUS activity in vegetative tissues.
Distinct tissues of 8 to 13 day-old seedlings grown *in vitro* were analyzed and photographed. For expression in leaves, plants were grown in soil. (a, f, k, p, u, z, ae, aj) Eight to Thirteen-day-old seedlings; arrows point to hypocotyl; (b, g, l, q, v, aa, af, ak) section of the root hair zone of 2-week-old seedlings; arrows designate endodermis (c, h, m, r, w, ab, ag, al) root tip of 2-week-old seedlings; (d, i, n, s, x, ac, ah, am) leaves of 3 week-old plants grown in soil; (e, j, o, t, y, ad, ai, an) flowers of 5- to 6-week-old plants grown in soil.

Nevertheless, all *PIP2* members exhibited GUS activity in the root hair zone important for nutrient and water uptake. Except for *PIP2;5* and *PIP2;6* all members were expressed in the root hairs as well (Fig. 8 and 9). By and large, these expression patterns of *PIP2* genes were corroborated by AtGenExpress array expression analyses in different anatomical structures (Fig. 10, see below).

The cellular expression in roots revealed additional differential patterns. *PIP2;3* and *PIP2;8* were strictly confined to cells within the vascular tissue clearly excluding the endodermis (Fig. 8). Instead, *PIP2;1*, *PIP2;2*, and *PIP2;7* were found to be highly expressed in several tissue layers in the stele and adjacent endodermis. In the elongation and maturation zone *PIP2;7* exhibited stronger and wider cellular expression throughout the root (Fig. 8ag; see below). *PIP2;5* had a rather similar pattern with expression in stele and in endodermis. In case of *PIP2;2*, expression was also extended into the cortex layer (Fig. 8). *PIP2;4* and *PIP2;6* were the only members which were not highly expressed within the stele tissue. *PIP2;4* was also found in outer cell layers, in particular in the cortex in contrast to array expression data. *PIP2;6* was mostly confined to endodermis (Fig. 8 and 10).

Differential expression was also detected in root tip. *PIP2;1*, *PIP2;2* and *PIP2;3* showed predominant GUS activity in the meristematic region (Fig. 8). *PIP2;4* and *PIP2;5* were not transcribed in this region; however, *PIP2;5* interestingly showed a particularly strong expression in emerging lateral roots (Fig. 9). Surprisingly, *PIP2;6* was confined to the quiescent center (Fig. 8ab). Although the highly homologous *PIP2;7* and *PIP2;8* clearly showed differential expression in all other parts, within the root tip region both were found in the emerging vascular bundle (Fig. 8).

In leaves, *PIP2;1*, *PIP2;2*, *PIP2;3*, *PIP2;5, PIP2;6* and *PIP2;7* were expressed in vascular tissues as well (Fig. 8). *PIP2;1, PIP2;2, PIP2;5, PIP2;7*, and in young leaves *PIP2;6* exhibited a broader pattern with expression also observed in mesophyll. Interestingly, significant GUS activity in stomata was only detected for *PIP2;3* (Fig. 9). Although microarray technique has been able to show expression of *PIP2;1* in guard cells (Leonhardt et al., 2004), we did not observe it with GUS histochemical assay. Similarly, using microarray, Leonhardt *et al.* (2004) detected expression of *PIP2;1*, *PIP2;2*, *PIP2;6* and *PIP2;7* in mesophyll cells.
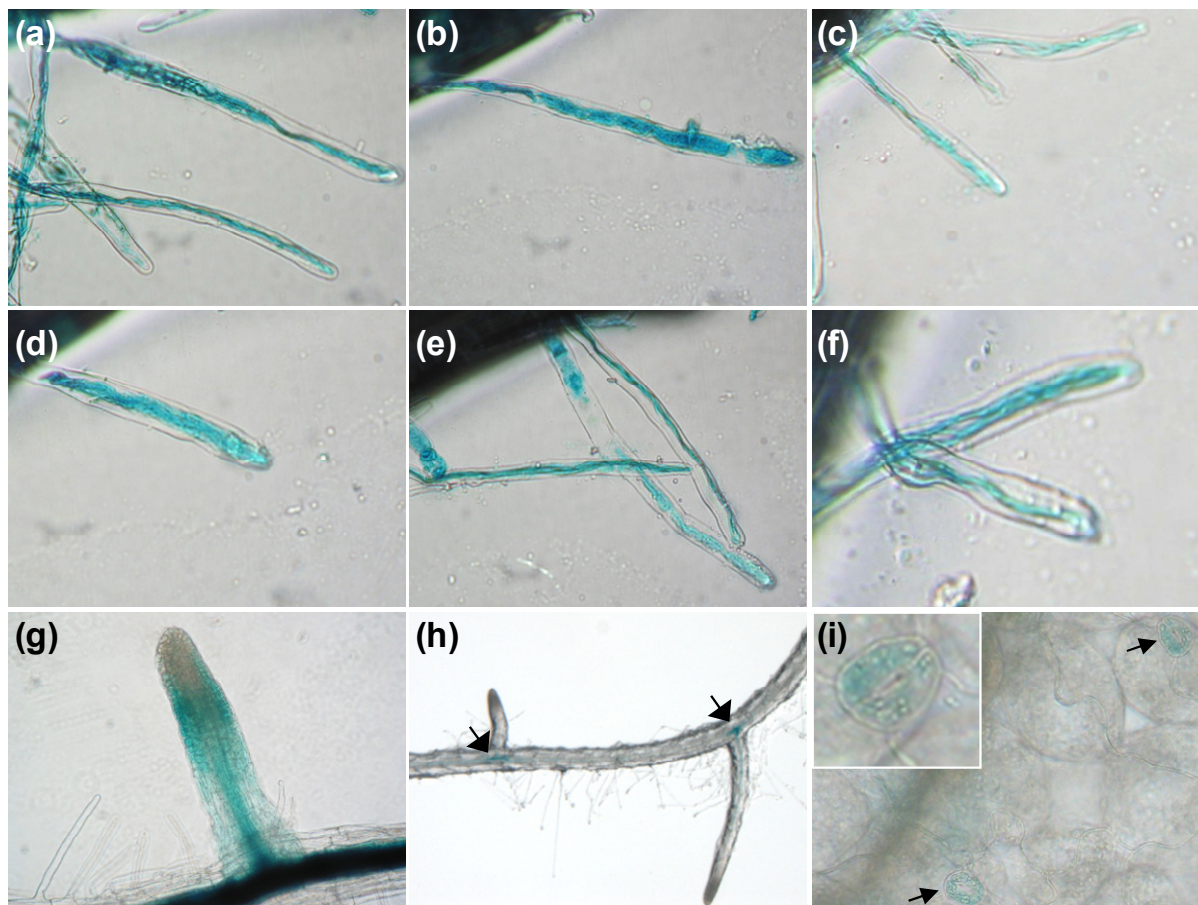
Figure 9. GUS expression in different cell types.
(a to f) Expression in root hairs of 2-week-old seedlings expressing *PIP2* promoter::GUS constructs: (a) *PIP2;1*, (b) *PIP2;2*, (c) *PIP2;3* promoter::GUS; (d) *PIP2;4*, (e) *PIP2;7*, and (f) *PIP2;8*. No expression could be detected for *PIP2;5* and *PIP2;6* promoter::GUS lines. (g) GUS Expression in young lateral root of 2-week-old seedling expressing a *PIP2;5* promoter::GUS construct. (h) Emerging lateral roots of 2-week-old plant expressing *PIP2;8*::GUS. (i) Leaf surface of 2-week-old transgenic seedling expressing a *PIP2;3* promoter::GUS construct. Stained stomata are indicated by arrows. The insert shows a magnification of a single stoma.

All *PIP2* genes were expressed in flowers and siliques, yet again in a differential manner with overlapping, but unique patterns (Fig. 8 and Supplementary Figure 1). Only *PIP2;1*, *PIP2;2*, *PIP2;3* or *PIP2;5* as well as *PIP2;6* were expressed in sepals and in petals similar to their expression in true leaves, whereas these genes and all other *PIP2* members were found in different parts of the reproductive organs (Fig. 8). In the filaments, *PIP2;1* and *PIP2;7* were strongly expressed, whereas *PIP2;2* and *PIP2;3* showed a weaker staining and *PIP2;6* was confined to their upper region. Only *PIP2;1* and *PIP2;4* were found in anthers, with *PIP2;4* being specifically confined to anthers in young unopened flowers. In the female part *PIP2;8* was specifically expressed in the upper part of the ovary just below the style similar to *PIP2;6*. Finally, *PIP2* gene expression in the stigma and style was only found for *PIP2;2*, while *PIP2;5*, was also expressed in the stigma and *PIP2;1* confined to the style. In

Arabidopsis ecotype Landsberg erecta, analysis of the stigma transcriptome also revealed expression of *PIP2;2* in the stigma but not of other isoforms (Swanson et al., 2005).

During flowering stage, *PIP2;5* was the only *PIP2* member active in the abscission zone, while several *PIP2* genes were located to that region in siliques (Fig. 8 and Supplementary Figure 1).

3.1.2   *PIP* gene expression profile based on microarray data

Transcripts expression profiling using microarray technology has become a powerful tool in biology and such studies contain a wealth of information that has been made available in public databases. Informations concerning one or more genes in multiple experiments can be queried using such tools. Thus, besides GUS histochemical assay, the Genevestigator Meta-Analyzer tool (Version 3; Zimmermann et al., 2005) was used to retrieve the gene expression profile of *PIP2* as well as *PIP1* genes in various tissues and organs in order to get insight into expression of the whole *PIP* family in *Arabidopsis*. Such analyses could give valuable information on the overlapping or differential expression profile between *PIP2* and *PIP1* members. Transcript profile of 40 anatomical structures (organ, tissue) was obtained and hierarchically clustered using the Genevestigator Meta-Analyzer tool (Fig. 10). Data were clustered by gene and profile using Pearson correlation. Unfortunately, one inconvenient of the data produced by commercial array Affymetrix whole genome ATH1 GeneChip is that it harbors several unspecific probesets that hybridize more than one gene. Thus, *PIP2;2* and *PIP2;3* as well as *PIP2;7* and *PIP2;8* hybridize the same probeset, respectively. Consequently, these genes can not be discriminated by the Affymetrix ATH1 array.

Regarding *PIP2* genes, the data retrieved from Genevestigator were in accordance with those obtained with *PIP2* promoter::GUS transgenic plants (see above). In case of *PIP1* genes, *PIP1;1*, *PIP1;2* and *PIP1;3* clustered together and showed nearly identical expression pattern and wide-spread organ expression (Fig. 10). *PIP1;4* exhibited a slight difference by showing higher expression in aerial parts than in roots but, yet, showed expression in all organs. *PIP1;5* was the only *PIP1* member not detected in root endodermis and cortex. Interestingly, *PIP1;1*, *PIP1;2* and *PIP1;3* showed an extremely similar expression with *PIP2;1*, *PIP2;2/2;3* and *PIP2;7/2;8* (Fig. 10).

Thus, differential expression pattern of *PIP2* members argue in favor of a different function of *PIP2* genes with implications in all plant tissues for some *PIP2*, e.g. *PIP2;1*, *PIP2;2* and *PIP2;7* that are co-expressed with *PIP1*.
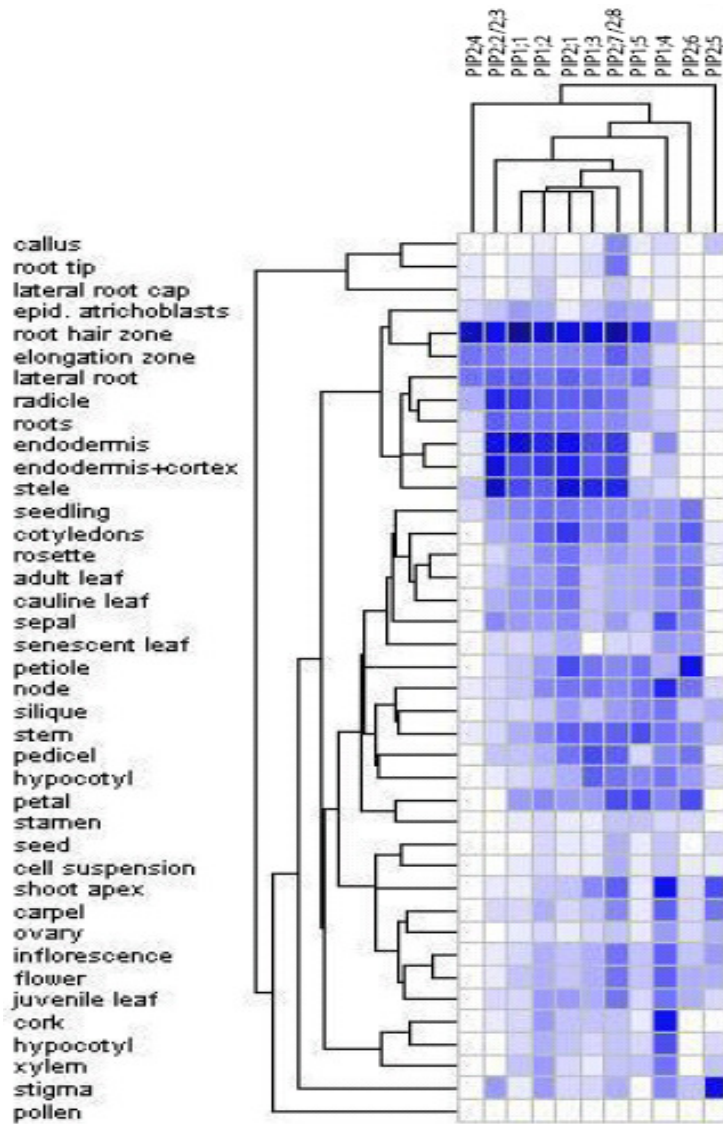
Figure 10. Hierarchical clustering of the 13 *Arabidopsis PIP* isoforms (Genevestigator, May 2007).
Expression of PIP2 in 40 anatomical structures. Data from about 3000 Affymetrix ATH1 GeneChip were retrieved using the Genevestigator Meta-Analyzer tool and then clustered by genes and profiles. A Pearson correlation was used for clustering.

3.1.3   PIP2;4 cellular and subcellular localization

The differential expression pattern observed for *PIP2;4* compared to other *PIP2* members using GUS histochemical assay prompted me to do more pronounced analyses. Thus, its cellular expression pattern was re-examined using transgenic plants expressing a *PIP2;4* promoter::*PIP2;4*-ORF-GFP fusion protein. Moreover, these transgenic plants did not only allow to visualize the cellular expression patterns, but also to investigate more precisely the subcellular localization of the PIP2;4-GFP fusion protein.

Transgenic plants expressing a *PIP2;1* promoter::*PIP2;1*-ORF-GFP fusion protein were also generated and use for comparison with PIP2;4 cellular pattern. Observations of roots from these *Arabidopsis* seedlings by Confocal Laser Scanning Microscopy showed GFP activity confined to the outer parts of the roots for PIP2;4 (Fig. 11b and d). Expression seemed to be localized to cortex and exodermis, while it was predominantly detected in vascular tissue in case of PIP2;1 (Fig. 11a and c). The visualization of GFP activity in these transgenic plants confirmed data observed using GUS histochemical assay (See above, Fig. 8).
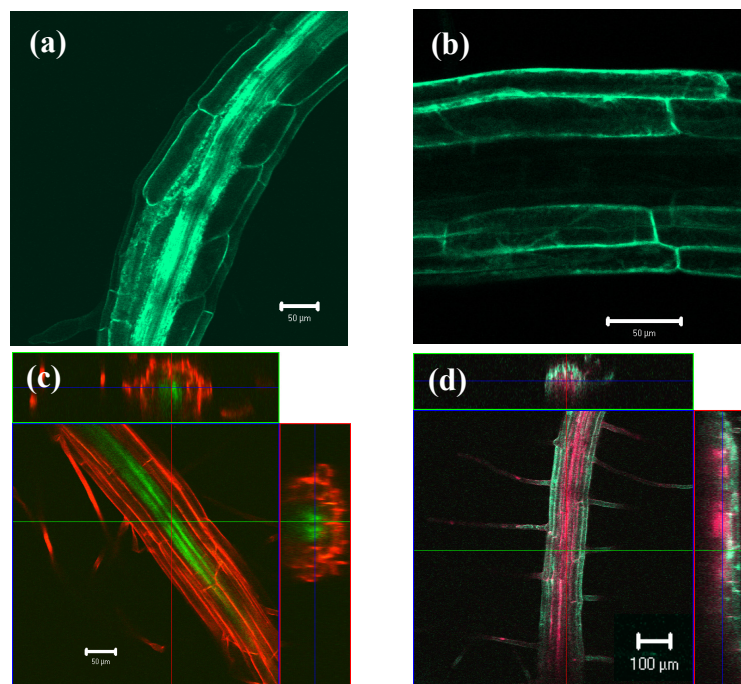
Figure 11. Cellular localization of PIP2 fused to GFP in *Arabidopsis* root seedlings.
The figures show laser-scanning confocal microscopy of GFP fluorescence emitted by root cells of 1 week old transgenic *Arabidopsis* seedlings grown in agar plate. All Panels are Z-stack confocal images (about 120 µm at 4 or 5 µm interval). In bottom panels, root cell walls were stained with propidium iodide for 30 min, washed and observed. Plants expressed the following fusion proteins: PIP2;1 Promoter::PIP2;1-ORF-GFP (a and c), PIP2;4 promoter::PIP2;4-ORF-GFP (b and d). Scale bar, 50 µm.

PIP2 proteins are assumed to be water channel localized to the plasma membrane and this plasma membrane location has been experimentally shown by immunocloning and biochemical analyses for PIP2;1, PIP2;2 and PIP2;3 (Daniels et al., 1994; Kammerloher et al., 1994) or using GFP fusion proteins for PIP2;1 and PIP2;7 (Cutler et al., 2000; Boursiac et al., 2005). The plasma membrane location of other PIP2 proteins, PIP2;5 being the only member for which no experimental evidence for plasma membrane localization is available, has been made highly likely based on protein identification using mass spectrometry (Elortza et al., 2003; Alexandersson et al., 2004; Nelson et al., 2006). However, it is impossible to completely exclude contaminants by endomembranes from such analyses. Moreover, evidence is increasing that suggests a location in more than one membrane and compartment, and, also, that MIPs may move depending on physiological states or environmental disturbances (Barkla et al., 1999; Vera-Estrella et al., 2004; Boursiac et al., 2005). Hence, precise analyses using a PIP2;4::PIP2;4-ORF-GFP fusion protein were carried out to check whether or not PIP2;4 was localized at the plasma membrane and/or other membranes. The PIP2;4 plasma membrane localization was confirmed using multiple fluorescence labeling observed by confocal microscopy (Fig. 12a to f).
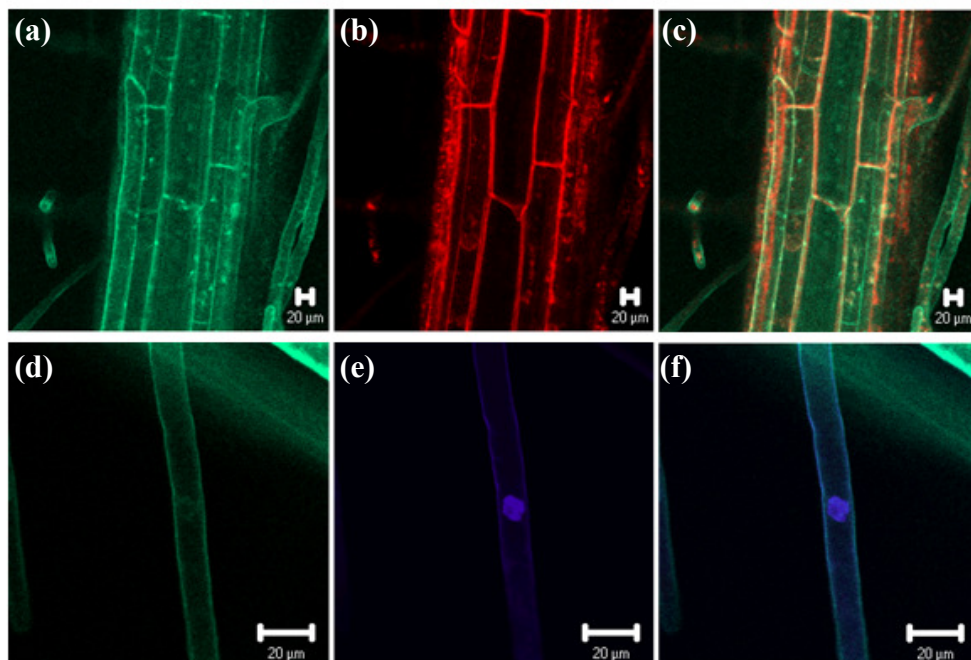
Figure 12. Plasma membrane localization of PIP2;4.
The figures show laser-scanning confocal micrographs of the fluorescence emitted by root cells of transgenic plants. Panels A to C are Z-stack confocal images (60 μm at 5 μm interval). (a and d) GFP fluorescence; (b) FM4-64 fluorescence; (c) merged image of a and b showing co-localization of PIP2;4::PIP2;4-ORF-GFP fusion protein with the vital dye FM4-64. (e) DAPI staining of nucleus; (f) merged image of d and e. Scale bar, 20 μm.

The GFP signal was easily observed at the plasma membrane of root cells and in particular

root hairs (Fig. 12a and d). The plasma membrane localization of PIP2;4 in *Arabidopsis* root cells was first demonstrated by the co-localization with the vital dye FM4-64, which stains specifically the plasma membrane phospholipids under the conditions used (Fig. 12a to c). Additionally, the labeling of the nucleus using DAPI clearly eliminated the vacuolar localization of PIP2;4, since no membrane invagination around the nucleus could be observed (Fig. 12d to f).

3.2 Isolation and molecular characterization of *pip2* insertional mutants

Reverse genetics and the use of loss-of-function mutants provide a reliable approach to explore the integrated function of a gene. Here, to investigate the function of individual PIP2 aquaporins in *Arabidopsis thaliana*, a collection of T-DNA or transposon insertion mutants was established (see Materials 2.1.1, Table 1).

3.2.1   Isolation of *pip2* single and double mutants

The *pip2* insertion mutant candidates were isolated by screening publicly accessible seed collections and characterized by PCR genotyping (Fig. 13; Method 2.2.5). Whenever possible, several independent T-DNA or transposon insertion lines were screened for each *PIP2* gene in order to obtain at least two independent alleles. Insertions lines were first tested for the presence of T-DNA or transposon and lines with insertion in both alleles (homozygous plants) were obtained. Insertions were first confirmed by PCR using reverse (or forward) *PIP*2 gene specific primer in combination with primer specific for the T-DNA left border. Homozygous plants were then revealed by PCR amplification of the *PIP2* coding sequence with reverse and forward gene-specific primers. DNA from homozygous plants gave no amplification product whereas DNA from heterozygous and wild-type plants did. All the PCR for screening of *PIP2* insertion mutants provided data essentially identical to those shown in Figure 13.

PIP2 are highly homologous in their amino-acid sequence and single knockout mutants may be compensated by other genes in case PIP2 members would share functional redundancies. Multiple mutants where two or more genes are mutated may help identifying functional redundancy or even interacting partners in biological pathways. Thus, double mutants where created by crossing single *pip2* mutants (Method 2.2.1.2). Progeny of F1 heterozygous plants were then screened for homozygosity of the insertions by PCR genotyping identical to the single mutants. The theoretical segregation was 1:15 among the F2 population, as long as there was no chromosomal linkage of the loci (Fig. 13c and d).

By sequencing the respective PCR products obtained with T-DNA and gene-specific primer combinations, the position of the insertion sites within the corresponding *PIP2* genomic sequence were established. The position of the insertions for each mutant is depicted in Figure 17.
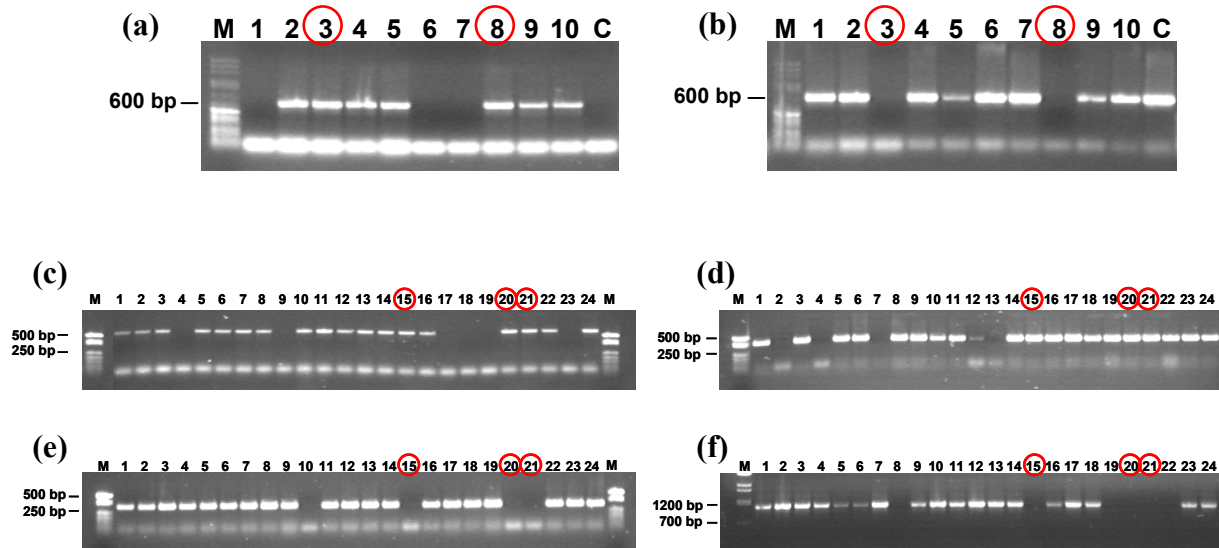
Figure 13. Screening of *pip2* T-DNA insertion mutants.
pip2 single and multiple mutants were characterized by PCR genotyping. **(a)** and **(b)** Ten *Arabidopsis* plants of a *PIP2;4-1* transposon insertion were screen to obtain homozygous mutants. T-DNA insertion was confirmed by PCR using reverse primer specific for *PIP2;4* and primer specific for the T-DNA left border (amplification using T-DNA primer and forward primer specific for *PIP2;4* did not give product in this mutant and is therefore not shown for better clarity). **(b)** PCR amplification of the *PIP2;4* coding sequence with *PIP2;4* reverse and forward gene-specific primers to reveal homozygous plants. **(c)** to **(f)** show PCR genotyping for a *pip2;2-3/ pip2;1-1* double mutant. F2 *Arabidopsis* plantlets were screened to obtain homozygous mutants. Confirmation of T-DNA insert by PCR using the required T-DNA left border primer and **(c)** *PIP2;1* or **(d)** *PIP2;2* gene specific primers. **(e)** and **(f)** show PCR amplification using reverse and forward gene specific primers of the *PIP2;1* and *PIP2;2* coding sequence, respectively. Red circles indicate homozygous T-DNA insertion mutant plants.

3.2.2   Molecular characterization of *pip2* insertional mutants

Since T-DNA or transposon insertion does not necessarily lead to loss of transcripts, the absence of the respective mRNA transcripts in the insertion lines had to be confirmed. Thus, *PIP2* mRNA expression in the mutant lines was tested by RT-PCR using gene specific primers for amplification of the gene (Fig. 14; Method 2.2.4.2). The gene specific-primer combinations were designed in regions flanking introns to generate PCR products from cDNA that were distinctly smaller than the products amplified from genomic DNA using the same primer combinations. Most insertion lines resulted in loss of transcripts and, hence, generated knockout mutants (Fig. 14; see Table 1 for a complete list of *pip2* mutants). In case of *PIP2;4* and *PIP2;8* only one knockout mutant could be isolated.
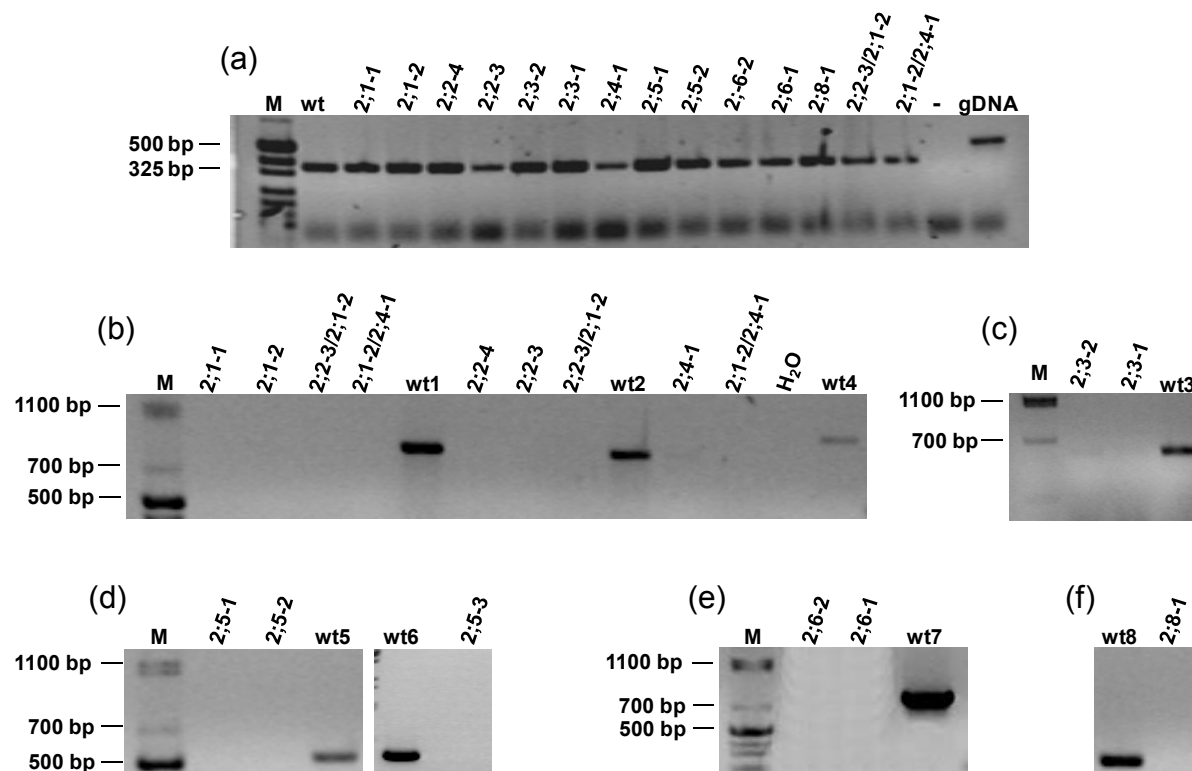
Figure 14. Agarose gel separation of PCR products amplified from cDNA of wild-type and *pip2* mutant lines.
RNA extracted from wild-type and *pip2* mutants was extracted and used to synthesized cDNA. The expression of Tubulin9 is shown as a control **(a)**. As expected, product amplified from genomic DNA (gDNA) was bigger than products polymerized using cDNA indicating that was no contamination with gDNA. Expression of the respective *PIP2* genes was then analyzed in *pip2* mutants and confirmed loss of transcripts in **(b)** *pip2;1*, *pip2;2*, *pip2;4* single and double mutants, **(c)** *pip2;3* mutants, **(d)** *pip2;5* mutants, **(e)** *pip2;6* mutants and **(f)** *pip2;8* mutant.

Since T-DNA insertions in the genome can result in local DNA rearrangement or loss of DNA, the integrity of the neighboring genome was confirmed by PCR using primer combination specific for that region. Thus, flanking genomic sequences were obtained using approximately 1.5 kb genomic fragments amplified by PCR, digested with restriction enzymes and characterized by their predicted size and characteristic restriction pattern. These analyses confirmed that for all mutants no aberrations of the directly flanking genomic region had occurred.

Eventually, since mutants have not been back-crossed into wild-type, a more careful examination of their insertion site and potential additional insertions was required, because independent insertions could also influence putative phenotypes. Therefore, Southern blot analyses were performed on *pip2* knockout mutants to analyze the structure of the T-DNA insertion lines. Genomic DNA from *pip2* mutant was digested with a restriction enzyme, blotted and hybridized with a probe generated by polymerization of a region of the T-DNA left border nearby the insertion sites (Fig. 15). Any T-DNA insertion would hybridize the

probe and generate a fragment visible on the blot (Fig. 15 and 16). Two or three different restriction enzymes had been selected. Using such strategy, it was therefore possible to identify whether *pip2* mutants exhibited additional T-DNA within their genome.
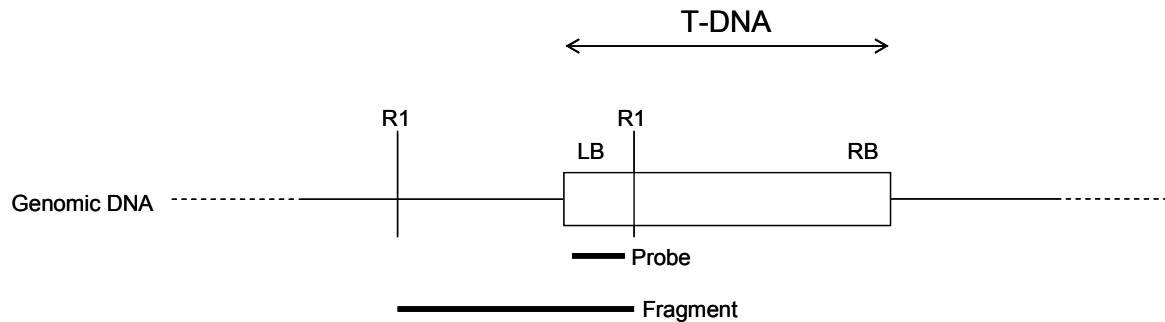
Figure 15. Southern blot strategy for analyzing T-DNA insertion in *pip2* mutant genomes.
Genomic DNA from *pip2* mutant plants is digested with restriction enzyme (R1), run on an agarose gel, and transferred to nylon membrane (Methods 2.2.4.8). The blot is hybridized with a T-DNA probe produced from PCR amplification of the T-DNA left border. Any digested T-DNA will produce a fragment that would hybridize with the radiolabeled probe and will be further visualized on the blot. LB: T-DNA left border; RB: T-DNA right border.

These analyses showed a single T-DNA insertion for both SM lines (*pip2;1-2* and *pip2;4-1*; Fig. 16 and Table 5) as well as both *pip2;2* mutant lines (*pip2;2-3* and *pip2;2-4*; Fig. 16 and Table 5). In the other single mutants, additional bands were found. They may mean insertions at independent loci or more complex T-DNA insertions at the *PIP2* loci. The latter has been already indicated by the fact that the inserts harbor two T-DNA left borders (see also Fig. 17). However, for these mutants, except for *pip2;8*, at least two independent mutant alleles were obtained. Therefore any phenotype observed in both lines, could consistently be attributed to the mutation at the corresponding *PIP2* locus. The *pip2;1-1* mutants has been previously characterized and several additional T-DNA insertions were observed (Affenzeller, 2003).

Two double mutants were also checked and showed exactly the same profile as their corresponding single mutants (Fig. 16).
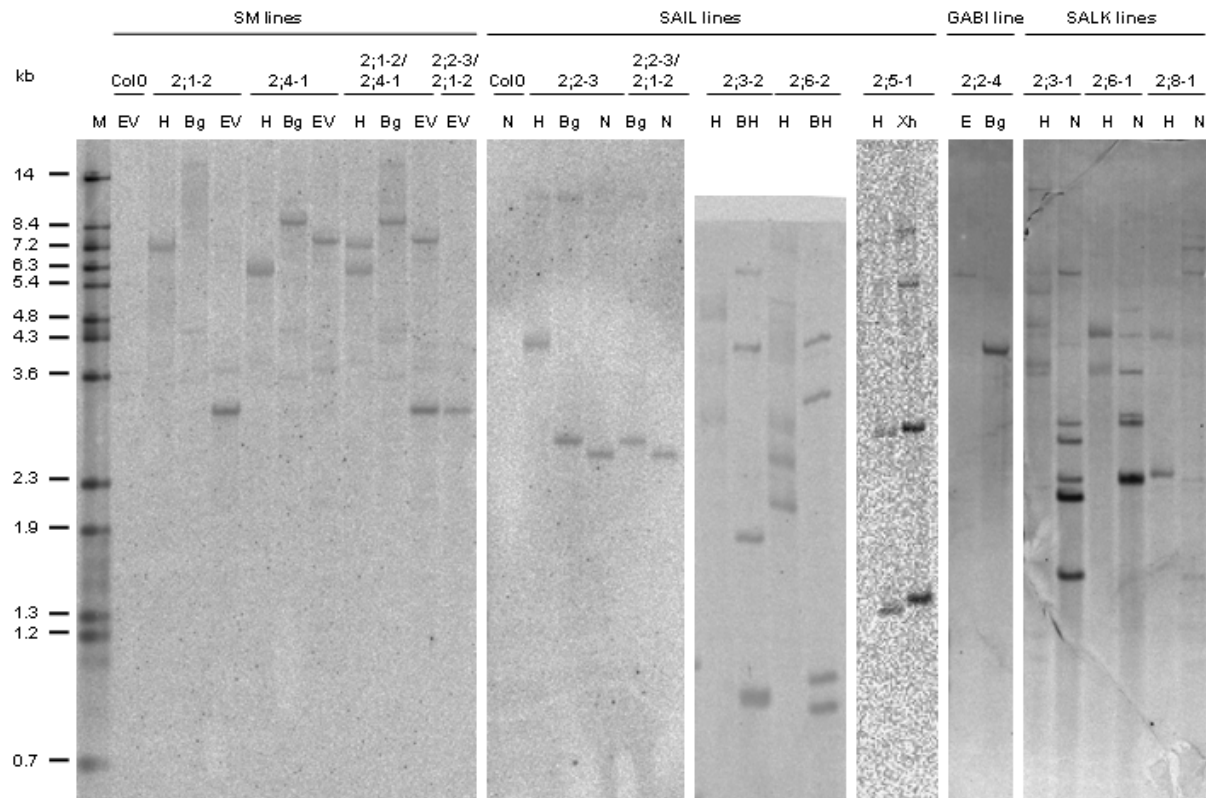
Figure 16. DNA blots of *pip2* knockout mutants.
Genomic DNA (2 μg) was digested, separated and transferred onto a positively charged nylon membrane and further hybridized with a radioactively labeled probe. Specific probes were produced by PCR amplification of the T-DNA left border of various T-DNA lines (SM, Sail, Gabi and Salk lines). Each line represents a DNA digest for a particular *pip2* mutant and enzyme. The respective T-DNA probes used are listed on the top of the Figure (e.g. SM lines, Sail lines). BH: BamHI; Bg: BglII; EV: EcoRV; H: Hind III; N: NcoI; M: DNA Marker.

Table 5. T-DNA or transposon flanking restriction fragments of *pip2* mutants.
Genomic DNA extracted from various *pip2* knockout mutants was extracted and submitted to restriction digest. Expected sizes for each digest are indicated. For several mutants (indicated by an asterisk), PCR genotyping revealed a T-DNA left border on both sides of the insertion, indicating a complex T-DNA insertion. Accordingly, two restriction fragments were expected.

Mutant	Insertion verified	Additional insertions	BamHI	BglII	EcoRI	EcoRV	HindIII	NcoI	XhoI
pip2;1-1	yes	yes				Affenzeller, 2003			
pip2;1-2	yes	no	-	9174	-	3144	7166	-	-
pip2;2-3	yes	no	-	2765	-	-	4133	2157	-
pip2;2-4	yes	no	-	4102	5963	-	-	-	-
pip2;3-1*	yes	yes	-	-	-	-	4971/ 4547	1607/ 6124	-
pip2;3-2*	yes	yes	1919/ 5614	-	-	-	3551/ 4328	-	-
pip2;4-1	yes	no	-	4153	-	7563	6067	-	-
pip2;5-1	yes	yes	-	-	-	-	6194	-	6106
pip2;6-1*	yes	yes	-	-	-	-	6858	3684	-
pip2;6-2*	yes	yes	3127/ 8000	-	-	-	3748/ 6675	-	-
pip2;8-1*	yes	possibly	-	-	-	-	2451/ 4284	7292/ 6124	-

Molecular characterization of *pip2* knockout mutants is a crucial step prior phenotypical characterization. Here, more than twenty *pip2* mutants were analyzed producing a valuable collection to study integrated function of *PIP2* genes. Figure 17 summarizes *pip2* single mutants characterized in this work (see also Table 1).
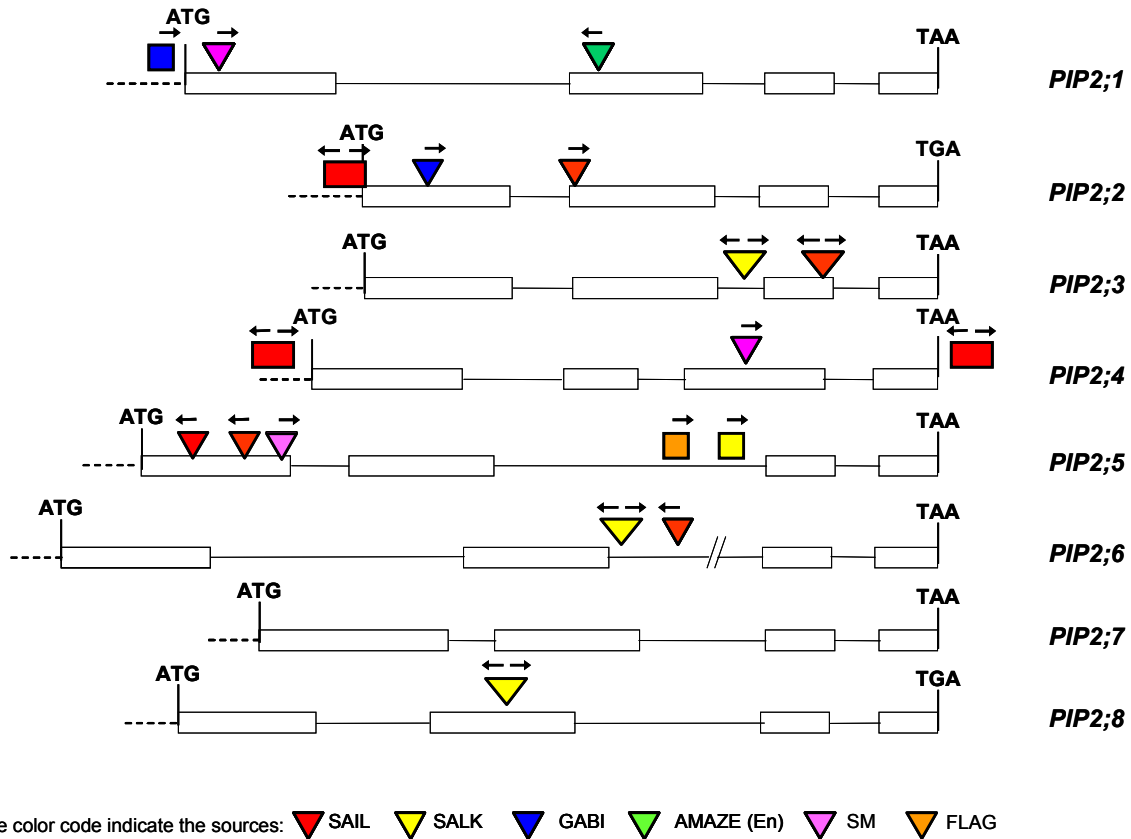
Figure 17. Collection of *pip2* insertional mutants in *Arabidopis thaliana.*
Except a *PIP2;5*_FLAG line which was in Ws ecotype, all *pip2* mutant were in the Columbia background. Position of the T-DNA insertions were verified by sequencing and arrows indicate orientation of T-DNA left border (two arrows indicate a left border on both sides of the insertion). Accordingly, the arrows indicate the En-1-element border for the transposon insertion in Amaze-(En) line or the nonautonomous defective *Spm* (d*Spm*) element in SM lines. Triangles represent knockout mutants, while squares indicate homozygous mutants in which transcripts were detected. Large boxes represent exons, while lines represent introns. Start (ATG) and stop codons (TAA/TGA) are indicated.

3.3 Phenotypical analysis of *pip2* knockout mutants

3.3.1 Growth responses of *pip2* mutants in standard and water stress conditions

PIP2 members are thought to be involved in water transport in plants and, as a consequence, a role in water deficit tolerance has been suggested. Plant responses to water deficit depend on the severity, i.e. on the amount of water lost, the rate of loss and the duration of the stress. Water deficit results from various stresses such as low (freezing) temperature, drought and salt enrichment in soil. For instance, application of NaCl to the root system of plants affects plant growth and development by exerting a strong osmotic water stress by lowering the water potential of the surrounding substrate, but it also exerts a toxic effect of the ions involved. Thus, both water relations are strongly affected by NaCl and toxicity of ions may harm the plants. Both pathways could influence the expression of aquaporins. Responses to abrupt water deficit as in many experimental approaches may occur in short time within a few minutes for the biophysical alterations and within hours or days for long-term adaptations depending on cellular and whole-plant mechanisms (Bray, 1997; Munns, 2002; Xiong and Zhu, 2002).

In *Arabidopsis*, *PIP* genes stress responsiveness has been shown at the transcriptional level (Kreps et al., 2002; Seki et al., 2002a; Affenzeller, 2003; Jang et al., 2004; Alexandersson et al., 2005; Boursiac et al., 2005). *Arabidopsis* plants with modulated expression of several PIPs also suggested their role in water stress conditions but none of them could demonstrate direct involvement of a particular *PIP* gene (Martre et al., 2002; Aharon et al., 2003; Jang et al., 2007a).

In order to check whether any PIP2 member plays a role in water stress tolerance, possible growth or developmental alterations of *pip2* mutants with respect to the wild-type were investigated. Whole plant growth including the roots was observed on vertical gelrite 0.5X MS plates supplemented with different concentrations of NaCl or sorbitol to account for ionic and osmotic stresses (see Method 2.2.1.6). Except for *pip2;4* and *pip2;8*, where only one mutant was available, two independent homozygous insertion lines were analyzed for each of the *PIP2* genes. *PIP2;7* was not included at all, because a knock-out mutant was not available. Since PIP2 proteins are highly homologous, a single knockout mutant may be covered by other genes. Thus, the use of multiple mutants should provide evidence toward either differential functions or functional redundancies or even interacting functions of *pip2* isoforms. Two selected *pip2* double mutants were generated and tested in the same way as for the single mutants asking the question whether these combinations would lead to additional phenotypes. Those double mutants were selected based on their expression pattern, e.g.

PIP2;1 and *PIP2;2* are highly expressed in all organs. The particular pattern observed for *PIP2;4* prompted us to generate double mutants including *PIP2;4* as well.

Germination was not affected in any of the mutants, if directly planted on standard medium or on plates with 50 mM NaCl, 100 mM NaCl or 200 mM sorbitol.

In order to impose water stress to young seedlings, four-day-old seedlings germinated on vertically orientated control plates were transferred to fresh 0.5X MS plates supplemented with either 50 mM NaCl, 100 mM NaCl or isoosmotic 200 mM sorbitol to impose water and/or ionic stress and onto control plates without additional solutes. Four-day-old seedlings did not show any growth phenotype before being transferred, with the exception of *pip2;5-1* seedlings that were slightly smaller in comparison to other wild-type control and other mutants (Fig. 18). However, this phenotype is likely not due to PIP2;5 loss-of-function since a second individual mutant, *pip2;5-3*, did not show this growth reduction phenotype (Fig. 18).
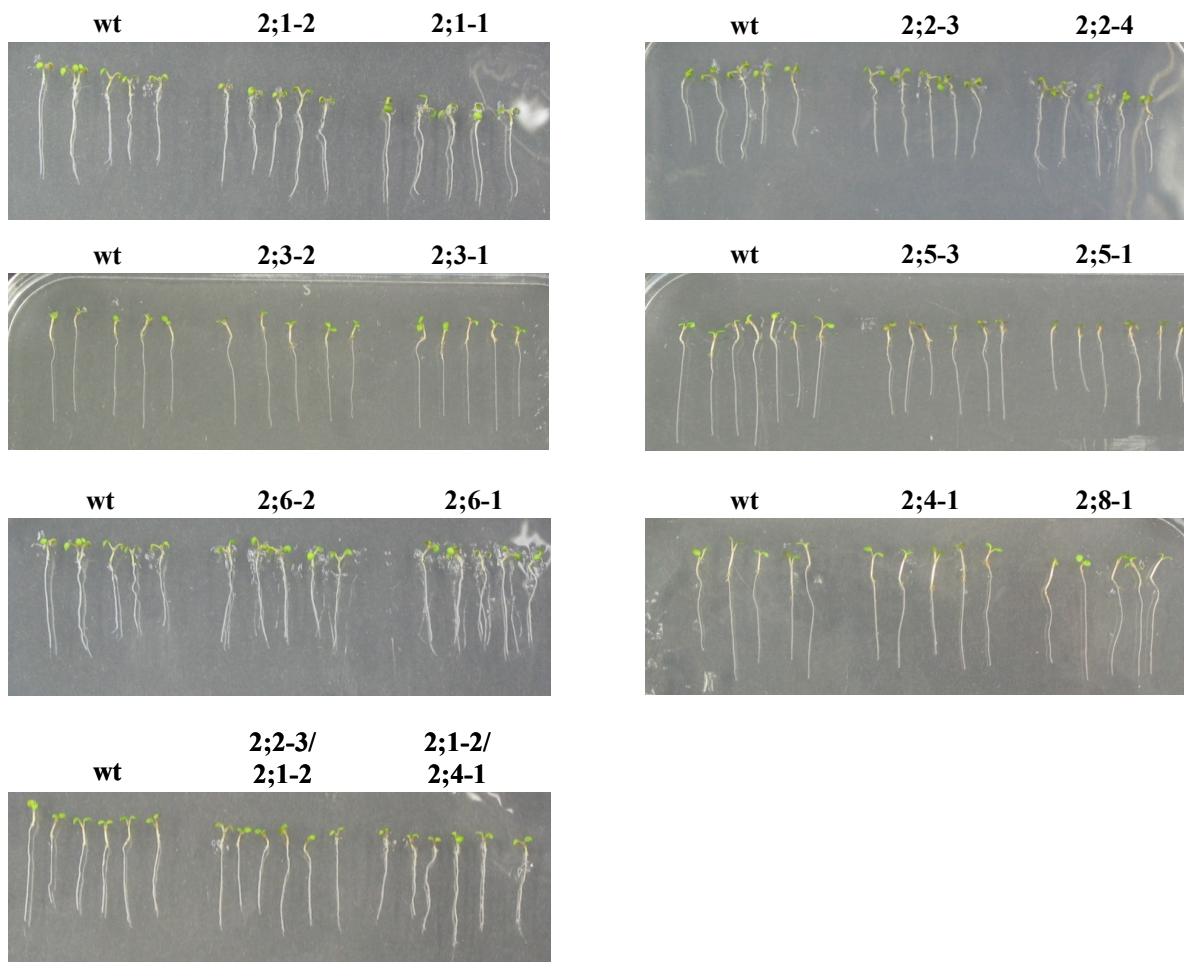
Figure 18. Four-day-old seedlings of wt and *pip2* mutant.
The *pip2* mutants and corresponding wild-type were grown on plates in a vertical orientation and seedlings were photographed after 4 days.

After transfer, plants were further grown for seven days in a vertical position and root growth was recorded by marking them daily and measuring root elongation (Fig. 19). Root elongation and whole plant phenotype were assessed separately. In standard medium, *pip2* mutants did not show any growth alteration (Fig. 19 and 20). Although *pip2;5-1* mutant showed slightly, but significantly reduced growth (about 20%), this phenotype was not confirmed by the independent *pip2;5-3* mutant (see below and Fig. 19 and 20).

However, when growth of roots and whole plants was assessed under different water stress conditions on vertical agar plates, differential sensitivity of *pip2* mutants could be observed. In general, growth of wild-type plants on 50 mM NaCl led to a reduced root elongation of about 25%, while it was around 55% in case of 100 mM NaCl. Osmotic stress imposed by sorbitol showed a reduced root elongation comparable to that of 100 mM NaCl, since root growth was inhibited by about 45%. These different conditions allowed the analysis of *pip2* mutants growth under mild as well as severe water stress. As shown in Figure 19, root elongation of most *pip2* mutants exposed to various water stresses was not affected with respect to the wild-type.
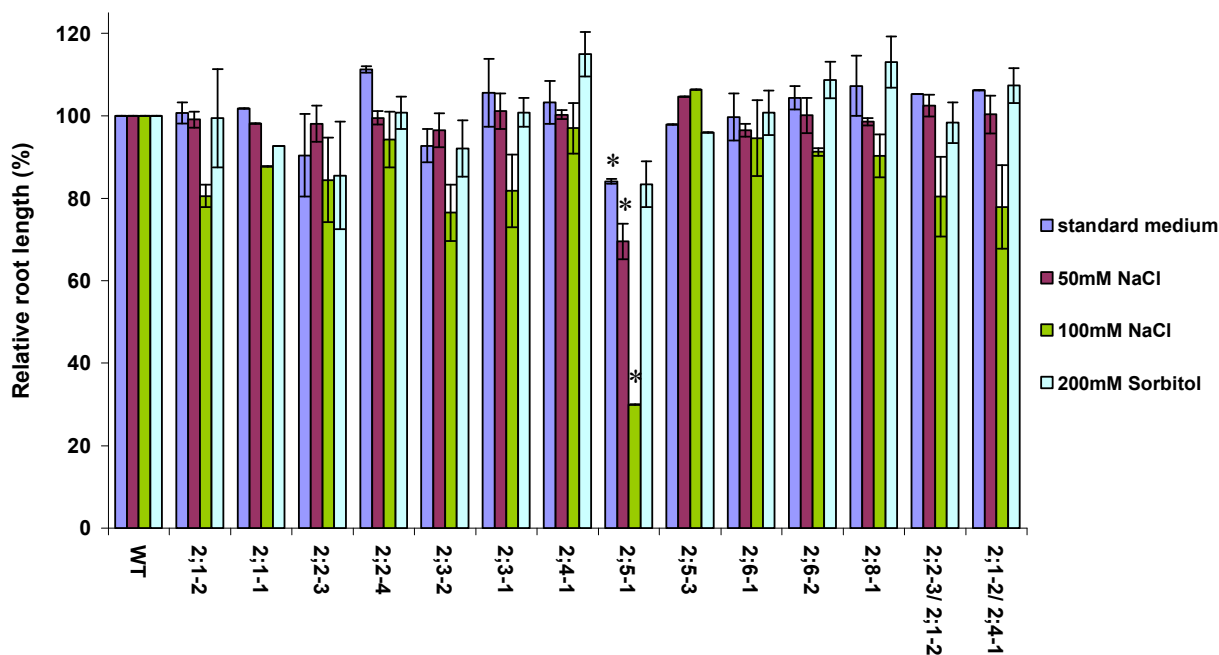
Figure 19. Relative root growth of *Arabidopsis* wild-type and *pip2* mutants under various water stresses.
Plants were germinated and grown for 4 days on standard medium plates, further transferred to gelrite plates containing standard medium supplemented or not with increasing concentrations of NaCl or sorbitol. Growth measurements were conducted up to seven days after seedlings were transferred on fresh plates. Relative Root Growth (RRG) of *pip2* mutants was calculated with wild-type root length set to 100%. Bars represent Relative Root Growth (RRG; percentage) of *pip2* mutants with respect to the wild-type 7 days after transfer. Bars are means ($\pm$ SE) of 3 to 5 independent experiment using 6 seedlings per genotype for each experiment. P-values were calculated using an unpaired Student's t-test assuming unequal variance to compare mean root length of wild-type and mutant plants. Asterisks indicate statistically significant differences ($p < 0.05$).

Actually, the most severe phenotype was observed for the *pip2;5-1* mutant. Its root growth was significantly retarded on 50 mM NaCl and was almost stopped on 100 mM NaCl (Fig. 19 and 20). The whole seedlings died under these conditions. However, the independent *pip2;5-5* mutant did not show this phenotype (Fig. 19). Nevertheless, it was tested via complementation, whether there could be any correlation of salt sensitivity and *pip2;5* knockout. Eventually a genomic construct encompassing the whole *PIP2;5* gene could not complement the salt sensitive phenotype of *pip2;5-1* (see Annex 2 which focuses on observations regarding *pip2;5* mutants) indicating that PIP2;5 is at least not directly responsible for the salt sensitivity observed. Indeed, *pip2;5-1* contains additional T-DNA inserts, as shown by Southern blotting (Results 3.2.2, Fig. 16), which likely contribute to the observed phenotype.

In addition, two independent *pip2;3* mutants also show water stress sensitivity. In case of mild salt stress (50 mM NaCl) no differences in growth were observed for any of the *pip2;3* mutants. However, *pip2;3* mutant leaves were found to be altered in case of severe salt stress (100 mM NaCl; Fig. 20 and 21). Indeed, when grown on 100 mM NaCl containing medium *pip2;3* seedlings become chlorotic and the leaf phenotype observed was correlated with a tendency for reduced root elongation (Fig. 19 and 21) indicating a severe damage on 100 mM NaCl plates. Importantly, in our conditions, *pip2;3* mutants showed an exclusively enhanced salt sensitivity since no phenotypical differences were observed when plants were grown under osmotic stress provoked by 200 mM sorbitol (Fig. 19 to 21). Since sorbitol can be metabolized by the plant, osmotic stress exerted by mannitol has also been tested for *pip2;3* mutants and results were similar to sorbitol (data not shown). Thus, *pip2;3* knockouts are exclusively sensitive to salt stress among *pip2* mutants, but not to purely isoosmotic stresses.

Regarding other mutants although no obvious phenotypes were observed, it is noteworthy that with 100 mM NaCl the final measured root length of *pip2;1* mutants was always lower than that of the wild-type. In fact, the double mutants tested, *2;2-3/ 2;1-2* and *2;1-2/ 2;4-1*, also showed the tendency for reduced root elongation that was observed for *pip2;1* single mutants under severe salt stress (Fig. 19). The root phenotype was more pronounced for *2;1-2/ 2;4-1*, however, the whole plants were also damaged including chlorosis of the leaves (Fig. 20). In addition, *2;1-2/ 2;4-1* double mutant developed less or shorter lateral roots in case of salt stress (Fig. 20). In comparison, osmotic stress imposed by 200 mM sorbitol did not lead to any reduced root elongation or visible phenotypical alteration in the conditions tested (Fig. 19 and 20).
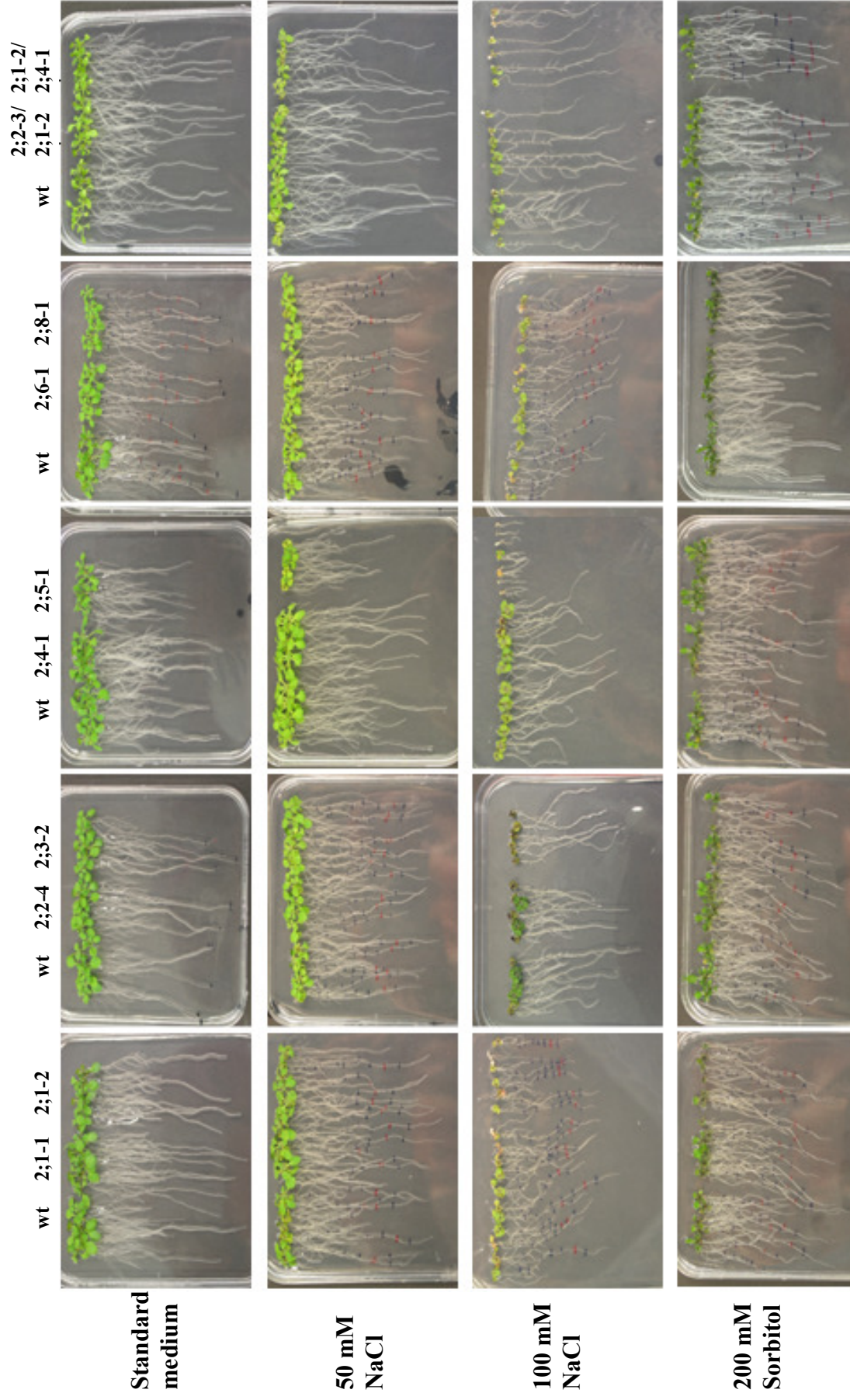
Figure 20. Growth of *pip2* single mutants under various water stresses show differential sensitivity.
Arabidopsis thaliana wild-type (WT) and *pip2* mutants were germinated on vertical MS gelrite plates and 4-day-old seedlings were then transferred to vertical gelrite plates containing various solutes (50 or 100 mM NaCl as well as 200 mM sorbitol) to imposed water stress. Seedlings were further grown for 7 days and subsequently photographed.
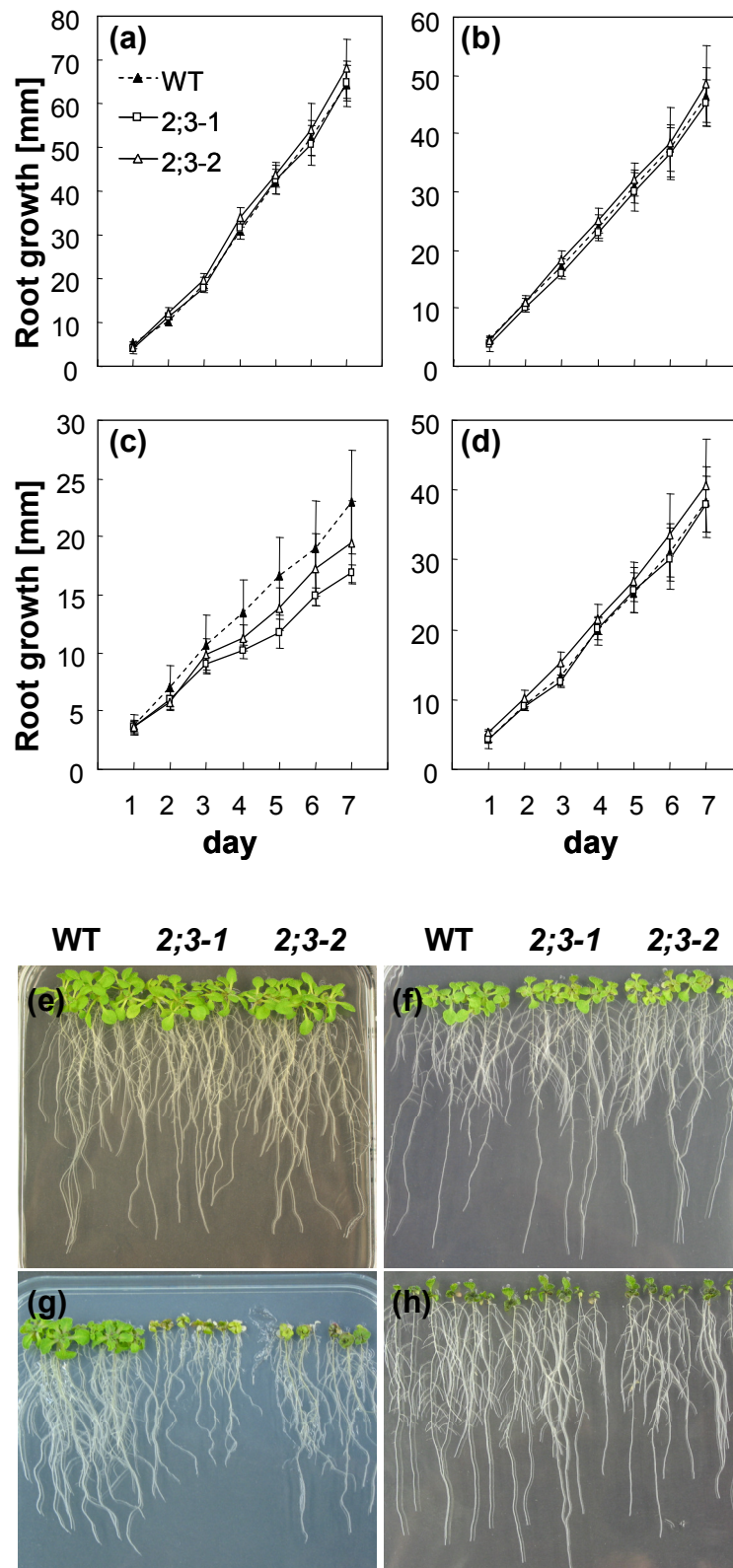
Figure 21. Growth of *pip2;3* mutants is sensitive to salt stress.
Root elongation and plant phenotype of *pip2;3* T-DNA insertional mutants and wild-type seedlings grown under various water stress conditions. Seeds were germinated on control medium and 4-day-old seedlings were transferred to vertically oriented plates containing control medium or control medium supplemented with different concentrations of NaCl or sorbitol to account for ionic and osmotic stresses. Seedlings were further grown for 7 days and root elongation was recorded daily (a to d). Wild-type and *pip2;3* mutant plantlets were photographed at the end of the treatment (e to f). Data in a, b, c and d are the means ± SD of measurements from six individual plants. Experiments were repeated five times. (a, e) controls; (b, f) 50 mM NaCl; (c, g) 100 mM NaCl and (d, h) 200 mM sorbitol.

3.3.2 Morphological analyses of *pip2* mutants

Although most *pip2* mutants did not showed any obvious visible phenotype under favorable growth or water stress conditions, a closer analysis of the root morphology has been carried out. Thus, roots of wild-type and *pip2* mutant seedlings grown under various conditions were observed by stereomicroscopy as well as confocal microscopy (LSM 510, Helmholtz Zentrum München-Institute of Pathology).
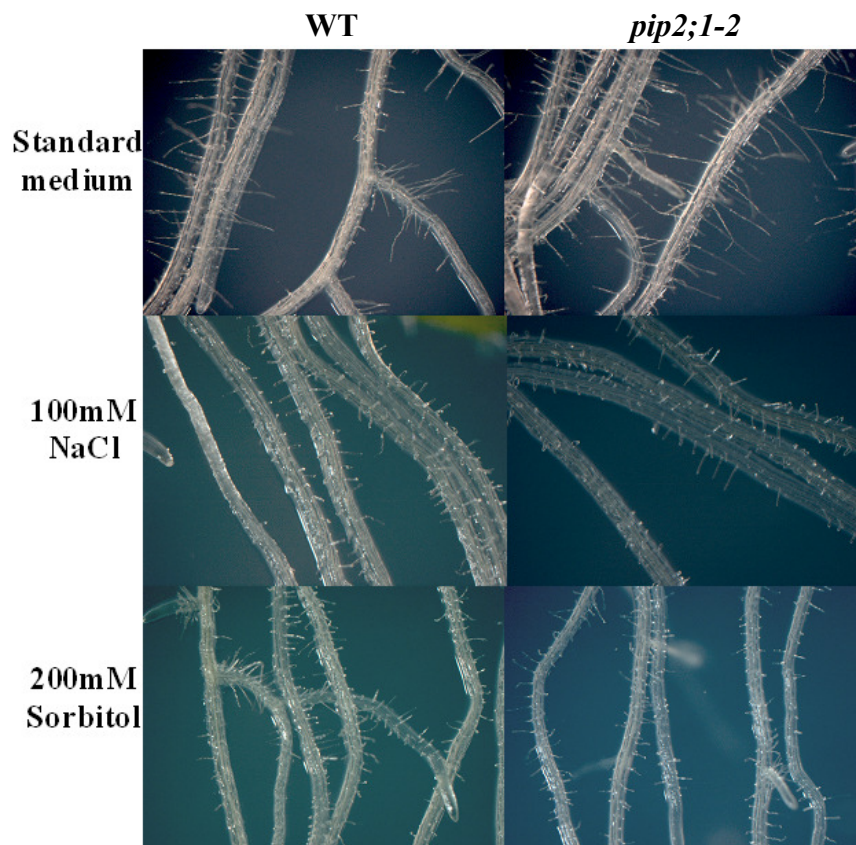
Figure 22. Stereomicroscopy images of WT and *pip2* mutant root seedlings.
Wt and pip2 mutants seeds were germinated on MS-gelrite control medium and 4-day-old seedlings were transferred to vertically oriented plates containing MS-gelrite control medium or MS-gelrite control medium supplemented with 100 mM NaCl or 200 mM sorbitol. Seedlings were further grown for 7 days, visualized with a stereomicroscope and photographed. Insertional *pip2* mutants did not show any root alterations with respect to the wild-type. As a representative example *pip2;1-2* is shown.

However, no morphological alterations could be observed between wild-type and *pip2* mutant plants under both standard and water stress conditions (Fig. 22). As expected, differences were observed between plants grown on standard medium and water-stressed plants. Thus, lateral root growth as well as root hair development was reduced, however, the morphology of the *pip2* mutants was affected in a similar way than the wild-type (Fig. 22).

3.3.3 Leaf water relations

Plant water relation is a complex process involving both below- and above-ground organs. In leaves, water loss via transpiration is the most critical parameter. It is mostly regulated by closure and opening of stomata, but also depends on water supply. To check whether PIP2 proteins play a role in regulation of water loss through the leaves, two independent types of experiments were performed. First, the rate of the loss of water from detached rosettes was recorded for *pip2* mutants and wild-type. Second, the transpiration and water use efficiency of selected mutants was analyzed.

3.3.3.1 Loss of water from detached rosettes

In order to record the loss of water from detached leaves, the aerial portion of three-week-old *pip2* mutant plants and wild-type controls grown on soil were removed from the roots, weighed, and the decline in fresh weight of the rosette leaves was measured for a period of four hours (Fig. 23 and 24).

The measured initial fresh weight was used to investigate differences in above ground part biomass. No significant differences could be observed in the initial fresh weight of 3 week-old plants grown on soil (Fig. 23).
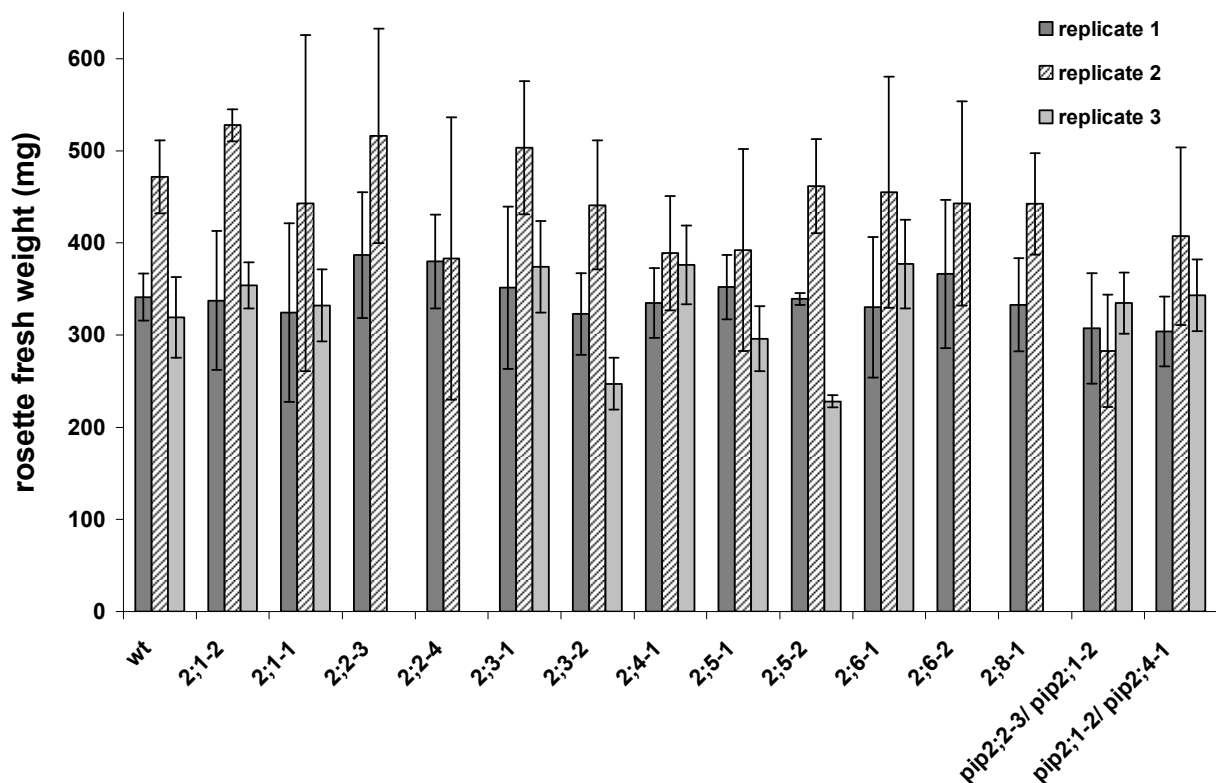
Figure 23. Rosette leaves fresh weight.
Rosette of three-week-old control and *pip2* mutant plants were detached and weighed. Bars represent fresh weight as a mean ± SD obtained from 4 individual plants. Experiments were repeated 3 times (or only twice *for pip2;2-3, pip2;2-4, pip2;6-2* and *pip2;8-1*).

The loss of water from detached leaves was then recorded under controlled temperature, light and humidity (Method 2.2.1.7). A gradual decline in leaf water content can be observed and this rate of leaf water loss was compared between mutants and wild-type. In this experiment, since the leaves are detached from the roots there is no water coming in and the rate of water loss is solely determined by the properties of the leaves such as stomatal conductance and leaf morphology. However, these analyses indicated that *pip2* single mutants did not alter the rate of water loss with respect to the wild-type (Fig. 24a to f). Although the *pip2;3-2* mutant deviated from the wild-type in showing an increased water loss, this phenotype was not confirmed by the independent *pip2;3-1* mutant.

However, detached-rosette assay showed that in the *pip2* double mutants decline in leaf water loss was slightly lower in comparison to wild-type (Fig. 24g and h). Although, this decline was relatively low (5%), it was significantly observed all over the time course of the experiment (Fig. 24g and h).
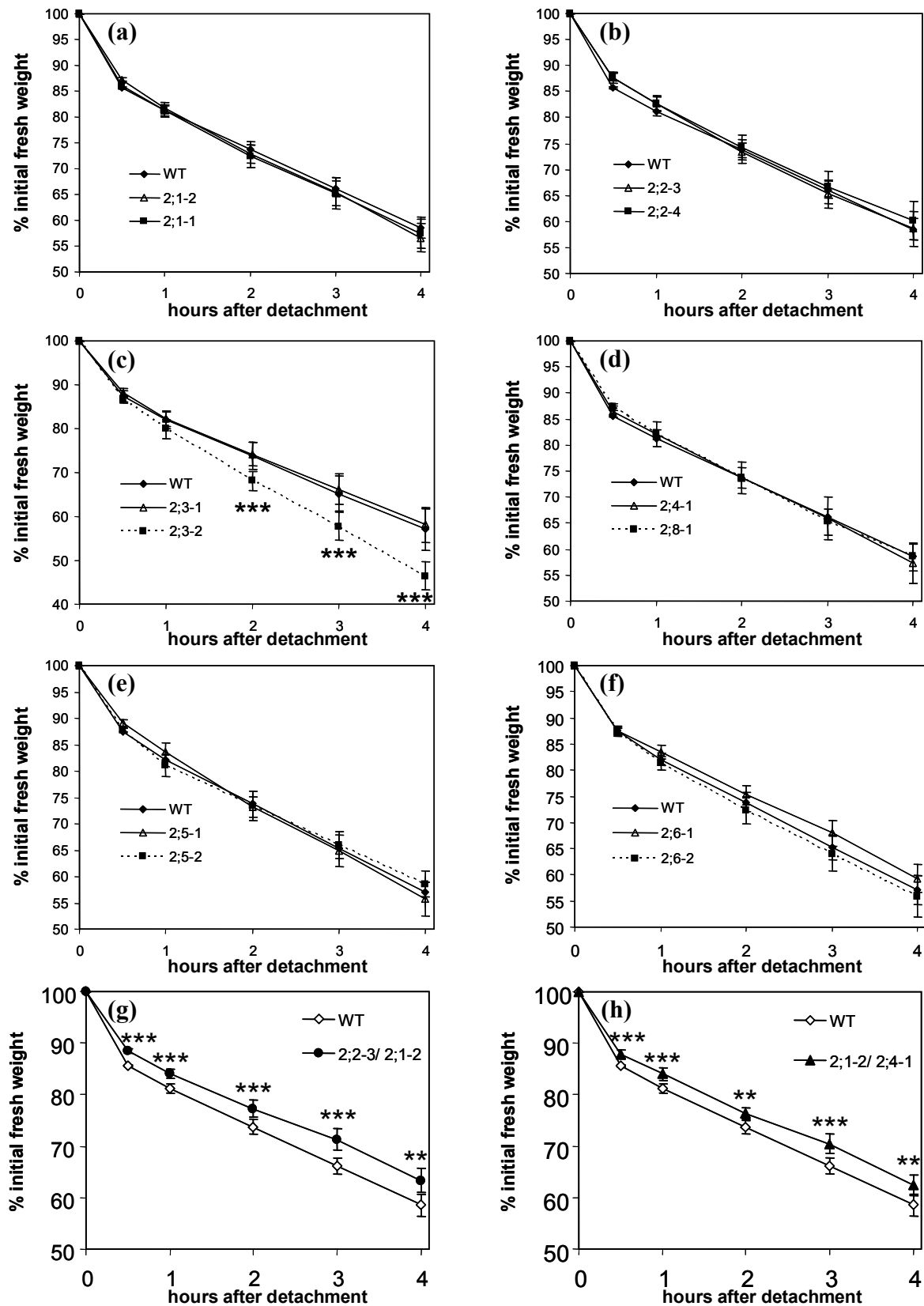
Figure 24. Water loss using detached rosette assay.
Relative water loss from rosette of three-week-old mutants and wild-type plants was assessed. Rosettes were detached and weighed every hour for 4 hours. Decline in fresh weight was expressed in percentage of the initial fresh weight. Percentage of initial fresh weight is displayed as mean ± SE obtained from three independent biological experiments (n = 3 with 4 separate plants for each experiment). The asterisks indicate statistically significant differences, as determined by two-tailed distribution student's t test assuming unequal variance (*** p < 0.005). (a to f) *pip2* single mutants. (g) *pip2;2-3/ pip2;1-2* and (h) *pip2;1-2/ pip2;4-1* double mutants.

3.3.3.2 Transpiration, stomatal conductance, net photosynthesis and water use efficiency measurements

To analyze potential additional effects of *pip2* loss-of-function on plant water relations, several physiological traits such as transpiration and water use efficiency were also measured. For these analyses, *pip2;1-2*, *pip2;2-3* and *pip2;2-3/ pip2;1-2* knockout mutants were chosen. First, they represent mutants of abundantly expressed aquaporins in both roots and leaves. Second, the slightly lower water loss observed for the double mutant suggested PIP2;1 and/or PIP2;2 may play an important role in plant water relations.

Measurements were done on three-week-old *pip2* mutant plants and wild-type controls grown on soil under either well-watered or water deficit conditions (Table 6). Water deficit condition was achieved by withholding watering four days before the measurements. Transpiration, stomatal conductance, net photosynthesis and water use efficiency were measured. Leaves were then cut and leaf area and leaf fresh and dry weight were determined (Table 6). In comparison to well-watered conditions, values under water deficit conditions were only little lower indicating a mild stress (Table 6).

There was no effect of *pip2* knockouts on leaf area or mass either under well-watered or water deficit conditions. Similarly, transpiration was not affected. Nevertheless, it was interesting to note that under well-watered conditions, net photosynthesis and water use efficiency was slightly lower in the single mutants than in wild-type plants (Table 6). Surprisingly, the double mutant was comparable to wild-type plants (Table 6).

In general, our measurements were in agreement with those obtained by Martre et al. (2002) who showed that stomatal conductance, leaf transpiration rate as well as leaf hydraulic conductance were not affected in PIP1 and PIP2 single and double antisense plants. Nevertheless, more replica are needed to confirm these results due to the high variability of the individual measurements.

Table 6. Transpiration, stomatal conductance, net photosynthesis and water use efficiency measurements.
Leaf fresh weight (LFW), leaf dry weight (LDW), leaf (LWC), leaf area, transpiration (E), Vapor-Pressure-Deficit (VPD), stomatal conductance (gH_2O), net photosynthesis (NP) and relative water content (RWC), leaf area, transpiration (E), Vapor-Pressure-Deficit (VPD), stomatal conductance (gH_2O), net photosynthesis (NP) and water use efficiency (WUE) were measured for wild-type and insertional *pip2* knockout mutant plants. Measurements were done using single plants (three-week old) grown in soil under well-watered or water deficit conditions. Values are means ± SE. n = number of individual plants. Environmental conditions were: 25°C, 53% relative humidity, light intensity was about 300 µmol m⁻² s⁻¹ and CO_2 abs. 380 ppm.

	well-watered conditions				water deficit conditions			
	WT (n = 4)	2;1-2 (n = 4)	2;2-3 (n = 3)	2;2-3/ 2;1-2 (n = 4)	WT (n = 6)	2;1-2 (n = 8)	2;2-3 (n = 7)	2;2-3/ 2;1-2 (n = 6)
LFW [mg]	52.3 ± 5.9	57.3 ± 7.7	52.0 ± 8.4	54.7 ± 4.6	42.4 ± 4.5	48.3 ± 6.4	41.1 ± 7.1	35.4 ± 5.4
LDW [mg]	6.6 ± 0.6	6.2 ± 1.0	6.2 ± 0.9	7.0 ± 0.6	5.8 ± 0.6	6.5 ± 0.9	5.5 ± 0.1	5.0 ± 0.1
LWC [mg]	45.7 ± 5.7	51.1 ± 6.9	45.9 ± 7.4	47.7 ± 4.0	36.6 ± 3.9	41.8 ± 5.6	35.7 ± 0.6	30.4 ± 0.5
RWC [%]	87.0 ± 1.4	89.0 ± 1.4	88.1 ± 0.5	87.3 ± 0.4	86.3 ± 0.7	86.6 ± 0.5	86.9 ± 0.8	85.3 ± 0.7
Leaf area [cm^2]	3.1 ± 0.4	3.4 ± 0.4	3.0 ± 0.4	2.8 ± 0.7	2.6 ± 0.2	3.0 ± 0.3	2.5 ± 0.4	2.3 ± 0.3
E [mmol m^{-2} s^{-1}]	2.6 ± 0.2	2.6 ± 0.2	2.9 ± 0.2	2.3 ± 0.2	2.1 ± 0.2	1.8 ± 0.2	2.0 ± 0.2	1.8 ± 0.3
VPD [Pa/kPa]	16.0 ± 0.2	15.9 ± 0.2	15.6 ± 0.5	16.2 ± 0.0	16.6 ± 0.1	16.7 ± 0.2	16.8 ± 0.2	17.1 ± 0.5
gH_2O [mmol m^{-2} s^{-1}]	163.8 ± 15.3	165.3 ± 10.4	209.5 ± 34.9	142.0 ± 13.4	124.1 ± 12.8	107.6 ± 13.7	121.6 ± 14.9	106.6 ± 21.6
NP [µmol m^{-2} s^{-1}]	5.0 ± 0.6	4.4 ± 0.8	3.5 ± 1.9	5.6 ± 0.4	5.2 ± 0.6	3.7 ± 0.5	4.9 ± 0.7	4.3 ± 0.7
WUE [µmol CO_2/ mmol H_2O] (=NP/ E)	2.0 ± 0.3	1.7 ± 0.2	1.0 ± 0.4	2.6 ± 0.4	2.7 ± 0.5	2.5 ± 0.5	2.6 ± 0.4	3.2 ± 0.9

3.3.4 Isotope tracing in plant water relations – deuterium content in leaf water

Many efforts have been made in the past to investigate water transport in plants. The use of stable isotopes techniques in plant research is increasing as the isotopes can serve as very valuable tracers allowing the nondestructive investigation of whole organisms and their interactions with biotic and abiotic environments. The isotopic content of leaf water (both D and ^{18}O) and its progressive enrichment due to e.g. transpiration and leaf compartmentation has been modeled (see below) to assess these processes in plant ecology and physiology. Thereby, the natural enrichment of D content in leaves was determined as well as changes of steady state after application of water with artificially enhanced D or ^{18}O content (Flanagan et al., 1991; West et al., 2006; Santrucek et al., 2007).

In contrast to these studies, I wanted to establish a dynamic tool using source water with artificially enhanced D content as a tracer to study the kinetics of water uptake and flux from roots into the aerial parts until a *new* equilibrium is reached. A particular advantage in contrast to most other techniques such as root exudation, pressure chamber or pressure bombs was that this approach would be non-invasive during the experiment.

Thus, water transfer into the rosette leaves was followed in a 24 h kinetic study by measuring the D translocation into whole rosette leaf water. Any genetic change *e.g.* an aquaporin knockout that will influence the water relations, may alter fluxes and thus the rate of establishing the new equilibrium.

3.3.4.1 Theory: Modeling leaf water isotope content

The isotopic composition of leaf water is generally different from the source water taken up by the roots and may become enriched or depleted in D depending on the relative humidity of the atmosphere, the D content of the soil water and that of the atmospheric moisture. Craig and Gordon (1965) established a model that depicts the stable isotope fractionation processes occurring during evaporation of water from the ocean. The processes result in a D enrichment of surface ocean water. The model was adapted for water transpired from a leaf and shown to be applicable to describe the D content of plant leaf water (Wershaw et al., 1966; Flanagan et al., 1991; Roden and Ehleringer, 1999a; Barnes et al., 2004).

The leaf water model considers the following processes (Fig. 2):

- Water evaporation from the leaf (leaf surface/ sub-stomatal spaces) into leaf intercellular air spaces. The water vapor in this layer is in thermodynamic equilibrium with the leaf water.

- Diffusional and turbulent transport of water vapor from this interface through stomata to the atmosphere. It was assumed that the turbulent transport was negligible in our experimental setting[1].

Fractionation factors describe the isotopic effects in the two processes. The equilibrium fractionation factor α_{eq} determines the relationship between the liquid water and water vapor in equilibrium:

$$\alpha_{eq} = R_l / R_v \tag{1}$$

where R is the molar ratio of the heavy and light isotope, i.e. D/H, and the subscripts l and v refer to liquid and vapor water, respectively. In the above definition it is assumed that the air is saturated with water vapor and that the liquid and vapor are at the same temperature. These conditions are satisfied for a leaf where water vapor in the intercellular air spaces is in equilibrium with leaf cell water. Majoube (1971) has measured the fractionation factor over a wide temperature range: $\alpha_{eq} = Exp(24844/T^2 - 76.248/T + 0,052612)$ (with T temperature in Kelvins). This expression was used to calculate values for α_{eq}.

The kinetic fractionation factor α_{kin} governs (beside the other mentioned parameters) the diffusional transport. It is defined as the ratio of the diffusion coefficients for water vapor molecules containing the light and heavy isotopes,

$$\alpha_{kin} = D_{^1H_2O} / D_{^1H^2HO} = D/D' \tag{2}$$

The different diffusion coefficients mainly result from the different molecular masses. In air this kinetic fractionation factor α_{kin} has been measured to be $\alpha_{kin} = 1.025$, indicating a 1.025 fold faster diffusion of H_2O *vs.* HDO (Merlivat, 1978). The transpirational flux due to diffusion is described according to Fick's law

$$Flux = -Diffusionfactor \cdot \frac{\partial Concentration}{\partial Dis\tan ce} \tag{3}$$

and thus, the transpirational flux E of the isotopically light water can be described as:

$$E = D \cdot \frac{\partial (e_i - e_a)/P}{\partial x} \tag{4}$$

---

[1] Several attempts have been made in modifying the model to account for turbulent conditions in a boundary layer and for boundary layer effects (e.g. Flanagan et al., 1991; Farquhar et al., 1989). The authors suggested that taking these modifications into account could improve the predictions for the leaf water D content. However, these parameters were shown to be negligible to the well ventilated *Arabidopsis* system, since the model predicted the actual leaf water D content quite reasonably (see below, verification of the model).

with e_i and e_a indicating the partial pressures of total water vapor in the leaf intercellular air spaces and the ambient air, respectively. The small portion of deuterated water can be neglected and, hence, $e_{i/a\ [H_2O]}$ is well approximated by $e_{i/a\ [total\ water]}$. P is the total air pressure, thus $e_{i,a}/P$ indicates the concentration of water in the two gas phases of compartments i and a.

A similar equation can be written to describe evaporation of heavy isotopes molecules (HDO):

$$E' = D' \cdot \frac{\partial (R_i e_i - R_a e_a)/P}{\partial x} \tag{5}$$

However, the partial pressure of deuterated water vapor in the leaf intercellular air spaces and the ambient air are only a fraction of e_i and e_a. Accordingly, they are to be multiplied by the molar ratios R_i and R_a of the heavy and light (i.e. approximately total) isotopes of water vapor in these compartments.

These equations depict the flux of light or heavy isotopes molecules transpired by the leaves. Hence, the isotopic composition of water evaporating and transpiring from a leaf R_{trans} can be described as the ratio of the fluxes of the heavy (E') and the light (E) isotopes:

$$R_{trans} \approx \frac{E'}{E} = \frac{1}{\alpha_{kin}} \frac{(R_i e_i - R_a e_a)}{(e_i - e_a)} = \frac{1}{\alpha_{kin}} \frac{\left(\dfrac{R_{leaf}}{\alpha_{eq}} e_i - R_a e_a \right)}{(e_i - e_a)} \tag{6}$$

with $R_i = \dfrac{R_{leaf}}{\alpha_{eq}}$ assuming water vapor in the intercellular air spaces in equilibrium with the leaf water.

Resolving equation 6 for R_{leaf} produces equation 7:

$$R_{leaf} = \alpha_{eq} \left[\alpha_{kin} R_{trans} \left(1 - \frac{e_a}{e_i} \right) + R_a \left(\frac{e_a}{e_i} \right) \right] \tag{7}$$

Since the air in the intercellular spaces is saturated with water vapor, e_i will be maximal (at the respective constant temperature). Hence, e_a/e_i equals the relative humidity h of the ambient air. The equation is then expressed in its simpler form describing R_{leaf} as being dependent on R_{trans}, R_a, and the ambient humidity:

$$R_{leaf} = \alpha_{eq} \left[\alpha_{kin} R_{trans} (1 - h) + R_a \cdot h \right] \tag{8}$$

It has to be noted that measuring the isotopic composition of the water of one leaf or even of a collection of leaves like the rosette leaves in this study and using this value in equation 8 treats the leaf water as being ideally mixed, which is a simplified view. Indeed, it has been

shown in various experiments that the model of Craig and Gordon predicts a greater isotopic enrichment than was actually observed in leaf water (Flanagan et al., 1991; Roden and Ehleringer, 1999a). The possibility that different fractions of water within a leaf are not necessarily uniform has been inferred to explain this discrepancy. It was suggested that the differences might result from unfractionated water in leaf tissue. Accordingly, several studies introduced a separation into two compartments reflected by the xylem vessels and the major rest of the leaf volume represented by the mesophyll cells . The portion of unfractionated water has often been calculated to be 13% to 30%. However, in our experimental set-up this portion was evaluated to be about 3% (data not shown) and the model predicted the actual leaf water D content quite reasonably (see below, verification of the model). Consequently, such effects were considered negligible.

According to equation 8 the isotopic composition of leaf water R_{leaf} depends only on the isotopic composition of the transpiration as long as the ambient humidity and isotopic composition of the atmosphere are constant.

Although it is true for a freely evaporating surface (like ocean), in case of a plant, water can exit the leaves not only by transpiration but also via the phloem flux back to lower leaves or roots (Fig. 2). Consequently, for a plant, the steady state of R_{leaf} described by equation 8 should be modified to account for water loss via phloem. If we call R_{loss} the total water loss by the leaves, then:

$$R_{loss} = R_{phloem} \cdot f + R_{trans}(1 - f) \tag{8a}$$

where R_{phloem} is the isotopic composition of phloem water and f is the fraction of the total lost leaf water attributed to phloem water flow.

The steady-state of R_{leaf} will be reached as soon as R_{loss} is equal to R_{xyl}, which will be the case when the isotopic composition of the water exiting the leaves (transpiring water and phloem water) will be the same as that of the resupplying water taken up by the roots through the xylem, R_{xyl}.

Assuming that phloem water takes on an isotopic composition identical to that of leaf water, R_{phloem} equals R_{leaf}. Thus, from eq. 8 and 8a follows equation 9 which describes the isotopic composition of the leaf water in steady state depending on the isotopic composition of the source water R_{xyl}:

$$R_{leaf} = \frac{1}{(1/\alpha_{eq}) \cdot (1-f) + f \cdot \alpha_{kin} \cdot (1-h)} \cdot \left(\alpha_{kin}(1-h)R_{xyl} + (1-f)h \cdot R_a \right)$$

(9)

$$where\ R_{xyl} = R_{loss}$$

If one transfers hydroponically grown plants to a new medium containing enhanced deuterium content, the isotopic composition of the leaf water R_{leaf} and that of the total water lost from the leaves R_{loss} is continuously changing until a new steady state is reached.

This temporal change of the isotopic composition of leaf water dR_{leaf}/dt can be expressed by equation 10.

$$\frac{dR_{leaf}}{dt} = \left(R_{xyl} - R_{loss}\right)q_{leaf}$$

(10)

where dR_{leaf}/dt is proportional to the relative turnover of leaf water q_{Leaf} ($q_{Leaf} = Q/V_{leaf}$ [s^{-1}] with Q: leaf water turnover and V_{leaf}: leaf water volume) as well as to the difference of the isotopic content of the incoming water R_{xyl} and isotopic content of the lost water comprising transpiring water and water that flows back to the root via the phloem.

R_{xyl} will be very close to that of the source water in soil or in a hydroponic tank. Water exchange occurring along the path through the xylem with the radially surrounding cells is rather quick and is assumed to be negligible in terms of volume in comparison to the high axial flow of water. Therefore, the water arriving in the leaf can be assumed to be isotopically equal to the soil water or water in the hydroponic tank: $R_{xyl} = R_{soil}$ (Fig. 2).

Finally, through a substitution of R_{loss} (eq. 8a) and R_{trans} (eq. 8) into equation 10, the differential equation reads:

$$\frac{dR_{leaf}}{dt} = \left[R_{xyl} - \left((1-f) \cdot \left(\frac{1}{\alpha_{kin}} \frac{R_{leaf}/\alpha_{eq} - h \cdot R_a}{1-h} \right) + f \cdot R_{phloem} \right) \right] \cdot q_{leaf}$$

(11)

The solution of this differential equation describes the temporal change of the isotopic content of rosette leaves water which approaches the new steady-state $R_{leaf,SS}$ (identical to R_{leaf} in equation 9) for high values of t:

$$R_{leaf}(t) = R_{leaf,SS}\left(1 - \exp(-aq_{leaf}t)\right) + R_{leaf,0}\exp(-aq_{leaf}t)$$

(12)

$R_{leaf,0}$ = Starting value

$R_{leaf,SS}$ = steady state = $\dfrac{1}{(1/\alpha_{eq})(1-f) + f \cdot \alpha_{kin} \cdot (1-h)} \cdot \left(\alpha_{kin} \cdot (1-h) \cdot R_{xyl} + (1-f)h \cdot R_a \right)$

$a = \dfrac{(1/\alpha_{eq}) \cdot (1-f)}{\alpha_{kin} \cdot (1-h)} + f$

q = water turnover rate

t = time

This equation was used to model the isotopic enrichment of rosette leaves water in the experiments described below after an intentional increase in source water D content in order to determine the relative turnover of leaf water q (equaling relative xylem flux) and the fractionation factor f (approximating phloem back flow).

3.3.4.2 Evaluation of the leaf water isotope model

The validity of the model was tested for the small, herbaceous model plant *Arabidopsis thaliana*. Equation 9 was to be used to model the steady-state isotopic content of leaf water for *Arabidopsis* rosettes before and after raising the D concentration of the tank water of hydroponically grown plants.

To be able to compare different plants/ genotypes, several parameters that might potentially influence water relations like light intensity, humidity and temperature had to be maintained constant and measured throughout the experiment. Thus, all experiments were done in a sun simulator with carefully controlled conditions (see Method 2.2.1.9). As mentioned above (see theory), the isotopic composition of the atmospheric water vapor influences the stable isotope composition of leaf water. According to equation 9 the steady-state of R_{leaf} will also vary with R_a. Therefore, the water vapor in the air of the sun simulator was collected and its isotopic content measured. It had in the sun simulator a δD value in the range of -120‰ to -150‰.

A prerequisite for applying the model is that the source water R_{xyl} equals a constant R_{tank} of the water supplied via the hydroponic solution. If the roots are submerged into D-enriched water, it is assumed that the water in the xylem that will supply the leaves will have the same isotopic composition as the tank water after a rather short lag phase. To control and measure the actual deuterium content of R_{xyl} that feeds into the model equations, water samples were collected both prior and after addition of deuterium in the tank water as well as throughout the experiment. The measurements demonstrated that tank water was well maintained throughout the experiment and that only minor changes occurred in tank water isotopic composition over the course of the experiment (Fig. 25).

Two steady-state situations occurring in our experiments were tested:

- Steady-state of plants grown in regular medium (i.e. starting point of the experiment)

- Steady-state after adding deuterium in the medium (considerable increase).

and the measured values compared with the value predicted by equation 9.

Three-week-old *Arabidopis* plants were transferred to a fresh medium enriched in deuterium. For the two steady-states, the modeled isotopic content of leaf water was in good agreement with the measured values when the fractionation factor f was fitted to a value of 0.15 (Table 7). The values predicted by the Craig and Gordon model were slightly different from the measured values demonstrating the improvement by the introduction of f.

Table 7. Isotopic composition of leaf water (δD, ‰) of hydroponically grown *Arabidopis thaliana* plants.
Isotopic content of leaf water was measured on samples collected right before starting the experiment (prior addition of D_2O in the medium) and at different time point after addition of D_2O in the medium. Environmental conditions were: 22°C, 50% relative humidity while light intensity was about 475 µmol m^{-2} s^{-1}. Isotopic content of water vapor was -130‰ and fractionation factor f fitted to 0.15.

Genotype	Initial steady state (time 0)				Final steady state (after 24 hours)			
	Measured source water	Measured	Phloem model	C & G model	Measured source water	Measured	Phloem model	C & G model
WT	-77.5 ± 0.1	- 20.7 ± 5	-22.5	-17.1	311.4 ± 1.7	212.3 ± 9.3	208.8	198.7
2;2-3	-77.7 ± 0.1	-19 ± 4.6	-22.6	-17.2	307.8 ± 2.4	203.3 ± 9.7	206.6	196.7
2;2-3/ 2;1-2	-77.8 ± 0.1	-21.3 ± 3	-22.7	-17.3	305.2 ± 1.3	209 ± 5.6	205.1	195.3

Furthermore, the second situation could be used to test the time required for leaf water to reach the new isotopic steady-state. The dynamic changes in leaf rosette D content were recorded over 24 h and modeled using equation 12 (Method 2.2.1.9). This experiment showed that the leaf isotopic steady-state was reached after the plants had been exposed to the new conditions for approximately 6 hours (Fig. 25). It is known that the relative humidity has an important impact on the model (see above, theory), because it influences the transpiration rate to the atmosphere. The model using 50% humidity as a parameter fits well to the measurement of the experiment carried out at 50% relative humidity (Figure 25, blue curve). However, changing the relative humidity parameter can drastically modify the steady-state (Fig. 25, red and green curve). Indeed, increasing the relative humidity will tend the leaf isotope content to the values of the atmospheric water vapor (Fig. 25, red curve). In a similar way, low humidity will shift the D content of the leaf water to the values of the xylem water and will increase the leaf isotope content (Fig. 25, green curve).
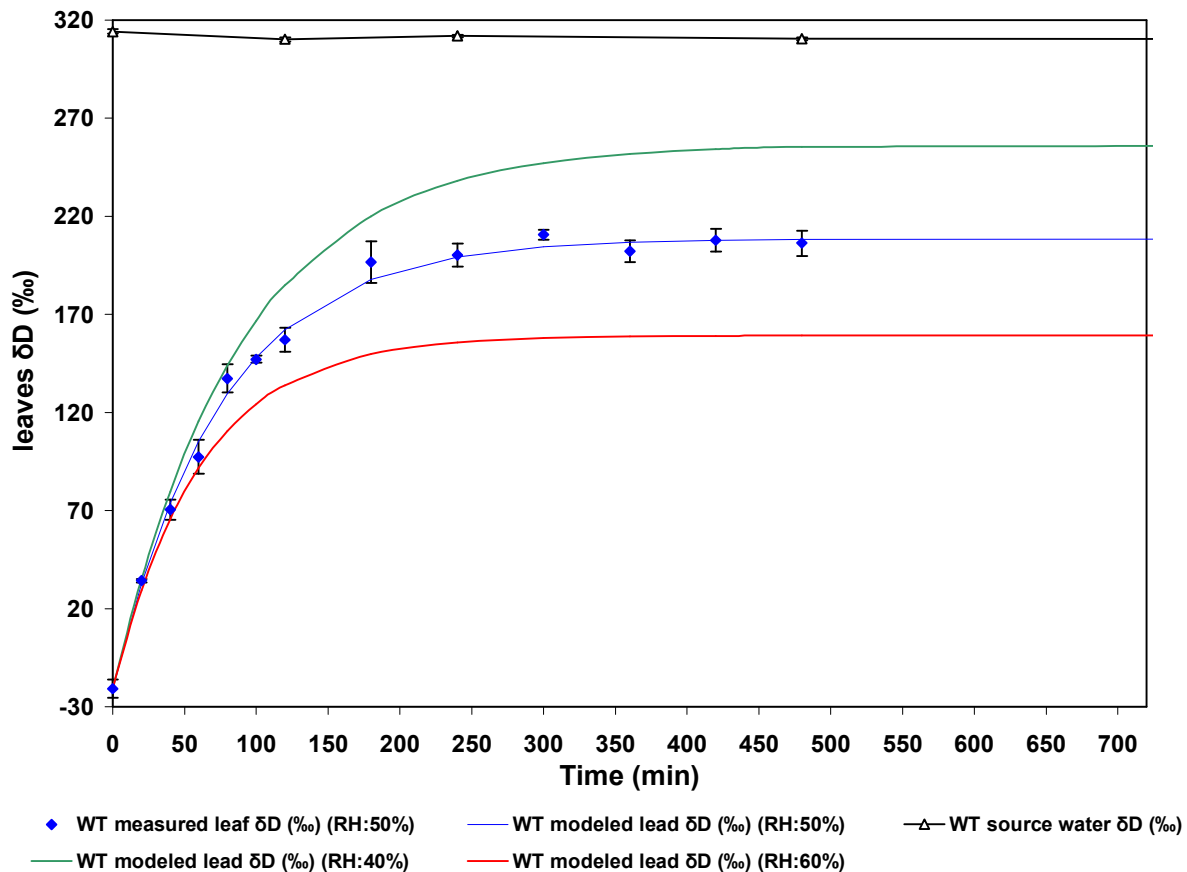
Figure 25. Modeling of isotopic content in leaf water of hydroponically grown *Arabidopsis* plants.
The different curves show the influence of relative humidity (RH) on the model. Solid circles are means (n = 3) and SD of measured isotopic content of rosette leaves water (some SD are contained within the symbol). Phloem fractionation factor f was 0.15 and q was 0.0079 min^{-1}.

The steady-states were well predicted by the modified model (Table 7). It was further investigated whether the dynamic change of isotopic content of the leaf water over time were in good agreement with the kinetic predictions of the model using equation 12. The comparison between measured and modeled isotopic content of leaf water revealed very good model predictions all over the course of the experiment allowing to accurately calculate the relative xylem flux q (Fig. 26; q = 0.0079 min^{-1}). Moreover, the model including a phloem fraction exiting the leaves (here f = 0.15) slightly improved the predicted values (slopes 1.0172 *vs.* 1.0694 in comparison to a perfect match of 1.0000; Fig. 26). The improvement due to the introduction of the fractionation factor f was even more pronounced under conditions of high humidity. Indeed, although the Craig & Gordon model predictions were still in reasonable agreement with measured values in case of experiments done with 50% humidity

(Fig. 26; red line), a strong discrepancy with measured values was observed in case of high humidity (Fig. 27).
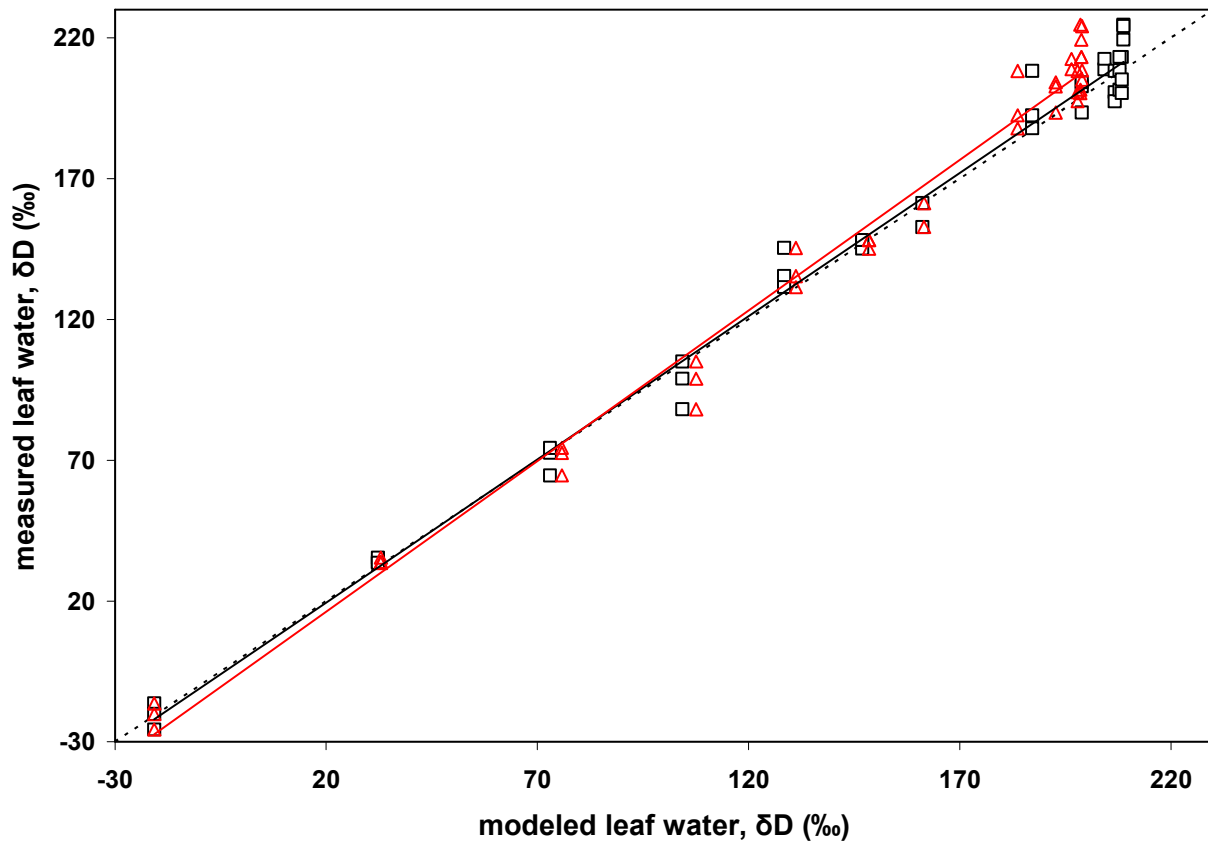
Figure 26. Relationship between the δD of modeled and measured leaf water in *Arabidopsis* plants. *Arabidopsis* wild-type plants were grown in hydroponic medium in a sun simulator. Relative humidity was set to 50% (for other environmental conditions, see Method 2.2.1.9). Black squares and red triangles represent the measured leaf δD over the course of the experiment (24 h) plotted against the phloem fractionated (with f = 0.15) and the original Craig & Gordon modeled values, respectively. In both model, the calculated relative turnover of leaf water q was 0.0079 min^{-1}. Three plants were measured for each time points with 14 time points. The equation for the regression lines was y = 1.0172x – 0.9236 (r^2 = 0.9900) and y = 1.0694x – 5.18 (r^2 = 0.9867) for the phloem fractionated (black line) and the original Craig & Gordon model (red line), respectively. The stippled line represents a 1:1 relationship.

In case of high humidity, transpiration is rather low and the fraction of phloem water flowing back is increasing in comparison to high transpiration situation. Indeed, in such an experiment, assuming a higher fraction f of water circulating via the phloem considerably improved the model prediction. By model fitting one can get a guess of the water fluxes in the phloem additional to the water fluxes in the xylem. It is important to note that the estimates of the phloem fluxes and their accuracies depend on model concept. Further experiments have to clarify, how close the concept of our model is to reality.

Figure 27 illustrates the utility of the adjusted model which fits well with the measured values when assuming a phloem fraction f = 0.7 and improves the Craig & Gordon derived leaf model. The Craig & Gordon model frequently predicts higher isotopic enrichment at the initial steady-state under natural conditions, while it will underestimates the experimental values after addition of deuterium in the source water in the experimental system used here (Fig. 27; see also Fig. 25 and 26).
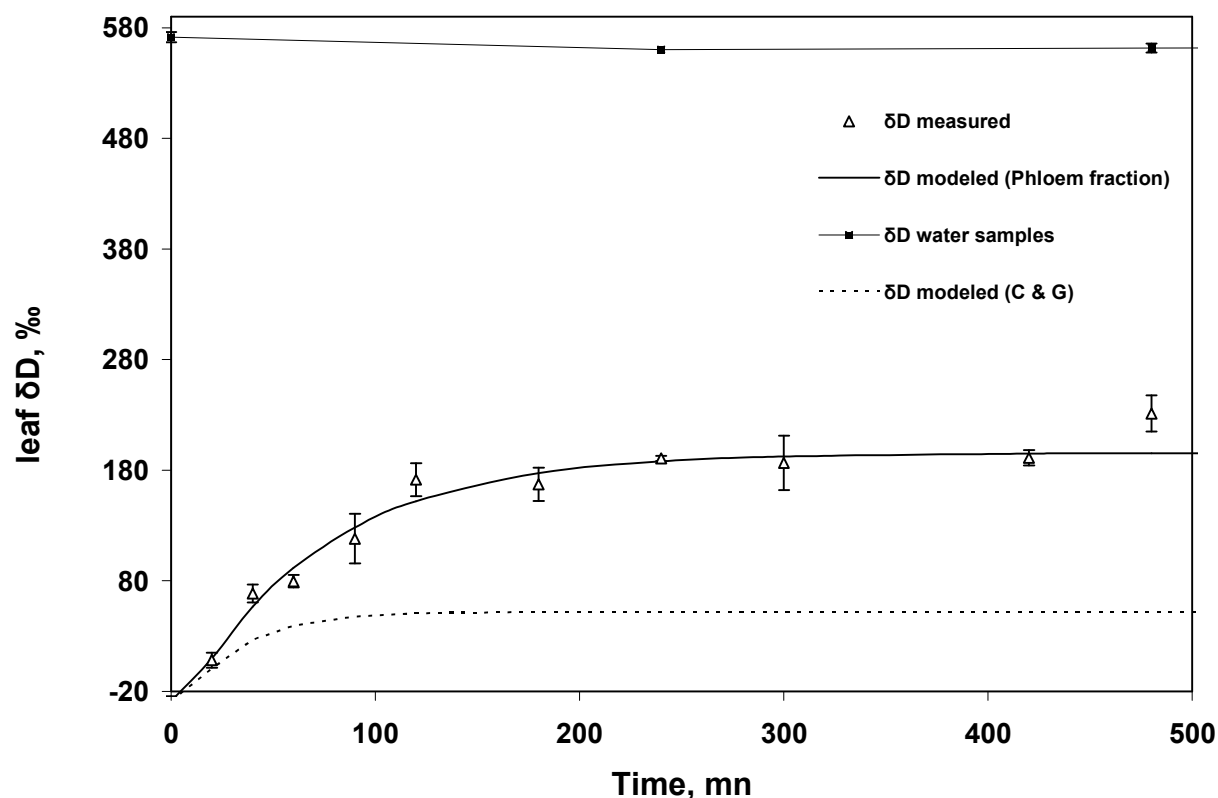
Figure 27. Modeling of isotopic content in leaf water of hydroponically grown *Arabidopsis* plants.
Experiment was done under high humidity (85%) (for other environmental conditions, see Method 2.2.1.9). Triangles are means (n = 3) and SDs of measured isotopic content of rosette leaf water. Using a phloem fractionation factor of 0.7, the modeled values predictions were in good agreement with the experimentally measured values while the Craig & Gordon (C & G) model underestimated the isotopic enrichment of leaf water.

To be able to compare different plant genotypes the influence of several plant-intrinsic parameters such as root and leaf fresh weight on the isotopic composition of bulk leaf water had to be examined as well.

After addition of D_2O to the hydroponic medium, the increase of D content in rosette leaves as well as the mass of the extracted leaf water (as a measure for the leaf water volume) and the individual root fresh weights were monitored during a period of 24 h. Clearly, the measured D content in the leaves was independent from both leaf and root masses at all time

points (Fig. 28a and b). There was also no correlation of leaf D concentration with the ratio of leaf to root mass (data not shown).

Plants were grown hydroponically and their roots were fully immersed in water. Thus, root water uptake was not limiting in our conditions, i.e. different root masses did not lead to different rates of uptake. The model equation 12 only allows the fitting of q (Q/ leaf mass) and fractionation factor f. Therefore, it was very important that the leaf isotopic content was independent from the water volume of rosette leaves, i.e. a larger rosette had taken up equivalently more water (xylem flux Q) from the medium at a certain time point to reach the same concentration of deuterium. Consequently, this feature was decisive for the applicability of the model and allowed comparing different plants irrespective of deviating leaf masses and extracting the relative flux q. The major properties influencing the model parameters q and f are the genetic and/or physiological traits of the plants.

Nevertheless, it is important to note that measurements of root fresh mass, leaf fresh and dry weight, and shoot/root ratio did not reveal mean differences between wild-type and several *pip2* mutant plants *per se* (*pip2;1*, *pip2;2*, *pip2;4-1* and *pip2;2-3-pip2;1-2*; data not shown). Eventually, growth is neglected in the short time frame of analysis.

(a) **(b)**

Time (min)	rosette leaves water volume (g)	root FW (g)	leaves δD (‰)
20	0.354	0.070	34
	0.393	0.081	35
	0.332	0.066	34
40	0.379	0.060	73
	0.400	0.077	65
	0.256	0.073	74
60	0.290	0.044	88
	0.248	0.058	105
	0.355	0.070	99
80	0.379	0.056	135
	0.260	0.052	145
	0.299	0.058	132
100	0.313	0.051	145
	0.346	0.058	148
	0.292	0.051	148
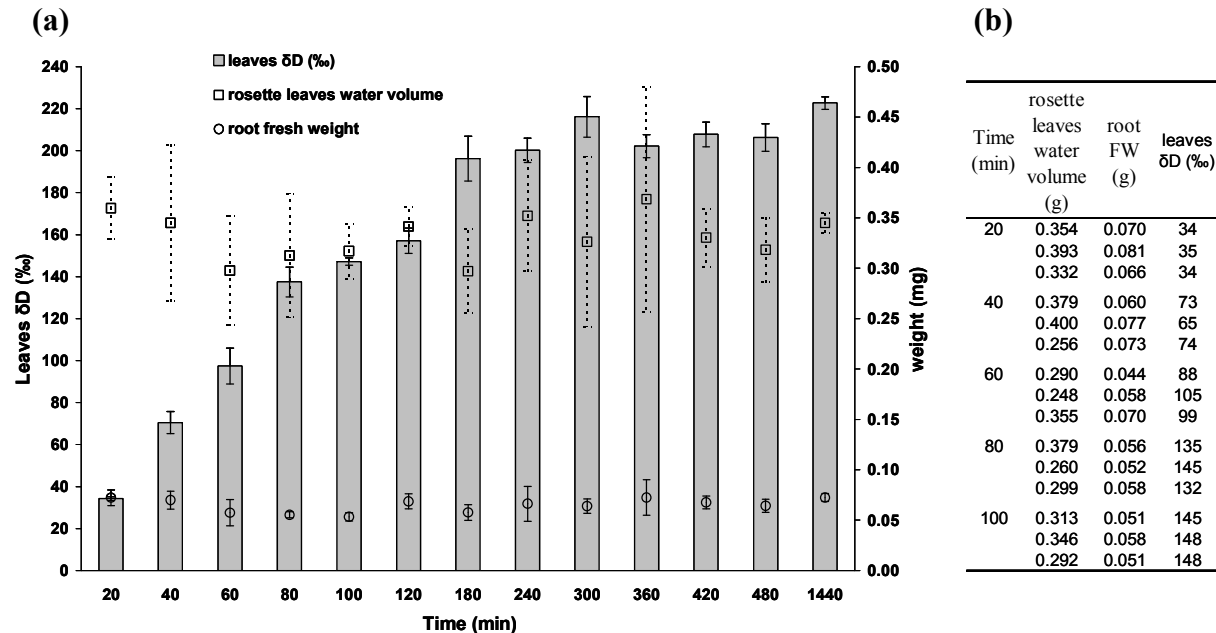
Figure 28. Influence of leaf water volume or root fresh weight on the isotopic content of *Arabidopsis* rosette leaves water.
At different time points, *Arabidopsis wild-type* plants were collected and their roots weighed. Water was extracted from rosette leaves and its volume and isotopic content measured. (a) Graphical display of the relation between leaf water volume or root fresh weight and the leaf δD. Bars, circles as well as squares represent means ± standard deviations (n = 3). (b) Leaf water volume, root fresh weight and leaf δD of individual plants harvested at different time points.

3.3.4.3 Comparison of deuterium content in rosette leaves water of wild-type and *pip2* mutants

Using this set-up and applying the developed model the dynamic change in isotopic content of rosette leaves, several *pip2* mutants were measured to investigate the involvement of PIP2 aquaporins in plant water transport. The *pip2;1* and *pip2;2* single mutants as well as *pip2;2-3/ pip2;1-2* double mutant were analyzed. As indicated above, *PIP2;1* and *PIP2;2* represent highly expressed isoforms in roots and leaves. In addition, their cellular expression profile (i.e. abundant in root cortex, endodermis as well as vascular tissue throughout the whole plant) together with the slight alteration of leaf water loss observed in double mutants may suggest a role in water transport between cells and tissues. Additionally, *pip2;4-1* single mutant was also analyzed. Although *PIP2;4* did not show expression in the leaves, its interesting root expression pattern (see Results 3.1) prompted us to analyze this mutant.

Figure 29 shows a typical experiment in which *pip2;2-3* single mutant exhibit a reduced leaf water isotopic enrichment in comparison to wild-type and *pip2;2-3/ pip2;1-2* double mutant plants.
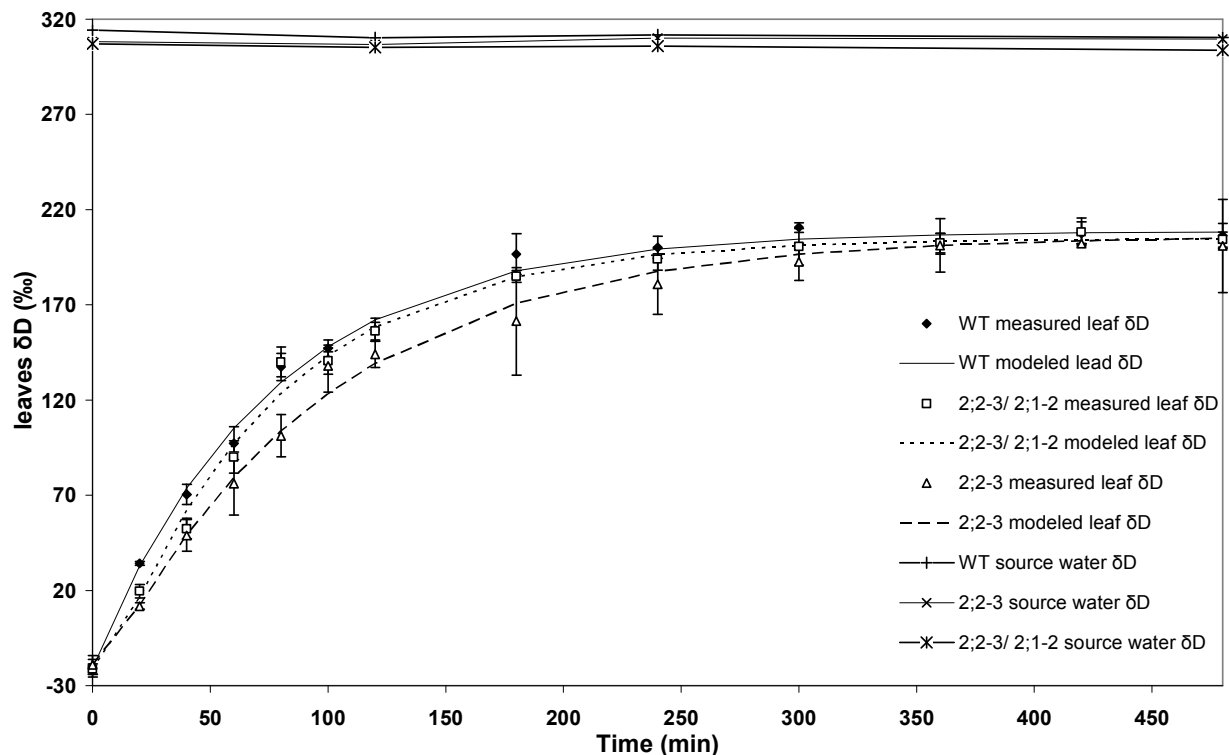
Figure 29. Comparison of deuterium translocation into rosette leaves water of wild-type and *pip2* mutants. Increase of the D content in rosette leaves water of *pip2;2-3* single mutant and *pip2;2-3/ pip2;1-2* double mutant was compared to that of wild-type plants (see Method 2.2.1.9 for environmental conditions). For each time points, symbols represent means ± standard deviations of 3 independent plants. In comparison to wild-type and *pip2;2-3/ pip2;1-2* mutant plants which exhibited a similar relative water turnover (q = 0.0079 min^{-1} and q = 0.0083 min^{-1}, respectively), *pip2;2-3* mutant showed a lower deuterium enrichment with a relative water turnover q = 0.0064 min^{-1}. Phloem fractionation factor were f_{wt} = 0.15; $f_{2;2-3/2;1-2}$ = 0.15 and $f_{2;2-3}$ = 0.10.

Both *pip2;1* and *pip2;2* single mutants exhibited a 15-20% slower increase of the D content (i.e. lower leaf water turnover q) in comparison to wild-type controls. In contrast, *pip2;4-1* did not show this reduction (Fig. 30). These data could suggest that a similar or even higher reduction would be observed in the *pip2;2-3/ pip2;1-2* double mutants. However, surprisingly no reduction was observed for the double mutant indicating a phenotypic recovery (Fig. 29 and 30).

It is noteworthy that no significant differences were found for the fractionation factor f (data not shown).
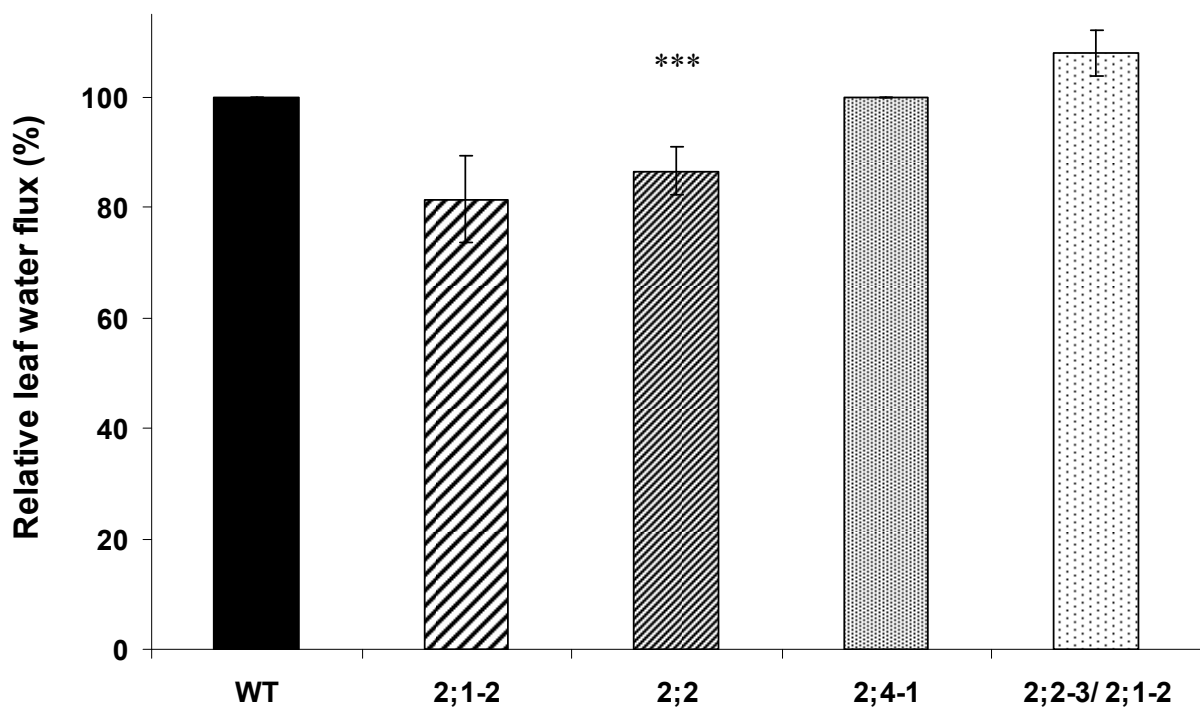
Figure 30. *pip2* single mutants exhibit a reduced leaf water translocation.
Increase of the D content in rosette leaves water of *pip2;1* and *pip2;2* is slower compared to that of the wild-type and a *pip2;2-3/ pip2;1-4* double mutant. Bars represent means ± standard deviations (n = 2 for *pip2;1-2* and *pip2;2-3/ pip2;1-2*, while *pip2;4-1* was done only once). Bar for *pip2;2* represent means of two independent *pip2;2* mutants (*pip2;2-3* and *pip2;2-4*) analyzed twice each.

3.3.5 Root gravitropism of *pip2* mutants

In addition to regular root growth, gravistimulated bending of root growth was also analyzed. Gravity provides a cue for downward orientation of plant roots and, hence, contributes to optimal utilization of available resources. Rotating seedlings grown on vertical agar plates by 90°C exerts a new stimulus that leads to a bending of the roots. All *pip2* single mutants were assessed for altered bending by this specific growth conditions requiring quick and differential growth to achieve bending and thus, the possible involvement of aquaporin-mediated water permeability. Seedlings were grown on vertical 0.5X MS-gelrite plates. Plates containing four-day-old seedlings were then gravistimulated and seedlings were photographed every 30 min for 8 h and then at 24 h (Fig. 31). Root bending was initiated after approximately 1 h for wild-type as well as *pip2* mutant plants. Although the bending angle kinetics were not measured, it was evident that the gravitropism response was not severely affected in any of the *pip2* mutant tested (Fig. 31).
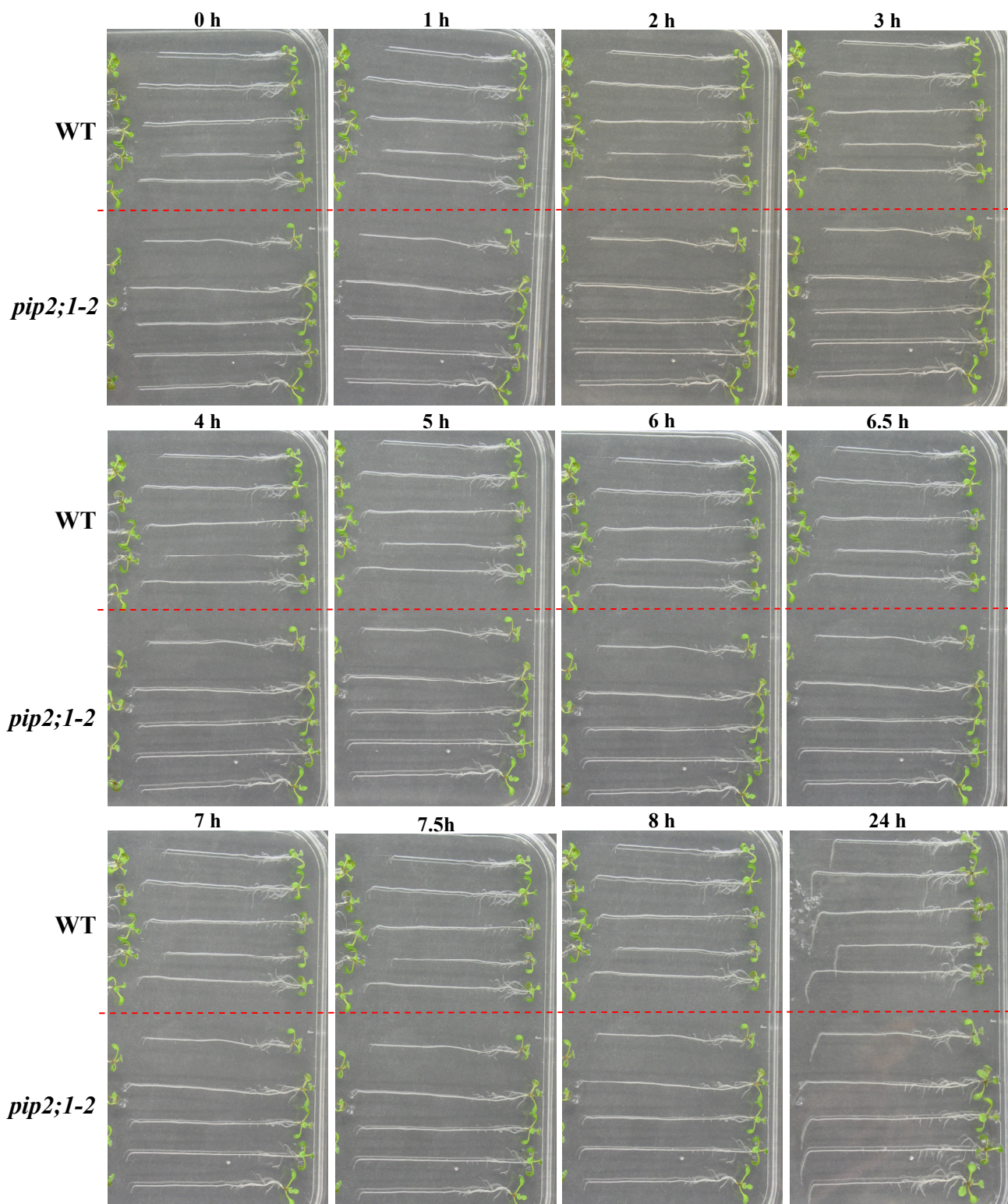
Figure 31. Gravitropism directs downward root growth in *Arabidopsis thaliana*.
Four-day-old wild-type and *pip2* mutant seedlings were grown on vertical gelrite-based medium in the light and positioned horizontally (gravistimulated). A *pip2;1-2* mutants is shown as a representative example. After 1 h, the roots have initiated a downward gravitropic curvature. In all panels the gravity vector is directed downward.

3.4 Transcriptional analyses of *pip2* knockout mutants

A particular mutation of a gene may lead to disturbance of other processes which may involve the deregulation of genes from these pathways. A suitable means to analyze changes at the transcriptional level of many genes is array hybridization technology. Here, two array technologies were used to measure changes in gene expression in the mutants with respect to the wild-type. The aim was to identify processes which might be disturbed in various *pip2* mutants and to compare the potential changes among the different *pip2* mutants.

3.4.1   Custom-made array covering target genes related to membrane transport

It is possible that the loss of individual *PIP2* may alter the natural expression of other endogenous aquaporins. In particular, it is important to know whether other *PIP* genes may be deregulated to compensate for a specific *pip2* loss-of-function, which, in turn, could influence the behavior of *pip2* mutant plants. Furthermore, the uptake and distribution of nutrients is directly linked to the bulk flow of water in the plant. Any transport across cellular membranes generates osmotic differences and thereby a driving force for the permeation of water. Thus, water and solute transport might influence each other. Previous analysis in roots have shown that transcription of aquaporins is highly sensitive to cation stresses and at the same time several members of other transporter families are deregulated (Maathuis et al., 2003). Analyses of *PIP2* expression indicated that all are present in roots (Results 3.1). Hence, the loss-of-function of any *PIP2* in the plant could lead to disturbance of the uptake and translocation or distribution of water and solutes.

Thus, the effect of *pip2* loss-of-function on other *MIP* genes as well as other transport processes was assessed at the transcriptional level in roots using a custom-made array. It harbored gene-specific DNA fragments of more than 500 genes encoding membrane proteins potentially mediating transports function as well as unrelated controls. Probes were designed and checked as previously described (Glombitza et al., 2004; Zhu et al., 2005) to ensure high specificity of the probes and to avoid cross-hybridization or provided by Eric van der Graaff, Sonja Hetfeld, Ulf-Ingo Flügge and Reinhard Kunze (Cologne, Germany; Unpublished data). The achieved probe specificity avoids e.g. also cross-hybridization of the closely related *PIP2;2* and *PIP2;3*, which are not distinguished by the Affymetrix ATH1 array (see below, Results 3.4.2; Affenzeller, 2003). A complete list of genes present on the array can be found in Supplementary Table 1.

Roots were harvested from wild-type and *pip2* mutant plants grown in hydroponic culture for three weeks. Two biologically independent replicates of twelve mutants and Columbia wild-type were analyzed in each case. In order to avoid a bias caused by additional T-DNA insertions in some mutants, replicates of independent mutant of the same *PIP2* gene were combined. Consequently, only genes consistently deregulated in both mutants were then seen as real changes.

The array was first evaluated by asking whether the knockout of a specific *PIP2* aquaporin may disturb the expression of other *MIPs* genes. Importantly, these analyses showed that in the conditions used all 35 aquaporin transcripts were detected in the plant roots. However, no significant changes in the transcript levels of *MIPs* were measured in the *pip2* knockout mutants with respect to the wild-type (Table 8). In particular, these results indicate that none of the single *pip2* mutations was compensated for by deregulation of other *PIP2* genes.

Movement of water is intricately linked to that of solutes or ions, which generate osmotic differences. Consequently, the array was also used to monitor transcriptional changes of membrane transport-related gene families (e.g. vacuolar ATPases, ABC transporters, sugar transporter, potassium channels, cyclic nucleotide gated channels, or amino acid permeases) in various *pip2* mutants. Transcript levels of transport-related genes present on the array were not noticeably varied in the mutant plants. Indeed, the expression of these genes was never consistently deregulated more than two-fold in at least two/ three independent biological replica (see Supplementary Table 1). Thus, at least at the transcriptional level the loss-of-function of individual *PIP2* genes did not interfere with these major transport processes.

Table 8. MIPs expression fold-change in roots of various *pip2* insertional mutants.
Wild-type and *pip2* mutants were grown hydroponically for 3 weeks and root expression of 35 MIPs genes was analyzed using DNA array. Two biologically independent replicates of twelve mutants and Columbia wild-type were analyzed. The signal intensity of each gene in the mutant plants was compared with the signal intensity of the same gene in the wild-type plants to calculate an expression ratio (mutant *versus* wild-type). In order to avoid a bias caused by T-DNA or transposon insertion, fold-changes (FC) were calculated by averaging expression ratios of the two biologically independent replica of two independent mutants each with the exception of *pip2;4-1* and *pip2;8-1*, for which only one mutant was available. Consequently, only genes consistently deregulated in both mutants were then seen as significant changes. Because specific probes spotted on the array correspond to 3'-UTR, the transcript level of several knockout genes seemed to be similar in the mutant and in the wild-type. However, loss-of-transcript of the respective *PIP2* genes in the *pip2* mutants had been clearly demonstrated by RT-PCR (Results 3.2.2; Fig. 14). Blue labeling indicates genes that were probed twice on the array and asterisks indicate probes designed in our lab. SD: standard deviation.

Mutation	pip2;1		pip2;2		pip2;3		pip2;4		pip2;5		pip2;6		pip2;8	
Combined mutants	pip2;1-1 + pip2;1-2		pip2;2-3 + pip2;2-4		pip2;3-1 + pip2;3-2		pip2;4-1		pip2;5-1 + pip2;5-3		pip2;6-1 + pip2;6-2		pip2;8-1	
Gene	FC	SD	FC	SD	FC	SD	FC	SD	FC	SD	FC	SD	FC	SD
PIP1;1	1.3	0.5	1.4	0.7	1.0	0.3	0.9	0.5	0.8	0.6	1.0	0.2	1.0	0.3
PIP1;2	1.3	0.5	1.5	0.6	1.0	0.2	1.2	0.4	0.9	0.7	1.1	0.4	0.8	0.1
PIP1;3	1.4	0.7	1.5	0.5	1.2	0.4	1.6	0.6	1.1	0.3	1.3	0.5	1.3	0.5
PIP1;4	1.2	0.3	1.3	0.4	1.0	0.1	1.4	0.5	1.0	0.1	1.2	0.2	1.2	0.2
PIP1;5	1.4	0.4	1.4	0.3	1.4	0.1	1.7	0.8	1.1	0.1	1.4	0.2	1.3	0.3
PIP2;1	n.d.	-	1.6	1.0	1.6	0.3	1.9	0.7	1.5	0.7	1.1	0.5	1.2	0.2
PIP2;2	1.1	0.3	0.3	0.1	1.2	0.3	1.5	0.1	0.9	0.3	1.0	0.4	1.0	0.1
PIP2;3	1.3	0.5	1.7	0.9	1.1	0.3	1.6	0.3	1.1	0.2	1.2	0.3	1.4	0.4
PIP2;4	1.4	0.5	1.5	0.4	2.0	0.7	1.4	0.1	1.0	0.1	1.3	0.1	1.2	0.3
PIP2;5	1.3	0.4	1.3	0.5	0.7	0.2	0.8	0.3	0.6	0.2	1.0	0.5	1.0	0.8
PIP2;6	1.1	0.2	1.1	0.4	0.8	0.1	0.6	0.2	0.8	0.2	1.1	0.2	0.7	0.1
PIP2;7	1.1	0.3	1.2	0.4	1.7	0.8	1.4	0.3	0.8	0.1	1.1	0.4	0.9	0.3
PIP2;8	1.3	0.4	1.4	0.7	0.7	0.2	0.7	0.2	0.8	0.2	1.1	0.5	1.1	0.5
TIP1;1	1.2	0.7	1.2	0.6	0.9	0.2	1.6	0.8	0.9	0.2	1.0	0.3	1.0	0.1
TIP1;2	0.9	0.3	0.8	0.1	0.7	0.1	0.8	0.2	0.9	0.2	0.7	0.2	0.7	0.3
TIP1;2*	1.4	0.5	1.3	0.5	1.1	0.3	1.4	0.7	1.0	0.3	1.1	0.2	1.0	0.3
TIP1;3	1.2	0.5	1.2	0.4	1.4	0.6	1.2	0.1	0.9	0.4	1.5	1.1	0.7	0.1
TIP2;1	1.1	0.1	0.9	0.1	0.7	0.2	0.9	0.1	0.8	0.3	0.6	0.0	1.0	0.1
TIP2;1*	1.3	0.6	1.3	0.6	1.1	0.5	1.3	0.6	1.0	0.3	1.2	0.5	1.0	0.6
TIP2;2	1.0	0.5	1.1	0.4	1.1	0.7	1.2	0.3	0.9	0.2	1.0	0.4	1.0	0.6
TIP2;3	1.4	0.7	1.5	0.8	1.8	0.7	1.8	0.7	1.4	0.3	1.5	1.0	1.9	1.1
TIP3;1	0.9	0.2	0.9	0.2	0.8	0.2	0.9	0.2	0.9	0.2	0.8	0.2	1.0	0.0
TIP3;1*	1.3	0.2	1.1	0.2	1.1	0.2	1.1	0.2	1.0	0.2	1.5	0.4	0.9	0.2
TIP3;2	1.0	0.3	0.9	0.2	1.3	0.8	1.1	0.1	0.9	0.1	1.2	1.1	0.9	0.2
TIP3;2*	1.4	0.6	1.4	0.6	1.4	0.3	2.3	0.3	1.7	0.4	1.9	0.8	1.4	0.4
TIP4;1	1.1	0.2	1.0	0.1	0.9	0.3	1.0	0.0	1.1	0.2	1.1	0.4	1.1	0.2
TIP4;1*	1.2	0.5	1.3	0.5	0.6	0.1	0.5	0.1	0.8	0.4	1.0	0.4	1.1	0.8
TIP5;1	1.5	0.5	1.5	0.5	0.7	0.2	0.7	0.2	0.8	0.4	1.3	0.6	1.3	1.2
NIP1;1	1.0	0.1	0.9	0.2	1.0	0.1	1.0	0.0	1.1	0.1	1.1	0.3	0.9	0.1
NIP1;1*	1.1	0.3	1.2	0.2	0.8	0.2	0.6	0.1	0.9	0.3	1.0	0.2	1.0	0.1
NIP1;2	1.0	0.7	1.0	0.3	0.9	0.3	1.1	0.2	1.3	0.5	1.4	0.7	1.0	0.1
NIP1;2*	1.1	0.2	1.2	0.2	1.0	0.3	0.9	0.3	1.1	0.3	1.3	0.2	1.0	0.1
NIP2;1	1.1	0.3	1.1	0.4	0.8	0.3	0.9	0.7	0.8	0.4	0.9	0.5	1.2	0.2
NIP3;1	1.2	0.4	1.2	0.3	1.3	0.3	1.3	0.4	1.2	0.3	1.0	0.2	0.9	0.3
NIP4;1	1.3	0.6	1.5	0.6	1.3	0.7	1.4	0.5	1.1	0.1	1.4	0.3	1.4	0.5
NIP4;2	1.0	0.2	1.2	0.3	1.0	0.1	1.0	0.1	1.2	0.2	1.1	0.3	1.3	0.2
NIP5;1	1.0	0.3	1.2	0.2	1.0	0.3	1.2	0.5	1.0	0.1	1.0	0.1	1.2	0.3
NIP6;1	1.1	0.5	1.2	0.4	1.1	0.4	1.0	0.4	0.9	0.1	1.1	0.1	0.9	0.4
NIP7;1*	1.1	0.6	1.2	0.2	1.0	0.3	0.6	0.1	1.0	0.5	1.1	0.4	1.0	0.1
NIP7;1	0.9	0.1	1.0	0.1	1.0	0.2	1.0	0.0	1.0	0.1	1.0	0.3	1.1	0.2
SIP1;1	1.1	0.2	1.1	0.2	1.1	0.2	1.4	0.7	1.1	0.2	1.1	0.4	0.9	0.1
SIP1;2	1.0	0.4	1.2	0.2	1.1	0.3	1.4	0.5	1.1	0.3	1.2	0.6	0.9	0.1
SIP2;1	1.1	0.2	1.2	0.2	0.7	0.1	0.6	0.3	0.9	0.3	1.2	0.2	0.8	0.0
PS-TIP	1.2	0.2	1.2	0.3	0.9	0.1	0.9	0.2	1.0	0.3	1.3	0.2	0.9	0.1
PS-NIP2;1	1.4	0.8	1.5	0.7	1.3	0.5	1.5	0.6	1.3	0.3	1.3	0.3	1.3	0.7
PS-NIP3;1	1.1	0.2	1.2	0.1	1.0	0.3	1.2	0.3	1.2	0.1	1.0	0.1	1.1	0.0

3.4.2 Whole genome transcriptional analysis using Affymetrix ATH1 GeneChip

Our custom-made microarray harbored about 500 gene-specific targets focusing on membrane transporter. Root expression analysis of the single mutants using this custom array did not reveal any transcriptional alteration (Results 3.4.1). Thus, it was reasoned whether a broader analysis could reveal a differentiation of these mutants. In order to extend the *pip2* insertional mutants root transcriptome analysis, the effect of selected mutations on global gene expression was investigated. Genome-wide analyses were carried out using the Affymetrix ATH1 GeneChip, which contains oligonucleotide probesets representing over 25,000 *Arabidopsis* gene sequences. Three single mutants *pip2;1-2*, *pip2;2-3* and *pip2;4-1* were chosen eliminating *PIP2;1*, *PIP2;2* and *PIP2;4*, which represent three of the most abundantly expressed *PIP2* isoforms in roots. Their expression pattern showed strong overlapping for *PIP2;1* and *PIP2;2* in the vasculature and endodermis, while *PIP2;4* was rather restricted to rhizodermis and cortex (see Results 3.1). The selected mutants showed a single T-DNA insertion in the genome and any observed transcriptional changes could therefore be attributed to the corresponding mutated gene. In addition, two double mutants, *pip2;2-3/ pip2;1-2* and *pip2;1-2/ pip2;4-1* were analyzed. *PIP2;1* and *PIP2;2* represent two of the most highly expressed *PIP2* isoforms in roots and leaves. Leaf water loss experiment (Results 3.3.3.1) indicated a lower decline in leaf water for the double mutants suggesting alteration of leaf water relations. Thus, root and leaf transcriptome of *pip2;2-3/ pip2;1-2* was analyzed to investigate whether the combined mutations lead to alteration of root and/ or leaf transcriptome and whether these alterations were different from the single mutants.

Using Affymetrix whole genome array, transcriptional profiles of the selected *pip2* mutants and wild-type plants were analyzed for three independent biological replicas each. The greater than twofold deregulated genes for each mutant were retrieved (Materials and Methods 2.2.9.2) and revealed distinct changes. Different numbers of deregulated genes, 237, 370 and over 1000, were found for *pip2;1-2*, *pip2;2-3* and *pip2;4-1* roots, respectively. For the double mutants, 94 genes were deregulated in roots of *pip2;2-3/ pip2;1-2*, whereas 802 were deregulated genes were found for *pip2;1-2/ pip2;4-1* corroborating the high number of altered gene transcripts in the *pip2;4* single mutant. The leaf transcriptional profile of the *pip2;2-3/ pip2;1-2* double mutant showed 293 deregulated genes. Due to biological as well as technical variations, a higher number of deregulated *per se* would not necessarily mean that one situation is more labile than another one[2]. In order to compare the different mutants and to

---

[2] The data may simply be more homogenous and therefore more genes may pass the filtering conditions.

investigate which genes and processes are most significantly deregulated, the top-hundred deregulated genes retrieved after gene filtering were used (Supplementary Table 2; Method 2.2.9.2).

These top-hundred genes were first assigned to functional categories based on MapMan classification (Thimm et al., 2004) to examine whether *pip2* mutations resulted in significant alterations of any category (Table 9). However, the functional representation of the top-hundred deregulated genes of the mutants was not different compare to that of the expected frequency (Table 9). *Cell wall* and *Miscellaneous* (i.e. various enzyme families) were the only categories exhibiting a statistically significant over-representation in the *pip2;2-3/ pip2;1-2* double mutant (Table 9). In particular, a high enrichment of cell wall-related genes was observed for *pip2;2-3/ pip2;1-2* in roots, but not in leaves (Table 9); 17% of the deregulated genes (i.e. 16 genes) in roots were assigned to this category. Moreover, nearly all these genes (15 genes), mainly related to cell wall synthesis or modification, were down-regulated indicating a significant, coordinated response in this mutant (Table 9 and Supplementary Table 2). Other mutants did not show such a significant enrichment, although *pip2;4-1* and *pip2;1-2/ pip2;4-1* exhibited four down-regulated cell wall-related genes (Table 9 and Supplementary Table 2).

The functional categories *Miscellaneous* showed an enrichment in all mutants, but it was significantly over-represented only in the top-hundred deregulated genes of the *pip2;2-3/ pip2;1-2* leaf transcriptome (Table 9 and Supplementary Table 2). In fact, miscellaneous was found to represent around 10% of the deregulated genes for most mutants and raised to 25% for the *pip2;2-3/ pip2;1-2* leaf transcriptome (Table 9). Within the miscellaneous category, a wide range of enzyme families were found altered such as cytochrome P450, peroxidases, glutathione-S-transferases or enzymes grouped to gluco-, galacto- and mannosidases family or GDSL-motif lipase family (Supplementary Table 2).

It is noteworthy that functional category representation using all deregulated genes was similar to that using top-hundred gene (data not shown).

Table 9. Classification of deregulated genes obtained by Affymetrix ATH1 expression analyses of *pip2* mutants.

Top-hundred deregulated genes for the indicated *pip2* single or double mutants were used and classified to determine functional category representation. Assignments into functional categories were taken from MapMan (Thimm et al., 2004). The functional profile was obtained by calculating the percentage of each category in the top hundred deregulated genes. For each category, percentage relative to all genes in the column, the number of assigned genes (in brackets) is indicated. The asterisks denote significance for over-representation based on p-values (two-sided Fisher's Exact test; see Materials and Methods 2.2.9.2): *** $< 10^{-5}$ and * < 0.002.

Category	Whole genome MapMan, 23322 probesets	Roots					Leaves
		pip2;1-2	*pip2;2-3*	*pip2;4-1*	*pip2;1-2/ pip2;4-1*	*pip2;2-3/ pip2;1-2*	*pip2;2-3/ pip2;1-2*
Photosynthesis	0.8 (177)	-	-	-	1	-	-
CHO metabol.	1.0 (222)	-	-	1	1	-	-
Glycolysis/ TCA	0.6 (132)	-	-	-	1	-	-
C, S, N metabol.	0.7 (153)	2	2	-	-	1 (1)	-
Cell wall	2.0 (477)	1	1	4	4	**17 (16)***	3
Lipid metabol.	1.6 (381)	4	4	2	2	4 (4)	3
A.a. metabol.	1.3 (297)	1	-	-	1	1 (1)	-
Metal handling	0.3 (73)	1	3	-	-	2 (2)	-
2ndary metabol.	1.8 (410)	5	2	3	3	-	5
Hormone	2.4 (553)	4	1	3	7	1 (1)	4
Tetrapyrrole	0.4 (88)	-	-	-	-	-	-
Mit. e⁻-transp/	0.4 (102)	-	-	-	1	1 (1)	-
Stress	3.5 (822)	8	6	7	7	9 (8)	2
Redox regulation	0.8 (177)	1	1	-	1	1 (1)	4
Nucleotide	0.6 (142)	-	-	-	-	-	-
Miscellaneous	**5.3 (1241)**	**10**	**13**	**8**	**13**	**12 (11)**	**24***
RNA metabol.	10.6 (2465)	5	3	7	7	4 (4)	5
DNA	3.8 (884)	10	8	8	6	1 (1)	2
Protein metabol.	12.5 (2924)	10	13	13	11	5 (5)	6
Signaling	4.6 (1079)	4	3	3	1	4 (4)	4
Cell	2.6 (597)	4	1	-	1	1 (1)	-
Development	2.2 (514)	2	3	2	-	-	6
Transport	3.7 (857)	5	2	2	3	5 (5)	4
Not assigned	36.7 (8555)	23	34	37	29	30 (28)	28

The observation that the functional representation of the top-hundred deregulated genes of the mutant was not different compared to that of the expected frequency raised the question whether deregulated genes would also be similar between the different mutants. It was therefore checked whether overlaps could be found between the root transcriptome of the *pip2* mutants, which were displayed by Venn diagrams (Figure 32). The Venn diagram showed a significant overlap between the top-hundred genes of the single mutants. The strongest overlap was observed between *pip2;1-2* and *pip2;2-3* with 41 common deregulated genes,

while *pip2;1-2* and *pip2;4-1* or *pip2;2-3* and *pip2;4-1* exhibited a relatively lower overlap (28 or 15 genes, respectively) (Fig. 32 and Supplementary Table 2). Interestingly, only 11 genes were common to all three single mutants (Fig. 32). These genes were either of unknown function or belonged to the DNA synthesis/chromatin structure/retrotransposon category (Supplementary Table 2). These overlapping genes were exclusively deregulated in the same way (Supplementary Table 2).

When single mutants were compared to double mutants, different results were observed. The double mutant *pip2;1-2/ pip2;4-1* showed significant overlap with the corresponding single mutants, i.e. 27 and 49 genes for *pip2;1-2* and *pip2;4-1*, respectively (Fig. 32). There were even 18 genes in common with the *pip2;2-3* mutant (Fig. 32). In fact, it is noteworthy that nine of the 11 genes common to all single mutants were also deregulated in the *pip2;1-2/ pip2;4-1* double mutant (Fig. 32; Supplementary Table 2). On the other hand, *pip2;2-3/ pip2;1-2* showed a different result, because only few deregulated genes were overlapping with the other mutants. Only 5, 6, 5 and 3 common deregulated genes with *pip2;1-2*, *pip2;2-3*, *pip2;4-1* and *pip2;1-2/ pip2;4-1*, respectively were found. In fact, only one gene, a lipid transfer protein gene LTP5 (At3g51600) was deregulated in the *pip2;2-3/ pip2;1-2* double mutant root transcriptome as well as in all single mutants. However, it was up-regulated in the double mutant, whereas it was down-regulated in the single mutants (Supplementary Table 2).
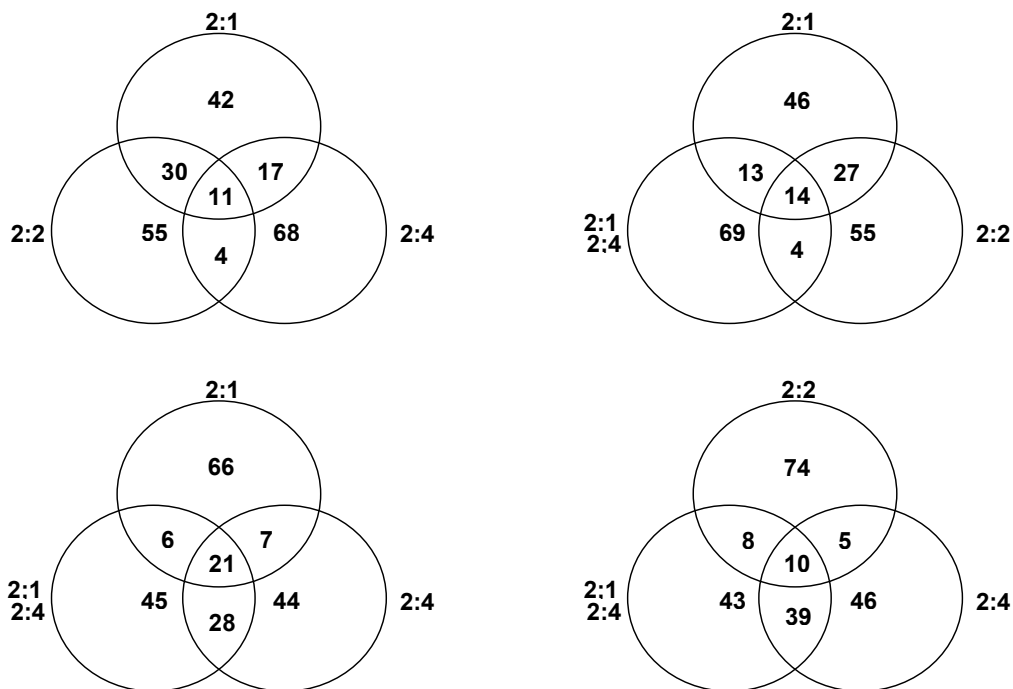
Figure 32. Venn diagram of genes deregulated in various *pip2* knockout mutants.
The numbers are based on the top-hundred deregulated genes for three single mutants and *pip2;1-4/ pip2;4-3* double mutant (see above; Method 2.2.9.2).

Eventually, there were three genes common to both double mutants. These genes were specific to double mutants and were deregulated in the same way. Two of them were genes of unknown function and one belonged to the proton-dependent oligopeptide transport family protein (Supplementary Table 2).

Thus, these analyses showed that deregulated genes were for the most part specific to a particular mutant indicating a different transcriptional response of each *pip2* mutant tested. Nevertheless, genes were mostly of unknown functions or involved in RNA or protein metabolism and thus did not give clear hints for the function of a PIP2 particular isoform (Supplementary Table 2).

The comparison of the leaf and root transcriptome of *pip2;2-3/ pip2;1-2* double mutant led to a similar conclusion. Based on the sole gene categories, several differences were observed. As mentioned above, cell wall and miscellaneous categories were particularly over-represented (p-value $< 10^{-5}$) in the top-hundred deregulated genes of roots and leaves, respectively (Table 9; Supplementary Table 2). In addition, six genes classified into development (e.g. senescence) were found to be deregulated in leaves, whereas no genes were found in roots (Supplementary Table 2). Other categories exhibited the expected frequency (see above; Table 9). When considering the individual genes that had been altered (Supplementary Table 2), only three differentially expressed genes were found in both roots and leaves; an iron superoxide dismutase (FSD1) and an acyl CoA reductase were downregulated, while an unknown protein was strongly upregulated. The latter was also upregulated in the *pip2;1-2* single mutant. In conclusion, these data suggested that *pip2* double mutation triggered a differential response in roots than in leaves.

3.5 *PIP2s* co-expression and stress responsiveness analyses using publicly available microarray data

The use of microarray in *Arabidopsis thaliana* has increased considerably in the past few years. They now represent an enormous volume of data that are made available on public databases, such as the Nottingham *Arabidopsis* Stock Center (NASC) (Craigon et al., 2004), The *Arabidopsis* Information Resource (TAIR) (Rhee et al., 2003) or the Gene Expression Omnibus (GEO) at the National Center for Biotechnology Information (Edgar et al., 2002). In addition, many web-based tools have been developed to assist the interpretation of these large microarray gene expression databases. One aim of microarray studies is to understand how genes are regulated and to integrate those regulations in biological processes. Here, the

primary goal was to extract information from existing microarray data using several web-based tools. The *Arabidopsis* Co-expression Tool (ACT) and the Bio-Array Resource (BAR) were used in order to find genes co-regulated with *PIP2* genes in a general manner or in specific contexts and, hence, to infer biological processes in which *PIP2* genes might be involved and that could lead to hypothesis on their biological functions. Furthermore, the Genevestigator Meta-Analyzer tool was used to extract the transcription profile of *PIP2* genes in a broad range of stress conditions to investigate whether *PIP2* genes can be distinguished based on their differential stress responsiveness.

3.5.1 Co-expression analyses revealed transcriptional interrelation of *PIP2* genes with *MIP* members and other processes.

Microarray data contain information on the coordinated expression level of nearly all genes in the analyzed condition. Gene co-expression analyses can identify genes involved in correlated processes based on their co-regulation and paralleled expression patterns across many different situations and experimental conditions. Web-based tools such as the Bio-Array Resource (Toufighi et al., 2005), CSB.DB (Steinhauser et al., 2004) and the *Arabidopsis* Co-expression Tool (Jen et al., 2006; Manfield et al., 2006) are allowing gene co-expression analyses based on *Arabidopsis* microarray data. In previous studies, co-expression tools have been used to search for genes involved in determined biological processes (Lisso et al., 2005; Persson et al., 2005; Rautengarten et al., 2005). Here, individual *PIP2* genes were used as a starting point to find information about correlated physiological pathways. Two different approaches were performed. First, the ACT was used to do co-expression analyses on mixed experiments encompassing a wide range of conditions (e.g. different tissues, growth conditions or ecotypes). Second, specific analyses using selected datasets, e.g. roots, leaves, abiotic or biotic stresses, were done using the Bio-Array resource.

Co-expression analyses on the *Arabidopsis* Co-expression Tool (ACT) are based on *Arabidopsis thaliana* data from 322 ATH1 microarray studies, which were all processed at NASC. Hence, this data set is more homogeneous in technical terms than other compilations and as a consequence the array results are more suited for comparison. On the other hand, these data also cover a wide range of biological processes and conditions. Positively and negatively co-regulated genes across a wide range of microarray experiments might reveal robust generalities toward a better understanding of *PIP2* functions.

To visualize the extent and significance of correlation between two genes with different Pearson correlation factors (r-value), two examples were chosen. The data for two genes

displaying all 322 experiments encompassed within the ACT were plotted. A Pearson correlation coefficient of 0.6 / -0.6 was chosen as a threshold for both positively and negatively correlated genes. Indeed, an r-value above 0.6 still gives a reasonable co-expression as shown in the scatter plots, whereas a value just below 0.6 results in a clearly more undirected, centered plot (Fig. 33).
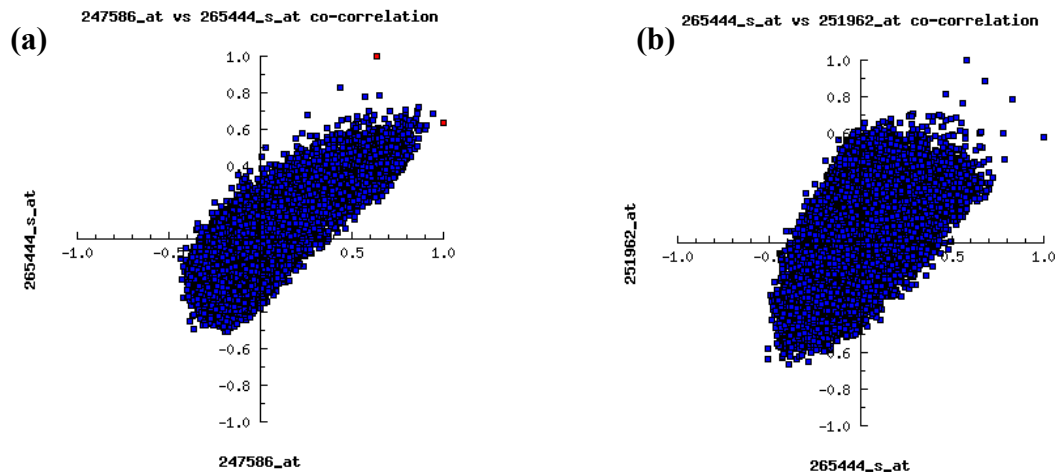
Figure 33. Co-correlation scatter plot of pairs of genes with different r-values.
The scatter plots show the expression values for 322 experiments included in the ACT for two genes with a Pearson correlation coefficient of 0.632 (a) or 0.581 (b). As an example *PIP2;2/PIP2;3* against *PIP2;4* (a) and *PIP2;1* against *PIP2;2/PIP2;3* (b) were chosen.

This experimental cut-off threshold (r-value ≥ 0.6) was also used for co-expression analyses based on other co-expression tools (e.g. BAR), since all web-based tools offer the Pearson correlation coefficient for statistical analyses, which was consistently selected here.

At last, it has to be noted that all the web-based tools based on Affymetrix whole genome arrays (ATH1) exhibit some non-specific probesets that cross-hybridize with other sequences. As indicated previously, *PIP2;2* and *PIP2;3* as well as *PIP2;7* and *PIP2;8* hybridize to the same probesets on the ATH1 array, respectively and therefore cannot be differentiated. Since *PIP2;2* and *PIP2;3* have been implicated with different functions (see above; also Javot et al., 2003), their combined expression could be problematic; however, most probably their expression values are dominated by the more highly expressed *PIP2;2*.

Each *PIP2* gene was submitted to a co-expression analysis using the ACT tool (Jen et al., 2006; Manfield et al., 2006), where Affymetrix ATH1 expression analyses encompassing a wide range of more than 300 conditions, but collectively hybridized at NASC can be approached. Both the positively (r-value ≥ 0.6) and negatively (r-value ≤ -0.6) co-regulated genes for each *PIP2* were then submitted to MapMan, another web-based tool that allows the

classification of genes into functional categories (Thimm et al., 2004) (Method 2.2.10; Table 11). Additional co-expression analyses were also performed using thematic datasets at Bio-Array Resource (BAR; Toufighi et al., 2005) primarily from AtGenExpress experiments (www.arabidopsis.org/info/expression/ATGenExpress.jsp; Kilian et al., 2007) to check the robustness of the enriched functional categories or to identify biological processes, which might involve *PIP2* genes in a specific context. In most cases, the conclusions based on mixed experiments from NASC (Table 10 and Supplementary Table 3) were validated when using distinct datasets generated from AtGenExpress such as hormone treatments, abiotic or biotic stresses (Supplementary Tables 4 to 8; see below).

Interestingly, the analysis of the broad ACT collection did not reveal genes showing significantly anti-correlated patterns with a *PIP2* gene; similarly, only a few negatively co-expressed genes were retrieved at BAR using several AtGenExpress datasets (see below; Supplementary Tables 4 to 8). However, different numbers of positively co-regulated genes were found. About 50 to 100 genes were co-expressed with *PIP2;1*, *PIP2;2/2;3*, *PIP2;5* and *PIP2;7/2;8*, whereas considerably more were found for *PIP2;4* and *PIP2;6* (Supplementary Table 3). With the exception of *PIP2;5* their classification according to MapMan revealed significantly enriched functional categories (p < 0.002), which clearly differed among the *PIP2* members (Table 10).

It should be noted that some gene categories were never or little represented in any of *PIP2* co-expression lists, e.g. CHO metabolism, C, S, N metabolism, amino acid metabolism, metal handling, mitochondrial electron transport and ATP synthesis, and nucleotide metabolism. This observation may indicate processes, which are not related to or not influenced by *PIP2* members.

Surprisingly, *PIP2;1* and *PIP2;6* showed a strong correlation with photosynthesis-related genes (10% and 17% of co-expressed genes, respectively). In addition, other gene categories related to photosynthesis such as tetrapyrrole synthesis or redox regulation were also significantly over-represented among *PIP2;6* co-expressed genes (Table 10).

Table 10. Functional categories assignment of *PIP2* correlated genes.
PIP2 correlated genes exhibiting a significant Pearson correlation coefficient were retrieved using the *Arabidopsis* Co-expression Tool and assigned to functional categories according to MapMan (Thimm et al., 2004) (see Materials and Methods). For each category, percentage relative to all genes in the column, the number of assigned genes (in brackets) is indicated. The asterisks denote different levels of significance based on p-values (two-sided Fisher's Exact test; Experimental Procedures): *** < 10^{-10}, ** < 10^{-5}, and * < 0.002.

Category	Expected Frequency Whole genome (MapMan, 23322)	Observed Frequency					
		PIP2;1 (out of 58)	PIP2;2/ PIP2;3 (out of 58)	PIP2;4 (out of 469)	PIP2;5 (out of 48)	PIP2;6 (out of 383)	PIP2;7/ PIP2;8 (out of 104)
Photosynthesis	0.8 (177)	10.3 (6)**	-	-	-	17.2 (66)***	1.9 (2)
CHO metabol.	1.0 (222)	-	1.7 (1)	0.4 (2)	-	0.8 (3)	1.0 (1)
Glycolysis/TCA	0.6 (132)	1.7 (1)	-	0.2 (1)	-	1.0 (4)	-
C, S, N metabol.	0.7 (153)	1.7 (1)	-	1.7 (8)	-	1.6 (6)	1.0 (1)
Cell wall	2.0 (477)	3.4 (2)	5.2 (3)	6.8 (32)**	10.4 (5)	1.0 (4)	7.7 (8)*
Lipid metabol.	1.6 (381)	5.2 (3)	-	1.1 (5)	2.1 (1)	1.0 (4)	5.8 (6)
A. a metabol.	1.3 (297)	-	-	0.6 (3)	-	0.8 (3)	-
Metal handling	0.3 (73)	-	-	1.1 (5)	-	-	-
Secondary metabol.	1.8 (410)	-	1.7 (1)	4.5 (21)*	-	2.3 (9)	1.9 (2)
Hormone metabol.	2.4 (555)	-	8.6 (5)	3.8 (18)	10.4 (5)	0.8 (3)	3.8 (4)
Tetrapyrrole	0.4 (88)	3.4 (2)	1.7 (1)	-	-	2.9 (11)**	-
Mit. e$^-$-transp/ ATP	0.4 (102)	-	-	-	-	0.3 (1)	-
Stress	3.5 (822)	-	5.2 (3)	7 (33)*	4.2 (2)	0.5 (2)	1.9 (2)
Redox regulation	0.8 (177)	5.2 (3)	-	0.2 (1)	-	3.9 (15)**	-
Nucleotide metabol.	0.6 (142)	-	1.7 (1)	0.2 (1)	2.1 (1)	0.3 (1)	-
Miscellaneous	5.3 (1241)	13.8 (8)	12.1 (7)	14.7 (69)***	4.2 (2)	4.4 (17)	13.5 (14)*
RNA metabol.	10.6 (2465)	3.4 (2)	3.4 (2)	6.4 (30)	18.8 (9)	5.7 (22)	6.7 (7)
DNA	3.8 (884)	-	1.7 (1)	1.3 (6)	-	0.3 (1)	1.0 (1)
Protein metabol.	12.5 (2924)	15.5 (9)	6.9 (4)	6.0 (28)	10.4 (5)	15.7 (60)	8.7 (9)
Signaling	4.6 (1079)	1.7 (1)	5.2 (3)	5.1 (24)	10.4 (5)	1.0 (4)	10.6 (11)
Cell	2.6 (597)	1.7 (1)	3.4 (2)	1.7 (8)	-	2.1 (8)	-
Development	2.2 (514)	1.7 (1)	1.7 (1)	2.8 (13)	4.2 (2)	0.8 (3)	1.9 (2)
Transport	3.7 (857)	15.5 (9)*	13.8 (8)*	4.1 (19)	4.2 (2)	3.7 (14)	5.8 (6)
Not assigned	36.7 (8553)	15.5 (9)	25.9 (15)	30.3 (142)	18.8 (9)	31.9 (122)	26.9 (28)

PIP2;6 is mostly detected in leaves and therefore co-regulation with other genes primarily expressed in leaves could be accidental. Therefore, to re-assess the correlation to photosynthesis, specific datasets based on leaf material only provided at BAR were used (www.arabidopsis.org/info/expression/ATGenExpress.jsp). However, when selecting expression analyses comprising biotic stresses applied to leaves both *PIP2;1* and *PIP2;6* co-

regulated genes were again significantly enriched with photosynthesis-related genes (p-values $5 \cdot 10^{-40}$ to $6 \cdot 10^{-58}$; Supplementary Tables 4 and 7). The *PIP2;6* co-regulated genes derived from the biotic stress response set revealed another strong association. Among the top twenty correlated genes with Pearson coefficients of 0.737 to 0.812 eight genes were related to cell wall biosynthesis, such as cellulose synthase genes CESA1, 2, 3, 5 and 6 as well as COBRA involved in anisotropic elongation (Table 11). Furthermore, stress category was significantly enriched with *PIP2;6* as well in the shoot abiotic stress dataset; the same was only observed for *PIP2;2/2;3* among all *PIP2* genes (Supplementary Tables 5 and 7).

Table 11. Twenty most highly co-expressed genes with *PIP2;6* among a dataset (AtGenExpress biotic stress dataset) covering pathogen responses in shoot.
Genes related to cell wall metabolism are clearly enriched.

Gene ID	r-value	Annotation
At2g39010	1.000	**PIP2;6, aquaporin**
At1g77060	0.812	mutase family protein
At5g05170	0.796	CESA3, cellulose synthase, catalytic subunit
At3g26520	0.794	**TIP1;2__tonoplast intrinsic protein**
At2g42320	0.791	expressed protein
At1g75680	0.791	glycosyl hydrolase family 9 protein
At5g60920	0.784	COBRA cell expansion protein
At2g42880	0.772	mitogen-activated protein kinase AtMPK20
At5g06710	0.766	homeobox-leucine zipper protein 14 (HAT14)
At1g05850	0.765	chitinase-like protein 1 (CTL1)
At5g62350	0.762	invertase/pectin methylesterase inhibitor family
At3g53420	0.760	**PIP2;1, aquaporin**
At4g27430	0.756	COP1-interacting protein 7 (CIP7)
At2g46910	0.755	plastid-lipid associated protein PAP / fibrillin family
At1g32220	0.754	expressed protein
At4g32410	0.752	CESA1/ RSW1__cellulose synthase
At1g75690	0.752	chaperone protein dnaJ-related
At1g77490	0.748	L-ascorbate peroxidase, thylakoid-bound (tAPX)
At3g46780	0.746	PTAC16__expressed protein
At4g09010	0.738	L-ascorbate peroxidase, APX4
At3g15480	0.737	expressed protein

Among NASC experiments a high number of genes encoding enzymes involved in oxidative stress response and secondary metabolism including peroxidases (13), glutathione-S-transferases (2), cytochrome P450 monooxygenases (16) and UDP-glycosyl transferases (8) were correlated with *PIP2;4*, which were listed by MapMan in part among the miscellaneous category (Table 10; Supplementary Table 3). A significant over-representation of stress category was also found among NASC experiments and among the thematic datasets for root abiotic stress responses (Table 10; Supplementary Tables 3 and 6).

Eventually, among NASC experiments *PIP2;7/2;8* exhibited significant over-representation of the cell wall and miscellaneous categories, where additional genes potentially related to cell wall metabolism such β-glucanases were assigned (Table 10; Supplementary Table 3). However, this correlation was not substantiated by analyses of abiotic, biotic, or hormone datasets from AtGenExpress. Instead, various over-representations of categories were found among different AtGenExpress datasets (Supplementary Table 8).

In addition to the differential co-regulation of *PIP2* genes with functional classes, the individual co-regulated genes were also different in most cases. However, there were a few notable exceptions (Fig. 34). The most striking instance is the overlap between *PIP2;2/2;3* and *PIP2;4*; two third out of 58 *PIP2;2/2;3* co-regulated genes were also co-regulated with *PIP2;4* (Fig. 34). Among many genes without a documented function a high affinity phosphate transporter *PHT1*, the peroxidase *RCI3* involved in cold and salt tolerance as well as - exclusively among *PIP2*s - two δ-*TIP* members *TIP2;2* and *TIP2;3* were co-regulated with both *PIP2* genes (Supplementary Table 3).
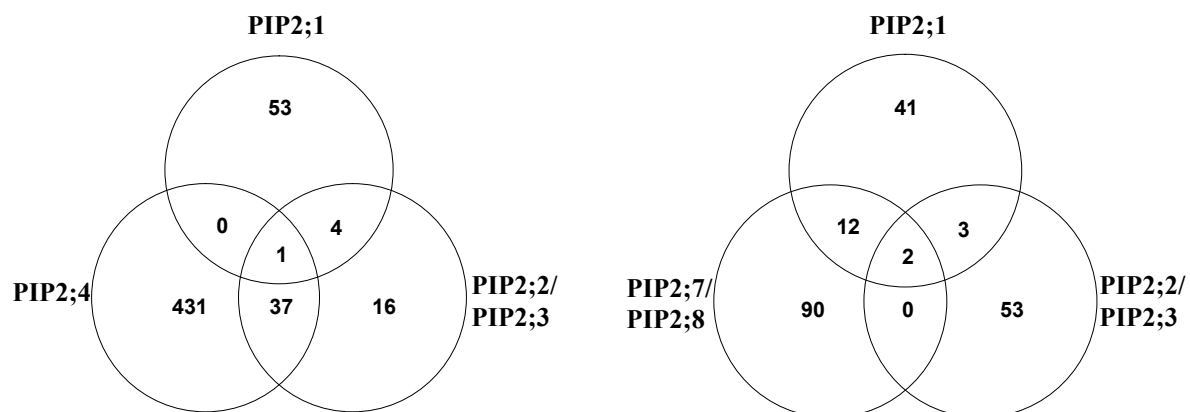
Figure 34. Venn diagram showing overlap for the positively correlated genes with the individual *PIP2*.
In the left diagram, an actin 8 gene was found to be common to *PIP2;1*, *PIP2;2/PIP2;3* and *PIP2;4*, whereas a *PIP1;2* gene was found to be common to *PIP2;1*, *PIP2;2/PIP2;3* and *PIP2;7/PIP2;8* (right diagram).

Furthermore, without taking into account the co-regulation among *PIP* or *TIP* genes (see below), only *PIP2;1* exhibited an considerable overlap with *PIP2;6* and *PIP2;7/2;8* (Fig. 34; Supplementary Table 3). Eventually, only two cases were found within the NASC data that revealed common co-regulated genes among more than two *PIP2* genes. Actin 8 (At1g49240) was associated with *PIP2;1*, *PIP2;2/2;3* as well as *PIP2;4*, whereas *PIP1;2* and a highly and ubiquitously expressed acid phosphatase (At5g44020) of unknown function were co-expressed with *PIP2;1, PIP2;2/2;3,* and *PIP2;7/2;8* (Fig. 34; Supplementary Table 3).

Surprisingly, a significant enrichment of transport-related genes was only detected among genes co-expressed with *PIP2;1* and *PIP2;2/2;3*, yet these were dominated by other *PIP* and *TIP* genes (Table 10; Supplementary Table 3). Four of the five *PIP1* genes (*PIP1;1*, *PIP1;2*, *PIP1;3*, *PIP1;5*) and three *TIP* genes (*TIP1;1*, *TIP1;2* and *TIP2;1*) were co-expressed with *PIP2;1*, while two *PIP1* genes (*PIP1;1*, *PIP1;2*), *PIP2;4*, and three *TIP* genes (*TIP1;1*, *TIP2;2*, *TIP2;3*) were correlated with *PIP2;2/2;3* (Table 12). Among other *PIP2* genes only *PIP2;4* and *PIP2;7/2;8* did show a correlation with other *PIP* and *TIP* as well, whereas *PIP2;5* and *PIP2;6* clearly did not, indicating a specific role among *PIP* members (Tables 12; Supplementary Table 3). In fact, *PIP2* genes showed a much better correlations with *PIP1* genes than with other *PIP2* members indicated by considerably high *PIP2-PIP1* correlation coefficients for the couples *PIP2;1 vs. PIP1;2*, *PIP2;2/2;3 vs. PIP1;1*, or *PIP2;7/2;8 vs. PIP1;3* (r > 0.82; Table 12). This observation may provide an independent hint towards a functional cooperation between PIP1 and PIP2 members.

Table 12. Correlation of *PIP2* members with *PIP* and *TIP* genes according to ACT co-expression analyses. Co-expression analyses were performed on the basis of 322 ATH1 microarray data at ACT (Manfield et al., 2006). For each *PIP2* gene, the Pearson correlation coefficients with other PIP1 or PIP2 as well as TIP members are indicated. All other *MIP* genes did not show correlations > 0.6. [1]The Affymetrix probeset for *TIP2;1* also hybridizes to At3g16250, which encodes a ferredoxin-related protein.

Genes	PIP2;1	PIP2;2/2;3	PIP2;4	PIP2;5	PIP2;6	PIP2;7/2;8
PIP2;1		0.581	0.225	-0.09	0.488	**0.636**
PIP2;2/2;3			**0.632**	-0.031	0.037	0.335
PIP2;4				-0.052	-0.183	0.202
PIP2;5					-0.056	0.059
PIP2;6						0.107
PIP1;1	**0.786**	**0.828**	0.438	-0.072	0.314	0.409
PIP1;2	**0.885**	**0.676**	0.258	-0.019	0.302	**0.675**
PIP1;3	**0.679**	0.496	0.376	-0.004	0.168	**0.863**
PIP1;4	0.354	0.284	-0.113	0.266	0.322	0.154
PIP1;5	**0.665**	0.395	0.358	-0.100	0.355	0.535
TIP1;1	**0.604**	**0.782**	0.573	-0.061	0.170	0.476
TIP1;2	**0.817**	0.466	0.247	-0.106	0.295	**0.783**
TIP2;1[1]	0.695	0.394	0.184	-0.047	0.390	0.780
TIP2;2	0.455	**0.782**	**0.652**	-0.168	0.140	0.048
TIP2;3	0.294	**0.701**	**0.859**	-0.087	-0.091	0.246
TIP4;1	0.298	0.506	**0.713**	-0.080	-0.275	0.339

3.5.2 Principal component analysis of *PIP2* transcriptional responses to various stimuli revealed differential reactions.

Public microarray databases can also be used to determine how genes of interest are expressed during specific growth stages or are responding to different conditions. Genevestigator (Zimmermann et al., 2004; Zimmermann et al., 2005) is a very valuable tool for analyzing such public microarray data. Previously, the Genevestigator Meta-Analyzer tool has been used to study *PIP* expression profile in various anatomical structures (Results 3.1.2). Here, the Meta-Analyzer tool (Version 3; Zimmermann et al., 2005) was used to examine the transcriptional changes of *PIP* genes in response to diverse abiotic and biotic stresses as well as to chemical and hormone treatments in order to identify differential reactions and functional involvements of *PIP* genes.

Expression ratios of *PIP2* genes in response to various treatments with respect to control experiments were extracted using the Genevestigator Meta-Analyzer tool (Method 2.2.11). In order to focus on typical conditions in which water channel regulation is supposed to occur, several atypical treatments were neglected (i.e. genotoxic stress (abiotic stress), cycloheximide, MG13 and PNO8 treatments (chemical treatments). Finally, expression ratios of *PIP2* genes in 54 conditions were retained (Methods 2.2.11; Supplementary Table 9 for *PIP2* genes expression ratio and list of all treatments). The selected conditions included 54 different data sets that had been obtained by the AtGenExpress consortium using *A. thaliana* Col-0 and a common Affymetrix ATH1 array platform (Kilian et al., 2007; www.arabidopsis.org/info/expression/ATGenExpress.jsp; Supplementary Table 9), which limits variability due to biological and technical differences. To identify similar and/or differential patterns among the transcriptional responses of *PIP* to the various conditions, the data were subjected to a principal component analysis (PCA; see Methods 2.2.11; Fig. 35).

The PCA defined distinct transcriptional responses of *PIP2* genes and only *PIP2;1* and *PIP2;7/2;8* exhibited an overlapping profile (Fig. 35a). The group formed by *PIP2;1* and *PIP2;7/2;8* showed a completely opposite response in comparison to *PIP2;4*, which was almost exclusively described by component 1. Component 1 was dominated by *Pseudomonas* infection and $AgNO_3$ treatment as the most discriminating variables. These two groups were independent from the responses of *PIP2;2/2;3*, *PIP2;5* and *PIP2;6*, which were also dependent on component 2. Yet, *PIP2;2/2;3* showed a roughly opposite responsiveness from *PIP2;5* and *PIP2;6* (Fig. 35a). Several different conditions that potentially affect plant water relation such as heat, cold stress, osmotic or salt stress contributed most to this distinction.
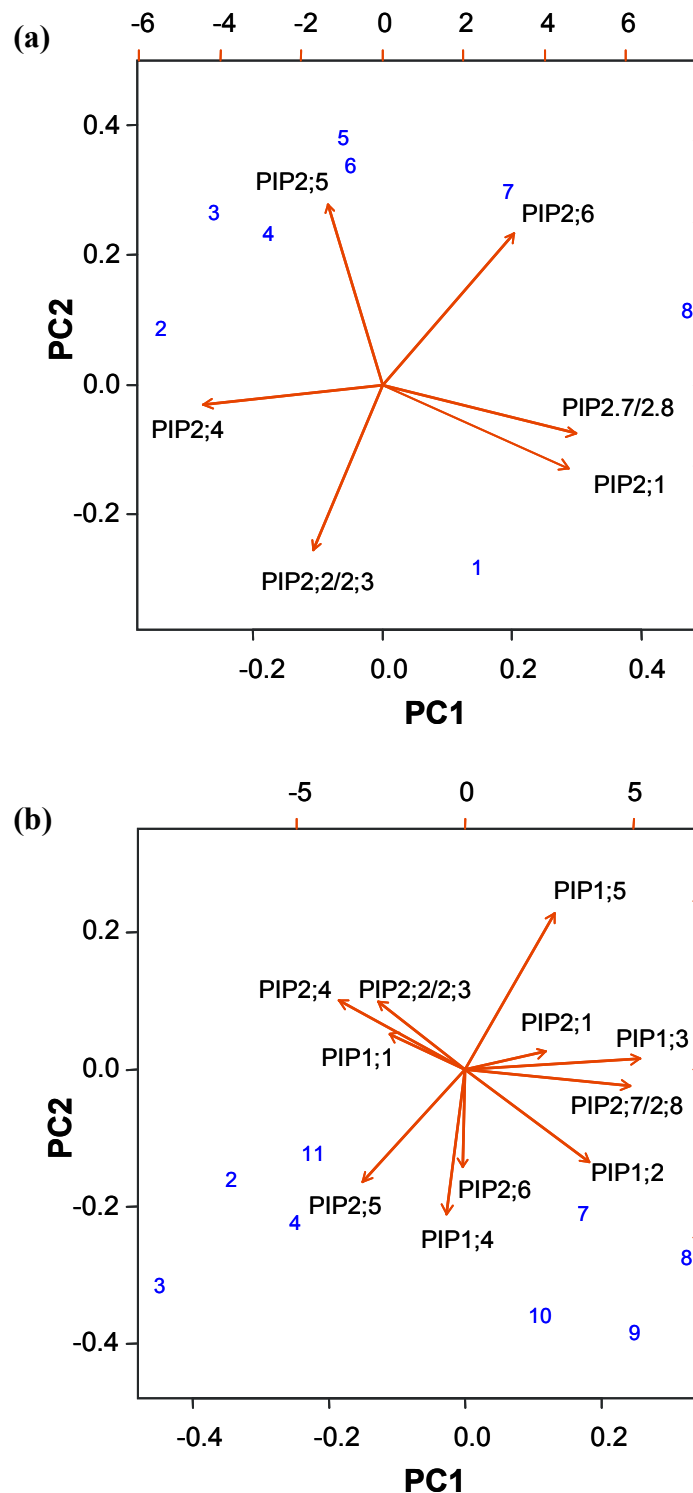
Figure 35. Principal component analyses of *PIP* transcriptional responses to diverse stimuli.
PCA were based on a large Affymetrix microarray dataset produced by the AtGenExpress consortium and extracted at Genevestigator using the Meta-Analyzer tool (Zimmermann et al., 2005). *PIP* expression ratios of 54 stress conditions and treatments were retrieved (Kilian et al., 2007; Method 2.2.11; Supplementary Table 9). PCA were performed using $\log_2$-transformed expression ratios and row-centered data (Method 2.2.11) for (a) *PIP2* genes and (b) *PIP2 + PIP1* genes. The total variance covered by the two components is 70% (a) and 62% (b). A radius of r > 3 was arbitrarily chosen from the polar coordinates to extract treatments most significantly contributing to the differentiation. The conditions that mostly influenced the PCA were: 1 heat stress in roots, 2 Pseudomonas syringae infection, 3 osmotic stress in green tissue (late/ 24 h), 4 salt stress in green tissue (Late/ 24 h), 5 cold stress in green tissue (late / 24 h), 6 cold stress in roots (late, 24 h), 7 TIBA, 8 AgNO3, 9 osmotic stress in roots (late/ 24 h), 10 salt stress in salt in roots (late/ 24 h), 11 *Botrytis cinerea* infection.

In terms of *PIP2* transcriptional reactions to individual cues, it is noteworthy that *PIP2;2/2;3*, *PIP2;4* and *PIP2;5* were more frequently deregulated than other *PIP2* genes (Supplementary Table 9). In particular, *PIP2;4* was often downregulated in all categories. *PIP2;5* was upregulated by several abiotic stresses and *Pseudomonas* infection, but rarely responsive to other conditions. *PIP2;2/2;3* also responded to several abiotic stresses, but showed both down- and upregulation. *PIP2;5* and *PIP2;6* were strongly upregulated by cold stress in both roots and leaves, while other genes did not respond or were affected in an opposite way (*PIP2;2/2;3*) (Supplementary Table 9).

Differential responses were also observed for *PIP2* genes upon salt stress in roots or green tissues. *PIP2;5* exhibited significant upregulation upon salt stress in green tissues. In contrast, all *PIP2* genes at least tended to be downregulated upon salt stress in roots. The gene-specific responses were also observed for drought, osmotic and heat treatments. Only *PIP2;2/2;3*, exhibited a significant upregulation in green tissue upon drought, whereas *PIP2;5* was induced in roots. Similarly, these two genes, in particular *PIP2;2/2;3*, were upregulated in green tissue upon heat stress. Finally, *PIP2;2/2;3*, *PIP2;4*, and *PIP2;7/2;8* were suppressed by osmotic stress, yet at different time points or in distinct organs (Supplementary Table 9).

PIP2 genes were only rarely deregulated upon exogenous application of plant hormones or chemicals interfering with hormone action. However, there was a noticeable suppression of *PIP2;4* by IAA and auxin (transport) inhibitors; only *PIP2;2/2;3* showed a similar tendency. Furthermore, *PIP2;1*, *PIP2;2/2;3*, and again *PIP2;4* were downregulated by salicylic acid and the ethylene inhibitor AgNO$_3$ (Supplementary Table 9).

Eventually, *PIP2* genes could also be differentiated by their responsiveness to biotic stresses. Infection by the avirulent pathogen *Pseudomonas syringae* pv. *tomato* DC3000 specifically triggered a strong upregulation of *PIP2;5*. In contrast, inoculations with fungi *Phythophtora infestans* or *Botrytis cinerea* downregulated *PIP2;5* and *PIP2;6* or *PIP2;4* and *PIP2;7/2;8*, respectively (Supplementary Table 9).

Recent publications demonstrated that PIP1 and PIP2 proteins might interact and synergistically enhanced water permeability when heterologously expressed (Fetter et al., 2004; Zelazny et al., 2007). In addition, certain *Arabidopsis PIP1* and *PIP2* genes are co-transcribed in many instances (see above). Therefore, it was interesting to extend the PCA analysis and include both *PIP1* and *PIP2* genes, which revealed several associations among *PIP1* and *PIP2* (Fig. 35b). *PIP2* gene responses were described by the first two components of this combined PCA similarly to the PCA using only *PIP2* genes, although some of the

most discriminating variables had changed and included responses to salt and osmotic stress as well as *Botrytis cinerea* infection (Fig. 35a and b). *PIP2;2/2;3* and *PIP2;4* were now grouped together and associated with *PIP1;1*. This association was dependent *e.g.* on a similar downregulation after *Pseudomonas syringae* infection or upon salt or osmotic stress in roots. A rather opposite response was exhibited by a group represented by *PIP2;1*, *PIP2;7/2;8,* and *PIP1;3* as well as by *PIP1;2* (Fig. 35b). They were in part characterized by their common downregulation upon osmotic stress or *B. cinerea* infection (Fig. 35b; Supplementary Table 9). A third group associated *PIP2;6* and *PIP1;4*. In contrast, *PIP2;5* and *PIP1;5* defined two distinct responses showing opposite reactions almost completely (*PIP1;5*) or partially (*PIP2;5*) independent from all other groups (Fig. 35b; Supplementary Table 9). This may suggest specific functions of these two genes. Besides *PIP1-PIP2* associations, it is important to emphasize that *PIP1* transcriptional reactions were also distinct from each other (Fig. 35b). Thus, these results do support the notion that *PIP2* as well as *PIP1* members may have evolved differential responsiveness and, consequently, gene-specific, non-redundant functions related to distinct stresses.

3.6 Interaction between PIP2 and PIP1 isoforms

Recent publications demonstrated interaction between maize *Zm*PIP2 and *Zm*PIP1 members at the protein level (Fetter et al., 2004; Zelazny et al., 2007). In oocytes, PIP1 members do not increase or do increase water permeability in a considerably weaker way in contrast to PIP2 members. However, co-expression of both PIP1 and PIP2 in *Xenopus* oocytes resulted in an increase in water permeability that was dependent on the amount of injected PIP1 (Fetter et al., 2004; Temmei et al., 2005). Using FRET/Fluorescence lifetime imaging microscopy in living maize cells Zelazny et al. (2007) demonstrated a PIP2-PIP1 heteromerization which regulated PIP1 subcellular localization. Interaction between PIPs is not restricted to maize since *Mimosa pudica Mp*PIP2;1 and *Mp*PIP1;1 were also shown to increase water permeability of the oocyte membrane and to interact in COS7 cells when co-expressed (Temmei et al., 2005).

It was then suggested that PIP2-PIP1 heteromerization could be a mean for PIPs to regulate their activity (Chaumont et al., 2005; Zelazny et al., 2007).

Fetter et al. (2004) demonstrated the importance of loop E in the interaction process although the influence should be indirect based on the MIP 3D-structure. By comparing the structural model of *Zm*PIP1;1 and *Zm*PIP1;2 and performing molecular dynamics simulation, it was suggested that the loop E residues affect the structure of the pore and possibly its channel activity (Chaumont et al., 2005). Thus, the amino acid sequence of the important region of loop E was compared in order to examine whether *Arabidopsis* PIPs harbor amino acids that had been suggested to be important for this type of isoform interactions (Fig. 36). Fetter et al. (2004) demonstrated the importance of four amino acids (amino acids in position 247, 251, 252 and 256 in Figure 36). However, in their experiment, Fetter et al. replaced the four amino acids altogether, therefore, it cannot be excluded that some of these amino acids do not account for the multimerization. Hence, with regard to these amino acids, heteromerization of PIP1 and PIP2 could also occur in *Arabidopsis* (Fig. 36). The position 247 is completely conserved among the PIP1 and PIP2 interacting members (Fig. 36). *Zm*PIP1;2 and *Mp*PIP1;1, which have been shown to interact with PIP2 have an isoleucine (I) in position 247. In contrast, it is a valine (V) for PIP2 or *Zm*PIP1;1. In this position, all *At*PIP1 have an I, whereas it is a V for all *At*PIP2 members except *At*PIP2;5.

Arginine251 of *Zm*PIP1;2 is replaced by a lysine (K) in all the *At*PIP1, which is usually considered a conservative exchange of basic side chains, although exact sizes and potential interactions may be different. Moreover, *Mp*PIP1;1 that was shown to interact with *Mp*PIP2;1 also has a K, indicating that the replacement of the R by a K should not abolish the interaction

per se. Similarly, at this position, members that do interact have different amino acid suggesting that the interaction is independent of the amino acid residue at position 251 (Fig. 36).

```
            220       230       240       250
            .|....|....|....|....|....|....|....|....
ZmPIP1-1    GFAVFLVHLATMGITGTGINPARSLGAAVIYNQHHAWADHW
ZmPIP1-2    GFAVFLVHLATIPITGTGINPARSLGAAIIYNRDHAWNDHW
ZmPIP1-5    GFAVFLVHLATIPITGTGINPARSLGAAIVYNRSHAWNDHW
ZmPIP2-1    GFAVFMVHLATIPVTGTGINPARSLGAAVIYNKDKPWDDHW
ZmPIP2-4    GFAVFMVHLATIPITGTGINPARSLGAAVIYNKDKAWDDQW
ZmPIP2-5    GFAVFMVHLATIPITGTGINPARSLGAAVIYNNDKAWDDHW
AtPIP1;1    GFAVFLVHLATIPITGTGINPARSLGAAIIYNKDHSWDDHW
AtPIP1;2    GFAVFLVHLATIPITGTGINPARSLGAAIIFNKDNAWDDHW
AtPIP1;3    GFAVFLVHLATIPITGTGINPARSLGAAIIYNKDHAWDDHW
AtPIP1;4    GFAVFLVHLATIPITGTGINPARSLGAAIIYNKDHSWDDHW
AtPIP1;5    GFAVFLVHLATIPITGTGINPARSLGAAIIYNKDHAWDDHW
AtPIP2;1    GFAVFMVHLATIPITGTGINPARSFGAAVIYNKSKPWDDHW
AtPIP2;2    GFAVFMVHLATIPITGTGINPARSFGAAVIYNKSKPWDDHW
AtPIP2;3    GFAVFMVHLATIPITGTGINPARSFGAAVIFNKSKPWDDHW
AtPIP2;4    GFAVFMVHLATIPITGTGINPARSFGAAVIYNNEKAWDDQW
AtPIP2;5    GFAVFIVHLATIPITGTGINPARSLGAAIIYNKDKAWDHHW
AtPIP2;6    GFSVFMVHLATIPITGTGINPARSFGAAVIYNNQKAWDDQW
AtPIP2;7    GFAVFMVHLATIPITGTGINPARSFGAAVIYNNEKAWDDQW
AtPIP2;8    GFAVFMVHLATIPITGTGINPARSFGAAVIYNNEKAWDDHW
MpPIP1;1    GFAVFLVHLATIPITGTGINPARSLGAAIVFNKHLGWHEHW
MpPIP2;1    GFAVFMVHLATIPVTGTGINPARSFGAAVIYNGSKAWDDHW
```

Figure 36. Sequence comparison of loop E of *Zm*PIP and *At*PIP.
The important amino acids are underlaid in yellow. *Zm*PIP1;1 did not show interaction unless loop E was replaced with *Zm*PIP1;2 loop E (amino acids 247 to 256) meaning that the amino acids 247, 251, 252 and 256 are probably involved in the interaction or recognition of the proteins. The numbering is referring to *Zm*PIP1;2, whereas other sequences are only aligned and actually numbering might slightly differ.

At position 252, both D and H may be in agreement with an interaction, since both *Zm*PIP1;2 and *Mp*PIP1;1 were shown to enhance water permeability. Nevertheless, all *At*PIP1 (and *At*PIP2;5) present a D at this position similarly as *Zm*PIP1;2. For PIP2 members shown to interact, amino acid D252 for *Zm*PIP2 or a S252 for *Mp*PIP2;1 was found. The same amino acids are present in *At*PIP2;1, *At*PIP2;2, *At*PIP2;3, and *At*PIP2;5 (Fig. 36).

A major difference of the interacting *Zm*PIP1;1 and *At*PIP1 members is the replacement of neutral asparagine N256 by an acidic aspartate D (Fig. 36). In addition, *Mp*PIP1;1 also possesses a charged, yet basic amino acid, H, at this position (Fig. 36).

Based on this amino acid sequences alignment, all *At*PIP1 and *At*PIP2 might be candidates for heteromerization. *At*PIP2;3 was also shown to have an effect on water permeability when co-expressed with *Zm*PIP1;2 (Fetter et al., 2004). Thus, *At*PIP2;1 and *At*PIP2;2 are good candidates, since they are highly similar to *At*PIP2;3. Interestingly, *At*PIP2;5 is very similar to *Zm*PIP1;2 or *Mp*PIP1;1 and, hence is likely to act in a manner similar to them.

3.6.1 Specificity of antisera against *At*PIP1 and *At*PIP2

To detect and analyze PIP protein expression polyclonal anti-*At*PIP1;1 and anti-*At*PIP2;2 antisera had been raised in our laboratory against the 42 N-terminal amino acids of *At*PIP1;1 and 17 C-terminal amino acids of *At*PIP2;2. According to the high amino acid sequence homology of the different members, the antisera should react with other isoforms (Fig. 37). Sequence alignment suggests that anti-*At*PIP1;1 antiserum should react with all *At*PIP1 isoforms. Only *At*PIP1;5 is somewhat more divergent, since three amino acids in a row are different in the central part (amino acids 27 to 29; Fig. 37).

```
                        10        20        30        40
              ....|....|....|....|....|....|....|....|....|
AtPIP1;1 epitope   MEGKEEDVRVGANKFPERQPIGTSAQS-DKDYKEPPPAPFFEP--
AtPIP1;1           MEGKEEDVRVGANKFPERQPIGTSAQS-DKDYKEPPPAPFFEPGE
AtPIP1;2           MEGKEEDVRVGANKFPERQPIGTSAQS-DKDYKEPPPAPLFEPGE
AtPIP1;3           MEGKEEDVRVGANKFPERQPIGTSAQT-DKDYKEPPPAPFFEPGE
AtPIP1;4           MEGKEEDVRVGANKFPERQPIGTSAQSTDKDYKEPPPAPLFEPGE
AtPIP1;5           MEGKEEDVNVGANKFPERQPIGTAAQTESKDYKEPPPAPFFEPGE


                       280       290
              ....|....|....|....|.
AtPIP2;2 epitope   RASGSKSLGSFRSAANV----
AtPIP2;1           RASGSKSLGSFRSAANV----
AtPIP2;2           RASGSKSLGSFRSAANV----
AtPIP2;3           RASGSKSLGSFRSAANV----
AtPIP2;4           RAAAIKALGSFGSFGSERSFA
AtPIP2;5           RAGAIKALGSFRSQPHV----
AtPIP2;6           RAGAMKAYGSVRSQLHELHA-
AtPIP2;7           RASAIKALGSFRSNATN----
AtPIP2;8           RAAATKAIASFRSNPTN----
```

Figure 37. Sequence alignment of *At*PIP1 and *At*PIP2 with the corresponding epitope used to raise anti-PIP1;1 or anti-PIP2;2 antisera.

*At*PIP2;1, *At*PIP2;2 and *At*PIP2;3 are absolutely identical in the epitope region and therefore collectively recognized by the antiserum, while other *At*PIP2 members are relatively different (Fig. 37).

To confirm experimentally with which PIP members the antisera would react, the N-terminal region of *At*PIP1;5 and the C-terminal region of *At*PIP2;4, *At*PIP2;5, *At*PIP2;6, *At*PIP2;7 and *At*PIP2;8 were amplified from genomic DNA by PCR and cloned via GATEWAY technology into the vector pDEST15, which allows the expression of recombinant fusion protein with glutathione-S-transferase (GST) in *E. coli* (Method 2.2.4.6). All fragments had been verified by DNA sequencing. The affinity-purified proteins were checked by SDS-PAGE and staining

with Coomassie brilliant blue (Fig. 38). A reference GST fusion protein carrying an extension of 23 amino acids due to flanking vector sequences was used as a control (Fig. 38, lane 1).
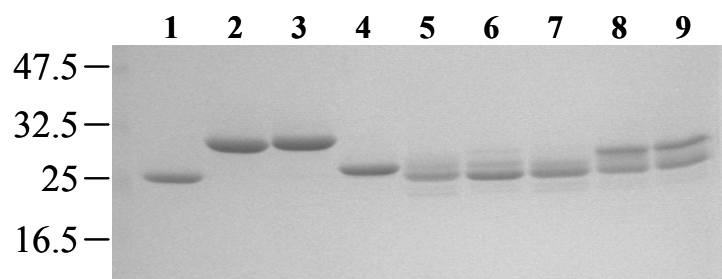
Figure 38. Identification of GST-PIP fusion proteins.
5 μg of GST reference protein (lane 1, MW 29.53 kDa), 10 μg of fusion protein GST-PIP1;1 (lane 2), GST-PIP1;5 (lane 3), 5 μg of fusion protein GST-PIP2;2 (lane 4), GST-PIP2;4 (lane 5), GST-PIP2;5 (lane 6), GST-PIP2;6 (lane 7), GST-PIP2;7 (lane 8) and GST-PIP2;8 (lane 9) were loaded on a 12% SDS-PAG and stained with Coomassie brilliant blue.

In a Western blot analysis the rabbit anti-*At*PIP1;1 antiserum indeed reacted with *At*PIP1;1 as well as with the more divergent *At*PIP1;5 fusion protein indicating the collective detection of all *At*PIP1 members (Fig. 39a). Since GST-PIP1;1 protein were used to raised the anti-PIP1;1 antiserum, it was pre-incubated with 10μg/mL GST protein for 1 hour to compete for the GST-directed antibodies prior to incubation with membrane. Nevertheless, the reactivity towards GST was not completely abolished (Fig. 39a, lane 1). However, signal with GST-PIP1;5 was much stronger indicating that the anti-PIP1;1 antiserum also recognized PIP1;5. In case of anti-PIP2;2 antiserum, a synthetic peptide coupled to keyhole limpet hemocyanin was used to raise the antibody and therefore GST protein could not interfere. However, the anti-PIP2;2 antiserum was treated similarly as anti-PIP1;1 antiserum. The GST-PIP2;2 fusion protein was used as a positive control to check the specificity of a rabbit anti-PIP2;2 antiserum against the other *At*PIP2 members except the identical *At*PIP2;1 and *At*PIP2;3. However, only *At*PIP2;2 was detected and neither *At*PIP2;4, *At*PIP2;5, *At*PIP2,6, *At*PIP2;7, or *At*PIP2;8 was recognized by the antiserum (Fig. 39b).
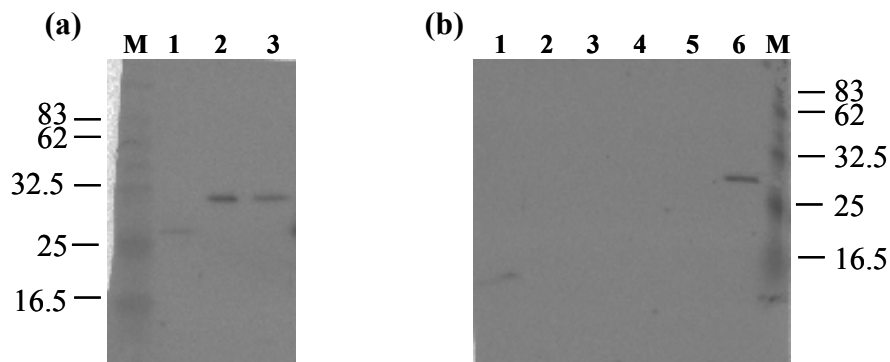
Figure 39. Specificity of anti-PIP1;1 and anti-PIP2;2 antisera.
GST-PIP fusion proteins were extracted and separated on a 12% SDS-PAG and blotted onto PVDF membrane. The membrane was incubated with rabbit (a) anti-PIP1;1 antiserum and (b) anti-PIP2;2 antiserum. Bound primary antibodies were detected with anti-rabbit-cy5-linked secondary antibodies and scanning with Fuji FLA3000 image reader. M: Protein Marker (kDa); (a) lane 1: 10 ng GST protein; lane 2: 10 ng GST-PIP1;1 protein and lane 3: 10 ng GST-PIP1;5 protein. (b) Lane 1 to 6: 10 ng GST-PIP2;4, -2;5, -2;6, -2;7, -2;8 and -2;2 protein. It should be noted that for GST-PIP protein, concentrations were adjusted to account for degradation observed previously (Fig. 38). Thus, a similar amount of protein was loaded by adjusting concentrations of each GST-PIP relative to the GST protein alone (set as 1).

Competition experiments with PIP-GST fusion proteins were also carried out to ensure the specificity against PIP1 or PIP2 proteins also in plant membrane preparations (Fig. 40). Microsomal fractions from *Arabidopsis* roots were prepared, separated on a SDS-PAG and probed using the antisera. The band could be competed by pre-incubation of antiserum with fusion protein GST-PIP1;1 or GST-PIP2;2 (Fig. 40).
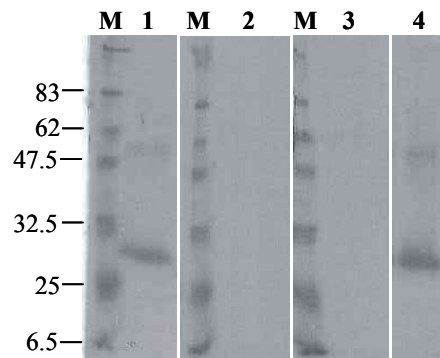
Figure 40. Anti-PIP1;1 and anti-PIP2;2 antisera specifically recognized PIP proteins.
Microsomal fractions from roots of 3-week-old *Arabidopsis* plants grown hydroponically were extracted, separated on a 12% SDS-PAG and blotted onto PVDF membrane. The membrane was incubated with: lane 1: rabbit anti-PIP2;2 antiserum; lane 2: rabbit anti-PIP2;2 antiserum and 10 μg/μl GST-PIP2;2 protein; lane 3: rabbit anti-PIP1;1 antiserum with 10 μg/μl GST-PIP1;1 protein and lane 4: rabbit anti-PIP1;1 antiserum. Bound primary antibodies were detected with anti-rabbit-cy5-linked secondary antibodies and scanning with Fuji FLA3000 image reader. M: Protein Marker (kDa).

3.3.1 Expression of PIP2 and PIP1 proteins in *pip2* knockout mutants

PIP1-PIP2 heteromerization has been demonstrated by transient co-expression or co-purification of PIP1 and PIP2 proteins (Fetter et al., 2004; Temmei et al., 2005). Data mining

of publicly available *Arabidopsis* microarray expression data revealed a high correlation at the transcriptional level between certain *PIP1* and *PIP2* members, such as *PIP1;2* and *PIP2;1*, *PIP1;1* and *PIP2;2/2;3* as well as with *PIP1;3* and *PIP2;7/2;8* (see Table 12, Results 3.5). Here, the *pip2* knock-out collection offered a different approach towards a PIP1-PIP2 interrelation by asking whether the complete loss of an individual PIP2 protein has an influence on PIP1 protein levels.

Microsomal fractions from roots and leaves of three week-old, hydroponically grown *Arabidopsis* plants were then monitored. Protein amount was measured according to the Esen test from denatured samples (Esen, 1978); equal amount of microsomal fraction was then separated by SDS-PAGE, blotted onto PVDF membrane and PIP expression was analyzed and quantified using ImageJ (version 1.37v; http://rsb.info.nih.gov/ij/) (Fig. 41). PIP protein expression was monitored collectively for *At*PIP1 isoforms using the anti-*At*PIP1;1 antiserum and for *At*PIP2;1, *At*PIP2;2 as well as *At*PIP2;3 using the anti-PIP2;2 antiserum. Hence, only changes in the expression of these proteins would be detectable.

As expected, a reduction of about 40% in the expression of PIP2 protein was observed in *pip2;1* and *pip2;2* knock-out mutants in roots (Fig. 41a and b). In the other *pip2* mutants, no significant changes of PIP2 protein level were measured indicating that PIP2;1, PIP2;2 and/ or PIP2;3 were not significantly influenced in these mutants (Fig. 41). Interestingly, *pip2;1* and *pip2;2* mutants showed a concomitant reduction of PIP1 proteins by 20 to 30%, whereas other *pip2* knockouts had no significant effect on PIP1 amounts (Fig. 41).

Two double mutants were tested and confirmed the results of single mutants (Fig. 41). Indeed, *pip2;2-3/ pip2;1-2* showed an additive phenotype and a barely detectable PIP2 signal in roots, while *pip2;1-2/ pip2;4-1* showed a reduction similar to that of *pip2;1-2* alone (Fig. 41). In those mutants, PIP1 expression level was also slightly reduced (Fig. 41). The *pip2;1-2/ pip2;4-1* double mutant showed a reduction similar to that of *pip2;1* single mutants (about 30%) while *pip2;2-3/ pip2;1-2* showed a more pronounced reduction (about 50%; Fig. 41).

PIP expression of two *pip1* knockout mutants, *pip1;1-1* and *pip1;2-1*, were analyzed as well. Although they showed a reduction in PIP1 antigens, PIP2 protein expression was not altered (Fig. 41). Thus, PIP1 levels are dependent on PIP2;1 or PIP2;2 proteins, whereas the reverse seems not to be the case. However, since antisera were not specific to one PIP2 isoform, it cannot be excluded that the expression of some PIP2 members is reduced, while the expression of another is increased at the same time.
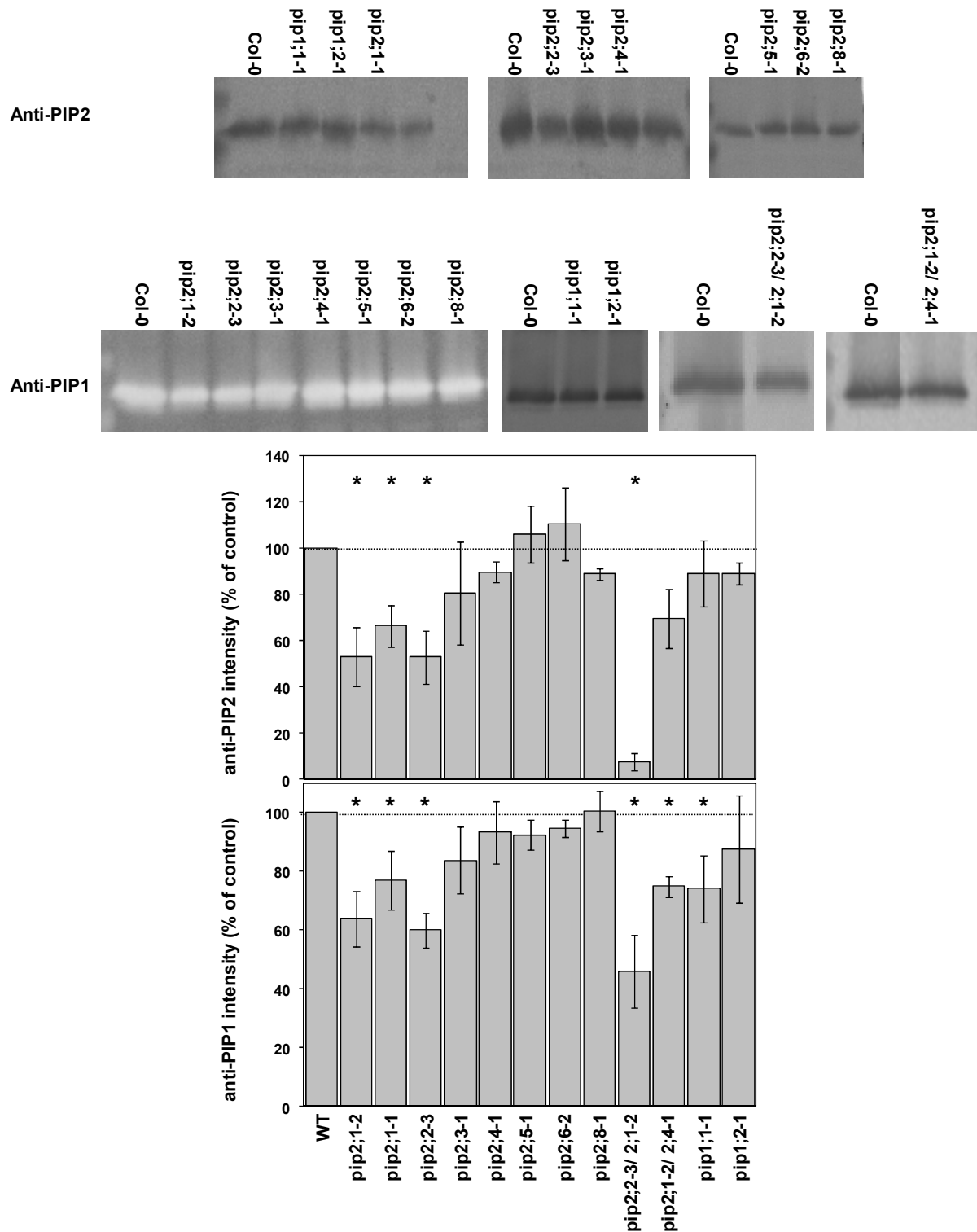
Figure 41. PIP protein expression level in *pip2* knockout mutants in roots.
(a) Microsomal fractions were extracted from roots. The fractions were separated on a 12% SDS-PAG and blotted onto PVDF membrane. Membranes were probed with rabbit anti-PIP2;2 or anti-PIP1;1 antisera and visualized using secondary Cy5-linked anti-rabbit antibodies and fluorescence scanning (Method 2.2.6.9). (b) Signal intensity was quantified using imageJ software. Values for each sample are expressed as a percentage of the wild-type value. Means ± SD are shown for two independent biological experiments that were separated, blotted and analyzed at least twice. For *pip2;5-1*, *pip2;6-2*, and *pip2;8-1*, data represent two independent blots of the same protein preparation. Asterisks above bars indicate statistically significant differences based on two-sided Student's T-test assuming unequal variance (* for p < 0.025).

Preliminar, similar results have been observed in leaves for *pip2;1* mutants which also showed a significant reduction of PIP1 protein (Fig. 42). Several double mutants obtained by crossing *pip2;1* single mutants with other *pip2* single mutants also showed a reduction, which, at least for *pip2;2-3/pip2;1-2*, was even stronger than the single mutants alone (Fig. 42).
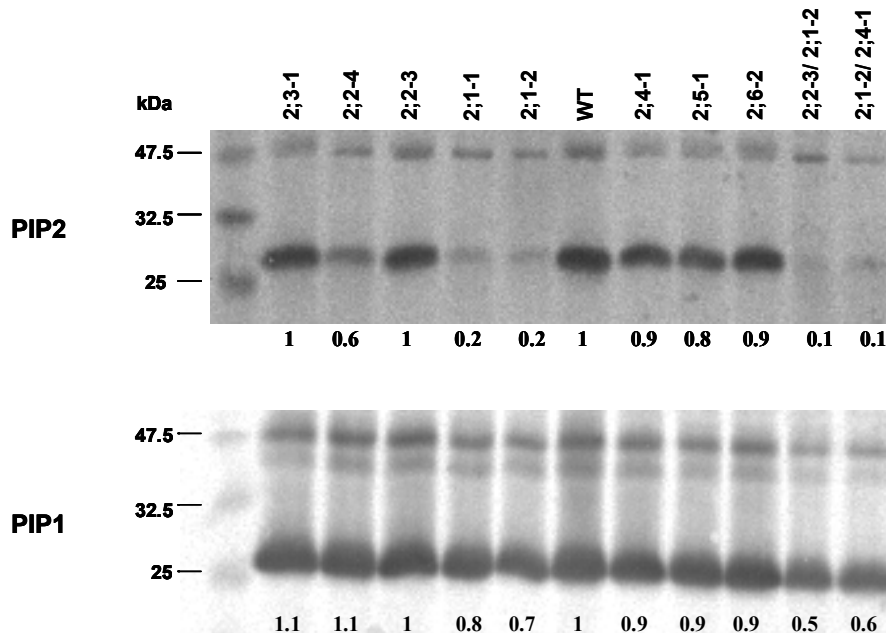
Figure 42. PIP protein expression level in *pip2* knockout mutants in leaves.
Microsomal fractions were isolated from *Arabidopsis* leaves, separated on a 12% SDS-PAG and blotted onto PVDF membrane. Membrane were probed with rabbit anti-PIP2;2 or anti-PIP1;1 antisera and visualized using secondary Cy5-linked anti-rabbit antibodies and fluorescence scanning (Method 2.2.6.9). Signals intensity was quantified using ImageJ software. Values for each sample are expressed as a ratio *pip2* mutant/wild-type. Single mutants as well as three double mutants are shown. It should be noted that these results are based on a single experiment.

In conclusion, PIP2 protein expression, in particular PIP2;1 levels, have an effect on PIP1 protein amounts, whereas no changes were observed at the transcription level for the same knockout mutants. Hence, the down-regulation of PIP had occurred at the post-transcriptional level and lack of PIP2 could negatively influence PIP1 protein amounts.

4   DISCUSSION

Despite the rapidly expanding literature on the isolation and regulation of aquaporins in various plant species, reports demonstrating the functions of individual *PIP* isoform in higher plants are limited to a mutation of a single PIP1 homolog in Brassica (Ikeda et al., 1997) and a single *pip2;2* knock-out line in *Arabidopsis* (Javot et al., 2003; see Introduction). Furthermore, the high isoform multiplicity may suggest that PIP2 aquaporins display functional redundancy. In the present study, several lines of evidence were elaborated arguing in favor of differential functions for the single *Arabidopsis PIP2* genes based on various expression analyses and *pip2* knockout mutants (Table 13): (1) *PIP2* genes exhibit differential expression pattern; based on these *in situ* expression analyses the integration of PIP2 members in plant water relations was tackled. In addition, the impact of two individual PIP2 proteins on plant water transport was demonstrated via translocation of D_2O through the roots into the leaves of *pip2* knockout mutant plants. (2) *PIP2* genes and *pip2* knockout mutants show differential stress-responsiveness, (3) *PIP2* genes and *pip2* knockout mutants display distinct co-expression and transcriptional profiles, respectively, and (4) *PIP2* genes are distinctly co-regulated with other *MIP* genes. Surprisingly, specific PIP2 proteins differentially influenced PIP1 expression at the protein level.

4.1 Distinct *PIP2* localizations allow for differential roles in water relation

The detailed promoter-reporter analysis presented here indicated a differential expression profile of *Arabidopsis PIP2* genes, which was in accordance with data based on array hybridization or RT-PCR at whole organ levels and in fluorescence-sorted root cells (Affenzeller, 2003; Alexandersson *et al.*, 2005; Birnbaum *et al.*, 2003; Boursiac *et al.*, 2005; Jang *et al.*, 2004; Schmid *et al.* 2005). Most *PIP2* genes exhibit a wide-spread organ expression pattern, but several members show predominant expression in roots (*PIP2;4*), young (*PIP2;6*) or emerging (*PIP2;8*) leaves. However, the cellular expression profile of individual *PIP2* aquaporins revealed significant additional differences.

Several transgenic lines constitutively altering PIP expression had supported their importance for plant water relations, yet did not allow to pinpoint roles of individual PIP members (see Introduction). Thus, provided that PIP2 indeed function as water channels (see below), their individual expression patterns would also suggest or preclude roles in water permeation like cellular osmoregulation, transcellular water transport, or cell growth.

All *PIP2* genes were expressed in the root hair zone and – except *PIP2;5* and *PIP2;6* – in root hairs themselves. This observation would comply with a function in absorption and/or conduction within this area most actively involved in nutrient and water uptake. Despite their biochemical function as water channels it has been questioned whether the sole function of PIP and aquaporins in general would be the enhancement of water permeation across membranes, since in several instances the reason for such a higher water conductance is obscure (Schäffner, 1998; Tyerman et al., 2002; Hill et al., 2004). Hill et al. (2004) proposed an alternative function for aquaporins as osmotic sensors. Although there is no supporting experimental evidence to date, the localization of the *PIP2* transcripts could allow such a role in the root hair cells exposed to the surrounding soil. In addition to root hair cells *PIP2;4* is the only *PIP2* that was specifically expressed in the roots including its outer cell layers, which would allow a role as an osmosensor as well as a specific function in transcellular water transport across the outer root cell layers. Interestingly, genes assigned to stress category were significantly co-expressed with *PIP2;4* (Tables 10, 13; Supplementary Table 6).

Abundant expression of *PIP2;1*, *PIP2;2* and *PIP2;7* and at a lower level *PIP2;3*, *PIP2;5*, and *PIP2;6* in vascular tissue in roots as well as in leaves could indicate that these genes exert functions in water loading into and disposal from vascular tissue in the whole plant, which is coupled to osmotic differences generated by active transport of ions or photosynthates (Fig. 8; Table 13). In the root, *PIP2;1*, *PIP2;2*, *PIP2;4*, *PIP2;5*, and *PIP2;7* could be involved in the water passage across endodermal cells with *PIP2;2* and *PIP2;4* being localized to the cortex layer as well. PIP2;2 had been previously related to root water uptake, since *pip2;2* knock-outs had shown reduced root exudation (Javot and Maurel, 2002).

Several aquaporin genes, e.g. *PIP2;5* and *PIP2;6*, have been shown to be deregulated in roots upon nematode infestation (Puthoff et al., 2003; Hammes et al., 2005; Jammes et al., 2005). *PIP2;6* was significantly induced throughout infested root while *PIP2;5* was preferentially induced in galls, including in giant cells (Hammes et al., 2005; Jammes et al., 2005). It is well known that giant cells are metabolically very active and, hence, that large amounts of water and solutes transport are required for gall development. Thus, the induction of aquaporin genes, in particular *PIP2;5*, under these conditions may suggest functions for these proteins in growth control and/ or cell osmoregulation via regulation of plasma membrane water permeability.

In particular in younger leaves the expression of *PIP2;1*, *PIP2;2*, *PIP2;6* and *PIP2;7* extended into the mesophyll, which would allow a main function in leaf water relations. In young seedlings *PIP2;6* was the only *PIP2* gene predominantly expressed in leaves.

Interestingly, genes related to photosynthesis were significantly enriched among genes co-expressed with *PIP2;6* and to a lesser extent with *PIP2;1* and *PIP2;7/2;8*. In addition, a significant link to genes involved in primary cell-wall biosynthesis could be deduced for *PIP2;6* from AtGenExpress biotic stress datasets. Thus, a role of PIP2;6 in growth and osmoregulation as well as in transpiration could be postulated among water related processes. *PIP2;5´*s expression in leaves would allow a similar function, although it showed a clearly distinct regulation and correlation of its expression.

In addition to its weak expression in the stele of roots similar to *PIP2;3*, *PIP2;8* could be involved in cellular osmoregulation and leaf growth at early stages (Fig. 8; Table 13). *PIP2;8* as well as *PIP2;1*, *PIP1;1, PIP1;2, PIP1;3*, and three *TIP* genes had been previously associated with growth, because reduced transcript levels were found in *cbb* mutants impaired in brassinosteroid-dependent cell elongation (Lisso et al., 2005). Interestingly, co-expression analyses also revealed a correlation of *PIP2;7/2;8* with brassinosteroid-associated and cell wall-related genes and, importantly with *PIP2;1, PIP1;2, PIP1;3,* and two of the *TIP* genes (Tables 10 and 13; Supplementary Table 3). Notably, abundant expression of several of these genes, *TIP1;1*, *TIP2;1* and *PIP1;2,* in growing/developing tissues, i.e. undergoing rapid growth have been demonstrated previously (Ludevid et al., 1992; Kaldenhoff et al., 1995; Daniels et al., 1996).

Eventually, *PIP2* genes showed a complex and differential expression in different parts of flowers, where water channels could be involved in pollen hydration and growth or in osmoregulation during deposition of nutrients. An implication for PIP aquaporins in such processes has been suggested in tobacco and tulip (Azad et al., 2004; Bots et al., 2005a; Bots et al., 2005b).

4.2 Establishment of a method for assessing in vivo plant water transport

So far, several methods have been used to assess aquaporin water permeability and function in plant water relation. At the cellular level, expression in heterologous system such as *Xenopus* oocytes (Maurel et al., 1993; Fetter et al., 2004; Temmei et al., 2005) or yeast (Loque et al., 2005; Bienert et al., 2006; Daniels et al., 2006) is widely used to functionally characterized aquaporin. Although helpful to determine the specificity of aquaporins, these systems are far from natural systems. The use of plant protoplast for single cell assay offers similar characteristic with the advantage of being in a plant cell environment (Kaldenhoff et al., 1998; Verkman, 2000). The involvement of aquaporins in plant water transport has also been investigated by measurement of hydraulic conductivity of plant organs and single cells.

For instance, pressure probes offer the advantage to continuously measure and manipulate the hydrostatic pressure of a single plant cell *in situ* but also of a whole tissue (Javot et al., 2003). At the organ level, root sap exudation measurement has proven useful to determine the contribution of PIP2;2 in water conductivity of whole *Arabidopsis* root water transport (Javot et al., 2003). A major disadvantage of these techniques is that plants are manipulated during the experiment or even destructed by decapitation, e.g. roots are separated from the leaves, for which water transport cannot be evaluated. Studies using the whole plant are a pre-requisite for an integrated knowledge of plant water relations. The use of stable isotopes as tracers is valuable since it allows dynamic investigations at the plant scale, which are non-destructive during the course of observation. The enrichment of naturally occurring stable isotopes of oxygen (^{16}O, ^{18}O) and hydrogen (H, D) have been largely used in plant physiology and ecology, mainly to study transpiration and/or photosynthesis and several models based on the Craig & Gordon model of the evaporation of water from the surface of an ocean have been developed (Craig and Gordon, 1965; Farquhar et al., 1989; Flanagan et al., 1991; Roden and Ehleringer, 1999a; Cuntz et al., 2007; Farquhar et al., 2007; Santrucek et al., 2007). These models have been applied to several plant and tree species such as *Phaseolus vulgaris*, *cornus stolonifera*, water birch, cottonwood, maize or snowgum (White, 1988; Flanagan et al., 1991; Flanagan and Ehleringer, 1991; Roden and Ehleringer, 1999a; Gan et al., 2003; Santrucek et al., 2007).

Artificially enhancing the D content of the source water like in hydroponic cultures should allow studying the kinetics of establishment of a new equilibrium and thus the contribution of individual gene products to water translocation if knockout mutants were analyzed. Similar additions of D_2O to source water have been already used to study its influence on the isotopic composition of leaf water and the accuracy of the Craig and Gordon model for predicting leaf water isotopic content in a wide range of environmental conditions (Roden and Ehleringer, 1999a; Roden and Ehleringer, 1999b). The authors demonstrated that Craig and Gordon model generated good predictions of leaf water isotopic content under a wide range of environmental conditions and in various tree species (alder, water birch and cottonwood).

Here, the current models had to be adapted to this experimental set-up and to *Arabidopsis*. Importantly, a new term to account for the fraction of phloem water recirculating back to the source was incorporated in the model. This modification essentially had an influence in steady-state situations. In particular, it considerably improved the Craig and Gordon model predictions at conditions of high humidity, i.e. when transpiration is low and consequently phloem shoot-to-root flow more dominant. In case of low humidity, fraction of phloem water

is minor compared to water loss through evapotranspiration and therefore almost negligible. Since phloem back flow could not be experimentally assessed it was calculated to give a best fit to the measured values. Thus, it is important that this "phloem fraction" encompasses any other loss of leaf water in addition to phloem transport and the separately treated transpiration.

Previous studies have often shown that Craig and Gordon models poorly predict the isotopic composition of leaf water in particular when transpiration is low (Allison et al., 1985; Flanagan et al., 1991; Wang and Yakir, 1995; Wang et al., 1998; Helliker and Ehleringer, 2000). These discrepancies are usually explained by isotopic heterogeneity of leaf water (e.g. compartmentation). Our fractionation factor may also account and correct the model for such effects.

Subsequently, several plant-intrinsic parameters such as root and leaf mass were analyzed. Importantly, leaf water volume did not alter the deuterium enrichment of leaf water. Recently, sensitivity analyses of leaf water enrichment models to varying mesophyll water volume have been made in other plant species (Cuntz et al., 2007). The authors demonstrated that mesophyll water volume was not critical for the model predictions and that a mean leaf water volume is sufficient to obtain a good prediction of the isotopic water enrichment although it seemed to have some influence during night time. In our experiment rosette leaves were used and treated as an ideally mixed compartment of constant volume. Although rather an approximation of reality, this situation was fairly well suited for our data sets.

Using hydroponic *Arabidopsis* cultures water translocation was not dependent on root mass. In fact, since plants were grown hydroponically, root water availability was not limiting in our system. These results indicated that the dynamic D enrichment was dominated by properties of the leaves under these conditions.

4.3 Non-invasive analyses of the impact of PIP2 on plant water translocation using *pip2* knockout mutants

These measurements demonstrated the applicability of the method and wild-type and mutant plants were then compared. Among the three single mutants tested, *pip2;1* and *pip2;2* showed a reduction of about 20% of the leaf water isotopic enrichment indicating that water relations were altered in these *pip2* knockouts. Importantly, no phenotypical or morphological changes were observed between *pip2* mutant and wild-type plants. According to Figure 2 depicting water transport and exchange in plants, a retarded D enrichment could be explained (1) by a

drop in water supply from roots, (2) by decreasing evapotranspiration, and/or (3) by a reduction of hydraulic exchange between leaf cells.

Detached leaf assay as well as transpiration measurements indicated that water loss and transpiration rate were similar in *pip2* mutants and in wild-type plants; thus evapotranspiration should play a minor role. Likewise, the phloem fraction should be negligible since it influences steady-state rather than the D enrichment time course.

In a previous study, root sap exudation measurements indicated a decline in osmotic hydraulic conductivity of *pip2;2* mutant roots (Javot et al., 2003). This would lead to a slower deuterium enrichment of leaf water assuming that the same phenomenon arose in the analyzed mutants and conditions here. However, for this hypothesis, the relative independence of the method from root mass still remains elusive. It is so far impossible with our data to determine how important the contribution of the root to the method is.

Alternatively, the reduction could be explained by a slower water exchange between leaves cells. Indeed, *pip2* knockout may alter leaf symplastic water flow. Thus, mixing of water is slower and evapotranspirating water via apoplastic path is then enriched in deuterium (see Introduction; Fig. 2). Consequently, leaf water will reach its isotopic steady-state more slowly. Recently, an influence of PIP2 aquaporin in leaf hydraulic conductance has been demonstrated (Cochard et al., 2007). The authors correlated downregulation or upregulation of *JrPIP2;1* and *JrPIP2;2* in walnut tree leaves in response to light with a low or high leaf hydraulic conductance, respectively. Their observation could be in agreement with the knockout results of this study.

These results demonstrated the involvement of PIP2;1 and PIP2;2 in plant water relation. Yet, so far, the data are not sufficient to determine whether the decline in water translocation is caused by root and/or leaf hydraulic conductance.

It is important to note that a *pip2;4* mutant did not exhibit retarded leaf isotopic enrichment. Thus, *PIP2;4* loss-of-function did not alter water translocation. The explanation may reside in its particular expression pattern; *PIP2;4* is not expressed in leaves and is predominant in outer root cell layers, yet expression in roots is much lower compared to *PIP2;1* and *PIP2;2*.

Surprisingly, the double mutant *pip2;2-3/ pip2;1-2* did not exhibit any decrease in its isotopic enrichment. While the decline observed in the single mutants indicated a disturbance in the plant water status, a phenotypical recovery was observed for the double mutant. Double mutant plants might be more severely affected that single mutant and, hence, have to develop a strategy to sustain stress and maintain a suitable water status. Consequently, the water translocation from root to shoot is unchanged and the plants would not be phenotypically

altered. To date, the explanation for such compensation is still obscure. However, such a phenomenon has already been observed using PIP antisense mutant plants (Kaldenhoff et al., 1998; Martre et al., 2002). A reduced osmotic hydraulic conductivity of root and leaf protoplasts from antisense plants with reduced amount of PIP1 and/ or PIP2 proteins was observed, while the hydraulic conductance of the whole plant was not affected (Martre et al., 2002). In fact, the authors did not observe alteration of the leaf hydraulic conductance while the root hydraulic conductivity was lower on a root dry mass basis but compensated by an increase in the root/leaf dry mass ratio.

Martre et al. (2002) used antisense constructs (*PIP1;2* and/ or *PIP2;3* cDNA) to reduce PIP protein expression. These antisense plants were characterized by reduction of several isoforms and therefore our *pip2;2-3/ pip2;1-2* double mutant may represent a slightly comparable situation. Nevertheless, our mutant is likely not as strongly disturbed as Martre et al. (2002) mutants since they observed a greater root dry mass to compensate for the lower root hydraulic conductance. Indeed, the increase or decrease of aquaporins in transgenic plants is hypothesized to increase or decrease root water permeability resulting in a smaller or larger root area to maintain a constant water uptake by roots, respectively (reviewed by Hachez et al., 2006a). However, no differences in root and shoot mass were observed in *pip2;2-3/ pip2;1-2* mutant. Possibly, in this mutant, a smaller root area was sufficient to supply enough water into the aerial parts. It may well be that in our hydroponic culture, double mutants do not need to adjust its root area to compensate for any reduction in root conductance but rather could optimize the uptake since water was not limiting under these conditions.

4.4 *PIP2s* differentially respond to stress

Several reports have shown the differential responsiveness of *PIP* genes to water stresses as well as to biotic cues or plant hormones (Kreps et al., 2002; Seki et al., 2002a; Seki et al., 2002b; Affenzeller, 2003; Maathuis et al., 2003; Jang et al., 2004; Kawaguchi et al., 2004; Alexandersson et al., 2005; Boursiac et al., 2005). However, in some instances, there is no agreement concerning the *PIP* members which are altered. For instance, Alexandersson et al. (2005) observed a strong down-regulation of *PIP2;2* upon drought stress while it was upregulated in another study (Kreps et al., 2002). Likewise, *PIP2;3* and *PIP2;6* were either upregulated (Seki et al., 2002a), downregulated (Jang et al., 2004) or not markedly altered (Alexandersson et al., 2005) upon drought stress. In contrast, Alexandersson et al. (2005) pointed out that *PIP1;4* and *PIP2;5* were consistently upregulated upon drought in these studies. These divergent results were mostly explained by experimental differences (e.g.

growth conditions, severity and duration of the stress). In this respect, the AtGenExpress consortium provided important information on plant stress responses under various treatments using Affymetrix microarray expression profiling (Kilian et al., 2007), which also supported the specific transcriptional deregulations of *PIP2* genes. Interestingly, *PIP2;2/2;3*, *PIP2;4* and *PIP2;5* were more frequently deregulated than other *PIP2* members, yet showed mostly responses to different cues (Supplementary Table 9). As a consequence, PCA based on these data demonstrated distinct stress-responsiveness. *PIP2* genes showed mostly opposite or independent projections and only *PIP2;1* and *PIP2;7/2;8* or *PIP2;2/2;3* and *PIP2;4* in context with *PIP1* genes were grouped together (Figure 35). On the other hand, *PIP1* genes themselves were associated with distinct *PIP2* groups or partially independent from these response patterns. Thus, these results do support the independent evolvement of stress responsiveness of *PIP2* as well as *PIP1* members and, consequently, gene-specific, non-redundant functions related to distinct stresses. PCA also highlighted stresses which contributed most to the *PIP2* differentiation. For instance, upregulation of *PIP2;5* under salt, osmotic or cold stress contributed to the particular pattern of this isoform. Such upregulation has been consistently demonstrated by other groups (Jang et al., 2004; Alexandersson et al., 2005). In addition enhanced GUS activity in transgenic seedlings expressing a *PIP2;5* promoter::GUS construct after several days of growth under salt stress was found, while seedlings grown on sorbitol did not show significant increase (See Annex 2 data *PIP2;5*).

4.5 PIP2;3 specifically required for NaCl resistance

Although *PIP* transcripts responded to salt or osmotic stresses and complex alterations of PIP expression in transgenic (overexpression and suppression) lines changed sensitivity towards water stresses, individual PIP functions had not been related to sensitivity towards osmotic or ionic stresses. A wide-spread down-regulation of *MIPs* genes was usually observed upon drought and osmotic stresses (Alexandersson et al., 2005; Jang et al., 2004) and may explain why none of the *pip2* knockouts showed enhanced sensitivity to sorbitol or mannitol; yet, enhanced resistance was not observed either. Surprisingly *pip2;3* mutants were sensitive to enhanced NaCl, whereas none of the other *pip2* mutants were affected. Indeed, mostly transient up-regulation of *PIP2;3* gene expression upon salt stress had been reported in roots or leaves (Boursiac et al., 2005; Jang et al., 2004; Maathuis et al., 2003), although adult plants did not show such a response (Affenzeller, 2003).

However in these contributions, transcription was analyzed shortly after salt treatment (2 to 96 h) implying a possible influence of *PIP2;3* in short-term ionic or purely osmotic stress

response. In contrast, our loss-of-function experiments indicated that *PIP2;3* expression was important to cope with a long-term challenge by enhanced NaCl irrespective of the osmotic stress. Importantly, there was no transcriptional compensation of *pip2;3* by any other aquaporin, in particular by its closest homologue *PIP2;2* (Table 8). In a previous report, *Arabidopsis pip2;2* knockout mutants did not show growth or developmental alterations under standard as well as water stress conditions but exhibited reduced root water uptake and endogenous *PIP* transcripts including *PIP2;3* were not altered either (Javot et al., 2003). Consequently, PIP2;2 is mainly involved in water uptake, whereas PIP2;3 has evolved with a non-redundant function and is specifically required for salt stress resistance in *Arabidopsis*.

The high homology of *PIP2;2* and *PIP2;3,* their water channel activity in *Xenopus* oocytes as well as their overlapping expression pattern in vegetative tissues strikingly contrasts such a differential function. Furthermore *PIP2;3´*s expression level was much weaker (this work; Affenzeller, 2003; Alexandersson et al., 2005; Boursiac et al., 2005; Daniels et al., 1994; Jang et al., 2004; Kammerloher et al., 1994). Thus it seems to be unlikely that sole water transport function is the major role of PIP2;3 in salt tolerance. Interestingly, PIP2;3 is expressed in stomata, which control transpiration. However the phenotype has been observed on plates with a high atmospheric water saturation that should diminish the influence of transpiration. Thus, a different regulation could distinguish both genes, although *PIP2;2* and *PIP2;3* share the same 3 kb upstream region in a head-to-head orientation, or a different property of PIP2;3 protein, which might also deviate from pure water channel activity (which would be PIP2;2´s part) either by allowing other molecules to permeate or through a regulatory role in salt tolerance. In fact, at least different putative transcription factor binding site could be found in the non-overlapping -1 kb upstream region of each gene (Supplementary Figure 2 and Supplementary Table 10). Only nine among 285 amino acids are altered in both proteins, yet modeling their position within the PIP structure (Törnroth-Horsefield et al., 2006) revealed that five are clustered within or in the vicinity of the extracellular loop C, where either the permeation or the interaction with extracellular partners could be influenced (Fig. 43). Two other changes are within helices 1 and 6 and might be of minor importance, although the T258 in PIP2;3 exposes a functional group in contrast to PIP2;2´s A258 that could be accessed within the membrane (Fig. 43). Interestingly, contrasting mercury sensitivities had been already reported for PIP2;2 and PIP2;3 despite their high homology and the absolute conservation of four cysteine residues (Daniels et al., 1994; Kammerloher et al., 1994), which also hints towards a structural difference.
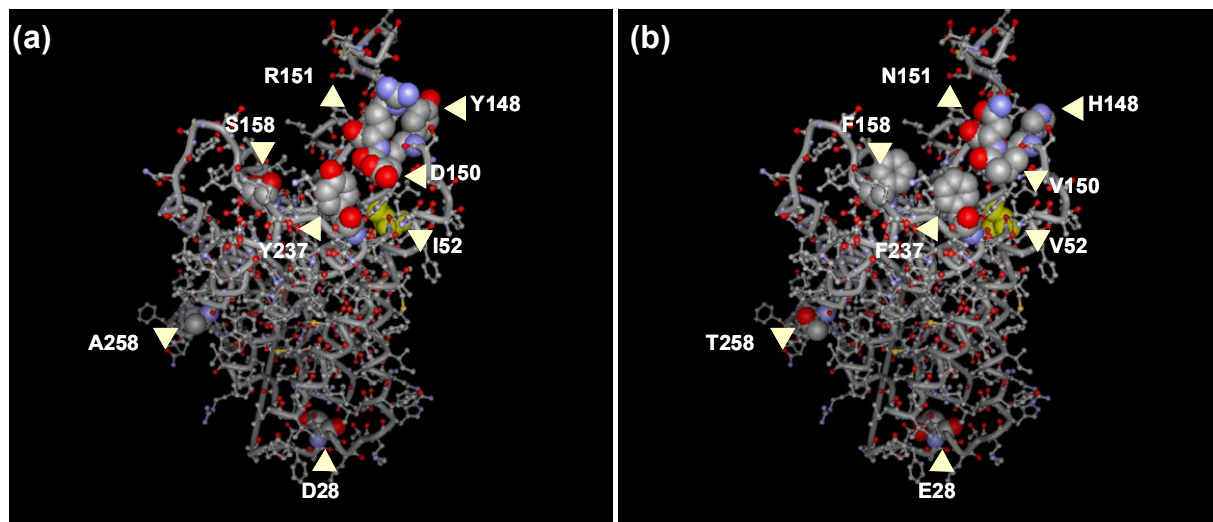
Figure 43. Structural models of PIP2;2 and PIP2;3 showing their different amino acids.
The three-dimensional structures of (a) PIP2;2 and (b) PIP2;3 were generated using SWISS-MODEL (Kopp and Schwede, 2004; Arnold et al., 2006) with the crystal structure of *So*PIP2;1 as template (PDB code: 1z98A). E9 in PIP2;2 which is replaced by D9 in PIP2;3 is not shown in the model. All other amino acids which diverge between PIP2;2 and PIP2;3 are shown and most are located within loop C or positioned nearby. Red spheres design oxygens, blue ones nitrogen, and grey ones carbon atoms; I52 and V52 in helix 1 are not coded for elements and highlighted in olive.

4.6 *PIP2* genes are embedded in different functional context

Given that aquaporins facilitate the permeation of water across biological membranes a major interest is now to integrate the contribution of aquaporin-water facilitation to physiological processes. Previous reports suggested a relation between aquaporin and various biological functions of plants including transport processes, nutrient acquisition, carbon fixation and stress responses. For instance, a relation between PIP1 and photosynthesis has been suggested in tobacco (Siefritz et al., 2002; Uehlein et al., 2003; Flexas et al., 2006) and *Arabidopsis* (Aharon et al., 2003). Data on PIP2 have been much more limited. In tobacco, PIP2 members are required for efficient anther dehiscence. Therefore, two different approaches were performed to investigate the functional context in which particular *PIP2* gene may be embedded. One approach consisted of analyzing the transcriptome of *pip2* knockout mutants while the other approach focused toward co-expression analyses. It is important to note that co-expression analyses are based on genes showing a pattern of expression correlated to that of a particular *PIP2* gene in a wide range of conditions. In contrast, array analyses were done to study the effect of a particular P*IP2* mutation on other transcripts.

In the first approach, transcriptome analyses of *pip2* mutants using two different array technologies revealed only minor changes but, nevertheless, supported the differential function hypothesis. Our custom-array indicated that transport-related families are not altered

in *pip2* mutants. The results were corroborated by whole genome Affymetrix analyses of *pip2;1-2*, *pip2;2-3* and *pip2;4-1* mutants since no deregulation of transport processes was observed in these mutants. Whole genome Affymetrix analyses also revealed different transcriptional profile of *pip2* mutants. However, functional categorization of the deregulated genes did not give clear hint on processes that could be affected in *pip2* mutants. In fact, apart from *pip2;2-3/ pip2;1-4* other single and double mutants tested did not exhibit significant alteration of a particular category. In *pip2;2-3/ pip2;1-4* root and leaf transcriptome, the over-representation of cell wall-related genes and of transcripts encoding enzymes involved in oxidative stress response and secondary metabolism (i.e. miscellaneous category), respectively, suggested an enhanced cell wall loosening.

To gain further insights into the PIP2 family, co-expression analyses were performed. Typically, a very poor, if any, overlap was observed at the gene level between *PIP2* co-expressed genes. However, the significant enrichment of genes assigned to the functional category revealed by co-expression analyses demonstrated that *PIP2* transcripts are differentially associated with other genes that are related to different functional contexts (Table 13). Surprisingly, only *PIP2;1* and *PIP2;2/2;3* exhibited enrichment of transport category supporting our array data which showed no alteration of transporter-related transcripts. These results suggest that the role of most PIP2 may not primarily be embedded in the functional context of transport. Interestingly, several members were linked to photosynthesis and/or cell wall-related processes, possibly indicating function in growth; other members were also correlated to hormone metabolism (e.g. *PIP2;7/2;8*; Table 13) or showed a higher enrichment of stress-related genes (e.g. *PIP2;2/2;3* and *PIP2;4*) (Tables 10 and 13). These observations provide a basis for further analysis on the integrated role of single PIP2 aquaporins.

4.7 Differential PIP2-MIP interactions

Relationships between PIP2 and PIP1 at both transcript and protein level were detected.
Co-expression analyses indicated differential and strong correlation of specific *PIP2* transcripts with other *PIP* and *TIP* genes in a wide range of conditions. Stress-based PCA also indicated a differential association of *PIP2* and *PIP1* genes. In fact, *PIP2* genes showed a much better correlations with *PIP1* genes than with other *PIP2* members indicated by considerably high *PIP2-PIP1* correlation coefficients for the couples *PIP2;1 vs. PIP1;2*, *PIP2;2/2;3 vs. PIP1;1*, or *PIP2;7/2;8 vs. PIP1;3* (r > 0.82; Tables 12 and 13). *PIP2;1*, *PIP2;2/2;3*, *PIP2;4* and *PIP2;7/2;8* also exhibited a strong correlation with several but

different *TIP* genes (Tables 12 and 13). These observations may provide an independent hint towards a partnership or functional cooperation of PIP2 isoforms with several PIP1s and TIPs members in order to maintain water status at the cellular and/ or tissue level. In fact, as a result of their subcellular localization, PIPs and TIPs are expected to function in concert in water relations. In contrast, *PIP2;5* and *PIP2;6* clearly did not show any correlations, indicating a specific role among *PIP* members (Tables 12 and 13).

Surprisingly, a direct influence of PIP2 on PIP1 protein levels was demonstrated by the specific reduction of PIP1 amounts in *pip2;1* and *pip2;2* knockout mutants. It is important to note that *pip2* mutants did not reveal significant alteration of any other *MIP* gene (this work; Javot et al., 2003). Importantly, these results pointed out the utility of knockout mutant to investigate a particular isoform contrasting to overexpression strategy (Jang et al., 2007a, b).

Recent reports demonstrated the importance of PIP2 and PIP1 protein interaction to regulate PIP1 targeting to the plasma membrane and consequently their activity (Fetter et al., 2004; Temmei et al., 2005; Zelazny et al., 2007). When expressed alone in maize protoplasts, PIP1 were not targeted to the plasma membrane, but retained in the endoplasmic reticulum. The authors speculated that PIP1 and PIP2 interaction is required for PIP1 trafficking to the plasma membrane to modulate plasma membrane permeability (Zelazny et al., 2007). In our work, the reduction of PIP1 protein level in *pip2* knockout mutants demonstrated the influence of PIP2 on PIP1 protein level. Interestingly, reduction of PIP2 protein level was not observed in two *pip1* knockout mutants suggesting that only PIP1 is regulated by PIP2;1 and PIP2;2, but the reverse may not be true. Thus, the expression level and/or stability of PIP1 protein may be closely linked to that of PIP2 proteins. Thus, a new type of interaction or a new type of regulation of expression at the protein level was identified. The dependence of PIP1 protein expression on PIP2;1 and PIP2;2 may be also related to the direct protein-protein interaction shown previously (Fetter et al., 2004; Temmei et al., 2005; Zelazny et al., 2007). PIP2-PIP1 interaction/heteromerization enhances PIP1 targeting to the plasma membrane and/or its stability and such heteromerization may lead to structural changes implicated in regulation of PIP activity (Chaumont et al., 2005; Zelazny et al., 2007). The present study suggests that PIP1 stability is altered; PIP1 is rather degraded than simply mistargeted to other membranes, because microsomal fractions were analyzed.

An important issue to address is whether this regulation process affects all or only particular PIP1 isoforms. Co-expression of both *At*PIP1;3 and *Zm*PIP1;2 in *Xenopus* oocytes resulted in an increase in water permeability (Fetter et al., 2004) and sequence comparison of PIPs indicates that all *Arabidopsis* isoforms harbor the critical amino acid residues which could be

responsible for the interaction as proposed by Fetter et al. (2004). *In planta*, such interactions/regulations would require a similar spatial expression of the genes in order to have a potential functional relevance. Interestingly, *PIP1;1*, *PIP1;2* and *PIP1;3* showed an extremely similar expression pattern and high correlation with *PIP2;1*, *PIP2;2/2;3* and *PIP2;7/2;8* suggesting that isoforms such as these PIP1 isoforms could potentially be involved. The presence of PIP2;1, PIP2;6, PIP2;7 and PIP2;8 as well as PIP1;1, PIP1;2, PIP1;3 and PIP1;5 has been demonstrated in detergent resistant membranes (i.e. lipid rafts) (Mongrand et al., 2004; Shahollari et al., 2004; Bhat and Panstruga, 2005).

4.8 Conclusion

This work demonstrated that the closely related PIP2 members exhibit differential functions. In addition, the functional context of single PIP2 members has been exposed and PIP2;3 has even been associated to salt stress. Such classification could definitely help identifying the physiological involvement of aquaporin in different key processes, e.g. elongation (PIP2;8) or photosynthesis (e.g. PIP2;6) and, consequently, provides a framework for future prospects. Complete characterizations whether any *PIP2* promoter are activated or repressed by stress or other treatments are still required for a clear distinction regarding different PIP2 isoforms.

Importantly, this study pointed out the utility of knockout mutant for the functional analysis of single PIP2 aquaporins demonstrating that even highly homologous isoforms (e.g. PIP2;2 and PIP2;3) exhibit non-redundant functions.

Aquaporins have been suggested to act as multifunctional channels but the lack of characterization of transport selectivity renders a complete comprehensive analysis difficult. In fact, aquaporins are often characterized exclusively in terms of their water transport ability; although a water channel activity has not been experimentally proven for most of them. The number of PIP2 isoforms in plants raises the question whether water is the only molecule capable of transiting through aquaporins, e.g. for PIP2;3, and what would be the physiological relevance of such permeation should be of major interest in future prospects?

A transcriptional interrelation of *PIPs* and even *TIPs* as well as a PIP protein relationship has been brought to light suggesting complex regulatory mechanisms. Several *MIPs* isoforms may work in combination for the maintenance of plant water status. Analysis of single and multiple knockout mutants (both PIPs and TIPs) and the effect of a particular MIP member on others may help integrate and interpret the function of plant aquaporins.

Eventually, the method using deuterated water as a tracer adapted in this study has proven useful and demonstrated that single aquaporin, i.e. PIP2;1 or PIP2;2 are involved in plant

water relations. Experiments isolating roots or leaves from each other could help to elucidate whether and to what extent PIP2 aquaporins contribute to root water uptake and/ or leaves hydraulic exchange.

Table 13. *Arabidopsis* PIP2 isoform classification.

[1]Using array hybridization Leonhardt et al. (2004) found weak evidence for *PIP2;1* transcripts in a guard cell fraction and for *PIP2;1, PIP2;2, PIP2;6,* and *PIP2;7* transcripts in mesophyll cells. [2]Abbreviations: D drought, H heat, C cold, O Osmotic, S Salt, *B.c. Botrytis cinerea, P.i. Phytophthora infestans, P.s. Pseudomonas syringae,* A Auxin, AT Auxin transport, ATI Auxin transport inhibitor, ET Ethylene inhibitor, CW Cell wall, HM Hormone metabolism, MC miscellaneous, PS Photosynthesis, RX redox, SA salicylic acid, ST stress, TP, transport. Arrows indicate up- or downregulation of transcripts.

Gene		PIP2;2	PIP2;1	PIP2;7	PIP2;3	PIP2;8	PIP2;5	PIP2;6	PIP2;4
Root	Hair	+	+	+	+	+	-	-	+
	Exodermis	-	-	-	-	-	-	-	(+)
	Cortex	(+)	-	(+)	-	-	-	-	+
	Endodermis	+	+	+	-	-	(+)	+	(+)
	Stele	+	+	+	+	+	+	-	-
Leaf	Vasculature	+	+	+	+	-	+	+	-
	Mesophyll	+[1]	(+)[1]	+[1]	-	leaf base	+	+[1]	-
	Stomata (n. s.)	-	-	-	+	-	-	-	-
Flower	Filament/ anther	+/-	+/+	+/-	+/-	-/-	-/-	+/-	-/+
	Pistil/ stigma	+/+	+/-	-/-	-/-	+/-	+/+	+/-	-/-
	Sepal/ petal	+/-	+/-	-/-	+/-	(+)/-	(+)/-	-/(+)	-/-
Expression level		high	high	high	low	low	Low	high	high
Water channel activity		+	+	+	+	predicted	Predicted	predicted	predicted
Relation with other *PIP2*		2;4	2;7/2;8	2;1	2;4	2;1	-	-	2;2/2;3
Relation with *PIP1* genes		1;1,1;2	1;1,1;2,1;3,1;5	1;2,1;3	1;1,1;2	1;2,1;3	-	-	-
Influence on PIP1 proteins		+	+	n.d.	-	-	-	-	-
Relation with other TIP		1;1, 2;2, 2;3	1;1, 1;2, 2;1	1;2, 2;1	1;1, 2;2, 2;3	1;2, 2;1	-	-	2;2,2;3,4;1
Abiotic stress responses[2]	Drought, heat, cold[2]	D↑, H↑	-	-	D↑, H↑	-	D↑, C↑, H↑	C↑	C↑
	Osmotic, salt[2]	O↓, S↓	-	O↓	O↓, S↓	O↓	S↑	-	O↓, S↓
	Others	Low nitrate↓	Low nitrate↓	-	-	-	-	Low nitrate↓	Oxidative↓
Biotic stress responses[2]		-	-	B.c.↓	-	B.c.↓	P.i↓, P.s.↑	P.i.↓	B.c.↓
Hormone responses[2]		SA↓, AT↓, ATI↓, EI↓	SA↓, ATI↓	-	SA↓, AT↓, ATI↓, EI↓	-	-	-	SA↓, A↓, AT↓, ATI↓, EI↓
Co-regulation with (ACT)[2]		TP	TP, PS	CW	TP	CW	No enrichment	PS, RX	ST, CW, MC
Co-regulation with (BAR)[2]		TP, ST	TP, PS	PS, ST, HM	TP, ST	PS, ST, HM	No enrichment	PS, RX, CW, ST	ST, CW, MC, TP

5 REFERENCES

Affenzeller MJ (2003) *Arabidopsis thaliana* unter Wasserstress: Transkriptionsprofile der MIP-Familie und von Genen aus dem Stress- und Sekundärstoffwechsel. Dissertation. Ludwig-Maximilians-Universität, München

Agre P, Saboori AM, Asimos A, Smith BL (1987) Purification and partial characterization of the Mr 30,000 integral membrane protein associated with the erythrocyte Rh(D) antigen. J Biol Chem **262:** 17497-17503

Aharon R, Shahak Y, Wininger S, Bendov R, Kapulnik Y, Galili G (2003) Overexpression of a plasma membrane aquaporin in transgenic tobacco improves plant vigor under favorable growth conditions but not under drought or salt stress. Plant Cell **15:** 439-447

Alexandersson E, Fraysse L, Sjovall-Larsen S, Gustavsson S, Fellert M, Karlsson M, Johanson U, Kjellbom P (2005) Whole gene family expression and drought stress regulation of aquaporins. Plant Mol Biol **59:** 469-484

Alexandersson E, Saalbach G, Larsson C, Kjellbom P (2004) Arabidopsis plasma membrane proteomics identifies components of transport, signal transduction and membrane trafficking. Plant Cell Physiol **45:** 1543-1556

Alleva K, Niemietz CM, Sutka M, Maurel C, Parisi M, Tyerman SD, Amodeo G (2006) Plasma membrane of Beta vulgaris storage root shows high water channel activity regulated by cytoplasmic pH and a dual range of calcium concentrations. J Exp Bot **57:** 609-621

Allison GB, Gat JR, Leaney FW (1985) The relationship between deuterium and oxygen-18 delta values in leaf water. Chemical Geology (Isotope Geoscience Section) **58:** 145 - 156

Alonso JM, Stepanova AN, Leisse TJ, Kim CJ, Chen H, Shinn P, Stevenson DK, Zimmerman J, Barajas P, Cheuk R, Gadrinab C, Heller C, Jeske A, Koesema E, Meyers CC, Parker H, Prednis L, Ansari Y, Choy N, Deen H, Geralt M, Hazari N, Hom E, Karnes M, Mulholland C, Ndubaku R, Schmidt I, Guzman P, Aguilar-Henonin L, Schmid M, Weigel D, Carter DE, Marchand T, Risseeuw E, Brogden D, Zeko A, Crosby WL, Berry CC, Ecker JR (2003) Genome-wide insertional mutagenesis of Arabidopsis thaliana. Science **301:** 653-657

Amiry-Moghaddam M, Lindland H, Zelenin S, Roberg BA, Gundersen BB, Petersen P, Rinvik E, Torgner IA, Ottersen OP (2005) Brain mitochondria contain aquaporin water channels: evidence for the expression of a short AQP9 isoform in the inner mitochondrial membrane. FASEB J **19:** 1459-1467

Arnold K, Bordoli L, Kopp J, Schwede T (2006) The SWISS-MODEL workspace: a web-based environment for protein structure homology modelling. Bioinformatics **22:** 195-201

Aroca R, Amodeo G, Fernandez-Illescas S, Herman EM, Chaumont F, Chrispeels MJ (2005) The role of aquaporins and membrane damage in chilling and hydrogen peroxide induced changes in the hydraulic conductance of maize roots. Plant Physiol **137:** 341-353

Ausubel FM, Brent R, Kingston RE, Moore DD, Seidman JG, Smith JA, Struhl K (1987 with quarterly updates) Current Protocols in Molecular Biology. John Wiley, New York, NY.

Azad AK, Sawa Y, Ishikawa T, Shibata H (2004) Phosphorylation of plasma membrane aquaporin regulates temperature-dependent opening of tulip petals. Plant Cell Physiol **45:** 608-617

Balzergue S, Dubreucq B, Chauvin S, Le-Clainche I, Le Boulaire F, de Rose R, Samson F, Biaudet V, Lecharny A, Cruaud C, Weissenbach J, Caboche M, Lepiniec L (2001) Improved PCR-walking for large-scale isolation of plant T-DNA borders. Biotechniques. Mar;30(3):496-8, 502, 504 **30:** 496-504

Barkla BJ, Vera-Estrella R, Pantoja O, Kirch HH, Bohnert HJ (1999) Aquaporin localization - how valid are the TIP and PIP labels? Trends Plant Sci **4:** 86-88

Barnes B, Farquhar G, Gan K (2004) Modelling the isotope enrichment of leaf water. J Math Biol **48:** 672-702

Barrieu F, Chaumont F, Chrispeels MJ (1998) High expression of the tonoplast aquaporin ZmTIP1 in epidermal and conducting tissues of maize. Plant Physiol **117:** 1153-1163

Benga G, Popescu O, Borza V, Pop VI, Muresan A, Mocsy I, Brain A, Wrigglesworth JM (1986) Water permeability in human erythrocytes: identification of membrane proteins involved in water transport. Eur J Cell Biol **41:** 252-262

Benjamini Y, Hochberg Y (1995) Controlling the false discovery rate: a practical and powerful approach to multiple testing. J. R. Stat. Soc. Ser. **B57:** 289–300

Bhat RA, Panstruga R (2005) Lipid rafts in plants. Planta **223:** 5-19

Biela A, Grote K, Otto B, Hoth S, Hedrich R, Kaldenhoff R (1999) The Nicotiana tabacum plasma membrane aquaporin NtAQP1 is mercury-insensitive and permeable for glycerol. Plant J **18:** 565-570

Bienert GP, Moller AL, Kristiansen KA, Schulz A, Moller IM, Schjoerring JK, Jahn TP (2007) Specific aquaporins facilitate the diffusion of hydrogen peroxide across membranes. J Biol Chem **282:** 1183-1192

Bienert GP, Schjoerring JK, Jahn TP (2006) Membrane transport of hydrogen peroxide. Biochim Biophys Acta **1758:** 994-1003

Birnbaum K, Shasha DE, Wang JY, Jung JW, Lambert GM, Galbraith DW, Benfey PN (2003) A gene expression map of the *Arabidopsis* root. Science **302:** 1956-1960

Bots M, Feron R, Uehlein N, Weterings K, Kaldenhoff R, Mariani T (2005a) PIP1 and PIP2 aquaporins are differentially expressed during tobacco anther and stigma development. J Exp Bot **56:** 113-121

Bots M, Vergeldt F, Wolters-Arts M, Weterings K, van As H, Mariani C (2005b) Aquaporins of the PIP2 class are required for efficient anther dehiscence in tobacco. Plant Physiol **137:** 1049-1056

Boursiac Y, Chen S, Luu DT, Sorieul M, van den Dries N, Maurel C (2005) Early effects of salinity on water transport in Arabidopsis roots. Molecular and cellular features of aquaporin expression. Plant Physiol **139:** 790-805

Bray EA (1997) Plant responses to water deficit. Trends in Plant Science **2:** 48-54

Bray EA (2004) Genes commonly regulated by water-deficit stress in Arabidopsis thaliana. J Exp Bot **55:** 2331-2341

Brown D (2003) The ins and outs of aquaporin-2 trafficking. Am J Physiol Renal Physiol **284:** F893-901

Cabanero FJ, Martinez-Ballesta MC, Teruel JA, Carvajal M (2006) New evidence about the relationship between water channel activity and calcium in salinity-stressed pepper plants. Plant Cell Physiol **47:** 224-233

Calamita G, Ferri D, Gena P, Liquori GE, Cavalier A, Thomas D, Svelto M (2005) The inner mitochondrial membrane has aquaporin-8 water channels and is highly permeable to water. J Biol Chem **280:** 17149-17153

Chang S, Puryear J, Cairney J (1993) A simple and efficient method for isolating RNA from pine trees. Plant Molecular Biology Reporter **11:** 113-116

Chaumont F, Barrieu F, Herman EM, Chrispeels MJ (1998) Characterization of a maize tonoplast aquaporin expressed in zones of cell division and elongation. Plant Physiol **117:** 1143-1152

Chaumont F, Barrieu F, Jung R, Chrispeels MJ (2000) Plasma membrane intrinsic proteins from maize cluster in two sequence subgroups with differential aquaporin activity. Plant Physiol **122:** 1025-1034

Chaumont F, Barrieu F, Wojcik E, Chrispeels MJ, Jung R (2001) Aquaporins constitute a large and highly divergent protein family in maize. Plant Physiol **125:** 1206-1215

Chaumont F, Moshelion M, Daniels MJ (2005) Regulation of plant aquaporin activity. Biol Cell **97:** 749-764

Cleveland W, Grosse E, Shyu W (1992) Local regression models. *In* JM Chambers, TJ Hastie, eds, Statistical Models in S. Wadsworth and Brooks, Pacific Grove, CA**:** 309-376

Clough SJ, Bent AF (1998) Floral dip: a simplified method for Agrobacterium-mediated transformation of Arabidopsis thaliana. Plant J **16:** 735-743

Cochard H, Venisse JS, Barigah TS, Brunel N, Herbette S, Guilliot A, Tyree MT, Sakr S (2007) Putative role of aquaporins in variable hydraulic conductance of leaves in response to light. Plant Physiol **143:** 122-133

Cooper GJ, Boron WF (1998) Effect of PCMBS on CO2 permeability of Xenopus oocytes expressing aquaporin 1 or its C189S mutant. Am J Physiol **275:** C1481-1486

Cooper GJ, Zhou Y, Bouyer P, Grichtchenko, II, Boron WF (2002) Transport of volatile solutes through AQP1. J Physiol **542:** 17-29

Craig H, Gordon LI (1965) Deuterium and oxygen-18 variations in the ocean and the marine atmosphere. E Tongiori, ed, Proceedings of a Conference on Stable Isotopes in Oceanographic studies and Paleotemperatures, Spoleto, Italy**:** 9-130

Craigon DJ, James N, Okyere J, Higgins J, Jotham J, May S (2004) NASCArrays: a repository for microarray data generated by NASC's transcriptomics service. Nucleic Acids Res **32:** D575-577

Cuntz M, Ogee J, Farquhar GD, Peylin P, Cernusak LA (2007) Modelling advection and diffusion of water isotopologues in leaves. Plant Cell Environ **30:** 892-909

Cutler SR, Ehrhardt DW, Griffitts JS, Somerville CR (2000) Random GFP::cDNA fusions enable visualization of subcellular structures in cells of Arabidopsis at a high frequency. Proc Natl Acad Sci U S A **97:** 3718-3723

Dainty J, Ginzburg BZ (1963) Irreversible thermodynamics and frictional models of membrane processes, with particular reference to the cell membrane. J Theor Biol **5:** 256-265

Daniels MJ, Chaumont F, Mirkov TE, Chrispeels MJ (1996) Characterization of a new vacuolar membrane aquaporin sensitive to mercury at a unique site. Plant Cell **8:** 587-599

Daniels MJ, Chrispeels MJ, Yeager M (1999) Projection structure of a plant vacuole membrane aquaporin by electron cryo-crystallography. J Mol Biol **294:** 1337-1349

Daniels MJ, Mirkov TE, Chrispeels MJ (1994) The plasma membrane of Arabidopsis thaliana contains a mercury-insensitive aquaporin that is a homolog of the tonoplast water channel protein TIP. Plant Physiol **106:** 1325-1333

Daniels MJ, Wood MR, Yeager M (2006) In vivo functional assay of a recombinant aquaporin in Pichia pastoris. Appl Environ Microbiol **72:** 1507-1514

de Groot BL, Grubmüller H (2001) Water Permeation Across Biological Membranes: Mechanism and Dynamics of Aquaporin-1 and GlpF. Science **294:** 2353-2357

Dean RM, Rivers RL, Zeidel ML, Roberts DM (1999) Purification and functional reconstitution of soybean nodulin 26. An aquaporin with water and glycerol transport properties. Biochemistry **38:** 347-353

del Martinez-Ballesta MC, Silva C, Lopez-Berenguer C, Cabanero FJ, Carvajal M (2006) Plant aquaporins: new perspectives on water and nutrient uptake in saline environment. Plant Biol (Stuttg) **8:** 535-546

Dixit R, Rizzo C, Nasrallah M, Nasrallah J (2001) The brassica MIP-MOD gene encodes a functional water channel that is expressed in the stigma epidermis. Plant Mol Biol **45:** 51-62

Dordas C, Chrispeels MJ, Brown PH (2000) Permeability and channel-mediated transport of boric acid across membrane vesicles isolated from squash roots. Plant Physiol **124:** 1349-1362

Dudoit S, Yang Y, Callow MJ, Speed TP (2000) Statistical methods for identifying differentially expressed genes in replicated cDNA microarray experiments. Technical reports 578. Stanford University School of Medicine, Stanford, CA.

Edgar R, Domrachev M, Lash AE (2002) Gene Expression Omnibus: NCBI gene expression and hybridization array data repository. Nucleic Acids Res **30:** 207-210

Elortza F, Nuhse TS, Foster LJ, Stensballe A, Peck SC, Jensen ON (2003) Proteomic analysis of glycosylphosphatidylinositol-anchored membrane proteins. Mol Cell Proteomics **2:** 1261-1270

Esen A (1978) A simple method for quantitative, semiquantitative, and qualitative assay of protein. Anal Biochem **89:** 264-273

Farquhar GD, Cernusak LA, Barnes B (2007) Heavy water fractionation during transpiration. Plant Physiol **143:** 11-18

Farquhar GD, Hubick KT, Condon AG, Richards RA (1989) Carbon isotope fractionation and plant water-use efficiency. *In* PW Rundel, JR Ehleringer, KA Nagy, eds, Stable Isotopes in Ecological Research. Springer-Verlag, Berlin**:** 21-40

Fetter K, Van Wilder V, Moshelion M, Chaumont F (2004) Interactions between plasma membrane aquaporins modulate their water channel activity. Plant Cell **16:** 215-228

Finkelstein A (1987) Water Movement through Lipid Bilayers, Pores, and Plasma Membranes. Theory and Reality. Distinguished Lectures Series of the Society of General Physiologists. New York: John Wiley & Sons **Vol. 4:** 1-228

Flanagan LB, Comstock JP, Ehleringer JR (1991) Comparison of Modeled and Observed Environmental Influences on the Stable Oxygen and Hydrogen Isotope Composition of Leaf Water in Phaseolus vulgaris L. Plant Physiol **96:** 588-596

Flanagan LB, Ehleringer JR (1991) Effects of Mild Water Stress and Diurnal Changes in Temperature and Humidity on the Stable Oxygen and Hydrogen Isotopic Composition of Leaf Water in Cornus stolonifera L. Plant Physiol **97:** 298-305

Flexas J, Ribas-Carbo M, Hanson DT, Bota J, Otto B, Cifre J, McDowell N, Medrano H, Kaldenhoff R (2006) Tobacco aquaporin NtAQP1 is involved in mesophyll conductance to CO2 in vivo. Plant J **48:** 427-439

Fotiadis D, Jeno P, Mini T, Wirtz S, Muller SA, Fraysse L, Kjellbom P, Engel A (2001) Structural characterization of two aquaporins isolated from native spinach leaf plasma membranes. J Biol Chem **276:** 1707-1714

Franck KI (1999) Untersuchungen zur Lokalisation, Genexpression und physiologischen Rolle der Plasmamembran-Aquaporine aus *Arabidopsis thaliana*. Dissertation. Ludwig-Maximilians-Universität, München

Frangne N, Maeshima M, Schäffner AR, Mandel T, Martinoia E, Bonnemain JL (2001) Expression and distribution of a vaculoar aquaporin in young and mature leaf tissues of Brassica napus in relation to water fluxes. Planta **212:** 270-278

Fray RG, Wallace A, Grierson D, Lycett GW (1994) Nucleotide sequence and expression of a ripening and water stress-related cDNA from tomato with homology to the MIP class of membrane channel proteins. Plant Mol Biol **24:** 539-543

Fu D, Libson A, Miercke LJ, Weitzman C, Nollert P, Krucinski J, Stroud RM (2000) Structure of a glycerol-conducting channel and the basis for its selectivity. Science **290:** 481-486

Fujiyoshi Y, Mitsuoka K, de Groot BL, Philippsen A, Grubmüller H, Agre P, Engel A (2002) Structure and function of water channels. Curr Opin Struct Biol **12:** 509-515

Gan KS, Wong SC, Yong JWH, Farquhar GD (2003) Evaluation of models of leaf water 18O enrichment using measurements of spatial patterns of vein xylem water, leaf water and dry matter in maize leaves. Plant, Cell & Environment **26:** 1479-1495

Gerbeau P, Amodeo G, Henzler T, Santoni V, Ripoche P, Maurel C (2002) The water permeability of Arabidopsis plasma membrane is regulated by divalent cations and pH. Plant J **30:** 71-81

Gerbeau P, Guclu J, Ripoche P, Maurel C (1999) Aquaporin Nt-TIPa can account for the high permeability of tobacco cell vacuolar membrane to small neutral solutes. Plant J **18:** 577-587

Gibeaut DM, Hulett J, Cramer GR, Seemann JR (1997) Maximal biomass of Arabidopsis thaliana using a simple, low-maintenance hydroponic method and favorable environmental conditions. Plant Physiol **115:** 317-319

Glombitza S, Dubuis PH, Thulke O, Welzl G, Bovet L, Götz M, Affenzeller M, Geist B, Hehn A, Asnaghi C, Ernst D, Seidlitz HK, Gundlach H, Mayer KF, Martinoia E, Werck-Reichhart D, Mauch F, Schäffner AR (2004) Crosstalk and differential response to abiotic and biotic stressors reflected at the transcriptional level of effector genes from secondary metabolism. Plant Mol Biol **54:** 817-835

Gonen T, Sliz P, Kistler J, Cheng Y, Walz T (2004) Aquaporin-0 membrane junctions reveal the structure of a closed water pore. Nature **429:** 193-197

Guenther JF, Chanmanivone N, Galetovic MP, Wallace IS, Cobb JA, Roberts DM (2003) Phosphorylation of soybean nodulin 26 on serine 262 enhances water permeability and is regulated developmentally and by osmotic signals. Plant Cell **15:** 981-991

Haberer G, Mader MT, Kosarev P, Spannagl M, Yang L, Mayer KF (2006) Large-scale cis-element detection by analysis of correlated expression and sequence conservation between Arabidopsis and Brassica oleracea. Plant Physiol **142:** 1589-1602

Hachez C, Moshelion M, Zelazny E, Cavez D, Chaumont F (2006b) Localization and quantification of plasma membrane aquaporin expression in maize primary root: a clue to understanding their role as cellular plumbers. Plant Mol Biol **62:** 305-323

Hachez C, Zelazny E, Chaumont F (2006a) Modulating the expression of aquaporin genes in planta: A key to understand their physiological functions? Biochim Biophys Acta **1758:** 1142-1156

Hammes UZ, Schachtman DP, Berg RH, Nielsen E, Koch W, McIntyre LM, Taylor CG (2005) Nematode-induced changes of transporter gene expression in Arabidopsis roots. Mol Plant Microbe Interact **18:** 1247-1257

Hanba YT, Shibasaka M, Hayashi Y, Hayakawa T, Kasamo K, Terashima I, Katsuhara M (2004) Overexpression of the barley aquaporin HvPIP2;1 increases internal CO(2) conductance and CO(2) assimilation in the leaves of transgenic rice plants. Plant Cell Physiol **45:** 521-529

Helliker BR, Ehleringer JR (2000) Establishing a grassland signature in veins: 18O in the leaf water of C3 and C4 grasses. Proc Natl Acad Sci U S A **97:** 7894-7898

Heymann JB, Engel A (1999) Aquaporins: Phylogeny, Structure, and Physiology of Water Channels. News Physiol Sci **14:** 187-193

Higuchi T, Suga S, Tsuchiya T, Hisada H, Morishima S, Okada Y, Maeshima M (1998) Molecular cloning, water channel activity and tissue specific expression of two isoforms of radish vacuolar aquaporin. Plant Cell Physiol **39:** 905-913

Hill AE, Shachar-Hill B, Shachar-Hill Y (2004) What are aquaporins for? J Membr Biol **197:** 1-32

Hiroaki Y, Tani K, Kamegawa A, Gyobu N, Nishikawa K, Suzuki H, Walz T, Sasaki S, Mitsuoka K, Kimura K, Mizoguchi A, Fujiyoshi Y (2006) Implications of the aquaporin-4 structure on array formation and cell adhesion. J Mol Biol **355:** 628-639

Holm LM, Jahn TP, Moller AL, Schjoerring JK, Ferri D, Klaerke DA, Zeuthen T (2005) NH3 and NH4+ permeability in aquaporin-expressing Xenopus oocytes. Pflugers Arch **450:** 415-428

Hukin D, Doering-Saad C, Thomas CR, Pritchard J (2002) Sensitivity of cell hydraulic conductivity to mercury is coincident with symplasmic isolation and expression of plasmalemma aquaporin genes in growing maize roots. Planta **215:** 1047-1056

Ikeda S, Nasrallah JB, Dixit R, Preiss S, Nasrallah ME (1997) An aquaporin-like gene required for the Brassica self-incompatibility response. Science **276:** 1564-1566

Ishikawa F, Suga S, Uemura T, Sato MH, Maeshima M (2005) Novel type aquaporin SIPs are mainly localized to the ER membrane and show cell-specific expression in Arabidopsis thaliana. FEBS Lett **579:** 5814-5820

Jahn TP, Moller AL, Zeuthen T, Holm LM, Klaerke DA, Mohsin B, Kuhlbrandt W, Schjoerring JK (2004) Aquaporin homologues in plants and mammals transport ammonia. FEBS Lett **574:** 31-36

Jammes F, Lecomte P, de Almeida-Engler J, Bitton F, Martin-Magniette ML, Renou JP, Abad P, Favery B (2005) Genome-wide expression profiling of the host response to root-knot nematode infection in Arabidopsis. Plant J **44:** 447-458

Jang JY, Kim DG, Kim YO, Kim JS, Kang H (2004) An expression analysis of a gene family encoding plasma membrane aquaporins in response to abiotic stresses in Arabidopsis thaliana. Plant Mol Biol **54:** 713-725

Jang JY, Lee SH, Rhee JY, Chung GC, Ahn SJ, Kang H (2007a) Transgenic Arabidopsis and tobacco plants overexpressing an aquaporin respond differently to various abiotic stresses. Plant Mol Biol **64:** 621-632

Jang JY, Rhee JY, Kim DG, Chung GC, Lee JH, Kang H (2007b) Ectopic expression of a foreign aquaporin disrupts the natural expression patterns of endogenous aquaporin genes and alters plant responses to different stress conditions. Plant Cell Physiol **48:** 1331-1339

Javot H, Lauvergeat V, Santoni V, Martin-Laurent F, Güclü J, Vinh J, Heyes J, Franck KI, Schäffner AR, Bouchez D, Maurel C (2003) Role of a single aquaporin isoform in root water uptake. Plant Cell **15:** 509-522

Javot H, Maurel C (2002) The role of aquaporins in root water uptake. Ann Bot (Lond) **90:** 301-313

Jefferson RA, Kavanagh TA, Bevan MW (1987) GUS fusions: beta-glucuronidase as a sensitive and versatile gene fusion marker in higher plants. Embo J **6:** 3901-3907

Jen CH, Manfield IW, Michalopoulos I, Pinney JW, Willats WG, Gilmartin PM, Westhead DR (2006) The Arabidopsis co-expression tool (ACT): a WWW-based tool and database for microarray-based gene expression analysis. Plant J **46:** 336-348

Johanson U, Gustavsson S (2002) A new subfamily of major intrinsic proteins in plants. Mol Biol Evol **19:** 456-461

Johanson U, Karlsson M, Johansson I, Gustavsson S, Sjovall S, Fraysse L, Weig AR, Kjellbom P (2001) The complete set of genes encoding major intrinsic proteins in Arabidopsis provides a framework for a new nomenclature for major intrinsic proteins in plants. Plant Physiol **126:** 1358-1369

Johansson I, Karlsson M, Johanson U, Larsson C, Kjellbom P (2000) The role of aquaporins in cellular and whole plant water balance. Biochim Biophys Acta **1465:** 324-342

Johansson I, Karlsson M, Shukla VK, Chrispeels MJ, Larsson C, Kjellbom P (1998) Water transport activity of the plasma membrane aquaporin PM28A is regulated by phosphorylation. Plant Cell **10:** 451-459

Johansson I, Larsson C, Ek B, Kjellbom P (1996) The major integral proteins of spinach leaf plasma membranes are putative aquaporins and are phosphorylated in response to Ca2+ and apoplastic water potential. Plant Cell **8:** 1181-1191

Johnson KD, Chrispeels MJ (1992) Tonoplast-Bound Protein Kinase Phosphorylates Tonoplast Intrinsic Protein. Plant Physiol **100:** 1787-1795

Jones AM, Thomas V, Bennett MH, Mansfield J, Grant M (2006) Modifications to the Arabidopsis defense proteome occur prior to significant transcriptional change in response to inoculation with Pseudomonas syringae. Plant Physiol **142:** 1603-1620

Jung JS, Preston GM, Smith BL, Guggino WB, Agre P (1994) Molecular structure of the water channel through aquaporin CHIP. The hourglass model. J Biol Chem **269:** 14648-14654

Kaldenhoff R, Fischer M (2006) Functional aquaporin diversity in plants. Biochimica et Biophysica Acta (BBA) - Biomembranes **1758:** 1134-1141

Kaldenhoff R, Grote K, Zhu JJ, Zimmermann U (1998) Significance of plasmalemma aquaporins for water-transport in Arabidopsis thaliana. Plant J **14:** 121-128

Kaldenhoff R, Kolling A, Meyers J, Karmann U, Ruppel G, Richter G (1995) The blue light-responsive AthH2 gene of Arabidopsis thaliana is primarily expressed in expanding as well as in differentiating cells and encodes a putative channel protein of the plasmalemma. Plant J **7:** 87-95

Kammerloher W, Fischer U, Piechottka GP, Schäffner AR (1994) Water channels in the plant plasma membrane cloned by immunoselection from a mammalian expression system. Plant J **6:** 187-199

Karimi M, Inze D, Depicker A (2002) GATEWAY vectors for Agrobacterium-mediated plant transformation. Trends Plant Sci **7:** 193-195

Katsuhara M, Akiyama Y, Koshio K, Shibasaka M, Kasamo K (2002) Functional analysis of water channels in barley roots. Plant Cell Physiol **43:** 885-893

Kawaguchi R, Girke T, Bray EA, Bailey-Serres J (2004) Differential mRNA translation contributes to gene regulation under non-stress and dehydration stress conditions in Arabidopsis thaliana. Plant J **38:** 823-839

Kilian J, Whitehead D, Horak J, Wanke D, Weinl S, Batistic O, D'Angelo C, Bornberg-Bauer E, Kudla J, Harter K (2007) The AtGenExpress global stress expression data set: protocols, evaluation and model data analysis of UV-B light, drought and cold stress responses. Plant J **50:** 347-363

Kirch HH, Vera-Estrella R, Golldack D, Quigley F, Michalowski CB, Barkla BJ, Bohnert HJ (2000) Expression of water channel proteins in Mesembryanthemum crystallinum. Plant Physiol **123:** 111-124

Kobae Y, Mizutani M, Segami S, Maeshima M (2006) Immunochemical analysis of aquaporin isoforms in Arabidopsis suspension-cultured cells. Biosci Biotechnol Biochem **70:** 980-987

Kopp J, Schwede T (2004) The SWISS-MODEL Repository of annotated three-dimensional protein structure homology models. Nucleic Acids Res **32:** D230-234

Kreps JA, Wu Y, Chang HS, Zhu T, Wang X, Harper JF (2002) Transcriptome changes for Arabidopsis in response to salt, osmotic, and cold stress. Plant Physiol **130:** 2129-2141

Kukulski W, Schenk AD, Johanson U, Braun T, de Groot BL, Fotiadis D, Kjellbom P, Engel A (2005) The 5A structure of heterologously expressed plant aquaporin SoPIP2;1. J Mol Biol **350:** 611-616

Laemmli UK (1970) Cleavage of structural proteins during the assembly of the head of bacteriophage T4. Nature **227:** 680-685

Lee JK, Kozono D, Remis J, Kitagawa Y, Agre P, Stroud RM (2005) Structural basis for conductance by the archaeal aquaporin AqpM at 1.68 A. Proc Natl Acad Sci U S A **102:** 18932-18937

Leonhardt N, Kwak JM, Robert N, Waner D, Leonhardt G, Schroeder JI (2004) Microarray expression analyses of Arabidopsis guard cells and isolation of a recessive abscisic acid hypersensitive protein phosphatase 2C mutant. Plant Cell **16:** 596-615

Lian HL, Yu X, Ye Q, Ding X, Kitagawa Y, Kwak SS, Su WA, Tang ZC (2004) The role of aquaporin RWC3 in drought avoidance in rice. Plant Cell Physiol **45:** 481-489

Lin W, Peng Y, Li G, Arora R, Tang Z, Su W, Cai W (2007) Isolation and functional characterization of PgTIP1, a hormone-autotrophic cells-specific tonoplast aquaporin in ginseng. J Exp Bot **58:** 947-956

Lisso J, Steinhauser D, Altmann T, Kopka J, Mussig C (2005) Identification of brassinosteroid-related genes by means of transcript co-response analyses. Nucleic Acids Res **33:** 2685-2696

Loque D, Ludewig U, Yuan L, von Wiren N (2005) Tonoplast intrinsic proteins AtTIP2;1 and AtTIP2;3 facilitate NH3 transport into the vacuole. Plant Physiol **137:** 671-680

Ludevid D, Hofte H, Himelblau E, Chrispeels MJ (1992) The Expression Pattern of the Tonoplast Intrinsic Protein gamma-TIP in Arabidopsis thaliana Is Correlated with Cell Enlargement. Plant Physiol **100:** 1633-1639

Ma JF, Tamai K, Yamaji N, Mitani N, Konishi S, Katsuhara M, Ishiguro M, Murata Y, Yano M (2006) A silicon transporter in rice. Nature **440:** 688-691

Ma S, Quist TM, Ulanov A, Joly R, Bohnert HJ (2004) Loss of TIP1;1 aquaporin in Arabidopsis leads to cell and plant death. Plant J **40:** 845-859

Maathuis FJ, Filatov V, Herzyk P, Krijger GC, Axelsen KB, Chen S, Green BJ, Li Y, Madagan KL, Sanchez-Fernandez R, Forde BG, Palmgren MG, Rea PA, Williams LE, Sanders D, Amtmann A (2003) Transcriptome analysis of root transporters reveals participation of multiple gene families in the response to cation stress. Plant J **35:** 675-692

Macey RI (1984) Transport of water and urea in red blood cells. Am J Physiol **246:** C195-203

Majoube M (1971) Fractionnement en oxygène-18 et en deutèrium entre l'eau et sa vapeur. J Chim Phys **58:** 1423-1436

Manfield IW, Jen CH, Pinney JW, Michalopoulos I, Bradford JR, Gilmartin PM, Westhead DR (2006) Arabidopsis Co-expression Tool (ACT): web server tools for microarray-based gene expression analysis. Nucleic Acids Res **34:** W504-509

Marin-Olivier M, Chevalier T, Fobis-Loisy I, Dumas C, Gaude T (2000) Aquaporin PIP genes are not expressed in the stigma papillae in Brassica oleracea. Plant J **24:** 231-240

Marmagne A, Rouet MA, Ferro M, Rolland N, Alcon C, Joyard J, Garin J, Barbier-Brygoo H, Ephritikhine G (2004) Identification of new intrinsic proteins in Arabidopsis plasma membrane proteome. Mol Cell Proteomics **3:** 675-691

Marples D, Frokiaer J, Knepper MA, Nielsen S (1998) Disordered water channel expression and distribution in acquired nephrogenic diabetes insipidus. Proc Assoc Am Physicians **110:** 401-406

Martre P, Morillon R, Barrieu F, North GB, Nobel PS, Chrispeels MJ (2002) Plasma membrane aquaporins play a significant role during recovery from water deficit. Plant Physiol **130:** 2101-2110

Maurel C (2007) Plant aquaporins: Novel functions and regulation properties. FEBS Lett **581:** 2227-2236

Maurel C, Javot H, Lauvergeat V, Gerbeau P, Tournaire C, Santoni V, Heyes J (2002) Molecular physiology of aquaporins in plants. Int Rev Cytol **215:** 105-148

Maurel C, Kado RT, Guern J, Chrispeels MJ (1995) Phosphorylation regulates the water channel activity of the seed-specific aquaporin alpha-TIP. Embo J **14:** 3028-3035

Maurel C, Reizer J, Schroeder JI, Chrispeels MJ (1993) The vacuolar membrane protein gamma-TIP creates water specific channels in Xenopus oocytes. Embo J **12:** 2241-2247

Maurel C, Tacnet F, Guclu J, Guern J, Ripoche P (1997) Purified vesicles of tobacco cell vacuolar and plasma membranes exhibit dramatically different water permeability and water channel activity. Proc Natl Acad Sci U S A **94:** 7103-7108

Merlivat L (1978) Molecular diffusivities of $H_2^{18}O$ in gases. J Chem Phys **69:** 2864-2871

Mongrand S, Morel J, Laroche J, Claverol S, Carde JP, Hartmann MA, Bonneu M, Simon-Plas F, Lessire R, Bessoule JJ (2004) Lipid rafts in higher plant cells: purification and characterization of Triton X-100-insoluble microdomains from tobacco plasma membrane. J Biol Chem **279:** 36277-36286

Moshelion M, Becker D, Biela A, Uehlein N, Hedrich R, Otto B, Levi H, Moran N, Kaldenhoff R (2002) Plasma membrane aquaporins in the motor cells of Samanea saman: diurnal and circadian regulation. Plant Cell **14:** 727-739

Munns R (2002) Comparative physiology of salt and water stress. Plant Cell Environ **25:** 239-250

Murata K, Mitsuoka K, Hirai T, Walz T, Agre P, Heymann JB, Engel A, Fujiyoshi Y (2000) Structural determinants of water permeation through aquaporin-1. Nature **407:** 599-605

Nakhoul NL, Davis BA, Romero MF, Boron WF (1998) Effect of expressing the water channel aquaporin-1 on the CO2 permeability of Xenopus oocytes. Am J Physiol **274:** C543-548

Nelson CJ, Hegeman AD, Harms AC, Sussman MR (2006) A quantitative analysis of Arabidopsis plasma membrane using trypsin-catalyzed (18)O labeling. Mol Cell Proteomics **5:** 1382-1395

Niemietz CM, Tyerman SD (1997) Characterization of Water Channels in Wheat Root Membrane Vesicles. Plant Physiol **115:** 561-567

Niemietz CM, Tyerman SD (2000) Channel-mediated permeation of ammonia gas through the peribacteroid membrane of soybean nodules. FEBS Lett **465:** 110-114

Niemietz CM, Tyerman SD (2002) New potent inhibitors of aquaporins: silver and gold compounds inhibit aquaporins of plant and human origin. FEBS Lett **531:** 443-447

Passioura JB (1980) The Transport of Water from Soil to Shoot in Wheat Seedlings. J. Exp. Bot. **31:** 333-345

Persson S, Wei H, Milne J, Page GP, Somerville CR (2005) Identification of genes required for cellulose synthesis by regression analysis of public microarray data sets. Proc Natl Acad Sci U S A **102:** 8633-8638

Prasad GV, Coury LA, Finn F, Zeidel ML (1998) Reconstituted aquaporin 1 water channels transport CO_2 across membranes. J Biol Chem **273:** 33123-33126

Preston GM, Agre P (1991) Isolation of the cDNA for erythrocyte integral membrane protein of 28 kilodaltons: member of an ancient channel family. Proc Natl Acad Sci U S A **88:** 11110-11114

Preston GM, Carroll TP, Guggino WB, Agre P (1992) Appearance of water channels in Xenopus oocytes expressing red cell CHIP28 protein. Science **256:** 385-387

Puthoff DP, Nettleton D, Rodermel SR, Baum TJ (2003) Arabidopsis gene expression changes during cyst nematode parasitism revealed by statistical analyses of microarray expression profiles. Plant J **33:** 911-921

Quigley F, Rosenberg JM, Shachar-Hill Y, Bohnert HJ (2002) From genome to function: the Arabidopsis aquaporins. Genome Biol **3:** RESEARCH0001

Rautengarten C, Steinhauser D, Bussis D, Stintzi A, Schaller A, Kopka J, Altmann T (2005) Inferring hypotheses on functional relationships of genes: Analysis of the Arabidopsis thaliana subtilase gene family. PLoS Comput Biol **1:** e40

Reisen D, Leborgne-Castel N, Ozalp C, Chaumont F, Marty F (2003) Expression of a cauliflower tonoplast aquaporin tagged with GFP in tobacco suspension cells correlates with an increase in cell size. Plant Mol Biol **52:** 387-400

Rhee SY, Beavis W, Berardini TZ, Chen G, Dixon D, Doyle A, Garcia-Hernandez M, Huala E, Lander G, Montoya M, Miller N, Mueller LA, Mundodi S, Reiser L, Tacklind J, Weems DC, Wu Y, Xu I, Yoo D, Yoon J, Zhang P (2003) The Arabidopsis Information Resource (TAIR): a model organism database providing a centralized, curated gateway to Arabidopsis biology, research materials and community. Nucleic Acids Res **31:** 224-228

Riederer M (2006) Thermodynamics of the water permeability of plant cuticles: characterization of the polar pathway. J Exp Bot **57:** 2937-2942

Ringler P, Borgnia MJ, Stahlberg H, Maloney PC, Agre P, Engel A (1999) Structure of the water channel AqpZ from Escherichia coli revealed by electron crystallography. J Mol Biol **291:** 1181-1190

Rivers RL, Dean RM, Chandy G, Hall JE, Roberts DM, Zeidel ML (1997) Functional analysis of nodulin 26, an aquaporin in soybean root nodule symbiosomes. J Biol Chem **272:** 16256-16261

Robinson DG, Sieber H, Kammerloher W, Schäffner AR (1996) PIP1 Aquaporins Are Concentrated in Plasmalemmasomes of Arabidopsis thaliana Mesophyll. Plant Physiol **111:** 645-649

Roden JS, Ehleringer JR (1999a) Observations of hydrogen and oxygen isotopes in leaf water confirm the craig-gordon model under wide-ranging environmental conditions. Plant Physiol **120:** 1165-1174

Roden JS, Ehleringer JR (1999b) Hydrogen and oxygen isotope ratios of tree-ring cellulose for riparian trees grown long-term under hydroponically controlled environments. Oecologia **121:** 467-477

Rosso MG, Li Y, Strizhov N, Reiss B, Dekker K, Weisshaar B (2003) An Arabidopsis thaliana T-DNA mutagenized population (GABI-Kat) for flanking sequence tag-based reverse genetics. Plant Mol Biol **53:** 247-259

Sakurai J, Ishikawa F, Yamaguchi T, Uemura M, Maeshima M (2005) Identification of 33 rice aquaporin genes and analysis of their expression and function. Plant Cell Physiol **46:** 1568-1577

Sandal NN, Marcker KA (1988) Soybean nodulin 26 is homologous to the major intrinsic protein of the bovine lens fiber membrane. Nucleic Acids Res **16:** 9347

Santoni V, Verdoucq L, Sommerer N, Vinh J, Pflieger D, Maurel C (2006) Methylation of aquaporins in plant plasma membrane. Biochem J **400:** 189-197

Santoni V, Vinh J, Pflieger D, Sommerer N, Maurel C (2003) A proteomic study reveals novel insights into the diversity of aquaporin forms expressed in the plasma membrane of plant roots. Biochem J **373:** 289-296

Santrucek J, Kveton J, Setlik J, Bulickova L (2007) Spatial variation of deuterium enrichment in bulk water of snowgum leaves. Plant Physiol **143:** 88-97

Saparov SM, Kozono D, Rothe U, Agre P, Pohl P (2001) Water and ion permeation of aquaporin-1 in planar lipid bilayers. Major differences in structural determinants and stoichiometry. J Biol Chem **276:** 31515-31520

Sarda X, Tousch D, Ferrare K, Legrand E, Dupuis JM, Casse-Delbart F, Lamaze T (1997) Two TIP-like genes encoding aquaporins are expressed in sunflower guard cells. Plant J **12:** 1103-1111

Savage DF, Egea PF, Robles-Colmenares Y, O'Connell JD, 3rd, Stroud RM (2003) Architecture and selectivity in aquaporins: 2.5 a X-ray structure of aquaporin Z. PLoS Biol **1:** E72

Schäffner AR (1998) Aquaporin function, structure, and expression: are there more surprises to surface in water relations? Planta **204:** 131-139

Schenk AD, Werten PJ, Scheuring S, de Groot BL, Muller SA, Stahlberg H, Philippsen A, Engel A (2005) The 4.5 A structure of human AQP2. J Mol Biol **350:** 278-289

Schmid M, Davison TS, Henz SR, Pape UJ, Demar M, Vingron M, Scholkopf B, Weigel D, Lohmann JU (2005) A gene expression map of Arabidopsis thaliana development. Nat Genet **37:** 501-506

Secchi F, Lovisolo C, Uehlein N, Kaldenhoff R, Schubert A (2007) Isolation and functional characterization of three aquaporins from olive (Olea europaea L.). Planta **225:** 381-392

Seki M, Ishida J, Narusaka M, Fujita M, Nanjo T, Umezawa T, Kamiya A, Nakajima M, Enju A, Sakurai T, Satou M, Akiyama K, Yamaguchi-Shinozaki K, Carninci P, Kawai J, Hayashizaki Y, Shinozaki K (2002b) Monitoring the expression pattern of around 7,000 Arabidopsis genes under ABA treatments using a full-length cDNA microarray. Funct Integr Genomics **2:** 282-291

Seki M, Narusaka M, Ishida J, Nanjo T, Fujita M, Oono Y, Kamiya A, Nakajima M, Enju A, Sakurai T, Satou M, Akiyama K, Taji T, Yamaguchi-Shinozaki K, Carninci P, Kawai J, Hayashizaki Y, Shinozaki K (2002a) Monitoring the expression profiles of 7000 Arabidopsis genes under drought, cold and high-salinity stresses using a full-length cDNA microarray. Plant J **31:** 279-292

Sessions A, Burke E, Presting G, Aux G, McElver J, Patton D, Dietrich B, Ho P, Bacwaden J, Ko C, Clarke JD, Cotton D, Bullis D, Snell J, Miguel T, Hutchison D, Kimmerly B, Mitzel T, Katagiri F, Glazebrook J, Law M, Goff SA (2002) A High-Throughput Arabidopsis Reverse Genetics System. Plant Cell **14:** 2985-2994

Shahollari B, Peskan-Berghofer T, Oelmuller R (2004) Receptor kinases with leucine-rich repeats are enriched in Triton X-100 insoluble plasma membrane microdomains from plants. . Physiol Plantarum **122:** 397–403

Siefritz F, Otto B, Bienert GP, van der Krol A, Kaldenhoff R (2004) The plasma membrane aquaporin NtAQP1 is a key component of the leaf unfolding mechanism in tobacco. Plant J **37:** 147-155

Siefritz F, Tyree MT, Lovisolo C, Schubert A, Kaldenhoff R (2002) PIP1 plasma membrane aquaporins in tobacco: from cellular effects to function in plants. Plant Cell **14:** 869-876

Sjovall-Larsen S, Alexandersson E, Johansson I, Karlsson M, Johanson U, Kjellbom P (2006) Purification and characterization of two protein kinases acting on the aquaporin SoPIP2;1. Biochim Biophys Acta **1758:** 1157-1164

Steinhauser D, Usadel B, Luedemann A, Thimm O, Kopka J (2004) CSB.DB: a comprehensive systems-biology database. Bioinformatics **20:** 3647-3651

Steudle E (1994) Water transport across roots. Plant and Soil **167:** 79-90

Steudle E (2001) The Cohesion-Tension Mechanism and the Acquisition of Water by Plant Roots. Annu Rev Plant Physiol Plant Mol Biol **52:** 847-875

Steudle E, Peterson C (1998) Review article. How does water get through roots? J. Exp. Bot. **49:** 775-788

Suga S, Imagawa S, Maeshima M (2001) Specificity of the accumulation of mRNAs and proteins of the plasma membrane and tonoplast aquaporins in radish organs. Planta **212:** 294-304

Sui H, Han BG, Lee JK, Walian P, Jap BK (2001) Structural basis of water-specific transport through the AQP1 water channel. Nature **414:** 872-878

Swanson R, Clark T, Preuss D (2005) Expression profiling of Arabidopsis stigma tissue identifies stigma-specific genes. Sexual Plant Reproduction **18:** 163-171

Takano J, Wada M, Ludewig U, Schaaf G, von Wiren N, Fujiwara T (2006) The Arabidopsis major intrinsic protein NIP5;1 is essential for efficient boron uptake and plant development under boron limitation. Plant Cell **18:** 1498-1509

Tamarappoo BK, Verkman AS (1998) Defective aquaporin-2 trafficking in nephrogenic diabetes insipidus and correction by chemical chaperones. J Clin Invest **101:** 2257-2267

Temmei Y, Uchida S, Hoshino D, Kanzawa N, Kuwahara M, Sasaki S, Tsuchiya T (2005) Water channel activities of Mimosa pudica plasma membrane intrinsic proteins are regulated by direct interaction and phosphorylation. FEBS Lett **579:** 4417-4422

Terashima I, Ono K (2002) Effects of HgCl(2) on CO(2) dependence of leaf photosynthesis: evidence indicating involvement of aquaporins in CO(2) diffusion across the plasma membrane. Plant Cell Physiol **43:** 70-78

Thimm O, Blasing O, Gibon Y, Nagel A, Meyer S, Kruger P, Selbig J, Muller LA, Rhee SY, Stitt M (2004) MAPMAN: a user-driven tool to display genomics data sets onto diagrams of metabolic pathways and other biological processes. Plant J **37:** 914-939

Tissier AF, Marillonnet S, Klimyuk V, Patel K, Torres MA, Murphy G, Jones JDG (1999) Multiple Independent Defective Suppressor-mutator Transposon Insertions in Arabidopsis: A Tool for Functional Genomics. Plant Cell **11:** 1841-1852

Törnroth-Horsefield S, Wang Y, Hedfalk K, Johanson U, Karlsson M, Tajkhorshid E, Neutze R, Kjellbom P (2006) Structural mechanism of plant aquaporin gating. Nature **439:** 688-694

Toufighi K, Brady SM, Austin R, Ly E, Provart NJ (2005) The Botany Array Resource: e-Northerns, Expression Angling, and promoter analyses. Plant J **43:** 153-163

Tournaire-Roux C, Sutka M, Javot H, Gout E, Gerbeau P, Luu DT, Bligny R, Maurel C (2003) Cytosolic pH regulates root water transport during anoxic stress through gating of aquaporins. Nature **425:** 393-397

Tyerman S, Bohnert H, Maurel C, Steudle E, Smith J (1999) Plant aquaporins: their molecular biology, biophysics and significance for plant water relations. J. Exp. Bot. **50:** 1055-1071

Tyerman SD, Niemietz CM, Bramley H (2002) Plant aquaporins: multifunctional water and solute channels with expanding roles. Plant Cell Environ **25:** 173-194

Uehlein N, Lovisolo C, Siefritz F, Kaldenhoff R (2003) The tobacco aquaporin NtAQP1 is a membrane CO2 pore with physiological functions. Nature **425:** 734-737

Vander Willigen C, Postaire O, Tournaire-Roux C, Boursiac Y, Maurel C (2006) Expression and inhibition of aquaporins in germinating Arabidopsis seeds. Plant Cell Physiol **47:** 1241-1250

Veenhoff LM, Heuberger EH, Poolman B (2002) Quaternary structure and function of transport proteins. Trends Biochem Sci **27:** 242-249

Vera-Estrella R, Barkla BJ, Bohnert HJ, Pantoja O (2004) Novel regulation of aquaporins during osmotic stress. Plant Physiol **135:** 2318-2329

Verkman AS (2000) Water permeability measurement in living cells and complex tissues. J Membr Biol **173:** 73-87

Wallace IS, Choi WG, Roberts DM (2006) The structure, function and regulation of the nodulin 26-like intrinsic protein family of plant aquaglyceroporins. Biochim Biophys Acta **1758:** 1165-1175

Wallace IS, Roberts DM (2004) Homology modeling of representative subfamilies of Arabidopsis major intrinsic proteins. Classification based on the aromatic/arginine selectivity filter. Plant Physiol **135:** 1059-1068

Wallace IS, Wills DM, Guenther JF, Roberts DM (2002) Functional selectivity for glycerol of the nodulin 26 subfamily of plant membrane intrinsic proteins. FEBS Lett **523:** 109-112

Wang XF, Yakir D (1995) Temporal and spatial variations in the oxygen-18 content of leaf water in different plant species. Plant, Cell & Environment **18:** 1377–1385

Wang XF, Yakir D, Avishai M (1998) Non-climatic variations in the oxygen isotopic compositions of plants. Global Change Biology **4:** 835– 849

Wayne R, Tazawa M (1990) Nature of the water channels in the internodal cells of Nitellopsis. J Membr Biol **116:** 31-39

Weig A, Deswarte C, Chrispeels MJ (1997) The major intrinsic protein family of Arabidopsis has 23 members that form three distinct groups with functional aquaporins in each group. Plant Physiol **114:** 1347-1357

Weig AR, Jakob C (2000) Functional identification of the glycerol permease activity of Arabidopsis thaliana NLM1 and NLM2 proteins by heterologous expression in Saccharomyces cerevisiae. FEBS Lett **481:** 293-298

Werner M, Uehlein N, Proksch P, Kaldenhoff R (2001) Characterization of two tomato aquaporins and expression during the incompatible interaction of tomato with the plant parasite Cuscuta reflexa. Planta **213:** 550-555

Wershaw RL, Friedman I, Heller SJ, Franck PA (1966) Hydrogen isotopic fractionation of water passing through trees. Advances in Organic Geochemistry (ed. G.D. Hobson). Pergamon Press, New York.**:** 55-67

West JB, Bowen GJ, Cerling TE, Ehleringer JR (2006) Stable isotopes as one of nature's ecological recorders. Trends Ecol Evol **21:** 408-414

White JWC (1988) Stable hydrogen ratio in plants: A review of current theory and some potential applications. *In* PW Rundel, JR Ehleringer, KA Nagy, eds, Stable Isotopes in Ecological Research. Springer-Verlag, Berlin**:** 142-162

Whittembury G, Gonzalez E, Gutierrez AM, Echevarria M, Hernandez CS (1997) Length of the selectivity filter of aquaporin-1. Biol Cell **89:** 299-306

Xiong L, Zhu JK (2002) Molecular and genetic aspects of plant responses to osmotic stress. Plant Cell Environ **25:** 131-139

Yamada S, Bohnert HJ (2000) Expression of the PIP aquaporin promoter-MipA from the common ice plant in tobacco. Plant Cell Physiol **41:** 719-725

Yamada S, Katsuhara M, Kelly WB, Michalowski CB, Bohnert HJ (1995) A family of transcripts encoding water channel proteins: tissue-specific expression in the common ice plant. Plant Cell **7:** 1129-1142

Yool AJ, Weinstein AM (2002) New roles for old holes: ion channel function in aquaporin-1. News Physiol Sci **17:** 68-72

Zardoya R (2005) Phylogeny and evolution of the major intrinsic protein family. Biol Cell **97:** 397-414

Zelazny E, Borst JW, Muylaert M, Batoko H, Hemminga MA, Chaumont F (2007) FRET imaging in living maize cells reveals that plasma membrane aquaporins interact to regulate their subcellular localization. Proc Natl Acad Sci U S A **104:** 12359-12364

Zhu C, Schraut D, Hartung W, Schäffner AR (2005) Differential responses of maize MIP genes to salt stress and ABA. J Exp Bot **56:** 2971-2981

Zimmermann P, Hennig L, Gruissem W (2005) Gene-expression analysis and network discovery using Genevestigator. Trends Plant Sci **10:** 407-409

Zimmermann P, Hirsch-Hoffmann M, Hennig L, Gruissem W (2004) GENEVESTIGATOR. Arabidopsis microarray database and analysis toolbox. Plant Physiol **136:** 2621-2632

6 SUPPLEMENTARY MATERIAL AND ANNEXES
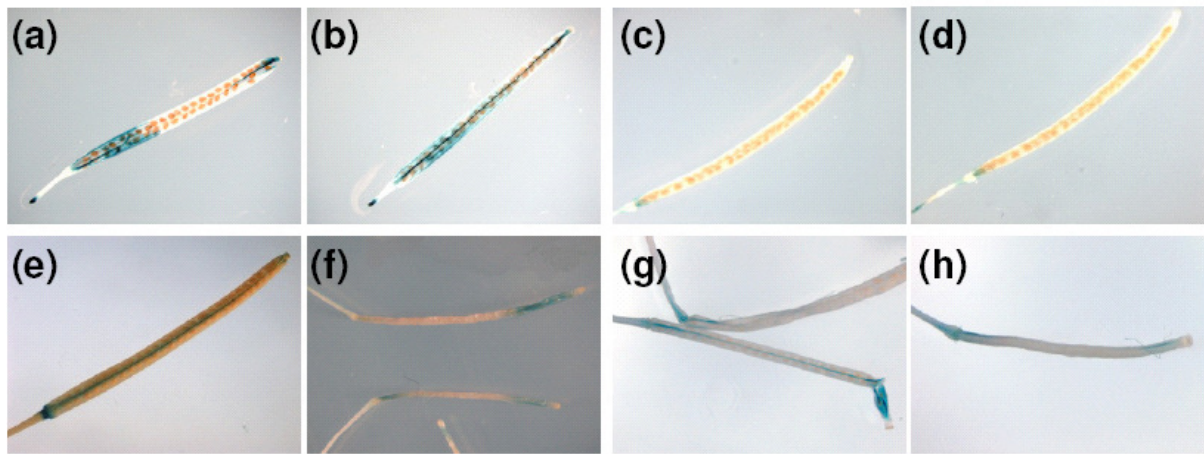
Supplementary Figure 1. Histochemical localization of PIP2::GUS activity in siliques. Expression in siliques of 5- to 6-week-old plants grown in soil expressing *PIP2* promoter::GUS constructs: (a) *PIP2;1*, (b) *PIP2;2*, (c) *PIP2;3* (d) *PIP2;4*, (e) *PIP2;5*, (f) *PIP2;6*, (g) *PIP2;7*, and (h) *PIP2;8* promoter::GUS.
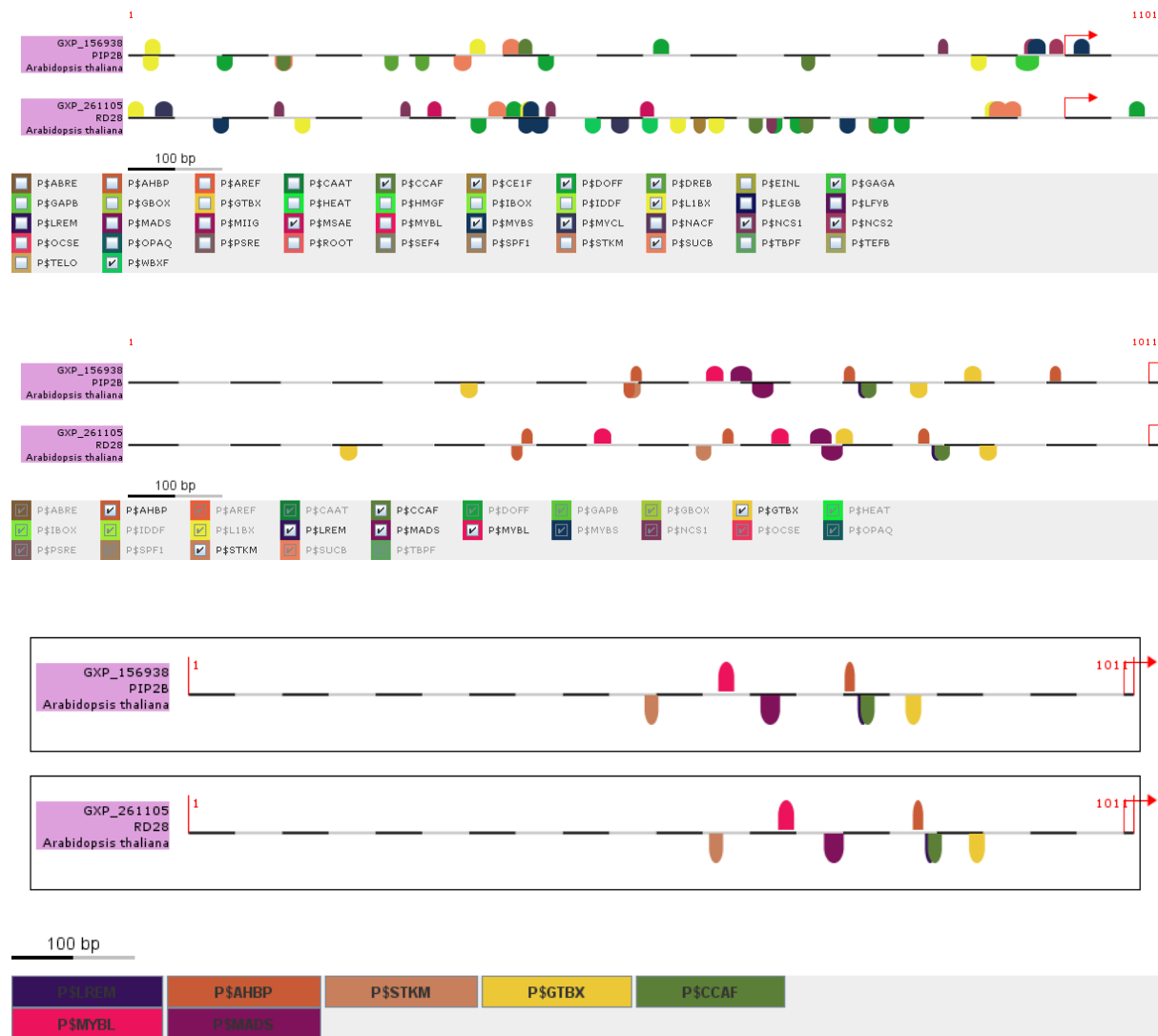
Supplementary Figure 2. Differential representation of promoter elements in *PIP2;3 (RD28)* vs. *PIP2;2 (PIP2B)*. (**a**) The regions -1000 until +100 with respect to the translation start site were examined for differential representation of all 68 families of plant transcription factor binding sites at MatInspector at www.genomatix.de. Differentially represented or arranged binding sites according to Supplementary Table 10 are depicted. (**b**) In addition to these differences, several framework motifs (i.e. combinations of binding sites with similar relative order and spacing) are found with FrameWorker at www.genomatix.de. (**c**) Shows an example of a randomly selected framework (1 out of 11 frameworks with up to 7 binding sites) consisting of seven binding sites. Interestingly, the included CCAF motif was also identified as a part of a differential representation and clustering of motifs (Supplementary Table 10).

Supplementary Table 1. Membrane transport-related gene expression in roots of *pip2* insertional mutants. Wild-type and *pip2* mutants were grown hydroponically for 3 weeks and root expression of about 500 transport-related genes were analyzed using a custom cDNA array harboring gene-specific 3´-UTR probes compiled within the DFG Priority program SPP1108 (Van der Graf, E., Kunze, R., Flügge, U., Neuschaefer-Rube, O. and Schäffner, A.R., unpublished; Glombitza et al., 2004; probe sequences are available upon request to schaeffner@helmholtz-muenchen.de). Two biologically independent replicates of twelve mutants and Columbia wild-type were analyzed. Signal intensity of each gene in the mutant plants was compared with the signal intensity of the same gene in the wild-type plants to calculate an expression ratio (mutant *versus* wild-type). Fold-changes (FC) were calculated by averaging expression ratios of the two biologically independent replica of two independent mutants each with the exception of *pip2;4* and *pip2;8*, for which only one mutant was available. Consequently, only genes consistently deregulated in both mutants were to be considered as significant changes.
SD: standard deviation. n.d.: not detected
(A) *MIP* gene expression. Probes corresponding to 3'-UTR regions detected *PIP2* transcripts of several knockouted genes similar to the wild-type. However, the loss of complete transcripts of the respective *PIP2* genes had been clearly demonstrated by RT-PCR with primers flanking the insertion site.
(B) Expression ratios for additional genes analyzed.

Mutation		pip2;1		pip2;2		pip2;3		pip2;4		pip2;5		pip2;6		pip2;8	
Combined mutants		pip2;1-1 + pip2;1-2		pip2;2-3 + pip2;2-4		pip2;3-1 + pip2;3-2		pip2;4-1		pip2;5-1 + pip2;5-3		pip2;6-1 + pip2;6-2		pip2;8-1	
AGI code	Gene annotation	FC	SD	FC	SD	FC	SD	FC	SD	FC	SD	FC	SD	FC	SD
(A) *MIP* genes															
At3g61430	PIP1;1	1.3	0.5	1.4	0.7	1.0	0.3	0.9	0.5	0.8	0.6	1.0	0.2	1.0	0.3
At2g45960	PIP1;2	1.3	0.5	1.5	0.6	1.0	0.2	1.2	0.4	0.9	0.7	1.1	0.4	0.8	0.1
At1g01620	PIP1;3	1.4	0.7	1.5	0.5	1.2	0.4	1.6	0.6	1.1	0.3	1.3	0.5	1.3	0.5
At4g00430	PIP1;4	1.2	0.3	1.3	0.4	1.0	0.1	1.4	0.5	1.0	0.1	1.2	0.2	1.2	0.2
At4g23400	PIP1;5	1.4	0.4	1.4	0.3	1.4	0.1	1.7	0.8	1.1	0.1	1.4	0.2	1.3	0.3
At3g53420	PIP2;1	0.9	0.4	1.6	1.0	1.6	0.3	1.9	0.7	1.5	0.7	1.1	0.5	1.2	0.2
At2g37170	PIP2;2	1.1	0.3	0.3	0.1	1.2	0.3	1.5	0.1	0.9	0.3	1.0	0.4	1.0	0.1
At2g37180	PIP2;3	1.3	0.5	1.7	0.9	1.1	0.3	1.6	0.3	1.1	0.2	1.2	0.3	1.4	0.4
At5g60660	PIP2;4	1.4	0.5	1.5	0.4	2.0	0.7	1.4	0.1	1.0	0.1	1.3	0.1	1.2	0.3
At3g54820	PIP2;5	1.3	0.4	1.3	0.5	0.7	0.2	0.8	0.3	0.6	0.2	1.0	0.5	1.0	0.8
At2g39010	PIP2;6	1.1	0.2	1.1	0.4	0.8	0.1	0.6	0.2	0.8	0.2	1.1	0.2	0.7	0.1
At4g35100	PIP2;7	1.1	0.3	1.2	0.4	1.7	0.8	1.4	0.3	0.8	0.1	1.1	0.4	0.9	0.3
At2g16850	PIP2;8	1.3	0.4	1.4	0.7	0.7	0.2	0.7	0.2	0.8	0.2	1.1	0.5	1.1	0.5
At2g36830	TIP1;1	1.2	0.7	1.2	0.6	0.9	0.2	1.6	0.8	0.9	0.2	1.0	0.3	1.0	0.1
At3g26520	TIP1;2	1.4	0.5	1.3	0.5	1.1	0.3	1.4	0.7	1.0	0.3	1.1	0.2	1.0	0.3
At4g01470	TIP1;3	1.2	0.5	1.2	0.4	1.4	0.6	1.2	0.1	0.9	0.4	1.5	1.1	0.7	0.1
At3g16240	TIP2;1	1.3	0.6	1.3	0.6	1.1	0.5	1.3	0.6	1.0	0.3	1.2	0.5	1.0	0.6
At4g17340	TIP2;2	1.0	0.5	1.1	0.4	1.1	0.7	1.2	0.3	0.9	0.2	1.0	0.4	1.0	0.6

ID	Name													
At5g47450	*TIP2;3*	**1.4**	0.7	**1.5**	0.8	**1.8**	0.7	**1.8**	0.7	**1.4**	0.3	**1.5**	1.0	**1.9**	1.1
At1g73190	*TIP3;1*	**1.3**	0.2	**1.1**	0.2	**1.1**	0.2	**1.1**	0.2	**1.0**	0.2	**1.5**	0.4	**0.9**	0.2
At1g17810	*TIP3;2*	**1.0**	0.3	**0.9**	0.2	**1.3**	0.8	**1.1**	0.1	**0.9**	0.1	**1.2**	1.1	**0.9**	0.2
At2g25810	*TIP4;1*	**1.2**	0.5	**1.3**	0.5	**0.6**	0.1	**0.5**	0.1	**0.8**	0.4	**1.0**	0.4	**1.1**	0.8
At3g47440	*TIP5;1*	**1.5**	0.5	**1.5**	0.5	**0.7**	0.2	**0.7**	0.2	**0.8**	0.4	**1.3**	0.6	**1.3**	1.2
At4g19030	*NIP1;1*	**1.1**	0.3	**1.2**	0.2	**0.8**	0.2	**0.6**	0.1	**0.9**	0.3	**1.0**	0.2	**1.0**	0.1
At4g18910	*NIP1;2*	**1.1**	0.2	**1.2**	0.2	**1.0**	0.3	**0.9**	0.3	**1.1**	0.3	**1.3**	0.2	**1.0**	0.1
At2g34390	*NIP2;1*	**1.1**	0.3	**1.1**	0.4	**0.8**	0.3	**0.9**	0.7	**0.8**	0.4	**0.9**	0.5	**1.2**	0.2
At1g31885	*NIP3;1*	**1.2**	0.4	**1.2**	0.3	**1.3**	0.3	**1.3**	0.4	**1.2**	0.3	**1.0**	0.2	**0.9**	0.3
At5g37810	*NIP4;1*	**1.3**	0.6	**1.5**	0.6	**1.3**	0.7	**1.4**	0.5	**1.1**	0.1	**1.4**	0.3	**1.4**	0.5
At5g37820	*NIP4;2*	**1.0**	0.2	**1.2**	0.3	**1.0**	0.1	**1.0**	0.1	**1.2**	0.2	**1.1**	0.3	**1.3**	0.2
At4g10380	*NIP5;1*	**1.0**	0.3	**1.2**	0.2	**1.0**	0.3	**1.2**	0.5	**1.0**	0.1	**1.0**	0.1	**1.2**	0.3
At1g80760	*NIP6;1*	**1.1**	0.5	**1.2**	0.4	**1.1**	0.4	**1.0**	0.4	**0.9**	0.1	**1.1**	0.1	**0.9**	0.4
At3g06100	*NIP7;1*	**0.9**	0.1	**1.0**	0.1	**1.0**	0.2	**1.0**	0.0	**1.0**	0.1	**1.0**	0.3	**1.1**	0.2
At3g04090	*SIP1;1*	**1.1**	0.2	**1.1**	0.2	**1.1**	0.2	**1.4**	0.7	**1.1**	0.2	**1.1**	0.4	**0.9**	0.1
At5g18290	*SIP1;2*	**1.0**	0.4	**1.2**	0.2	**1.1**	0.3	**1.4**	0.5	**1.1**	0.3	**1.2**	0.6	**0.9**	0.1
At3g56950	*SIP2;1*	**1.1**	0.2	**1.2**	0.2	**0.7**	0.1	**0.6**	0.3	**0.9**	0.3	**1.2**	0.2	**0.8**	0.0
At1g52180	*pseudo-delta-TIP*	**1.2**	0.2	**1.2**	0.3	**0.9**	0.1	**0.9**	0.2	**1.0**	0.3	**1.3**	0.2	**0.9**	0.1
At2g29870	*pseudo-NIP2;1*	**1.4**	0.8	**1.5**	0.7	**1.3**	0.5	**1.5**	0.6	**1.3**	0.3	**1.3**	0.3	**1.3**	0.7
At2g21020	*pseudo-NIP3;1*	**1.1**	0.2	**1.2**	0.1	**1.0**	0.3	**1.2**	0.3	**1.2**	0.1	**1.0**	0.1	**1.1**	0.0

(B) Other genes encoding transmembrane proteins (including unrelated genes)

ID	Name													
At1g01340	*AtCNGC10*	**1.0**	0.1	**1.1**	0.1	**1.3**	0.2	**1.1**	0.2	**1.1**	0.1	**1.0**	0.2	**1.4**	0.5
At1g01440	*extra-large G-protein-related*	**1.1**	0.2	**1.2**	0.2	**1.0**	0.4	**0.7**	0.5	**1.0**	0.1	**1.4**	0.3	**0.9**	0.6
At1g02510	*AtKCO4*	**1.0**	0.1	**1.0**	0.1	**1.0**	0.3	**1.0**	0.0	**1.0**	0.2	**1.0**	0.2	**1.1**	0.2
At1g02730	*CSLD5 cellulose synthase*	**0.9**	0.2	**1.0**	0.1	**1.0**	0.1	**1.0**	0.0	**1.0**	0.1	**1.0**	0.4	**1.0**	0.0
At1g04120	*AtMRP5*	**1.2**	0.2	**1.0**	0.1	**1.2**	0.3	**1.2**	0.3	**1.3**	0.3	**1.5**	1.1	**1.1**	0.1
At1g05140	*membrane-associated zinc metalloprotease, put,*	**1.0**	0.1	**1.0**	0.1	**0.9**	0.2	**0.7**	0.5	**1.0**	0.1	**1.0**	0.2	**0.9**	0.2
At1g05200	*AtGLR3.4*	**1.0**	0.4	**1.1**	0.3	**0.8**	0.3	**0.6**	0.5	**0.9**	0.3	**1.0**	0.3	**0.9**	0.9
At1g05300	*ZIP5, ZINC TRANSPORTER 5*	**1.0**	0.2	**0.9**	0.1	**1.2**	0.5	**1.0**	0.0	**0.9**	0.2	**0.8**	0.3	**0.8**	0.2
At1g05560	*UDP-glycosyl transferase UGT75B1*	**0.9**	0.1	**0.9**	0.1	**0.9**	0.2	**0.8**	0.3	**0.9**	0.2	**0.9**	0.4	**0.7**	0.4
At1g05940	*CAT9, CATIONIC AMINO ACID TRANSPORTER 9*	**1.4**	0.8	**1.0**	0.1	**1.8**	0.8	**1.3**	0.1	**1.0**	0.3	**1.5**	1.3	**1.0**	0.1
At1g07110	*F2KP, FRUCTOSE-2,6-BISPHOSPHATASE*	**1.0**	0.0	**1.0**	0.0	**1.0**	0.1	**1.0**	0.0	**1.0**	0.1	**0.9**	0.1	**1.0**	0.0
At1g07340	*STP2, SUGAR TRANSPORTER 2*	**1.0**	0.0	**1.1**	0.1	**1.1**	0.1	**1.4**	0.5	**1.2**	0.2	**1.0**	0.2	**1.2**	0.3
At1g07890	*APX1, ASCORBATE PEROXIDASE 1*	**0.9**	0.2	**0.9**	0.3	**1.0**	0.2	**1.6**	0.4	**1.0**	0.3	**1.1**	0.4	**1.0**	0.2
At1g08890	*SUGTL4; Sugar transporter-like protein 4*	**1.2**	0.2	**1.1**	0.2	**1.1**	0.4	**1.4**	0.5	**1.0**	0.1	**1.3**	0.6	**1.3**	0.4
At1g08920	*SUGTL2*	**1.0**	0.2	**1.0**	0.2	**0.8**	0.3	**0.9**	0.2	**0.9**	0.3	**0.8**	0.4	**1.1**	0.0
At1g08930	*ERD6, EARLY RESPONSE TO DEHYDRATION 6*	**0.7**	0.2	**0.8**	0.3	**0.7**	0.4	**0.7**	0.1	**0.7**	0.3	**0.6**	0.4	**0.3**	0.3
At1g09500	*SAG26, cinnamyl-alcohol dehydrogenase*	**1.0**	0.1	**1.1**	0.2	**1.2**	0.1	**1.2**	0.3	**1.1**	0.2	**1.2**	0.2	**1.3**	0.4

Gene	Description													
At1g09860	*AtPUP9 purine permease-related*	**1.0**	0.2	**1.1**	0.1	**1.3**	0.4	**1.1**	0.2	**1.1**	0.1	**1.2**	0.2	**1.1**	0.1
At1g09930	*OPT2, oligopeptide transporter 2*	**1.0**	0.2	**1.0**	0.1	**0.9**	0.3	**1.3**	0.4	**1.0**	0.1	**1.2**	0.6	**0.9**	0.1
At1g09960	*SUT4*	**0.9**	0.3	**0.9**	0.3	**0.6**	0.3	**0.5**	0.4	**0.8**	0.2	**1.0**	0.1	**0.5**	0.2
At1g10010	*AAP8*	**0.9**	0.1	**1.0**	0.0	**1.0**	0.1	**1.0**	0.0	**1.1**	0.1	**1.0**	0.1	**1.1**	0.1
At1g10140	*SAG103*	**0.9**	0.3	**0.9**	0.3	**1.5**	0.3	**1.4**	0.4	**1.3**	0.2	**1.4**	0.3	**1.3**	0.1
At1g10400	*UDP-glycosyltransferase UGT90A2*	**0.8**	0.1	**1.0**	0.3	**0.6**	0.3	**0.7**	0.1	**0.7**	0.5	**0.9**	0.7	**0.6**	0.1
At1g10680	*PGP10/MDR10 (P-GLYCOPROTEIN 10)*	**0.9**	0.2	**1.1**	0.3	**1.1**	0.0	**1.6**	0.3	**1.3**	0.1	**1.1**	0.1	**1.5**	0.1
At1g10760	*SEX1 (STARCH EXCESS 1)*	**1.2**	0.4	**1.1**	0.2	**2.3**	2.7	**0.9**	0.2	**0.9**	0.3	**1.2**	0.5	**0.9**	0.6
At1g10830	*sodium symporter-related*	**1.0**	0.2	**1.0**	0.1	**1.2**	0.5	**1.0**	0.0	**1.0**	0.1	**1.0**	0.5	**1.0**	0.0
At1g10980	*similar to unknown membrane protein*	**1.2**	0.3	**1.2**	0.3	**1.1**	0.3	**1.3**	0.5	**1.1**	0.1	**1.2**	0.6	**1.1**	0.2
At1g11260	*STP1 (SUGAR TRANSPORTER 1)*	**1.0**	0.2	**1.0**	0.1	**1.0**	0.3	**0.7**	0.0	**1.0**	0.3	**1.4**	0.3	**0.8**	0.5
At1g12840	*vATPC*	**1.1**	0.2	**0.9**	0.2	**1.1**	0.3	**1.0**	0.3	**1.4**	0.6	**1.3**	0.6	**1.1**	0.2
At1g13210	*haloacid dehalogenase-like hydrolase*	**1.1**	0.1	**1.1**	0.2	**1.0**	0.3	**1.2**	0.3	**1.1**	0.3	**1.2**	0.5	**1.1**	0.2
At1g13560	*AAPT1 (AMINOALCOHOLPHOSPHOTRANSFERASE 1)*	**0.9**	0.2	**1.0**	0.2	**0.7**	0.1	**0.5**	0.1	**0.7**	0.3	**0.8**	0.2	**0.8**	0.1
At1g14360	*UTR3 (UDP-GALACTOSE TRANSPORTER 3)*	**0.9**	0.3	**0.9**	0.2	**1.0**	0.2	**0.9**	0.2	**0.9**	0.2	**0.9**	0.5	**0.9**	0.1
At1g15210	*AtPDR7 (PLEIOTROPIC DRUG RESISTANCE 7)*	**1.0**	0.2	**0.9**	0.1	**1.0**	0.1	**1.0**	0.1	**0.9**	0.2	**0.9**	0.4	**0.9**	0.1
At1g15500	*AtATP2 chloroplast ADP, ATP carrier protein, putative*	**1.1**	0.5	**0.9**	0.2	**1.0**	0.4	**1.1**	0.3	**1.0**	0.3	**1.1**	0.1	**0.9**	0.5
At1g15990	*CNGC7 (CYCLIC NUCLEOTIDE GATED CHANNEL 7)*	**1.0**	0.1	**1.1**	0.1	**0.7**	0.3	**1.1**	0.9	**0.9**	0.3	**1.0**	0.2	**0.7**	0.1
At1g16010	*MRS2-1, magnesium transporter CorA-like family*	**1.0**	0.4	**1.0**	0.3	**1.4**	0.7	**1.0**	0.3	**1.4**	0.9	**1.2**	0.3	**1.0**	0.1
At1g16370	*OCT6 ORGANIC CATION/CARNITINE TRANSPORTER6*	**1.0**	0.0	**1.1**	0.1	**1.1**	0.1	**1.1**	0.2	**1.1**	0.2	**1.3**	0.5	**1.2**	0.3
At1g16390	*OCT3 ORGANIC CATION/CARNITINE TRANSPORTER2*	**0.8**	0.1	**0.9**	0.2	**1.5**	0.7	**1.3**	0.2	**1.0**	0.1	**1.1**	0.4	**0.9**	0.0
At1g17870	*S2P-like putative metalloprotease*	**1.0**	0.1	**1.0**	0.1	**0.8**	0.3	**0.7**	0.4	**1.0**	0.0	**1.0**	0.1	**0.9**	0.2
At1g19450	*integral membrane protein, putative / sugar transporter family protein*	**1.1**	0.1	**1.2**	0.2	**0.9**	0.2	**0.7**	0.3	**1.1**	0.3	**1.3**	0.4	**1.1**	0.2
At1g19770	*PUP14 (purine permease 14)*	**1.6**	0.5	**1.2**	0.3	**1.2**	0.4	**1.3**	0.4	**1.4**	0.5	**1.1**	0.4	**1.2**	0.3
At1g19780	*AtCNGC8 (CYCLIC NUCLEOTIDE GATED CHANNEL 8)*	**1.2**	0.2	**1.0**	0.1	**1.2**	0.2	**1.4**	0.6	**1.1**	0.1	**1.5**	0.6	**1.2**	0.3
At1g19910	*AtvATPC2*	**1.0**	0.2	**1.0**	0.5	**1.1**	0.3	**1.1**	0.1	**1.2**	0.4	**0.9**	0.3	**1.1**	0.2
At1g19920	*APS2 (ATP SULFURYLASE PRECURSOR)*	**1.1**	0.4	**1.0**	0.1	**1.3**	0.3	**1.4**	0.6	**1.2**	0.6	**1.3**	0.7	**n.d.**	n.d.
At1g20260	*VHA-B3*	**1.2**	0.3	**1.2**	0.4	**0.8**	0.4	**0.7**	0.4	**0.9**	0.3	**1.1**	0.1	**1.2**	1.3
At1g20620	*CAT3 (CATALASE 3)*	**1.1**	0.4	**1.1**	0.4	**0.8**	0.2	**0.6**	0.0	**0.8**	0.2	**0.7**	0.3	**0.6**	0.2
At1g20630	*CAT1 (CATALASE 1)*	**1.4**	0.9	**1.7**	0.6	**1.7**	0.3	**1.5**	0.8	**1.2**	0.4	**1.1**	0.3	**1.1**	0.5
At1g20810	*immunophilin / FKBP-type peptidyl-prolyl cis-trans isomerase 1*	**0.8**	0.2	**0.9**	0.2	**0.7**	0.2	**0.5**	0.3	**1.0**	0.3	**1.1**	0.4	**0.8**	0.1
At1g20816	*similar to chloroplast channel forming outer membrane*	**1.1**	0.2	**1.3**	0.3	**1.5**	0.5	**1.5**	0.6	**1.3**	0.4	**1.3**	0.4	**1.2**	0.3
At1g20840	*TMT1 (TONOPLAST MONOSACCHARIDE TRANSPORTER1)*	**1.0**	0.2	**0.9**	0.1	**0.9**	0.1	**0.8**	0.3	**0.9**	0.2	**1.1**	0.4	**0.9**	0.1
At1g20950	*PPFK pyrophosphate-dependent 6-phosphofructose-1-kinase-related*	**1.2**	0.4	**1.1**	0.4	**0.6**	0.3	**0.5**	0.3	**0.7**	0.2	**1.0**	0.3	**0.9**	0.9
At1g22360	*UDP-glycosyltransferase UGT85A2*	**1.1**	0.4	**1.3**	0.4	**1.6**	0.4	**1.9**	0.4	**1.6**	0.5	**1.4**	0.7	**1.1**	0.1
At1g22710	*SUC2 (SUCROSE-PROTON SYMPORTER 2)*	**1.1**	0.2	**1.0**	0.2	**1.3**	0.5	**1.0**	0.0	**1.0**	0.1	**1.0**	0.5	**1.0**	0.1
At1g22850	*similar to unknown protein*	**1.2**	0.3	**1.0**	0.0	**n.d.**	n.d.	**1.4**	0.6	**n.d.**	n.d.	**n.d.**	n.d.	**n.d.**	n.d.
At1g24400	*LHT2 (LYSINE HISTIDINE TRANSPORTER 2)*	**0.9**	0.1	**0.9**	0.1	**0.8**	0.3	**0.7**	0.5	**1.0**	0.1	**1.0**	0.2	**0.8**	0.3
At1g24490	*ALB4 (ALBINA 4)*	**1.0**	0.3	**1.0**	0.3	**1.1**	0.2	**1.0**	0.0	**1.0**	0.2	**0.8**	0.1	**1.0**	0.0
At1g25500	*choline transporter-related*	**1.1**	0.3	**1.0**	0.3	**1.2**	0.2	**1.1**	0.2	**1.0**	0.0	**1.2**	0.7	**1.0**	0.0
At1g26130	*haloacid dehalogenase-like hydrolase family protein*	**1.1**	0.2	**1.2**	0.2	**1.1**	0.2	**1.3**	0.5	**1.0**	0.0	**1.2**	0.2	**1.2**	0.3

Gene	Description														
At1g26440	UPS5 (ARABIDOPSIS THALIANA UREIDE PERMEASE 5)	1.1	0.5	1.1	0.3	1.9	0.9	1.2	0.0	1.0	0.3	1.1	0.6	1.1	0.3
At1g27080	proton-dependent oligopeptide transport (POT) family protein	1.0	0.2	1.0	0.1	1.3	0.6	1.2	0.2	1.1	0.1	1.1	0.6	1.0	0.1
At1g28220	PUP3 (purine permease 3)	0.9	0.1	1.0	0.1	0.8	0.2	0.9	0.1	0.9	0.1	0.7	0.2	1.1	0.2
At1g28230	AtPUP1 (PURINE PERMEASE 1); purine transporter	0.9	0.2	0.8	0.2	0.6	0.3	0.6	0.5	0.8	0.2	0.8	0.2	0.6	0.6
At1g30220	ATINT2 (INOSITOL TRANSPORTER 2)	1.1	0.1	1.2	0.2	1.1	0.2	1.2	0.3	1.2	0.2	1.0	0.1	1.2	0.3
At1g30400	AtMRP1	0.8	0.4	1.0	0.4	0.6	0.3	0.6	0.4	0.7	0.1	1.1	0.5	0.6	0.4
At1g30420	MRP12, ABC transporter	0.9	0.4	1.2	0.7	0.7	0.3	0.8	0.0	0.8	0.5	1.0	0.7	1.0	0.5
At1g30560	transporter, putative	1.0	0.0	1.1	0.2	1.0	0.4	1.1	0.1	1.0	0.2	1.1	0.3	1.1	0.2
At1g30840	PUP4 (purine permease 4)	1.0	0.1	1.1	0.3	1.0	0.2	1.0	0.3	1.0	0.2	1.1	0.3	1.2	0.1
At1g31260	ZIP10 (ZINC TRANSPORTER 10 PRECURSOR)	0.9	0.2	1.0	0.5	0.7	0.4	0.6	0.4	0.7	0.3	1.2	0.5	0.7	0.6
At1g31930	XLG3 (extra-large GTP-binding protein 3); signal transducer	1.1	0.3	1.2	0.2	0.9	0.2	0.6	0.2	1.0	0.3	1.1	0.4	1.2	0.3
At1g32080	membrane protein, putative	0.6	0.2	0.8	0.4	0.5	0.3	1.0	1.0	0.6	0.3	0.8	0.5	0.6	0.4
At1g32090	early-responsive to dehydration protein-related	1.1	0.1	1.0	0.1	0.9	0.4	1.1	0.1	1.0	0.0	1.0	0.4	1.0	0.0
At1g34580	monosaccharide transporter, putative	1.0	0.3	0.9	0.2	1.0	0.3	1.0	0.0	1.0	0.2	1.2	1.2	1.0	0.0
At1g36160	ACC1 (ACETYL-COENZYME A CARBOXYLASE 1)	0.8	0.2	0.8	0.4	1.0	0.5	1.0	0.1	1.3	0.4	1.3	0.3	0.9	0.7
At1g37130	NIA2 (NITRATE REDUCTASE 2)	0.9	0.2	0.9	0.4	1.4	0.2	1.3	0.3	1.0	0.2	0.9	0.3	1.2	0.6
At1g42540	GLR3.3	0.9	0.1	1.0	0.1	1.0	0.1	1.0	0.0	1.0	0.1	0.8	0.1	1.1	0.1
At1g42560	MLO9 (MILDEW RESISTANCE LOCUS O 9)	0.9	0.2	1.1	0.4	0.8	0.3	0.6	0.5	1.0	0.2	1.1	0.3	0.8	0.7
At1g42970	GAPDH glyceraldehyde-3-phosphate dehydrogenase	1.1	0.3	1.0	0.1	0.9	0.4	0.7	0.5	0.9	0.1	1.0	0.1	0.7	0.4
At1g44750	PUP11	0.9	0.1	1.0	0.3	0.8	0.1	0.7	0.3	0.9	0.2	0.9	0.2	1.0	0.2
At1g45170	similar to unknown protein; similar to pore protein of 24 kD (OEP24)	1.0	0.2	1.1	0.5	0.7	0.3	0.6	0.3	0.9	0.1	1.1	0.3	0.8	0.8
At1g47603	PUP19	0.8	0.2	0.8	0.2	0.7	0.3	0.6	0.5	0.9	0.2	0.9	0.3	0.7	0.4
At1g47670	LHT4/ AtAATL1 amino acid transporter family	1.2	0.2	1.2	0.2	1.5	0.3	1.2	0.3	1.0	0.0	0.9	0.2	1.2	0.2
At1g48635	peroxin-3 family (next to lysine and histidine specific transporter, putative)	1.2	0.3	1.1	0.2	0.9	0.2	0.7	0.3	1.0	0.3	1.1	0.3	1.1	0.1
At1g48860	EPSP 5-enolpyruvylshikimate-3-phosphate	1.2	0.3	1.4	0.3	1.9	0.4	1.7	0.3	1.7	0.2	1.5	0.3	1.5	0.2
At1g49530	GGPS6 (GERANYLGERANYL PYROPHOSPHATE SYNTHASE 6)	1.0	0.1	1.1	0.3	0.7	0.2	0.7	0.3	0.9	0.2	1.3	0.2	0.7	0.1
At1g50310	STP9 monosaccharide transporter	0.9	0.0	0.7	0.4	1.1	0.3	1.0	0.0	1.1	0.1	1.3	0.6	1.0	0.0
At1g51680	4CL1 4-coumarate-CoA ligase	0.8	0.1	0.8	0.2	1.0	0.3	1.1	0.2	0.9	0.3	0.9	0.3	0.7	0.3
At1g52580	rhomboid family protein	1.1	0.2	1.1	0.2	1.3	0.5	1.1	0.1	1.1	0.2	1.3	0.6	1.2	0.3
At1g53390	WBC25; ATPase	1.0	0.1	1.0	0.2	0.7	0.3	0.6	0.3	0.8	0.2	1.0	0.1	0.8	0.1
At1g54730	sugar transporter, putative	0.8	0.2	0.9	0.4	1.4	0.7	1.1	0.1	1.0	0.2	1.1	0.5	0.8	0.1
At1g55120	AtFRUCT5 (BETA-FRUCTOFURANOSIDASE 5)	1.0	0.1	1.1	0.1	1.0	0.3	1.1	0.2	0.9	0.1	1.0	0.3	1.1	0.2
At1g58030	CAT2 (CATIONIC AMINO ACID TRANSPORTER 2)	1.5	0.6	1.4	0.4	2.0	0.5	1.8	0.5	2.1	0.8	2.1	1.2	1.6	0.2
At1g58360	AAP1 (AMINO ACID PERMEASE 1); amino acid permease	0.9	0.1	1.0	0.1	0.7	0.3	0.6	0.4	1.0	0.1	1.2	0.2	0.7	0.6
At1g59870	PDR8/PEN3 (PLEIOTROPIC DRUG RESISTANCE8)	1.1	0.3	0.9	0.2	1.2	0.5	1.1	0.0	1.2	0.2	1.3	0.7	0.9	0.1
At1g61270	LHT3 lysine and histidine specific transporter	1.1	0.4	1.0	0.1	0.8	0.4	0.7	0.5	0.9	0.1	1.1	0.3	0.7	0.4
At1g61800	GPT2 (glucose-6-phosphate/phosphate translocator 2)	1.2	0.3	1.2	0.3	1.5	0.4	1.1	0.1	1.1	0.2	1.1	0.2	1.3	0.5
At1g62300	WRKY6 (WRKY DNA-binding protein 6); transcription factor	0.9	0.2	0.9	0.2	1.1	0.2	1.1	0.4	1.0	0.1	1.0	0.3	0.7	0.4
At1g62320	ERD protein-related/early-responsive to dehydration protein-related	1.3	0.6	1.1	0.1	1.1	0.4	1.1	0.2	1.2	0.2	1.2	0.5	1.1	0.2
At1g62430	CDS1 (CDP-diacylglycerol synthase 1); phosphatidate cytidylyltransferase	1.2	0.2	1.1	0.3	1.3	0.2	1.3	0.1	1.2	0.1	1.4	0.5	1.0	0.5
At1g63440	HMA5 (HEAVY METAL ATPASE 5)	0.9	0.1	1.0	0.2	0.9	0.3	1.0	0.0	0.9	0.1	0.9	0.2	1.0	0.1

Locus	Description														
At1g64150	VHA-E3 (VACUOLAR H+-ATPASE SUBUNIT E ISOFORM 3)	0.7	0.2	0.8	0.3	0.8	0.3	0.8	0.0	1.1	0.4	0.9	0.5	0.9	0.0
At1g64150	Protein of unknown function	1.1	0.1	1.1	0.1	1.2	0.2	1.2	0.3	1.2	0.2	1.7	1.2	1.1	0.1
At1g64550	GCN3 (general control non-repressible 3)	1.2	0.2	1.4	0.5	1.6	0.3	2.0	0.4	1.6	0.4	1.4	0.1	1.3	0.5
At1g64780	AMT1;2 (AMMONIUM TRANSPORTER 1;2)	1.1	0.1	1.2	0.3	1.1	0.1	1.4	0.6	1.1	0.1	1.2	0.2	1.0	0.1
At1g65060	4CL3 (4-coumarate:CoA ligase 3)	1.1	0.1	1.1	0.1	1.3	0.4	0.7	0.4	1.1	0.1	1.4	0.4	1.3	0.4
At1g65930	isocitrate dehydrogenase, putative	0.8	0.4	0.8	0.3	0.8	0.1	1.0	0.0	0.8	0.2	0.7	0.3	0.7	0.0
At1g66270	betaGLUC beta-glucosidase (PSR3.2)	1.4	0.6	1.4	0.8	0.8	0.3	0.7	0.2	0.7	0.4	1.1	0.4	1.0	0.5
At1g66580	SAG24 (60S ribosomal protein L10C)	0.8	0.3	1.0	0.3	1.0	0.3	1.2	0.1	0.9	0.2	0.8	0.4	1.1	0.4
At1g66780	MATE efflux family protein	0.9	0.1	1.0	0.1	0.9	0.1	0.8	0.3	1.1	0.1	1.1	0.2	1.0	0.0
At1g67070	DIN9 (DARK INDUCIBLE 9); mannose-6-phosphate isomerase	1.0	0.1	0.9	0.3	1.1	0.3	1.1	0.1	1.2	0.5	1.1	0.7	1.0	0.1
At1g67080	unknown protein	0.9	0.1	0.9	0.2	1.0	0.0	0.9	0.1	0.9	0.1	0.8	0.2	0.9	0.2
At1g67300	hexose transporter, putative	1.1	0.4	1.1	0.2	1.8	0.9	1.2	0.6	1.4	0.2	1.4	0.8	0.9	0.5
At1g67640	lysine and histidine specific transporter, putative	0.9	0.1	0.9	0.1	0.8	0.3	0.7	0.5	0.9	0.2	1.0	0.2	0.8	0.3
At1g68070	zinc finger (C3HC4-type RING finger) family protein	0.9	0.1	1.3	0.4	1.3	0.6	1.1	0.2	1.0	0.1	n.d.	n.d.	n.d.	n.d.
At1g68100	IAR1 (IAA-ALANINE RESISTANT 1); metal ion transporter	1.4	0.5	1.2	0.3	1.3	0.3	1.5	0.1	1.3	0.3	1.2	0.1	1.6	0.4
At1g69830	AMY3 (ALPHA-AMYLASE-LIKE 3)	1.0	0.1	1.1	0.2	0.9	0.2	1.1	0.1	1.1	0.1	1.1	0.4	0.8	0.7
At1g70610	TAP1 (transporter associated with antigen processing protein 1)	0.9	0.1	0.9	0.1	0.9	0.1	0.7	0.4	1.0	0.0	0.9	0.2	0.9	0.2
At1g71880	SUC1 (SUCROSE-PROTON SYMPORTER 1); carbohydrate transporter	1.0	0.2	1.0	0.3	1.0	0.2	1.2	0.2	1.0	0.5	1.0	0.3	0.7	0.4
At1g71890	AtSUC5 (SUCROSE-PROTON SYMPORTER 5); carbohydrate transporter	1.0	0.0	1.1	0.3	1.0	0.5	1.0	0.1	1.0	0.1	0.9	0.2	1.0	0.0
At1g72120	proton-dependent oligopeptide transport (POT) family protein	1.0	0.0	1.2	0.3	1.0	0.4	1.1	0.1	1.0	0.1	1.0	0.1	1.1	0.1
At1g72700	haloacid dehalogenase-like hydrolase family protein	0.9	0.1	0.9	0.2	0.8	0.4	0.7	0.4	0.8	0.2	0.8	0.2	0.7	0.5
At1g73220	sugar transporter family protein	1.2	0.4	1.0	0.1	1.2	0.6	1.1	0.1	1.0	0.2	1.2	0.9	0.9	0.2
At1g73650	unknown protein	1.0	0.2	1.0	0.2	0.8	0.2	0.7	0.5	1.2	0.6	1.6	0.7	0.8	0.2
At1g74920	ALDH10A8 (Aldehyde dehydrogenase 10A8)	1.1	0.3	1.1	0.3	1.4	0.3	1.4	0.0	1.4	0.3	1.1	0.5	1.1	0.3
At1g75220	integral membrane protein, putative	1.2	0.2	1.2	0.1	1.2	0.1	1.3	0.1	1.2	0.3	1.2	0.4	1.3	0.0
At1g75330	OTC (ORNITHINE CARBAMOYLTRANSFERASE)	1.0	0.2	1.1	0.3	0.9	0.2	1.2	0.4	1.2	0.4	0.9	0.4	0.9	0.1
At1g75470	PUP15 (Arabidopsis thaliana purine permease 15)	1.1	0.2	1.3	0.4	1.2	0.3	1.3	0.5	1.3	0.4	1.1	0.4	1.5	0.8
At1g75630	vATPC4 (AVA-P4)	0.6	0.2	0.7	0.1	0.6	0.2	0.5	0.0	0.6	0.2	0.5	0.1	0.5	0.0
At1g76030	vATPB1	0.8	0.2	0.9	0.4	0.9	0.2	0.8	0.2	0.8	0.2	0.9	0.4	1.1	0.3
At1g76405	unknown protein	0.9	0.2	1.0	0.2	0.7	0.2	0.5	0.3	0.8	0.1	0.8	0.0	0.7	0.2
At1g76490	HMG1 (3-HYDROXY-3-METHYLGLUTARYL COA REDUCTASE)	0.9	0.4	0.9	0.3	0.8	0.5	1.0	0.2	1.1	0.3	1.1	0.2	1.0	0.6
At1g77210	sugar transporter, putative	0.9	0.2	0.9	0.1	1.0	0.2	1.0	0.0	0.9	0.1	0.9	0.1	0.9	0.1
At1g77380	AAP3 (amino acid permease 3); amino acid permease	0.8	0.3	0.8	0.1	1.0	0.3	1.0	0.4	1.1	0.2	1.2	0.9	0.8	0.2
At1g77490	TAPX; L-ascorbate peroxidase	1.1	0.2	1.0	0.2	0.8	0.3	0.7	0.4	0.9	0.2	1.2	0.5	0.7	0.4
At1g78090	TPPB (TREHALOSE-6-PHOSPHATE PHOSPHATASE)	1.1	0.1	1.0	0.1	1.1	0.2	n.d.	n.d.	0.9	0.1	1.1	0.6	0.9	0.1
At1g78560	bile acid:sodium symporter family protein	1.1	0.2	1.0	0.1	1.0	0.3	1.1	0.1	1.1	0.4	1.1	0.4	1.1	0.0
At1g78580	ATTPS1 (TREHALOSE-6-PHOSPHATE SYNTHASE)	1.1	0.1	1.0	0.0	1.1	0.3	1.2	0.3	1.0	0.1	1.0	0.4	1.0	0.0
At1g78620	integral membrane family protein	0.9	0.1	0.8	0.2	1.5	0.6	1.2	0.1	1.2	0.2	1.0	0.3	1.0	0.1
At1g78900	VHA-A	0.8	0.2	0.8	0.3	0.7	0.1	0.8	0.1	0.8	0.2	0.8	0.2	0.8	0.2
At1g79360	OCT2 (ORGANIC CATION/CARNITINE TRANSPORTER2)	1.0	0.1	1.1	0.2	1.4	0.3	1.2	0.3	1.3	0.3	1.3	0.4	n.d.	n.d.
At1g79410	OCT5 (ORGANIC CATION/CARNITINE TRANSPORTER5)	1.0	0.1	1.1	0.2	1.1	0.2	1.0	0.1	1.1	0.2	1.0	0.2	1.2	0.2

At1g79820	SGB1; carbohydrate transporter/ sugar porter	**1.0**	0.2	**1.1**	0.2	**1.0**	0.4	**0.9**	0.3	**1.1**	0.4	**1.0**	0.4	**1.2**	0.1
At1g79900	MBAC2/BAC2 (mitochondrial basic amino acid carrier 2)	**0.9**	0.1	**1.0**	0.0	**0.9**	0.2	**0.8**	0.3	**1.0**	0.0	**0.9**	0.1	**1.0**	0.1
At1g80300	ATP1 (chloroplast ADP, ATP carrier protein 1)	**1.2**	0.5	**1.0**	0.1	**1.1**	0.4	**1.3**	0.3	**1.2**	0.3	**1.3**	0.8	**1.0**	0.3
At1g80900	magnesium transporter CorA-like family protein (MGT1) (MRS2)	**1.0**	0.2	**0.9**	0.1	**0.7**	0.3	**0.7**	0.4	**0.9**	0.1	**1.1**	0.1	**1.0**	0.9
At2g01110	APG2 (ALBINO AND PALE GREEN 2)	**0.9**	0.2	**0.9**	0.2	**1.1**	0.4	**1.1**	0.2	**1.0**	0.0	**0.9**	0.3	**1.0**	0.3
At2g01320	ABC transporter family protein	**n.d.**	n.d.	**1.0**	0.1	**1.0**	0.0	**1.0**	0.0	**0.8**	0.3	**n.d.**	n.d.	**n.d.**	n.d.
At2g01420	PIN4 (PIN-FORMED 4); auxin:hydrogen symporter/ transporter	**0.9**	0.1	**1.0**	0.0	**1.0**	0.1	**1.0**	0.1	**1.0**	0.0	**0.9**	0.1	**1.0**	0.1
At2g01980	SOS1 (=AtNHX7) (SALT OVERLY SENSITIVE 1)	**1.1**	0.1	**1.2**	0.2	**1.1**	0.1	**1.2**	0.3	**1.1**	0.1	**1.0**	0.3	**1.2**	0.3
At2g02380	GSTZ2 (Glutathione S-transferase (class zeta)	**1.5**	0.8	**1.6**	0.5	**1.6**	0.8	**1.5**	0.3	**1.3**	0.2	**1.4**	0.6	**1.4**	0.4
At2g02590	similar to Putative small multi-drug export [Medicago truncatula]	**1.1**	0.2	**1.0**	0.1	**0.9**	0.3	**1.3**	0.4	**1.1**	0.1	**1.1**	0.4	**1.2**	0.3
At2g02860	SUT2/ SUC3	**0.9**	0.5	**0.7**	0.3	**1.0**	0.4	**0.9**	0.1	**0.9**	0.4	**1.0**	0.3	**0.7**	0.5
At2g03140	CAAX amino terminal protease family protein	**0.9**	0.2	**0.9**	0.2	**0.8**	0.3	**0.8**	0.3	**0.9**	0.2	**0.8**	0.2	**1.3**	0.4
At2g03520	UPS4 (ureide permease 4)	**0.9**	0.1	**1.1**	0.2	**0.9**	0.4	**1.0**	0.1	**0.9**	0.2	**0.9**	0.2	**1.0**	0.1
At2g03530	UPS2 (ureide permease 2)	**1.0**	0.2	**1.1**	0.2	**1.2**	0.4	**1.2**	0.3	**1.0**	0.1	**1.1**	0.3	**1.0**	0.0
At2g03590	UPS1 (ureide permease 1)	**1.0**	0.1	**0.9**	0.1	**0.8**	0.3	**0.7**	0.4	**0.9**	0.1	**0.8**	0.1	**0.8**	0.3
At2g03600	UPS3 (ureide permease 3)	**1.2**	0.5	**1.1**	0.1	**1.0**	0.3	**1.1**	0.1	**0.9**	0.1	**1.0**	0.2	**1.1**	0.2
At2g03620	MRS2-5 magnesium transporter CorA-like family protein	**0.9**	0.2	**0.8**	0.1	**0.5**	0.1	**0.5**	0.4	**0.8**	0.1	**1.2**	0.4	**0.6**	0.2
At2g04032	ZIP7 (ZINC TRANSPORTER 7 PRECURSOR); cation transporter	**1.1**	0.2	**1.0**	0.0	**1.2**	0.4	**1.2**	0.3	**1.0**	0.0	**1.2**	0.6	**1.1**	0.1
At2g07680	MRP11 (multidrug resistance-associated protein 11)	**1.0**	0.3	**0.9**	0.2	**0.9**	0.1	**0.9**	0.1	**0.9**	0.1	**0.9**	0.3	**0.9**	0.2
At2g13360	AGT (ALANINE:GLYOXYLATE AMINOTRANSFERASE)	**1.0**	0.1	**1.0**	0.2	**0.8**	0.3	**0.6**	0.3	**0.8**	0.3	**1.1**	0.2	**0.9**	0.3
At2g14670	ATSUC8 (SUCROSE-PROTON SYMPORTER 8)	**0.8**	0.2	**0.8**	0.3	**0.5**	0.3	**0.6**	0.6	**0.8**	0.2	**1.1**	0.6	**0.5**	0.2
At2g15620	NIR1 (NITRITE REDUCTASE); ferredoxin-nitrate reductase	**0.9**	0.3	**0.9**	0.4	**1.4**	0.2	**1.2**	0.3	**1.2**	0.4	**1.2**	0.2	**1.1**	0.6
At2g16120	mannitol transporter, putative	**1.0**	0.1	**1.2**	0.2	**1.2**	0.2	**1.2**	0.3	**1.2**	0.2	**1.2**	0.3	**1.2**	0.2
At2g16510	vATPC3	**1.1**	0.2	**1.1**	0.4	**1.1**	0.3	**1.1**	0.3	**1.1**	0.1	**0.9**	0.4	**1.5**	0.2
At2g16800	high-affinity nickel-transport family protein	**1.0**	0.2	**0.9**	0.3	**1.3**	0.2	**1.2**	0.2	**1.3**	0.5	**1.4**	0.4	**1.1**	0.1
At2g17260	GLR2 (GLUTAMATE RECEPTOR 2)	**0.9**	0.1	**1.0**	0.2	**0.9**	0.3	**0.7**	0.4	**1.0**	0.2	**1.2**	0.3	**0.9**	0.5
At2g17430	MLO7 (MILDEW RESISTANCE LOCUS O 7)	**1.0**	0.1	**1.0**	0.1	**1.0**	0.2	**0.8**	0.3	**1.0**	0.1	**1.0**	0.2	**1.1**	0.1
At2g17840	ERD7 (EARLY-RESPONSIVE TO DEHYDRATION 7)	**0.8**	0.2	**0.7**	0.2	**1.1**	0.3	**1.1**	0.2	**1.0**	0.2	**0.9**	0.4	**0.8**	0.1
At2g18480	mannitol transporter, putative	**1.2**	0.2	**1.3**	0.3	**1.3**	0.3	**1.3**	0.3	**1.5**	0.4	**1.3**	0.2	**1.9**	0.0
At2g19500	CKX2 (CYTOKININ OXIDASE 2); cytokinin dehydrogenase	**0.9**	0.1	**0.9**	0.2	**0.7**	0.3	**0.7**	0.5	**0.9**	0.2	**1.0**	0.0	**0.7**	0.4
At2g19600	KEA4 (K+ efflux antiporter 4); potassium:hydrogen antiporter	**1.1**	0.1	**1.1**	0.2	**1.1**	0.3	**1.3**	0.5	**1.2**	0.4	**1.3**	0.7	**1.1**	0.1
At2g19860	HXK2 (HEXOKINASE 2)	**1.2**	0.3	**0.9**	0.2	**1.0**	0.1	**1.1**	0.4	**1.2**	0.3	**1.1**	0.5	**0.7**	0.4
At2g20310	expressed protein	**1.2**	0.3	**1.0**	0.1	**1.1**	0.5	**1.2**	0.3	**1.0**	0.1	**1.2**	0.7	**1.0**	0.0
At2g20780	mannitol transporter, putative	**1.2**	0.7	**1.1**	0.1	**1.2**	0.4	**1.4**	0.3	**1.5**	0.7	**1.2**	0.2	**1.4**	0.4
At2g21340	DTX46, putative MATE-related efflux carrier	**1.0**	0.1	**1.1**	0.3	**1.1**	0.3	**1.2**	0.3	**1.1**	0.1	**1.3**	0.9	**1.2**	0.3
At2g21410	vATPv1	**1.0**	0.1	**1.2**	0.5	**1.2**	0.3	**1.1**	0.1	**1.2**	0.3	**1.0**	0.3	**1.2**	0.3
At2g21940	SKK shikimate kinase, putative	**0.9**	0.1	**1.1**	0.2	**1.2**	0.2	**1.2**	0.3	**1.1**	0.2	**1.1**	0.3	**1.2**	0.3
At2g23260	UDP-glycosyltransferase UGT84B1	**1.1**	0.1	**1.1**	0.1	**1.0**	0.3	**0.9**	0.2	**1.1**	0.1	**1.0**	0.1	**0.9**	0.1
At2g23460	XLG1 (EXTRA-LARGE G-PROTEIN 1); signal transducer	**1.0**	0.2	**1.0**	0.0	**0.9**	0.1	**1.1**	0.1	**0.9**	0.1	**1.0**	0.4	**1.0**	0.0
At2g23800	GGPS2 (GERANYLGERANYL PYROPHOSPHATE SYNTHASE 2)	**1.0**	0.1	**1.2**	0.4	**1.0**	0.1	**1.2**	0.3	**1.0**	0.2	**1.1**	0.2	**1.1**	0.2
At2g23810	TET8 (TETRASPANIN8)	**1.7**	0.4	**1.3**	0.4	**1.2**	0.3	**1.2**	0.3	**1.3**	0.3	**1.1**	0.4	**1.2**	0.6

Locus	Description													
At2g23980	CNGC6	**1.2**	0.3	**1.1**	0.2	**0.9**	0.2	**0.7**	0.4	**1.0**	0.1	**1.3**	0.7	**1.0**	0.0
At2g24220	PUP5	**1.0**	0.0	**1.0**	0.0	**0.9**	0.2	**0.7**	0.4	**1.0**	0.1	**1.1**	0.3	**1.0**	0.0
At2g24610	CNGC14	**1.0**	0.1	**1.1**	0.1	**1.2**	0.3	**1.1**	0.1	**1.1**	0.1	**1.1**	0.1	**1.2**	0.0
At2g24710	GLR2.3	**0.8**	0.1	**0.8**	0.2	**1.1**	0.1	**0.8**	0.1	**0.9**	0.2	**1.1**	0.3	**0.9**	0.1
At2g24720	GLR2.2	**1.2**	0.3	**1.1**	0.1	**1.5**	0.3	**1.0**	0.0	**1.0**	0.1	**1.1**	0.3	**1.1**	0.3
At2g25520	PPT3 phosphate translocator-related	**1.0**	0.2	**1.1**	0.4	**1.6**	0.3	**1.8**	0.5	**1.5**	0.4	**1.2**	0.3	**1.2**	0.5
At2g25600	SPIK (SHAKER POLLEN INWARD K+ CHANNEL)	**1.0**	0.2	**0.9**	0.1	**0.8**	0.3	**0.6**	0.5	**0.9**	0.1	**1.1**	0.2	**0.8**	0.3
At2g25610	vATPc2b	**1.0**	0.2	**0.9**	0.1	**0.6**	0.0	**0.6**	0.3	**0.8**	0.2	**0.8**	0.2	**1.0**	0.0
At2g26300	GPA1 (G PROTEIN ALPHA SUBUNIT 1); signal transducer	**0.8**	0.3	**0.9**	0.2	**0.8**	0.2	**0.6**	0.1	**0.9**	0.2	**0.8**	0.3	**1.1**	0.5
At2g26510	PDE135 (PIGMENT DEFECTIVE EMBRYO 135); permease	**1.0**	0.1	**1.1**	0.1	**0.9**	0.3	**0.7**	0.5	**1.3**	0.3	**1.7**	0.8	**1.1**	0.1
At2g26650	AKT1 (ARABIDOPSIS K TRANSPORTER 1)	**0.8**	0.3	**0.8**	0.2	**1.0**	0.5	**1.2**	0.2	**1.1**	0.3	**1.2**	0.3	**1.0**	0.6
At2g26900	bile acid:sodium symporter family protein	**1.1**	0.3	**1.1**	0.2	**1.0**	0.2	**1.2**	0.3	**1.0**	0.2	**0.9**	0.6	**1.1**	0.1
At2g26910	PDR4 (PLEIOTROPIC DRUG RESISTANCE 4)	**1.0**	0.1	**1.0**	0.1	**1.1**	0.1	**1.1**	0.2	**1.1**	0.1	**1.0**	0.3	**1.0**	0.0
At2g27810	NAT12, putative nucleobase ascorbate transporter	**1.0**	0.1	**1.0**	0.1	**0.9**	0.4	**1.0**	0.0	**1.0**	0.0	**1.0**	0.1	**1.1**	0.2
At2g28070	WBC3, ABC transporter	**0.9**	0.1	**0.9**	0.1	**0.7**	0.3	**0.5**	0.3	**0.9**	0.1	**1.0**	0.3	**0.6**	0.2
At2g28260	CNGC15 (cyclic nucleotide gated channel 15)	**0.9**	0.2	**0.9**	0.2	**0.7**	0.3	**0.8**	0.3	**1.0**	0.2	**1.0**	0.1	**0.8**	0.3
At2g28520	vATPv3 (VHA-A1)	**1.0**	0.1	**1.0**	0.1	**1.1**	0.1	**1.0**	0.0	**0.9**	0.1	**0.9**	0.1	**1.2**	0.3
At2g28800	ALBINO3	**1.0**	0.1	**0.9**	0.1	**1.0**	0.5	**0.7**	0.4	**0.9**	0.1	**1.0**	0.4	**0.9**	0.1
At2g28900	OEP16 (OUTER ENVELOPE PROTEIN 16); protein translocase	**1.3**	0.5	**1.3**	0.3	**1.0**	0.2	**0.7**	0.2	**1.1**	0.2	**1.1**	0.4	**1.3**	0.3
At2g29100	GLR2.9 (glutamate receptor 2.9)	**1.0**	0.1	**1.0**	0.1	**1.1**	0.2	**1.1**	0.2	**1.1**	0.1	**1.0**	0.2	**1.1**	0.2
At2g29110	GLR2.8 (glutamate receptor 2.8)	**1.0**	0.2	**1.0**	0.1	**1.1**	0.1	**1.0**	0.0	**0.9**	0.1	**1.0**	0.3	**1.2**	0.2
At2g29120	GLR2.7 (glutamate receptor 2.7)	**0.9**	0.2	**1.0**	0.2	**0.9**	0.1	**1.0**	0.7	**1.4**	0.6	**1.1**	0.2	**1.0**	0.2
At2g29350	SAG13 (Senescence-associated gene 13); oxidoreductase	**0.9**	0.1	**1.0**	0.0	**0.9**	0.2	**0.7**	0.5	**0.9**	0.1	**1.0**	0.1	**0.9**	0.1
At2g29450	GSTU5 (Glutathione S-transferase)	**1.5**	0.6	**1.2**	1.0	**0.5**	0.4	**0.5**	0.2	**0.8**	0.3	**1.3**	0.4	**0.8**	0.5
At2g29650	inorganic phosphate transporter, putative	**0.9**	0.1	**0.9**	0.1	**0.8**	0.3	**0.6**	0.5	**0.9**	0.1	**1.0**	0.3	**0.7**	0.4
At2g29940	PDR3 (PLEIOTROPIC DRUG RESISTANCE 3)	**1.0**	0.1	**1.0**	0.1	**0.9**	0.1	**1.0**	0.1	**0.9**	0.1	**1.4**	0.6	**1.0**	0.0
At2g30860	GST (Glutathione S-transferase)	**1.0**	0.3	**1.0**	0.2	**1.3**	0.3	**1.7**	0.0	**1.2**	0.5	**1.1**	0.4	**1.2**	0.1
At2g30970	ASP1 aspartate aminotransferase, mitochondrial / transaminase A	**1.1**	0.1	**1.2**	0.3	**1.0**	0.2	**1.1**	0.1	**1.1**	0.2	**1.2**	0.4	**1.0**	0.0
At2g31790	UDP-glycosyltransferase UGT74C1	**1.0**	0.3	**1.3**	0.3	**1.3**	0.2	**2.0**	0.0	**1.8**	0.5	**1.4**	0.2	**1.3**	0.6
At2g32040	integral membrane transporter family protein	**1.1**	0.1	**1.1**	0.1	**1.1**	0.2	**1.2**	0.3	**1.3**	0.4	**1.2**	0.4	**1.3**	0.4
At2g32270	ZIP3 (ZINC TRANSPORTER 3 PRECURSOR); zinc ion transporter	**1.0**	0.2	**1.0**	0.2	**1.0**	0.3	**0.9**	0.4	**0.9**	0.3	**1.0**	0.0	**1.1**	0.4
At2g32390	GLR3.5 (GLUTAMATE RECEPTOR 6)	**0.9**	0.1	**0.9**	0.2	**1.0**	0.4	**1.1**	0.1	**1.0**	0.0	**1.0**	0.4	**1.0**	0.0
At2g32400	GLR5 (Glutamate receptor 5)	**0.9**	0.1	**1.1**	0.4	**1.0**	0.3	**1.0**	0.1	**1.0**	0.1	**0.9**	0.1	**1.0**	0.1
At2g33750	PUP2	**1.1**	0.1	**1.1**	0.2	**1.1**	0.2	**1.2**	0.3	**1.1**	0.2	**1.4**	0.9	**1.2**	0.3
At2g34660	MRP2	**1.0**	0.3	**1.2**	0.3	**0.7**	0.3	**0.7**	0.1	**0.8**	0.3	**1.1**	0.4	**1.0**	0.7
At2g34960	CAT5 (CATIONIC AMINO ACID TRANSPORTER 5)	**0.9**	0.2	**1.0**	0.1	**1.2**	0.3	**1.1**	0.1	**1.0**	0.1	**1.4**	0.7	**1.0**	0.1
At2g35260	expressed protein T4C15.7	**1.0**	0.0	**1.0**	0.0	**0.9**	0.2	**0.9**	0.1	**1.0**	0.1	**1.0**	0.0	**1.0**	0.0
At2g35370	GDCH (Glycine decarboxylase complex H)	**1.2**	0.4	**1.1**	0.1	**1.8**	0.9	**1.6**	0.1	**1.6**	0.6	**1.5**	0.9	**1.0**	0.4
At2g35740	INT3 (INOSITOL TRANSPORTER 3	**0.9**	0.1	**0.8**	0.2	**0.7**	0.2	**0.6**	0.6	**0.9**	0.2	**0.9**	0.1	**0.9**	0.2
At2g35840	sucrose-phosphatase 1 (SPP1)	**1.0**	0.3	**0.9**	0.1	**0.7**	0.2	**1.1**	0.7	**1.1**	0.3	**0.9**	0.2	**1.2**	0.1
At2g36300	integral membrane Yip1 protein family	**1.1**	0.2	**1.0**	0.0	**1.2**	0.1	**1.3**	0.4	**1.0**	0.1	**1.3**	0.5	**1.1**	0.2

Gene	Description													
At2g36380	*PDR6 (PLEIOTROPIC DRUG RESISTANCE 6)*	**1.0**	0.1	**1.2**	0.3	**1.1**	0.2	**1.3**	0.4	**1.2**	0.2	**1.3**	0.9	**1.3**	0.4
At2g36580	*PK; pyruvate kinase, putative*	**1.1**	0.2	**1.2**	0.2	**1.3**	0.1	**1.2**	0.2	**1.2**	0.1	**1.2**	0.2	**1.6**	0.4
At2g36590	*PROT3 (PROLINE TRANSPORTER 3)*	**1.0**	0.2	**1.0**	0.3	**1.0**	0.4	**0.8**	0.5	**1.2**	0.4	**1.8**	1.0	**0.9**	0.0
At2g36910	*PGP1/MDR1*	**1.0**	0.2	**1.0**	0.2	**1.1**	0.1	**1.1**	0.1	**0.9**	0.1	**1.2**	0.8	**0.9**	0.2
At2g37040	*PAL1*	**1.1**	0.3	**0.9**	0.1	**1.0**	0.3	**1.0**	0.6	**1.2**	0.6	**1.0**	0.5	**0.7**	0.1
At2g37280	*PDR5*	**0.7**	0.3	**0.9**	0.5	**1.1**	0.5	**1.0**	0.6	**1.2**	0.4	**1.1**	0.2	**0.8**	0.6
At2g38060	*transporter-related*	**1.1**	0.1	**1.1**	0.1	**0.9**	0.2	**0.8**	0.6	**1.1**	0.4	**1.4**	0.5	**1.1**	0.2
At2g38100	*proton-dependent oligopeptide transport (POT) family*	**1.3**	0.4	**1.4**	0.5	**1.6**	1.0	**1.7**	1.0	**1.3**	0.5	**1.7**	1.0	**1.6**	0.9
At2g38170	*CAX1 (CATION EXCHANGER 1)*	**0.9**	0.3	**0.8**	0.3	**0.6**	0.4	**0.6**	0.5	**0.8**	0.2	**1.1**	0.5	**0.6**	0.5
At2g38550	*similar to non-green plastid inner envelope membrane protein precursor*	**1.1**	0.5	**1.2**	0.2	**1.5**	0.7	**1.4**	0.6	**1.3**	0.3	**1.5**	0.8	**1.2**	0.4
At2g38860	*YLS5 (yellow-leaf-specific gene 5)*	**0.8**	0.5	**0.8**	0.4	**1.5**	0.4	**1.6**	0.3	**1.5**	0.3	**1.2**	0.6	**1.2**	0.3
At2g39130	*amino acid transporter family protein*	**1.0**	0.1	**1.0**	0.1	**0.8**	0.3	**0.7**	0.4	**0.9**	0.1	**0.9**	0.1	**0.7**	0.4
At2g39480	*PGP6; Multidrug resistance protein 6*	**1.0**	0.2	**1.0**	0.2	**0.8**	0.3	**1.0**	0.0	**1.0**	0.1	**0.9**	0.1	**0.9**	0.1
At2g39800	*P5CS1 DELTA1-PYRROLINE-5-CARBOXYLATE SYNTHASE 1*	**1.1**	0.2	**1.1**	0.1	**1.0**	0.3	**1.4**	0.5	**1.0**	0.0	**1.0**	0.4	**1.1**	0.2
At2g40380	*prenylated rab acceptor (PRA1) family protein*	**1.2**	0.5	**1.0**	0.1	**1.1**	0.3	**1.1**	0.1	**0.9**	0.1	**1.4**	1.2	**1.0**	0.1
At2g40420	*amino acid transporter family protein*	**0.9**	0.1	**0.9**	0.1	**1.0**	0.4	**1.0**	0.1	**0.9**	0.1	**1.0**	0.3	**0.9**	0.1
At2g41190	*amino acid transporter family protein*	**0.9**	0.1	**1.1**	0.2	**1.0**	0.2	**1.1**	0.1	**1.1**	0.2	**1.0**	0.1	**1.1**	0.1
At2g41220	*GLU2*	**0.9**	0.3	**1.1**	0.2	**0.9**	0.1	**0.6**	0.2	**1.0**	0.2	**1.1**	0.4	**0.9**	0.0
At2g41700	*AOH1, ABC transporter*	**1.4**	0.4	**1.5**	0.4	**1.8**	0.4	**2.1**	0.5	**1.8**	0.5	**1.7**	0.3	**1.6**	0.6
At2g42210	*OEP16-3; protein translocase*	**0.9**	0.3	**1.0**	0.3	**1.4**	0.4	**1.4**	0.6	**1.0**	0.2	**0.8**	0.1	**0.7**	0.3
At2g43330	*INT1 (INOSITOL TRANSPORTER 1)*	**1.1**	0.1	**1.0**	0.1	**0.9**	0.3	**1.1**	0.5	**1.3**	0.2	**1.3**	0.3	**1.2**	0.2
At2g43820	*UDP-glycosyltransferase UGT74F2*	**1.5**	0.7	**1.6**	0.3	**1.6**	0.3	**1.5**	0.2	**1.5**	0.1	**1.4**	0.3	**1.5**	0.0
At2g43840 a	*UDP-glycosyltransferase UGT74F1*	**1.2**	0.4	**1.3**	0.3	**1.1**	0.1	**1.3**	0.4	**1.2**	0.2	**1.0**	0.1	**1.1**	0.2
At2g43950	*OEP37; ion channel*	**1.2**	0.2	**1.1**	0.2	**1.3**	0.5	**1.2**	0.3	**1.1**	0.1	**1.1**	0.5	**1.1**	0.1
At2g44290	*putative lipid transfer protein*	**0.9**	0.1	**0.9**	0.1	**0.9**	0.1	**0.8**	0.3	**1.0**	0.1	**1.1**	0.4	**0.9**	0.1
At2g45570	*CYP76C2 cytochrome P450 monooxygenase*	**0.9**	0.1	**0.9**	0.1	**0.8**	0.3	**0.7**	0.4	**0.9**	0.1	**1.0**	0.0	**0.7**	0.4
At2g46380	*similar to unknown protein*	**1.1**	0.2	**1.1**	0.2	**1.3**	0.4	**1.1**	0.1	**1.0**	0.1	**1.0**	0.2	**1.1**	0.1
At2g46430	*CNGC3*	**1.0**	0.1	**1.1**	0.1	**1.2**	0.3	**1.4**	0.6	**1.2**	0.2	**1.2**	0.3	**1.2**	0.4
At2g47000	*MDR4/ PGP4 (P-GLYCOPROTEIN 4, P-GLYCOPROTEIN4)*	**1.0**	0.3	**0.9**	0.3	**0.8**	0.2	**0.8**	0.5	**0.8**	0.3	**1.2**	0.5	**0.8**	0.1
At2g47760	*ALG3 family protein*	**0.8**	0.2	**0.9**	0.1	**0.9**	0.1	**0.9**	0.1	**1.0**	0.1	**0.8**	0.1	**1.0**	0.0
At2g47800	*MRP4*	**0.9**	0.2	**0.9**	0.1	**0.9**	0.1	**1.2**	0.3	**0.9**	0.1	**1.2**	0.5	**1.0**	0.0
At2g48020	*sugar transporter, putative*	**1.2**	0.1	**1.1**	0.1	**1.2**	0.1	**1.4**	0.0	**1.3**	0.4	**1.4**	0.5	**1.3**	0.4
At3g01120	*MTO1 (METHIONINE OVERACCUMULATION 1)*	**1.1**	0.2	**1.3**	0.3	**1.2**	0.2	**1.3**	0.3	**1.4**	0.7	**1.0**	0.4	**1.0**	0.1
At3g01280	*porin, putative*	**1.0**	0.4	**1.1**	0.3	**0.8**	0.2	**0.9**	0.1	**1.0**	0.1	**0.8**	0.1	**1.0**	0.1
At3g01390	*vATPG1*	**1.1**	0.5	**0.9**	0.2	**1.1**	0.4	**1.5**	0.7	**1.0**	0.4	**0.9**	0.3	**0.8**	0.0
At3g01550	*PPT5*	**1.0**	0.3	**0.9**	0.4	**1.1**	0.4	**1.0**	0.0	**0.9**	0.1	**1.1**	0.3	**1.0**	0.0
At3g01760	*lysine and histidine specific transporter*	**1.0**	0.1	**1.2**	0.3	**1.0**	0.1	**1.1**	0.2	**1.1**	0.1	**0.9**	0.1	**1.1**	0.1
At3g02050	*KUP3 (K+ uptake permease 3); potassium ion transporter*	**0.9**	0.1	**0.9**	0.1	**0.9**	0.3	**0.7**	0.4	**1.0**	0.1	**1.1**	0.4	**0.9**	0.1
At3g02690	*integral membrane family protein*	**0.9**	0.2	**0.9**	0.3	**1.1**	0.2	**0.8**	0.1	**0.9**	0.1	**1.1**	0.4	**0.8**	0.1
At3g02850	*SKOR*	**1.2**	0.2	**0.9**	0.3	**0.5**	0.3	**0.5**	0.2	**0.8**	0.2	**1.0**	0.3	**1.5**	1.6
At3g03090	*sugar transporter family*	**1.1**	0.3	**1.0**	0.1	**0.8**	0.2	**0.7**	0.4	**0.9**	0.1	**1.1**	0.3	**1.2**	0.3

At3g03110	XPO1B (exportin 1B); protein transporter	**1.4**	0.4	**1.1**	0.2	**1.1**	0.4	**1.3**	0.4	**1.0**	0.1	**1.4**	0.8	**1.2**	0.4
At3g03250	UGP (UDP-glucose pyrophosphorylase)	**1.2**	0.5	**1.0**	0.3	**1.5**	0.9	**1.2**	0.0	**0.9**	0.4	**1.0**	0.5	**0.7**	0.0
At3g03720	CAT4 (CATIONIC AMINO ACID TRANSPORTER 4)	**0.9**	0.1	**0.9**	0.2	**0.8**	0.3	**0.7**	0.5	**0.9**	0.1	**0.9**	0.1	**0.8**	0.3
At3g04110	GLR1.1	**1.0**	0.1	**1.0**	0.2	**1.2**	0.3	**1.1**	0.2	**1.1**	0.3	**1.0**	0.1	**1.2**	0.2
At3g05150	sugar transporter family protein	**1.2**	0.4	**1.1**	0.2	**1.2**	0.2	**1.1**	0.1	**0.9**	0.1	**1.0**	0.1	**1.4**	0.5
At3g05160/	sugar transporter, putative (both genes)	**1.0**	0.2	**1.0**	0.3	**1.0**	0.2	**0.9**	0.4	**1.1**	0.3	**1.1**	0.2	**0.8**	0.1
At3g05400	SUGTL5	**1.0**	0.2	**0.9**	0.1	**1.0**	0.2	**0.8**	0.3	**1.0**	0.0	**1.3**	0.8	**0.9**	0.1
At3g05940	expressed protein F10A16.24	**1.1**	0.3	**1.0**	0.2	**1.0**	0.1	**0.7**	0.4	**1.0**	0.0	**0.8**	0.1	**0.9**	0.1
At3g05960	STP6 sugar transporter, putative	**1.1**	0.1	**1.1**	0.3	**0.9**	0.3	**1.0**	0.0	**1.0**	0.1	**0.9**	0.2	**1.2**	0.3
At3g06483	PDK (PYRUVATE DEHYDROGENASE KINASE)	**1.1**	0.3	**1.1**	0.2	**0.7**	0.2	**0.6**	0.4	**0.9**	0.2	**1.0**	0.1	**1.2**	0.8
At3g06500	beta-fructofuranosidase, putative	**1.3**	0.2	**1.2**	0.3	**1.2**	0.3	**1.8**	0.3	**1.6**	0.5	**1.4**	0.7	**1.5**	0.2
At3g07020	UDP-glycosyltransferase UGT80A2	**0.8**	0.4	**0.9**	0.3	**1.3**	0.7	**0.9**	0.4	**0.9**	0.5	**0.9**	0.4	**0.7**	0.3
At3g07520	GLR1.4	**1.5**	0.4	**1.4**	0.2	**2.2**	0.9	**1.9**	0.6	**1.0**	0.1	**1.7**	0.9	**1.4**	0.0
At3g07568	expressed protein	**1.0**	0.3	**1.1**	0.3	**1.5**	0.5	**1.3**	0.4	**1.1**	0.3	**0.9**	0.2	**0.8**	0.3
At3g08560	VHA-E2 (VACUOLAR H+-ATPASE SUBUNIT E ISOFORM 2)	**0.9**	0.1	**1.1**	0.2	**1.2**	0.1	**1.1**	0.1	**1.1**	0.1	**1.2**	0.2	**1.2**	0.3
At3g08650	metal transporter family	**1.2**	0.3	**1.1**	0.1	**1.2**	0.3	**1.2**	0.1	**1.4**	0.5	**1.2**	0.3	**1.3**	0.3
At3g10970	haloacid dehalogenase-like hydrolase family protein	**1.3**	0.5	**1.2**	0.2	**1.5**	0.7	**1.7**	0.9	**1.1**	0.2	**1.6**	0.8	**1.0**	0.4
At3g11170	FAD7 omega-3 fatty acid desaturase, chloroplast precursor	**1.2**	0.1	**1.1**	0.1	**1.4**	0.6	**1.2**	0.3	**1.1**	0.2	**1.3**	0.5	**1.5**	0.2
At3g12590	Hypothetical protein	**0.9**	0.1	**0.8**	0.3	**0.7**	0.3	**n.d.**	n.d.	**0.9**	0.1	**0.8**	0.3	**0.7**	0.4
At3g12750	ZIP1	**1.0**	0.1	**0.9**	0.2	**1.0**	0.2	**1.0**	0.1	**0.8**	0.2	**1.0**	0.6	**0.9**	0.1
At3g13080	MRP3	**1.3**	0.3	**1.4**	0.3	**0.9**	0.3	**0.6**	0.0	**0.9**	0.3	**1.1**	0.3	**0.9**	0.0
At3g13090	ABC-V	**1.1**	0.1	**1.2**	0.2	**1.3**	0.4	**1.3**	0.3	**1.3**	0.3	**1.3**	0.4	**0.8**	0.1
At3g13090	MRP8	**0.9**	0.2	**0.9**	0.1	**0.9**	0.2	**0.7**	0.5	**0.8**	0.2	**1.1**	0.1	**0.9**	0.2
At3g13100	MRP7 (Arabidopsis thaliana multidrug resistance-associated protein 7)	**1.1**	0.3	**0.9**	0.1	**0.8**	0.3	**0.6**	0.5	**0.9**	0.1	**1.1**	0.2	**0.7**	0.2
At3g14940	PPC3 (PHOSPHOENOLPYRUVATE CARBOXYLASE 3)	**1.0**	0.1	**1.0**	0.2	**1.0**	0.1	**1.0**	0.0	**1.0**	0.1	**1.0**	0.3	**1.1**	0.1
At3g15520	bAMY peptidyl-prolyl cis-trans isomerase	**1.0**	0.2	**1.0**	0.1	**1.0**	0.2	**1.1**	0.1	**1.0**	0.1	**1.2**	0.6	**1.1**	0.2
At3g15990	SULTR3;4 (SULTR3;4); sulfate transporter	**1.0**	0.2	**1.0**	0.1	**0.9**	0.4	**1.2**	0.2	**1.0**	0.2	**1.2**	0.5	**1.1**	0.1
At3g16340	PDR1	**1.1**	0.4	**1.1**	0.2	**1.5**	0.4	**1.4**	0.1	**1.4**	0.4	**1.5**	0.8	**1.0**	0.4
At3g16520	UDP-glycosyltransferase UGT88A1	**1.0**	0.2	**1.1**	0.2	**0.8**	0.3	**0.6**	0.2	**0.8**	0.2	**1.0**	0.2	**0.7**	0.0
At3g17690	CNGC19 (cyclic nucleotide gated channel 19)	**1.0**	0.0	**1.0**	0.1	**1.0**	0.1	**1.1**	0.1	**1.0**	0.1	**1.0**	0.2	**1.0**	0.0
At3g17700	CNGC20 (CNBT1; cyclic nucleotide-binding transporter 1)	**1.1**	0.1	**1.1**	0.1	**1.0**	0.2	**1.1**	0.1	**1.1**	0.2	**1.4**	0.5	**1.1**	0.2
At3g17820	GSKB6 (glutamine synthase clone KB6)	**0.9**	0.1	**0.9**	0.2	**1.1**	0.1	**1.1**	0.1	**1.3**	0.4	**1.5**	0.9	**1.2**	0.1
At3g18830	PLT5 (POLYOL TRANSPORTER 5)	**1.2**	0.4	**1.3**	0.3	**1.4**	0.6	**1.7**	0.5	**1.5**	0.2	**1.6**	0.4	**1.5**	0.5
At3g19450	CAD4 (CINNAMYL ALCOHOL DEHYDROGENASE 4)	**0.6**	0.3	**0.5**	0.1	**0.7**	0.2	**0.8**	0.0	**0.8**	0.2	**0.7**	0.1	**0.7**	0.1
At3g19490	NHD1 putative sodium-proton antiporter, NhaD subfamily	**1.2**	0.3	**1.3**	0.4	**1.3**	0.2	**1.2**	0.2	**1.1**	0.1	**1.0**	0.2	**1.3**	0.4
At3g19640	MRS2-3	**1.2**	0.3	**1.2**	0.2	**1.3**	0.3	**1.6**	0.7	**1.5**	0.3	**1.3**	0.5	**1.1**	0.3
At3g19930	STP4	**1.1**	0.3	**1.1**	0.3	**1.6**	0.5	**1.2**	0.3	**1.2**	0.4	**1.2**	0.7	**1.4**	0.1
At3g19940	STP10	**0.9**	0.1	**1.1**	0.2	**1.0**	0.0	**1.0**	0.0	**1.0**	0.1	**0.9**	0.3	**1.0**	0.1
At3g20460	sugar transporter, putative	**0.9**	0.1	**0.9**	0.1	**0.7**	0.4	**0.6**	0.5	**0.9**	0.1	**1.0**	0.3	**0.9**	0.9
At3g20660	OCT4 ORGANIC CATION/CARNITINE TRANSPORTER4	**1.0**	0.1	**1.1**	0.2	**0.9**	0.3	**0.7**	0.1	**1.0**	0.3	**1.1**	0.4	**1.2**	0.1
At3g21560	UDP-glycosyltransferase UGT84A2; sinapate 1-glucosyltransferase	**1.0**	0.2	**1.2**	0.4	**1.3**	0.2	**1.7**	0.3	**1.4**	0.1	**1.4**	0.4	**1.5**	0.0

Gene	Description													
At3g21640	*TWD1 (TWISTED DWARF 1); peptidyl-prolyl cis-trans isomerase*	**1.3**	0.6	**1.1**	0.3	**1.2**	0.3	**1.2**	0.3	**1.1**	0.2	**1.2**	0.5	**1.2**	0.3
At3g21690	*DTX40, putative MATE-related efflux carrier*	**1.0**	0.1	**1.0**	0.1	**1.0**	0.1	**0.8**	0.3	**1.0**	0.1	**1.0**	0.1	**1.1**	0.1
At3g21720	*ICL isocitrate lyase, putative*	**0.9**	0.1	**1.0**	0.0	**0.8**	0.2	**0.7**	0.5	**1.0**	0.1	**1.1**	0.1	**1.0**	0.0
At3g22890	*APS1 (ATP sulfurylase 3)*	**1.0**	0.2	**1.1**	0.3	**1.1**	0.2	**1.6**	0.3	**1.5**	0.5	**1.3**	1.0	**n.d.**	n.d.
At3g23580	*RNR2/RNR2A (RIBONUCLEOTIDE REDUCTASE 2A)*	**0.9**	0.3	**0.7**	0.3	**1.0**	0.1	**0.8**	0.3	**0.9**	0.2	**0.9**	0.1	**0.9**	0.1
At3g24170	*GR1; glutathione-disulfide reductase*	**1.0**	0.3	**0.9**	0.3	**0.8**	0.1	**1.0**	0.1	**1.0**	0.3	**1.2**	0.4	**1.0**	0.2
At3g24290	*AMT1.5*	**1.2**	0.2	**1.1**	0.1	**1.2**	0.2	**1.4**	0.6	**1.1**	0.2	**1.7**	0.9	**1.4**	0.6
At3g24300	*AMT1.3*	**1.0**	0.1	**1.0**	0.2	**0.9**	0.3	**0.7**	0.4	**0.9**	0.2	**1.0**	0.0	**0.8**	0.3
At3g25410	*MWL2.2 bile acid:sodium symporter family protein*	**0.8**	0.1	**1.0**	0.2	**0.8**	0.2	**1.1**	0.2	**0.9**	0.0	**0.9**	0.4	**1.2**	0.0
At3g25585	*AAPT2 (AMINOALCOHOLPHOSPHOTRANSFERASE)*	**0.7**	0.2	**0.8**	0.1	**0.7**	0.1	**0.5**	0.1	**0.8**	0.2	**0.8**	0.2	**0.7**	0.0
At3g25620	*WBC21, ABC transporter*	**0.9**	0.2	**0.8**	0.3	**0.7**	0.4	**0.7**	0.5	**0.8**	0.2	**0.8**	0.2	**0.6**	0.5
At3g26570	*PHT2;1 (phosphate transporter 2;1)*	**1.1**	0.3	**0.9**	0.1	**1.1**	0.3	**1.0**	0.0	**0.9**	0.2	**1.0**	0.6	**0.9**	0.1
At3g28710	*vATPd1*	**0.9**	0.3	**1.0**	0.1	**0.8**	0.2	**0.9**	0.2	**1.1**	0.2	**1.0**	0.2	**1.0**	0.1
At3g28715	*vATPd2*	**1.0**	0.2	**1.1**	0.2	**0.9**	0.2	**0.8**	0.2	**1.1**	0.2	**1.2**	0.4	**1.2**	0.1
At3g29320	*glucan phosphorylase, putative*	**0.9**	0.2	**1.0**	0.1	**0.7**	0.2	**0.6**	0.2	**0.9**	0.1	**0.9**	0.2	**0.8**	0.0
At3g30390	*amino acid transporter family protein*	**1.2**	0.4	**1.2**	0.4	**1.2**	0.1	**1.4**	0.1	**1.2**	0.4	**1.4**	0.4	**1.2**	0.1
At3g30775	*ERD5 osmotic stress-responsive proline dehydrogenase (POX) (PRO1)*	**0.7**	0.3	**0.7**	0.0	**0.9**	0.4	**1.1**	0.0	**0.9**	0.2	**0.9**	0.3	**1.2**	0.6
At3g42050	*vATPH*	**1.1**	0.1	**0.9**	0.2	**0.6**	0.2	**0.5**	0.3	**0.7**	0.2	**0.9**	0.1	**0.9**	0.4
At3g44160 a	*plastid outer envelope porin, putative*	**1.0**	0.1	**1.0**	0.1	**0.7**	0.3	**0.7**	0.4	**1.0**	0.1	**1.0**	0.2	**0.8**	0.3
At3g44770	*similar to unknown protein*	**1.1**	0.3	**0.9**	0.1	**1.2**	0.3	**1.1**	0.1	**0.9**	0.1	**1.3**	1.0	**1.0**	0.0
At3g47340	*ASN1 (DARK INDUCIBLE 6)*	**0.9**	0.2	**1.0**	0.2	**0.8**	0.3	**0.7**	0.4	**1.0**	0.1	**1.1**	0.3	**0.7**	0.4
At3g47520	*MDH (malate dehydrogenase); malate dehydrogenase*	**1.1**	0.2	**1.1**	0.1	**0.8**	0.2	**0.7**	0.3	**1.8**	1.6	**0.9**	0.3	**1.1**	0.5
At3g48010	*CNGC16*	**1.1**	0.1	**1.1**	0.2	**0.9**	0.4	**1.2**	0.3	**1.1**	0.1	**1.1**	0.2	**1.1**	0.2
At3g48170	*ALDH10A9 (Aldehyde dehydrogenase 10A9)*	**1.0**	0.2	**1.2**	0.3	**1.7**	0.7	**1.5**	0.3	**1.5**	0.6	**1.2**	0.6	**1.0**	0.2
At3g49620	*DIN11 (DARK INDUCIBLE 11); oxidoreductase*	**1.0**	0.0	**1.1**	0.2	**1.1**	0.1	**1.0**	0.1	**1.0**	0.1	**0.9**	0.2	**1.1**	0.2
At3g49920	*porin, putative*	**1.2**	0.2	**1.2**	0.2	**1.1**	0.2	**1.6**	0.8	**1.4**	0.4	**1.3**	0.5	**1.3**	0.4
At3g51430	*YLS2 (yellow-leaf-specific gene 2); strictosidine synthase*	**1.0**	0.1	**0.9**	0.1	**1.0**	0.2	**0.9**	0.1	**0.8**	0.2	**0.9**	0.1	**0.9**	0.1
At3g51480	*GLR3.6*	**1.1**	0.5	**1.0**	0.2	**1.2**	0.2	**1.2**	0.1	**1.3**	0.5	**1.0**	0.3	**1.2**	0.2
At3g51490	*TMT3 (TONOPLAST MONOSACCHARIDE TRANSPORTER3)*	**1.1**	0.2	**1.0**	0.1	**1.0**	0.4	**1.1**	0.1	**0.9**	0.2	**1.3**	0.7	**1.2**	0.3
At3g51860	*CAX3 (cation exchanger 3); cation:cation antiporter*	**1.0**	0.2	**1.0**	0.0	**1.3**	0.5	**1.0**	0.1	**1.1**	0.1	**1.2**	0.4	**1.1**	0.1
At3g52420	*outer envelope membrane protein, putative*	**0.8**	0.3	**0.8**	0.2	**0.6**	0.2	**0.6**	0.1	**0.8**	0.1	**0.7**	0.1	**0.7**	0.1
At3g52760	*integral membrane Yip1 protein family*	**1.1**	0.2	**1.1**	0.1	**1.3**	0.5	**1.1**	0.2	**1.1**	0.1	**1.4**	1.0	**1.1**	0.1
At3g53260	*PAL2*	**0.9**	0.4	**1.8**	1.8	**0.7**	0.1	**0.6**	0.4	**1.1**	0.5	**1.1**	0.5	**0.8**	0.0
At3g53480	*PDR9/PDR11*	**0.9**	0.5	**1.1**	0.6	**0.8**	0.2	**0.9**	0.4	**0.9**	0.2	**0.9**	0.5	**1.1**	0.4
At3g54660	*GR (GLUTATHIONE REDUCTASE)*	**1.1**	0.1	**1.1**	0.3	**1.1**	0.1	**0.8**	0.2	**1.0**	0.0	**1.1**	0.1	**1.1**	0.2
At3g55610	*PCSB*	**0.8**	0.1	**1.0**	0.2	**1.1**	0.4	**1.4**	0.0	**1.2**	0.1	**1.1**	0.2	**1.3**	0.2
At3g56160	*bile acid:sodium symporter*	**1.2**	0.2	**1.1**	0.1	**1.2**	0.3	**1.1**	0.2	**1.1**	0.1	**1.2**	0.6	**1.1**	0.1
At3g56200	*amino acid transporter family protein*	**1.0**	0.1	**1.0**	0.1	**0.9**	0.1	**1.1**	0.2	**1.0**	0.1	**0.6**	0.3	**1.0**	0.0
At3g57330	*ACA11 calcium-transporting ATPase, plasma membrane-type*	**0.9**	0.2	**0.8**	0.2	**0.8**	0.2	**0.4**	0.1	**0.8**	0.2	**0.8**	0.3	**0.7**	0.0
At3g58730	*vATPD*	**1.0**	0.2	**0.9**	0.3	**1.0**	0.2	**1.5**	0.2	**1.3**	0.4	**0.9**	0.6	**1.1**	0.1
At3g58970	*MRS2-6*	**1.4**	0.7	**1.1**	0.2	**1.1**	0.4	**1.0**	0.0	**1.2**	0.5	**1.2**	0.4	**1.0**	0.6

Gene	Description													
At3g60130	YLS1, glycosyl hydrolase family 1	1.1	0.1	1.1	0.1	1.1	0.2	1.1	0.2	1.1	0.1	1.1	0.2	1.1	0.2
At3g60140	DIN2 (DARK INDUCIBLE 2); hydrolyzing O-glycosyl compounds	0.9	0.1	1.0	0.3	1.9	1.4	1.4	0.1	2.0	1.2	2.0	1.4	1.1	0.1
At3g61670	similar to unknown protein	1.0	0.2	1.0	0.1	0.8	0.4	0.7	0.2	1.1	0.2	0.9	0.4	1.1	0.6
At3g62150	PGP21 (P-GLYCOPROTEIN 21) Pot. cross-hybridization At2g47000	1.0	0.2	0.9	0.2	1.0	0.1	1.0	0.0	0.9	0.2	1.3	0.7	1.0	0.0
At3g62880	OEP16-4; protein translocase	1.0	0.4	1.0	0.4	1.2	0.4	1.0	0.0	1.2	0.1	0.9	0.1	1.1	0.2
At3g63160	similar to outer envelope membrane protein, putative	1.1	0.1	1.1	0.2	1.5	0.6	1.2	0.3	1.1	0.2	1.3	1.0	1.0	0.0
At3g63210	MARD1/SAG102 (MEDIATOR OF ABA-REGULATED DORMANCY 1)	1.3	0.3	1.3	0.4	1.6	0.3	1.1	0.2	1.1	0.2	1.1	0.1	1.2	0.3
At3g63250	HMT-2; homocysteine S-methyltransferase	0.7	0.3	0.9	0.3	0.9	0.2	1.1	0.1	1.1	0.2	0.8	0.3	1.0	0.2
At3g63380	ACA12, calcium-transporting ATPase, plasma membrane-type, putative	1.1	0.1	1.1	0.1	1.2	0.3	1.1	0.2	1.0	0.0	1.1	0.1	1.4	0.6
At4g01010	CNGC13	0.8	0.2	0.9	0.1	1.0	0.0	0.7	0.4	1.0	0.1	1.0	0.0	1.0	0.0
At4g01090	extra-large G-protein-related	1.0	0.1	1.0	0.3	1.0	0.3	1.1	0.2	1.0	0.0	0.9	0.2	1.0	0.0
At4g01820	AtPGP3/AtMDR3	1.0	0.2	1.1	0.1	0.8	0.2	0.6	0.0	1.0	0.3	1.1	0.1	0.8	0.1
At4g01830	AtPGP5/AtMDR5	0.9	0.1	1.0	0.1	0.8	0.1	1.0	0.0	1.0	0.1	1.0	0.3	1.1	0.1
At4g01840	KCO5	0.9	0.1	1.0	0.1	0.8	0.3	0.7	0.4	1.0	0.0	1.2	0.1	0.8	0.3
At4g01850	MAT2/SAM-2 (S-adenosylmethionine synthetase 2)	1.0	0.2	1.0	0.3	0.9	0.3	0.9	0.4	0.7	0.4	0.8	0.2	0.7	0.1
At4g02050	STP7 sugar transporter, putative	1.0	0.1	1.0	0.2	1.2	0.2	1.0	0.1	1.0	0.2	1.0	0.1	1.1	0.1
At4g02380	SAG21	0.5	0.3	0.8	0.3	0.8	0.3	1.0	0.3	0.7	0.2	0.8	0.2	1.0	0.4
At4g02620	vATPF	0.8	0.1	0.7	0.5	1.0	0.2	1.0	0.6	1.0	0.3	1.1	0.4	0.9	0.0
At4g03560	TPC1, vacuolar two pore Ca2+-channel	0.8	0.3	0.9	0.2	1.2	0.2	1.1	0.4	0.9	0.3	1.0	0.1	1.0	0.1
At4g04040	MEE51; diphosphate-fructose-6-phosphate 1-phosphotransferase	1.3	0.6	1.2	0.2	1.7	0.4	1.3	0.0	1.3	0.5	1.5	0.7	1.2	0.2
At4g04750	carbohydrate transporter/ sugar porter	0.9	0.2	0.8	0.2	0.7	0.4	0.6	0.5	0.8	0.2	0.9	0.2	0.6	0.5
At4g04760	sugar transporter family protein	1.2	0.2	1.2	0.2	1.1	0.3	1.3	0.4	1.1	0.1	0.9	0.1	1.1	0.2
At4g04970	callose/1,3-beta-glucan synthase (GSL1/ CalS11)	1.1	0.2	1.2	0.2	1.2	0.2	1.1	0.2	1.1	0.1	0.9	0.3	1.4	0.3
At4g08620	high-affinity sulfate transporter (HST1/ Sultr1.1)	1.2	0.5	1.3	0.4	1.6	0.3	1.6	0.2	1.7	0.6	1.7	0.9	1.3	0.5
At4g08700 a	PUP13 and PUP12	1.2	0.2	1.4	0.5	1.3	0.4	1.3	0.4	1.2	0.4	1.1	0.3	1.5	0.7
At4g11150	vATPE1	0.7	0.3	0.7	0.3	0.7	0.3	0.5	0.3	0.7	0.1	0.7	0.3	0.6	0.1
At4g11230	RBOH, respiratory burst oxidase homolog / NADPH oxidase, putative	1.1	0.3	1.1	0.1	1.0	0.3	0.7	0.5	1.0	0.1	1.1	0.2	1.4	0.5
At4g11570	haloacid dehalogenase-like hydrolase family protein	1.4	0.6	1.5	0.3	1.8	0.8	1.5	0.3	1.7	0.5	1.7	0.6	1.5	0.3
At4g11680	zinc finger (C3HC4-type RING finger) family protein	1.0	0.0	1.1	0.2	1.0	0.3	1.1	0.1	1.0	0.1	1.1	0.4	0.8	0.1
At4g13510	AMT1.1	1.0	0.1	1.0	0.1	0.9	0.2	0.8	0.3	0.9	0.2	1.3	0.7	0.8	0.2
At4g14680	APS3	1.0	0.3	1.0	0.3	1.5	0.3	1.2	0.0	1.5	0.7	1.3	0.5	1.1	0.3
At4g15480	UDP-glycosyltransferase UGT84A1	1.1	0.1	1.2	0.2	1.3	0.5	1.3	0.2	1.2	0.3	1.3	0.6	1.0	0.3
At4g15490	UDP-glycosyltransferase UGT84A3	1.0	0.1	1.0	0.1	1.0	0.2	0.9	0.1	1.0	0.1	0.9	0.1	0.8	0.2
At4g15530	PPDK	1.0	0.4	0.9	0.1	1.2	0.1	1.3	0.2	1.1	0.2	1.0	0.2	1.3	0.1
At4g15550	UDP-glycosyltransferase UGT75D1	1.1	0.2	1.2	0.2	0.9	0.2	0.7	0.4	1.1	0.3	1.4	0.3	0.8	0.2
At4g16160	OEP16-2/OEP16-S; protein translocase	0.9	0.1	0.9	0.1	0.8	0.3	0.7	0.4	1.0	0.1	1.0	0.1	0.7	0.4
At4g16480	INT4 (INOSITOL TRANSPORTER 4)	0.8	0.2	0.8	0.2	0.7	0.3	0.6	0.6	0.9	0.2	0.9	0.1	0.8	0.3
At4g17550	transporter-related	0.9	0.2	0.9	0.2	0.8	0.4	0.8	0.7	0.9	0.3	1.1	0.3	0.7	0.3
At4g17840	expressed protein	1.2	0.2	1.1	0.2	1.0	0.3	1.1	0.2	1.1	0.1	1.0	0.1	1.1	0.1
At4g18050	PGP9/AtMDR9	1.0	0.2	1.1	0.1	1.1	0.4	1.2	0.3	1.1	0.3	1.1	0.2	1.0	0.0
At4g18160	KCO6, TPK3 tandem-pore potassium channel	1.2	0.2	1.2	0.2	1.3	0.3	1.2	0.3	1.3	0.3	1.3	0.4	1.5	0.7

At4g18190	*PUP4*	**1.1**	0.1	**1.2**	0.3	**1.3**	0.2	**1.1**	0.1	**1.1**	0.1	**1.0**	0.1	**1.3**	0.2
At4g18200	*PUP5*	**1.1**	0.1	**1.2**	0.3	**1.3**	0.2	**1.3**	0.4	**1.2**	0.2	**1.2**	0.2	**1.2**	0.4
At4g18220 a	*PUP8 and PUP7*	**1.0**	0.1	**1.1**	0.2	**1.0**	0.2	**1.2**	0.2	**1.1**	0.2	**1.1**	0.8	**1.1**	0.2
At4g18290	*KAT2*	**1.0**	0.1	**1.1**	0.1	**1.1**	0.2	**1.2**	0.3	**1.0**	0.0	**1.2**	0.5	**1.2**	0.2
At4g19680	*IRT2 (iron-responsive transporter 2)*	**1.0**	0.1	**0.9**	0.1	**0.8**	0.2	**0.7**	0.5	**0.9**	0.1	**1.0**	0.1	**0.9**	0.2
At4g21480	*glucose transporter, putative*	**1.0**	0.1	**1.0**	0.2	**0.7**	0.3	**0.7**	0.5	**1.1**	0.2	**1.3**	0.5	**0.7**	0.3
At4g22200	*AKT2 (Arabidopsis K+ transporter 2)*	**1.0**	0.1	**0.9**	0.1	**0.8**	0.3	**0.7**	0.4	**0.9**	0.1	**1.0**	0.2	**0.7**	0.5
At4g23710	*vATPG2*	**1.0**	0.1	**1.0**	0.1	**1.2**	0.2	**1.7**	0.5	**1.1**	0.2	**1.3**	0.2	**1.2**	0.3
At4g24090	*similar to unknown protein*	**1.0**	0.2	**1.1**	0.5	**1.3**	0.3	**1.0**	0.0	**1.1**	0.2	**0.9**	0.1	**1.1**	0.1
At4g24460	*similar to unknown protein*	**1.0**	0.2	**0.9**	0.1	**1.0**	0.1	**0.9**	0.1	**1.1**	0.1	**1.2**	0.5	**1.0**	0.0
At4g25640	*DTX35, putative MATE*	**1.0**	0.2	**1.1**	0.2	**1.4**	0.3	**1.1**	0.2	**1.2**	0.2	**1.2**	0.2	**1.2**	0.2
At4g25950	*vATPG3*	**1.1**	0.2	**1.2**	0.2	**1.3**	0.4	**1.4**	0.5	**1.0**	0.1	**1.4**	0.7	**1.2**	0.3
At4g25960	*PGP2/ MDR2*	**1.1**	0.2	**1.2**	0.2	**1.1**	0.2	**1.3**	0.4	**1.1**	0.1	**1.2**	0.3	**1.3**	0.2
At4g26180	*put. mitoch. Carrier protein*	**0.9**	0.3	**0.8**	0.3	**0.8**	0.2	**0.6**	0.5	**0.8**	0.2	**1.0**	0.5	**0.9**	0.2
At4g26770	*phosphatidate cytidylyltransferase, putative*	**1.2**	0.2	**1.1**	0.2	**1.1**	0.1	**1.1**	0.2	**1.1**	0.2	**1.0**	0.1	**1.1**	0.2
At4g28210	*EMB1923 (EMBRYO DEFECTIVE 1923)*	**0.8**	0.1	**0.8**	0.2	**0.7**	0.3	**0.5**	0.1	**0.8**	0.2	**0.9**	0.4	**0.6**	0.0
At4g28580	*MRS2-6*	**1.0**	0.2	**1.0**	0.2	**0.8**	0.3	**0.9**	0.1	**1.0**	0.2	**1.1**	0.2	**1.1**	0.1
At4g28700	*AMT1.4*	**0.9**	0.1	**1.1**	0.1	**0.9**	0.2	**0.7**	0.4	**1.0**	0.1	**1.2**	0.3	**1.0**	0.1
At4g29130	*HXK1 (GLUCOSE INSENSITIVE 2)*	**0.9**	0.2	**0.8**	0.2	**0.5**	0.2	**0.5**	0.5	**1.1**	0.7	**0.9**	0.3	**0.6**	0.5
At4g29660	*EMB2752 (EMBRYO DEFECTIVE 2752)*	**1.1**	0.2	**1.3**	0.3	**1.1**	0.2	**1.2**	0.3	**1.2**	0.3	**1.0**	0.1	**1.3**	0.4
At4g30110	*HMA2 (Heavy metal ATPase 2); cadmium-transporting ATPase*	**1.0**	0.3	**1.0**	0.0	**1.0**	0.3	**0.7**	0.4	**1.0**	0.0	**1.0**	0.2	**1.1**	0.4
At4g30270	*MERI5B (MERISTEM-5); hydrolase, acting on glycosyl bonds*	**1.1**	0.1	**1.0**	0.1	**1.3**	0.4	**1.2**	0.1	**1.1**	0.2	**1.2**	0.4	**1.4**	0.5
At4g30360	*CNGC17*	**1.3**	0.6	**1.0**	0.2	**1.7**	0.7	**1.2**	0.3	**1.4**	0.6	**1.5**	0.8	**1.2**	0.1
At4g30560	*CNGC9*	**1.0**	0.1	**1.1**	0.3	**0.8**	0.2	**1.3**	1.2	**0.9**	0.1	**1.1**	0.1	**0.8**	0.1
At4g31710	*GLR2.4*	**1.0**	0.1	**1.0**	0.0	**1.3**	0.4	**1.1**	0.2	**1.1**	0.1	**1.3**	0.6	**1.3**	0.2
At4g32500	*AKT5*	**1.0**	0.1	**0.9**	0.1	**0.9**	0.1	**0.6**	0.5	**0.9**	0.1	**1.2**	0.2	**1.0**	0.0
At4g32650	*KC1/KAT3/AKT4 (K+ RECTIFYING CHANNEL 1)*	**1.2**	0.4	**1.2**	0.4	**1.6**	0.6	**2.1**	0.5	**1.4**	0.2	**1.6**	0.1	**1.8**	1.2
At4g32770	*VTE1 (VITAMIN E DEFICIENT 1)*	**1.2**	0.2	**1.1**	0.1	**1.0**	0.3	**1.2**	0.3	**1.1**	0.1	**1.2**	0.5	**1.0**	0.1
At4g33510	*DHS2 (3-deoxy-D-arabino-heptulosonate 7-phosphate synthase)*	**0.9**	0.2	**1.1**	0.4	**1.3**	0.4	**1.1**	0.2	**1.0**	0.1	**1.2**	0.4	**0.8**	0.6
At4g34100	*protein binding / zinc ion binding*	**0.9**	0.3	**1.9**	1.8	**0.9**	0.1	**0.5**	0.0	**1.0**	0.3	**0.9**	0.2	**0.8**	0.0
At4g34230	*CAD5 (cinnamyl-alcohol dehydrogenase 5)*	**0.9**	0.2	**0.8**	0.1	**0.6**	0.3	**0.5**	0.2	**0.8**	0.2	**0.8**	0.3	**0.7**	0.1
At4g34390	*XLG2 (extra-large GTP-binding protein 2); signal transducer*	**0.9**	0.4	**1.0**	0.2	**1.4**	0.6	**1.3**	0.3	**1.3**	0.4	**1.5**	0.9	**1.0**	0.3
At4g34720	*vATPC1*	**1.3**	0.5	**1.5**	0.5	**1.3**	0.4	**1.4**	0.6	**1.3**	0.5	**1.2**	0.5	**1.6**	0.8
At4g35080	*high-affinity nickel-transport family protein*	**1.0**	0.2	**1.0**	0.3	**0.8**	0.4	**0.6**	0.3	**0.7**	0.2	**1.2**	0.3	**0.8**	0.6
At4g35090	*CAT2 (CATALASE 2)*	**1.1**	0.3	**1.1**	0.2	**0.9**	0.2	**1.2**	0.1	**0.9**	0.3	**1.1**	0.3	**1.0**	0.2
At4g35180	*LHT7 (LYS/HIS TRANSPORTER 7)*	**1.0**	0.1	**1.0**	0.1	**1.1**	0.2	**1.1**	0.1	**1.1**	0.1	**0.9**	0.4	**1.0**	0.0
At4g35290	*GLR3.2 (Glutamate receptor 2)*	**1.0**	0.3	**0.9**	0.2	**0.6**	0.2	**0.8**	0.7	**0.9**	0.2	**1.1**	0.2	**0.7**	0.2
At4g35300	*TMT2 (TONOPLAST MONOSACCHARIDE TRANSPORTER2)*	**0.9**	0.1	**0.9**	0.1	**1.0**	0.1	**0.7**	0.4	**0.9**	0.1	**0.9**	0.1	**0.9**	0.1
At4g35830	*ACO; aconitate hydratase*	**1.0**	0.2	**0.9**	0.2	**0.7**	0.2	**0.7**	0.4	**0.9**	0.3	**1.0**	0.3	**0.9**	0.0
At4g36670	*PLT6, putative polyol (linear)-proton symporter*	**0.9**	0.2	**1.1**	0.1	**1.0**	0.3	**1.8**	0.1	**1.3**	0.1	**1.3**	0.4	**1.5**	0.6
At4g37270	*HMA1 (Heavy metal ATPase 1); copper-exporting ATPase*	**0.9**	0.1	**1.0**	0.4	**1.1**	0.4	**1.0**	0.2	**1.0**	0.3	**1.2**	0.5	**0.8**	0.1

At4g38250	*amino acid transporter family protein*	**1.1**	0.4	**1.1**	0.2	**1.6**	0.6	**1.5**	0.0	**1.6**	0.5	**1.5**	0.6	**1.2**	0.1
At4g38510	*vATPB2*	**1.1**	0.1	**1.0**	0.3	**1.0**	0.2	**1.1**	0.2	**1.1**	0.3	**1.2**	0.4	**1.1**	0.0
At4g38920	*VHA-C3/AVA-P3 (vacuolar-type H(+)-ATPase C3); ATPase*	**1.0**	0.2	**1.0**	0.1	**0.9**	0.2	**1.0**	0.4	**1.1**	0.3	**1.0**	0.5	**0.8**	0.1
At4g39080	*VHA-A3 (VACUOLAR PROTON ATPASE A3); ATPase*	**0.9**	0.2	**1.0**	0.3	**0.8**	0.4	**0.8**	0.3	**1.0**	0.2	**1.1**	0.4	**0.8**	0.2
At4g39330	*mannitol dehydrogenase, putative*	**1.0**	0.3	**1.0**	0.3	**0.8**	0.2	**0.6**	0.6	**0.9**	0.1	**1.2**	0.5	**0.8**	0.0
At4g39980	*DHS1 (3-deoxy-D-arabino-heptulosonate 7-phosphate synthase 1)*	**1.1**	0.5	**1.0**	0.4	**0.6**	0.2	**0.6**	0.5	**0.9**	0.2	**0.9**	0.1	**0.8**	0.2
At5g01340	*ACR1 mitochondrial succinate/fumarate translocator (mSFC1)*	**1.0**	0.2	**1.0**	0.1	**0.9**	0.2	**1.1**	0.3	**1.1**	0.2	**1.0**	0.1	**1.4**	0.0
At5g01460	*LMBR1 integral membrane family protein*	**1.0**	0.1	**1.0**	0.2	**0.9**	0.2	**1.0**	0.1	**0.9**	0.1	**1.1**	0.4	**1.0**	0.1
At5g01490	*CAX4, Ca2+/H+ antiporter/cation exchanger*	**0.9**	0.2	**1.1**	0.2	**1.2**	0.2	**1.0**	0.1	**1.1**	0.1	**1.1**	0.5	**1.3**	0.1
At5g02180	*amino acid transporter family protein*	**1.0**	0.0	**1.0**	0.1	**0.9**	0.1	**1.1**	0.1	**1.0**	0.1	**1.0**	0.1	**1.1**	0.1
At5g03860	*malate synthase, putative*	**n.d.**	n.d.	**n.d.**	n.d.	**0.9**	0.1	**n.d.**	n.d.	**n.d.**	n.d.	**n.d.**	n.d.	**n.d.**	n.d.
At5g04140	*GLU1 (FERREDOXIN-DEPENDENT GLUTAMATE SYNTHASE 1)*	**0.9**	0.1	**1.0**	0.2	**0.9**	0.2	**1.2**	0.2	**1.1**	0.2	**1.2**	0.4	**1.2**	0.3
At5g04160	*phosphate translocator-related*	**1.1**	0.1	**1.0**	0.2	**0.7**	0.2	**0.6**	0.5	**1.0**	0.1	**1.2**	0.4	**0.9**	0.1
At5g04770	*CAT6 (CATIONIC AMINO ACID TRANSPORTER 6)*	**1.3**	0.3	**1.2**	0.2	**1.4**	0.3	**1.2**	0.3	**1.1**	0.2	**1.1**	0.1	**1.1**	0.2
At5g05170	*CESA3 (CELLULASE SYNTHASE 3)*	**1.0**	0.3	**0.8**	0.2	**0.7**	0.4	**0.5**	0.3	**0.7**	0.1	**0.8**	0.1	**0.6**	0.0
At5g05920	*EDA22 EMBRYO SAC DEVELOPMENT ARREST 22*	**1.0**	0.2	**1.2**	0.4	**1.2**	0.3	**0.9**	0.1	**1.2**	0.1	**1.3**	0.5	**1.0**	0.0
At5g08100	*L-asparaginase / L-asparagine amidohydrolase*	**1.2**	0.6	**1.1**	0.1	**1.1**	0.4	**1.1**	0.0	**1.5**	0.7	**1.3**	0.5	**1.2**	0.2
At5g08290	*YLS8 (yellow-leaf-specific gene 8)*	**0.8**	0.2	**0.9**	0.3	**1.1**	0.2	**1.1**	0.2	**1.0**	0.1	**1.0**	0.2	**1.2**	0.4
At5g08640	*FLS (FLAVONOL SYNTHASE)*	**1.1**	0.3	**1.1**	0.2	**1.2**	0.2	**1.3**	0.3	**1.3**	0.4	**1.4**	0.5	**1.2**	0.1
At5g09220	*AAP2 (AMINO ACID PERMEASE 2); amino acid permease*	**1.0**	0.3	**1.1**	0.1	**1.4**	0.4	**1.4**	0.5	**1.4**	0.3	**1.1**	0.2	**1.0**	0.4
At5g09690	*MRS2-7*	**1.0**	0.1	**1.1**	0.3	**0.9**	0.2	**0.8**	0.5	**1.3**	0.4	**1.4**	0.5	**1.0**	0.1
At5g09710	*MRS2-9*	**1.0**	0.2	**1.1**	0.2	**1.0**	0.2	**1.2**	0.5	**1.2**	0.4	**1.2**	0.5	**1.2**	0.3
At5g09720	*MRS2-8*	**1.1**	0.2	**1.1**	0.2	**1.1**	0.2	**1.0**	0.0	**1.0**	0.1	**1.1**	0.1	**1.2**	0.0
At5g10240	*ASN3 (ASPARAGINE SYNTHETASE 3)*	**0.9**	0.2	**1.1**	0.3	**1.4**	0.7	**1.3**	0.5	**1.3**	0.6	**1.6**	1.0	**1.4**	0.4
At5g11180	*GLR2.6 (Arabidopsis thaliana glutamate receptor 2.6)*	**1.0**	0.2	**0.9**	0.2	**0.7**	0.3	**0.6**	0.5	**0.8**	0.2	**1.2**	0.4	**0.7**	0.5
At5g11870	*similar to SAG18 (Senescence associated gene 18)*	**0.9**	0.1	**0.9**	0.3	**0.6**	0.3	**0.6**	0.2	**0.8**	0.2	**1.0**	0.3	**0.8**	0.3
At5g13170	*nodulin MtN3 family protein*	**1.1**	0.2	**1.2**	0.3	**1.1**	0.3	**1.5**	0.6	**1.2**	0.3	**1.0**	0.1	**1.2**	0.3
At5g13280	*AK-LYS1 (ASPARTATE KINASE 1)*	**0.9**	0.2	**1.1**	0.3	**0.9**	0.1	**0.7**	0.4	**0.9**	0.1	**1.0**	0.2	**0.9**	0.1
At5g13400	*proton-dependent oligopeptide transport (POT) family*	**1.0**	0.2	**1.0**	0.2	**1.0**	0.1	**1.0**	0.0	**1.0**	0.0	**0.9**	0.2	**1.0**	0.0
At5g13550	*SULTR4;1 (Sulfate transporter 4.1); sulfate transporter*	**1.0**	0.0	**0.9**	0.1	**1.0**	0.2	**1.0**	0.0	**1.0**	0.0	**0.9**	0.1	**1.0**	0.0
At5g13750	*ZIFL1 (ZINC INDUCED FACILITATOR-LIKE 1)*	**1.1**	0.0	**1.1**	0.2	**0.6**	0.2	**0.6**	0.4	**0.9**	0.2	**1.1**	0.1	**1.0**	0.7
At5g13930	*CHS (CHALCONE SYNTHASE); naringenin-chalcone synthase*	**0.9**	0.1	**1.1**	0.3	**1.3**	0.5	**1.1**	0.1	**1.1**	0.2	**1.2**	0.7	**1.2**	0.3
At5g14800	*P5CR (PYRROLINE-5- CARBOXYLATE (P5C) REDUCTASE)*	**0.8**	0.5	**0.9**	0.3	**0.8**	0.0	**1.0**	0.1	**1.1**	0.2	**0.8**	0.4	**1.0**	0.1
At5g14870	*CNGC18 (cyclic nucleotide-gated ion channel 18)*	**0.9**	0.2	**0.9**	0.2	**0.9**	0.2	**1.0**	0.1	**1.0**	0.1	**1.1**	0.8	**0.9**	0.1
At5g14930	*SAG101 (SENESCENCE-ASSOCIATED GENE 101); triacylglycerol lipase*	**1.3**	0.5	**1.2**	0.2	**1.8**	0.4	**1.3**	0.4	**1.6**	0.3	**1.2**	0.2	**1.4**	0.0
At5g15090	*porin / voltage-dependent anion-selective channel protein, putative*	**1.1**	0.4	**1.1**	0.2	**0.9**	0.2	**1.2**	0.2	**1.2**	0.1	**0.9**	0.2	**1.1**	0.0
At5g15240	*amino acid transporter family protein*	**1.0**	0.1	**1.0**	0.1	**1.0**	0.0	**1.0**	0.0	**0.9**	0.1	**0.8**	0.2	**1.0**	0.0
At5g15410	*CNGC2/AtDND1 (DEFENSE NO DEATH 1)*	**0.9**	0.1	**0.9**	0.2	**0.9**	0.1	**1.0**	0.0	**1.0**	0.0	**1.2**	0.8	**0.9**	0.1
At5g16150	*GLT1/PGLCT (GLUCOSE TRANSPORTER 1)*	**0.9**	0.1	**0.9**	0.1	**0.7**	0.2	**0.5**	0.1	**0.9**	0.3	**1.0**	0.2	**0.8**	0.3
At5g17010	*sugar transporter family protein*	**0.8**	0.2	**1.0**	0.0	**0.7**	0.3	**0.7**	0.4	**1.0**	0.0	**0.9**	0.4	**0.7**	0.4
At5g17020	*XPO1A (exportin 1A); protein transporter*	**1.1**	0.2	**1.1**	0.1	**1.1**	0.5	**1.3**	0.4	**0.9**	0.1	**1.2**	0.7	**1.1**	0.1

Gene ID	Description													
At5g17230	PSY (phytoene synthase)	1.0	0.1	1.1	0.2	1.2	0.2	1.3	0.4	1.3	0.3	1.3	0.2	1.4	0.5
At5g17330	GAD (Glutamate decarboxylase 1); calmodulin binding	0.8	0.4	0.8	0.1	0.8	0.2	0.8	0.0	0.7	0.2	0.8	0.2	0.8	0.0
At5g17630	glucose-6-phosphate/phosphate translocator, putative; similar to GPT1	1.1	0.1	1.1	0.2	1.2	0.2	1.3	0.5	1.1	0.1	1.2	0.1	1.2	0.3
At5g17850	CAX8 cation exchanger, putative	1.3	0.3	1.0	0.2	1.0	0.2	1.1	0.2	1.0	0.2	1.3	0.5	0.9	0.1
At5g18170	GDH1 (GLUTAMATE DEHYDROGENASE 1); oxidoreductase	1.2	0.6	1.2	0.3	1.0	0.4	0.7	0.4	1.1	0.3	1.3	0.3	1.1	0.3
At5g18840	sugar transporter, putative	1.0	0.1	1.0	0.1	1.0	0.3	1.5	0.3	1.3	0.2	1.2	0.4	1.3	0.2
At5g20250	DIN10 (dark inducible 10), raffinose synthase family protein	0.8	0.2	0.8	0.2	1.0	0.2	1.0	0.4	1.1	0.3	0.9	0.2	1.1	0.3
At5g20280	SPS1F (sucrose phosphate synthase 1F)	1.1	0.1	1.1	0.2	1.1	0.3	1.2	0.3	1.1	0.3	0.9	0.1	1.2	0.3
At5g20830	SUS1 (SUCROSE SYNTHASE 1)	1.2	0.5	1.0	0.1	1.3	0.3	1.6	0.3	1.6	0.9	1.5	0.3	1.3	0.4
At5g22830	MRS2-11/MGT10, putative Mg2+ magnesium transporter	1.0	0.2	1.0	0.1	0.9	0.2	0.9	0.1	0.9	0.3	1.1	0.5	0.9	0.1
At5g23270	STP11 pollen tube-specific monosaccharide-proton symporter	0.9	0.1	0.8	0.2	0.7	0.3	0.7	0.5	1.1	0.5	1.0	0.3	0.8	0.6
At5g23810	AAP7 (amino acid permease 7)	0.9	0.2	1.1	0.3	0.9	0.3	0.7	0.2	1.2	0.1	1.5	0.7	1.0	0.1
At5g23990	FRO5 putative ferric-chelate reductase	1.1	0.1	1.1	0.1	1.0	0.2	1.2	0.2	1.0	0.0	1.2	0.4	1.2	0.2
At5g24000	similar to unknown protein (TAIR:AT5G52540.1)	1.0	0.1	1.0	0.2	1.1	0.4	1.0	0.0	1.0	0.1	0.9	0.2	1.1	0.1
At5g24130	similar to Os02g0257200 [Oryza sativa (japonica cultivar-group)]	1.2	0.2	1.2	0.2	1.2	0.4	0.9	0.1	1.2	0.3	1.3	0.2	1.2	0.6
At5g26250	STP8, putative monosaccharide-proton symporter	1.2	0.2	1.1	0.2	1.1	0.5	1.2	0.2	1.0	0.1	1.2	0.5	1.2	0.3
At5g26340	MSS1 (SUGAR TRANSPORT PROTEIN 13)	1.0	0.2	1.1	0.1	0.8	0.2	0.7	0.4	1.3	0.4	1.6	0.6	0.9	0.1
At5g27100	GLR2.1	1.0	0.2	0.9	0.2	1.3	0.7	1.0	0.0	0.9	0.1	0.9	0.1	1.0	0.0
At5g27150	NHX1 (NA+/H+ EXCHANGER); sodium:hydrogen antiporter	1.0	0.2	1.0	0.4	0.7	0.4	0.6	0.3	0.7	0.1	1.0	0.4	1.0	1.1
At5g27350	SFP1 putative MFS superfamily monosaccharide transporter	1.1	0.2	1.1	0.3	0.8	0.3	1.3	1.2	0.9	0.1	1.1	0.2	0.7	0.1
At5g27360	SFP2 putative MFS superfamily monosaccharide transporter	1.1	0.3	0.9	0.1	0.7	0.4	0.7	0.4	0.9	0.1	1.1	0.3	1.3	1.3
At5g27380	GSH2 (GLUTATHIONE SYNTHETASE 2)	1.1	0.1	1.1	0.1	1.1	0.3	1.5	0.3	1.3	0.2	1.3	0.4	1.4	0.4
At5g33320	PPT1 PHOSPHATE/PHOSPHOENOLPYRUVATE TRANSLOCATOR	1.1	0.1	1.0	0.3	0.6	0.4	0.7	0.3	0.8	0.1	1.0	0.2	0.9	0.4
At5g35630	GS2 (GLUTAMINE SYNTHETASE 2); glutamate-ammonia ligase	0.9	0.2	0.9	0.2	1.2	0.3	1.2	0.1	1.0	0.2	0.9	0.2	1.0	0.0
At5g36940	CAT3 (CATIONIC AMINO ACID TRANSPORTER 3)	1.0	0.2	1.1	0.2	0.8	0.2	0.7	0.5	1.0	0.1	1.1	0.3	0.9	0.0
At5g37500	GORK (GATED OUTWARDLY-RECTIFYING K+ CHANNEL)	1.0	0.2	0.9	0.1	0.9	0.0	0.7	0.4	0.9	0.1	1.2	0.4	0.9	0.1
At5g37610	porin-like protein	1.1	0.4	0.9	0.1	0.8	0.3	0.7	0.5	1.0	0.1	1.0	0.1	0.9	0.4
At5g40780	LHT1 (LYSINE HISTIDINE TRANSPORTER 1)	1.1	0.3	1.1	0.3	0.9	0.2	0.7	0.1	0.8	0.3	0.7	0.3	0.8	0.2
At5g41760	nucleotide-sugar transporter family protein	1.2	0.2	1.2	0.3	1.5	0.6	1.5	0.7	1.4	0.4	1.1	0.3	1.3	0.4
At5g42690	similar to unknown protein (TAIR:AT4G37080.2)	1.2	0.3	1.1	0.2	1.4	0.4	1.5	0.0	1.4	0.3	1.2	0.3	1.2	0.0
At5g42960	similar to unknown protein (TAIR:AT1G45170.1)	1.0	0.2	1.1	0.3	0.6	0.1	0.5	0.2	0.8	0.2	0.6	0.3	1.0	0.5
At5g43610	SUC6 (SUCROSE-PROTON SYMPORTER 6)	1.0	0.2	0.9	0.1	0.7	0.2	0.6	0.6	0.9	0.1	1.2	0.5	0.7	0.1
At5g43780	APS4	1.0	0.4	1.4	0.5	1.5	0.5	1.4	0.1	1.7	0.5	1.2	0.8	n.d.	n.d.
At5g44070	CAD1/ PCS1 (CADMIUM SENSITIVE 1/ phytochelatin synthase 1)	1.1	0.1	1.1	0.2	1.3	0.5	1.0	0.0	0.9	0.2	1.0	0.3	1.2	0.3
At5g44370	ANTR5, putative anion transporter	1.0	0.2	1.1	0.1	0.8	0.0	0.7	0.3	1.0	0.2	1.1	0.4	1.1	0.2
At5g45890	SAG12 (senescence-associated gene 12); cysteine-type peptidase	0.9	0.1	0.9	0.1	0.8	0.3	0.7	0.5	1.0	0.1	1.0	0.2	0.8	0.3
At5g46110	TPT/APE2; antiporter/ triose-phosphate transporter	1.0	0.1	1.0	0.1	1.0	0.1	0.7	0.4	1.0	0.1	1.1	0.1	1.0	0.0
At5g46240	KAT1 (K+ ATPase 1)	1.0	0.1	0.9	0.1	0.8	0.1	0.7	0.4	0.9	0.1	1.0	0.1	1.0	0.0
At5g46360	KCO3 (Ca2+ activated outward rectifying K+ channel 3)	1.0	0.2	1.0	0.1	1.0	0.3	1.1	0.1	0.9	0.1	1.1	0.5	1.0	0.0
At5g46370	KCO2 (CA2+ ACTIVATED OUTWARD RECTIFYING K+ CHANNEL 2)	1.2	0.2	1.2	0.3	1.2	0.2	1.3	0.4	1.2	0.3	1.0	0.2	1.2	0.3
At5g47530	auxin-induced protein, putative	0.9	0.2	0.9	0.1	1.1	0.4	0.7	0.4	0.9	0.1	1.1	0.3	1.1	0.4

At5g47560	SDAT/ TDT tonoplast dicarboxylate transporter	**n.d.**	n.d.	**0.9**	0.1	**0.8**	0.2	**n.d.**	n.d.	**n.d.**	n.d.	**n.d.**	n.d.	**n.d.**	n.d.
At5g48400	GLR1.2	**0.8**	0.3	**0.8**	0.2	**0.8**	0.1	**0.8**	0.2	**0.8**	0.3	**1.0**	0.7	**0.9**	0.1
At5g48410	GLR1.3	**0.9**	0.1	**1.0**	0.1	**1.0**	0.1	**1.1**	0.1	**1.0**	0.1	**0.9**	0.2	**1.1**	0.1
At5g49190	SUS2 (SUCROSE SYNTHASE 2)	**1.2**	0.2	**1.0**	0.1	**0.9**	0.4	**0.7**	0.4	**0.9**	0.1	**1.1**	0.2	**0.7**	0.4
At5g49630	AAP6	**1.0**	0.3	**1.1**	0.3	**1.1**	0.2	**1.4**	0.1	**1.4**	0.1	**1.4**	0.3	**1.3**	0.3
At5g49740	FRO7, putative ferric-chelate reductase	**0.8**	0.2	**0.8**	0.3	**0.7**	0.2	**0.6**	0.4	**0.8**	0.1	**0.9**	0.4	**0.7**	0.3
At5g51070	ERD1 (EARLY RESPONSIVE TO DEHYDRATION 1)	**n.d.**	n.d.	**n.d.**	n.d.	**n.d.**	n.d.	**n.d.**	n.d.	**n.d.**	n.d.	**n.d.**	n.d.	**n.d.**	n.d.
At5g51460	TPPA (trehalose-6-phosphate phosphatase)	**1.1**	0.1	**1.1**	0.1	**1.3**	0.2	**1.4**	0.2	**1.3**	0.5	**1.4**	0.2	**1.5**	0.2
At5g51820	PGM (PHOSPHOGLUCOMUTASE)	**1.0**	0.3	**0.9**	0.1	**0.8**	0.4	**0.7**	0.5	**1.0**	0.1	**1.2**	0.7	**0.9**	0.1
At5g52540	Protein of unknown function	**0.9**	0.3	**0.9**	0.2	**1.2**	0.5	**1.3**	0.0	**1.2**	0.4	**0.9**	0.4	**0.9**	0.0
At5g53130	CNGC1	**1.1**	0.5	**0.9**	0.1	**0.9**	0.2	**0.9**	0.1	**0.9**	0.2	**1.0**	0.4	**1.0**	0.0
At5g54250	CNGC4	**1.1**	0.1	**1.1**	0.1	**1.1**	0.1	**1.2**	0.3	**1.0**	0.1	**1.2**	0.1	**1.2**	0.3
At5g54800	GPT1 (glucose-6-phosphate transporter 1)	**1.0**	0.2	**0.9**	0.3	**1.0**	0.3	**1.2**	0.1	**1.1**	0.2	**0.9**	0.2	**1.0**	0.3
At5g54810	TSB1, tryptophan synthase, beta subunit 1	**0.9**	0.3	**0.8**	0.2	**0.7**	0.2	**0.6**	0.3	**0.8**	0.2	**0.8**	0.3	**0.9**	0.1
At5g55630	KCO1	**1.4**	0.5	**1.1**	0.1	**1.2**	0.4	**1.2**	0.3	**1.0**	0.1	**1.5**	1.1	**1.2**	0.3
At5g55970	zinc finger (C3HC4-type RING finger) family protein	**1.1**	0.2	**1.1**	0.2	**1.0**	0.2	**1.1**	0.2	**1.0**	0.1	**0.9**	0.1	**1.2**	0.3
At5g56080	NAS2, nicotianamine synthase	**1.1**	0.2	**1.0**	0.1	**0.8**	0.3	**0.7**	0.4	**0.9**	0.1	**1.1**	0.1	**0.9**	0.7
At5g57090	PIN2/ EIR1 (ETHYLENE INSENSITIVE ROOT 1)	**1.0**	0.5	**0.9**	0.2	**1.1**	0.2	**1.2**	0.1	**2.0**	2.0	**0.8**	0.2	**0.9**	0.1
At5g57490	porin, putative	**0.9**	0.2	**0.9**	0.1	**0.7**	0.3	**0.6**	0.3	**0.8**	0.2	**0.8**	0.1	**0.6**	0.3
At5g57940	CNGC5	**0.8**	0.2	**1.0**	0.1	**1.0**	0.1	**1.2**	0.2	**1.1**	0.2	**1.0**	0.1	**1.1**	0.3
At5g59250	sugar transporter family	**0.9**	0.1	**0.8**	0.2	**0.9**	0.2	**0.7**	0.4	**0.9**	0.1	**0.8**	0.2	**0.8**	0.2
At5g59520	ZIP2	**1.1**	0.3	**1.2**	0.2	**1.2**	0.4	**1.3**	0.2	**1.3**	0.3	**1.1**	0.4	**1.3**	0.1
At5g60070	ankyrin repeat protein	**1.2**	0.2	**1.2**	0.2	**1.0**	0.4	**1.3**	0.4	**1.2**	0.4	**1.1**	0.1	**1.3**	0.5
At5g61520	STP3 monosaccharide-proton symporter	**n.d.**	n.d.	**0.9**	0.1	**0.7**	0.4	**n.d.**	n.d.	**n.d.**	n.d.	**n.d.**	n.d.	**n.d.**	n.d.
At5g62160	ZIP12 (ZINC TRANSPORTER 12 PRECURSOR)	**0.9**	0.1	**1.0**	0.3	**0.7**	0.2	**0.6**	0.4	**0.9**	0.2	**1.3**	0.4	**0.5**	0.0
At5g62530	P5CDH/ALDH12A1 (delta-1-pyrroline-5-carboxylate dehydrogenase/ Aldehyde dehydrogenase 12A1)	**1.0**	0.0	**1.0**	0.2	**0.9**	0.3	**1.0**	0.0	**1.0**	0.4	**1.1**	0.6	**0.9**	0.1
At5g63850	AAP4 (amino acid permease 4)	**0.9**	0.1	**1.0**	0.2	**1.1**	0.3	**1.2**	0.3	**1.0**	0.2	**0.9**	0.4	**0.7**	0.2
At5g64280	DiT2.2/ pDCT2putative plastidic glutamate/malate translocator	**1.1**	0.2	**1.2**	0.1	**0.9**	0.2	**0.8**	0.6	**1.4**	0.2	**1.5**	0.4	**1.0**	0.0
At5g64290	DiT2.1/ pDCT1, plastidic glutamate/malate-translocator	**0.9**	0.1	**1.1**	0.1	**1.1**	0.1	**1.1**	0.1	**1.1**	0.1	**0.9**	0.1	**1.2**	0.3
At5g64560	MRS2-2	**1.0**	0.2	**1.0**	0.3	**0.7**	0.2	**0.5**	0.3	**1.0**	0.2	**1.5**	0.3	**0.8**	0.3
At5g65010	ASN2 (ASPARAGINE SYNTHETASE 2)	**1.0**	0.2	**1.1**	0.4	**1.5**	0.6	**1.5**	0.5	**1.2**	0.3	**1.4**	0.6	**1.0**	n.d.
At5g65750	2-oxoglutarate dehydrogenase E1 component, putative	**0.9**	0.1	**1.0**	0.1	**1.0**	0.0	**1.1**	0.1	**1.1**	0.1	**0.9**	0.1	**1.1**	0.1
At5g66170	senescence-associated protein	**0.9**	0.2	**0.8**	0.3	**2.0**	1.3	**0.9**	0.2	**1.3**	0.5	**1.2**	0.6	**1.1**	0.4
At5g67500	porin, putative	**0.9**	0.1	**1.0**	0.1	**0.9**	0.1	**1.0**	0.0	**1.0**	0.2	**1.0**	0.3	**1.3**	0.5

Supplementary Table 2. Top hundred deregulated genes in various *pip2* knockout mutants. Mutants transcriptional profile were analyzed using Affymetrix ATH1 GeneChip. After statistical analyses, differentially expressed genes were extracted and the top hundred were submitted to functional classification according to MapMan. Expression ratios are expressed as log2 values.

mutant	ROOTS pip 2;1	wt	ratio 2;1/wt	p-value	pip 2;2	wt	ratio pip2;2/wt	p-value	pip 2;4	wt	ratio pip2;4/wt	p-value	pip 2;1-2;4	wt	ratio 2;1-2;4/wt	p-value	pip 2;2-2;1	wt	ratio 2;2-2;1/wt	p-value	LEAVES pip 2;2-2;1	wt	ratio 2;2-2;1/wt	p-value	Functional categories	description
AGI code																										
AT2G12300	2.6	6.8	-4.2	0.021	2.6	6.8	-4.2	0.020	2.3	6.8	-4.5	0.020	2.3	6.8	-4.5	0.017									DNA.synthesis/chromatin structure.retrotransposon	
AT2G10640	4.5	8.1	-3.6	0.013	4.1	8.1	-4.0	0.010	4.2	8.1	-3.9	0.012	3.9	8.1	-4.2	0.010									DNA.synthesis/chromatin structure.retrotransposon	
AT1G36470	2.4	6.3	-3.8	0.023	1.3	6.3	-4.9	0.013	2.7	6.3	-3.5	0.031	2.5	6.3	-3.7	0.024									DNA.synthesis/chromatin structure.retrotransposon	
AT2G04770	4.7	8.3	-3.6	0.007	4.6	8.3	-3.7	0.006	5.0	8.3	-3.2	0.009	4.8	8.3	-3.5	0.008									DNA.synthesis/chromatin structure.retrotransposon	
AT1G36240	4.3	6.6	-2.2	0.026	4.5	6.6	-2.1	0.031	4.4	6.6	-2.1	0.030	4.4	6.6	-2.1	0.032									protein.synthesis.misc ribososomal protein	60S ribosomal protein L30
AT4G16630	6.4	7.4	-0.9	0.051	6.4	7.4	-1.0	0.037	6.3	7.4	-1.1	0.035	6.0	7.4	-1.4	0.018									DNA.synthesis/chromatin structure	
AT2G23630	7.0	7.7	-0.8	0.078	6.7	7.7	-1.0	0.059	6.4	7.7	-1.3	0.027	6.5	7.7	-1.2	0.033									not assigned.no ontology	SKS16 (SKU5 Similar 16); copper ion binding / pectinesterase
AT3G15230	6.6	7.5	-0.8	0.052	6.6	7.5	-0.9	0.059	6.1	7.5	-1.3	0.017	6.6	7.5	-0.8	0.055									not assigned.unknown	
AT3G49790	7.7	6.9	0.8	0.051	7.7	6.9	0.8	0.052	7.8	6.9	0.9	0.037	7.7	6.9	0.8	0.046									not assigned.unknown	similar to ATPP2-A10 (Phloem protein 2-A10)
AT5G59240	6.8	7.6	-0.8	0.067	6.7	7.6	-1.0	0.052	6.5	7.6	-1.1	0.031													protein.synthesis.misc ribososomal protein	40S ribosomal protein S8
AT3G51600	8.1	9.0	-1.0	0.029	7.8	9.0	-1.2	0.020	8.0	9.0	-1.0	0.030					8.9	8.2	0.6	0.035					lipid metabolism.lipid transfer proteins etc	LTP5 (LIPID TRANSFER PROTEIN 5)
AT2G15560	4.1	6.2	-2.1	0.033	4.3	6.2	-1.8	0.038					4.0	6.2	-2.2	0.028									not assigned.disagreeing hits	
AT3G47330	4.7	6.1	-1.4	0.029	4.7	6.1	-1.4	0.028					4.9	6.1	-1.2	0.052									not assigned.disagreeing hits	similar to unknown protein
AT4G00640	5.4	6.2	-0.8	0.083	5.2	6.2	-1.0	0.061					5.2	6.2	-1.0	0.051									not assigned.unknown	similar to unknown protein
AT1G11530	8.9	8.2	0.7	0.046	9.0	8.2	0.8	0.034					9.0	8.2	0.7	0.030									redox.thioredoxin	AtCXXS1 C-TER CYSTEINE residue is changed to a serine 1
AT2G31730	7.7	6.8	1.0	0.033	8.0	6.8	1.2	0.011					7.6	6.8	0.8	0.034	6.7	7.9	-1.2	0.066					hormone metabolism.ethylene	ethylene-responsive protein, putative
AT5G35940	5.7	7.3	-1.6	0.019	5.5	7.3	-1.9	0.013									7.1	7.7	-0.6	0.357					misc.myrosinases-lectin-jacalin	jacalin lectin family protein
AT1G62510	7.1	5.9	1.2	0.030	6.9	5.9	1.0	0.047									6.4	5.8	0.6	0.087					misc.protease inhibitor/seed storage/LTP	protease inhibitor/seed storage/lipid transfer protein (LTP)
AT1G29660	6.3	7.4	-1.1	0.036	6.2	7.4	-1.2	0.054																	misc.GDSL-motif lipase	GDSL-motif lipase/hydrolase family protein
AT2G42840	7.3	8.3	-1.0	0.037	7.2	8.3	-1.1	0.036													8.4	9.4	-1.0	0.039	not assigned.no ontology	PDF1 (PROTODERMAL FACTOR 1)
AT5G51750	5.6	6.5	-0.8	0.075	5.4	6.5	-1.0	0.058													8.2	8.9	-0.7	0.044	protein.degradation.subtilases	ATSBT1.3__subtilase family protein
AT3G60140	4.0	7.1	-3.1	0.007	3.9	7.1	-3.2	0.007																	misc.gluco-, galacto- and mannosidases	DIN2 (DARK INDUCIBLE 2); hydrolase
AT3G26200	3.6	6.4	-2.8	0.025	4.1	6.4	-2.3	0.034																	misc.cytochrome P450	CYP71B22 cytochrome P450
AT4G15370	7.5	9.0	-1.5	0.014	7.6	9.0	-1.4	0.045																	secondary metabolism.isoprenoids.terpenoids	pentacyclic triterpene synthase, putative
AT1G49570	8.8	10.0	-1.1	0.053	8.8	10.0	-1.2	0.067																	misc.peroxidases	peroxidase, putative
AT4G33070	8.1	8.9	-0.8	0.059	7.7	8.9	-1.2	0.032																	fermentation.PDC	pyruvate decarboxylase, putative
AT3G49090	5.9	6.8	-0.8	0.079	5.7	6.8	-1.1	0.048																	not assigned.disagreeing hits	
AT4G38410	6.6	7.5	-0.9	0.049	6.4	7.5	-1.1	0.034																	stress.abiotic.unspecified	dehydrin, putative
AT1G27950	7.2	8.1	-0.9	0.053	7.1	8.1	-1.1	0.044																	lipid metabolism.lipid transfer proteins etc	lipid transfer protein-related
AT5G01510	6.7	7.4	-0.7	0.071	6.4	7.4	-1.0	0.030																	development.unspecified	AIL6 (AINTEGUMENTA-LIKE 6); DNA binding / transcription factor
AT5G01870	10.3	11.2	-0.9	0.031	10.3	11.2	-1.0	0.036																	lipid metabolism.lipid transfer proteins etc	lipid transfer protein, putative
AT3G16370	7.0	7.8	-0.8	0.079	6.9	7.8	-0.9	0.056																	misc.GDSL-motif lipase	GDSL-motif lipase/hydrolase family protein
AT3G59690	8.9	8.3	0.6	0.058	8.9	8.3	0.6	0.059																	signalling.calcium	IQD13 (IQ-domain 13); calmodulin binding
AT3G16920	9.2	8.4	0.8	0.025	9.0	8.4	0.6	0.046																	stress.biotic	chitinase
AT2G37950	7.4	6.7	0.7	0.065	7.3	6.7	0.6	0.063																	protein.degradation.ubiquitin.E3.RING	zinc finger (C3HC4-type RING finger) family protein
AT2G22570	10.1	9.5	0.6	0.066	10.2	9.5	0.7	0.056																	misc.protease inhibitor/seed storage/LTP	protease inhibitor/seed storage/lipid transfer protein (LTP)
AT3G56730	7.6	6.9	0.7	0.083	7.6	6.9	0.7	0.062																	not assigned.unknown	similar to unknown protein
AT1G71740	8.1	7.5	0.6	0.077	8.2	7.5	0.7	0.053																	not assigned.unknown	similar to unknown protein
AT3G53770	7.1	6.4	0.7	0.060	7.1	6.4	0.8	0.045																	development.late embryogenesis abundant	late embryogenesis abundant protein-related / LEA protein-related
AT5G23840	9.2	8.5	0.8	0.060	9.3	8.5	0.9	0.034																	not assigned.no ontology	MD-2-related lipid recognition domain-containing protein
AT2G22980	6.2	5.1	1.1	0.042	6.3	5.1	1.2	0.034																	protein.degradation.serine protease	SCPL13 (serine carboxypeptidase)
AT2G28790	8.9	9.7	-0.9	0.022					8.7	9.7	-1.1	0.012	8.9	9.7	-0.8	0.031					8.2	9.6	-1.4	0.026	stress.abiotic	osmotin-like protein, putative
AT1G35590	1.8	6.5	-4.7	0.038					1.4	6.5	-5.0	0.026	0.4	6.5	-6.0	0.009									DNA.unspecified	
AT1G43800	7.1	8.2	-1.0	0.064					7.0	8.2	-1.1	0.033	6.9	8.2	-1.2	0.032									lipid metabolism+	acyl-(acyl-carrier-protein) desaturase, putative
AT5G50730	7.0	7.7	-0.7	0.081					5.8	7.7	-1.9	0.009	6.5	7.7	-1.2	0.023									not assigned.unknown	
AT1G33750	6.8	7.6	-0.8	0.063					6.1	7.6	-1.5	0.021	6.6	7.6	-1.0	0.051									secondary metabolism.isoprenoids.terpenoids	terpene synthase/cyclase family protein
AT2G23050	5.7	6.8	-1.0	0.038					5.3	6.8	-1.5	0.016	5.8	6.8	-1.0	0.048									signalling.light	phototropic-responsive NPH3 family protein
AT2G25980	9.3	10.0	-0.7	0.060					8.6	10.0	-1.4	0.009	9.0	10.0	-1.0	0.020									hormone metabolism.jasmonate	jacalin lectin family protein
AT4G25630	10.0	10.9	-0.9	0.018					10.0	10.9	-0.8	0.022	10.0	10.9	-0.9	0.019									RNA.processing	FIB2__FIB2 (FIBRILLARIN 2)
AT1G27390	8.1	8.8	-0.8	0.035					7.9	8.8	-1.0	0.019	8.1	8.8	-0.7	0.052									protein.targeting.mitochondria	TOM20-2 (TRANSLOCASE OUTER MEMBRANE 20-2)
AT1G67500	6.8	6.0	0.8	0.062					7.1	6.0	1.0	0.024	7.0	6.0	0.9	0.042									DNA.synthesis/chromatin structure	AtREV3 (Arabidopsis thaliana recovery protein 3); DNA binding
AT3G25830	7.6	6.8	0.8	0.083					8.2	6.8	1.3	0.021	8.2	6.8	1.4	0.022									secondary metabolism.isoprenoids.terpenoids	ATTPS-CIN (TERPENE SYNTHASE-LIKE SEQUENCE-1,8-CINEOLE)
AT5G37990	8.5	7.5	1.0	0.063					9.0	7.5	1.5	0.024	9.1	7.5	1.5	0.030									hormone metabolism.salicylic acid	S-adenosylmethionine-dependent methyltransferase
AT3G30720	8.3	7.4	0.9	0.074					5.2	7.4	-2.2	0.015					7.5	4.6	2.9	0.002	8.2	6.9	1.3	0.022	not assigned.unknown	unknown protein

Gene	v1	v2	log	p	v1	v2	log	p	v1	v2	log	p	v1	v2	log	p	v1	v2	log	p	v1	v2	log	p	Functional category	Description
AT4G26600	5.9	6.7	-0.8	0.058					5.3	6.7	-1.4	0.017													DNA.synthesis/chromatin structure	nucleolar protein, putative
AT1G56680	7.9	8.6	-0.7	0.082					7.7	8.6	-0.9	0.031													stress.biotic	glycoside hydrolase family 19 protein
AT3G57150	9.7	10.3	-0.6	0.069					9.5	10.3	-0.9	0.029													DNA.synthesis/chromatin structure	NAP57 (ARABIDOPSIS THALIANA HOMOLOGUE OF NAP57)
AT3G07050	8.2	8.9	-0.7	0.061					8.1	8.9	-0.8	0.037													signalling.G-proteins	GTP-binding family protein
AT3G53420	9.1	12.7	-3.6	0.000									8.9	12.7	-3.7	0.000	8.0	13.0	-5.0	0.000	8.1	12.0	-3.9	0.000	transport (PIP)	PIP2;1
AT1G78180	4.9	6.1	-1.2	0.054																					transport (transport at the mitochondrial membrane)	binding
AT3G43720	6.4	7.5	-1.1	0.038																					misc.protease inhibitor/seed storage/LTP	lipid binding
AT2G17580	5.6	6.5	-1.0	0.047																					RNA.processing	polynucleotide adenylyltransferase family protein
AT3G20470	6.0	6.9	-0.9	0.051																					not assigned.no ontology.glycine rich proteins	GRP-5__
AT4G29020	8.6	9.4	-0.9	0.048																					not assigned.no ontology.glycine rich proteins	glycine-rich protein
AT3G50900	7.3	8.1	-0.8	0.070																					DNA.unspecified	similar to unknown protein
AT5G59030	5.9	6.7	-0.8	0.071																					transport.metal	COPT1 (COPPER TRANSPORTER 1)
AT3G20240	6.2	7.0	-0.8	0.066																					transport (transport at the mitochondrial membrane)	mitochondrial substrate carrier family protein
AT1G77120	10.2	11.0	-0.8	0.043																					fermentation.ADH	ALCOHOL DEHYDROGENASE 1
AT5G48940	7.3	8.1	-0.8	0.077																					signalling.receptor kinases.leucine rich repeat XI	leucine-rich repeat transmembrane protein kinase, putative
AT4G37490	6.1	6.8	-0.7	0.081																					cell.cycle	CYCLIN 1; cyclin-dependent protein kinase regulator
AT2G30130	5.7	6.4	-0.7	0.085																					RNA.regulation of transcription (Lateral Organ Boundaries)	ASL5/ LBD12/ PCK1 (phosphoenolpyruvate carboxykinase1)
AT3G03130	6.2	6.9	-0.7	0.084																					not assigned.unknown	similar to unknown protein
AT3G62720	7.3	8.1	-0.7	0.079																					cell wall.hemicellulose synthesis	AtXT1; transferase/ transferase, transferring glycosyl groups
AT4G26760	7.9	8.6	-0.7	0.064																					cell.organisation	microtubule associated protein (MAP65/ASE1) family protein
AT4G33720	11.6	12.3	-0.7	0.057																					stress.biotic	pathogenesis-related protein, putative
AT1G32190	6.6	7.3	-0.7	0.076																					not assigned.unknown	similar to unknown protein
AT2G36230	6.6	7.3	-0.7	0.074																					amino acid metabolism.synthesis.histidine	APG10 (ALBINO AND PALE GREEN 10)
AT5G27330	7.2	7.9	-0.7	0.080																					not assigned.unknown	similar to unknown protein
AT4G05410	7.8	8.4	-0.6	0.084																					not assigned.no ontology	transducin family protein / WD-40 repeat family protein
AT1G72230	8.6	8.0	0.6	0.073																					misc.plastocyanin-like	plastocyanin-like domain-containing protein
AT1G62415	9.3	8.8	0.6	0.079																					not assigned.disagreeing hits	
AT5G03170	9.0	8.4	0.6	0.061																					not assigned.disagreeing hits	FLA11__FLA11 (fasciclin-like arabinogalactan-protein 11)
AT5G01360	7.7	7.0	0.6	0.079																					not assigned.unknown	similar to unknown protein
AT2G29130	8.5	7.9	0.6	0.083																					secondary metabolism.simple phenols	LAC2 (laccase 2); copper ion binding / oxidoreductase
AT4G35060	10.2	9.5	0.6	0.047																					metal handling.binding, chelation and storage	heavy-metal-associated domain-containing protein / CCH-related
AT1G52250	8.5	7.9	0.6	0.082																					cell.organisation	dynein light chain type 1 family protein
AT1G69080	7.3	6.7	0.6	0.076																					stress.abiotic.unspecified	universal stress protein (USP) family protein
AT2G38080	9.5	8.8	0.7	0.049																					secondary metabolism.simple phenols	IRX12/LAC4 (laccase 4); copper ion binding / oxidoreductase
AT1G20850	11.1	10.4	0.7	0.041																					protein.degradation.cysteine protease	XCP2 (XYLEM CYSTEINE PEPTIDASE 2); cysteine-type peptidase
AT1G70890	7.9	7.2	0.7	0.059																					stress.abiotic.unspecified	MLP43__major latex protein-related / MLP-related
AT1G27920	6.5	5.9	0.7	0.084																					cell.organisation	microtubule associated protein (MAP65/ASE1) family protein
AT5G40020	9.0	8.3	0.7	0.070																					stress.biotic	pathogenesis-related thaumatin family protein
AT5G12870	6.1	5.3	0.7	0.080																					RNA.regulation of transcription (MYB)	AtMYB46 (myb domain protein); DNA binding / transcription factor
AT2G28270	8.5	7.8	0.7	0.034																					not assigned.no ontology	DC1 domain-containing protein
AT5G59845	6.9	6.2	0.8	0.085																					hormone metabolism.gibberelin	gibberellin-regulated family protein
AT1G61750	8.5	7.7	0.8	0.060																					protein.postranslational modification	similar to protein kinase-related
AT5G01930	7.7	6.9	0.8	0.037																					not assigned.disagreeing hits	(1-4)-beta-mannan endohydrolase, putative
AT5G59250	6.3	5.4	0.9	0.076																					transporter.sugars	sugar transporter family protein
AT5G37260	8.0	7.1	0.9	0.068																					RNA.regulation of transcription (MYB)	myb family transcription factor
AT1G24030	6.6	5.7	0.9	0.053																					protein.postranslational modification/kinase receptor like	protein kinase family protein
AT1G33680					6.0	7.0	-1.0	0.058	5.9	7.0	-1.1	0.035	6.1	7.0	-0.9	0.051									not assigned.no ontology	nucleic acid binding
AT1G19515					7.0	7.9	-0.9	0.067	6.8	7.9	-1.1	0.020														
AT4G38680					8.9	9.8	-0.9	0.061	8.7	9.8	-1.1	0.015													stress.abiotic.cold	GRP2 (COLD SHOCK DOMAIN PROTEIN 2); nucleic acid binding
AT2G18900					7.1	7.9	-0.8	0.062	6.9	7.9	-1.0	0.029													not assigned.no ontology	transducin family protein / WD-40 repeat family protein
AT4G03900					5.7	6.8	-1.1	0.052					5.5	6.8	-1.2	0.040									DNA.synthesis/chromatin structure.retrotransposon	
AT1G65510					9.2	8.6	0.7	0.053					9.2	8.6	0.6	0.049									not assigned.unknown	similar to unknown protein
AT1G80180					10.4	9.8	0.6	0.066					10.5	9.8	0.7	0.047									not assigned.unknown	similar to unknown protein
AT2G18680					6.6	5.8	0.9	0.065									5.6	6.4	-0.8	0.207					not assigned.unknown	similar to unknown protein
AT1G07690					9.1	8.5	0.6	0.051									7.2	7.8	-0.6	0.244					not assigned.unknown	similar to unknown protein
AT1G24280					8.1	9.4	-1.3	0.021																	OPP.oxidative PP.G6PD	G6PD3 (glucose-6-phosphate 1-dehydrogenase)
AT5G34900					5.0	6.1	-1.1	0.050																	not assigned.no ontology	Ulp1 protease family protein
AT1G77050					5.6	6.7	-1.0	0.043																	DNA.synthesis/chromatin structure	DEAD/DEAH box helicase, putative
AT5G50740					5.6	6.6	-1.0	0.054																	metal handling.binding, chelation and storage	similar to ATFP3 (Arabidopsis thaliana farnesylated protein 3)
AT2G02740					5.5	6.5	-0.9	0.061																	RNA.regulation of transcription.plant TF (pbf2)	AtWHY3/PTAC11 (A. THALIANA WHIRLY 3)
AT2G27840					8.8	9.6	-0.9	0.059																	RNA.regulation of transcription.HDA	HDT4/HDA13 (histone deacetylase 13)
AT1G22530					10.8	10.2	0.6	0.062																	DNA.unspecified	SEC14 cytosolic factor family protein
AT3G27150					7.8	7.2	0.6	0.058																	protein.degradation.ubiquitin.E3.SCF.FBOX	kelch repeat-containing F-box family protein

Gene	v1	v2	ratio	p	v1	v2	ratio	p	v1	v2	ratio	p	v1	v2	ratio	p	v1	v2	ratio	p	Category	Description
AT1G16170	9.6	9.0	0.6	0.059																	not assigned.unknown	similar to unknown protein
AT1G63840	10.5	9.9	0.6	0.063																	protein.degradation.ubiquitin.E3.RING	zinc finger (C3HC4-type RING finger) family protein
AT1G01170	7.9	7.3	0.6	0.055																	stress.abiotic.unspecified	ozone-responsive stress-related protein, putative
AT3G26290	7.9	7.3	0.6	0.065																	misc.cytochrome P450	CYP71B26 (cytochrome P450)
AT5G58520	7.9	7.3	0.6	0.056																	protein.postranslational modification	protein kinase family protein
AT1G22990	9.7	9.1	0.6	0.048																	metal handling.binding, chelation and storage	heavy-metal-associated domain-containing protein / CCH-related
AT2G39430	8.9	8.3	0.6	0.063																	stress.biotic	disease resistance-responsive protein-related
AT2G01880	8.4	7.7	0.6	0.050																	misc.acid and other phosphatases	AtPAP7/PAP7 (purple acid phosphatase 7)
AT4G35350	10.8	10.2	0.7	0.034																	protein.degradation.cysteine protease	XCP1 (XYLEM CYSTEINE PEPTIDASE 1); cysteine-type peptidase
AT1G79620	7.4	6.7	0.7	0.051																	signalling.receptor kinases.leucine rich repeat VIII-1	leucine-rich repeat transmembrane protein kinase, putative
AT3G25790	9.1	8.4	0.7	0.038																	RNA.regulation of transcription (G2-like TF)	myb family transcription factor
AT3G11370	8.4	7.8	0.7	0.065																	not assigned.no ontology	DC1 domain-containing protein
AT5G48290	8.5	7.8	0.7	0.050																	not assigned.no ontology	metal ion binding
AT5G38610	7.8	7.1	0.7	0.045																	not assigned.disagreeing hits	invertase/pectin methylesterase inhibitor family protein
AT5G16490	7.5	6.8	0.7	0.059																	not assigned.no ontology	RIC4 (ROP-INTERACTIVE CRIB MOTIF-CONTAINING PROTEIN 4)
AT1G58070	7.4	6.7	0.7	0.055																	not assigned.unknown	similar to Os11g0195800
AT2G20670	8.0	7.3	0.7	0.064																	not assigned.unknown	similar to unknown protein
AT2G45180	9.4	8.7	0.7	0.060																	misc.protease inhibitor/seed storage/LTP	protease inhibitor/seed storage/lipid transfer protein (LTP)
AT1G76360	7.5	6.8	0.7	0.063																	protein.postranslational modification/kinase receptor like	protein kinase, putative
AT5G15600	8.5	7.8	0.7	0.060																	not assigned.unknown	SP1L4__SP1L4 (SPIRAL1-LIKE4)
AT2G38760	8.0	7.2	0.7	0.044																	cell.organisation	ANNAT3 (ANNEXIN ARABIDOPSIS 3); calcium ion binding
AT5G02790	8.3	7.6	0.7	0.048																	not assigned.no ontology	In2-1 protein, putative
AT4G28290	6.6	5.8	0.7	0.067																	not assigned.unknown	unknown protein
AT2G22000	7.3	6.5	0.8	0.063																	not assigned.unknown	PROPEP6__PROPEP6 (Elicitor peptide 6 precursor)
AT1G03660	8.9	8.1	0.8	0.044																	not assigned.unknown	similar to ankyrin repeat family protein
AT5G44130	8.4	7.6	0.8	0.068																	cell wall.cell wall proteins.AGPs	FLA13__fasciclin-like arabinogalactan-protein, putative
AT5G47950	8.3	7.5	0.8	0.048																	secondary metabolism.phenylpropanoids	transferase family protein
AT3G49780	8.1	7.4	0.8	0.046																	not assigned.no ontology	AtPSK4 (PHYTOSULFOKINE 4 PRECURSOR); growth factor
AT1G79110	6.5	5.7	0.8	0.066																	protein.degradation.ubiquitin.E3.RING	protein binding / zinc ion binding
AT1G52190	6.4	5.6	0.8	0.065																	transport.peptides and oligopeptides	proton-dependent oligopeptide transport (POT) family protein
AT4G00240	6.9	6.1	0.8	0.049																	lipid metabolism.lipid degradation	PLDBETA2__PLDBETA2 (phospholipase D beta 2)
AT1G17250	6.5	5.6	0.8	0.057																	stress.biotic	leucine-rich repeat family protein
AT1G17960	6.4	5.6	0.8	0.066																	protein.aa activation	threonyl-tRNA synthetase / threonine--tRNA ligase, putative
AT1G50700	6.5	5.7	0.8	0.068																	signalling.calcium	CPK33 (calcium- and calmodulin-dependent protein kinase)
AT5G17450	6.2	5.3	0.8	0.059																	metal handling.binding, chelation and storage	heavy-metal-associated domain-containing protein / CCH-related
AT4G23810	8.3	7.5	0.8	0.041																	not assigned.disagreeing hits	WRKY53 (WRKY DNA-binding protein 53); transcription factor
AT5G45380	7.2	6.3	0.9	0.042																	transport.unspecified cations	sodium:solute symporter family protein
AT3G09240	6.1	5.2	0.9	0.051																	protein.postranslational modification	protein kinase-related
AT1G79760	6.2	5.3	0.9	0.046																	not assigned.unknown	DTA4__DTA4 (DOWNSTREAM TARGET OF AGL15-4)
AT1G66800	7.1	6.2	0.9	0.041																	misc.alcohol dehydrogenases	cinnamyl-alcohol dehydrogenase family / CAD family
AT3G20100	6.9	5.9	1.0	0.027																	misc.cytochrome P450	CYP705A19 (cytochrome P450)
AT5G20240	6.8	5.5	1.3	0.023																	development.unspecified	PI__PI (PISTILLATA); DNA binding / transcription factor
AT1G72140					6.3	5.0	1.4	0.036	6.3	5.0	1.3	0.048	6.2	5.5	0.7	0.070					transport.peptides and oligopeptides	proton-dependent oligopeptide transport (POT) family protein
AT3G49620					6.1	4.6	1.5	0.024	6.3	4.6	1.7	0.027					6.3	2.1	4.2	0.030	not assigned.no ontology	DIN11 (DARK INDUCIBLE 11); oxidoreductase
AT5G60660					5.4	10.8	-5.4	0.000	3.7	10.8	-7.0	0.000									transport (PIP)	PIP2;4
AT4G37160					5.9	8.0	-2.1	0.017	6.5	8.0	-1.5	0.040									not assigned.no ontology	SKS15__SKS15 (SKU5 Similar 15); copper ion binding
AT3G62760					6.8	8.3	-1.5	0.012	7.1	8.3	-1.2	0.021									misc.glutathione S transferases	AtGSTF13 (Glutathione S-transferase (class phi) 13)
AT2G04160					6.7	8.0	-1.3	0.026	6.8	8.0	-1.1	0.035									protein.degradation.subtilases	AIR3 (Auxin-Induced in Root cultures 3); subtilase
AT5G62340					9.4	11.0	-1.6	0.013	9.9	11.0	-1.1	0.020									misc.invertase/pectin methylesterase inhibitor family	invertase/pectin methylesterase inhibitor family protein
AT1G57590					6.8	8.2	-1.4	0.017	7.1	8.2	-1.1	0.047									cell wall.pectin*esterases.acetyl esterase	carboxylic ester hydrolase
AT5G13870					6.9	8.0	-1.1	0.036	7.0	8.0	-1.1	0.042									cell wall.modification	EXGT-A4 (ENDOXYLOGLUCAN TRANSFERASE A4); hydrolase
AT4G00730					6.2	7.5	-1.3	0.019	6.5	7.5	-1.1	0.041									RNA.regulation of transcription (Homeobox)	ANL2 (ANTHOCYANINLESS 2); transcription factor
AT1G73620					7.8	9.0	-1.2	0.015	8.0	9.0	-1.0	0.022									stress.biotic	thaumatin-like protein, putative / pathogenesis-related protein
AT3G17990					5.9	7.1	-1.2	0.023	6.1	7.1	-1.0	0.048										
AT5G10130					8.3	9.5	-1.3	0.035	8.6	9.5	-1.0	0.047									stress.abiotic.unspecified	pollen Ole e 1 allergen and extensin family protein
AT5G12940					8.0	9.1	-1.1	0.036	8.1	9.1	-1.0	0.042									not assigned.no ontology	leucine-rich repeat family protein
AT5G56320					6.8	8.2	-1.4	0.018	7.3	8.2	-0.9	0.048									cell wall.modification	AtEXPA14 (ARABIDOPSIS THALIANA EXPANSIN A14)
AT1G31950					7.2	8.3	-1.1	0.033	7.4	8.3	-0.9	0.051									secondary metabolism.isoprenoids.terpenoids	terpene synthase/cyclase family protein
AT5G22440					11.0	11.6	-0.7	0.037	11.0	11.6	-0.6	0.045									protein.synthesis.misc ribosomal protein	60S ribosomal protein L10A (RPL10aC)
AT2G18370					9.6	8.7	0.9	0.037	9.5	8.7	0.8	0.047									misc.protease inhibitor/seed storage/LTP	protease inhibitor/seed storage/lipid transfer protein (LTP)
AT4G10510					7.3	6.2	1.1	0.023	7.1	6.2	0.9	0.041									protein.degradation.subtilases	subtilase family protein
AT2G33850					9.9	8.9	1.1	0.027	9.8	8.9	0.9	0.042									not assigned.unknown	similar to unknown protein
AT5G49450					9.4	8.4	1.0	0.026	9.3	8.4	0.9	0.037									RNA.regulation of transcription (bZIP)	ATBZIP1__bZIP family transcription factor

Gene													Function	Description
AT3G16450	11.3	10.2	1.1	0.026	11.2	10.2	1.0	0.042					hormone metabolism.jasmonate	jacalin lectin family protein
AT4G23670	11.4	10.2	1.2	0.020	11.3	10.2	1.1	0.027					stress.abiotic.unspecified	major latex protein-related / MLP-related
AT2G39310	10.1	8.7	1.4	0.026	9.9	8.7	1.2	0.040					misc.myrosinases-lectin-jacalin	jacalin lectin family protein
AT3G26460	7.8	6.3	1.5	0.031	7.8	6.3	1.5	0.027					stress.abiotic.unspecified	major latex protein-related / MLP-related
AT1G14120	7.8	6.1	1.8	0.021	7.8	6.1	1.7	0.025					misc.oxidases - copper, flavone etc.	2-oxoglutarate-dependent dioxygenase, putative
AT2G16005	6.5	4.5	2.0	0.020	6.5	4.5	1.9	0.054					not assigned.no ontology	MD-2-related lipid recognition domain-containing protein
AT1G26250	12.3	11.7	0.7	0.036					11.4	12.0	-0.6	0.114	cell wall.cellulose	
AT2G34180	8.0	7.1	0.9	0.038					6.8	7.4	-0.6	0.277	protein.postranslational modification	SnRK3.7_CIPK13__CIPK13 (CIPK13); kinase
AT2G43160	4.7	6.5	-1.8	0.015									not assigned.no ontology	epsin N-terminal homology (ENTH) domain-containing protein
AT5G51490	4.8	6.4	-1.6	0.027									cell wall.pectin*esterases.misc	pectinesterase family protein
AT3G16855	5.4	6.8	-1.3	0.020										
AT1G74500	8.1	9.2	-1.1	0.031									RNA.regulation of transcription (bHLH)	bHLH family protein
AT2G07370	6.8	7.8	-1.1	0.024										
AT2G41800	8.3	9.3	-1.1	0.023									not assigned.unknown	similar to unknown protein
AT3G15357	7.3	8.3	-1.1	0.024									not assigned.unknown	similar to zinc finger protein-related
AT1G75710	7.0	8.0	-1.0	0.029									RNA.regulation of transcription (C2H2 zinc finger)	zinc finger (C2H2 type) family protein
AT1G13730	7.5	8.5	-1.0	0.018									protein.targeting.nucleus	nuclear transport factor 2 (NTF2) / (RRM)-containing protein
AT4G28190	6.7	7.7	-1.0	0.025									not assigned.unknown	ULT1_ULT__ULT1 (ULTRAPETALA1); DNA binding
AT1G79150	6.8	7.8	-1.0	0.027									not assigned.unknown	binding
AT3G15240	6.8	7.8	-1.0	0.031									not assigned.unknown	similar to unknown protein
AT5G62450	8.3	9.3	-0.9	0.024										
AT3G17160	8.3	9.2	-0.9	0.026									not assigned.unknown	similar to unknown protein
AT2G34020	6.9	7.8	-0.9	0.031									signalling.calcium	calcium ion binding
AT4G39800	8.0	8.9	-0.9	0.036									minor CHO metabolism.myo-inositol.InsP Synthases	MI-1-P SYNTHASE (Myo-inositol-1-phosphate synthase)
AT1G64880	8.6	9.5	-0.9	0.026									protein.synthesis.chloroplast/mito	ribosomal protein S5 family protein
AT5G02050	8.3	9.2	-0.9	0.033									not assigned.no ontology	mitochondrial glycoprotein family protein / MAM33 family protein
AT4G30800	8.2	9.0	-0.9	0.036									protein.synthesis.misc ribososomal protein	40S ribosomal protein S11 (RPS11B)
AT5G50375	8.6	9.5	-0.9	0.036									not assigned.no ontology	CPI1__CPI1 (CYCLOPROPYL ISOMERASE)
AT3G18600	8.6	9.4	-0.8	0.036									DNA.synthesis/chromatin structure	DEAD/DEAH box helicase, putative
AT1G49600	9.2	10.0	-0.8	0.035									RNA.regulation of transcription.unclassified	AtRBP47A (RNA-BINDING PROTEIN 47A); RNA binding
AT3G20000	9.2	9.9	-0.8	0.035									not assigned.no ontology	TOM40 (translocase of the outer mitochondrial membrane 40)
AT1G22885	10.0	9.3	0.7	0.036									not assigned.unknown	similar to unknown protein
AT2G36690	8.6	7.9	0.8	0.033									misc.oxidases - copper, flavone etc.	oxidoreductase, 2OG-Fe(II) oxygenase family protein
AT5G22920	11.2	10.5	0.8	0.038									protein.degradation.ubiquitin.E3.RING	zinc finger (C3HC4-type RING finger) family protein
AT1G76590	8.5	7.7	0.8	0.038									not assigned.no ontology	zinc-binding family protein
AT1G01070	8.7	7.8	0.8	0.036									development.unspecified	nodulin MtN21 family protein
AT3G14280	10.3	9.4	0.8	0.029									not assigned.unknown	similar to hypothetical protein MtrDRAFT
AT1G13260	10.4	9.6	0.8	0.037									RNA.regulation of transcription (AP2/EREBP, APETALA2)	RAV1 (Related to ABI3/VP 1); DNA binding / transcription factor
AT4G37610	9.9	9.0	0.9	0.033									protein.degradation.ubiquitin.E3.BTB/POZ	BTB7 TAZ domain protein 5; protein binding / transcription regulator
AT3G54500	8.4	7.5	0.9	0.035									not assigned.unknown	similar to dentin sialophosphoprotein-related
AT1G80440	10.8	9.9	0.9	0.033									protein.degradation.ubiquitin.E3.SCF.FBOX	kelch repeat-containing F-box family protein
AT2G46940	6.8	5.8	1.0	0.032									not assigned.unknown	similar to unknown protein
AT4G22610	8.6	7.4	1.2	0.031									misc.protease inhibitor/seed storage/LTP	protease inhibitor/seed storage/lipid transfer protein (LTP)
AT3G46700	6.2	4.9	1.2	0.033									misc.UDP glucosyl and glucoronyl transferases	UDP-glycosyltransferase/ transferase
AT3G48450	7.6	6.3	1.3	0.036									not assigned.no ontology	nitrate-responsive NOI protein, putative
AT4G35770	7.9	6.5	1.4	0.038									development.unspecified	SEN1_DIN1__SEN1 (DARK INDUCIBLE 1)
AT1G15045	7.1	5.6	1.5	0.023										
AT5G14330					3.4	6.0	-2.6	0.011	5.2	6.3	-1.2	0.167	not assigned.unknown	similar to unknown protein
AT4G27652					7.2	6.3	0.9	0.050	7.9	7.0	1.0	0.027	not assigned.unknown	similar to unknown protein
AT1G74490					5.3	6.5	-1.3	0.039					protein.postranslational modification/kinase receptor like	protein kinase, putative
AT5G04970					6.2	7.3	-1.1	0.054					cell wall.pectin*esterases.misc	pectinesterase, putative
AT2G45050					6.7	7.8	-1.1	0.051					RNA.regulation of transcription (C2C2(Zn) GATA)	zinc finger (GATA type) family protein
AT4G11610					6.3	7.3	-1.0	0.053					amino acid metabolism.synthesis.aromatic aa.tryptophan	NTRB (NADPH-dependent thioredoxin reductase B)
AT2G43480					5.5	6.5	-1.0	0.054					misc.peroxidases	peroxidase, putative
AT3G60530					7.2	8.1	-1.0	0.046					RNA.regulation of transcription (C2C2(Zn) GATA)	zinc finger (GATA type) family protein
AT5G53290					5.7	6.7	-0.9	0.055					RNA.regulation of transcription (AP2/EREBP, APETALA2)	CRF3 (Cytokinin response factor 3); transcription factor
AT3G03680					6.4	7.3	-0.9	0.049					not assigned.no ontology	C2 domain-containing protein
AT3G18000					7.8	8.6	-0.8	0.051					lipid metabolism.Phospholipid synthesis	XIPOTL1/ NMT1; phosphoethanolamine N-methyltransferase
AT3G09890					7.5	8.3	-0.8	0.051					cell.organisation	ankyrin repeat family protein
AT3G11250					8.7	9.5	-0.8	0.048					protein.synthesis.misc ribososomal protein	60S acidic ribosomal protein P0 (RPP0C)
AT3G03250					10.0	10.7	-0.8	0.044					glycolysis.UGPase	UGP (UDP-glucose pyrophosphorylase)
AT3G18190					10.3	11.0	-0.7	0.046					protein.folding	chaperonin, putative
AT3G58550					9.3	8.6	0.7	0.052					misc.protease inhibitor/seed storage/LTP	protease inhibitor/seed storage/lipid transfer protein (LTP)

Gene										Functional category	Description
AT2G37090	7.9	7.2	**0.7**	0.054						not assigned.no ontology	IRX9 (IRREGULAR XYLEM 9); transferase
AT4G16190	10.8	10.1	**0.7**	0.050						protein.degradation.cysteine protease	cysteine proteinase, putative
AT5G05320	8.6	7.9	**0.7**	0.047						misc.oxidases - copper, flavone etc.	monooxygenase, putative (MO3)
AT3G16770	9.4	8.6	**0.8**	0.050						RNA.regulation of transcription (AP2/EREBP, APETALA2)	AtEBP (RELATED TO AP2 3); DNA binding / transcription factor
AT2G01670	10.5	9.6	**0.8**	0.039						not assigned.no ontology	AtNUDT17 (Arabidopsis thaliana Nudix hydrolase homolog 17)
AT1G05575	8.4	7.6	**0.8**	0.053						not assigned.unknown	similar to unknown protein
AT3G56360	10.2	9.4	**0.9**	0.032						not assigned.unknown	similar to unknown protein
AT2G44420	6.9	6.0	**0.9**	0.044						not assigned.no ontology	protein N-terminal asparagine amidohydrolase family protein
AT4G36430	10.6	9.7	**0.9**	0.048						misc.peroxidases	peroxidase, putative
AT5G61600	9.5	8.5	**0.9**	0.046						hormone metabolism.ethylene.signal transduction	ethylene-responsive element-binding family protein
AT5G38020	8.2	7.3	**0.9**	0.054						hormone metabolism.salicylic acid	S-adenosyl-L-methionine:carboxyl methyltransferase family protein
AT2G04795	8.6	7.6	**0.9**	0.052						not assigned.unknown	similar to unknown protein
AT5G19110	7.9	7.0	**1.0**	0.040						not assigned.no ontology	extracellular dermal glycoprotein-related / EDGP-related
AT5G12110	7.3	6.4	**1.0**	0.047						protein.synthesis.elongation	elongation factor 1B alpha-subunit 1 (eEF1Balpha1)
AT2G43535	10.6	9.6	**1.0**	0.045						stress.biotic	trypsin inhibitor, putative
AT1G58340	7.4	6.4	**1.0**	0.029						not assigned.no ontology	ZF14__ZF14; transporter
AT1G53990	8.0	6.9	**1.1**	0.037						misc.GDSL-motif lipase	GLIP3 (GDSL-motif lipase 3); carboxylic ester hydrolase/ lipase
AT5G47990	7.1	6.0	**1.1**	0.034						misc.cytochrome P450	CYP705A5 (cytochrome P450)
AT5G25450	7.2	6.1	**1.1**	0.048						mitochondrial electron transport / ATP synthesis	ubiquinol-cytochrome C reductase complex 14 kDa, putative
AT4G14060	8.7	7.6	**1.1**	0.037						stress.abiotic.unspecified	major latex protein-related / MLP-related
AT5G06720	6.8	5.6	**1.2**	0.048						misc.peroxidases	peroxidase, putative
AT2G47180	8.9	7.6	**1.2**	0.034						minor CHO metabolism	ATGOLS1 (GALACTINOL SYNTHASE 1); transferase
AT3G24500	8.3	7.1	**1.2**	0.051						hormone metabolism.ethylene	AtMBF1C/MBF1C (MULTIPROTEIN BRIDGING FACTOR 1C)
AT5G06730	7.5	6.2	**1.3**	0.047						misc.peroxidases	peroxidase, putative
AT5G02780	6.4	4.9	**1.5**	0.025						not assigned.no ontology	In2-1 protein, putative
AT1G53960	6.7	4.9	**1.7**	0.038							
AT4G25100					6.8	7.6	**-0.8**	0.112	9.1 9.9 **-0.8** 0.045	redox.dismutases and catalases	FSD1 (Fe iron superoxide dismutase 1)
AT4G33790					6.3	6.9	**-0.6**	0.266	5.8 6.7 **-0.8** 0.026	lipid metabolism.lipid degradation	acyl CoA reductase, putative
AT5G06630					5.2	6.4	**-1.3**	0.061		cell wall, cellulose	proline-rich extensin-like family protein
AT5G26130					8.8	9.9	**-1.1**	0.131		stress.biotic	pathogenesis-related protein, putative
AT4G12360					5.0	6.1	**-1.0**	0.098		misc.protease inhibitor/seed storage/LTP	protease inhibitor/seed storage/lipid transfer protein (LTP)
AT3G49960					5.8	6.8	**-1.0**	0.120		misc.peroxidases	peroxidase, putative
AT4G30320					5.8	6.8	**-0.9**	0.110		stress.abiotic.unspecified	allergen V5/Tpx-1-related family protein
AT4G02270					9.0	10.0	**-0.9**	0.058		stress.abiotic.unspecified	pollen Ole e 1 allergen and extensin family protein
AT4G08380					6.9	7.8	**-0.9**	0.098		cell wall, cellulose	proline-rich extensin-like family protein
AT5G49870					5.3	6.2	**-0.9**	0.138		misc.myrosinases-lectin-jacalin	jacalin lectin family protein
AT4G25790					6.9	7.8	**-0.9**	0.097		stress.abiotic.unspecified	allergen V5/Tpx-1-related family protein
AT1G65570					5.3	6.2	**-0.9**	0.134		cell wall.degradation	polygalacturonase, putative / pectinase, putative
AT5G05500					7.2	8.0	**-0.9**	0.094		stress.abiotic.unspecified	pollen Ole e 1 allergen and extensin family protein
AT4G25820					7.9	8.8	**-0.9**	0.104		cell wall.modification	XTR9 (XYLOGLUCAN ENDOTRANSGLYCOSYLASE 9); hydrolase
AT5G49080					6.9	7.8	**-0.8**	0.088		cell wall, cellulose	
AT2G41970					5.3	6.2	**-0.8**	0.162		protein.postranslational modification/kinase receptor like	protein kinase, putative
AT3G16990					7.1	7.9	**-0.8**	0.132		not assigned.no ontology	TENA/THI-4 family protein
AT3G62680					7.4	8.2	**-0.8**	0.149		cell wall.cell wall proteins.proline rich proteins	PRP3 (Proline-rich protein 3); structural constituent of cell wall
AT4G33730					5.5	6.3	**-0.8**	0.191		stress.biotic	pathogenesis-related protein, putative
AT1G30870					7.8	8.6	**-0.8**	0.145		misc.peroxidases	cationic peroxidase, putative
AT1G63560					5.3	6.1	**-0.8**	0.205		signalling.receptor kinases.misc	similar to protein kinase-related
AT2G37820					6.4	7.1	**-0.8**	0.146		not assigned.no ontology	DC1 domain-containing protein
AT2G24980					8.5	9.2	**-0.7**	0.140		cell wall, cellulose	proline-rich extensin-like family protein
AT1G12560					6.3	7.0	**-0.7**	0.213		cell wall.modification	AtEXPA7 (ARABIDOPSIS THALIANA EXPANSIN A7)
AT5G67400					8.9	9.7	**-0.7**	0.141		misc.peroxidases	peroxidase 73 (PER73) (P73) (PRXR11)
AT4G37430					5.6	6.4	**-0.7**	0.195		misc.cytochrome P450	CYP91A2 (CYTOCHROME P450 MONOOXYGENASE 91A2)
AT5G06640					7.1	7.8	**-0.7**	0.156		cell wall, cellulose	proline-rich extensin-like family protein
AT4G15290					6.0	6.7	**-0.7**	0.252		cell wall.cellulose synthesis	AtCSLB05 (Cellulose synthase-like B5)
AT5G04730					7.1	7.8	**-0.7**	0.209		not assigned.unknown	similar to unknown protein
AT1G53680					6.7	7.4	**-0.7**	0.295		misc.glutathione S transferases	AtGSTU28 (Glutathione S-transferase (class tau) 28)
AT5G04960					6.5	7.2	**-0.7**	0.201		cell wall.pectin*esterases.PME	pectinesterase family protein
AT1G19900					6.9	7.5	**-0.7**	0.237		Biodegradation of Xenobiotics	glyoxal oxidase-related
AT2G34730					7.4	8.0	**-0.7**	0.180		not assigned.disagreeing hits	
AT3G51540					5.4	6.1	**-0.7**	0.275		not assigned.no ontology	similar to unknown protein
AT5G07780					5.7	6.4	**-0.7**	0.241		not assigned.no ontology	formin homology 2 (FH2) domain-containing protein
AT2G16760					6.5	7.2	**-0.7**	0.261		not assigned.unknown	similar to unknown protein
AT3G28550					7.3	7.9	**-0.7**	0.218		cell wall, cellulose	

Gene									Functional category	Description
AT4G08620	7.3	8.0	-0.7	0.224					transport.sulphate	SULTR1;1 (sulfate transporter 1;1)
AT4G26180	5.5	6.2	-0.6	0.272					transport (transport at the mitochondrial membrane)	mitochondrial substrate carrier family protein
AT4G17483	5.9	6.5	-0.6	0.257					lipid metabolism.lipid degradation	palmitoyl protein thioesterase family protein
AT3G61300	5.9	6.6	-0.6	0.253					amino acid metabolism.synthesis.aromatic aa.tryptophan	C2 domain-containing protein
AT4G13340	6.0	6.7	-0.6	0.248					cell wall.cell wall proteins.LRR	leucine-rich repeat family protein / extensin family protein
AT5G14650	7.0	7.7	-0.6	0.385					cell wall.degradation	polygalacturonase, putative / pectinase, putative
AT4G10500	7.1	7.7	-0.6	0.217					not assigned.no ontology	oxidoreductase, 2OG-Fe(II) oxygenase family protein
AT1G33910	5.4	6.1	-0.6	0.286					stress.biotic	avirulence induced gene (AIG1) family protein
AT4G40091	6.8	7.4	-0.6	0.236					not assigned.disagreeing hits	
AT3G24400	5.4	6.1	-0.6	0.349					signalling.receptor kinases.proline extensin like	
AT5G66080	5.4	6.0	-0.6	0.295					protein.postranslational modification	protein phosphatase 2C family protein / PP2C family protein
AT5G57000	6.3	6.9	-0.6	0.244					not assigned.unknown	similar to unknown protein
AT3G47780	6.0	6.6	-0.6	0.306					transport.ABC transporters and MDR	AtATH6 (ABC2 homolog 6); ATPase
AT1G02740	5.9	6.5	-0.6	0.362					RNA.regulation of transcription (HAT)	chromatin binding
AT3G44520	5.4	6.0	-0.6	0.334					lipid metabolism.lipid degradation	esterase/lipase/thioesterase family protein
AT5G22555	6.7	7.3	-0.6	0.283					not assigned.unknown	unknown protein
AT5G25810	7.7	8.3	-0.6	0.252					RNA.regulation of transcription (AP2/EREBP, APETALA2)	TNY__TNY (TINY); DNA binding / transcription factor
AT5G49270	5.7	6.3	-0.6	0.404					metal handling	COBL9/MRH4 (COBRA-LIKE 9); hydrolyzing O-glycosyl compounds
AT1G28040	6.3	6.9	-0.6	0.253					protein.degradation.ubiquitin.E3.RING	protein binding / zinc ion binding
AT5G59650	6.2	6.8	-0.6	0.272					signalling.receptor kinases.leucine rich repeat I	leucine-rich repeat protein kinase, putative
AT1G01750	6.5	7.1	-0.6	0.370					cell.organisation	actin-depolymerizing factor, putative
AT1G43160	7.4	8.0	-0.6	0.301					RNA.regulation of transcription (AP2/EREBP, APETALA2)	RAP2.6 (related to AP2 6); DNA binding / transcription factor
AT2G19950	5.8	6.3	-0.6	0.301					not assigned.disagreeing hits	
AT5G59490	6.3	6.8	-0.6	0.307					not assigned.no ontology	haloacid dehalogenase-like hydrolase family protein
AT1G26180	6.2	5.6	0.6	0.143					not assigned.disagreeing hits	
AT1G27730	9.2	8.5	0.6	0.063					stress	STZ (SALT TOLERANCE ZINC FINGER); transcription factor
AT4G15850	6.2	5.6	0.6	0.098					DNA.synthesis/chromatin structure	ATRH1 (Arabidopsis thaliana RNA helicase 1)
AT3G27400	6.9	6.2	0.6	0.068					cell wall.degradation	pectate lyase family protein
AT3G03020	6.1	5.5	0.6	0.097					not assigned.unknown	unknown protein
AT5G37770	7.9	7.3	0.7	0.033					signalling.calcium	TCH2_CML24 (TOUCH 2); calcium ion binding
AT2G24762	8.0	7.4	0.7	0.036					not assigned.unknown	ATGDU4__similar to GDU1 (GLUTAMINE DUMPER 1)
AT5G02590	6.1	5.4	0.7	0.076					not assigned.no ontology	chloroplast lumen common family protein
AT1G72970	6.6	5.9	0.7	0.049					misc.nitrilases	EDA17_HTH__HTH (HOTHEAD); aldehyde-lyase
AS4G19070	6.2	5.5	0.7	0.057					metal handling	cadmium-responsive protein / cadmium induced protein (AS8)
AT3G17180	7.5	6.8	0.7	0.027					protein.degradation.serine protease	SCPL33 (serine carboxypeptidase-like 33)
AT3G18050	6.2	5.4	0.7	0.069					not assigned.unknown	similar to unknown protein
AT3G10930	6.6	5.9	0.8	0.053					not assigned.unknown	unknown protein
AT5G38140	6.1	5.4	0.8	0.103					RNA.regulation of transcription (CCAAT box)	histone-like transcription factor (CBF/NF-Y) family protein
AT5G51190	8.0	7.2	0.8	0.058					hormone metabolism.ethylene.signal transduction	AP2 domain-containing transcription factor, putative
AT3G44260	6.9	6.1	0.8	0.073					not assigned.no ontology	CCR4-NOT transcription complex protein, putative
AT4G24570	7.2	6.3	0.8	0.068					mitochondrial electron transport / ATP synthesis	mitochondrial substrate carrier family protein
AT1G73540	7.6	6.6	0.9	0.022					not assigned.no ontology	AtNUDT21 (Arabidopsis thaliana Nudix hydrolase homolog 21)
AT1G09670	6.0	5.1	1.0	0.088					not assigned.disagreeing hits	
AT3G47880	6.6	4.9	1.7	0.037					not assigned.disagreeing hits	
At2g20870					5.2	8.3	-3.1	0.001	not assigned.no ontology	cell wall protein precursor, putative
At4g29030					7.2	8.8	-1.6	0.030	RNA.regulation of transcription.Trihelix	glycine-rich protein
At5g33370					6.0	7.5	-1.6	0.006	misc.GDSL-motif lipase	GDSL-motif lipase/hydrolase family protein
At4g22490					5.9	7.4	-1.5	0.046	misc.protease inhibitor/seed storage/LTP	protease inhibitor/seed storage/lipid transfer protein (LTP)
At5g52390					5.0	6.4	-1.4	0.030	signalling.in sugar and nutrient physiology	photoassimilate-responsive protein, putative
At4g02290					6.0	7.4	-1.4	0.029	misc.gluco-, galacto- and mannosidases	glycosyl hydrolase family 9 protein
At3g28500					6.3	7.7	-1.3	0.022	protein.synthesis.misc ribososomal protein	60S acidic ribosomal protein P2 (RPP2C)
At5g13170					6.2	7.5	-1.3	0.025	development.unspecified	nodulin MtN3 family protein
At3g08770					9.4	10.7	-1.3	0.015	lipid metabolism.lipid transfer proteins etc	LTP6 (Lipid transfer protein 6); lipid binding
At2g02850					6.3	7.5	-1.2	0.044	misc.plastocyanin-like	ARPN__ARPN (PLANTACYANIN); copper ion binding
At5g07030					8.7	9.8	-1.1	0.026	RNA.regulation of transcription. DNA-binding protein	pepsin A
At2g37870					7.9	9.0	-1.1	0.029	misc.protease inhibitor/seed storage/LTP	protease inhibitor/seed storage/lipid transfer protein (LTP)
At5g23940					6.1	7.2	-1.1	0.041	not assigned.no ontology	EMB3009 (EMBRYO DEFECTIVE 3009); transferase
At2g39330					6.7	7.8	-1.1	0.021	misc.myrosinases-lectin-jacalin	jacalin lectin family protein
At3g25580					5.1	6.1	-1.0	0.019	redox.thioredoxin	thioredoxin-related
At5g62210					6.8	7.8	-1.0	0.020	development.unspecified	embryo-specific protein-related
At5g54060					6.6	7.5	-1.0	0.034	secondary metabolism.flavonoids.dihydroflavonols	UF3GT (UDP-Glucose:flavonoid 3-O-glucosyltransferase)
At4g17470					7.3	8.3	-1.0	0.012	lipid metabolism.lipid degradation	palmitoyl protein thioesterase family protein
At4g31840					7.4	8.3	-1.0	0.028	misc.plastocyanin-like	plastocyanin-like domain-containing protein

Gene				Val1	Val2	Diff	p	Category	Description
At4g26070				6.9	7.8	-0.9	0.016	signalling.MAP kinases	NMAPKK/MEK1 (MAP kinase kinase 1)
At5g60910				5.3	6.3	-0.9	0.024	development.unspecified	AGL8_FUL__AGL8 (AGAMOUS-LIKE 8)
At1g25450				6.9	7.9	-0.9	0.031	secondary metabolism.wax	very-long-chain fatty acid condensing enzyme, putative
At5g55180				7.5	8.4	-0.9	0.025	not assigned.no ontology	glycosyl hydrolase family 17 protein
At4g14090				6.4	7.3	-0.9	0.042	misc.UDP glucosyl and glucoronyl transferases	UDP-glucoronosyl/UDP-glucosyl transferase family protein
At5g10430				7.0	7.9	-0.9	0.031	cell wall.cell wall proteins.AGPs	AGP4__AGP4 (ARABINOGALACTAN-PROTEIN 4)
At5g08640				5.9	6.7	-0.9	0.028	secondary metabolism.flavonoids.flavonols	FLS__FLS (FLAVONOL SYNTHASE)
At5g25090				5.2	6.0	-0.9	0.046	misc.plastocyanin-like	plastocyanin-like domain-containing protein
At4g33550				7.1	8.0	-0.9	0.046	misc.protease inhibitor/seed storage/LTP	similar to protease inhibitor/seed storage/lipid transfer protein (LTP)
At3g16470				8.5	9.3	-0.9	0.040	hormone metabolism.jasmonate	JR1__JR1 (Jacalin lectin family protein)
At3g52170				5.3	6.1	-0.8	0.025	RNA.regulation of transcription. DNA-binding protein	DNA binding
At1g08470				6.8	7.6	-0.8	0.021	secondary metabolism.N misc.alkaloid-like	strictosidine synthase family protein
At2g43800				7.0	7.7	-0.8	0.038	not assigned.no ontology	formin homology 2 (FH2) domain-containing protein
At3g25290				5.3	6.1	-0.8	0.037	hormone metabolism.auxin	auxin-responsive family protein
At3g53190				7.3	8.1	-0.8	0.039	cell wall.degradation	pectate lyase family protein
At1g65450				5.7	6.5	-0.8	0.035	not assigned.no ontology	transferase family protein
At3g08850				7.1	7.9	-0.8	0.021	not assigned.no ontology	RAPTOR1B (RAPTOR1); nucleotide binding / protein binding
At1g78490				7.9	8.7	-0.8	0.032	misc.cytochrome P450	CYP708A3 (cytochrome P450)
At5g42110				7.8	8.6	-0.8	0.041	not assigned.unknown	unknown protein
At3g01100				6.1	6.9	-0.8	0.031	stress.abiotic.drought/salt	HYP1 (HYPOTHETICAL PROTEIN 1)
At5g14420				5.5	6.3	-0.8	0.040	protein.degradation.ubiquitin.E3.RING	RGLG2__copine-related
At4g30450				6.9	7.7	-0.8	0.036	not assigned.no ontology.glycine rich proteins	glycine-rich protein
At1g26690				5.9	6.6	-0.8	0.028	transport.misc	emp24/gp25L/p24 family protein
At4g10955				5.7	6.4	-0.7	0.041		lipase class 3 family protein
At2g21690				6.3	7.1	-0.7	0.033	DNA.synthesis/chromatin structure	EMB1968__EMB1968 (EMBRYO DEFECTIVE 1968); ATPase
At1g59740				6.1	6.9	-0.7	0.031	transport.peptides and oligopeptides	proton-dependent oligopeptide transport (POT) family protein
At1g52400				10.8	11.5	-0.7	0.046	misc.gluco-, galacto- and mannosidases	BGL1 (BETA-GLUCOSIDASE HOMOLOG 1)
At1g57820				6.2	7.0	-0.7	0.044	protein.degradation.ubiquitin.E3.RING	ORTH2/VIM1 (VARIANT IN METHYLATION 1); DNA binding
At1g14900				6.1	6.8	-0.7	0.043	DNA.synthesis/chromatin structure	HMGA__high-mobility-group protein / HMG-I/Y protein
At1g55360				7.5	8.2	-0.7	0.028	not assigned.unknown	similar to unknown protein
At1g65370				6.4	7.1	-0.7	0.030	not assigned.no ontology	meprin and TRAF homology domain-containing protein
At2g44670				7.5	8.2	-0.7	0.025	development.unspecified	senescence-associated protein-related
At2g39220				5.9	6.6	-0.7	0.041	development.storage proteins	PLA IIB/PLP6 (Patatin-like protein 6); nutrient reservoir
At2g45640				7.8	8.5	-0.7	0.022	not assigned.no ontology	SAP18 (SIN3 associated polypeptide P18); transcription regulator
At3g14120				6.1	6.8	-0.7	0.042	not assigned.no ontology	similar to Nuclear pore complex, rNup107
At3g22845				7.1	7.8	-0.7	0.031	not assigned.no ontology	emp24/gp25L/p24 protein-related
At4g26400				6.8	7.5	-0.7	0.031	protein.degradation.ubiquitin.E3.RING	zinc finger (C3HC4-type RING finger) family protein
At2g14560				7.6	8.3	-0.7	0.032	not assigned.unknown	similar to unknown protein
At4g39510				7.3	7.9	-0.6	0.039	misc.cytochrome P450	CYP96A12 (cytochrome P450)
At5g12190				6.8	7.4	-0.6	0.038	not assigned.no ontology	RNA recognition motif (RRM)-containing protein
At5g02410				6.1	6.7	-0.6	0.043	not assigned.no ontology	DIE2/ALG10 family
At2g07350				7.4	8.0	-0.6	0.034		
At2g04570				7.7	8.3	-0.6	0.039	misc.GDSL-motif lipase	GDSL-motif lipase/hydrolase family protein
At4g23990				7.5	8.1	-0.6	0.040	cell wall.cellulose synthesis	AtCSLG3 (Cellulose synthase-like G3)
At5g20890				8.9	9.5	-0.6	0.029	protein.folding	chaperonin, putative
At3g22231				10.8	11.4	-0.6	0.036	not assigned.unknown	PCC1 (PATHOGEN AND CIRCADIAN CONTROLLED 1)
At1g06640				9.0	9.6	-0.6	0.038	redox.ascorbate and glutathione	2-oxoglutarate-dependent dioxygenase, putative
At2g42200				6.6	7.2	-0.6	0.034	development.unspecified	squamosa promoter-binding protein-like 9 (SPL9)
At5g04900				8.0	7.2	0.8	0.042	misc.short chain dehydrogenase/reductase (SDR)	short-chain dehydrogenase/reductase (SDR) family protein
At5g27760				8.7	8.0	0.8	0.042	not assigned.no ontology	hypoxia-responsive family protein
At4g34590				7.7	6.9	0.8	0.041	RNA.regulation of transcription.bZIP	AtBZIP11/GBF6 (G-box binding factor 6)
At5g61820				10.5	9.6	0.8	0.033	not assigned.unknown	similar to hypothetical protein
At2g41100				7.3	6.4	1.0	0.033	signalling.calcium	TCH3_ATCAL4__TCH3 (TOUCH 3)
At5g22300				7.6	6.6	1.0	0.033	misc.nitrilases	NIT4__NIT4 (NITRILASE 4)
At1g02850				8.1	7.2	1.0	0.047	misc.gluco-, galacto- and mannosidases	similar to glycosyl hydrolase family 1 protein
At4g27820				7.9	6.9	1.0	0.043	misc.gluco-, galacto- and mannosidases	glycosyl hydrolase family 1 protein
At5g49480				9.4	8.3	1.0	0.033	signalling.calcium	AtCP1 (CA2+-BINDING PROTEIN 1)
At2g05380				10.2	9.0	1.1	0.018	not assigned.no ontology.glycine rich proteins	GRP3S__GRP3S (GLYCINE-RICH PROTEIN 3 SHORT ISOFORM)
At1g06830				6.5	5.3	1.2	0.026	redox.glutaredoxins	glutaredoxin family protein
At3g51860				8.3	7.0	1.3	0.047	transport.metal	CAX3/ A7HCX1 (cation exchanger 3)
At4g01870				8.7	7.4	1.3	0.037	not assigned.no ontology	tolB protein-related
At2g29490				7.6	6.1	1.5	0.027	misc.glutathione S transferases	A7GSTU1/ GST19 (GLUTATHIONE S-TRANSFERASE 19)
At4g37990				7.6	6.0	1.6	0.028	secondary metabolism.phenylpropanoids	ELI3-2_ELI3__ELI3-2 (ELICITOR-ACTIVATED GENE 3)

At5g20230						9.6	8.0	1.6	0.021 misc.plastocyanin-like	AtBCB (BLUE-COPPER-BINDING PROTEIN)
At1g17170						8.5	6.9	1.6	0.014 misc.glutathione S transferases	AtGSTU24 (Glutathione S-transferase (class tau) 24)
At3g04720						7.6	5.9	1.7	0.008 not assigned.no ontology	PR4_HEL_PR-4__PR4 (PATHOGENESIS-RELATED 4)
At3g16530						7.7	5.9	1.7	0.029 misc.myrosinases-lectin-jacalin	legume lectin family protein
At1g67810						6.4	4.6	1.7	0.023 not assigned.no ontology	Fe-S metabolism associated domain-containing protein
At1g10585						6.6	4.8	1.8	0.029 RNA.regulation of transcription.bHLH	transcription factor
At1g05680						8.5	6.6	1.9	0.010 hormone metabolism.salicylic acid	UDP-glucoronosyl/UDP-glucosyl transferase family protein
At1g60730						6.2	3.9	2.4	0.032 hormone metabolism.auxin	aldo/keto reductase family protein
At2g02930						6.7	4.1	2.6	0.006 misc.glutathione S transferases	AtGSTF3/ GST16 (GLUTATHIONE S-TRANSFERASE 16)
At3g26830						6.0	3.1	2.9	0.032 misc.cytochrome P450	PAD3/ CYP71B15 (PHYTOALEXIN DEFICIENT 3)

Supplementary Table 3. Functional categories according to MapMan classification (Thimm et al., 2004) of genes co-regulated with *PIP2* genes retrieved from ACT. Italic labeling indicates probesets that recognize several genes. Genes co-expressed with several *PIP2* genes are compiled separately as well.

PIP2;1 (251962_at/ At3g534207)

ProbeSet	r-value	p-value	e-value	GeneID	Annotation	MAPMAN classification
245318_at	0.699	0.00E+00	3.90E-44	AT4G16980	arabinogalactan-protein family	cell wall.cell wall proteins.AGPs
265066_at	0.607	8.10E-34	1.80E-29	AT1G03870	fasciclin-like arabinogalactan-protein (FLA9)	cell wall.cell wall proteins.AGPs
257749_at	*0.606*	*1.30E-33*	*2.90E-29*	*AT1G49240* *AT3G18780*	*actin 8 (ACT8)* *actin 2 (ACT2)*	*cell.organisation*
245281_at	0.648	8.50E-40	1.90E-35	AT4G15560	1-deoxy-D-xylulose 5-phosphate synthase, putative	development.unspecified
254102_at	0.667	8.10E-43	1.80E-38	AT4G25050	acyl carrier family protein / ACP family protein	lipid metabolism.FA synthesis and FA elongation
246267_at	0.634	1.20E-37	2.50E-33	AT1G31812	acyl-CoA binding protein / ACBP identical to acyl-CoA-binding protein	lipid metabolism.FA synthesis and FA elongation
261667_at	0.702	0.00E+00	9.80E-45	AT1G18460	lipase family protein similar to triacylglycerol lipase	lipid metabolism.lipid degradation.lipases
249073_at	0.602	3.40E-33	7.40E-29	AT5G44020	acid phosphatase class B family protein	misc.acid and other phosphatases
262826_at	0.636	7.80E-38	1.70E-33	AT1G13080	cytochrome P450 family protein	misc.cytochrome P450
259375_at	0.696	0.00E+00	1.40E-43	AT3G16370	GDSL-motif lipase/hydrolase family protein	misc.GDSL-motif lipase
265646_at	0.611	2.10E-34	4.70E-30	AT2G27360	Lipase/Acylhydrolase with GDSL-like motif	misc.GDSL-motif lipase
262980_at	0.615	6.50E-35	1.40E-30	AT1G75680	glycosyl hydrolase family 9 protein similar to endo-beta-1,4-glucanase	misc.gluco-, galacto- and mannosidases
266123_at	0.659	2.00E-41	4.30E-37	AT2G45180	protease inhibitor/seed storage/lipid transfer protein (LTP) family protein	misc.protease inhibitor/seed storage/lipid transfer prot.
264371_at	0.634	1.40E-37	3.00E-33	AT1G12090	protease inhibitor/seed storage/lipid transfer protein (LTP) family protein	misc.protease inhibitor/seed storage/lipid transfer prot.
267635_at	0.600	6.80E-33	1.50E-28	AT2G42220	rhodanese-like domain-containing protein	misc.rhodanese
249710_at	0.656	5.10E-41	1.10E-36	AT5G35630	glutamine synthetase (GS2), chloroplast precursor	N-metabolism.ammonia metabolism
263345_s_at	*0.627*	*1.40E-36*	*3.10E-32*	*AT2G05070* *AT2G05100*	*chlorophyll A-B binding protein / LHCII type II (LHCB2.2)* *chlorophyll A-B binding protein / LHCII type II (LHCB2.1) (LHCB2.3)*	*not assigned.disagreeing hits*
246294_at	0.608	6.90E-34	1.50E-29	AT3G56910	expressed protein	not assigned.disagreeing hits
265149_at	0.605	1.50E-33	3.40E-29	AT1G51400	photosystem II 5 kD protein 100% identical to GI:4836947 (F5D21.10)	not assigned.disagreeing hits
258412_at	0.710	0.00E+00	0.00E+00	AT3G17210	stable protein 1-related similar to stable protein 1	not assigned.no ontology
257974_at	0.621	1.20E-35	2.60E-31	AT3G20820	leucine-rich repeat family protein contains similarity to Cf-2.1	not assigned.no ontology
258432_at	0.619	1.80E-35	3.80E-31	AT3G16570	rapid alkalinization factor (RALF) family protein	not assigned.no ontology
258535_at	0.692	0.00E+00	7.40E-43	AT3G06750	hydroxyproline-rich glycoprotein family protein	not assigned.no ontology.hydroxyproline rich proteins
261049_at	0.695	0.00E+00	1.60E-43	AT1G01430	expressed protein	not assigned.unknown
267000_at	0.651	3.70E-40	8.10E-36	AT2G34310	expressed protein	not assigned.unknown
267262_at	0.619	1.80E-35	3.90E-31	AT2G22990	sinapoylglucose:malate sinapoyltransferase (SNG1)	protein.degradation.serine protease
258060_at	0.602	4.40E-33	9.60E-29	AT3G26030	serine/threonine protein phosphatase 2A (PP2A) regulatory subunit B'	protein.postranslational modification
261954_at	0.642	8.90E-39	1.90E-34	AT1G64510	ribosomal protein S6 family protein	protein.synthesis.chloroplast/mito - plastid ribosomal prot.
251883_at	0.628	8.60E-37	1.90E-32	AT3G54210	ribosomal protein L17 family protein	protein.synthesis.chloroplast/mito - plastid ribosomal prot.
260898_at	0.621	1.20E-35	2.60E-31	AT1G29070	ribosomal protein L34 family protein	protein.synthesis.chloroplast/mito - plastid ribosomal prot.
262029_at	0.605	1.40E-33	3.10E-29	AT1G35680	50S ribosomal protein L21, chloroplast / CL21 (RPL21)	protein.synthesis.chloroplast/mito - plastid ribosomal prot.
265247_at	0.618	2.90E-35	6.40E-31	AT2G43030	ribosomal protein L3 family protein	protein.synthesis.chloroplast/mito - plastid ribosomal prot.
257190_at	0.614	8.20E-35	1.80E-30	AT3G13120	30S ribosomal protein S10, chloroplast	protein.synthesis.chloroplast/mito - plastid ribosomal prot.
253201_at	0.623	5.50E-36	1.20E-31	AT4G34620	ribosomal protein S16 family protein	protein.synthesis.misc ribososomal protein
260481_at	0.635	9.90E-38	2.20E-33	AT1G10960	ferredoxin, chloroplast, putative	PS.lightreaction.other electron carrier (ox/red).ferredoxin
259727_at	0.612	2.00E-34	4.40E-30	AT1G60950	ferredoxin, chloroplast (PETF)	PS.lightreaction.other electron carrier (ox/red).ferredoxin
247320_at	0.610	3.80E-34	8.30E-30	AT5G64040	photosystem I reaction center subunit PSI-N, chloroplast	PS.lightreaction.photosystem I.PSI polypeptide subunits

251031_at	0.624	3.80E-36	8.30E-32	AT5G02120	thylakoid membrane one helix protein (OHP)	PS.lightreaction.photosystem II.PSII polypeptide subunits
264837_at	0.612	1.90E-34	4.10E-30	AT1G03600	photosystem II family protein	PS.lightreaction.photosystem II.PSII polypeptide subunits
261388_at	0.601	5.30E-33	1.20E-28	AT1G05385	photosystem II 11 kDa protein-related	PS.lightreaction.photosystem II.PSII polypeptide subunits
245238_at	0.766	0.00E+00	0.00E+00	AT4G25570	cytochrome B561 family protein	redox.ascorbate and glutathione
253174_at	0.671	2.10E-43	4.50E-39	AT4G35090	identical to catalase 2	redox.dismutases and catalases
259237_at	0.600	6.40E-33	1.40E-28	AT3G11630	2-cys peroxiredoxin, chloroplast (BAS1)	redox.periredoxins
260956_at	0.679	7.00E-45	1.50E-40	AT1G06040	zinc finger (B-box type) family protein / salt-tolerance protein (STO)	RNA.regulation of transcription.C2C2(Zn) CO-like
259476_at	0.623	5.50E-36	1.20E-31	AT1G19000	myb family transcription factor	RNA.regulation of transcription.MYB-related
267517_at	0.693	0.00E+00	3.80E-43	AT2G30520	signal transducer of phototropic response (RPT2)	signalling.light
264313_at	0.688	0.00E+00	4.30E-42	AT1G70410	carbonic anhydrase, putative / carbonate dehydratase	TCA / org. transformation.carbonic anhydrases
254105_at	0.605	1.40E-33	3.00E-29	AT4G25080	magnesium-protoporphyrin O-methyltransferase, putative	tetrapyrrole synthesis
251664_at	0.655	8.50E-41	1.90E-36	AT3G56940	dicarboxylate diiron protein, putative (Crd1)	tetrapyrrole synthesis
266927_at	0.885	0.00E+00	0.00E+00	AT2G45960	**PIP1;2**	transport.Major Intrinsic Proteins.PIP
251324_at	0.786	0.00E+00	0.00E+00	AT3G61430	**PIP1;1**	transport.Major Intrinsic Proteins.PIP
259431_at	0.679	8.40E-45	1.80E-40	AT1G01620	**PIP1;3**	transport.Major Intrinsic Proteins.PIP
254239_at	0.665	1.90E-42	4.10E-38	AT4G23400	**PIP1;5**	transport.Major Intrinsic Proteins.PIP
266533_s_at	0.637	5.60E-38	1.20E-33	AT2G16850	**PIP2;8**	transport.Major Intrinsic Proteins.PIP
257313_at	0.817	0.00E+00	0.00E+00	AT3G26520	**TIP1;2**	transport.Major Intrinsic Proteins.TIP
258054_at	*0.695*	*0.00E+00*	*1.60E-43*	*AT3G16240*	***TIP2;1***	*transport.Major Intrinsic Proteins.TIP*
				AT3G16250	*ferredoxin-related (2Fe-2S iron-sulfur cluster binding domains)*	
263867_at	0.604	2.50E-33	5.40E-29	AT2G36830	**TIP1;1**	transport.Major Intrinsic Proteins.TIP
249327_at	0.658	2.40E-41	5.20E-37	AT5G40890	chloride channel protein (CLC-a)	transport.unspecified anions

PIP2;2/PIP2;3 (265444_s_at/ At2g37170 and At2g37180)

ProbeSet	r-value	p-value	e-value	GeneID	Annotation	MAPMAN classification
247189_at	0.644	4.30E-39	9.50E-35	AT5G65390	arabinogalactan-protein (AGP7)	cell wall.cell wall proteins.AGPs
256900_at	0.623	4.50E-36	9.80E-32	AT3G24670	pectate lyase family protein	cell wall degradation pectate lyases and polygalacturonases
264157_at	0.623	5.40E-36	1.20E-31	AT1G65310	xyloglucan:xyloglucosyl transferase, putative	cell wall.modification
257749_at	*0.655*	*7.80E-41*	*1.70E-36*	*AT1G49240*	*actin 8 (ACT8)*	*cell.organisation*
				AT3G18780	*actin 2 (ACT2)*	
260765_at	0.601	5.30E-33	1.20E-28	AT1G49240	actin 8 (ACT8)	cell.organisation
263137_at	0.620	1.30E-35	2.90E-31	AT1G78660	gamma-glutamyl hydrolase, putative	Co-factor and vitamine metabolism
265439_at	0.706	0.00E+00	1.40E-45	AT2G21045	senescence-associated family protein	development.unspecified
257798_at	0.637	4.70E-38	1.00E-33	AT3G15950	DNA topoisomerase-related similar to DNA topoisomerase IV subunit A	DNA.unspecified
263664_at	0.648	8.70E-40	1.90E-35	AT1G04250	auxin-responsive protein / indoleacetic acid-induced protein 17 (IAA17)	hormone metabolism.auxin
246216_at	0.674	6.20E-44	1.30E-39	AT4G36380	cytochrome P450 90C1 (CYP90C1) / rotundifolia3 (ROT3)	hormone metabolism.brassinosteroid
261727_at	0.656	5.50E-41	1.20E-36	AT1G76090	S-adenosyl-methionine-sterol-C-methyltransferase	hormone metabolism.brassinosteroid
246390_at	0.611	2.80E-34	6.10E-30	AT1G77330	1-aminocyclopropane-1-carboxylate oxidase, putative / ACC oxidase	hormone metabolism.ethylene
266838_at	0.649	8.00E-40	1.80E-35	AT2G25980	jacalin lectin family protein	hormone metabolism.jasmonate
265118_at	0.674	6.40E-44	1.40E-39	AT1G62660	beta-fructosidase (BFRUCT3)	major CHO metabolism
249073_at	0.651	3.10E-40	6.70E-36	AT5G44020	acid phosphatase class B family protein	misc.acid and other phosphatases
249045_at	0.603	2.90E-33	6.40E-29	AT5G44380	FAD-binding domain-containing protein	misc.nitrilases, *nitrile lyases, berberine bridge enzymes
266356_at	0.634	1.20E-37	2.50E-33	AT2G32300	uclacyanin I	misc.oxidases - copper, flavone etc.

247091_at	0.604	2.10E-33	4.70E-29	AT5G66390	peroxidase 72 (PER72)	misc.peroxidases
247297_at	0.703	0.00E+00	5.60E-45	AT5G64100	peroxidase, putative	misc.peroxidases
259276_at	0.613	1.40E-34	3.00E-30	AT3G01190	peroxidase 27 (PER27)	misc.peroxidases
254820_s_at	*0.695*	*0.00E+00*	*1.80E-43*	*AT4G12510*	*protease inhibitor/seed storage/lipid transfer protein (LTP) family protein* *AT4G12520 protease inhibitor/seed storage/lipid transfer protein (LTP) family protein*	*misc.protease inhibitor/seed storage/lipid transfer prot.*
254718_at	*0.647*	*1.30E-39*	*2.90E-35*	*AT4G13580*	*disease resistance-responsive family protein* *AT4G13590 expressed protein*	*not assigned.disagreeing hits*
250663_at	0.607	7.90E-34	1.70E-29	AT5G07110	prenylated rab acceptor (PRA1) family protein	not assigned.no ontology
250717_at	0.658	2.20E-41	4.70E-37	AT5G06200	integral membrane family protein similar to unknown protein	not assigned.no ontology
256785_at	0.619	1.80E-35	3.90E-31	AT3G13720	prenylated rab acceptor (PRA1) family protein	not assigned.no ontology
259291_at	0.618	2.40E-35	5.40E-31	AT3G11550	integral membrane family protein similar to unknown protein	not assigned.no ontology
263284_at	0.724	0.00E+00	0.00E+00	AT2G36100	integral membrane family protein	not assigned.no ontology
265645_at	0.657	3.50E-41	7.60E-37	AT2G27370	integral membrane family protein	not assigned.no ontology
266884_at	0.703	0.00E+00	7.00E-45	AT2G44790	uclacyanin II	not assigned.no ontology
253629_at	0.681	2.80E-45	7.20E-41	AT4G30450	glycine-rich protein	not assigned.no ontology.glycine rich proteins
246142_at	0.665	2.00E-42	4.30E-38	AT5G19970	expressed protein ; expression supported by MPSS	not assigned.unknown
250844_at	0.604	2.10E-33	4.60E-29	AT5G04470	expressed protein	not assigned.unknown
261456_at	0.607	9.60E-34	2.10E-29	AT1G21050	expressed protein	not assigned.unknown
263227_at	0.646	2.40E-39	5.20E-35	AT1G30750	expressed protein	not assigned.unknown
264998_at	0.649	7.60E-40	1.70E-35	AT1G67330	expressed protein	not assigned.unknown
246702_at	0.656	5.40E-41	1.20E-36	AT5G28050	cytidine/deoxycytidylate deaminase family protein	nucleotide metabolism.degradation
252622_at	0.614	9.00E-35	2.00E-30	AT3G45310	cysteine proteinase, putative similar to AALP protein	protein.degradation.cysteine protease
247755_at	0.619	1.70E-35	3.70E-31	AT5G59090	subtilase family protein contains similarity to prepro-cucumisin	protein.degradation.subtilases
259854_at	0.685	1.40E-45	1.50E-41	AT1G72200	zinc finger (C3HC4-type RING finger) family protein	protein.degradation.ubiquitin.E3.RING
265031_at	0.689	0.00E+00	2.80E-42	AT1G61590	protein kinase, putative contains protein kinase domain	protein.postranslational modification.kinase.receptor like
250697_at	0.602	4.20E-33	9.10E-29	AT5G06800	myb family transcription factor	RNA.regulation of transcription.G2-like transcription factor
259274_at	0.631	3.30E-37	7.30E-33	AT3G01220	homeobox-leucine zipper protein, putative / HD-ZIP transcription factor	RNA.regulation of transcription.Homeobox transcription factor
258619_at	0.636	6.00E-38	1.30E-33	AT3G02780	isopentenyl-diphosphate delta-isomerase II	secondary metabolism.isoprenoids.mevalonate pathway
252915_at	0.605	1.70E-33	3.80E-29	AT4G38810	calcium-binding EF hand family protein	signalling.calcium
259853_at	0.665	2.10E-42	4.60E-38	AT1G72300	leucine-rich repeat transmembrane protein kinase	signalling.receptor kinases.leucine rich repeat X
254506_at	0.610	3.60E-34	7.90E-30	AT4G20140	leucine-rich repeat transmembrane protein kinase	signalling.receptor kinases.leucine rich repeat XI
264577_at	0.621	9.60E-36	2.10E-31	AT1G05260	peroxidase 3 (PER3) / rare cold-inducible protein (RCI3A)	stress.abiotic.cold
263437_at	0.630	4.80E-37	1.00E-32	AT2G28670	disease resistance-responsive family protein	stress.biotic
266978_at	0.624	4.00E-36	8.70E-32	AT2G39430	disease resistance-responsive protein-related	stress.biotic
247586_at	0.632	2.20E-37	4.90E-33	AT5G60660	**PIP2;4**	transport.Major Intrinsic Proteins.PIP
251324_at	0.828	0.00E+00	0.00E+00	AT3G61430	**PIP1;1**	transport.Major Intrinsic Proteins.PIP
266927_at	0.676	2.20E-44	5.00E-40	AT2G45960	**PIP1;2**	transport.Major Intrinsic Proteins.PIP
245399_at	0.782	0.00E+00	0.00E+00	AT4G17340	**TIP2;2**	transport.Major Intrinsic Proteins.TIP
248790_at	0.701	0.00E+00	1.50E-44	AT5G47450	**TIP2;3**	transport.Major Intrinsic Proteins.TIP
263867_at	0.782	0.00E+00	0.00E+00	AT2G36830	**TIP1;1**	transport.Major Intrinsic Proteins.TIP
249152_s_at	*0.626*	*2.10E-36*	*4.70E-32*	*AT5G43350*	*inorganic phosphate transporter (PHT1) (PT1)* *AT5G43370 inorganic phosphate transporter (PHT2)*	*transport.phosphate*
256751_at	0.627	1.50E-36	3.30E-32	AT3G27170	chloride channel protein (CLC-b)	transport.unspecified anions
259247_at	0.600	6.60E-33	1.40E-28	AT3G07570	membrane protein, putative similar to membrane protein SDR2	transport.unspecified anions

PIP2;4 (247586_at/ At5g60660)

ProbeSet	r-value	p-value	e-value	GeneID	Annotation	MAPMAN classification
248690_at	0.623	5.00E-36	1.10E-31	AT5G48230	acetyl-CoA C-acyltransferase, putative / 3-ketoacyl-CoA thiolase	amino acid metabolism.degradation.aspartate family.lysine
256531_at	0.621	8.60E-36	1.90E-31	AT1G33320	cystathionine gamma-synthase / O-succinylhomoserine (Thiol)-lyase	amino acid metabolism.synthesis
262646_at	0.618	3.00E-35	6.50E-31	AT1G62800	aspartate aminotransferase, cytoplasmic isozyme 2 / transaminase A	amino acid metabolism.synthesis
255814_at	0.754	0.00E+00	0.00E+00	AT1G19900	glyoxal oxidase-related	Biodegradation of Xenobiotics
262972_at	0.604	2.20E-33	4.70E-29	AT1G75620	glyoxal oxidase-related	Biodegradation of Xenobiotics
248636_at	0.648	1.10E-39	2.40E-35	AT5G49080	proline-rich extensin-like family protein	cell wall
263628_at	0.728	0.00E+00	0.00E+00	AT2G04780	fasciclin-like arabinogalactan-protein (FLA7)	cell wall.cell wall proteins.AGPs
253957_at	0.863	0.00E+00	0.00E+00	AT4G26320	arabinogalactan-protein (AGP13)	cell wall.cell wall proteins.AGPs
250437_at	0.689	0.00E+00	2.40E-42	AT5G10430	arabinogalactan-protein (AGP4)	cell wall.cell wall proteins.AGPs
247965_at	0.811	0.00E+00	0.00E+00	AT5G56540	arabinogalactan-protein (AGP14)	cell wall.cell wall proteins.AGPs
264347_at	0.614	1.00E-34	2.20E-30	AT1G12040	leucine-rich repeat family protein / extensin family protein (LRX1)	cell wall.cell wall proteins.LRR
265114_at	0.693	0.00E+00	5.40E-43	AT1G62440	leucine-rich repeat family protein / extensin family protein	cell wall.cell wall proteins.LRR
256352_at	0.624	4.20E-36	9.10E-32	AT1G54970	proline-rich family protein	cell wall.cell wall proteins.proline rich proteins
245546_at	0.725	0.00E+00	0.00E+00	AT4G15290	cellulose synthase family protein	cell wall.cellulose synthesis
263229_s_at	*0.636*	*7.90E-38*	*1.70E-33*	*AT1G05650* *AT1G05660*	*polygalacturonase, putative / pectinase* *polygalacturonase, putative / pectinase*	*cell wall.degradation.pectate lyases and polygalacturonases*
265350_at	0.629	6.70E-37	1.50E-32	AT2G22620	expressed protein	cell wall.degradation.pectate lyases and polygalacturonases
256900_at	0.798	0.00E+00	0.00E+00	AT3G24670	pectate lyase family protein	cell wall.degradation.pectate lyases and polygalacturonases
257613_at	0.733	0.00E+00	0.00E+00	AT3G26610	polygalacturonase, putative / pectinase	cell wall.degradation.pectate lyases and polygalacturonases
254338_s_at	*0.618*	*2.80E-35*	*6.10E-31*	*AT4G22080* *AT4G22090*	*pectate lyase family protein similar to pectate lyase 2* *pectate lyase family protein similar to pectate lyase 2*	*cell wall.degradation.pectate lyases and polygalacturonases*
262666_at	0.742	0.00E+00	0.00E+00	AT1G14080	xyloglucan fucosyltransferase, putative (FUT6)	cell wall.hemicellulose synthesis
261404_at	0.639	2.00E-38	4.50E-34	AT1G18690	galactosyl transferase GMA12/MNN10 family protein	cell wall.hemicellulose synthesis
263560_s_at	0.707	0.00E+00	1.40E-45	AT2G15370	xyloglucan fucosyltransferase, putative (FUT5)	cell wall.hemicellulose synthesis
261099_at	0.636	7.30E-38	1.60E-33	AT1G62980	expansin, putative (EXP18)	cell wall.modification
264157_at	0.806	0.00E+00	0.00E+00	AT1G65310	xyloglucan:xyloglucosyl transferase, putative	cell wall.modification
266066_at	0.753	0.00E+00	0.00E+00	AT2G18800	xyloglucan:xyloglucosyl transferase, putative	cell wall.modification
258388_at	0.646	2.30E-39	5.10E-35	AT3G15370	expansin, putative (EXP12)	cell wall.modification
252607_at	0.619	2.00E-35	4.40E-31	AT3G44990	xyloglucan:xyloglucosyl transferase, putative	cell wall.modification
255591_at	0.640	1.40E-38	3.10E-34	AT4G01630	expansin, putative (EXP17)	cell wall.modification
247871_at	*0.604*	*2.20E-33*	*4.90E-29*	*AT5G57530* *AT5G57540*	*xyloglucan:xyloglucosyl transferase, putative* *xyloglucan:xyloglucosyl transferase, putative*	*cell wall.modification*
247914_at	*0.647*	*1.60E-39*	*3.50E-35*	*AT5G57530* *AT5G57540*	*xyloglucan:xyloglucosyl transferase, putative* *xyloglucan:xyloglucosyl transferase, putative*	*cell wall.modification*
262198_at	0.786	0.00E+00	0.00E+00	AT1G53830	pectinesterase family protein	cell wall.pectin*esterases.misc
250802_at	0.731	0.00E+00	0.00E+00	AT5G04970	pectinesterase, putative	cell wall.pectin*esterases.misc
258765_at	0.612	1.60E-34	3.50E-30	AT3G10710	pectinesterase family protein	cell wall.pectin*esterases.PME
250801_at	0.619	1.90E-35	4.20E-31	AT5G04960	pectinesterase family protein	cell wall.pectin*esterases.PME
247094_at	0.705	0.00E+00	2.80E-45	AT5G66280	GDP-D-mannose 4,6-dehydratase, putative	cell wall.precursor synthesis.GMD

249057_at	0.711	0.00E+00	0.00E+00	AT5G44480	NAD-dependent epimerase/dehydratase family protein	cell wall.precursor synthesis.MUR4
261953_at	0.629	7.70E-37	1.70E-32	AT1G64440	UDP-glucose 4-epimerase / UDP-galactose 4-epimerase, putative	cell wall.precursor synthesis.UGE
255432_at	0.648	8.50E-40	1.90E-35	AT4G03330	syntaxin, putative (SYP123)	cell. vesicle transport
261562_at	0.699	0.00E+00	3.80E-44	AT1G01750	actin-depolymerizing factor, putative	cell.organisation
264263_at	0.673	9.20E-44	2.00E-39	AT1G09155	SKP1 interacting partner 3-related	cell.organisation
260765_at	0.620	1.20E-35	2.70E-31	AT1G49240	actin 8 (ACT8)	cell.organisation
266701_at	0.688	0.00E+00	3.20E-42	AT2G19760	profilin 1 (PRO1) (PFN1) (PRF1) / allergen Ara t 8 identical to profilin 1	cell.organisation
257241_at	0.741	0.00E+00	0.00E+00	AT3G24210	ankyrin repeat family protein contains ankyrin repeats	cell.organisation
255632_at	0.641	1.00E-38	2.20E-34	AT4G00680	actin-depolymerizing factor, putative	cell.organisation
247210_at	0.608	6.60E-34	1.50E-29	AT5G65020	annexin 2 (ANN2)	cell.organisation
247634_at	*0.604*	*2.30E-33*	*4.90E-29*	*AT5G60510* *AT5G60520*	*undecaprenyl pyrophosphate synthetase family protein* *late embryogenesis abundant protein-related*	*development.late embryogenesis abundant*
253699_at	0.658	2.70E-41	5.90E-37	AT4G29800	patatin-related	development.storage proteins
261335_at	0.648	1.00E-39	2.30E-35	AT1G44800	nodulin MtN21 family protein	development.unspecified
265935_at	0.606	1.20E-33	2.70E-29	AT2G19580	senescence-associated protein-related	development.unspecified
265439_at	0.795	0.00E+00	0.00E+00	AT2G21045	senescence-associated family protein	development.unspecified
259005_at	*0.624*	*3.90E-36*	*8.60E-32*	*AT3G01920* *AT3G01930*	*yrdC family protein* *nodulin family protein*	*development.unspecified*
256273_at	0.632	3.00E-37	6.70E-33	AT3G12090	senescence-associated family protein	development.unspecified
258421_at	0.706	0.00E+00	1.40E-45	AT3G16690	nodulin MtN3 family protein	development.unspecified
258145_at	0.816	0.00E+00	0.00E+00	AT3G18200	nodulin MtN21 family protein	development.unspecified
256847_at	0.723	0.00E+00	0.00E+00	AT3G27950	early nodule-specific protein	development.unspecified
254756_at	0.611	2.70E-34	5.80E-30	AT4G13235	hypothetical protein late embryogenesis abundant protein	development.unspecified
254644_at	0.714	0.00E+00	0.00E+00	AT4G18510	Clavata3 / ESR-Related-2 (CLE2)	development.unspecified
253618_at	0.737	0.00E+00	0.00E+00	AT4G30420	nodulin MtN21 family protein	development.unspecified
266011_at	0.722	0.00E+00	0.00E+00	AT2G37440	endonuclease/exonuclease/phosphatase family protein	DNA.synthesis/chromatin structure
254392_at	0.621	1.10E-35	2.50E-31	AT4G21600	bifunctional nuclease, putative	DNA.synthesis/chromatin structure
261926_at	0.667	8.70E-43	1.90E-38	AT1G22530	SEC14 cytosolic factor family protein/ phosphoglyceride transfer protein	DNA.unspecified
266546_at	0.665	1.80E-42	3.90E-38	AT2G35270	DNA-binding protein-related	DNA.unspecified
245139_at	0.712	0.00E+00	0.00E+00	AT2G45430	DNA-binding protein-related	DNA.unspecified
256647_at	*0.633*	*2.10E-37*	*4.60E-33*	*AT3G13610* *AT3G13620*	*oxidoreductase, 2OG-Fe(II) oxygenase family protein* *amino acid permease family protein*	*DNA.unspecified*
254141_at	0.604	2.00E-33	4.40E-29	AT4G24620	glucose-6-phosphate isomerase, putative	glycolysis.G6PIsomerase
263664_at	0.609	5.10E-34	1.10E-29	AT1G04250	auxin-responsive protein / indoleacetic acid-induced protein 17 (IAA17)	hormone metabolism.auxin
256137_at	0.720	0.00E+00	0.00E+00	AT1G48690	auxin-responsive GH3 family protein	hormone metabolism.auxin
264941_at	0.831	0.00E+00	0.00E+00	AT1G60680	aldo/keto reductase family protein	hormone metabolism.auxin
264928_at	0.696	0.00E+00	1.10E-43	AT1G60710	aldo/keto reductase family protein	hormone metabolism.auxin
258648_at	0.701	0.00E+00	1.80E-44	AT3G07900	expressed protein	hormone metabolism.auxin
245412_at	0.755	0.00E+00	0.00E+00	AT4G17280	auxin-responsive family protein	hormone metabolism.auxin
253515_at	0.826	0.00E+00	0.00E+00	AT4G31320	auxin-responsive protein, putative / small auxin up RNA (SAUR_C)	hormone metabolism.auxin
259680_at	0.867	0.00E+00	0.00E+00	AT1G77690	amino acid permease, putative similar to AUX1	hormone metabolism.auxin.signal transduction
246216_at	0.768	0.00E+00	0.00E+00	AT4G36380	cytochrome P450 90C1 (CYP90C1) / rotundifolia3 (ROT3)	hormone metabolism.brassinosteroid
261727_at	0.677	1.70E-44	3.70E-40	AT1G76090	S-adenosyl-methionine-sterol-C-methyltransferase	hormone metabolism.brassinosteroid
262915_at	0.608	5.80E-34	1.30E-29	AT1G59940	two-component responsive regulator / response regulator 3 (ARR3)	hormone metabolism.cytokinin.signal transduction

258184_at	0.613	1.20E-34	2.60E-30	AT3G21510	two-component phosphorelay mediator 3 (HP3) identical to ATHP3	hormone metabolism.cytokinin.signal transduction
249972_at	0.712	0.00E+00	0.00E+00	AT5G19040	adenylate isopentenyltransferase 5 / cytokinin synthase (IPT5)	hormone metabolism.cytokinin.synthesis-degradation
254404_at	0.742	0.00E+00	0.00E+00	AT4G21340	ethylene-responsive protein-related	hormone metabolism.ethylene
255264_at	0.817	0.00E+00	0.00E+00	AT4G05170	basic helix-loop-helix (bHLH) family protein	hormone metabolism.ethylene.signal transduction
246390_at	0.640	1.60E-38	3.50E-34	AT1G77330	1-aminocyclopropane-1-carboxylate oxidase, putative / ACC oxidase	hormone metabolism.ethylene.synthesis-degradation
248443_at	0.608	7.10E-34	1.60E-29	AT5G51310	gibberellin 20-oxidase-related	hormone metabolism.gibberelin.synthesis-degradation
266838_at	0.614	9.10E-35	2.00E-30	AT2G25980	jacalin lectin family protein similar to myrosinase-binding protein homolog	hormone metabolism.jasmonate
259388_at	0.778	0.00E+00	0.00E+00	AT1G13420	sulfotransferase family protein similar to steroid sulfotransferase 1	lipid metabolism.'exotics' (steroids, squalene etc)
252605_s_at	0.768	0.00E+00	0.00E+00	AT3G45070	sulfotransferase family protein similar to steroid sulfotransferase 3	lipid metabolism.'exotics' (steroids, squalene etc)
249108_at	0.719	0.00E+00	0.00E+00	AT5G43690	sulfotransferase family protein similar to steroid sulfotransferase 3	lipid metabolism.'exotics' (steroids, squalene etc)
260950_s_at	*0.695*	*0.00E+00*	*1.70E-43*	*AT1G06090*	*fatty acid desaturase family protein*	*lipid metabolism.FA desaturation.desaturase*
				AT1G06120	*fatty acid desaturase family protein*	
258473_s_at	*0.614*	*9.90E-35*	*2.20E-30*	*AT3G02610*	*acyl-[acyl-carrier-protein] desaturase, putative / stearoyl-ACP desaturase*	*lipid metabolism.FA synthesis and FA elongation*
				AT3G02620	*acyl-[acyl-carrier-protein] desaturase, putative / stearoyl-ACP desaturase*	
259251_at	0.644	4.50E-39	9.90E-35	AT3G07600	heavy-metal-associated domain-containing protein	metal handling
257197_at	0.684	1.40E-45	2.00E-41	AT3G23800	selenium-binding family protein	metal handling
248652_at	0.734	0.00E+00	0.00E+00	AT5G49270	phytochelatin synthetase-related	metal handling
253172_at	0.650	4.40E-40	9.70E-36	AT4G35060	heavy-metal-associated domain-containing prot./ copper chaperone related	metal handling.binding, chelation and storage
248048_at	0.642	8.50E-39	1.90E-34	AT5G56080	nicotianamine synthase, putative similar to nicotianamine synthase	metal handling.binding, chelation and storage
259264_at	0.797	0.00E+00	0.00E+00	AT3G01260	aldose 1-epimerase family protein	minor CHO metabolism.others
260059_at	0.748	0.00E+00	0.00E+00	AT1G78090	trehalose-6-phosphate phosphatase (TPPB)	minor CHO metabolism.trehalose.TPP
256368_at	0.684	1.40E-45	2.30E-41	AT1G66800	cinnamyl-alcohol dehydrogenase family / CAD family	misc.alcohol dehydrogenases
254344_at	0.746	0.00E+00	0.00E+00	AT4G22110	alcohol dehydrogenase, putative similar to alcohol dehydrogenase ADH	misc.alcohol dehydrogenases
261690_at	0.701	0.00E+00	1.80E-44	AT1G50090	aminotransferase class IV family protein	misc.aminotransferases.aminotransferase class IV family prot.
259424_at	0.719	0.00E+00	0.00E+00	AT1G13830	beta-1,3-glucanase-related similar to beta-1,3-glucanase-like protein	misc.beta 1,3 glucan hydrolases
251280_at	0.687	0.00E+00	5.80E-42	AT3G61810	glycosyl hydrolase family 17 protein	misc.beta 1,3 glucan hydrolases
261185_at	0.611	2.50E-34	5.50E-30	AT1G34540	cytochrome P450 family protein similar to Cytochrome P450 94A1	misc.cytochrome P450
261879_at	0.731	0.00E+00	0.00E+00	AT1G50520	cytochrome P450 family protein similar to CYTOCHROME P450 93A3	misc.cytochrome P450
261878_at	0.758	0.00E+00	0.00E+00	AT1G50560	cytochrome P450, putative similar to CYTOCHROME P450 93A3	misc.cytochrome P450
262865_at	*0.622*	*7.50E-36*	*1.60E-31*	*AT1G64930*	*cytochrome P450, putative similar to cytochrome P450 CYP89*	*misc.cytochrome P450*
				AT2G12190	*cytochrome P450, putative*	
264470_at	0.608	6.40E-34	1.40E-29	AT1G67110	cytochrome P450, putative similar to Cytochrome P450 72A1	misc.cytochrome P450
245728_at	0.640	1.50E-38	3.20E-34	AT1G73340	cytochrome P450 family protein similar to Cytochrome P450 90A1	misc.cytochrome P450
264404_at	0.805	0.00E+00	0.00E+00	AT2G25160	cytochrome P450, putative similar to cytochrome p450(CYP82C1p)	misc.cytochrome P450
266307_at	0.725	0.00E+00	0.00E+00	AT2G27000	cytochrome P450 family protein	misc.cytochrome P450
263970_at	0.731	0.00E+00	0.00E+00	AT2G42850	cytochrome P450 family protein similar to taxane 13-alpha-hydroxylase	misc.cytochrome P450
257143_at	0.743	0.00E+00	0.00E+00	AT3G20110	cytochrome P450 family protein similar to Cytochrome P450 93A1	misc.cytochrome P450
257113_at	0.648	8.90E-40	1.90E-35	AT3G20130	cytochrome P450 family protein	misc.cytochrome P450
245550_at	0.679	5.60E-45	1.30E-40	AT4G15330	cytochrome P450 family protein	misc.cytochrome P450
245554_at	0.688	0.00E+00	3.70E-42	AT4G15380	cytochrome P450 family protein similar to CYTOCHROME P450 93A3	misc.cytochrome P450
246978_at	0.620	1.30E-35	2.80E-31	AT5G24910	cytochrome P450 family protein similar to Cytochrome P450 72A1	misc.cytochrome P450
249203_at	0.613	1.20E-34	2.60E-30	AT5G42590	cytochrome P450 71A16, putative	misc.cytochrome P450
248727_at	0.702	0.00E+00	8.40E-45	AT5G47990	cytochrome P450 family protein similar to Cytochrome P450 93A3	misc.cytochrome P450
267439_at	0.631	4.10E-37	8.90E-33	AT2G19060	GDSL-motif lipase/hydrolase family protein	misc.GDSL-motif lipase

251255_at	0.683	1.40E-45	3.00E-41	AT3G62280	GDSL-motif lipase/hydrolase family protein	misc.GDSL-motif lipase
264861_at	0.643	6.30E-39	1.40E-34	AT1G24320	alpha-glucosidase, putative similar to alpha-glucosidase I	misc.gluco-, galacto- and mannosidases
260944_at	0.710	0.00E+00	0.00E+00	AT1G45130	beta-galactosidase, putative / lactase, putative	misc.gluco-, galacto- and mannosidases
260758_at	0.634	1.20E-37	2.60E-33	AT1G48930	endo-1,4-beta-glucanase, putative / cellulase, putative	misc.gluco-, galacto- and mannosidases
262516_at	0.674	6.60E-44	1.40E-39	AT1G17190	glutathione S-transferase, putative	misc.glutathione S transferases
259964_at	0.738	0.00E+00	0.00E+00	AT1G53680	glutathione S-transferase, putative	misc.glutathione S transferases
254056_at	0.652	2.50E-40	5.50E-36	AT4G25250	invertase/pectin methylesterase inhibitor family protein	misc.invertase/pectin methylesterase inhibitor family protein
260812_at	0.696	0.00E+00	1.30E-43	AT1G43650	integral membrane family protein / nodulin MtN21-related	misc.misc2
249516_s_at	0.760	0.00E+00	0.00E+00	AT5G38550	jacalin lectin family protein similar to myrosinase-binding protein homolog	misc.myrosinases-lectin-jacalin
248577_at	0.601	5.70E-33	1.30E-28	AT5G49870	jacalin lectin family protein similar to myrosinase-binding protein homolog	misc.myrosinases-lectin-jacalin
260344_at	0.676	2.80E-44	6.20E-40	AT1G69240	hydrolase, alpha/beta fold family protein	misc.nitrilases, *nitrile lyases, berberine bridge enzymes, etc.
267128_at	0.746	0.00E+00	0.00E+00	AT2G23620	esterase, putative similar to ethylene-induced esterase	misc.nitrilases, *nitrile lyases, berberine bridge enzymes, etc.
266356_at	0.834	0.00E+00	0.00E+00	AT2G32300	uclacyanin I	misc.oxidases - copper, flavone etc.
265882_at	0.623	4.80E-36	1.00E-31	AT2G42490	copper amine oxidase, putative	misc.oxidases - copper, flavone etc.
258852_at	0.614	9.00E-35	2.00E-30	AT3G06300	oxidoreductase, 2OG-Fe(II) oxygenase family protein	misc.oxidases - copper, flavone etc.
265102_at	0.623	5.20E-36	1.10E-31	AT1G30870	cationic peroxidase, putative similar to cationic peroxidase	misc.peroxidases
261606_at	0.731	0.00E+00	0.00E+00	AT1G49570	peroxidase, putative identical to peroxidase ATP5a	misc.peroxidases
266191_at	0.768	0.00E+00	0.00E+00	AT2G39040	peroxidase, putative similar to cationic peroxidase isozyme 38K precursor	misc.peroxidases
259276_at	0.764	0.00E+00	0.00E+00	AT3G01190	peroxidase 27 (PER27) (P27) (PRXR7)	misc.peroxidases
257952_at	0.772	0.00E+00	0.00E+00	AT3G21770	peroxidase 30 (PER30) (P30) (PRXR9)	misc.peroxidases
254914_at	0.735	0.00E+00	0.00E+00	AT4G11290	peroxidase, putative identical to peroxidase ATP19a	misc.peroxidases
253667_at	0.763	0.00E+00	0.00E+00	AT4G30170	peroxidase, putative identical to peroxidase ATP8a	misc.peroxidases
250157_at	0.699	0.00E+00	3.60E-44	AT5G15180	peroxidase, putative similar to peroxidase ATP12a	misc.peroxidases
250059_at	0.622	6.40E-36	1.40E-31	AT5G17820	peroxidase 57 (PER57) (P57) (PRXR10)	misc.peroxidases
246149_at	0.746	0.00E+00	0.00E+00	AT5G19890	peroxidase, putative	misc.peroxidases
249934_at	0.627	1.20E-36	2.70E-32	AT5G22410	peroxidase, putative identical to peroxidase ATP14a	misc.peroxidases
249227_at	0.620	1.40E-35	3.00E-31	AT5G42180	peroxidase 64 (PER64)	misc.peroxidases
247091_at	0.779	0.00E+00	0.00E+00	AT5G66390	peroxidase 72 (PER72)	misc.peroxidases
261745_at	0.681	2.80E-45	6.90E-41	AT1G08500	plastocyanin-like domain-containing protein	misc.plastocyanin-like
265656_at	0.601	5.10E-33	1.10E-28	AT2G13820	protease inhibitor/seed storage/lipid transfer protein (LTP) family	misc.protease inhibitor/seed storage/lipid transfer prot.
256935_at	0.793	0.00E+00	0.00E+00	AT3G22570	protease inhibitor/seed storage/lipid transfer protein (LTP) family	misc.protease inhibitor/seed storage/lipid transfer prot.
256937_at	0.600	6.30E-33	1.40E-28	AT3G22620	protease inhibitor/seed storage/lipid transfer protein (LTP) family	misc.protease inhibitor/seed storage/lipid transfer prot.
254820_s_at	*0.795*	*0.00E+00*	*0.00E+00*	*AT4G12510* *AT4G12520*	*protease inhibitor/seed storage/lipid transfer protein (LTP) family* *protease inhibitor/seed storage/lipid transfer protein (LTP) family*	*misc.protease inhibitor/seed storage/lipid transfer prot.*
254828_at	0.783	0.00E+00	0.00E+00	AT4G12550	protease inhibitor/seed storage/lipid transfer protein (LTP) family	misc.protease inhibitor/seed storage/lipid transfer prot.
248844_s_at	0.608	6.40E-34	1.40E-29	AT5G46900	protease inhibitor/seed storage/lipid transfer protein (LTP) family	misc.protease inhibitor/seed storage/lipid transfer prot.
257774_at	0.749	0.00E+00	0.00E+00	AT3G29250	short-chain dehydrogenase/reductase (SDR) family protein	misc.short chain dehydrogenase/reductase (SDR)
252070_at	0.652	2.20E-40	4.90E-36	AT3G51680	short-chain dehydrogenase/reductase (SDR) family protein	misc.short chain dehydrogenase/reductase (SDR)
256053_at	0.699	0.00E+00	3.60E-44	AT1G07260	UDP-glucoronosyl/UDP-glucosyl transferase family protein	misc.UDP glucosyl and glucoronyl transferases
261550_at	0.673	8.30E-44	1.80E-39	AT1G63450	exostosin family protein	misc.UDP glucosyl and glucoronyl transferases
262863_at	0.635	8.70E-38	1.90E-33	AT1G64910	glycosyltransferase family protein	misc.UDP glucosyl and glucoronyl transferases
262371_at	0.612	2.00E-34	4.30E-30	AT1G73160	glycosyl transferase family 1 protein	misc.UDP glucosyl and glucoronyl transferases
260563_at	0.698	0.00E+00	4.80E-44	AT2G43840	UDP-glucoronosyl/UDP-glucosyl transferase family protein	misc.UDP glucosyl and glucoronyl transferases
252490_at	0.642	8.60E-39	1.90E-34	AT3G46720	UDP-glucoronosyl/UDP-glucosyl transferase family protein	misc.UDP glucosyl and glucoronyl transferases

245561_at	0.626	2.30E-36	5.00E-32	AT4G15500	UDP-glucoronosyl/UDP-glucosyl transferase family protein	misc.UDP glucosyl and glucoronyl transferases
253379_at	0.664	2.60E-42	5.70E-38	AT4G33330	glycogenin glucosyltransferase (glycogenin)-related	misc.UDP glucosyl and glucoronyl transferases
250746_at	0.699	0.00E+00	3.50E-44	AT5G05880	UDP-glucoronosyl/UDP-glucosyl transferase family protein	misc.UDP glucosyl and glucoronyl transferases
246826_at	*0.780*	*0.00E+00*	*0.00E+00*	*AT5G26310*	*UDP-glucoronosyl/UDP-glucosyl transferase family protein*	*misc.UDP glucosyl and glucoronyl transferases*
				AT5G66690	*UDP-glucoronosyl/UDP-glucosyl transferase family protein*	
266365_at	0.675	3.80E-44	8.40E-40	AT2G41220	glutamate synthase, chloroplast / ferredoxin-dependent glutamate synthase	N-metabolism.ammonia metabolism.glutamate synthase
248518_at	*0.802*	*0.00E+00*	*0.00E+00*	*AT5G50560*	*expressed protein*	*not assigned.disagreeing hits*
				AT5G50660	*expressed protein*	
251045_s_at	0.674	4.60E-44	1.00E-39	AT5G02360	DC1 domain-containing protein	not assigned.disagreeing hits
251116_at	*0.762*	*0.00E+00*	*0.00E+00*	*AT3G63470*	*serine carboxypeptidase, putative*	*not assigned.disagreeing hits*
				AT3G63480	*kinesin heavy chain*	
251438_s_at	*0.736*	*0.00E+00*	*0.00E+00*	*AT3G59930*	*expressed protein*	*not assigned.disagreeing hits*
				AT5G33355	*expressed protein*	
254718_at	*0.811*	*0.00E+00*	*0.00E+00*	*AT4G13580*	*disease resistance-responsive family protein*	*not assigned.disagreeing hits*
				AT4G13590	*expressed protein*	
261464_at	*0.857*	*0.00E+00*	*0.00E+00*	*AT1G07730*	*disease resistance-responsive family protein*	*not assigned.disagreeing hits*
				AT1G07740	*pentatricopeptide (PPR) repeat-containing protein*	
261729_s_at	0.730	0.00E+00	0.00E+00	AT1G47840	hexokinase, putative similar to hexokinase 1	not assigned.disagreeing hits
262655_s_at	0.758	0.00E+00	0.00E+00	AT1G14190	glucose-methanol-choline (GMC) oxidoreductase family protein	not assigned.disagreeing hits
265435_s_at	0.762	0.00E+00	0.00E+00	AT1G31885	major intrinsic family protein / MIP family proteiN	not assigned.disagreeing hits
264643_at	0.721	0.00E+00	0.00E+00	AT1G08990	glycogenin glucosyltransferase (glycogenin)-related	not assigned.no ontology
262756_at	0.624	3.30E-36	7.20E-32	AT1G16370	transporter-related low similarity to organic cation transporter OCTN1	not assigned.no ontology
259454_at	0.823	0.00E+00	0.00E+00	AT1G44050	DC1 domain-containing protein	not assigned.no ontology
262444_at	0.816	0.00E+00	0.00E+00	AT1G47480	expressed protein similar to PrMC3 [Pinus radiata]	not assigned.no ontology
260646_at	0.653	1.50E-40	3.20E-36	AT1G53340	DC1 domain-containing protein	not assigned.no ontology
256350_at	0.684	1.40E-45	2.00E-41	AT1G54940	glycogenin glucosyltransferase (glycogenin)-related	not assigned.no ontology
256360_at	0.640	1.60E-38	3.60E-34	AT1G66440	DC1 domain-containing protein	not assigned.no ontology
256362_at	0.630	4.70E-37	1.00E-32	AT1G66450	DC1 domain-containing protein	not assigned.no ontology
267217_at	*0.691*	*0.00E+00*	*1.10E-42*	*AT2G02610*	*DC1 domain-containing protein*	*not assigned.no ontology*
				AT2G02640	*DC1 domain-containing protein*	
263616_at	0.669	4.60E-43	1.00E-38	AT2G04680	DC1 domain-containing protein	not assigned.no ontology
265645_at	0.850	0.00E+00	0.00E+00	AT2G27370	integral membrane family protein	not assigned.no ontology
266209_at	0.656	4.70E-41	1.00E-36	AT2G27550	centroradialis protein, putative	not assigned.no ontology
263284_at	0.864	0.00E+00	0.00E+00	AT2G36100	integral membrane family protein	not assigned.no ontology
266083_at	0.606	1.10E-33	2.50E-29	AT2G37820	DC1 domain-containing protein	not assigned.no ontology
266884_at	0.708	0.00E+00	0.00E+00	AT2G44790	uclacyanin II	not assigned.no ontology
265766_at	0.689	0.00E+00	2.40E-42	AT2G48080	oxidoreductase, 2OG-Fe(II) oxygenase family protein	not assigned.no ontology
259106_at	0.629	6.70E-37	1.50E-32	AT3G05490	rapid alkalinization factor (RALF) family protein	not assigned.no ontology
258745_at	0.900	0.00E+00	0.00E+00	AT3G05920	heavy-metal-associated domain-containing protein	not assigned.no ontology
259260_at	0.692	0.00E+00	7.00E-43	AT3G11370	DC1 domain-containing protein	not assigned.no ontology
259291_at	0.906	0.00E+00	0.00E+00	AT3G11550	integral membrane family protein	not assigned.no ontology
257105_at	0.731	0.00E+00	0.00E+00	AT3G15300	VQ motif-containing protein	not assigned.no ontology
257720_at	0.605	1.80E-33	3.90E-29	AT3G18450	expressed protein similar to PGPS/D12 [Petunia x hybrida]	not assigned.no ontology
258013_at	0.713	0.00E+00	0.00E+00	AT3G19320	leucine-rich repeat family protein	not assigned.no ontology

257924_at	0.809	0.00E+00	0.00E+00	AT3G23190	lesion inducing protein-related similar to ORF, able to induce HR-like lesions	not assigned.no ontology
259369_s_at	*0.709*	*0.00E+00*	*0.00E+00*	*AT1G69150*	*DC1 domain-containing protein*	*not assigned.no ontology*
				AT3G43890	*DC1 domain-containing protein*	
252396_at	0.644	4.40E-39	9.50E-35	AT3G47980	integral membrane HPP family protein	not assigned.no ontology
252397_at	0.682	1.40E-45	4.00E-41	AT3G47980	integral membrane HPP family protein	not assigned.no ontology
256673_at	0.658	2.20E-41	4.70E-37	AT3G52370	beta-Ig-H3 domain-containing protein / fasciclin domain-containing proteing	not assigned.no ontology
245328_at	0.630	4.40E-37	9.60E-33	AT4G14465	DNA-binding protein-related	not assigned.no ontology
245555_at	0.836	0.00E+00	0.00E+00	AT4G15390	transferase family protein	not assigned.no ontology
245556_at	0.677	1.40E-44	3.20E-40	AT4G15400	transferase family protein	not assigned.no ontology
245382_at	0.741	0.00E+00	0.00E+00	AT4G17800	DNA-binding protein-related	not assigned.no ontology
253732_at	0.601	6.00E-33	1.30E-28	AT4G29140	MATE efflux protein-related	not assigned.no ontology
251044_at	0.747	0.00E+00	0.00E+00	AT5G02350	DC1 domain-containing protein	not assigned.no ontology
250717_at	0.790	0.00E+00	0.00E+00	AT5G06200	integral membrane family protein	not assigned.no ontology
250663_at	0.736	0.00E+00	0.00E+00	AT5G07110	prenylated rab acceptor (PRA1) family protein	not assigned.no ontology
250618_at	0.659	1.50E-41	3.20E-37	AT5G07220	BAG domain-containing protein	not assigned.no ontology
249812_at	0.736	0.00E+00	0.00E+00	AT5G23830	MD-2-related lipid recognition domain-containing protein	not assigned.no ontology
249814_at	0.638	3.20E-38	7.10E-34	AT5G23840	MD-2-related lipid recognition domain-containing protein	not assigned.no ontology
255860_at	0.630	5.10E-37	1.10E-32	AT5G34940	glycosyl hydrolase family 79 N-terminal domain-containing protein	not assigned.no ontology
249364_at	0.672	1.30E-43	2.80E-39	AT5G40590	DC1 domain-containing protein	not assigned.no ontology
249166_at	0.648	1.10E-39	2.30E-35	AT5G42840	DC1 domain-containing protein	not assigned.no ontology
249185_at	0.611	2.60E-34	5.70E-30	AT5G43030	DC1 domain-containing protein	not assigned.no ontology
249186_at	0.640	1.50E-38	3.30E-34	AT5G43040	DC1 domain-containing protein	not assigned.no ontology
248715_at	0.682	1.40E-45	4.00E-41	AT5G48290	heavy-metal-associated domain-containing protein	not assigned.no ontology
248183_at	0.603	2.60E-33	5.80E-29	AT5G54040	DC1 domain-containing protein	not assigned.no ontology
247797_at	0.680	4.20E-45	8.90E-41	AT5G58780	dehydrodolichyl diphosphate synthase/ DEDOL-PP synthase, putative	not assigned.no ontology
247674_at	0.728	0.00E+00	0.00E+00	AT5G59930	DC1 domain-containing protein / UV-B light-insensitive protein	not assigned.no ontology
247568_at	0.615	6.00E-35	1.30E-30	AT5G61260	chromosome scaffold protein-related	not assigned.no ontology
264794_at	0.618	2.80E-35	6.00E-31	AT1G08670	epsin N-terminal homology (ENTH) domain-containing protein	not assigned.no ontology.ENTH domain-containing protein
252851_at	0.607	8.10E-34	1.80E-29	AT4G40080	epsin N-terminal homology (ENTH) domain-containing protein	not assigned.no ontology.ENTH domain-containing protein
253629_at	0.618	2.60E-35	5.60E-31	AT4G30450	glycine-rich protein	not assigned.no ontology.glycine rich proteins
245967_at	0.602	3.50E-33	7.80E-29	AT5G19800	hydroxyproline-rich glycoprotein family protein similar to extensin	not assigned.no ontology.hydroxyproline rich proteins
260053_at	0.636	7.40E-38	1.60E-33	AT1G78120	tetratricopeptide repeat (TPR)-containing protein	not assigned.no ontology.PPR repeat-containing protein
262315_at	0.796	0.00E+00	0.00E+00	AT1G70990	proline-rich family protein	not assigned.no ontology.proline rich family
252222_at	0.661	7.40E-42	1.60E-37	AT3G49840	proline-rich family protein	not assigned.no ontology.proline rich family
254772_at	0.602	3.50E-33	7.60E-29	AT4G13390	proline-rich extensin-like family protein	not assigned.no ontology.proline rich family
251723_at	0.738	0.00E+00	0.00E+00	AT3G56230	speckle-type POZ protein-related	not assigned.no ontology.speckle-type POZ protein-related
249033_at	0.651	3.60E-40	7.80E-36	AT5G44920	Toll-Interleukin-Resistance (TIR) domain-containing protein	not assigned.no ontology.TIR domain-containing protein
264466_at	0.687	0.00E+00	5.60E-42	AT1G10380	expressed protein	not assigned.unknown
264342_at	0.662	5.80E-42	1.30E-37	AT1G12080	expressed protein	not assigned.unknown
256191_at	0.610	2.90E-34	6.30E-30	AT1G30130	expressed protein	not assigned.unknown
263227_at	0.749	0.00E+00	0.00E+00	AT1G30750	expressed protein	not assigned.unknown
261991_at	0.663	3.90E-42	8.60E-38	AT1G33700	expressed protein	not assigned.unknown
261999_at	0.779	0.00E+00	0.00E+00	AT1G33800	expressed protein	not assigned.unknown
259624_at	0.740	0.00E+00	0.00E+00	AT1G43020	expressed protein	not assigned.unknown

261297_at	0.676	2.40E-44	5.30E-40	AT1G48500 expressed protein ; expression supported by MPSS	not assigned.unknown
256208_at	0.636	6.30E-38	1.40E-33	AT1G50930 hypothetical protein	not assigned.unknown
260151_at	0.666	1.30E-42	2.90E-38	AT1G52910 expressed protein	not assigned.unknown
264287_at	0.628	1.00E-36	2.30E-32	AT1G61930 expressed protein	not assigned.unknown
264998_at	0.813	0.00E+00	0.00E+00	AT1G67330 expressed protein	not assigned.unknown
261509_at	0.715	0.00E+00	0.00E+00	AT1G71740 hypothetical protein	not assigned.unknown
261778_at	0.708	0.00E+00	0.00E+00	AT1G76220 hypothetical protein	not assigned.unknown
262045_at	0.703	0.00E+00	5.60E-45	AT1G80240 expressed protein	not assigned.unknown
261893_at	0.661	7.20E-42	1.60E-37	AT1G80690 expressed protein	not assigned.unknown
265710_at	0.619	1.60E-35	3.60E-31	AT2G03370 hypothetical protein	not assigned.unknown
263513_at	0.616	5.80E-35	1.30E-30	AT2G12400 expressed protein	not assigned.unknown
266525_at	0.667	7.60E-43	1.70E-38	AT2G16970 expressed protein ; expression supported by MPSS	not assigned.unknown
266526_at	0.786	0.00E+00	0.00E+00	AT2G16980 expressed protein	not assigned.unknown
263575_at	0.753	0.00E+00	0.00E+00	AT2G17070 expressed protein	not assigned.unknown
266561_at	0.661	7.50E-42	1.60E-37	AT2G23960 defense-related protein, putative similar to defense-related protein	not assigned.unknown
263436_at	0.604	1.90E-33	4.30E-29	AT2G28690 expressed protein	not assigned.unknown
265845_at	0.723	0.00E+00	0.00E+00	AT2G35610 expressed protein	not assigned.unknown
267037_at	0.660	1.40E-41	3.00E-37	AT2G38320 expressed protein	not assigned.unknown
263387_at	0.608	6.20E-34	1.40E-29	AT2G40160 expressed protein	not assigned.unknown
245113_at	0.630	4.40E-37	9.60E-33	AT2G41660 expressed protein	not assigned.unknown
266913_at	0.677	1.50E-44	3.40E-40	AT2G45890 expressed protein	not assigned.unknown
259191_at	0.675	4.20E-44	9.30E-40	AT3G01720 expressed protein	not assigned.unknown
259195_at	0.606	1.20E-33	2.70E-29	AT3G01730 expressed protein	not assigned.unknown
259345_s_at	*0.641*	*1.00E-38*	*2.20E-34*	*AT3G03700 expressed protein, Protein of unknown function, DUF580* *AT3G04440 expressed protein, Protein of unknown function, DUF580*	*not assigned.unknown*
258728_at	0.666	1.20E-42	2.60E-38	AT3G11800 expressed protein	not assigned.unknown
256283_at	0.674	6.20E-44	1.30E-39	AT3G12540 expressed protein	not assigned.unknown
256600_at	0.740	0.00E+00	0.00E+00	AT3G14850 expressed protein	not assigned.unknown
258143_at	0.764	0.00E+00	0.00E+00	AT3G18170 expressed protein	not assigned.unknown
256563_at	0.655	7.70E-41	1.70E-36	AT3G29780 expressed protein	not assigned.unknown
252458_at	0.664	2.40E-42	5.30E-38	AT3G47210 expressed protein	not assigned.unknown
251517_at	0.765	0.00E+00	0.00E+00	AT3G59370 expressed protein	not assigned.unknown
251368_at	0.643	5.60E-39	1.20E-34	AT3G61380 expressed protein	not assigned.unknown
255757_at	0.658	2.70E-41	5.90E-37	AT4G00460 expressed protein	not assigned.unknown
255528_at	0.721	0.00E+00	0.00E+00	AT4G02090 expressed protein	not assigned.unknown
255005_at	0.789	0.00E+00	0.00E+00	AT4G09990 expressed protein	not assigned.unknown
245610_at	0.746	0.00E+00	0.00E+00	AT4G14380 expressed protein	not assigned.unknown
245568_at	0.641	1.10E-38	2.30E-34	AT4G14650 expressed protein	not assigned.unknown
245300_at	0.605	1.40E-33	3.10E-29	AT4G16350 calcineurin B-like protein 6 (CBL6) identical to calcineurin B-like protein 6	not assigned.unknown
245495_at	0.648	9.40E-40	2.10E-35	AT4G16400 expressed protein	not assigned.unknown
254361_at	0.668	5.80E-43	1.30E-38	AT4G22212 expressed protein	not assigned.unknown
254324_at	0.724	0.00E+00	0.00E+00	AT4G22640 expressed protein	not assigned.unknown
254029_at	0.716	0.00E+00	0.00E+00	AT4G25870 expressed protein	not assigned.unknown
253179_at	0.736	0.00E+00	0.00E+00	AT4G35200 hypothetical protein	not assigned.unknown

253180_at	0.627	1.20E-36	2.70E-32	AT4G35210	hypothetical protein	not assigned.unknown
250907_at	0.635	1.10E-37	2.40E-33	AT5G03670	expressed protein	not assigned.unknown
250844_at	0.686	0.00E+00	1.00E-41	AT5G04470	expressed protein	not assigned.unknown
250472_at	0.676	2.50E-44	5.40E-40	AT5G10210	expressed protein	not assigned.unknown
250438_at	0.756	0.00E+00	0.00E+00	AT5G10580	expressed protein	not assigned.unknown
250224_at	0.724	0.00E+00	0.00E+00	AT5G14150	expressed protein	not assigned.unknown
250145_at	0.682	1.40E-45	4.00E-41	AT5G14690	expressed protein	not assigned.unknown
246534_at	*0.721*	*0.00E+00*	*0.00E+00*	*AT5G15880* expressed protein *AT5G15890* expressed protein		*not assigned.unknown*
246535_at	0.734	0.00E+00	0.00E+00	AT5G15900	expressed protein	not assigned.unknown
246142_at	0.744	0.00E+00	0.00E+00	AT5G19970	expressed protein	not assigned.unknown
249756_at	0.606	1.20E-33	2.60E-29	AT5G24313	expressed protein	not assigned.unknown
249533_at	0.769	0.00E+00	0.00E+00	AT5G38790	expressed protein	not assigned.unknown
249358_at	0.791	0.00E+00	0.00E+00	AT5G40510	expressed protein	not assigned.unknown
249332_at	0.683	1.40E-45	2.90E-41	AT5G40980	expressed protein	not assigned.unknown
249167_at	0.633	2.10E-37	4.60E-33	AT5G42860	expressed protein	not assigned.unknown
249136_at	0.624	4.10E-36	9.10E-32	AT5G43180	expressed protein	not assigned.unknown
249143_at	0.642	9.50E-39	2.10E-34	AT5G43230	hypothetical protein	not assigned.unknown
249153_s_at	0.735	0.00E+00	0.00E+00	AT5G43390	hypothetical protein	not assigned.unknown
248572_at	0.622	8.10E-36	1.80E-31	AT5G49800	expressed protein	not assigned.unknown
248212_at	0.673	7.70E-44	1.70E-39	AT5G54020	expressed protein	not assigned.unknown
247522_at	0.804	0.00E+00	0.00E+00	AT5G61340	expressed protein	not assigned.unknown
247070_at	0.729	0.00E+00	0.00E+00	AT5G66815	expressed protein	not assigned.unknown
252152_at	0.671	1.70E-43	3.80E-39	AT3G51350	aspartyl protease family protein	not assigned
257393_at	0.656	5.80E-41	1.30E-36	AT2G20080	expressed protein	not assigned
254816_at	0.601	4.70E-33	1.00E-28	AT4G12440	adenine phosphoribosyltransferase, putative	nucleotide metabolism.salvage.phosphoribosyltransferases
261806_at	0.739	0.00E+00	0.00E+00	AT1G30510	ferredoxin--NADP(+) reductase, putative / adrenodoxin reductase, putative	OPP.electron transfer
262323_at	0.720	0.00E+00	0.00E+00	AT1G64190	6-phosphogluconate dehydrogenase family protein	OPP.oxidative PP.6-phosphogluconate dehydrogenase
249729_at	0.818	0.00E+00	0.00E+00	AT5G24410	glucosamine/galactosamine-6-phosphate isomerase-related	OPP.oxidative PP.6-phosphogluconolactonase
264859_at	0.700	0.00E+00	2.50E-44	AT1G24280	glucose-6-phosphate 1-dehydrogenase, putative / G6PD, putative	OPP.oxidative PP.G6PD
245977_at	0.657	4.40E-41	9.70E-37	AT5G13110	glucose-6-phosphate 1-dehydrogenase, putative / G6PD, putative	OPP.oxidative PP.G6PD
255216_s_at	0.712	0.00E+00	0.00E+00	AT4G07670	protease-associated (PA) domain-containing protein	protein.degradation
256626_at	0.769	0.00E+00	0.00E+00	AT3G20015	aspartyl protease family protein	protein.degradation.aspartate protease
252692_at	0.749	0.00E+00	0.00E+00	AT3G43960	cysteine proteinase, putative	protein.degradation.cysteine protease
260092_at	0.714	0.00E+00	0.00E+00	AT1G73280	serine carboxypeptidase S10 family protein	protein.degradation.serine protease
257500_s_at	*0.756*	*0.00E+00*	*0.00E+00*	*AT1G73300* serine carboxypeptidase S10 family protein *AT5G36180* serine carboxypeptidase S10 family protein		*protein.degradation.serine protease*
247755_at	0.871	0.00E+00	0.00E+00	AT5G59090	subtilase family protein contains similarity to prepro-cucumisin	protein.degradation.subtilases
259472_at	0.664	3.20E-42	6.90E-38	AT1G18910	zinc finger (C3HC4-type RING finger) family protein	protein.degradation.ubiquitin.E3.RING
261927_at	0.667	7.00E-43	1.50E-38	AT1G22500	zinc finger (C3HC4-type RING finger) family protein	protein.degradation.ubiquitin.E3.RING
259576_at	0.755	0.00E+00	0.00E+00	AT1G35330	zinc finger (C3HC4-type RING finger) family protein	protein.degradation.ubiquitin.E3.RING
259699_at	0.727	0.00E+00	0.00E+00	AT1G68940	armadillo/beta-catenin repeat protein-related/ U-box domain-containing protein	protein.degradation.ubiquitin.E3.RING
259854_at	0.942	0.00E+00	0.00E+00	AT1G72200	zinc finger (C3HC4-type RING finger) family protein	protein.degradation.ubiquitin.E3.RING
262218_at	0.608	6.60E-34	1.40E-29	AT1G74760	zinc finger (C3HC4-type RING finger) family protein	protein.degradation.ubiquitin.E3.RING

267418_at	0.749	0.00E+00	0.00E+00	AT2G35000	zinc finger (C3HC4-type RING finger) family protein	protein.degradation.ubiquitin.E3.RING
255074_at	0.677	1.40E-44	3.10E-40	AT4G09100	zinc finger (C3HC4-type RING finger) family protein	protein.degradation.ubiquitin.E3.RING
253741_at	0.805	0.00E+00	0.00E+00	AT4G28890	zinc finger (C3HC4-type RING finger) family protein	protein.degradation.ubiquitin.E3.RING
252834_at	0.614	9.00E-35	2.00E-30	AT4G40070	expressed protein	protein.degradation.ubiquitin.E3.RING
246135_at	0.694	0.00E+00	3.20E-43	AT5G20885	zinc finger (C3HC4-type RING finger) family protein	protein.degradation.ubiquitin.E3.RING
262732_at	0.643	5.60E-39	1.20E-34	AT1G16440	protein kinase, putative similar to viroid symptom modulation protein	protein.postranslational modification
261605_at	0.609	5.00E-34	1.10E-29	AT1G49580	calcium-dependent protein kinase / CDPK, putative	protein.postranslational modification
259947_at	0.646	2.10E-39	4.50E-35	AT1G71530	protein kinase contains Serine/Threonine prot. kinases active-site signature	protein.postranslational modification
258367_at	0.658	2.60E-41	5.80E-37	AT3G14370	protein kinase family protein contains protein kinase domain	protein.postranslational modification
251423_at	0.787	0.00E+00	0.00E+00	AT3G60550	cyclin family protein	protein.postranslational modification
250905_at	0.604	1.90E-33	4.10E-29	AT5G03640	protein kinase contains serine/threonine protein kinase domain	protein.postranslational modification
247531_at	0.612	1.70E-34	3.60E-30	AT5G61550	protein kinase family protein	protein.postranslational modification kinase receptor
249588_at	0.614	9.00E-35	2.00E-30	AT5G37790	protein kinase family protein contains protein kinase domain	protein.postranslational modification kinase receptor
265003_at	0.645	2.60E-39	5.70E-35	AT1G26970	protein kinase, putative similar to protein kinase	protein.postranslational modification kinase receptor
265031_at	0.857	0.00E+00	0.00E+00	AT1G61590	protein kinase, putative contains protein kinase domain	protein.postranslational modification kinase receptor
252224_at	0.759	0.00E+00	0.00E+00	AT3G49860	ADP-ribosylation factor, putative	protein.targeting.secretory pathway.unspecified
262905_at	0.636	5.70E-38	1.20E-33	AT1G59730	thioredoxin, putative	redox.thioredoxin
254738_at	0.716	0.00E+00	0.00E+00	AT4G13860	glycine-rich RNA-binding protein	RNA
262657_at	0.605	1.40E-33	3.00E-29	AT1G14210	ribonuclease T2 family protein	RNA.processing.ribonucleases
257386_at	0.695	0.00E+00	1.70E-43	AT2G42440	LOB domain protein 17 / lateral organ boundaries domain protein 17	RNA.regulation of transcription.AS2,Lateral Organ Boundaries
256944_at	0.656	4.60E-41	1.00E-36	AT3G18990	transcriptional factor B3 family protein	RNA.regulation of transcription.B3 transcription factor family
261647_at	0.640	1.90E-38	4.20E-34	AT1G27740	basic helix-loop-helix (bHLH) family protein	RNA.regulation of transcription.bHLH family
248559_at	0.672	1.40E-43	3.10E-39	AT5G50010	expressed protein	RNA.regulation of transcription.bHLH family
247895_at	0.633	2.20E-37	4.80E-33	AT5G58010	basic helix-loop-helix family protein bHLH transcription factor GBOF-1	RNA.regulation of transcription.bHLH family
247199_at	0.672	1.30E-43	2.90E-39	AT5G65210	bZIP family transcription factor (TGA1)	RNA.regulation of transcription.bZIP transcription factor family
259028_at	0.719	0.00E+00	0.00E+00	AT3G09290	zinc finger (C2H2 type) family protein	RNA.regulation of transcription.C2H2 zinc finger family
259365_at	0.760	0.00E+00	0.00E+00	AT1G13300	myb family transcription factor	RNA.regulation of transcription.G2-like transcription factor
257645_at	0.729	0.00E+00	0.00E+00	AT3G25790	myb family transcription factor	RNA.regulation of transcription.G2-like transcription factor
250697_at	0.693	0.00E+00	4.80E-43	AT5G06800	myb family transcription factor	RNA.regulation of transcription.G2-like transcription factor
259274_at	0.791	0.00E+00	0.00E+00	AT3G01220	homeobox-leucine zipper protein / HD-ZIP transcription factor, putative	RNA.regulation of transcription.Homeobox transcription factor
261504_at	0.667	7.60E-43	1.70E-38	AT1G71692	MADS-box protein (AGL12)	RNA.regulation of transcription.MADS box transcription factor
263892_at	0.712	0.00E+00	0.00E+00	AT2G36890	myb family transcription factor (MYB38)	RNA.regulation of transcription.MYB domain
255538_at	0.603	3.30E-33	7.20E-29	AT4G01680	myb family transcription factor (MYB55)	RNA.regulation of transcription.MYB domain
250173_at	0.801	0.00E+00	0.00E+00	AT5G14340	myb family transcription factor (MYB40)	RNA.regulation of transcription.MYB domain
246844_at	0.719	0.00E+00	0.00E+00	AT5G26660	myb family transcription factor (MYB4) (MYB86)	RNA.regulation of transcription.MYB domain
248343_at	0.653	1.60E-40	3.50E-36	AT5G52260	myb family transcription factor (MYB19)	RNA.regulation of transcription.MYB domain
247868_at	0.647	1.70E-39	3.60E-35	AT5G57620	myb family transcription factor (MYB36)	RNA.regulation of transcription.MYB domain
250741_at	0.716	0.00E+00	0.00E+00	AT5G05790	myb family transcription factor	RNA.regulation of transcription.MYB-related
247768_at	0.641	1.10E-38	2.40E-34	AT5G58900	myb family transcription factor	RNA.regulation of transcription.MYB-related
261945_at	0.616	5.20E-35	1.10E-30	AT1G64530	RWP-RK domain-containing protein similar to nodule inception protein	RNA.regulation of transcription.NIN-like bZIP-related family
267216_at	0.668	6.00E-43	1.30E-38	AT2G02620	DC1 domain-containing protein / PHD finger protein-related	RNA.regulation of transcription.unclassified
252341_at	0.641	1.00E-38	2.20E-34	AT3G48940	remorin family protein	RNA.regulation of transcription.unclassified
251710_at	0.662	5.90E-42	1.30E-37	AT3G56930	zinc finger (DHHC type) family protein	RNA.regulation of transcription.unclassified
260882_at	0.672	1.10E-43	2.40E-39	AT1G29280	WRKY family transcription factor similar to DNA binding protein WRKY3	RNA.regulation of transcription.WRKY transcription factor

267427_at	0.649	7.50E-40	1.60E-35	AT2G34830	WRKY family transcription factor	RNA.regulation of transcription.WRKY transcription factor
251553_at	0.806	0.00E+00	0.00E+00	AT3G58710	WRKY family transcription factor	RNA.regulation of transcription.WRKY transcription factor
251857_at	0.710	0.00E+00	0.00E+00	AT3G54770	RNA recognition motif (RRM)-containing protein	RNA.RNA binding
266828_at	0.740	0.00E+00	0.00E+00	AT2G22930	glycosyltransferase family protein	secondary metabolism.flavonoids.dihydroflavonols
266670_at	0.658	2.80E-41	6.20E-37	AT2G29740	UDP-glucoronosyl/UDP-glucosyl transferase family protein	secondary metabolism.flavonoids.dihydroflavonols
266669_at	0.797	0.00E+00	0.00E+00	AT2G29750	UDP-glucoronosyl/UDP-glucosyl transferase family protein	secondary metabolism.flavonoids.dihydroflavonols
262416_at	0.661	7.60E-42	1.70E-37	AT1G49390	oxidoreductase, 2OG-Fe(II) oxygenase family protein	secondary metabolism.flavonoids.flavonols
253334_at	0.615	7.90E-35	1.70E-30	AT4G33360	terpene cyclase/mutase-related	secondary metabolism.flavonoids.flavonols
254726_at	0.656	5.20E-41	1.10E-36	AT4G13660	pinoresinol-lariciresinol reductase, putative	secondary metabolism.flavonoids.isoflavonoids
248718_at	0.640	1.50E-38	3.30E-34	AT5G47770	farnesyl pyrophosphate synthetase 1, mitochondrial (FPS1)	secondary metabolism.isoprenoids.mevalonate pathway
258619_at	0.773	0.00E+00	0.00E+00	AT3G02780	isopentenyl-diphosphate delta-isomerase II	secondary metabolism.isoprenoids.mevalonate pathway
246778_at	0.698	0.00E+00	4.50E-44	AT5G27450	mevalonate kinase (MK)	secondary metabolism.isoprenoids.mevalonate pathway
245258_at	0.648	1.10E-39	2.40E-35	AT4C15340	pentacyclic triterpene synthase (04C11)	secondary metabolism.isoprenoids.terpenoids
254510_at	0.673	9.10E-44	2.00E-39	AT4G20210	terpene synthase/cyclase family protein	secondary metabolism.isoprenoids.terpenoids
262744_at	0.687	0.00E+00	5.50E-42	AT1G28680	transferase family protein similar to elicitor inducible gene product EIG-I24	secondary metabolism.phenylpropanoids
252202_at	0.783	0.00E+00	0.00E+00	AT3G50300	transferase family protein	secondary metabolism.phenylpropanoids
253483_at	0.678	1.30E-44	2.80E-40	AT4G31910	transferase family protein	secondary metabolism.phenylpropanoids
248723_at	0.700	0.00E+00	2.80E-44	AT5G47950	transferase family protein similar to deacetylvindoline 4-O-acetyltransferase	secondary metabolism.phenylpropanoids
248725_at	0.728	0.00E+00	0.00E+00	AT5G47980	transferase family protein similar to alcohol acyltransferase	secondary metabolism.phenylpropanoids
247837_at	0.661	8.80E-42	1.90E-37	AT5G57840	transferase family protein	secondary metabolism.phenylpropanoids
247059_at	0.780	0.00E+00	0.00E+00	AT5G26310	UDP-glucoronosyl/UDP-glucosyl transferase family protein	secondary metabolism.phenylpropanoids.lignin biosynthesis
253985_at	0.801	0.00E+00	0.00E+00	AT4G26220	caffeoyl-CoA 3-O-methyltransferase, putative	secondary metabolism.phenylpropanoids.lignin biosynthesis
256128_at	0.672	1.10E-43	2.40E-39	AT1G18140	laccase family protein / diphenol oxidase family protein	secondary metabolism.simple phenols
267307_at	0.782	0.00E+00	0.00E+00	AT2G30210	laccase, putative / diphenol oxidase, putative	secondary metabolism.simple phenols
262743_at	0.655	7.90E-41	1.70E-36	AT1G29020	calcium-binding EF hand family protein	signalling.calcium
265688_at	0.698	0.00E+00	4.90E-44	AT2G24300	calmodulin-binding protein similar to calmodulin-binding protein TCB60	signalling.calcium
254774_at	0.709	0.00E+00	0.00E+00	AT4G13440	calcium-binding EF hand family protein low similarity to Polcalcin	signalling.calcium
245257_at	0.651	3.40E-40	7.50E-36	AT4G14640	calmodulin-8 (CAM8)	signalling.calcium
261042_at	0.721	0.00E+00	0.00E+00	AT1G01200	Ras-related GTP-binding protein, putative	signalling.G-proteins
263876_at	0.624	3.70E-36	8.20E-32	AT2G21880	Ras-related GTP-binding protein, putative	signalling.G-proteins
265666_at	0.624	3.20E-36	7.10E-32	AT2G27440	rac GTPase activating protein, putative	signalling.G-proteins
251918_at	0.633	1.70E-37	3.60E-33	AT3G54040	photoassimilate-responsive protein-related	signalling.in sugar and nutrient physiology
248535_at	0.601	5.30E-33	1.20E-28	AT5G50120	transducin family protein / WD-40 repeat family protein	signalling.in sugar and nutrient physiology
262131_at	0.685	1.40E-45	1.70E-41	AT1G02900	rapid alkalinization factor (RALF) family protein	signalling.misc
252964_at	0.666	1.20E-42	2.50E-38	AT4G38830	protein kinase family protein	signalling.receptor kinases.DUF 26
256811_at	0.753	0.00E+00	0.00E+00	AT3G21340	leucine-rich repeat protein kinase, putative	signalling.receptor kinases.leucine rich repeat I
250102_at	0.624	3.50E-36	7.60E-32	AT5G16590	leucine-rich repeat transmembrane protein kinase, putative	signalling.receptor kinases.leucine rich repeat III
249768_at	0.751	0.00E+00	0.00E+00	AT5G24100	leucine-rich repeat transmembrane protein kinase, putative	signalling.receptor kinases.leucine rich repeat III
258357_at	0.604	2.40E-33	5.20E-29	AT3G14350	leucine-rich repeat transmembrane protein kinase, putative	signalling.receptor kinases.leucine rich repeat V
250640_at	0.636	7.00E-38	1.50E-33	AT5G07150	leucine-rich repeat family protein	signalling.receptor kinases.leucine rich repeat VI
264804_at	0.758	0.00E+00	0.00E+00	AT1G08590	CLAVATA1 receptor kinase (CLV1)	signalling.receptor kinases.leucine rich repeat XI
254506_at	0.854	0.00E+00	0.00E+00	AT4G20140	leucine-rich repeat transmembrane protein kinase, putative Cf-2.2	signalling.receptor kinases.leucine rich repeat XI
253786_at	0.755	0.00E+00	0.00E+00	AT4G28650	leucine-rich repeat transmembrane protein kinase, putative	signalling.receptor kinases.leucine rich repeat XI
252510_at	0.627	1.30E-36	2.90E-32	AT3G46270	receptor protein kinase-related	signalling.receptor kinases.misc

260366_at	0.604	1.90E-33	4.10E-29	AT1G70460	protein kinase, putative	signalling.receptor kinases.proline extensin like
253910_at	0.630	4.50E-37	9.90E-33	AT4G27290	S-locus protein kinase, putative	signalling.receptor kinases.S-locus glycoprotein like
248324_at	0.793	0.00E+00	0.00E+00	AT5G52790	CBS domain-containing protein-related	Signaling
253227_at	0.730	0.00E+00	0.00E+00	AT4G35030	protein kinase family protein	Signaling
264577_at	0.871	0.00E+00	0.00E+00	AT1G05260	peroxidase 3 (PER3) (P3) / rare cold-inducible protein (RCI3A) (PRC)	stress.abiotic.cold
245510_at	0.665	1.60E-42	3.40E-38	AT4G15740	C2 domain-containing protein similar to cold-regulated gene SRC2	stress.abiotic.cold
262838_at	0.764	0.00E+00	0.00E+00	AT1G14960	major latex protein-related / MLP-related low similarity to major latex protein	stress.abiotic.unspecified
265155_at	0.641	1.00E-38	2.20E-34	AT1G30990	major latex protein-related / MLP-related low similarity to major latex protein	stress.abiotic.unspecified
264029_at	0.623	5.40E-36	1.20E-31	AT2G03720	universal stress protein (USP) family protein	stress.abiotic.unspecified
245172_at	0.729	0.00E+00	0.00E+00	AT2G47540	pollen Ole e 1 allergen and extensin family protein	stress.abiotic.unspecified
258080_at	0.728	0.00E+00	0.00E+00	AT3G25930	universal stress protein (USP) family protein	stress.abiotic.unspecified
254025_at	0.665	1.80E-42	3.90E-38	AT4G25790	allergen V5/Tpx-1-related family protein	stress.abiotic.unspecified
253613_at	0.614	9.50E-35	2.10E-30	AT4G30320	allergen V5/Tpx-1-related family protein	stress.abiotic.unspecified
249477_s_at	*0.758*	*0.00E+00*	*0.00E+00*	*AT5G38930* germin-like protein, putative similar to germin-like portein GLP9 *AT5G38940* germin-like protein, putative similar to germin-like portein GLP9	*stress.abiotic.unspecified*
262318_at	0.746	0.00E+00	0.00E+00	AT1G27620	transferase protein, similar to hypersensitivity-related gene product HSR201	stress.biotic
262138_at	0.700	0.00E+00	2.50E-44	AT1G52660	similar to NBS/LRR disease resistance protein	stress.biotic
266851_at	0.687	0.00E+00	4.90E-42	AT2G26820	avirulence-responsive family protein / avirulence induced gene family	stress.biotic
263437_at	0.751	0.00E+00	0.00E+00	AT2G28670	disease resistance-responsive family protein / fibroin-related	stress.biotic
266978_at	0.823	0.00E+00	0.00E+00	AT2G39430	disease resistance-responsive protein-related / dirigent protein-related	stress.biotic
260549_at	0.663	4.60E-42	1.00E-37	AT2G43535	trypsin inhibitor, putative	stress.biotic
267191_at	0.651	3.60E-40	8.00E-36	AT2G44110	seven transmembrane MLO family protein / MLO-like protein 15 (MLO15)	stress.biotic
256781_at	0.679	8.40E-45	1.70E-40	AT3G13650	disease resistance response protein-related/ dirigent protein-related	stress.biotic
254907_at	0.613	1.40E-34	3.10E-30	AT4G11190	disease resistance-responsive family protein / dirigent family protein	stress.biotic
254909_at	0.739	0.00E+00	0.00E+00	AT4G11210	disease resistance-responsive family protein / dirigent family protein	stress.biotic
254313_at	0.719	0.00E+00	0.00E+00	AT4G22460	protease inhibitor/seed storage/lipid transfer protein (LTP) family protein	stress.biotic
254264_at	0.679	8.40E-45	1.90E-40	AT4G23510	disease resistance protein (TIR class)	stress.biotic
254226_at	0.700	0.00E+00	2.00E-44	AT4G23690	disease resistance-responsive family protein / dirigent family protein	stress.biotic
254206_at	0.685	0.00E+00	1.30E-41	AT4G24180	pathogenesis-related thaumatin family protein	stress.biotic
253527_at	0.846	0.00E+00	0.00E+00	AT4G31470	pathogenesis-related protein, putative	stress.biotic
250771_at	0.655	7.80E-41	1.70E-36	AT5G05400	disease resistance protein (CC-NBS-LRR class), putative	stress.biotic
249195_s_at	0.814	0.00E+00	0.00E+00	AT5G42500	disease resistance-responsive family protein	stress.biotic
249110_at	0.616	5.70E-35	1.30E-30	AT5G43730	disease resistance protein (CC-NBS-LRR class)	stress.biotic
248416_at	0.619	1.90E-35	4.10E-31	AT5G51630	disease resistance protein (TIR-NBS-LRR class)	stress.biotic
264647_at	0.796	0.00E+00	0.00E+00	AT1G09090	respiratory burst oxidase protein B (RbohB) / NADPH oxidase	stress.biotic.respiratory burst
254912_at	0.698	0.00E+00	6.20E-44	AT4G11230	respiratory burst oxidase, putative / NADPH oxidase	stress.biotic.respiratory burst
254092_at	0.669	3.90E-43	8.60E-39	AT4G25090	respiratory burst oxidase, putative / NADPH oxidase	stress.biotic.respiratory burst
250629_at	0.635	9.00E-38	2.00E-33	AT5G07390	respiratory burst oxidase protein A (RbohA) / NADPH oxidase	stress.biotic.respiratory burst
262575_at	0.760	0.00E+00	0.00E+00	AT1G15210	ABC transporter family protein	transport.ABC transporters and multidrug resistance systems
246580_at	0.746	0.00E+00	0.00E+00	AT1G31770	ABC transporter family protein	transport.ABC transporters and multidrug resistance systems
256141_at	0.672	1.20E-43	2.70E-39	AT1G48640	lysine and histidine specific transporter	transport.amino acids
263795_at	0.678	1.10E-44	2.30E-40	AT2G24610	cyclic nucleotide-regulated ion channel, putative (CNGC14)	transport.cyclic nucleotide or calcium regulated channels
265444_s_at	0.632	2.20E-37	4.90E-33	AT2G37180	**PIP2;2/PIP2;3**	transport.Major Intrinsic Proteins.PIP
266649_at	0.713	0.00E+00	0.00E+00	AT2G25810	**TIP4;1**	transport.Major Intrinsic Proteins.TIP

245399_at	0.652	2.70E-40	6.00E-36	AT4G17340	**TIP2;2**	transport.Major Intrinsic Proteins.TIP
248790_at	0.859	0.00E+00	0.00E+00	AT5G47450	**TIP2;3**	transport.Major Intrinsic Proteins.TIP
266336_at	0.814	0.00E+00	0.00E+00	AT2G32270	zinc transporter (ZIP3)	transport.metal
250952_at	0.659	1.70E-41	3.80E-37	AT5G03570	iron-responsive transporter-related	transport.metal
262813_at	0.631	3.70E-37	8.10E-33	AT1G11670	MATE efflux family protein similar to ripening regulated protein DDTFR18	transport.misc
261514_at	0.737	0.00E+00	0.00E+00	AT1G71870	MATE efflux family protein	transport.misc
264497_at	0.682	1.40E-45	4.20E-41	AT1G30840	purine permease-related low similarity to purine permease	transport.nucleotides
261924_at	0.615	6.30E-35	1.40E-30	AT1G22550	proton-dependent oligopeptide transport (POT) family protein	transport.peptides and oligopeptides
252589_s_at	0.709	0.00E+00	0.00E+00	AT3G45650	proton-dependent oligopeptide transport (POT) family protein	transport.peptides and oligopeptides
252536_at	0.816	0.00E+00	0.00E+00	AT3G45700	proton-dependent oligopeptide transport (POT) family protein	transport.peptides and oligopeptides
252537_at	0.802	0.00E+00	0.00E+00	AT3G45710	proton-dependent oligopeptide transport (POT) family protein	transport.peptides and oligopeptides
258293_at	0.640	1.90E-38	4.10E-34	AT3G23430	phosphate transporter, putative (PHO1) identical to PHO1 protein	transport.phosphate
249152_s_at	*0.700*	*0.00E+00*	*2.50E-44*	*AT5G43350*	*inorganic phosphate transporter (PHT1) (PT1)*	*transport.phosphate*
				AT5G43370	*inorganic phosphate transporter (PHT2)*	

PIP2;5 (251858_at/ At3g54820)

ProbeSet	r-value	p-value	e-value	GeneID	Annotation	MAPMAN classification
258914_at	0.645	3.00E-39	6.50E-35	AT3G06360	arabinogalactan-protein (AGP27)	cell wall.cell wall proteins.AGPs
254754_at	0.630	5.10E-37	1.10E-32	AT4G13210	pectate lyase family protein	cell wall.degradation.pectate lyases and polygalacturonases
260333_at	0.842	0.00E+00	0.00E+00	AT1G70500	polygalacturonase, putative / pectinase, putative	cell wall.degradation.pectate lyases and polygalacturonases
265174_s_at	0.623	5.90E-36	1.30E-31	AT1G23460	polygalacturonase, putative / pectinase, putative	cell wall.degradation.pectate lyases and polygalacturonases
248732_at	0.654	1.10E-40	2.50E-36	AT5G48070	xyloglucan:xyloglucosyl transferase, putative	cell wall.modification
267012_at	0.616	5.90E-35	1.30E-30	AT2G39220	patatin family protein similar to patatin-like latex allergen	development.storage proteins
247196_at	0.761	0.00E+00	0.00E+00	AT5G65510	ovule development protein, putative similar to AINTEGUMENTA	development.unspecified
256190_at	0.662	6.90E-42	1.50E-37	AT1G30100	9-cis-epoxycarotenoid dioxygenase / neoxanthin cleavage enzyme, putative	hormone metabolism.abscisic acid.synthesis-degradation
267452_at	0.650	4.70E-40	1.00E-35	AT2G33860	auxin-responsive factor (ARF3) / ETTIN protein (ETT)	hormone metabolism.auxin.signal transduction
264790_at	0.820	0.00E+00	0.00E+00	AT2G17820	histidine kinase 1	hormone metabolism.cytokinin.signal transduction
245108_at	0.640	1.90E-38	4.20E-34	AT2G41510	FAD-binding domain-containing protein / cytokinin oxidase family protein	hormone metabolism.cytokinin.synthesis-degradation
245713_at	0.628	1.10E-36	2.30E-32	AT5G04370	S-adenosyl-L-methionine:carboxyl methyltransferase family protein	hormone metabolism.salicylic acid.synthesis-degradation
252640_at	0.739	0.00E+00	0.00E+00	AT3G44560	acyl CoA reductase, putative	lipid metabolism.lipid degradation.beta-oxidation.
261311_at	0.739	0.00E+00	0.00E+00	AT1G05770	jacalin lectin family protein	misc.myrosinases-lectin-jacalin
246228_at	0.641	1.30E-38	2.80E-34	AT4G36430	peroxidase, putative	misc.peroxidases
267597_at	0.783	0.00E+00	0.00E+00	AT2G33020	leucine-rich repeat family protein	not assigned.no ontology
245784_at	0.731	0.00E+00	0.00E+00	AT1G32190	expressed protein	not assigned.unknown
247948_at	0.745	0.00E+00	0.00E+00	AT5G57130	expressed protein	not assigned.unknown
248154_at	0.854	0.00E+00	0.00E+00	AT5G54400	expressed protein	not assigned.unknown
249824_at	0.675	4.10E-44	8.90E-40	AT5G23380	expressed protein	not assigned.unknown
250756_at	0.607	7.50E-34	1.60E-29	AT5G05940	expressed protein	not assigned.unknown
251751_at	0.783	0.00E+00	0.00E+00	AT3G55720	expressed protein	not assigned.unknown
257815_at	0.620	1.30E-35	2.90E-31	AT3G25130	expressed protein	not assigned.unknown
262922_at	0.744	0.00E+00	0.00E+00	AT1G79420	expressed protein	not assigned.unknown
254490_at	0.669	3.90E-43	8.60E-39	AT4G20320	CTP synthase, putative / UTP--ammonia ligase, putative	nucleotide metabolism.synthesis.pyrimidine.CTP synthetase
253935_at	0.686	0.00E+00	1.10E-41	AT4G26870	aspartyl-tRNA synthetase, putative / aspartate--tRNA ligase, putative	protein.aa activation
256991_at	0.617	3.80E-35	8.30E-31	AT3G28600	AAA-type ATPase family protein	protein.degradation.AAA type

266565_at	0.900	0.00E+00	0.00E+00	AT2G24010	serine carboxypeptidase S10 family protein	protein.degradation.serine protease
252751_at	0.677	1.30E-44	3.00E-40	AT3G43430	zinc finger (C3HC4-type RING finger) family protein	protein.degradation.ubiquitin.E3.RING
245623_s_at	0.609	4.50E-34	9.80E-30	AT4G14103	F-box family protein contains F-box domain	protein.degradation.ubiquitin.E3.SCF.FBOX
257467_at	0.643	6.30E-39	1.40E-34	AT1G31320	LOB domain protein 4 / lateral organ boundaries domain protein 4 (LBD4)	RNA.regulation of transcription.AS2,Lateral Organ Boundaries
247625_at	0.629	6.70E-37	1.50E-32	AT5G60200	Dof-type zinc finger domain-containing protein	RNA.regulation of transcription.C2C2(Zn) DOF zinc finger
261800_at	0.622	8.00E-36	1.80E-31	AT1G30490	homeobox-leucine zipper transcription factor (HB-9)	RNA.regulation of transcription.Homeobox transcription factor
263013_at	0.623	5.60E-36	1.20E-31	AT1G23380	homeobox transcription factor (KNAT6)	RNA.regulation of transcription.Homeobox transcription factor
246834_at	0.847	0.00E+00	0.00E+00	AT5G26630	MADS-box protein (AGL35)	RNA.regulation of transcription.MADS box transcription factor
249858_at	0.603	2.60E-33	5.80E-29	AT5G23000	myb family transcription factor (MYB37)	RNA.regulation of transcription.MYB domain
266469_at	0.840	0.00E+00	0.00E+00	AT2G31180	myb family transcription factor (MYB14)	RNA.regulation of transcription.MYB domain
250908_at	0.753	0.00E+00	0.00E+00	AT5G03680	trihelix DNA-binding protein, putative	RNA.regulation of transcription.Triple-Helix transcription factor
253617_at	0.707	0.00E+00	1.40E-45	AT4G30410	expressed protein similar to cDNA bHLH transcription factor	RNA.regulation of transcription.unclassified
266507_at	0.665	1.90E-42	4.20E-38	AT2G47860	phototropic-responsive NPH3 family protein contains NPH3 family domain	signalling.light
254898_at	0.870	0.00E+00	0.00E+00	AT4G11480	protein kinase family protein	signalling.receptor kinases.DUF 26
256899_at	0.672	1.20E-43	2.60E-39	AT3G24660	leucine-rich repeat transmembrane protein kinase, putative	signalling.receptor kinases.leucine rich repeat III
248237_at	0.666	1.00E-42	2.30E-38	AT5G53890	leucine-rich repeat transmembrane protein kinase, putative	signalling.receptor kinases.leucine rich repeat X
255879_at	0.786	0.00E+00	0.00E+00	AT1G67000	protein kinase family protein contains protein kinase domain	signalling.receptor kinases.wheat LRK10 like
249495_at	0.725	0.00E+00	0.00E+00	AT5G39100	germin-like protein (GLP6)	stress.abiotic.unspecified
265588_at	0.817	0.00E+00	0.00E+00	AT2G19970	pathogenesis-related protein, putative	stress.biotic
255726_at	0.681	2.80E-45	6.90E-41	AT1G25530	lysine and histidine specific transporter, putative	transport.amino acids
262912_at	0.783	0.00E+00	0.00E+00	AT1G59740	proton-dependent oligopeptide transport (POT) family protein	transport.peptides and oligopeptides

PIP2;6 (266172_at/ At2g39010)

ProbeSet	r-value	p-value	e-value	GeneID	Annotation	MAPMAN classification
264394_at	0.658	2.30E-41	5.10E-37	AT1G11860	aminomethyltransferase, putative	amino acid metabolism.degradation
258281_at	0.667	9.80E-43	2.20E-38	AT3G26900	shikimate kinase family protein	amino acid metabolism.synthesis
260566_at	0.661	8.70E-42	1.90E-37	AT2G43750	cysteine synthase, chloroplast / O-acetylserine (thiol)-lyase	amino acid metabolism.synthesis
247931_at	0.604	2.40E-33	5.20E-29	AT5G57040	lactoylglutathione lyase family protein / glyoxalase I family protein	Biodegradation of Xenobiotics
264970_at	0.604	2.30E-33	5.00E-29	AT1G67280	lactoylglutathione lyase, putative / glyoxalase I, putative	Biodegradation of Xenobiotics
252971_at	0.699	0.00E+00	3.10E-44	AT4G38770	proline-rich family protein (PRP4)	cell wall.cell wall proteins.proline rich proteins
258003_at	0.632	3.00E-37	6.60E-33	AT3G29030	expansin, putative (EXP5)	cell wall.modification
253372_at	0.632	2.60E-37	5.70E-33	AT4G33220	pectinesterase family protein	cell wall.pectin*esterases.misc
252255_at	0.610	2.90E-34	6.40E-30	AT3G49220	pectinesterase family protein	cell wall.pectin*esterases.PME
246644_at	0.692	0.00E+00	8.20E-43	AT5G35100	peptidyl-prolyl cis-trans isomerase cyclophilin-type family protein	cell.cycle
251305_at	0.628	1.10E-36	2.40E-32	AT3G62030	peptidyl-prolyl cis-trans isomerase/ cyclophilin/ cyclosporin A-binding protein	cell.cycle
245744_at	0.610	3.20E-34	7.10E-30	AT1G51110	plastid-lipid associated protein PAP / fibrillin family protein	cell.organisation
246154_at	0.711	0.00E+00	0.00E+00	AT5G19940	plastid-lipid associated protein PAP-related / fibrillin-related	cell.organisation
253139_at	0.709	0.00E+00	0.00E+00	AT4G35450	ankyrin repeat family protein / AFT protein (AFT) contains ankyrin repeats	cell.organisation
253956_at	0.617	4.30E-35	9.40E-31	AT4G26700	fimbrin-like protein (FIM1)	cell.organisation
258295_at	0.622	7.10E-36	1.50E-31	AT3G23400	plastid-lipid associated protein PAP / fibrillin family protein	cell.organisation
266767_at	0.615	7.60E-35	1.70E-30	AT2G46910	plastid-lipid associated protein PAP / fibrillin family protein	cell.organisation
252132_at	0.601	6.00E-33	1.30E-28	AT3G50790	late embryogenesis abundant protein / LEA protein, putative	development.late embryogenesis abundant

Probe	r	p1	p2	AGI	Description	Functional category
245281_at	0.617	3.40E-35	7.40E-31	AT4G15560	1-deoxy-D-xylulose 5-phosphate synthase/ DXP-synthase, putative	development.unspecified
252409_at	0.632	2.70E-37	6.00E-33	AT3G47650	bundle-sheath defective protein 2 family	development.unspecified
245123_at	0.671	1.70E-43	3.80E-39	AT2G47450	chloroplast signal recognition particle component (CAO)	DNA.synthesis/chromatin structure
250498_at	0.715	0.00E+00	0.00E+00	AT5G09660	malate dehydrogenase, glyoxysomal	gluconeogenesis.Malate DH
257699_at	0.724	0.00E+00	0.00E+00	AT3G12780	phosphoglycerate kinase, putative	glycolysis.phosphoglycerate kinase
247025_at	0.625	2.90E-36	6.20E-32	AT5G67030	zeaxanthin epoxidase (ZEP)	hormone metabolism.abscisic acid
252425_at	0.623	4.50E-36	9.80E-32	AT3G47620	TCP family transcription factor, putative auxin-induced bHLH TF	hormone metabolism.auxin
252965_at	0.601	4.70E-33	1.00E-28	AT4G38860	auxin-responsive protein, putative auxin-induced protein 10A	hormone metabolism.auxin
258250_at	0.616	4.40E-35	9.70E-31	AT3G15850	fatty acid desaturase family protein similar to delta 9 acyl-lipid desaturase	lipid metabolism.FA desaturation.desaturase
253547_at	0.624	3.50E-36	7.60E-32	AT4G30950	omega-6 fatty acid desaturase, chloroplast (FAD6) (FADC)	lipid metabolism.FA desaturation.omega 6 desaturase
262176_at	0.681	2.80E-45	6.40E-41	AT1G74960	3-ketoacyl-ACP synthase, putative	lipid metabolism.FA synthesis and FA elongation
266421_at	0.645	2.80E-39	6.10E-35	AT2G38540	nonspecific lipid transfer protein 1 (LTP1)	lipid metabolism.lipid transfer proteins etc
248687_at	0.603	2.90E-33	6.40E-29	AT5G48300	glucose-1-phosphate adenylyltransferase small subunit 1 (APS1)	major CHO metabolism.synthesis.starch.AGPase
249927_at	0.726	0.00E+00	0.00E+00	AT5G19220	glucose-1-phosphate adenylyltransferase large subunit 1 (APL1)	major CHO metabolism.synthesis.starch.AGPase
266207_at	0.677	1.40E-44	3.20E-40	AT2G27680	aldo/keto reductase family protein	minor CHO metabolism.others
254021_at	0.601	5.70E-33	1.20E-28	AT4G25650	Rieske [2Fe-2S] domain-containing protein	misc. other Ferredoxins and Rieske domain
256468_at	0.607	8.70E-34	1.90E-29	AT1G32550	ferredoxin family protein	misc. other Ferredoxins and Rieske domain
259896_at	0.719	0.00E+00	0.00E+00	AT1G71500	Rieske [2Fe-2S] domain-containing protein	misc. other Ferredoxins and Rieske domain
245532_at	0.616	5.40E-35	1.20E-30	AT4G15110	cytochrome P450 97B3, putative (CYP97B3)	misc.cytochrome P450
253886_at	0.609	4.30E-34	9.50E-30	AT4G27710	cytochrome P450 family protein	misc.cytochrome P450
259786_at	0.728	0.00E+00	0.00E+00	AT1G29660	GDSL-motif lipase/hydrolase family protein	misc.GDSL-motif lipase
251996_at	0.678	1.30E-44	2.60E-40	AT3G52840	beta-galactosidase, putative / lactase, putative	misc.gluco-, galacto- and mannosidases
264435_at	0.656	5.70E-41	1.20E-36	AT1G10360	glutathione S-transferase, putative	misc.glutathione S transferases
260106_at	0.672	1.20E-43	2.60E-39	AT1G35420	dienelactone hydrolase family protein	misc.misc2
266293_at	0.701	0.00E+00	1.50E-44	AT2G29360	tropinone reductase, putative / tropine dehydrogenase, putative	misc.nitrilases, *nitrile lyases, berberine bridge enzymes, etc…
253875_at	0.605	1.50E-33	3.30E-29	AT4G27520	plastocyanin-like domain-containing protein	misc.plastocyanin-like
265400_at	0.681	4.20E-45	8.60E-41	AT2G10940	protease inhibitor/seed storage/lipid transfer protein (LTP) family protein	misc.protease inhibitor/seed storage/lipid transfer prot.
253860_at	0.653	1.70E-40	3.70E-36	AT4G27700	rhodanese-like domain-containing protein contains rhodanese-like domain	misc.rhodanese
258989_at	0.646	1.90E-39	4.20E-35	AT3G08920	rhodanese-like domain-containing protein contains rhodanese-like domain	misc.rhodanese
267635_at	0.673	6.90E-44	1.50E-39	AT2G42220	rhodanese-like domain-containing protein contains rhodanese-like domain	misc.rhodanese
256033_at	0.640	1.70E-38	3.80E-34	AT1G07250	UDP-glucoronosyl/UDP-glucosyl transferase family protein	misc.UDP glucosyl and glucoronyl transferases
257205_at	0.662	4.80E-42	1.10E-37	AT3G16520	UDP-glucoronosyl/UDP-glucosyl transferase family protein	misc.UDP glucosyl and glucoronyl transferases
245716_at	0.603	2.60E-33	5.80E-29	AT5G08740	pyridine nucleotide-disulphide oxidoreductase family protein	mitochondrial electron transport / ATP synthesis
245701_at	0.667	7.20E-43	1.60E-38	AT5G04140	glutamate synthase (GLU1) / ferredoxin-dependent glutamate synthase	N-metabolism.ammonia metabolism.glutamate synthase
249710_at	0.640	1.90E-38	4.10E-34	AT5G35630	glutamine synthetase (GS2) identical to glutamine synthetase	N-metabolism.ammonia metabolism.glutamine synthase
246294_at	0.601	5.60E-33	1.20E-28	AT3G56910	expressed protein	not assigned.disagreeing hits
246880_s_at	0.627	1.60E-36	3.50E-32	AT5G25980	glycosyl hydrolase family 1 protein	not assigned.disagreeing hits
248151_at	0.639	2.00E-38	4.40E-34	AT5G54270 / AT5G54280	chlorophyll A-B binding protein / LHCII type III (LHCB3) / myosin heavy chain, putative similar to myosin	not assigned.disagreeing hits
255997_s_at	0.671	1.50E-43	3.30E-39	AT1G29910 / AT1G29920 / AT1G29930	chlorophyll A-B binding protein 2, chloroplast / LHCII type I / chlorophyll A-B binding protein 165/180, chloroplast / LHCII type I / chlorophyll A-B binding protein 2, chloroplast / LHCII type I	not assigned.disagreeing hits
259491_at	0.751	0.00E+00	0.00E+00	AT1G15810 / AT1G15820	ribosomal protein S15 family protein / chlorophyll A-B binding protein, chloroplast (LHCB6)	not assigned.disagreeing hits

262368_at	*0.646*	*2.00E-39*	*4.30E-35*	*AT1G73060 expressed protein*	*not assigned.disagreeing hits*
				AT1G73070 leucine-rich repeat family protein	
259914_at	0.627	1.50E-36	3.30E-32	AT1G72640 expressed protein	not assigned.disagreeing hits
265374_at	*0.614*	*8.80E-35*	*1.90E-30*	*AT2G06510 replication protein, putative similar to replication protein A*	*not assigned.disagreeing hits*
				AT2G06520 membrane protein, putative contains 2 transmembrane domains	
245201_at	0.631	4.20E-37	9.20E-33	AT1G67840 ATP-binding region, ATPase-like domain-containing protein	not assigned.no ontology
245924_at	0.610	3.50E-34	7.70E-30	AT5G28750 thylakoid assembly protein, putative	not assigned.no ontology
248128_at	0.603	3.10E-33	6.70E-29	AT5G54770 thiazole biosynthetic enzyme, chloroplast (ARA6) (THI1) (THI4)	not assigned.no ontology
248224_at	0.733	0.00E+00	0.00E+00	AT5G53490 thylakoid lumenal 17.4 kDa protein, chloroplast	not assigned.no ontology
248287_at	0.632	2.20E-37	4.90E-33	AT5G52970 thylakoid lumen 15.0 kDa protein	not assigned.no ontology
248560_at	0.600	7.10E-33	1.60E-28	AT5G49970 pyridoxamine 5'-phosphate oxidase-related	not assigned.no ontology
249524_at	0.644	4.00E-39	8.80E-35	AT5G38520 hydrolase, alpha/beta fold family protein	not assigned.no ontology
251353_at	0.664	2.80E-42	6.10E-38	AT3G61080 fructosamine kinase family protein	not assigned.no ontology
252366_at	0.609	3.90E-34	8.60E-30	AT3G48420 haloacid dehalogenase-like hydrolase family protein	not assigned.no ontology
252876_at	0.618	2.70E-35	6.00E-31	AT4G39970 haloacid dehalogenase-like hydrolase family protein	not assigned.no ontology
253197_at	0.666	1.10E-42	2.50E-38	AT4G35250 vestitone reductase-related	not assigned.no ontology
253251_at	0.603	3.30E-33	7.30E-29	AT4G34730 ribosome-binding factor A family protein	not assigned.no ontology
253823_at	0.681	4.20E-45	8.20E-41	AT4G28030 GCN5-related N-acetyltransferase (GNAT) family protein	not assigned.no ontology
254137_at	0.674	4.90E-44	1.10E-39	AT4G24930 thylakoid lumenal 17.9 kDa protein, chloroplast	not assigned.no ontology
254388_at	0.647	1.30E-39	2.70E-35	AT4G21860 methionine sulfoxide reductase domain-containing protein	not assigned.no ontology
254737_at	0.641	1.30E-38	2.70E-34	AT4G13840 transferase family protein low	not assigned.no ontology
255440_at	0.678	9.80E-45	2.20E-40	AT4G02530 chloroplast thylakoid lumen protein	not assigned.no ontology
255692_at	0.655	8.80E-41	1.90E-36	AT4G00400 phospholipid/glycerol acyltransferase family protein	not assigned.no ontology
255719_at	0.602	3.90E-33	8.50E-29	AT1G32080 membrane protein, putative contains 12 transmembrane domains	not assigned.no ontology
256115_at	0.669	4.00E-43	8.80E-39	AT1G16880 uridylyltransferase-related similar to [Protein-PII] uridylyltransferase	not assigned.no ontology
259603_at	0.678	9.80E-45	2.20E-40	AT1G56500 haloacid dehalogenase-like hydrolase family protein	not assigned.no ontology
259633_at	0.627	1.50E-36	3.20E-32	AT1G56500 haloacid dehalogenase-like hydrolase family protein	not assigned.no ontology
260529_at	0.762	0.00E+00	0.00E+00	AT2G47400 CP12 domain-containing protein	not assigned.no ontology
260709_at	0.623	5.60E-36	1.20E-31	AT1G32500 ATP-binding-cassette transporter	not assigned.no ontology
261351_at	0.626	1.90E-36	4.20E-32	AT1G79790 haloacid dehalogenase-like hydrolase family protein	not assigned.no ontology
262151_at	0.614	9.90E-35	2.20E-30	AT1G52510 hydrolase, alpha/beta fold family protein	not assigned.no ontology
262202_at	0.695	0.00E+00	2.20E-43	AT2G01110 thylakoid membrane formation protein / cpTatC (APG2)	not assigned.no ontology
264158_at	0.761	0.00E+00	0.00E+00	AT1G65260 PspA/IM30 family protein	not assigned.no ontology
264185_at	0.735	0.00E+00	0.00E+00	AT1G54780 thylakoid lumen 18.3 kDa protein	not assigned.no ontology
266224_at	0.718	0.00E+00	0.00E+00	AT2G28800 chloroplast membrane protein (ALBINO3) Oxa1p homolog	not assigned.no ontology
266704_at	0.607	7.50E-34	1.60E-29	AT2G19940 semialdehyde dehydrogenase family protein	not assigned.no ontology
266813_at	0.664	2.70E-42	5.90E-38	AT2G44920 thylakoid lumenal 15 kDa protein, chloroplast	not assigned.no ontology
267005_at	0.610	3.20E-34	7.10E-30	AT2G34460 flavin reductase-related	not assigned.no ontology
255572_at	0.764	0.00E+00	0.00E+00	AT4G01050 hydroxyproline-rich glycoprotein family protein	not assigned.no ontology.hydroxyproline rich proteins
249247_at	0.631	4.30E-37	9.30E-33	AT5G42310 pentatricopeptide (PPR) repeat-containing protein	not assigned.no ontology.PPR repeat-containing protein
262104_at	0.645	2.80E-39	6.10E-35	AT1G02910 tetratricopeptide repeat (TPR)-containing protein	not assigned.no ontology.PPR repeat-containing protein
264199_at	0.644	3.50E-39	7.70E-35	AT1G22700 tetratricopeptide repeat (TPR)-containing protein	not assigned.no ontology.PPR repeat-containing protein
250668_at	0.677	1.40E-44	3.10E-40	AT5G07020 proline-rich family protein	not assigned.no ontology.proline rich family
257172_at	0.723	0.00E+00	0.00E+00	AT3G23700 S1 RNA-binding domain-containing protein	not assigned.no ontology

245019_at	0.677	1.40E-44	3.00E-40	AtCg00530	hypothetical protein	not assigned.unknown
245321_at	0.647	1.40E-39	3.20E-35	AT4G15545	expressed protein	not assigned.unknown
245388_at	0.610	3.00E-34	6.50E-30	AT4G16410	expressed protein	not assigned.unknown
245795_at	0.606	1.20E-33	2.60E-29	AT1G32160	expressed protein	not assigned.unknown
246449_at	0.636	6.90E-38	1.50E-33	AT5G16810	expressed protein	not assigned.unknown
246487_at	0.614	9.30E-35	2.00E-30	AT5G16030	expressed protein	not assigned.unknown
246792_at	0.672	1.40E-43	3.20E-39	AT5G27290	expressed protein	not assigned.unknown
247889_at	0.617	4.20E-35	9.20E-31	AT5G57930	expressed protein	not assigned.unknown
248449_at	0.661	8.10E-42	1.80E-37	AT5G51110	expressed protein	not assigned.unknown
248459_at	0.626	2.10E-36	4.60E-32	AT5G51020	expressed protein	not assigned.unknown
248624_at	0.708	0.00E+00	1.40E-45	AT5G48790	expressed protein	not assigned.unknown
248663_at	0.621	1.10E-35	2.50E-31	AT5G48590	expressed protein	not assigned.unknown
249120_at	0.654	1.10E-40	2.30E-36	AT5G43750	expressed protein	not assigned.unknown
249230_at	0.638	2.90E-38	6.40E-34	AT5G42070	expressed protein	not assigned.unknown
249519_at	0.610	3.70E-34	8.20E-30	AT5G38660	expressed protein	not assigned.unknown
249610_at	0.665	1.60E-42	3.60E-38	AT5G37360	expressed protein	not assigned.unknown
250366_at	0.662	5.30E-42	1.20E-37	AT5G11420	expressed protein	not assigned.unknown
250563_at	0.649	7.30E-40	1.60E-35	AT5G08050	expressed protein	not assigned.unknown
250728_at	0.673	8.50E-44	1.90E-39	AT5G06440	expressed protein	not assigned.unknown
250865_at	0.612	1.80E-34	4.00E-30	AT5G03900	expressed protein	not assigned.unknown
250867_at	0.633	1.80E-37	4.00E-33	AT5G03880	expressed protein	not assigned.unknown
251036_at	0.727	0.00E+00	0.00E+00	AT5G02160	expressed protein	not assigned.unknown
251243_at	0.671	2.00E-43	4.30E-39	AT3G61870	expressed protein	not assigned.unknown
251810_at	0.693	0.00E+00	4.40E-43	AT3G55250	expressed protein predicted pectate-lyase	not assigned.unknown
252116_at	0.697	0.00E+00	8.40E-44	AT3G51510	expressed protein	not assigned.unknown
252181_at	0.656	6.00E-41	1.30E-36	AT3G50685	expressed protein	not assigned.unknown
252441_at	0.705	0.00E+00	2.80E-45	AT3G46780	expressed protein	not assigned.unknown
252463_at	0.660	1.00E-41	2.20E-37	AT3G47070	expressed protein	not assigned.unknown
252922_at	0.605	1.70E-33	3.70E-29	AT4G39040	expressed protein	not assigned.unknown
253283_at	0.625	3.00E-36	6.50E-32	AT4G34090	expressed protein	not assigned.unknown
253530_at	0.667	7.60E-43	1.70E-38	AT4G31530	expressed protein	not assigned.unknown
253548_at	0.659	2.00E-41	4.30E-37	AT4G30993	expressed protein	not assigned.unknown
253686_at	0.618	2.40E-35	5.20E-31	AT4G29750	expressed protein	not assigned.unknown
253825_at	0.694	0.00E+00	3.20E-43	AT4G28025	expressed protein	not assigned.unknown
254117_at	0.601	6.10E-33	1.30E-28	AT4G24750	expressed protein	not assigned.unknown
254298_at	0.695	0.00E+00	2.40E-43	AT4G22890	expressed protein	not assigned.unknown
254460_at	0.623	5.20E-36	1.10E-31	AT4G21210	expressed protein	not assigned.unknown
254638_at	0.729	0.00E+00	0.00E+00	AT4G18740	expressed protein	not assigned.unknown
254755_at	0.630	5.10E-37	1.10E-32	AT4G13220	expressed protein	not assigned.unknown
255456_at	0.702	0.00E+00	1.10E-44	AT4G02920	expressed protein	not assigned.unknown
255764_at	0.631	3.60E-37	7.90E-33	AT1G16720	expressed protein	not assigned.unknown
255774_at	0.638	3.00E-38	6.60E-34	AT1G18620	expressed protein	not assigned.unknown
256076_at	0.696	0.00E+00	1.20E-43	AT1G18060	expressed protein	not assigned.unknown
256215_at	0.639	2.30E-38	5.00E-34	AT1G50900	expressed protein	not assigned.unknown

257717_at	0.614	1.00E-34	2.20E-30	AT3G18390	expressed protein	not assigned.unknown
258156_at	0.661	7.30E-42	1.60E-37	AT3G18050	expressed protein	not assigned.unknown
259658_at	0.604	2.30E-33	5.00E-29	AT1G55370	expressed protein	not assigned.unknown
259838_at	0.624	3.80E-36	8.20E-32	AT1G52220	expressed protein	not assigned.unknown
260127_at	0.617	4.10E-35	8.90E-31	AT1G36320	expressed protein	not assigned.unknown
261422_at	0.674	5.20E-44	1.10E-39	AT1G18730	expressed protein	not assigned.unknown
261788_at	0.653	1.80E-40	4.00E-36	AT1G15980	expressed protein	not assigned.unknown
261948_at	0.628	8.90E-37	1.90E-32	AT1G64680	expressed protein	not assigned.unknown
262168_at	0.694	0.00E+00	2.60E-43	AT1G74730	expressed protein	not assigned.unknown
262955_at	0.612	1.60E-34	3.60E-30	AT1G54520	expressed protein	not assigned.unknown
263048_s_at	0.656	5.30E-41	1.20E-36	AT2G05310	expressed protein	not assigned.unknown
263142_at	0.656	4.90E-41	1.10E-36	AT1G65230	expressed protein	not assigned.unknown
263298_at	0.615	7.90E-35	1.70E-30	AT2G15290	expressed protein	not assigned.unknown
263410_at	0.635	9.20E-38	2.00E-33	AT2G04039	expressed protein	not assigned.unknown
263676_at	0.719	0.00E+00	0.00E+00	AT1G09340	expressed protein	not assigned.unknown
263709_at	0.617	4.10E-35	9.10E-31	AT1G09310	expressed protein	not assigned.unknown
263880_at	0.675	3.50E-44	7.70E-40	AT2G21960	expressed protein	not assigned.unknown
264201_at	0.609	4.80E-34	1.00E-29	AT1G22630	expressed protein (DnaJ central domain (4 repeats))	not assigned.unknown
264728_at	0.682	1.40E-45	4.00E-41	AT1G22850	expressed protein	not assigned.unknown
265073_at	0.687	0.00E+00	5.10E-42	AT1G55480	expressed protein	not assigned.unknown
265415_at	0.710	0.00E+00	0.00E+00	AT2G20890	expressed protein	not assigned.unknown
265773_at	0.632	2.20E-37	4.90E-33	AT2G48070	expressed protein	not assigned.unknown
266329_at	0.614	1.00E-34	2.20E-30	AT2G01590	expressed protein	not assigned.unknown
266521_at	0.612	1.80E-34	3.90E-30	AT2G24020	expressed protein	not assigned.unknown
266551_at	0.665	2.10E-42	4.70E-38	AT2G35260	expressed protein	not assigned.unknown
266716_at	0.707	0.00E+00	1.40E-45	AT2G46820	expressed protein	not assigned.unknown
267172_at	0.638	3.50E-38	7.70E-34	AT2G37660	expressed protein	not assigned.unknown
267294_at	0.620	1.60E-35	3.50E-31	AT2G23670	expressed protein	not assigned.unknown
267344_at	0.625	2.60E-36	5.60E-32	AT2G44230	expressed protein	not assigned.unknown
267379_at	0.633	1.90E-37	4.20E-33	AT2G26340	expressed protein	not assigned.unknown
267630_at	0.613	1.50E-34	3.20E-30	AT2G42130	expressed protein contains weak hit to Pfam PF04755: PAP_fibrillin	not assigned.unknown
246651_at	0.656	5.50E-41	1.20E-36	AT5G35170	adenylate kinase family protein	nucleotide metabolism.phosphotransfer and pyrophosphatase
249694_at	0.631	3.80E-37	8.30E-33	AT5G35790	glucose-6-phosphate 1-dehydrogenase / G6PD (APG1)	OPP.oxidative PP.G6PD
246226_at	0.604	2.00E-33	4.50E-29	AT4G37200	thioredoxin family protein	protein assembly and cofactor ligation
248962_at	0.650	4.50E-40	9.80E-36	AT5G45680	FK506-binding protein 1 (FKBP13)	protein assembly and cofactor ligation
249875_at	0.760	0.00E+00	0.00E+00	AT5G23120	photosystem II stability/assembly factor, chloroplast (HCF136)	protein assembly and cofactor ligation
262954_at	0.662	5.90E-42	1.30E-37	AT1G54500	rubredoxin family protein	protein assembly and cofactor ligation
245198_at	0.735	0.00E+00	0.00E+00	AT1G67700	expressed protein	protein.degradation
252048_at	0.632	2.90E-37	6.30E-33	AT3G52500	aspartyl protease family protein	protein.degradation
259296_at	0.601	4.90E-33	1.10E-28	AT3G05350	aminopeptidase P, cytosolic, putative	protein.degradation
261118_at	0.613	1.40E-34	3.10E-30	AT1G75460	ATP-dependent protease La (LON) domain-containing protein	protein.degradation
261141_at	0.653	1.50E-40	3.30E-36	AT1G19740	ATP-dependent protease La (LON) domain-containing protein	protein.degradation
261483_at	0.612	2.00E-34	4.40E-30	AT1G14270	CAAX amino terminal protease family protein	protein.degradation
249244_at	0.650	4.50E-40	9.80E-36	AT5G42270	FtsH protease, putative	protein.degradation.metalloprotease

262473_at	0.608	5.40E-34	1.20E-29	AT1G50250	cell division protein ftsH homolog 1, chloroplast (FTSH1) (FTSH)	protein.degradation.metalloprotease
264584_at	0.623	5.00E-36	1.10E-31	AT1G05140	membrane-associated zinc metalloprotease, putative	protein.degradation.metalloprotease
267196_at	*0.713*	*0.00E+00*	*0.00E+00*	*AT2G30950 AT2G30960*	*FtsH protease (VAR2) identical to zinc dependent protease VAR2 expressed protein*	*protein.degradation.metalloprotease*
245263_at	0.606	1.20E-33	2.60E-29	AT4G17740	C-terminal processing protease, putative	protein.degradation.serine protease
248950_at	0.648	1.20E-39	2.60E-35	AT5G45390	ATP-dependent Clp protease proteolytic subunit (ClpP4)	protein.degradation.serine protease
257222_at	0.646	1.70E-39	3.80E-35	AT3G27925	DegP protease, putative	protein.degradation.serine protease
259521_at	0.654	1.20E-40	2.60E-36	AT1G12410	ATP-dependent Clp protease proteolytic subunit (ClpP2)	protein.degradation.serine protease
266509_at	0.640	1.80E-38	3.90E-34	AT2G47940	DegP2 protease (DEGP2) identical to DegP2 protease	protein.degradation.serine protease
267262_at	0.682	1.40E-45	3.90E-41	AT2G22990	sinapoylglucose:malate sinapoyltransferase (SNG1)	protein.degradation.serine protease
248177_at	0.700	0.00E+00	2.70E-44	AT5G54630	zinc finger protein-related	protein.degradation.ubiquitin.E3.RING
256446_at	0.602	3.80E-33	8.20E-29	AT3G11110	zinc finger (C3HC4-type RING finger) family protein	protein.degradation.ubiquitin.E3.RING
250262_at	0.655	8.90E-41	1.90E-36	AT5G13410	immunophilin / FKBP-type peptidyl-prolyl cis-trans isomerase family protein	protein.folding
256088_at	0.706	0.00E+00	1.40E-45	AT1G20810	immunophilin / FKBP-type peptidyl-prolyl cis-trans isomerase family protein	protein.folding
258929_at	0.698	0.00E+00	6.40E-44	AT3G10060	immunophilin / FKBP-type peptidyl-prolyl cis-trans isomerase, putative	protein.folding
259193_at	0.661	7.90E-42	1.70E-37	AT3G01480	peptidyl-prolyl cis-trans isomerase/ cyclophilin/ rotamase, putative	protein.folding
260044_at	0.630	5.40E-37	1.20E-32	AT1G73655	immunophilin / FKBP-type peptidyl-prolyl cis-trans isomerase family protein	protein.folding
260542_at	0.690	0.00E+00	1.70E-42	AT2G43560	immunophilin / FKBP-type peptidyl-prolyl cis-trans isomerase family protein	protein.folding
262970_at	0.758	0.00E+00	0.00E+00	AT1G75690	chaperone protein dnaJ-related	protein.folding
267430_at	0.689	0.00E+00	2.40E-42	AT2G34860	chaperone protein dnaJ-related	protein.folding
248034_at	0.614	9.00E-35	2.00E-30	AT5G55910	protein kinase, putative contains protein kinase domain	protein.postranslational modification
251068_at	0.614	9.50E-35	2.10E-30	AT5G01920	protein kinase family protein contains eukaryotic protein kinase domain	protein.postranslational modification
252543_at	0.657	3.90E-41	8.40E-37	AT3G45780	protein kinase / nonphototropic hypocotyl protein 1 (NPH1)	protein.postranslational modification
259080_at	0.638	3.30E-38	7.30E-34	AT3G04910	protein kinase family protein contains protein kinase domain	protein.postranslational modification
260036_at	0.607	8.80E-34	1.90E-29	AT1G68830	protein kinase family protein contains eukaryotic protein kinase domain	protein.postranslational modification
259437_at	0.632	3.10E-37	6.80E-33	AT1G01540	protein kinase family protein contains protein kinase domain	protein.postranslational modification.kinase
244968_at	0.647	1.20E-39	2.70E-35	AtCg00640	encodes a chloroplast ribosomal protein L33	protein.synthesis.chloroplast/mito - plastid ribosomal protein
244988_s_at	0.691	0.00E+00	9.90E-43	AtCg00840, AtCg01300	flag_XH2	protein.synthesis.chloroplast/mito - plastid ribosomal protein
246673_at	0.616	5.10E-35	1.10E-30	AT5G30510	30S ribosomal protein S1, putative	protein.synthesis.chloroplast/mito - plastid ribosomal protein
248174_at	0.679	8.40E-45	1.90E-40	AT5G54600	50S ribosomal protein L24, chloroplast	protein.synthesis.chloroplast/mito - plastid ribosomal protein
250190_at	0.697	0.00E+00	8.40E-44	AT5G14320	30S ribosomal protein S13, chloroplast (CS13)	protein.synthesis.chloroplast/mito - plastid ribosomal protein
251120_at	0.671	2.10E-43	4.50E-39	AT3G63490	ribosomal protein L1 family protein	protein.synthesis.chloroplast/mito - plastid ribosomal protein
251744_at	0.637	4.10E-38	9.00E-34	AT3G56010	expressed protein	protein.synthesis.chloroplast/mito - plastid ribosomal protein
256753_at	0.633	1.90E-37	4.20E-33	AT3G27160	ribosomal protein S21 family protein	protein.synthesis.chloroplast/mito - plastid ribosomal protein
260898_at	0.617	4.20E-35	9.30E-31	AT1G29070	ribosomal protein L34 family protein	protein.synthesis.chloroplast/mito - plastid ribosomal protein
261078_at	0.662	6.80E-42	1.50E-37	AT1G07320	50S ribosomal protein L4, chloroplast	protein.synthesis.chloroplast/mito - plastid ribosomal protein
261119_at	0.615	6.40E-35	1.40E-30	AT1G75350	ribosomal protein L31 family protein	protein.synthesis.chloroplast/mito - plastid ribosomal protein
261190_at	0.621	1.10E-35	2.40E-31	AT1G32990	ribosomal protein L11 family protein	protein.synthesis.chloroplast/mito - plastid ribosomal protein
264575_at	0.669	4.10E-43	8.90E-39	AT1G05190	ribosomal protein L6 family protein	protein.synthesis.chloroplast/mito - plastid ribosomal protein
247201_at	0.603	2.70E-33	5.90E-29	AT5G65220	ribosomal protein L29 family protein	protein.synthesis.chloroplast/mito - plastid ribosomal protein
249742_at	0.606	1.20E-33	2.70E-29	AT5G24490	30S ribosomal protein, putative	protein.synthesis.chloroplast/mito - plastid ribosomal protein
256855_at	0.619	2.10E-35	4.70E-31	AT3G15190	chloroplast 30S ribosomal protein S20, putative	protein.synthesis.chloroplast/mito - plastid ribosomal protein
267088_at	0.655	7.40E-41	1.60E-36	AT2G38140	chloroplast 30S ribosomal protein S31 (PSRP4)	protein.synthesis.chloroplast/mito - plastid ribosomal protein

254480_at	0.679	7.00E-45	1.50E-40	AT4G20360	elongation factor Tu / EF-Tu (TUFA)	protein.synthesis.elongation
262645_at	0.613	1.30E-34	2.80E-30	AT1G62750	elongation factor Tu family protein	protein.synthesis.elongation
254910_at	0.604	2.30E-33	5.00E-29	AT4G11175	translation initiation factor IF-1, chloroplast, putative	protein.synthesis.initiation
262172_at	0.650	5.50E-40	1.20E-35	AT1G74970	ribosomal protein S9 (RPS9)	protein.synthesis.misc ribososomal protein
263131_at	0.645	3.10E-39	6.90E-35	AT1G78630	ribosomal protein L13 family protein	protein.synthesis.misc ribososomal protein
255540_at	0.667	8.80E-43	1.90E-38	AT4G01800	preprotein translocase secA subunit, putative	protein.targeting.chloroplast
254072_at	0.654	1.20E-40	2.60E-36	AT4G25370	Clp amino terminal domain-containing protein	protein.targeting.unknown
262988_at	0.730	0.00E+00	0.00E+00	AT1G23310	glutamate:glyoxylate aminotransferase 1 (GGT1)	PS.aminotransferases peroxisomal
263350_at	0.739	0.00E+00	0.00E+00	AT2G13360	serine-glyoxylate aminotransferase-related	PS.aminotransferases peroxisomal
264018_at	0.632	2.60E-37	5.60E-33	AT2G21170	triosephosphate isomerase, chloroplast, putative	PS.calvin cycle.TPI
252929_at	0.744	0.00E+00	0.00E+00	AT4G38970	fructose-bisphosphate aldolase, putative	PS.calvin cyle.aldolase
263761_at	0.716	0.00E+00	0.00E+00	AT2G21330	fructose-bisphosphate aldolase, putative	PS.calvin cyle.aldolase
251885_at	0.740	0.00E+00	0.00E+00	AT3G54050	D-fructose-1,6-bisphosphate 1-phosphohydrolase, putative	PS.calvin cyle.FBPase
257807_at	0.605	1.70E-33	3.80E-29	AT3G26650	glyceraldehyde 3-phosphate dehydrogenase A, chloroplast (GAPA)	PS.calvin cyle.GAP
259625_at	0.684	1.40E-45	2.10E-41	AT1G42970	glyceraldehyde-3-phosphate dehydrogenase B, chloroplast (GAPB)	PS.calvin cyle.GAP
261197_at	0.617	4.00E-35	8.80E-31	AT1G12900	glyceraldehyde 3-phosphate dehydrogenase, chloroplast, putative	PS.calvin cyle.GAP
265998_at	0.670	3.20E-43	6.90E-39	AT2G24270	NADP-dependent glyceraldehyde-3-phosphate dehydrogenase, putative	PS.calvin cyle.GAP
255720_at	0.735	0.00E+00	0.00E+00	AT1G32060	phosphoribulokinase (PRK) / phosphopentokinase	PS.calvin cyle.PRK
259098_at	0.633	2.10E-37	4.60E-33	AT3G04790	ribose 5-phosphate isomerase-related	PS.calvin cyle.Rib5P Isomerase
245061_at	0.671	1.80E-43	4.00E-39	AT2G39730	ribulose bisphosphate carboxylase/oxygenase activase / RuBisCO activase	PS.calvin cyle.rubisco interacting
262377_at	0.606	1.10E-33	2.30E-29	AT1G73110	ribulose bisphosphate carboxylase/oxygenase activase / RuBisCO activase	PS.calvin cyle.rubisco interacting
251762_at	0.634	1.30E-37	2.90E-33	AT3G55800	sedoheptulose-1,7-bisphosphatase, chloroplast	PS.calvin cyle.seduheptulose bisphosphatase
251396_at	0.602	4.20E-33	9.30E-29	AT3G60750	transketolase, putative	PS.calvin cyle.transketolase
245025_at	0.674	6.00E-44	1.30E-39	AtCg00130	ATPase F subunit	PS.lightreaction.ATP synthase
253420_at	0.731	0.00E+00	0.00E+00	AT4G32260	ATP synthase family	PS.lightreaction.ATP synthase
255046_at	0.757	0.00E+00	0.00E+00	AT4G09650	ATP synthase delta chain, chloroplast, putative	PS.lightreaction.ATP synthase
255290_at	0.726	0.00E+00	0.00E+00	AT4G04640	ATP synthase gamma chain 1, chloroplast (ATPC1)	PS.lightreaction.ATP synthase
244936_at	0.623	5.50E-36	1.20E-31	AtCg01100	NADH dehydrogenase ND1	PS.lightreaction.cyclic electron flow-chlororespiration
245012_at	0.659	1.50E-41	3.30E-37	AtCg00440	NADH dehydrogenase D3 subunit of the NAD(P)H dehydrogenase complex	PS.lightreaction.cyclic electron flow-chlororespiration
265569_at	0.601	5.60E-33	1.20E-28	AT2G05620	expressed protein	PS.lightreaction.cyclic electron flow-chlororespiration
245044_at	0.604	2.40E-33	5.30E-29	AT2G26500	cytochrome b6f complex subunit (petM), putative	PS.lightreaction.cytochrome b6/f
255435_at	0.710	0.00E+00	0.00E+00	AT4G03280	cytochrome B6-F complex iron-sulfur subunit, chloroplast	PS.lightreaction.cytochrome b6/f
253391_at	0.635	8.60E-38	1.90E-33	AT4G32590	ferredoxin-related	PS.lightreaction.other electron carrier (ox/red).ferredoxin
247131_at	0.687	0.00E+00	7.30E-42	AT5G66190	ferredoxin--NADP(+) reductase, putative / adrenodoxin reductase, putative	PS.lightreaction.other electron carrier (ox/red)
261218_at	0.636	7.90E-38	1.70E-33	AT1G20020	ferredoxin--NADP(+) reductase, putative / adrenodoxin reductase, putative	PS.lightreaction.other electron carrier (ox/red)
255886_at	0.601	4.60E-33	1.00E-28	AT1G20340	plastocyanin	PS.lightreaction.other electron carrier (ox/red).plastocyanin
261769_at	0.646	1.80E-39	4.00E-35	AT1G76100	plastocyanin	PS.lightreaction.other electron carrier (ox/red).plastocyanin
245806_at	0.665	2.00E-42	4.40E-38	AT1G45474	chlorophyll A-B binding protein, putative (LHCA5)	PS.lightreaction.photosystem I.LHC-I
245007_at	0.612	1.80E-34	3.90E-30	AtCg00350	Encodes psaA protein comprising reaction center for PSI along with psaB protein	PS.lightreaction.photosystem I.PSI polypeptide subunits
247320_at	0.703	0.00E+00	5.60E-45	AT5G64040	photosystem I reaction center subunit PSI-N, chloroplast, putative	PS.lightreaction.photosystem I.PSI polypeptide subunits
253738_at	0.685	1.40E-45	1.60E-41	AT4G28750	photosystem I reaction center subunit IV, chloroplast/ PSI-E, putative	PS.lightreaction.photosystem I.PSI polypeptide subunits
255457_at	0.666	1.30E-42	2.90E-38	AT4G02770	photosystem I reaction center subunit II, chloroplast, putative	PS.lightreaction.photosystem I.PSI polypeptide subunits
256309_at	0.666	1.50E-42	3.20E-38	AT1G30380	photosystem I reaction center subunit psaK, chloroplast, putative	PS.lightreaction.photosystem I.PSI polypeptide subunits

258285_at	0.710	0.00E+00	0.00E+00	AT3G16140	photosystem I reaction center subunit VI, chloroplast/ PSI-H, putative	PS.lightreaction.photosystem I.PSI polypeptide subunits
259840_at	0.670	2.80E-43	6.20E-39	AT1G52230	photosystem I reaction center subunit VI, chloroplast/ PSI-H, putative	PS.lightreaction.photosystem I.PSI polypeptide subunits
261746_at	0.602	4.30E-33	9.50E-29	AT1G08380	expressed protein	PS.lightreaction.photosystem I.PSI polypeptide subunits
262557_at	0.635	8.70E-38	1.90E-33	AT1G31330	photosystem I reaction center subunit III family protein	PS.lightreaction.photosystem I.PSI polypeptide subunits
263114_at	0.682	1.40E-45	4.10E-41	AT1G03130	photosystem I reaction center subunit II, chloroplast, putative	PS.lightreaction.photosystem I.PSI polypeptide subunits
265287_at	0.673	8.30E-44	1.80E-39	AT2G20260	photosystem I reaction center subunit IV, chloroplast/ PSI-E, putative	PS.lightreaction.photosystem I.PSI polypeptide subunits
251082_at	0.648	8.90E-40	2.00E-35	AT5G01530	chlorophyll A-B binding protein CP29 (LHCB4)	PS.lightreaction.photosystem II.LHC-II
258239_at	0.622	8.50E-36	1.90E-31	AT3G27690	chlorophyll A-B binding protein (LHCB2:4)	PS.lightreaction.photosystem II.LHC-II
258993_at	0.714	0.00E+00	0.00E+00	AT3G08940	chlorophyll A-B binding protein (LHCB4.2)	PS.lightreaction.photosystem II.LHC-II
244975_at	0.633	1.80E-37	3.90E-33	AtCg00710	phosphoprotein that is a component of the PS II oxygen evolving core	PS.lightreaction.photosystem II.PSII polypeptide subunits
245004_at	0.621	1.10E-35	2.30E-31	AtCg00300	PsbZ, which is a subunit of PS II	PS.lightreaction.photosystem II.PSII polypeptide subunits
245195_at	0.723	0.00E+00	0.00E+00	AT1G67740	photosystem II core complex proteins psbY, chloroplast (PSBY)	PS.lightreaction.photosystem II.PSII polypeptide subunits
247073_at	0.748	0.00E+00	0.00E+00	AT5G66570	oxygen-evolving enhancer protein 1-1	PS.lightreaction.photosystem II.PSII polypeptide subunits
251031_at	0.609	4.40E-34	9.50E-30	AT5G02120	thylakoid membrane one helix protein (OHP)	PS.lightreaction.photosystem II.PSII polypeptide subunits
251701_at	0.691	0.00E+00	9.80E-43	AT3G56650	thylakoid lumenal 20 kDa protein	PS.lightreaction.photosystem II.PSII polypeptide subunits
251784_at	0.671	1.60E-43	3.40E-39	AT3G55330	photosystem II reaction center PsbP family protein	PS.lightreaction.photosystem II.PSII polypeptide subunits
252130_at	0.733	0.00E+00	0.00E+00	AT3G50820	oxygen-evolving enhancer protein, chloroplast, putative	PS.lightreaction.photosystem II.PSII polypeptide subunits
254398_at	0.677	2.00E-44	4.30E-40	AT4G21280	oxygen-evolving enhancer protein 3, chloroplast, putative (PSBQ1) (PSBQ)	PS.lightreaction.photosystem II.PSII polypeptide subunits
255248_at	0.709	0.00E+00	0.00E+00	AT4G05180	oxygen-evolving enhancer protein 3, chloroplast, putative (PSBQ2)	PS.lightreaction.photosystem II.PSII polypeptide subunits
255982_at	0.671	1.80E-43	3.90E-39	AT1G34000	light stress-responsive one-helix protein (OHP2)	PS.lightreaction.photosystem II.PSII polypeptide subunits
256979_at	0.654	1.20E-40	2.70E-36	AT3G21055	photosystem II 5 kD protein, putative	PS.lightreaction.photosystem II.PSII polypeptide subunits
259981_at	0.685	1.40E-45	1.60E-41	AT1G76450	oxygen-evolving complex-related	PS.lightreaction.photosystem II.PSII polypeptide subunits
262632_at	0.662	4.70E-42	1.00E-37	AT1G06680	photosystem II oxygen-evolving complex 23 (OEC23)	PS.lightreaction.photosystem II.PSII polypeptide subunits
264837_at	0.742	0.00E+00	0.00E+00	AT1G03600	photosystem II family protein	PS.lightreaction.photosystem II.PSII polypeptide subunits
264959_at	0.632	2.70E-37	6.00E-33	AT1G77090	thylakoid lumenal 29.8 kDa protein	PS.lightreaction.photosystem II.PSII polypeptide subunits
260704_at	0.683	1.40E-45	3.70E-41	AT1G32470	glycine cleavage system H protein, mitochondrial, putative	PS.photorespiration.glycine cleavage
266636_at	0.604	2.40E-33	5.20E-29	AT2G35370	glycine cleavage system H protein 1, mitochondrial (GDCSH) (GCDH)	PS.photorespiration.glycine cleavage
258359_s_at	*0.709*	*0.00E+00*	*0.00E+00*	*AT3G14415* *AT3G14420*	*(S)-2-hydroxy-acid oxidase, peroxisomal/ glycolate oxidase, putative* *(S)-2-hydroxy-acid oxidase, peroxisomal/ glycolate oxidase, putative*	*PS.photorespiration.glycolate oxydase*
260014_at	0.617	3.90E-35	8.60E-31	AT1G68010	glycerate dehydrogenase / NADH-dependent hydroxypyruvate reductase	PS.photorespiration.hydroxypyruvate reductase
249658_s_at	*0.643*	*5.30E-39*	*1.20E-34*	*AT5G36700* *AT5G36790*	*phosphoglycolate phosphatase, putative* *phosphoglycolate phosphatase, putative*	*PS.photorespiration.phosphoglycolate phosphatase*
264383_at	0.692	0.00E+00	8.90E-43	AT2G25080	phospholipid hydroperoxide glutathione peroxidase, chloroplast	redox.ascorbate and glutathione
255078_at	0.676	2.40E-44	5.30E-40	AT4G09010	L-ascorbate peroxidase, chloroplast, putative	redox.ascorbate and glutathione.ascorbate
259707_at	0.708	0.00E+00	0.00E+00	AT1G77490	L-ascorbate peroxidase, thylakoid-bound (tAPX)	redox.ascorbate and glutathione.ascorbate
251860_at	0.660	1.20E-41	2.60E-37	AT3G54660	gluthatione reductase, chloroplast	redox.ascorbate and glutathione.glutathione
250733_at	0.636	6.10E-38	1.30E-33	AT5G06290	2-cys peroxiredoxin, chloroplast	redox.periredoxins
258087_at	0.629	7.70E-37	1.70E-32	AT3G26060	peroxiredoxin Q, putative similar to peroxiredoxin Q	redox.periredoxins
259237_at	0.654	1.10E-40	2.40E-36	AT3G11630	2-cys peroxiredoxin, chloroplast (BAS1)	redox.periredoxins
250133_at	0.644	3.90E-39	8.50E-35	AT5G16400	thioredoxin, putative	redox.thioredoxin
255379_at	0.606	1.00E-33	2.30E-29	AT4G03520	thioredoxin M-type 2, chloroplast (TRX-M2)	redox.thioredoxin
258398_at	0.763	0.00E+00	0.00E+00	AT3G15360	thioredoxin M-type 4, chloroplast (TRX-M4)	redox.thioredoxin
258607_at	0.698	0.00E+00	6.40E-44	AT3G02730	thioredoxin, putative	redox.thioredoxin
262418_at	0.686	0.00E+00	1.00E-41	AT1G50320	thioredoxin x	redox.thioredoxin

262721_at	0.613	1.20E-34	2.60E-30	AT1G43560	thioredoxin family protein	redox.thioredoxin
263624_at	0.657	3.20E-41	7.00E-37	AT2G04700	ferredoxin thioredoxin reductase catalytic beta chain family protein	redox.thioredoxin
264845_at	0.661	9.50E-42	2.10E-37	AT1G03680	thioredoxin M-type 1, chloroplast (TRX-M1)	redox.thioredoxin
263656_at	0.626	2.20E-36	4.80E-32	AT1G04240	auxin-responsive protein / indoleacetic acid-induced protein 3 (IAA3)	RNA.regulation of transcription.Aux/IAA family
246977_at	0.682	2.80E-45	5.20E-41	AT5G24930	zinc finger (B-box type) family protein similar to CONSTANS-like protein 1	RNA.regulation of transcription.C2C2(Zn) CO-like
266110_at	0.653	1.70E-40	3.60E-36	AT2G02080	zinc finger (C2H2 type) family protein	RNA.regulation of transcription.C2H2 zinc finger family
266120_at	0.654	1.00E-40	2.20E-36	AT2G02070	zinc finger (C2H2 type) family protein	RNA.regulation of transcription.C2H2 zinc finger family
249035_at	0.653	1.50E-40	3.30E-36	AT5G44190	myb family transcription factor (GLK2)	RNA.regulation of transcription.G2-like transcription factor
263715_at	0.623	4.60E-36	1.00E-31	AT2G20570	golden2-like transcription factor (GLK1)	RNA.regulation of transcription.G2-like transcription factor
245354_at	0.677	1.80E-44	4.00E-40	AT4G17600	lil3 protein	RNA.regulation of transcription.HSF transcription factor
261206_at	0.665	1.80E-42	3.80E-38	AT1G12800	S1 RNA-binding domain-containing protein	RNA.regulation of transcription.HSF transcription factor
258333_at	0.645	3.20E-39	7.10E-35	AT3G16000	matrix-localized MAR DNA-binding protein-related	RNA.regulation of transcription.Orphan family
264177_at	0.621	9.70E-36	2.10E-31	AT1G02150	pentatricopeptide (PPR) repeat-containing protein	RNA.regulation of transcription.putative DNA-binding protein
250170_at	0.652	2.10E-40	4.50E-36	AT5G14260	SET domain-containing protein	RNA.regulation of transcription.SET-domain
245774_at	0.627	1.40E-36	3.10E-32	AT1G30210	TCP family transcription factor, putative	RNA.regulation of transcription.TCP transcription factor
248828_at	0.661	9.00E-42	2.00E-37	AT5G47110	lil3 protein, putative similar to Lil3 protein	RNA.regulation of transcription.unclassified
251157_at	0.723	0.00E+00	0.00E+00	AT3G63140	mRNA-binding protein, putative	RNA.regulation of transcription.unclassified
263946_at	0.633	1.80E-37	3.90E-33	AT2G36000	mitochondrial transcription termination factor-related / mTERF-related	RNA.regulation of transcription.unclassified
264954_at	0.677	1.80E-44	3.90E-40	AT1G77060	mutase family protein	RNA.regulation of transcription.unclassified
254126_at	0.706	0.00E+00	1.40E-45	AT4G24770	31 kDa ribonucleoprotein, chloroplast/ RNA-binding protein RNP-T, putative	RNA.RNA binding
256678_at	0.607	8.30E-34	1.80E-29	AT3G52380	33 kDa ribonucleoprotein, chloroplast/ RNA-binding protein cp33, putative	RNA.RNA binding
265966_at	0.667	7.10E-43	1.60E-38	AT2G37220	29 kDa ribonucleoprotein, chloroplast/ RNA-binding protein cp29, putative	RNA.RNA binding
262879_at	0.630	5.70E-37	1.20E-32	AT1G64860	RNA polymerase sigma subunit SigA (sigA) / sigma factor 1 (SIG1)	RNA.transcription
263846_at	0.629	6.60E-37	1.40E-32	AT2G36990	RNA polymerase sigma subunit SigF (sigF) / sigma-like factor (SIG6)	RNA.transcription
264781_at	0.623	4.70E-36	1.00E-31	AT1G08540	RNA polymerase sigma subunit SigB (sigB) / sigma factor 2 (SIG2)	RNA.transcription
258755_at	0.656	4.80E-41	1.00E-36	AT3G11950	UbiA prenyltransferase family protein	secondary metabolism.isoprenoids
264799_at	0.614	1.10E-34	2.30E-30	AT1G08550	violaxanthin de-epoxidase precursor, putative (AVDE1)	secondary metabolism.isoprenoids.carotenoids
250095_at	0.601	6.10E-33	1.30E-28	AT5G17230	phytoene synthase (PSY)	secondary metabolism.isoprenoids.carotenoids
260236_at	0.731	0.00E+00	0.00E+00	AT1G74470	geranylgeranyl reductase	secondary metabolism.isoprenoids.non-mevalonate pathway
253235_at	0.615	7.60E-35	1.70E-30	AT4G34350	LytB family protein	secondary metabolism.isoprenoids.non-mevalonate pathway
247637_at	0.630	5.40E-37	1.20E-32	AT5G60600	1-hydroxy-2-methyl-2-(E)-butenyl 4-diphosphate synthase, putative	secondary metabolism.isoprenoids.non-mevalonate pathway
251118_at	0.703	0.00E+00	5.60E-45	AT3G63410	chloroplast inner envelope membrane protein, putative (APG1)	secondary metabolism.isoprenoids.tocopherol biosynthesis
266099_at	0.634	1.20E-37	2.50E-33	AT2G38040	acetyl co-enzyme A carboxylase carboxyltransferase alpha subunit family	secondary metabolism.unspecified
260267_at	0.624	4.20E-36	9.10E-32	AT1G68530	very-long-chain fatty acid condensing enzyme (CUT1)	secondary metabolism.wax
263494_at	0.678	1.30E-44	2.60E-40	AT2G42590	14-3-3 protein GF14 mu (GRF9)	signalling.14-3-3 proteins
250531_at	0.684	1.40E-45	2.10E-41	AT5G08650	GTP-binding protein LepA, putative	signalling.G-proteins
256655_at	0.623	4.90E-36	1.10E-31	AT3G18890	expressed protein similar to UV-B and ozone similarly regulated protein 1	signalling.light
261480_at	0.722	0.00E+00	0.00E+00	AT1G14280	phytochrome kinase, putative	signalling.light
253272_at	0.707	0.00E+00	1.40E-45	AT4G34190	stress enhanced protein 1 (SEP1)	stress
254034_at	0.655	7.60E-41	1.70E-36	AT4G25960	multidrug resistance P-glycoprotein, putative	stress.biotic
246596_at	0.654	9.40E-41	2.10E-36	AT5G14740	carbonic anhydrase 2 / carbonate dehydratase 2 (CA2) (CA18)	TCA / org. transformation.carbonic anhydrases
259161_at	0.707	0.00E+00	1.40E-45	AT3G01500	carbonic anhydrase 1, chloroplast / carbonate dehydratase 1 (CA1)	TCA / org. transformation.carbonic anhydrases
247813_at	0.601	6.00E-33	1.30E-28	AT5G58330	malate dehydrogenase [NADP], chloroplast	TCA / org. transformation.other organic acid transformations
264820_at	0.621	9.60E-36	2.10E-31	AT1G03475	coproporphyrinogen III oxidase/ coproporphyrinogenase, putative	tetrapyrrole synthesis.coproporphyrinogen III oxidase

256020_at	0.608	5.60E-34	1.20E-29	AT1G58290	glutamyl-tRNA reductase 1 / GluTR (HEMA1)	tetrapyrrole synthesis.glu-tRNA reductase
250243_at	0.681	2.80E-45	7.40E-41	AT5G13630	magnesium-chelatase subunit chlH, chloroplast, putative	tetrapyrrole synthesis.magnesium chelatase
254623_at	0.650	5.00E-40	1.10E-35	AT4G18480	magnesium-chelatase subunit chlI, chloroplast	tetrapyrrole synthesis.magnesium chelatase
261695_at	0.679	5.60E-45	1.40E-40	AT1G08520	magnesium-chelatase subunit chlD, chloroplast, putative	tetrapyrrole synthesis.magnesium chelatase
254105_at	0.667	7.40E-43	1.60E-38	AT4G25080	magnesium-protoporphyrin O-methyltransferase, putative	tetrapyrrole synthesis.Mg protoporphyrin IX methyltransferase
251664_at	0.703	0.00E+00	7.00E-45	AT3G56940	dicarboxylate diiron protein, putative (Crd1)	tetrapyrrole synthesis.Mg-protoporphyrin IX ester cyclase
246033_at	0.604	2.00E-33	4.40E-29	AT5G08280	hydroxymethylbilane synthase / porphobilinogen deaminase, chloroplast	tetrapyrrole synthesis.porphobilinogen deaminase
255537_at	0.654	1.20E-40	2.50E-36	AT4G01690	protoporphyrinogen oxidase (PPOX)	tetrapyrrole synthesis.protoporphyrin IX oxidase
251519_at	0.680	5.60E-45	1.20E-40	AT3G59400	expressed protein	tetrapyrrole synthesis.regulation
255826_at	0.618	3.00E-35	6.50E-31	AT2G40490	uroporphyrinogen decarboxylase, putative / UPD, putative	tetrapyrrole synthesis.uroporphyrinogen decarboxylase
260490_at	0.743	0.00E+00	0.00E+00	AT1G51500	ABC transporter family protein	transport.ABC transporters and multidrug resistance systems
261353_at	0.629	8.10E-37	1.80E-32	AT1G79600	ABC1 family protein	transport.ABC transporters and multidrug resistance systems
251815_at	0.709	0.00E+00	0.00E+00	AT3G54900	CAX-interacting protein 1 (CAXIP1)	transport.calcium
246510_at	0.781	0.00E+00	0.00E+00	AT5G15410	cyclic nucleotide-gated channel (CNGC2)	transport.cyclic nucleotide or calcium regulated channels
248886_at	0.679	7.00E-45	1.50E-40	AT5G46110	phosphate/triose-phosphate translocator, putative	transport.metabolite transporters at the envelope membrane
247289_at	0.601	4.70E-33	1.00E-28	AT5G64290	oxoglutarate/malate translocator, putative	transport.metabolite transporters at the mito. membrane
250278_at	0.647	1.50E-39	3.30E-35	AT5G12860	oxoglutarate/malate translocator, putative	transport.metabolite transporters at the mito. membrane
260082_at	0.606	1.30E-33	2.80E-29	AT1G78180	mitochondrial substrate carrier family protein	transport.metabolite transporters at the mito. membrane
267093_at	0.632	2.80E-37	6.20E-33	AT2G38170	calcium exchanger CAX1 identical to high affinity calcium antiporter CAX1	transport.metal
267027_at	0.616	5.90E-35	1.30E-30	AT2G38330	MATE efflux family protein	transport.misc
266672_at	0.608	5.70E-34	1.20E-29	AT2G29650	inorganic phosphate transporter, putative	transport.phosphate
261536_at	0.674	6.60E-44	1.40E-39	AT1G01790	K+ efflux antiporter, putative (KEA1)	transport.potassium
249864_at	0.697	0.00E+00	9.70E-44	AT5G22830	magnesium transporter CorA-like family protein	transport.unspecified cations
247709_at	0.723	0.00E+00	0.00E+00	AT5G59250	sugar transporter similar to D-xylose-H+ symporter from Lactobacillus brevis	transporter.sugars

PIP2;7/2;8 (266533_s_at/ At2g16850 and At4g35100)

ProbeSet	r-value	p-value	e-value	GeneID	Annotation	MAPMAN classification
245318_at	0.661	7.90E-42	1.70E-37	AT4G16980	arabinogalactan-protein family	cell wall.cell wall proteins.AGPs
256964_at	0.664	2.80E-42	6.20E-38	AT3G13520	arabinogalactan-protein (AGP12)	cell wall.cell wall proteins.AGPs
259664_at	0.810	0.00E+00	0.00E+00	AT1G55330	arabinogalactan-protein (AGP21)	cell wall.cell wall proteins.AGPs
265066_at	0.722	0.00E+00	0.00E+00	AT1G03870	fasciclin-like arabinogalactan-protein (FLA9)	cell wall.cell wall proteins.AGPs
266588_at	0.698	0.00E+00	6.70E-44	AT2G14890	arabinogalactan-protein (AGP9)	cell wall.cell wall proteins.AGPs
260914_at	0.644	4.40E-39	9.70E-35	AT1G02640	glycosyl hydrolase family 3 protein	cell wall.degradation.mannan-xylose-arabinose-fucose
257203_at	0.746	0.00E+00	0.00E+00	AT3G23730	xyloglucan:xyloglucosyl transferase, putative	cell wall.modification
266215_at	0.690	0.00E+00	2.00E-42	AT2G06850	xyloglucan:xyloglucosyl transferase (EXT) (EXGT-A1)	cell wall.modification
245138_at	0.649	6.60E-40	1.40E-35	AT2G45190	axial regulator YABBY1/ abnormal floral organs protein	development.unspecified
255709_at	0.633	1.90E-37	4.10E-33	AT4G00180	axial regulator YABBY3	development.unspecified
262840_at	0.611	2.30E-34	5.10E-30	AT1G14900	high-mobility-group protein / HMG-I/Y protein	DNA.synthesis/chromatin structure
258402_at	*0.650*	*5.70E-40*	*1.20E-35*	*AT3G15450*	*expressed protein similar to auxin down-regulated protein ARG10*	*hormone metabolism.auxin*
				AT3G15460	*brix domain-containing protein*	
257938_at	0.636	7.00E-38	1.50E-33	AT3G19820	cell elongation protein / DWARF1 / DIMINUTO (DIM)	hormone metabolism.brassinosteroid
264374_at	0.652	2.50E-40	5.40E-36	AT2G25180	two-component responsive regulator family protein	hormone metabolism.cytokinin.signal transduction

250109_at	0.650	5.00E-40	1.10E-35	AT5G15230	gibberellin-regulated protein 4 (GASA4)	hormone metabolism.gibberelin
251736_at	0.745	0.00E+00	0.00E+00	AT3G56130	biotin/lipoyl attachment domain-containing protein	lipid metabolism.FA synthesis and FA elongation
254102_at	0.612	2.10E-34	4.50E-30	AT4G25050	acyl carrier family protein / ACP family protein	lipid metabolism.FA synthesis and FA elongation
250470_at	0.606	1.20E-33	2.60E-29	AT5G10160	beta-hydroxyacyl-ACP dehydratase, putative	lipid metabolism.FA synthesis and FA elongation
250891_at	0.624	3.70E-36	8.10E-32	AT5G04530	beta-ketoacyl-CoA synthase family protein	lipid metabolism.FA synthesis and FA elongation
253285_at	0.601	5.60E-33	1.20E-28	AT4G34250	fatty acid elongase, putative	lipid metabolism.FA synthesis and FA elongation
252950_at	0.650	4.50E-40	9.90E-36	AT4G38690	1-phosphatidylinositol phosphodiesterase-related	lipid metabolism.lipid degradation.lysophospholipases
246114_at	0.600	6.60E-33	1.40E-28	AT5G20250	raffinose synthase family protein / seed imbibition protein, putative (din10)	minor CHO metabolism.raffinose family.raffinose synthases
245637_at	0.785	0.00E+00	0.00E+00	AT1G25230	purple acid phosphatase family protein	misc.acid and other phosphatases
247362_at	0.616	4.90E-35	1.10E-30	AT5G63140	calcineurin-like phosphoesterase family protein	misc.acid and other phosphatases
249073_at	0.686	0.00E+00	7.40E-42	AT5G44020	acid phosphatase class B family protein	misc.acid and other phosphatases
249718_at	0.658	2.80E-41	6.20E-37	AT5G35740	glycosyl hydrolase family protein 17	misc.beta 1,3 glucan hydrolases
255779_at	0.652	2.70E-40	5.90E-36	AT1G18650	glycosyl hydrolase family protein 17 similar to beta-1,3-glucanase	misc.beta 1,3 glucan hydrolases
248912_at	0.641	1.10E-38	2.50E-34	AT5G45670	GDSL-motif lipase/hydrolase family protein	misc.GDSL-motif lipase
254609_at	0.657	3.30E-41	7.30E-37	AT4G18970	GDSL-motif lipase/hydrolase family protein	misc.GDSL-motif lipase
259375_at	0.658	2.60E-41	5.70E-37	AT3G16370	GDSL-motif lipase/hydrolase family protein	misc.GDSL-motif lipase
262980_at	0.619	2.10E-35	4.70E-31	AT1G75680	glycosyl hydrolase family 9 protein similar to endo-beta-1,4-glucanase	misc.gluco-, galacto- and mannosidases
262376_at	0.606	1.20E-33	2.60E-29	AT1G72970	glucose-methanol-choline (GMC) oxidoreductase family protein	misc.nitrilases, *nitrile lyases, berberine bridge enzymes, etc.
250110_at	0.655	8.80E-41	1.90E-36	AT5G15350	plastocyanin-like domain-containing protein	misc.plastocyanin-like
252711_at	0.611	2.40E-34	5.20E-30	AT3G43720	protease inhibitor/seed storage/lipid transfer protein (LTP) family protein	misc.protease inhibitor/seed storage/lipid transfer prot.
259660_at	0.619	2.00E-35	4.30E-31	AT1G55260	protease inhibitor/seed storage/lipid transfer protein (LTP) family protein	misc.protease inhibitor/seed storage/lipid transfer prot.
264371_at	0.620	1.30E-35	2.90E-31	AT1G12090	protease inhibitor/seed storage/lipid transfer protein (LTP) family protein	misc.protease inhibitor/seed storage/lipid transfer prot.
259382_s_at	*0.608*	*5.50E-34*	*1.20E-29*	*AT3G16420* *AT3G16430*	*jacalin lectin family protein similar to myrosinase binding protein* *jacalin lectin family protein similar to myrosinase binding protein*	*not assigned.disagreeing hits*
248622_at	0.653	1.60E-40	3.40E-36	AT5G49360	glycosyl hydrolase family 3 protein	not assigned.no ontology
254041_at	0.685	0.00E+00	1.40E-41	AT4G25830	integral membrane family protein	not assigned.no ontology
254815_at	0.615	7.20E-35	1.60E-30	AT4G12420	multi-copper oxidase, putative (SKU5)	not assigned.no ontology
257974_at	0.605	1.50E-33	3.20E-29	AT3G20820	leucine-rich repeat family protein	not assigned.no ontology
259009_at	0.658	2.40E-41	5.20E-37	AT3G09260	glycosyl hydrolase family 1 protein	not assigned.no ontology
259235_at	0.608	5.90E-34	1.30E-29	AT3G11600	expressed protein weak similarity to B-type cyclin	not assigned.no ontology
262539_at	0.686	0.00E+00	8.90E-42	AT1G17200	integral membrane family protein	not assigned.no ontology
263979_at	0.656	5.70E-41	1.30E-36	AT2G42840	protodermal factor 1 (PDF1)	not assigned.no ontology
264307_at	0.796	0.00E+00	0.00E+00	AT1G61900	expressed protein contains similarity to glutamic acid/alanine-rich protein	not assigned.no ontology
267034_at	0.677	1.80E-44	4.00E-40	AT2G38310	expressed protein low similarity to early flowering protein 1	not assigned.no ontology
253754_at	0.680	5.60E-45	1.10E-40	AT4G29020	glycine-rich protein	not assigned.no ontology.glycine rich proteins
246063_at	0.764	0.00E+00	0.00E+00	AT5G19340	expressed protein	not assigned.unknown
251141_at	0.686	0.00E+00	1.00E-41	AT5G01075	expressed protein	not assigned.unknown
253286_at	0.663	3.30E-42	7.10E-38	AT4G34260	expressed protein	not assigned.unknown
254260_at	0.617	3.60E-35	7.80E-31	AT4G23440	expressed protein	not assigned.unknown
254954_at	0.631	4.30E-37	9.40E-33	AT4G10910	expressed protein	not assigned.unknown
255962_at	0.670	2.90E-43	6.40E-39	AT1G22335	expressed protein ; expression supported by MPSS	not assigned.unknown
257171_at	0.614	9.00E-35	2.00E-30	AT3G23760	expressed protein	not assigned.unknown
258393_at	0.653	1.80E-40	4.00E-36	AT3G15480	expressed protein	not assigned.unknown
258836_at	0.674	6.30E-44	1.40E-39	AT3G07210	expressed protein	not assigned.unknown

259023_at	0.618	2.50E-35	5.50E-31	AT3G07510	expressed protein	not assigned.unknown
259131_at	0.663	3.30E-42	7.10E-38	AT3G02180	expressed protein	not assigned.unknown
259586_at	0.619	2.20E-35	4.70E-31	AT1G28100	expressed protein	not assigned.unknown
259996_at	0.614	9.80E-35	2.20E-30	AT1G67910	expressed protein	not assigned.unknown
261740_at	0.655	9.30E-41	2.00E-36	AT1G47740	expressed protein	not assigned.unknown
265265_at	0.710	0.00E+00	0.00E+00	AT2G42900	expressed protein	not assigned.unknown
266591_at	0.610	3.80E-34	8.30E-30	AT2G46225	expressed protein	not assigned.unknown
260967_at	0.658	2.20E-41	4.90E-37	AT1G12230	transaldolase, putative	OPP.non-reductive PP.transaldolase
249847_at	0.662	5.50E-42	1.20E-37	AT5G23210	serine carboxypeptidase S10 family protein	protein.degradation.serine protease
258857_at	0.730	0.00E+00	0.00E+00	AT3G02110	serine carboxypeptidase S10 family protein	protein.degradation.serine protease
249862_at	0.640	1.50E-38	3.20E-34	AT5G22920	zinc finger (C3HC4-type RING finger) family protein	protein.degradation.ubiquitin.E3.RING
259741_at	0.651	3.60E-40	7.80E-36	AT1G71020	armadillo/beta-catenin repeat family protein/ U-box domain-containing protein	protein.degradation.ubiquitin.E3.RING
256914_at	0.693	0.00E+00	5.50E-43	AT3G23880	F-box family protein contains F-box domain	protein.degradation.ubiquitin.E3.SCF.FBOX
250428_at	0.694	0.00E+00	3.60E-43	AT5G10480	protein tyrosine phosphatase-like protein, putative (PAS2)	protein.postranslational modification
251500_at	0.607	8.00E-34	1.80E-29	AT3G59110	protein kinase family protein contains protein kinase domain	protein.postranslational modification.kinase
245898_at	0.632	3.00E-37	6.50E-33	AT5G11020	protein kinase family protein contains protein kinase domain	protein.postranslational modification.kinase
265816_s_at	*0.615*	*7.90E-35*	*1.70E-30*	*AT1G30230* *AT2G18110*	*elongation factor 1-beta / EF-1-beta* *elongation factor 1-beta, putative / EF-1-beta, putative*	*protein.synthesis.elongation*
248975_at	0.648	8.60E-40	1.90E-35	AT5G45040	cytochrome c6 (ATC6)	PS.lightreaction.other electron carrier (ox/red)
260481_at	0.627	1.30E-36	2.90E-32	AT1G10960	ferredoxin, chloroplast, putative	PS.lightreaction.other electron carrier (ox/red).ferredoxin
255675_at	0.662	6.70E-42	1.50E-37	AT4G00480	myc-related transcription factor (MYC1)	RNA.regulation of transcription.bHLH family
257198_at	0.613	1.10E-34	2.40E-30	AT3G23690	basic helix-loop-helix (bHLH) family protein	RNA.regulation of transcription.bHLH family
264517_at	0.651	3.10E-40	6.70E-36	AT1G10120	basic helix-loop-helix (bHLH) family protein	RNA.regulation of transcription.bHLH family
245576_at	0.636	6.10E-38	1.30E-33	AT4G14770	tesmin/TSO1-like CXC domain-containing protein	RNA.regulation of transcription.CPP(Zn) transcription factor
253065_at	0.634	1.20E-37	2.70E-33	AT4G37740	expressed protein identical to transcription activator GRL2	RNA.regulation of transcription.General Transcription
249290_at	0.643	6.70E-39	1.50E-34	AT5G41060	zinc finger (DHHC type) family protein	RNA.regulation of transcription.unclassified
260806_at	0.667	9.60E-43	2.10E-38	AT1G78260	RNA recognition motif (RRM)-containing protein	RNA.RNA binding
267377_at	0.622	7.90E-36	1.70E-31	AT2G26250	beta-ketoacyl-CoA synthase family (FIDDLEHEAD) (FDH)	secondary metabolism.isoprenoids
245199_at	0.688	0.00E+00	4.60E-42	AT1G67730	b-keto acyl reductase, putative (GLOSSY8) similar to b-keto acyl reductase	secondary metabolism.wax
262729_at	*0.707*	*0.00E+00*	*1.40E-45*	*AT1G20090* *AT1G75840*	*Rac-like GTP-binding protein (ARAC4) / Rho-like GTP-binding protein (ROP2)* *Rac-like GTP-binding protein (ARAC5) / Rho-like GTP-binding protein (ROP4)*	*signalling.G-proteins*
253062_at	0.639	2.30E-38	5.00E-34	AT4G37590	phototropic-responsive NPH3 family protein	signalling.light
266745_at	0.626	1.70E-36	3.80E-32	AT2G02950	phytochrome kinase substrate 1 (PKS1)	signalling.light
267517_at	0.602	3.60E-33	7.90E-29	AT2G30520	signal transducer of phototropic response (RPT2)	signalling.light
258704_at	0.613	1.30E-34	2.80E-30	AT3G09780	protein kinase family protein contains eukaryotic protein kinase domain	signalling.receptor kinases.crinkly like
246244_at	0.666	1.00E-42	2.30E-38	AT4G37250	leucine-rich repeat family protein / protein kinase family protein	signalling.receptor kinases.leucine rich repeat III
250102_at	0.609	4.00E-34	8.70E-30	AT5G16590	leucine-rich repeat transmembrane protein kinase, putative	signalling.receptor kinases.leucine rich repeat III
261308_at	0.615	7.00E-35	1.50E-30	AT1G48480	leucine-rich repeat transmembrane protein kinase, putative	signalling.receptor kinases.leucine rich repeat III
256516_at	0.625	2.70E-36	6.00E-32	AT1G66150	leucine-rich repeat protein kinase, putative (TMK1)	signalling.receptor kinases.leucine rich repeat IX
257202_at	0.628	8.70E-37	1.90E-32	AT3G23750	leucine-rich repeat family protein / protein kinase family protein	signalling.receptor kinases.leucine rich repeat IX
267481_at	0.666	1.10E-42	2.40E-38	AT2G02780	leucine-rich repeat transmembrane protein kinase, putative	signalling.receptor kinases.leucine rich repeat VI
262195_at	0.684	1.40E-45	2.40E-41	AT1G78040	pollen Ole e 1 allergen and extensin family protein	stress.abiotic.unspecified
248763_at	0.724	0.00E+00	0.00E+00	AT5G47550	cysteine protease inhibitor, putative / cystatin	stress.biotic
256970_at	0.611	2.20E-34	4.80E-30	AT3G21090	ABC transporter family protein	transport.ABC transporters and multidrug resistance systems

251962_at	0.637	5.60E-38	1.20E-33	AT3G53420 **PIP2;1**	transport.Major Intrinsic Proteins.PIP
259431_at	0.863	0.00E+00	0.00E+00	AT1G01620 **PIP1;3**	transport.Major Intrinsic Proteins.PIP
266927_at	0.675	3.50E-44	7.70E-40	AT2G45960 **PIP1;2**	transport.Major Intrinsic Proteins.PIP
257313_at	0.783	0.00E+00	0.00E+00	AT3G26520 **TIP1;2**	transport.Major Intrinsic Proteins.TIP
258054_at	*0.780*	*0.00E+00*	*0.00E+00*	*AT3G16240* ***TIP2;1*** *AT3G16250 ferredoxin-related (2Fe-2S iron-sulfur cluster binding domains)*	*transport.Major Intrinsic Proteins.TIP*

Genes co-expressed with more than one *PIP2* gene				
Genes common to *PIP2;1* and *PIP2;6*				
Probe Set	r-value PIP2;1	r-value PIP2;6	AGI code	Annotation	MAPMAN classification

Probe Set	r-value PIP2;1	r-value PIP2;6	AGI code	Annotation	MAPMAN classification
245281_At	0.648	0.617	At4g15560	1-deoxy-D-xylulose 5-phosphate synthase _CLA1_CLA_DEF_DXPS2_DXS	development.unspecified
267635_At	0.600	0.673	At2g42220	rhodanese-like domain-containing protein	misc.rhodanese
249710_At	0.656	0.640	At5g35630	ATGSL1_GLN2__GS2 (GLUTAMINE SYNTHETASE 2)	N-metabolism.ammonia metabolism.glutamine synthase
246294_At	0.608	0.601	At3g56910	PSRP5 (PLASTID-SPECIFIC 50S RIBOSOMAL PROTEIN 5)	not assigned.disagreeing hits
267262_At	0.619	0.682	At2g22990	SNG1_SCPL8__SNG1 (SINAPOYLGLUCOSE 1); serine carboxypeptidase	protein.degradation.serine protease
260898_At	0.621	0.617	At1g29070	ribosomal protein L34 family protein	protein.synthesis.chloroplast/mito - plastid ribosomal protein
247320_At	0.610	0.703	At5g64040	PSAN (photosystem I reaction center subunit PSI-N); calmodulin binding	PS.lightreaction.photosystem I.PSI polypeptide subunits
251031_At	0.624	0.609	At5g02120	OHP (ONE HELIX PROTEIN)	PS.lightreaction.photosystem II.PSII polypeptide subunits
264837_At	0.612	0.742	At1g03600	photosystem II family protein	PS.lightreaction.photosystem II.PSII polypeptide subunits
259237_At	0.600	0.654	At3g11630	2-cys peroxiredoxin, chloroplast (BAS1)	redox.periredoxins
254105_At	0.605	0.667	At4g25080	CHLM (MAGNESIUM-PROTOPORPHYRIN IX METHYLTRANSFERASE)	tetrapyrrole synthesis.Mg protoporphyrin IX methyltransferase
251664_At	0.655	0.703	At3g56940	ACSF_CHL27_CRD1__AT103 (DICARBOXYLATE DIIRON 1)	tetrapyrrole synthesis.Mg-protoporphyrin IX ester cyclase

Genes common to *PIP2;1* and *PIP2;7/2;8*				
Probe Set	r-value PIP2;1	r-value PIP2;7/ PIP2;8	AGI code	Annotation	MAPMAN classification

Probe Set	r-value PIP2;1	r-value PIP2;7/ PIP2;8	AGI code	Annotation	MAPMAN classification
265066_At	0.607	0.722	At1g03870	FLA9	cell wall.cell wall proteins.AGPs
245318_At	0.699	0.661	At4g16980	arabinogalactan-protein family	cell wall.cell wall proteins.AGPs
254102_At	0.667	0.612	At4g25050	ACP4 (ACYL CARRIER PROTEIN 4)	lipid metabolism.FA synthesis and elongation
249073_At	0.602	0.686	At5g44020	acid phosphatase class B family protein	misc.acid and other phosphatases
259375_At	0.696	0.658	At3g16370	GDSL-motif lipase/hydrolase family protein	misc.GDSL-motif lipase
262980_At	0.615	0.619	At1g75680	glycosyl hydrolase family 9 protein	misc.gluco-, galacto- and mannosidases
264371_At	0.634	0.620	At1g12090	ELP (EXTENSIN-LIKE PROTEIN); lipid binding	misc.protease inhibitor/seed storage/lipid transfer prot.
257974_At	0.621	0.605	At3g20820	leucine-rich repeat family protein	not assigned.no ontology
260481_At	0.635	0.627	At1g10960	ATFD1 (FERREDOXIN 1); electron carrier/ iron ion binding	PS.lightreaction.other electron carrier (ox/red).ferredoxin
267517_At	0.693	0.602	At2g30520	RPT2 (ROOT PHOTOTROPISM 2)	signalling.light
259431_At	0.679	0.863	At1g01620	**PIP1;3**	transport.Major Intrinsic Proteins.PIP

266927_At	0.885	0.675	At2g45960 **PIP1;2**	transport.Major Intrinsic Proteins.PIP
258054_At	0.695	0.780	At3g16240 **TIP2;1**	transport.Major Intrinsic Proteins.TIP
257313_At	0.817	0.783	At3g26520 **TIP1;2**	transport.Major Intrinsic Proteins.TIP

Genes common to *PIP2;1* and *PIP2;2/2;3*				
Probe Set	r-value PIP2;2 / 2;3	r-value PIP2;1	AGI code Annotation	MAPMAN classification
257749_at	*0.606*	*0.655*	*AT1G49240 actin 8 (ACT8)* *AT3G18780 actin 2 (ACT2)*	*cell.organisation*
249073_At	0.651	0.602	AT5G44020 acid phosphatase class B family protein	misc.acid and other phosphatases
266927_At	0.676	0.885	AT2G45960 **PIP1;2**	transport.Major Intrinsic Proteins.PIP
251324_At	0.828	0.786	AT3G61430 **PIP1;1**	transport.Major Intrinsic Proteins.PIP
263867_At	0.782	0.604	AT2G36830 **TIP1;1**	transport.Major Intrinsic Proteins.TIP

Genes common to *PIP2;4* and *PIP2;2/2;3*				
Probe Set	r-value PIP2;2 / 2;3	r-value PIP2;4	AGI code Annotation	MAPMAN classification
256900_at	0.623	0.798	AT3G24670 pectate lyase family protein	cell wall.degradation.pectate lyases and polygalacturonases
264157_at	0.623	0.806	AT1G65310 xyloglucan:xyloglucosyl transferase, putative	cell wall.modification
260765_at	0.601	0.620	AT1G49240 actin 8 (ACT8)	cell.organisation
265439_at	0.706	0.795	AT2G21045 senescence-associated family protein	development.unspecified
263664_at	0.648	0.609	AT1G04250 auxin-responsive protein / indoleacetic acid-induced protein 17 (IAA17)	hormone metabolism.auxin
246216_at	0.674	0.768	AT4G36380 cytochrome P450 90C1 (CYP90C1) / rotundifolia3 (ROT3)	hormone metabolism.brassinosteroid
261727_at	0.656	0.677	AT1G76090 S-adenosyl-methionine-sterol-C-methyltransferase	hormone metabolism.brassinosteroid
246390_at	0.611	0.640	AT1G77330 1-aminocyclopropane-1-carboxylate oxidase/ ACC oxidase, putative	hormone metabolism.ethylene
266838_at	0.649	0.614	AT2G25980 jacalin lectin family protein	hormone metabolism.jasmonate
266356_at	0.634	0.834	AT2G32300 uclacyanin I	misc.oxidases - copper, flavone etc.
247091_at	0.604	0.779	AT5G66390 peroxidase 72 (PER72) (P72) (PRXR8)	misc.peroxidases
259276_at	0.613	0.764	AT3G01190 peroxidase 27 (PER27) (P27) (PRXR7)	misc.peroxidases
254820_s_at	0.695	0.795	AT4G12510 protease inhibitor/seed storage/lipid transfer protein (LTP) family protein	misc.protease inhibitor/seed storage/lipid transfer prot.
254718_at	0.647	0.811	AT4G13580 disease resistance-responsive family protein	not assigned.disagreeing hits
250663_at	0.607	0.736	AT5G07110 prenylated rab acceptor (PRA1) family protein	not assigned.no ontology
250717_at	0.658	0.790	AT5G06200 integral membrane family protein	not assigned.no ontology
259291_at	0.618	0.906	AT3G11550 integral membrane family protein	not assigned.no ontology
263284_at	0.724	0.864	AT2G36100 integral membrane family protein	not assigned.no ontology
265645_at	0.657	0.850	AT2G27370 integral membrane family protein	not assigned.no ontology
266884_at	0.703	0.708	AT2G44790 uclacyanin II	not assigned.no ontology

253629_at	0.681	0.618	AT4G30450	glycine-rich protein	not assigned.no ontology.glycine rich proteins
246142_at	0.665	0.744	AT5G19970	expressed protein ; expression supported by MPSS	not assigned.unknown
250844_at	0.604	0.686	AT5G04470	expressed protein	not assigned.unknown
263227_at	0.646	0.749	AT1G30750	expressed protein	not assigned.unknown
264998_at	0.649	0.813	AT1G67330	expressed protein	not assigned.unknown
247755_at	0.619	0.871	AT5G59090	subtilase family protein contains similarity to prepro-cucumisin	protein.degradation.subtilases
259854_at	0.685	0.942	AT1G72200	zinc finger (C3HC4-type RING finger) family protein	protein.degradation.ubiquitin.E3.RING
265031_at	0.689	0.857	AT1G61590	protein kinase, putative	protein.postranslational modification.kinase
250697_at	0.602	0.693	AT5G06800	myb family transcription factor	RNA.regulation of transcription.G2-like transcription factor
259274_at	0.631	0.791	AT3G01220	homeobox-leucine zipper protein/ HD-ZIP transcription factor, putative	RNA.regulation of transcription.Homeobox transcription factor
258619_at	0.636	0.773	AT3G02780	isopentenyl-diphosphate delta-isomerase II	secondary metabolism.isoprenoids.mevalonate pathway
254506_at	0.610	0.854	AT4G20140	leucine-rich repeat transmembrane protein kinase	signalling.receptor kinases.leucine rich repeat XI
264577_at	0.621	0.871	AT1G05260	peroxidase 3 (PER3) (P3) / rare cold-inducible protein (RCI3A) (PRC)	stress.abiotic.cold
263437_at	0.630	0.751	AT2G28670	disease resistance-responsive family protein/ fibroin-related	stress.biotic
266978_at	0.624	0.823	AT2G39430	disease resistance-responsive protein-related / dirigent protein-related	stress.biotic
245399_at	0.782	0.652	AT4G17340	**TIP2;2**	transport.Major Intrinsic Proteins.TIP
248790_at	0.701	0.859	AT5G47450	**TIP2;3**	transport.Major Intrinsic Proteins.TIP
249152_s_at	0.626	0.700	AT5G43350	inorganic phosphate transporter (PHT1) (PT1)	transport.phosphate

Genes in common with PIP2;4 and PIP2;7/PIP2;8					
Probe Set	r-value PIP2;4	r-value PIP2;7/2;8	AGI code	Annotation	MAPMAN classification
250102_at	0.624	0.609	AT5G16590	leucine-rich repeat transmembrane protein kinase, putative	signalling.receptor kinases.leucine rich repeat III

PIP1;2 and acid phosphatase B in common among *PIP2;1, PIP2;2/2;3* and *PIP2;7/2;8*					
Probe Set	r-value PIP2;1	r-value PIP2;2/2;3	r-value PIP2;7/2;8	AGI code	Annotation	MAPMAN classification
249073_At	0.602	0.651	0.686	At5g44020	acid phosphatase class B family protein	misc.acid and other phosphatases
266927_At	0.885	0.676	0.675	At2g45960	**PIP1;2**	transport.Major Intrinsic Proteins.PIP

ACTIN2/8 were co-expressed with *PIP2;1*, *PIP2;2/2;3* and *PIP2;4*, but detected with two different probe sets					
Probe Set	r-value PIP2;1	r-value PIP2;2/2;3	r-value PIP2;4	AGI code	Annotation	MAPMAN classification
257749_at	*0.606*	*0.655*	-	*AT1G49240* actin 8 (ACT8) *AT3G18780* actin 2 (ACT2)	*cell.organisation*
260765_at	-	0.601	0.620	AT1G49240 actin 8 (ACT8)	cell.organisation

Supplementary Table 4 to 8. *PIP2* **correlated genes classified into functional categories based on MapMan (Thimm et al., 2004).** Correlated genes were retrieved at BAR using distinct AtGenExpress array datasets. All datasets showing *PIP2* correlated genes with a Pearson correlation coefficient above 0.6 (or below 0.6 for negative correlation) were analyzed. For each category, percentage relative to all genes in the column, the number of assigned genes (in brackets) is indicated. Significance of over-representation for each functional category was determined using a Fisher's exact test (two-sided). The asterisks denote different levels of significance based on p-values (two-sided Fisher's Exact test; Methods 2.2.10): $***$ $< 10^{-10}$, $**$ $< 10^{-5}$, and $*$ < 0.002. +/- correspond to positively or negatively correlated gene lists, respectively.

Supplementary Table 4. Functional categories assignment of *PIP2;1* correlated genes.

Category	Expected Frequency Whole genome (MapMan)	Observed Frequency					
		Abiotic root + (out of 39)	Abiotic shoot + (out of 198)	Hormone + (out of 116)	Biotic + (out of 404)	Biotic – (out of 162)	Abiotic shoot – (out of 171)
Photosynthesis	0.8% (177)	-	16.2% (32)***	31% (36)***	15.8% (64)***	-	-
CHO metabolism	1% (222)	2.6% (1)	0.5% (1)	-	1.5% (6)	-	1.8% (3)
Glycolysis/ TCA	0.6% (132)	-	1% (2)	6% (7)**	1% (4)	2.5% (4)	2.9% (5)
C, S, N metabolism	0.7% (153)	-	-	1.7% (2)	1% (4)	-	1.8% (3)
Cell wall	2% (477)	5.1% (2)	1% (2)	0.9% (1)	2.2% (9)	-	0.6% (1)
Lipid metabolism	1.6% (381)	-	2% (4)	0.9% (1)	3.5% (14)	2.5% (4)	1.8% (3)
Amino acid metabolism	1.3% (297)	-	1% (2)	3.4% (4)	1.5% (6)	-	2.9% (5)
Metal handling	0.3% (73)	-	0.5% (1)	0.9% (1)	0.2% (1)	0.6% (1)	0.6% (1)
Secondary metabolism	1.8% (410)	-	4.5% (9)	-	2.2% (9)	-	1.2% (2)
Hormone metabolism	2.4% (555)	2.6% (1)	5.1% (10)	0.9% (1)	2.2% (9)	0.6% (1)	2.3% (4)
Tetrapyrrole synthesis	0.4% (88)	-	3% (6) *	2.6% (3)	3.2% (13)**	0.6% (1)	1.2% (2)
Mito. e- transport/ ATP ∑	0.4% (102)	2.6% (1)	0.5% (1)	0.9% (1)	0.7% (3)	1.2% (2)	-
Stress	3.5% (822)	2.6% (1)	2% (4)	1.7% (2)	1.7% (7)	3.7% (6)	1.8% (3)
Redox regulation	0.8% (177)	2.6% (1)	1.5% (3)	2.6% (3)	2.5% (10)*	1.9% (3)	2.3% (4)
Nucleotide metabolism	0.6% (142)	-	1% (2)	0.9% (1)	0.5% (2)	0.6% (1)	-
Miscellaneous	5.3% (1241)	5.1% (2)	7.1% (14)	5.2% (6)	5.2% (21)	5.6% (9)	5.8% (10)
RNA metabolism	10.6% (2465)	15.4% (6)	6.1% (12)	0.9% (1)	4.2% (17)	6.2% (10)	9.4% (16)
DNA	3.8% (884)	2.6% (1)	-	-	1% (4)	0.6% (1)	1.2% (2)
Protein metabolism	12.5% (2924)	2.6% (1)	4.5% (9)	15.5% (18)	9.4% (38)	17.9% (29)	18.1% (31)
Signaling	4.6% (1079)	2.6% (1)	2.5% (5)	-	2.5% (10)	4.3% (7)	3.5% (6)
Cell	2.6% (597)	-	0.5% (1)	3.4% (4)	2% (8)	3.1% (5)	2.9% (5)
Development	2.2% (514)	2.6% (1)	2.5% (5)	1.7% (2)	1.2% (5)	1.2% (2)	2.3% (4)
Transport	3.7% (857)	25.6% (10)**	8.1% (16)	6.9% (8)	4.2% (17)	6.8% (11)	7% (12)
Not assigned	36.7% (8553)	25.6% (10)	28.8% (57)	12.1% (14)	30.4% (123)	40.1% (65)	28.7% (49)

Supplementary Table 5. Functional categories assignment of *PIP2;2/PIP2;3* correlated genes.

Category	Expected Frequency		Observed Frequency	
	Whole genome (MapMan)	Abiotic root + (out of 125)	Abiotic root - (out of 74)	Abiotic shoot + (out of 165)
Photosynthesis	0.8% (177)	-	1.4% (1)	0.6% (1)
CHO metabolism	1% (222)	-	2.7% (2)	0.6% (1)
Glycolysis/ TCA	0.6% (132)	0.8% (1)	-	0.6% (1)
C, S, N metabolism	0.7% (153)	1.6% (2)	-	-
Cell wall	2% (477)	5.6% (7)	2.7% (2)	0.6% (1)
Lipid metabolism	1.6% (381)	1.6% (2)	2.7% (2)	0.6% (1)
Amino acid metabolism	1.3% (297)	-	2.7% (2)	0.6% (1)
Metal handling	0.3% (73)	-	-	0.6% (1)
Secondary metabolism	1.8% (410)	1.6% (2)	2.7% (2)	-
Hormone metabolism	2.4% (555)	3.2% (4)	5.4% (4)	1.8% (3)
Tetrapyrrole synthesis	0.4% (88)	0.8% (1)	1.4% (1)	-
Mito. e- transp./ ATP $\sum$	0.4% (102)	**4% (5)***	-	1.2% (2)
Stress	3.5% (822)	4.8% (6)	4.1% (3)	**20% (33)*****
Redox regulation	0.8% (177)	2.4% (3)	-	0.6% (1)
Nucleotide metabolism	0.6% (142)	1.6% (2)	-	-
Miscellaneous	5.3% (1241)	4.8% (6)	**18.9% (14)***	1.2% (2)
RNA metabolism	10.6% (2465)	4% (5)	8.1% (6)	9.1% (15)
DNA	3.8% (884)	-	-	0.6% (1)
Protein metabolism	12.5% (2924)	12.8% (16)	4.1% (3)	11.5% (19)
Signaling	4.6% (1079)	8.8% (11)	5.4% (4)	4.2% (7)
Cell	2.6% (597)	2.4% (3)	1.4% (1)	3.6% (6)
Development	2.2% (514)	2.4% (3)	8.1% (6)	0.6% (1)
Transport	3.7% (857)	**12% (15)***	9.5% (7)	4.2% (7)
Not assigned	36.7% (8553)	24.8% (31)	18.9% (14)	37% (61)

Supplementary Table 6. Functional categories assignment of *PIP2;4* and *PIP2;5* correlated genes.

Category	Expected Frequency	Observed Frequency		
		PIP2;4		*PIP2;5*
	Whole genome (MapMan)	Abiotic root + (out of 155)	Hormone (out of 71)	Abiotic shoot + (out of 133)
Photosynthesis	0.8% (177)	-	-	-
CHO metabolism	1% (222)	0.6% (1)	-	3.8% (5)
Glycolysis/ TCA	0.6% (132)	-	-	1.5% (2)
C, S, N metabolism	0.7% (153)	1.3% (2)	-	0.8% (1)
Cell wall	2% (477)	**15.5% (24)********	**12.7% (9)***	6% (8)
Lipid metabolism	1.6% (381)	1.3% (2)	1.4% (1)	3% (4)
Amino acid metabolism	1.3% (297)	-	-	1.5% (2)
Metal handling	0.3% (73)	0.6% (1)	-	0.8% (1)
Secondary metabolism	1.8% (410)	3.2% (5)	2.8% (2)	1.5% (2)
Hormone metabolism	2.4% (555)	3.9% (6)	1.4% (1)	1.5% (2)
Tetrapyrrole synthesis	0.4% (88)	-	1.4% (1)	-
Mito. e- transport/ ATP $\sum$	0.4% (102)	-	-	-
Stress	3.5% (822)	**11.6% (18)***	7% (5)	7.5% (10)
Redox regulation	0.8% (177)	-	-	-
Nucleotide metabolism	0.6% (142)	-	-	0.8% (1)
Miscellaneous	5.3% (1241)	**13.5% (21)***	**19.7% (14)***	6.8% (9)
RNA metabolism	10.6% (2465)	3.2% (5)	5.6% (4)	9.8% (13)
DNA	3.8% (884)	1.9% (3)	-	-
Protein metabolism	12.5% (2924)	5.2% (8)	4.2% (3)	10.5% (14)
Signaling	4.6% (1079)	7.1% (11)	7% (5)	2.3% (3)
Cell	2.6% (597)	3.2% (5)	1.4% (1)	2.3% (3)
Development	2.2% (514)	4.5% (7)	1.4% (1)	2.3% (3)
Transport	3.7% (857)	6.5% (10)	**16.9% (12)***	5.3% (7)
Not assigned	36.7% (8553)	16.8% (26)	16.9% (12)	32.3% (43)

Supplementary Table 7. Functional categories assignment of *PIP2;6* correlated genes.

Category	Expected Frequency	Observed Frequency			
	Whole genome (MapMan)	Abiotic shoot + (out of 176)	hormone + (out of 87)	Biotic + (out of 334)	Biotic - (out of 288)
Photosynthesis	0.8% (177)	-	**14.9% (13)***	**13.8% (46)***	-
CHO metabolism	1% (222)	1.7% (3)	-	1.5% (5)	0.3% (1)
Glycolysis/ TCA	0.6% (132)	-	2.3% (2)	1.2% (4)	**4.2% (12)***
C, S, N metabolism	0.7% (153)	1,1% (2)	-	2.7% (4)	0.3% (1)
Cell wall	2% (477)	4.5% (8)	1.1% (1)	**6% (20)***	1% (3)
Lipid metabolism	1.6% (381)	2.8% (5)	1.1% (1)	3.6% (12)	2.8% (8)
Amino acid metabol.	1.3% (297)	0.6% (1)	3.4% (3)	0.6% (2)	0.7% (2)
Metal handling	0.3% (73)	0.6% (1)	-	0.6% (2)	0.3% (1)
Secondary metabol.	1.8% (410)	1.1% (2)	1.1% (1)	1.8% (6)	-
Hormone metabol.	2.4% (555)	4.5% (8)	2.3% (2)	2.7% (9)	1% (3)
Tetrapyrrole synth.	0.4% (88)	-	-	**2.1% (7)***	0.3% (1)
Mito. e- transp./ ATP $\sum$.	0.4% (102)	-	-	-	1.4% (4)
Stress	3.5% (822)	**10.2% (18)***	1.1% (1)	3.3% (11)	3.1% (9)
Redox regulation	0.8% (177)	-	**5.7% (5)***	**2.7% (9)***	**3.5% (10)***
Nucleotide metabolism	0.6% (142)	1.7% (3)	1.1% (1)	0.6% (2)	0.7% (2)
Miscellaneous	5.3% (1241)	7.4% (13)	5.7% (5)	5.4% (18)	7.3% (21)
RNA metabolism	10.6% (2465)	11.4% (20)	3.4% (3)	4.2% (14)	4.2% (12)
DNA	3.8% (884)	2.3% (4)	1.1% (1)	0.6% (2)	0.3% (1)
Protein metabolism	12.5% (2924)	6.3% (11)	11.5 % (10)	9.3% (31)	**22.9% (66)***
Signaling	4.6% (1079)	4% (7)	-	3.3% (11)	4.9% (14)
Cell	2.6% (597)	1.7% (3)	5.7% (5)	2.7% (9)	1.7% (5)
Development	2.2% (514)	2.3% (4)	2.3% (2)	1.2% (4)	0.7% (2)
Transport	3.7% (857)	5.7% (10)	6.9% (6)	2.7% (9)	4.9% (14)
Not assigned	36.7% (8553)	30.1% (53)	28.7% (25)	29% (97)	33.3% (96)

Supplementary Table 8. Functional categories assignment of *PIP2;7/PIP2;8* correlated genes.

Category	Expected Frequency	Observed Frequency				
	Whole genome (MapMan)	Abiotic root + (out of 245)	Abiotic shoot + (out of 280)	Abiotic shoot - (out of 232)	Hormone + (out of 154)	Biotic + (out of 92)
Photosynthesis	0.8% (177)	2% (5)	7.1% (20)***	-	22.7% **(35)*****	1.1% (1)
CHO metabolism	1% (222)	0.4% (1)	0.7% (2)	1.7% (4)	-	-
Glycolysis/ TCA	0.6% (132)	1.2% (3)	0.4% (1)	5.6% **(13)****	2.6% (4)	-
C, S, N metabolism	0.7% (153)	-	1.4% (4)	1.7% (4)	2.6% (4)	-
Cell wall	2% (477)	0.8% (2)	2.5% (7)	0.9% (2)	3.9% (6)	6.5% (6)
Lipid metabolism	1.6% (381)	1.6% (4)	2.5% (7)	1.7% (4)	1.3% (2)	4.3% (4)
Amino acid metabol.	1.3% (297)	0.8% (2)	0.4% (1)	1.3% (3)	1.3% (2)	-
Metal handling	0.3% (73)	0.4% (1)	0.4% (1)	1.3% (3)	-	-
Secondary metabol.	1.8% (410)	0.8% (2)	2.1% (6)	1.7% (4)	0.6% (1)	2.2% (2)
Hormone metabol.	2.4% (555)	1.6% (4)	8.2% **(23)****	1.3% (3)	1.3% (2)	3.3% (3)
Tetrapyrrole synthesis	0.4% (88)	0.4% (1)	1.8% (5)	0.4% (1)	1.3% (2)	-
Mito. e- transport/ ATP $\sum$	0.4% (102)	1.2% (3)	-	-	0.6% (1)	-
Stress	3.5% (822)	11.8% **(29)****	1.1% (3)	2.2% (5)	3.2% (5)	1.1% (1)
Redox regulation	0.8% (177)	2% (5)	1.4% (4)	1.7% (4)	4.5% **(7)***	-
Nucleotide metabolism	0.6% (142)	-	0.4% (1)	0.9% (2)	0.6% (1)	-
Miscellaneous	5.3% (1241)	1.6% (4)	7.5% (21)	11.2% **(26)***	3.2% (5)	7.6% (7)
RNA metabolism	10.6% (2465)	9.4% (23)	8.9% (25)	9.5% (22)	1.3% (2)	6.5% (6)
DNA	3.8% (884)	0.4% (1)	0.7% (2)	0.9% (2)	-	1.1% (1)
Protein metabolism	12.5% (2924)	18% (44)	7.9% (22)	11.6% (27)	29.9% **(46)****	3.3% (3)
Signaling	4.6% (1079)	2.4% (6)	5.4% (15)	5.2% (12)	1.3% (2)	12% (11)
Cell	2.6% (597)	4.1% (10)	1.8% (5)	2.2% (5)	3.2% (5)	2.2% (2)
Development	2.2% (514)	1.2% (3)	2.1% (6)	1.3% (3)	0.6% (1)	2.2% (2)
Transport	3.7% (857)	3.7% (9)	5% (14)	4.7% (11)	3.9% (6)	4.3% (4)
Not assigned	36.7% (8553)	33.9% (83)	30.4% (85)	31% (72)	9.7% (15)	42.4% (39)

Supplementary Table 9. Expression ratios (log2) of *PIP* transcripts with respect to control plants for 54 stress conditions and treatments extracted using the Meta-Analyzer tool at Genevestigator (Version 3; Zimmermann et al., 2005). Repression < -0.74 (< 0.6-fold) were underlined in blue, inductions > 0.74 (>1.67-fold) were labeled in red. Accordingly, total number of deregulations for each PIP members is listed.

Stress/Treatment		PIP2;1	PIP2;2/ PIP2;3	PIP2;4	PIP2;5	PIP2;6	PIP2;7/ PIP2;8	PIP1,1	PIP1;2	PIP1;3	PIP1,4	PIP1;5
BIOTIC	B. cinerea (+)	-0.6	-0.3	-1.0	0.1	-0.4	-1.1	0.0	-0.6	-1.1	0.3	-1.0
	E. orontii (+)	0.0	0.3	-0.3	-0.1	-0.1	0.2	0.0	0.1	0.2	-0.2	0.1
	P. infestans (+)	-0.6	-0.5	0.5	-0.8	-0.8	-0.7	0.2	-0.3	-1.1	-0.8	-0.9
	Ps. syringae pv. Tomato DC3000 (+)	-0.2	0.6	0.4	1.4	-0.2	-0.4	0.6	0.0	-0.2	0.9	-1.2
HORMONE-INHIBITORS	2,4,6 T (+) (auxin inhibitor)	-0.2	-1.0	-1.2	-0.5	-0.2	-0.2	-0.5	-0.4	-0.3	-0.2	-0.6
	AgNO3 (+) (ethylene inhibitor)	-0.7	-1.3	-3.5	-0.4	-0.7	-0.1	-0.7	-0.6	-0.6	-1.1	-1.9
	AVG (+) (ethylene inhibitor)	0.1	0.0	0.6	0.5	0.0	-0.1	0.1	-0.1	0.5	0.2	0.4
	brz220 (+) (brassinosteroid biosynthesis inhibitor)	-0.2	-0.2	-0.2	-0.2	-0.3	-0.1	0.0	-0.3	-0.2	-0.3	-0.3
	brz91 (+) (brassinosteroid biosynthesis inhibitor)	-0.1	-0.3	-0.6	-0.5	-0.2	0.1	-0.1	-0.2	0.0	-0.3	0.0
	daminozide (+) (ethylene inhibitor)	0.2	-0.1	0.0	-0.4	0.0	0.3	0.1	0.0	0.2	0.1	0.0
	ibuprofen (+) (jasmonic acid biosynthesis inhibitor)	-0.1	-0.6	-0.5	0.1	-0.3	0.4	0.0	-0.2	-0.3	0.0	-0.6
	NPA (+) (auxin transport inhibitor)	-0.1	-0.3	-1.1	0.1	0.0	-0.2	-0.1	-0.2	-0.3	-0.2	-0.2
	paclobutrazole (+) (gibberellic acid biosynthesis inhibitor)	0.0	0.0	0.4	-0.5	-0.1	-0.1	0.1	-0.1	0.1	-0.3	0.1
	PCIB (+) (auxin inhibitor)	0.2	-0.2	-0.7	0.1	0.0	0.1	0.0	0.0	0.3	-0.2	0.0
	prohexadione (+) (gibberellic acid biosynthesis inhibitor)	0.3	0.1	0.2	-0.5	0.3	0.3	0.4	0.2	0.5	0.0	0.2
	propiconazole (+) (gibberellic acid biosynthesis inhibitor)	-0.2	-0.3	-0.6	-0.4	-0.3	0.0	-0.1	-0.4	-0.3	-0.3	-0.4
	TIBA (+) (auxin transport inhibitor)	-0.9	-1.3	-1.6	0.0	-0.1	0.1	-0.8	-0.5	-0.3	-0.4	-0.8
	uniconazole (+) (gibberellic acid biosynthesis inhibitor)	0.0	-0.1	0.0	-0.1	-0.2	0.0	0.1	-0.2	-0.1	-0.3	-0.2
HORMONE	Abscisic acid (+)	0.2	0.1	-0.4	0.5	0.2	0.0	0.2	0.4	0.5	0.7	0.0
	ACC (+)	-0.4	-0.2	0.0	-0.1	-0.3	-0.2	-0.1	-0.2	-0.4	-0.4	-0.1
	BL (+) (Brassinolide)	-0.1	0.0	0.3	0.1	-0.2	0.1	0.0	0.2	0.2	-0.1	0.2
	GA3 (+) (Gibberellic acid)	-0.1	-0.1	0.1	0.2	-0.1	0.0	-0.1	-0.1	0.1	-0.1	0.3
	IAA (auxin)	-0.5	-0.4	-1.0	-0.5	0.0	0.0	-0.4	-0.1	-0.2	-0.2	-0.3
	Methyl-Jasmonate (+)	-0.1	-0.1	0.2	0.2	-0.2	0.0	0.1	-0.2	-0.3	-0.2	-0.1
	salicylic acid (+)	-0.8	-0.9	-1.3	-0.7	-0.4	0.0	-0.8	-0.7	-0.3	-0.5	-0.6
	zeatin (+) (cytokinins family)	-0.2	-0.3	0.3	0.0	0.0	0.1	-0.4	-0.1	0.2	0.1	0.0
ABIOTIC	Nutrient: Nitrate_low	-0.7	-0.4	0.5	0.1	-0.7	0.1	-0.5	-0.4	-0.4	0.3	0.1
	Nutrient: S deprivation	-0.1	-0.3	-0.1	-0.2	-0.1	-0.1	-0.2	0.0	-0.1	0.0	-0.1
	cold_green_early	0.2	0.3	-0.3	0.2	-0.1	0.0	0.2	0.1	-0.2	0.0	-0.3
	cold_green_late	0.0	-0.4	0.4	1.0	0.9	-0.2	-0.3	-0.3	-0.6	-0.2	-0.4
	cold_roots_early	0.2	0.3	0.5	-0.2	0.6	0.0	0.3	0.2	0.3	0.4	0.1
	cold_roots_late	0.5	-0.3	0.8	1.2	1.0	-0.2	-0.4	0.0	0.0	-0.3	-0.4
	drought_green_early	0.1	1.3	-0.1	0.6	0.1	0.0	0.2	0.1	-0.1	0.1	-0.5
	drought_green_late	0.2	0.8	0.4	-0.1	0.1	0.1	0.4	0.2	0.1	0.0	0.2
	drought _roots_early	-0.3	0.0	-0.6	0.2	0.0	0.1	-0.2	-0.1	0.0	-0.1	-0.5
	drought _roots_late	-0.1	-0.1	-0.2	1.1	-0.1	0.0	0.1	0.2	-0.1	-0.1	-0.5
	heat_green	0.3	1.9	-0.2	0.8	0.2	0.4	0.1	0.2	0.1	0.5	0.1
	heat_roots	0.5	0.5	-0.3	-0.3	0.0	0.6	0.3	0.5	0.3	1.1	0.2
	osmotic_green_early	0.0	0.6	-0.3	0.1	-0.1	-0.3	0.2	-0.2	-0.3	-0.1	-0.8
	osmotic_green_late	-0.7	-0.4	0.4	0.5	0.1	-0.9	0.3	-0.7	-1.2	0.6	-2.5
	osmotic_roots_early	-0.1	0.0	-0.9	0.0	0.0	0.1	-0.1	0.2	-0.1	0.5	-0.7
	osmotic_roots_late	-0.2	-0.8	-0.7	-0.2	-0.2	0.2	-0.8	0.5	0.2	0.9	-1.4
	oxidative_green_early	-0.1	0.1	-0.1	0.1	0.0	0.1	0.0	0.0	-0.1	0.0	-0.2
	oxidative_green_late	-0.1	0.2	0.1	-0.1	0.1	0.1	-0.1	-0.1	-0.3	0.0	0.0
	oxidative_roots_early	-0.1	0.0	-0.8	0.0	-0.1	0.0	0.0	0.0	-0.1	0.0	-0.1
	oxidative_roots_late	-0.1	-0.1	-0.4	0.1	-0.2	-0.1	-0.3	0.1	0.0	0.0	-0.2
	salt_green_early	0.2	0.5	-0.1	0.5	0.1	-0.1	0.3	0.1	0.0	0.1	-0.4
	salt_green_late	-0.1	0.0	0.4	1.0	0.4	-0.4	0.0	-0.1	-0.5	0.5	-1.2
	salt_roots_early	-0.2	-0.3	-1.3	0.1	0.0	0.0	-0.2	0.0	-0.2	0.2	-0.7
	salt_roots_late	-0.7	-1.0	-0.6	-0.5	-0.4	-0.5	-1.0	0.0	-0.3	0.7	-1.7
	wounding_green_early	0.0	0.1	-0.2	0.0	0.3	-0.1	-0.1	-0.2	-0.4	-0.3	-0.5
	wounding_green_late	0.0	-0.2	-0.2	-0.4	-0.3	-0.1	0.1	-0.2	-0.2	-0.2	-0.2
	wounding_roots_early	0.0	0.1	-0.1	0.2	0.0	0.1	0.3	0.1	0.1	0.0	0.1
	wounding_roots_late	0.1	0.1	0.2	-0.1	0.1	0.0	0.1	0.0	0.2	-0.4	0.3

	PIP2;1	PIP2;2/ PIP2;3	PIP2;4	PIP2;5	PIP2;6	PIP2;7/ PIP2;8	PIP1,1	PIP1;2	PIP1;3	PIP1,4	PIP1;5
Total number of deregulations	**3**	**9**	**11**	**7**	**4**	**2**	**4**	**0**	**3**	**5**	**10**
Responses to biotic stresses	0	0	1	2	1	1	0	0	**2**	**2**	3
Responses to chemicals/ hormone inhibitors	1	3	**4**	0	0	0	1	0	0	1	2
Responses to hormones	1	1	2	0	0	0	1	0	0	0	0
Responses to abiotic stresses	1	**5**	4	5	3	1	**2**	0	1	2	5

Supplementary Table 10. Promoter elements in *PIP2;2* and *PIP2;3*. (a) A summary of the families related to transcription factor binding sites that were found in both promoters with -1000 and +100 bp sequences with respect to the translation start site. Families labelled in bold were selected and depicted in Supplementary Figure 2. (b) All individual sites for both promoters are listed with their exact position, sequence and similarities to both the consensus matrix and the four-nucleotide core sequence. In a few cases (e.g. CCAF) the same number of sites were found, yet with a different distribution.
[MatInspectorprofessional 7.6.2, November 2007; Search Jan 17, 2008 at www.genomatix.de].

(a)

Family	PIP2;2	PIP2;3	Comment
ABRE	1	2	
AHBP	15	10	
AREF	1	1	
CAAT	1	1	
CCAF	3	3	different arrangement in PIP2;3
CE1F	0	1	only found in PIP2;3
DOFF	3	8	two additional duplicated sites in PIP2;3
DREB	2	0	only found in PIP2;2
EINL	2	1	
GAGA	1	0	only found in PIP2;2
GAPB	2	2	
GBOX	4	6	
GTBX	7	8	
HEAT	4	1	
HMGF	1	0	
IBOX	4	2	
IDDF	3	2	
L1BX	4	6	additional duplett in PIP2;3
LEGB	0	2	
LFYB	1	0	
LREM	4	2	
MADS	5	6	
MIIG	1	1	
MSAE	0	2	only found in PIP2;3
MYBL	9	15	
MYBS	3	6	additional sites with one triplett in PIP2;3
MYCL	0	2	only found in PIP2;3
NACF	0	2	
NCS1	1	4	three adiitonal sites in PIP2;3
NCS2	2	0	only found in PIP2;2
OCSE	4	4	
OPAQ	2	5	
PSRE	2	2	
ROOT	1	0	
SEF4	1	0	
SPF1	2	2	
STKM	2	2	
SUCB	3	3	duplett just before translation start in PIP2;3
TBPF	2	10	
TEFB	1	1	
TELO	1	1	
WBXF	0	2	only found in PIP2;3

(b)

PIP	Family/Matrix	Opt. thre-shold	Start pos.	End pos.	Str and	Matri x sim.	Core sim.	Sequence
2;2	HEAT/ HSE.01	0.81	9	23	+	0.820	1	agctccttctAGAAa
2;2	GTBX/ SBF1.01	0.87	17	33	+	0.876	1	ctagaaaTTAAatgaag
2;2	L1BX/ ATML1.02	0.76	17	33	-	0.765	1	cttCATTtaatttctag
2;2	L1BX/ PDF2.01	0.85	19	35	+	0.885	1	agaaatTAAAtgaagga
2;2	LREM/ ATCTA.01	0.85	41	51	+	0.888	1	gaATCTagata
2;2	LREM/ ATCTA.01	0.85	42	52	-	0.902	1	ttATCTagatt
2;2	SPF1/ SP8BF.01	0.87	61	73	+	0.936	1	ttTACTattgatc
2;2	DOFF/ DOF2.01	0.98	96	112	-	0.983	1	ttaacgatAAAGctttt
2;2	IBOX/ GATA.01	0.93	96	112	-	0.958	1	ttaacGATAaagctttt
2;2	GTBX/ SBF1.01	0.87	102	118	+	0.878	1	tttatcgTTAacaagta
2;2	MYBL/ NTMYBAS1.01	0.96	112	128	-	0.962	1	tgaaagttGTTActtgt
2;2	MYBL/ CARE.01	0.83	115	131	-	0.861	1	acttgaaAGTTgttact
2;2	MADS/ AGL1.01	0.84	131	151	+	0.865	1	tatTGCCcaaatagataaggt
2;2	IBOX/ GATA.01	0.93	139	155	+	0.975	1	aaataGATAaggttcat
2;2	EINL/ TEIL.01	0.92	147	155	-	0.991	0.964	aTGAAcctt
2;2	SUCB/ SUCROSE.01	0.81	158	176	-	0.815	1	atAAATaaaaaatatgaag
2;2	**CCAF/ CCA1.01**	0.85	**160**	**174**	-	0.861	0.757	aaataaaaAATAtga
2;2	HMGF/ HMG_IY.01	0.89	170	184	+	0.919	1	tattTATTttatgtg
2;2	AREF/ SEBF.01	0.96	188	200	-	0.983	1	gacTGTCactctt
2;2	AHBP/ BLR.01	0.90	201	211	+	0.929	1	tatATTAttct
2;2	IDDF/ ID1.01	0.92	235	247	-	0.923	1	tctcTTGTcctat
2;2	HEAT/ HSE.01	0.81	249	263	+	0.923	1	agaaaaatatAGAAg
2;2	SPF1/ SP8BF.01	0.87	262	274	-	0.877	1	taTACTatatgct
2;2	DREB/ CRT_DRE.01	0.89	275	289	-	0.924	1	ttggaCCGAccctaa
2;2	GAPB/ GAP.01	0.88	286	300	+	0.993	1	ccaaATGAaaacaac
2;2	DREB/ HVDRF1.01	0.89	308	322	-	0.910	0.826	cctcGCCGccccata
2;2	GTBX/ GT1.01	0.85	327	343	-	0.976	1	tttgtgGTTAatttaac
2;2	MIIG/ PALBOXP.01	0.81	328	342	-	0.823	0.936	ttGTGGttaatttaa
2;2	IBOX/ GATA.01	0.93	343	359	-	0.936	1	tggttGATAatggagtt
2;2	SUCB/ SUCROSE.01	0.81	349	367	-	0.843	1	taAAATtatggttgataat
2;2	L1BX/ HDG9.01	0.77	366	382	+	0.785	1	tagaatTAAAaggtctc
2;2	SUCB/ SUCROSE.01	0.81	401	419	+	0.855	0.75	caCAATcattcttttaaat
2;2	AHBP/ ATHB5.01	0.89	402	412	+	0.978	0.936	acaATCAttct
2;2	AHBP/ ATHB5.01	0.89	402	412	-	0.904	0.83	agaATGAttgt
2;2	**CCAF/ CCA1.01**	0.85	**418**	**432**	+	0.890	1	ataatcagAATCtca
2;2	AHBP/ BLR.01	0.90	431	441	-	0.924	0.791	gaaCTTAtttg
2;2	OCSE/ OCSL.01	0.69	433	453	-	0.691	0.769	gtaactaaagatgaACTTatt
2;2	EINL/ TEIL.01	0.92	435	443	-	0.926	0.964	aTGAActta
2;2	DOFF/ DOF1.01	0.98	439	455	-	0.997	1	ctgtaactAAAGatgaa
2;2	MYBL/ MYBPH3.02	0.76	441	457	+	0.772	1	catcttTAGTtacagat
2;2	AHBP/ HAHB4.01	0.87	487	497	-	0.923	1	attattATTAt
2;2	STKM/ STK.01	0.85	489	503	-	0.882	1	aacTAAAttattatt
2;2	AHBP/ ATHB5.01	0.89	490	500	+	0.903	0.83	ataATAAttta
2;2	AHBP/ BLR.01	0.90	490	500	-	0.998	1	taaATTAttat
2;2	MYBL/ MYBPH3.02	0.76	493	509	+	0.867	1	ataattTAGTtatagtt
2;2	AHBP/ BLR.01	0.90	494	504	+	0.920	0.826	taaTTTAgtta
2;2	GTBX/ SBF1.01	0.87	501	517	+	0.913	1	gttatagTTAAttttgt
2;2	IDDF/ ID1.01	0.92	510	522	+	0.929	1	aattTTGTcaaca
2;2	MYBL/ MYBPH3.02	0.76	529	545	-	0.814	1	atatgaTAGTtaaggta
2;2	IDDF/ ID1.01	0.92	545	557	-	0.924	1	gtgtTTGTcataa
2;2	TELO/ ATPURA.01	0.85	550	564	+	0.855	0.75	acaaACACtaattga
2;2	DOFF/ PBOX.01	0.75	562	578	+	0.756	0.761	tgagatgaAAAActctt
2;2	GAPB/ GAP.01	0.88	562	576	+	0.886	1	tgagATGAaaaactc
2;2	MYBL/ MYBPH3.01	0.80	568	584	+	0.809	0.75	gaaaaactCTTAgcagt
2;2	MADS/ AGL15.01	0.79	592	612	+	0.813	1	tctTACTatcatcagttaatt
2;2	MYBL/ MYBPH3.01	0.80	598	614	+	0.810	1	tatcatcaGTTAattat
2;2	AHBP/ HAHB4.01	0.87	607	617	-	0.914	1	agtataATTAa

2;2	MADS/ MADS.01	0.75	613	633	-	0.771	1	aatttCCATatacattagtat
2;2	PSRE/ GAAA.01	0.83	623	639	+	0.869	1	atatgGAAAttctgctt
2;2	LFYB/ LFY.01	0.93	649	661	-	0.969	1	tTCCactgtttt
2;2	AHBP/ ATHB5.01	0.89	703	713	-	0.940	0.936	ctaATCAttgc
2;2	AHBP/ HAHB4.01	0.87	703	713	+	0.967	1	gcaatgATTAg
2;2	LREM/ ATCTA.01	0.85	707	717	-	0.902	1	caATCTaatca
2;2	STKM/ STK.01	0.85	711	725	-	0.851	1	atcTAAAccaatcta
2;2	CAAT/ CAAT.01	0.97	712	720	-	0.975	1	aaCCAtct
2;2	LREM/ ATCTA.01	0.85	717	727	-	0.961	1	taATCTaaacc
2;2	**CCAF/ CCA1.01**	0.85	**720**	**734**	-	0.868	1	tgatatatAATCtaa
2;2	OPAQ/ O2.01	0.87	723	739	+	0.872	1	gattatataTCATcatg
2;2	OCSE/ OCSL.01	0.69	747	767	-	0.742	0.769	ttcactaattaattACCTagc
2;2	GTBX/ SBF1.01	0.87	749	765	+	0.881	1	taggtaaTTAAttagtg
2;2	GTBX/ S1F.01	0.79	768	784	-	0.793	0.75	ttttGTGGaaactttct
2;2	AHBP/ HAHB4.01	0.87	785	795	-	0.907	1	attatgATTAt
2;2	ROOT/ RHE.02	0.77	790	814	-	0.772	0.75	tagaattgtgtgtatGACGattatg
2;2	HEAT/ HSE.01	0.81	809	823	-	0.831	1	aaatgaatatAGAAt
2;2	GTBX/ S1F.01	0.79	821	837	+	0.816	0.75	tttcATTGaaacgaata
2;2	SEF4/ SEF4.01	0.98	836	846	-	0.998	1	tgTTTTtatta
2;2	IBOX/ GATA.01	0.93	866	882	-	0.955	1	attacGATAatgttttc
2;2	NCS1/ NCS1.01	0.85	866	876	+	0.856	1	gAAAAcattat
2;2	GBOX/ GBF1.01	0.94	890	910	-	0.968	1	aattgtatACGTgttattgat
2;2	ABRE/ ABRE.01	0.82	893	909	-	0.842	1	attgtatACGTgttatt
2;2	OCSE/ OCSL.01	0.69	896	916	-	0.766	1	gttaataattgtatACGTgtt
2;2	L1BX/ ATML1.01	0.82	901	917	-	0.834	0.75	cgttaaTAATtgtatac
2;2	OCSE/ OCSL.01	0.69	901	921	+	0.753	1	gtatacaattattaACGTata
2;2	AHBP/ ATHB5.01	0.89	905	915	+	1.000	1	acaATTAttaa
2;2	AHBP/ ATHB5.01	0.89	905	915	-	0.903	0.83	ttaATAAttgt
2;2	GBOX/ HBP1B.01	0.83	906	926	-	0.839	1	gtcaatatACGTtaataattg
2;2	AHBP/ BLR.01	0.90	931	941	+	1.000	1	aaaATTAatga
2;2	GAGA/ BPC.01	1.00	949	973	-	1.000	1	atatagAGAGactatagctatagtg
2;2	NCS2/ NCS2.01	0.79	958	972	+	0.794	1	tatagtCTCTctata
2;2	MYBS/ ZMMRP1.01	0.79	962	978	+	0.878	0.778	gtctctcTATAtaaaca
2;2	MYBS/ ZMMRP1.01	0.79	964	980	+	0.829	0.778	ctctctaTATAaacaac
2;2	TBPF/ TATA.02	0.90	965	979	+	0.950	1	tctcTATAtaaacaa
2;2	TBPF/ TATA.01	0.88	967	981	+	0.941	1	tctaTATAaacaact
2;2	NCS2/ NCS2.01	0.79	985	999	+	0.832	1	attcgtCTCTtcagt
2;2	MYBS/ OSMYBS.01	0.82	1011	1027	+	0.843	1	caacaTATCcacaatac
2;2	MYBL/ GAMYB.01	0.91	1042	1058	-	0.915	1	cttttttttGTTAtatat
2;2	MADS/ SQUA.01	0.90	1043	1063	-	0.908	0.837	tataactTTTTttgttatata
2;2	MYBL/ MYBPH3.01	0.80	1050	1066	+	0.813	1	caaaaaaaGTTAtagaa
2;2	HEAT/ HSE.01	0.81	1053	1067	+	0.815	1	aaaaagttatAGAAa
2;2	MADS/ SQUA.01	0.90	1055	1075	-	0.904	1	tttggccATTTctataactttt
2;2	PSRE/ GAAA.01	0.83	1059	1075	+	0.834	1	ttataGAAAtggccaaa
2;2	TEFB/ TEF1.01	0.76	1065	1085	+	0.787	0.839	aaATGGccaaagacgtggaag
2;2	GBOX/ HBP1A.01	0.88	1068	1088	-	0.918	1	gtccttcCACGtctttggcca
2;2	GBOX/ GBF1.01	0.94	1069	1089	+	0.971	1	ggccaaagACGTggaaggacc
2;2	OPAQ/ O2.02	0.87	1070	1086	-	0.961	1	ccttCCACGtctttggc
2;3	L1BX/ ATML1.02	0.76	1	17	+	0.777	0.89	taaCAATgaatccacaa
2;3	MYBL/ GAMYB.01	0.91	13	29	-	0.926	1	tatgatctGTTAttgtg
2;3	MYCL/ ICE.01	0.95	30	48	+	0.953	1	aaattACATctgactcata
2;3	OPAQ/ GCN4.01	0.81	35	51	-	0.887	1	acataTGAGtcagatgt
2;3	OPAQ/ GCN4.01	0.81	65	81	+	0.877	1	tatgtTGAGtcaatata
2;3	TBPF/ TATA.02	0.90	73	87	-	0.918	1	cgacTATAtattgac
2;3	TBPF/ TATA.02	0.90	90	104	+	0.932	1	ggagTATAatagag
2;3	TBPF/ TATA.02	0.90	91	105	-	0.966	1	actcTATAtatactc
2;3	MYBS/ ZMMRP1.01	0.79	92	108	-	0.817	0.778	ataactcTATAtatact
2;3	NCS1/ NCS1.01	0.85	157	167	+	0.852	1	aAAAAgttaag
2;3	OCSE/ OCSL.01	0.69	157	177	-	0.702	0.769	ttatttgagacttaACTTttt
2;3	OCSE/ OCSL.01	0.69	167	187	+	0.767	1	gtctcaaataaattACGTatt
2;3	AHBP/ BLR.01	0.90	171	181	-	0.936	0.826	taaTTTAtttg
2;3	GBOX/ HBP1B.01	0.83	172	192	-	0.865	1	gcataaatACGTaatttattt

2;3	L1BX/ PDF2.01	0.85	179	195	-	0.874	1	aacgcaTAAAtacgtaa
2;3	AHBP/ BLR.01	0.90	199	209	+	0.924	0.791	taaCTTAttat
2;3	GTBX/ GT1.01	0.85	209	225	-	0.899	0.844	ttttagGTCAttttgta
2;3	TBPF/ TATA.02	0.90	238	252	+	0.905	1	ttccTATAcaaatat
2;3	PSRE/ GAAA.01	0.83	241	257	+	0.856	0.75	ctataCAAAtattcgct
2;3	MADS/ AGL15.01	0.79	255	275	+	0.809	1	gctTACTatatatactatatg
2;3	TBPF/ TATA.02	0.90	257	271	+	0.966	1	ttacTATAtatacta
2;3	TBPF/ TATA.02	0.90	258	272	-	0.926	1	atagTATAtatagta
2;3	SPF1/ SP8BF.01	0.87	265	277	+	0.877	1	taTACTatatgtt
2;3	MYBL/ MYBPH3.02	0.76	272	288	-	0.787	0.779	gatagtTGGTaaacata
2;3	MYBL/ CARE.01	0.83	276	292	-	0.884	1	tcatgatAGTTggtaaa
2;3	GAPB/ GAP.01	0.88	285	299	+	0.926	1	tatcATGAaaaagat
2;3	NCS1/ NCS1.01	0.85	292	302	+	0.907	1	aAAAAgatgca
2;3	HEAT/ HSE.01	0.81	303	317	+	0.932	1	cgaatgatccAGAAt
2;3	NACF/ TANAC69.01	0.68	315	337	+	0.716	0.812	aatgtgcttgaAACGgcagaaaa
2;3	MSAE/ MSA.01	0.80	321	335	+	0.883	1	cttgaAACGgcagaa
2;3	AREF/ ARE.01	0.93	347	359	-	0.952	1	tcgTGTCacacga
2;3	IDDF/ ID1.01	0.92	360	372	-	0.923	1	gtatTTGTctcga
2;3	DOFF/ PBOX.01	0.75	367	383	-	0.791	1	tgattagtAAAGtattt
2;3	AHBP/ HAHB4.01	0.87	377	387	-	0.893	1	tatatgATTAg
2;3	TBPF/ TATA.01	0.88	380	394	+	0.907	1	atcaTATAaaatcat
2;3	SUCB/ SUCROSE.01	0.81	386	404	+	0.846	1	taAAATcattatttatcaa
2;3	AHBP/ ATHB5.01	0.89	387	397	-	0.903	0.83	ataATGAtttt
2;3	AHBP/ HAHB4.01	0.87	387	397	+	0.967	1	aaaatcATTAt
2;3	DOFF/ DOF3.01	0.99	405	421	+	0.996	1	aaacttaaAAAGcacct
2;3	MYBS/ TAMYB80.01	0.83	418	434	-	0.913	1	ttgcATATActgtaggt
2;3	L1BX/ ATML1.01	0.82	420	436	+	0.829	0.75	ctacagTATAtgcaatg
2;3	MYBS/ TAMYB80.01	0.83	423	439	+	0.894	1	cagtATATgcaatgtgg
2;3	MYBS/ MYBST1.01	0.90	431	447	-	0.919	1	agctgtATCCacattgc
2;3	MYBS/ ZMMRP1.01	0.79	433	449	-	0.819	1	ttagctgTATCcacatt
2;3	IBOX/ GATA.01	0.93	447	463	+	0.996	1	taaaaaGATAaggtatgt
2;3	NCS1/ NCS1.01	0.85	447	457	+	0.951	1	tAAAAgataag
2;3	MYBL/ GAMYB.01	0.91	458	474	+	0.913	1	gtatgtatGTTAacaca
2;3	EINL/ TEIL.01	0.92	460	468	+	0.922	1	aTGTAtgtt
2;3	MYBL/ GAMYB.01	0.91	463	479	-	0.915	1	acttgtgtGTTAacata
2;3	WBXF/ WRKY.01	0.92	489	505	-	0.939	1	catatTTGAcaatgatg
2;3	OPAQ/ O2_GCN4.01	0.81	503	519	+	0.819	0.829	atgttcACTTatataat
2;3	OCSE/ OCSL.01	0.69	511	531	+	0.864	1	ttatataattgctcACGTttt
2;3	GBOX/ HBP1B.01	0.83	516	536	-	0.849	1	ccgataaaACGTgagcaatta
2;3	MYCL/ MYCRS.01	0.93	517	535	-	0.931	1	cgataaaACGTgagcaatt
2;3	ABRE/ ABRE.01	0.82	519	535	-	0.839	1	cgataaaACGTgagcaa
2;3	MYBL/ MYBPH3.01	0.80	526	542	-	0.823	0.75	caaaaaccGATAaaacg
2;3	IDDF/ ID1.01	0.92	544	556	+	0.934	1	ttttTTGTcaacg
2;3	MYBL/ ATMYB77.01	0.87	547	563	-	0.881	0.857	atttgaCCGTtgacaaa
2;3	MSAE/ MSA.01	0.80	548	562	+	0.891	1	ttgtcAACGgtcaaa
2;3	WBXF/ ERE.01	0.89	550	566	-	0.967	1	aaaattTGACcgttgac
2;3	STKM/ STK.01	0.85	558	572	-	0.888	0.833	accCAAAaaatttga
2;3	MYBL/ MYBPH3.02	0.76	574	590	-	0.806	0.817	taaattTTGTtaggcat
2;3	L1BX/ ATML1.02	0.76	580	596	-	0.831	1	cgtCATTaaattttgtt
2;3	GTBX/ SBF1.01	0.87	582	598	-	0.927	1	cacgtcaTTAAattttg
2;3	AHBP/ WUS.01	0.94	584	594	+	1.000	1	aaattTAATga
2;3	GBOX/ HBP1B.01	0.83	585	605	-	0.947	1	caagagtcACGTcattaaatt
2;3	GBOX/ TGA1.01	0.90	586	606	+	0.987	1	atttaaTGACgtgactcttgg
2;3	ABRE/ ABF1.03	0.82	587	603	+	0.854	1	tttaatgaCGTgactct
2;3	NACF/ TANAC69.01	0.68	587	609	-	0.685	0.896	gtcccaagagtcACGtcattaaa
2;3	OPAQ/ RITA1.01	0.95	588	604	+	0.976	1	ttaatgACGTgactctt
2;3	CE1F/ ABI4.01	0.87	605	617	-	0.924	1	agatCACCgtccc
2;3	L1BX/ PDF2.01	0.85	621	637	-	0.888	1	gattgtTAAAtgctact
2;3	MYBL/ MYBPH3.02	0.76	625	641	-	0.833	0.817	actagaTTGTtaaatgc
2;3	MYBL/ MYBPH3.02	0.76	632	648	+	0.776	1	acaatcTAGTtatttgg
2;3	**CCAF/ CCA1.01**	0.85	**664**	**678**	-	0.868	1	atagtataAATCtca
2;3	TBPF/ TATA.02	0.90	664	678	-	0.907	1	atagTATAaatctca

2;3	MADS/ SQUA.01	0.90	670	690	+	0.931	1	ttatactATTTgtataaactt
2;3	PSRE/ GAAA.01	0.83	670	686	-	0.845	0.75	ttataCAAAtagtataa
2;3	SPF1/ SP8BF.01	0.87	671	683	+	0.948	1	taTACTatttgta
2;3	MADS/ AG.01	0.80	681	701	-	0.804	0.963	catTTCCtgaaaagtttatac
2;3	DOFF/ PBOX.01	0.75	683	699	-	0.816	1	tttcctgaAAAGttttat
2;3	NCS1/ NCS1.01	0.85	683	693	-	0.904	1	gAAAAgtttat
2;3	GTBX/ SBF1.01	0.87	695	711	+	0.879	1	ggaaatgTTAAattata
2;3	DOFF/ DOF1.01	0.98	708	724	-	0.985	1	aatctcctAAAGatata
2;3	**CCAF/ CCA1.01**	0.85	**718**	**732**	-	0.981	1	atacaaaaAATCtcc
2;3	CAAT/ CAAT.01	0.97	729	737	-	0.977	1	aaCCAatac
2;3	LREM/ ATCTA.01	0.85	744	754	-	0.971	1	taATCTaaatc
2;3	GTBX/ GT1.01	0.85	753	769	+	0.856	1	tatcaaGTTActgagat
2;3	AHBP/ BLR.01	0.90	756	766	+	0.914	0.826	caaGTTActga
2;3	MYBS/ ZMMRP1.01	0.79	761	777	-	0.808	1	ttttttTATCtcagta
2;3	IBOX/ GATA.01	0.93	762	778	+	0.943	1	actgaGATAaaaaaaaa
2;3	AHBP/ BLR.01	0.90	776	786	+	1.000	1	aaaATTAatac
2;3	LREM/ ATCTA.01	0.85	789	799	-	0.990	1	aaATCTaaaac
2;3	**CCAF/ CCA1.01**	0.85	**792**	**806**	-	0.861	1	ctaaaggaAATCtaa
2;3	DOFF/ DOF1.01	0.98	796	812	-	0.983	1	tggtaactAAAGgaaat
2;3	MYBL/ GAMYB.01	0.91	798	814	+	0.919	1	ttcctttaGTTAccact
2;3	MYBL/ MYBPH3.02	0.76	809	825	-	0.788	0.779	agaagtTGGTcagtggt
2;3	STKM/ STK.01	0.85	817	831	-	0.872	1	tgcTAAAgaagttgg
2;3	DOFF/ DOF1.01	0.98	819	835	-	0.985	1	tttttgctAAAGaagtt
2;3	GTBX/ GT1.01	0.85	836	852	-	0.859	0.969	ttagtgGTAAttttttt
2;3	MYBL/ MYBPH3.02	0.76	846	862	-	0.833	0.779	ataagtTGGTttagtgg
2;3	GTBX/ GT3A.01	0.83	863	879	+	0.838	1	gcattcGTTAcaaaaaa
2;3	GTBX/ S1F.01	0.79	876	892	-	0.888	1	ttttATGGtattttttt
2;3	MYBL/ CARE.01	0.83	904	920	+	0.857	1	tgttgtaAGTTgtgaca
2;3	OCSE/ OCSL.01	0.69	904	924	+	0.730	0.808	tgttgtaagttgtgACATtaa
2;3	GTBX/ SBF1.01	0.87	914	930	+	0.879	1	tgtgacaTTAAatcaaa
2;3	L1BX/ ATML1.02	0.76	916	932	+	0.821	1	tgaCATTaaatcaaaag
2;3	AHBP/ WUS.01	0.94	918	928	-	1.000	1	tgattTAATgt
2;3	DOFF/ PBF.01	0.97	921	937	+	0.983	1	ttaaatcaAAAGtgtca
2;3	SUCB/ SUCROSE.01	0.81	921	939	+	0.903	1	ttAAATcaaaagtgtcaaa
2;3	SUCB/ SUCROSE.01	0.81	936	954	+	0.812	1	caAAATcaacagtagcaca
2;3	MADS/ AGL15.01	0.79	964	984	-	0.792	0.925	aggTTCTttatatagagtgag
2;3	MADS/ AGL3.01	0.83	965	985	+	0.842	0.791	tcactCTATataaagaacctt
2;3	TBPF/ TATA.02	0.90	967	981	+	0.946	1	actcTATAtaaagaa
2;3	TBPF/ TATA.01	0.88	969	983	+	0.930	1	tctaTATAaagaacc
2;3	GAPB/ GAP.01	0.88	985	999	-	0.956	1	tgagATGAagaataa
2;3	TELO/ RPBX.01	0.84	1005	1019	+	0.898	1	acaagCCCTacaaca
2;3	MIIG/ PALBOXP.01	0.81	1012	1026	-	0.842	0.936	ttGTGGttgttgtag
2;3	MYBL/ MYBPH3.01	0.80	1028	1044	+	0.807	0.75	gcaaacaCTTActtag
2;3	LEGB/ LEGB.01	0.59	1049	1075	+	0.611	0.75	tccagaaACATccattaacacatatgg
2;3	LEGB/ LEGB.01	0.59	1056	1082	-	0.648	1	tctttagCCATatgtgttaatggatgt
2;3	AHBP/ WUS.01	0.94	1060	1070	-	1.000	1	tgtgtTAATgg
2;3	MADS/ MADS.01	0.75	1060	1080	-	0.765	1	tttagCCATatgtgttaatgg
2;3	DOFF/ DOF1.01	0.98	1070	1086	+	0.985	1	atatggctAAAGacgtg
2;3	TEFB/ TEF1.01	0.76	1070	1090	+	0.782	0.839	atATGGctaaagacgtggaag
2;3	GBOX/ HBP1A.01	0.88	1073	1093	-	0.918	1	gtccttcCACGtctttagcca
2;3	GBOX/ GBF1.01	0.94	1074	1094	+	0.971	1	ggctaaagACGTggaaggacc
2;3	OPAQ/ O2.02	0.87	1075	1091	-	0.961	1	ccttCCACgtctttagc

Annex 1. Oligonucleotides.

1.1. Gene specific primers for insertion mutant screening. f and r designate forward and reverse primers, respectively. * indicates primer giving product in combination with insertion mutant collection specific primer (Annex 1.2). [1]indicates gene-specific primer pair for verification on genomic DNA.

Gene	Insertion line	Primer name	Sequence 5´→ 3´
PIP2;1	6AAS98(En-1)	6AA-f*	GCTTGTTGTACCTTAATTCTCAAGT
		6AA-r	AGAGAAGACGGTGTAGACAAGAAC
	SM_3_35928	2;1_SM-f[1]	AACATATAACGTTGGCAAAAA
		2;1_SM-r[1]	TTAATTTCGAATAAACAAACCA
		2;1_SM-re*	TGGTTAAGACAGGGTTAGTCA
	SALK_040961	No insertion detected	
	GABI_158B11	SAIL1283_f*	GAAATTTACTGGCTAACTTATTTG
		SAIL1283_r*	GGAGCTGGTGGCGGATCTT
	GABI_895D12	2;1_SM-f	AACATATAACGTTGGCAAAAA
		2;1_SM-r	TTAATTTCGAATAAACAAACCA
PIP2;2	SAIL_169_A03	SAIL_169_A03-f	CGGCGGCGTCGGAATCCT
		SAIL_169_A03-r*	ACCGGAACGTGGGAGTCTC
	GABI_098_D07	2b-f0	AAGTTATAGAAATGGCCAAAGAC
		2b-r874*	CTCAAAGCTTGGCTGCACTTCT
	SAIL_80_A06	SAIL_80_A06-f*	GTGAAAGAAAGTTTCCACAAAAAT
		SAIL_80_A06-r*	CGACGCCGCCGCAGTCAA
PIP2;3	SAIL_1215_D03	SAIL_1215_D03-f[1]*	GGACTCGCGGCAGAGATCA
		SAIL_1215_D03-r*	AAACGTTGGCTGCACTTCTGA
		2c_rn[1]	GAAGAAAAAGTTGTCTTTCTC
	SALK_117876	2;3_f430[1]*	TTGTAGGTGGTCACATAAACC
		2;3_r960*	GGCTTGCTCTTGTTAAAGATTA
		2c_rn[1]	GAAGAAAAAGTTGTCTTTCTC
PIP2;4	SM_3_20853	2;4_SM-f[1]	CAAAGCATTCCAAAGTTCTTA
		2e-r*	GATTTTATCTTAAAGCAACAT
		SAIL_1251_G12-r[1]	AAAGCAACATTAATTAAAACCACA
	SAIL_1251_G12	SAIL_1251_G12-f*	CTAGCCGATGGCTACAACA
		SAIL_1251_G12-r*	AAAGCAACATTAATTAAAACCACA
	SAIL_535_D05	SAIL_535_D05-f*	ATCGCACTCTAAGTCATAATGG
		SAIL_535_D05-r*	GTGGTCCACTCTCGTTCACA
PIP2;5	SAIL_452_H09	SAIL_452_H09-f*	CGAAGGAAGTGGTTGGTGATA
		SAIL_452_H09-r	AGGCACTGAGCCACCATGTA
	SAIL_1179_F10	SAIL_1179_F10-f*	CAGAGTCCAAAGCCTCGTCA
		SAIL_1179_F10-r	TGTGAGCTTTAACACCAAACCA
	SALK_072405	PIP2;5_f970	CGTAGAAATTGTAGTCTTGTTG
		PIP2;5_r1500*	AAGCTTTGTCCTTGTTGTAGAT
PIP2;6	SALK_029718	PIP2;6_f1180*	TGAATTACTAAATCGAAGTTTTGC
		PIP2;6_r1770	ATCTATCCTAATATTTCTTCCATTATTT
	SAIL_1286_G02	SAIL_1286_G02-f*	ACCGACCCTAAGCGAAATGC
		SAIL_1286_G02-r*	GGAGCTGGTGGCGGATCTT
PIP2;8	SALK_099098	PIP2;8_f400*	AAATACCTTTTTAGCAAGAAGG
		PIP2;8_r820*	AACTGGTTTGCAAAGTTTTACT
PIP1;1	GABI_437_B11	437B11-f*	CAGAGCTTTACAATTTCTCTCTACA
		437B11-r*	CACAGTGTTAGCTCCTCCTCCT
PIP1;2	SALK_145347 and SALK_019794	PIP1;2_f890*	CTGGTTTCTCCGATCTAACGA
		PIP1;2_r1440*	GCATTTTGATCCGATGTTACAA

1.2. Insertion mutant collection specific primers

Collection	Primer name	Sequence 5´→ 3´
Amaze (En)	6AA-En	GGTGCTTGTGTTATGTTATGTTGA
FLAG	FLAG_TAILB	CGGCTATTGGTAATAGGACACTGG
GABI-Kat	GABI_LB2	CCATTTGGACGTGAATGTAGACAC
JIC SM	dSpm1	CTTATTTCAGTAAGAGTGTGGGGTTTTGG
SAIL	SAIL_L	TTCATAACCAATCTCGATACAC
SALK	Lba1_mod	GGTTCACGTAGTGGGCCATC

1.3. RT-PCR primers

Gene name	For. primer	Sequence 5´→ 3´
PIP2;1	2a_f0	AAGAAGTTAACTATGGCAAAGGA
	2a_r890	TTGAGAAATCTGGTTTGGTGT
PIP2;2	2bf0*	AAGTTATAGAAATGGCCAAAGAC
	2br+874	CTCAAAGCTTGGCTGCACTTCTG
PIP2;3	2;3_1215D03f	GGACTCGCGGCAGAGATCA
	2c_rn	GAAGAAAAGTTGTCTTTCTC
PIP2;4	2e_qRTf	TTGGATGTGAACGAGAGTGGACC
	1251G12r	AAAGCAACATTAATTAAAACCACA
PIP2;5	2f_qRTf	GTGGTTGGTGATAAGAGATCTTTCTCC
	2;5_r1500	AAGCTTTGTCCTTGTTGTAGAT
PIP2;6	2h_qRTf	AGTTGACGGAGGAAGAGTCGCTC
	2;6_r2610	GCTCTCAACACAAACTGATGGTAA
PIP2;8	2;8_qRTf	AGTGAGTGAAGAAGGAAGACA
	2;8_qRTr	CAATAATCTCAGCACCAAGAG
PIP1;1	437B11-f	CAGAGCTTTACAATTTCTCTCTACA
	437B11-r	CACAGTGTTAGCTCCTCCTCCT
PIP1;2	PIP1;2cDNA_F	CAACACATAACCCACTCACAGAAAAACCT
	PIP1;2cDNA_R	CCAGATTTTAAATAGAACTCAATCAGCTTTAGC

1.4. Primers for amplification of DNA blot probes

Collection	primer	Sequence 5´→ 3´
GABI	Gabi_Lbsouthern_f	CTACATGGATCAGCAATGAGT
	Gabi_Lbsouthern_r	TGAAGATGAAATGGGTATCTG
SAIL	probesail-south_f	CGGACGTTTTTAATGTACTGA
	probesail-south_r	CGGGTATTCTGTTTCTATTCC
SALK	Salkprobe_f	AATGTACTGGGGTGGTTTTTC
	Lba1 mod	GGTTCACGTAGTGGGCCATC
SM	probesm-south_f	CTGAAATAAGCCGACACTCTA
	probesm-south_r	TTCGTATGGACTTGAACTTGT

1.5. Primers for amplification of PIP2 promoters and PIP2 promoters and open reading frame for fusion constructs.

Construct	Name	Sequence 5´ → 3´
PIP2;1-ORF-GFP	PIP2;1-ORF-GFPf	GGGGACAAGTTTGTACAAAAAAGCAGGCTGGAGTGACTAAAAAGGACAA
	PIP2;1-ORF-GFPr	GGGGACCACTTTGTACAAGAAAGCTGGGTCGACGTTGGCAGCACTTCT
PIP2;4-ORF-GFP	PIP2;4-attBP-f695	GGGGACAAGTTTGTACAAAAAAGCAGGCTATCATCTCCTCCTCATTATTT
	PIP2;4-ORF-GFP-rB	GGGGACCACTTTGTACAAGAAAGCTGGGTAATAAATGTATATTGAGCAAAGC
PIP2;6::GUS	PIP2-6_Pro_GW_F-2500	GGGGACAAGTTTGTACAAAAAAGCAGGCTGATGTCGCTTGAATTGTCA
	PIP2-6_Pro_GW_R0	GGGGACCACTTTGTACAAGAAAGCTGGGTGTCATTCTTTCAGACTTAGCCTTC
PIP2;7::GUS	PIP2-7_Pro_GW_F-2500	GGGGACAAGTTTGTACAAAAAAGCAGGCTGGAAAAAGGAATTGCGAGAA
	PIP2-7_Pro_GW_R0	GGGGACCACTTTGTACAAGAAAGCTGGGTGACATCTTTGTTCTTTTTACTCTCTAGC
PIP2;8::GUS	PIP2-8_Pro_GW_F-2500	GGGGACAAGTTTGTACAAAAAAGCAGGCTCTTTTGGCGGGAGTTAGAAG
	PIP2-8_Pro_GW_R0	GGGGACCACTTTGTACAAGAAAGCTGGGTGACATTTTTCTTAGCTCAGCTCTAAGA

1.6. C-terminal peptides in PIP2-GST fusion proteins

Construct	Sequence
PIP2;4 epitope	GAAAAAFYHQFILRAAAIKALGSFGSFGSFRSFA
PIP2;5 epitope	GAAIAAFYHQFVLRAGAIKALGSFRSQPHV
PIP2;6 epitope	GAAIAAFYHQFVLRAGAMKAYGSVRSQLHELHA
PIP2;7 epitope	GALAAAAYHQYILRASAIKALGSFRSNATN
PIP2;8 epitope	GALAAAAYHQYILRAAAIKALASFRSNPTN

Annex 2. Data *PIP2;5*

Interestingly, the *pip2;5-1* mutant showed a drastic salt sensitivity. This mutant did not show any phenotype under normal growth as well as under purely osmotic stress (see Results 3.3). However, this mutant exhibited additional T-DNA insertions as shown by Southern blotting (see Results 3.2) and the phenotype was not confirmed by a second independent T-DNA insertional mutant (Results 3.3). Hence, a involvement of PIP2;5 in salt resistance seemed to be less likely; yet the interesting phenotype possibly due to another mutation was examined in more detail.

First, the salt sensitivity had been observed with NaCl. Thus, to check whether this sensitivity was specific to NaCl or could be extended to other salts, growth of *pip2;5-1* mutant under potassium chloride stress (KCl) was assessed. Interestingly, the reduced growth observed under NaCl stress was also observed under KCl stress arguing against a sole Na^+ toxicity (Fig. 1).
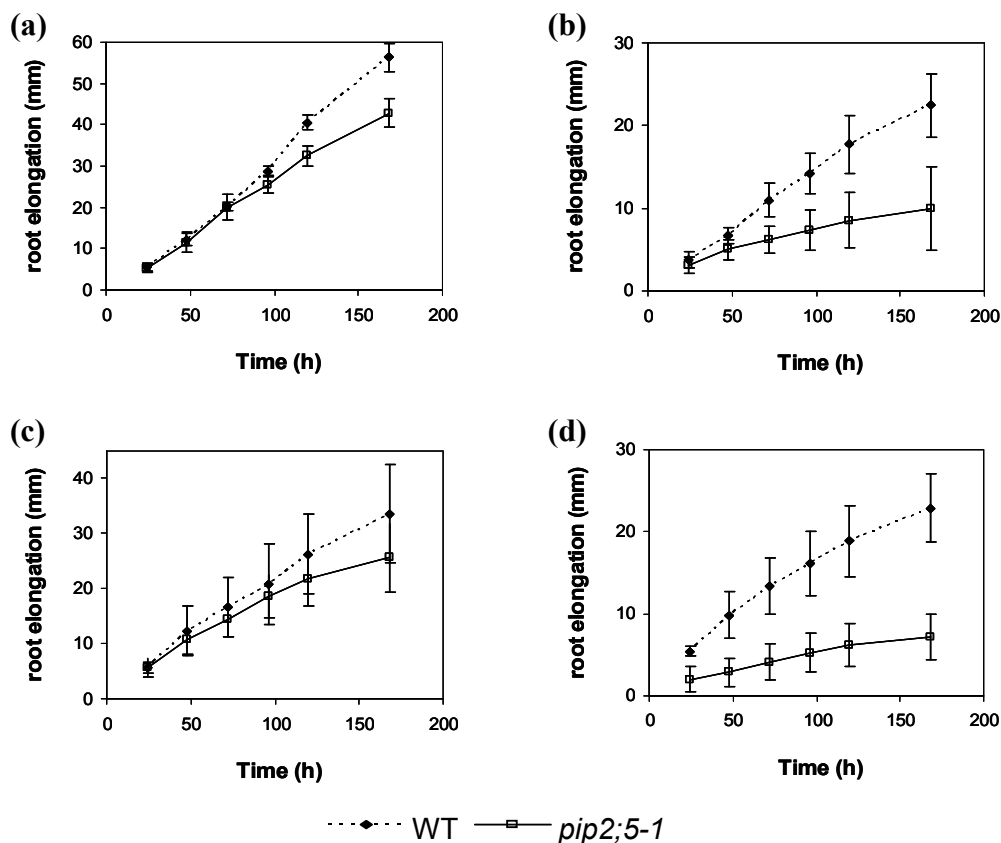
Figure 1. Root elongation of wild-type and *pip2;5-1* mutant under salt stress.
Four-day-old seedlings germinated in standard medium were transferred to vertically orientated plates containing various salt: (a) 50 mM NaCl; (b) 100 mM NaCl; (c) 50 mM KCl and (d) 100 mM KCl. Seedlings were grown for 7 additional days and root elongation was recorded daily. Symbols are means ± SDs of 6 to 7 plants.

Both salts provoked reduced growth to a similar extent with a slight reduction under 50 mM salt (Fig. 1a and c) and an often lethal phenotype under 100 mM salt (Fig. 1b and d). It is noteworthy that the phenotype observed for *pip2;5-1* seems to be the consequence of the duration of the stress since normal growth was observed during the first days of stress. The first symptoms of death appeared only after 2 to 3 days of growth under salt stress (Fig. 1).

In addition, *pip2;5-1* mutant was grown on enhanced, isoosmotic 200 mM mannitol to check sensitivity under purely osmotic stress. The use of mannitol, similar to sorbitol, did not lead to the strong phenotype observed with salt indicating that *pip2;5-1* was exclusively salt sensitive (Fig. 2).
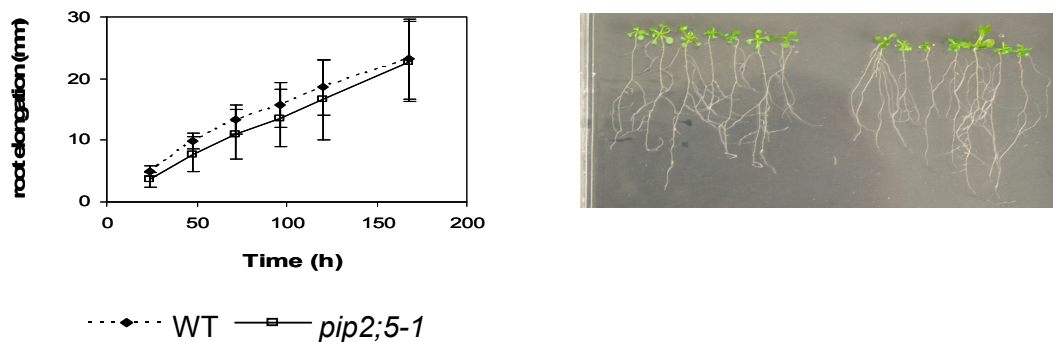
Figure 2. Root elongation of wild-type and *pip2;5-1* mutant under Mannitol.
Four-day-old seedlings germinated in standard medium were transferred to vertically orientated plates containing 200 mM Mannitol. Seedlings were grown for 7 additional days; root elongation was recorded daily (left panel) and plants were photographed (right panel). Symbols are means ± SDs of 6 to 7 plants.

Since the *pip2;5-1* mutant has additional T-DNA insertions, the line showing the phenotype has been backcrossed into wild-type in order to get rid of additional insertions. Five lines have been recovered from these backcrosses and their segregation on BASTA selection indicated a 1:5 segregation suggesting that these five backcrossed lines may contain a single T-DNA insert. All five lines showed the lethal phenotype previously observed when grown in presence of high NaCl concentration whereas a hemizygous line did not exhibit salt sensitivity (Fig. 3).
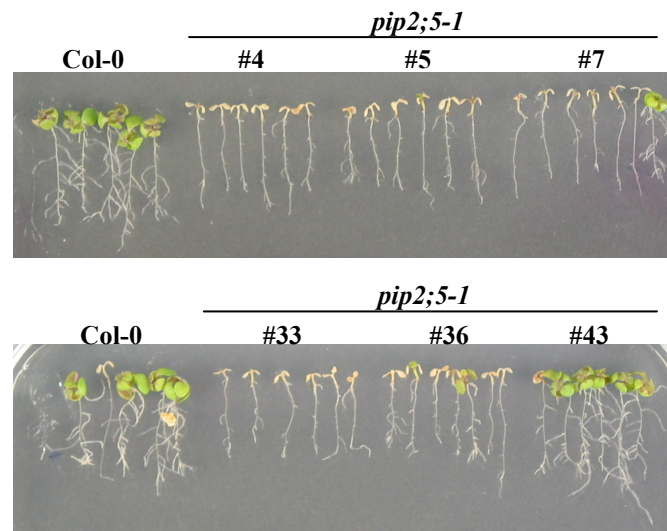
Figure 3. Several *pip2;5-1* backcrossed mutant lines exhibit salt sensitivity.
Six *pip2;5* backcrossed mutant lines were grown under salt stress (100 mM NaCl). Lines 4 to 36 were homozygous and exhibited salt sensitivity whereas a hemizygous line (line 43) did not exhibit any phenotype.

Furthermore, transgenic plants expressing a *PIP2;5* promoter::GUS fusion protein were used to investigate *PIP2;5* expression under salt stress. Expression of *PIP2;5* in seedlings grown on standard medium was compared with *PIP2;5* expression in seedlings grown under osmotic and salt stress conditions to check whether these conditions would alter *PIP2;5* expression in plants. The histochemical GUS assay was carried out on transgenic seedlings. An induction of GUS activity was observed in leaves when seedlings were submitted to 100 mM NaCl stress but not with 200 mM sorbitol (Fig. 4). Indeed, 4 days-old transgenic plants expressing a *PIP2;5* promoter::GUS construct were transferred to vertical plates containing 100 mM NaCl or 200 mM Sorbitol and GUS expression was tested after 1 day and after 6 days. As a control, transgenic plants were also transferred in plates containing standard medium. Interestingly, no differences were observed after 1 day. Similar GUS expression could be detected in both seedlings grown in standard medium as well as in water stress medium (data not shown). However, after 6 days, transgenic seedlings exhibited a differential response. Although GUS activity was detected in control seedlings as well as in stress conditions, GUS activity was stronger in seedlings grown under salt stress (100 mM NaCl) than in seedlings grown under standard or osmotic stress conditions (Fig. 4). These results indicate that *PIP2;5* responds to water stress provoked by salt.
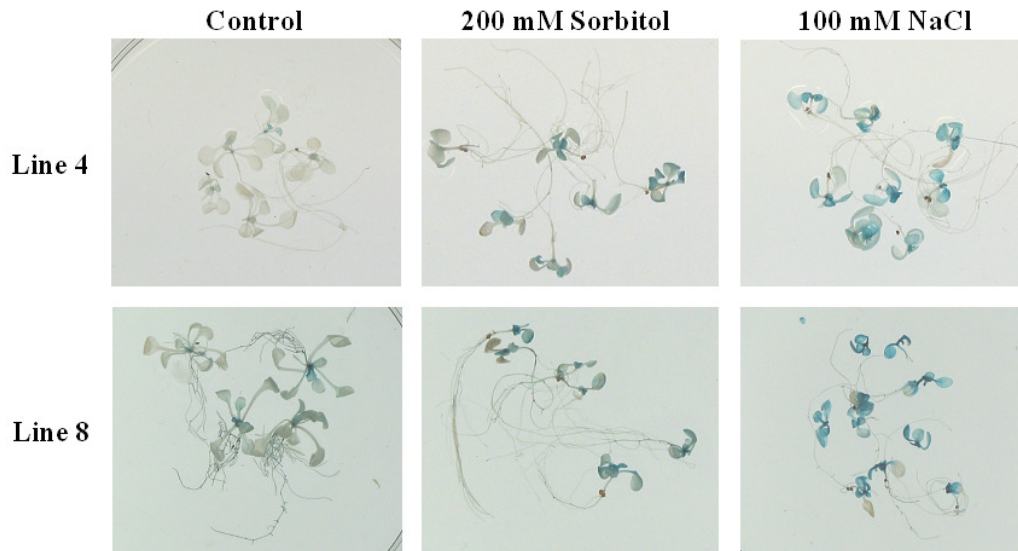
Figure 4. Histochemical GUS analysis of transgenic plants expressing a *PIP2;5* promoter::GUS fusion protein.
GUS activity was tested in transgenic seedlings grown under normal and water stress conditions. Different lines were tested and exhibited similar results although expression level was different.

All together, these observations suggested an involvement of *PIP2;5* to withstand salt stress (in particular ionic stress). Indeed, several backcrossed lines for which segregation analyses indicated a single insertion showed a strong phenotype when grown under salt stress. GUS analyses revealed induction of *PIP2;5* after salt exposure. However, this phenotype was only observed with the particular *pip2;5-1* mutant and was not confirmed by a second independent mutant (*pip2;5-3*, see Results 3.3). Genomic analyses revealed that *pip2;5-1* mutant carried additional insertions. Therefore, complementation analyses were performed to test whether there could be any correlation of salt sensitivity and *pip2;5* knock-out. Complementation analyses constitute the ultimate proof to link the observed phenotype to *PIP2;5* loss-of-function. Hence, the *PIP2;5* genomic region was introduced into *pip2;5-1* mutant plants. Transformed plants were selected by their resistance to kanamycin and the presence and expression of the transgene in these plants were confirmed by PCR amplification of the *PIP2;5* cDNA (Fig. 5a). Transformed lines carrying the introduced PIP2;5 genomic sequence were then tested for their salt sensitivity. The complementation did not rescue the phenotype of *pip2;5-1* plants suggesting that PIP2;5 is probably not, at least not directly and/or not alone, responsible of the salt sensitivity observed (Fig. 5b).

(a)
1 2 C2 C3

Tubulin

PIP2 ;5

(b)
WT   2;5-C2   pip2;5-1
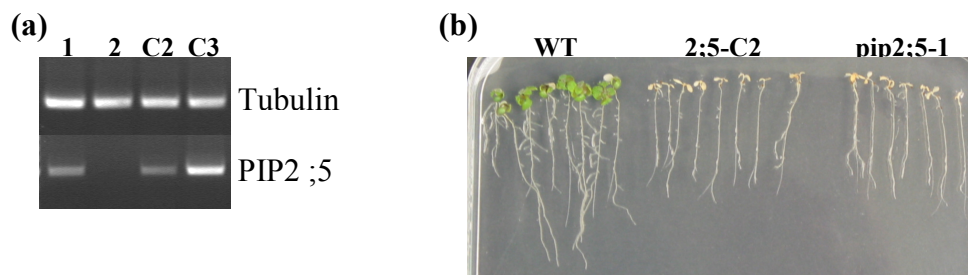
Figure 5. *PIP2;5* **genomic sequence does not rescue** *pip2;5-1* **salt phenotype.**
(a) Agarose gel electrophoresis of Col-0 (1), *pip2;5-1* mutant (2) and *PIP2;5* complemented plants (C2-C3) cDNA amplification products. Total RNA was isolated from *Arabidopsis* seedlings and cDNA synthesized. Amplification products were further visualized by ethidium bromide staining. For control, cDNA fragments for Tubulin (*TUB9*, At4g20890) were amplified. Expression of the *PIP2;5* gene was not detectable in *pip2;5-1* mutant whereas it was detected in col-0 wt and complemented plants. No signals were detected in the controls (-RT; not shown).
(b) wt, complemented plant and *pip2;5-1* mutant seedlings grown on 100 mM NaCl. Four-day-old seedlings germinated in standard medium were transferred to vertically orientated plates containing 100 mM NaCl and further grown for 7 days.

To conclude, a salt sensitivity was observed for a particular *pip2;5-1* but could not be complemented by *PIP2;5* coding sequence. The *pip2;5-1* phenotype was still observed after backcrosses for homozygous lines, while hemizygous lines did not exhibit the phenotype. Molecular characterization of *pip2;5-1* mutant indicated additional T-DNA insertion but the integrity of the genome flanking *PIP2;5* gene was confirmed by PCR and restriction digest (see Results 3.2). Thus, all these results suggest that the *pip2;5-1* phenotype could be the result of the mutation of a single recessive gene which might be closely linked to *PIP2;5* gene. It is noteworthy that a second mutant, *pip2;5-2,* was strongly growth retarded. The salt sensitivity of this *pip2;5-2* mutant could not be tested since four-day-old seedlings did not have cotyledons, while root growth was relatively normal. Cotyledons were fully developed only after about 7 days and then this mutant could not be compared with any other genotype. Nevertheless, *pip2;5-1* and *pip2;5-2* mutants showed a T-DNA insertion in the first exon and oriented in the same direction (see Results 3.2, Fig. 17). Hence, it may well be that the T-DNA insertion in this region alters another part of the genome.

ACKNOWLEDGEMENTS

Finally, I thank my family and friends for their endless and unselfish support throughout. Particularly, I am grateful for the love and concerns of my parents, my sister Julie, my brother David, and my Girlfriend Mercedes. Completing the Ph.D. would have been impossible without their love and encouragement.

CURRICULUM VITAE

PERSONAL DETAILS

Name	DA INES Olivier
Date of birth	June 19, 1978
Place of birth	Mâcon (France)
Nationality	French
Marital status	Single

EDUCATION

11/2003- 05/2008   Ph.D. at the Ludwig-Maximilians University, Munich, Germany. Title: "Functional Analysis of PIP2 Aquaporins in *Arabidopsis thaliana*". *Advisor:* PD. Dr. Anton R. Schäffner. Helmholtz Zentrum München. German Research Center for Environmental Health. Neuherberg, Germany. Institute for Biochemical Plant Pathology.

2001-2003   Master of Science (Biochemistry, Cellular and Molecular Biology) University of Burgundy, France.

1999-2001   Bachelor of Science (Biochemistry degree) University of Burgundy, France.

1997-1999   Pharmaceutical School University of Burgundy, France.

1993-1997   Mathematics, Physics, Chemistry and Life Sciences Lycée Lamartine, Mâcon, France.

PROFESSIONAL EXPERIENCE

2002-2003**. Master Thesis** on UMR INRA/CNRS Plante-Microbe-Environnement. University of Burgundy, France. Title: "Modulation of Tonoplastic Aquaporins expression in *Arabidopsis thaliana* using sense and anti-sense strategies". Advisor: Prof. Francis Marty; Supervisor: Dr. Karim Bouhidel.

June-September 2001**. Training period** in the laboratory of Immunology. Nottingham Trent University. Nottingham, UK. Title: "Identification of new tumor Antigens using SEREX". Director: Prof. R. Rees. Supervisor: Dr. Amanda Miles.

PUBLICATIONS

Olivier Da Ines, Katja J. Franck, Birgit Geist, Ulrich Hammes, Gerhard Welzl and Anton R. Schäffner. 2008. Differential roles of PIP2 aquaporins in *Arabidopsis thaliana*. (submitted to Plant Physiology).

Aniela Sommer, Birgit Geist, Olivier Da Ines, Renate Gehwolf, Anton R. Schäffner, and Gerhard Obermeyer. Ectopic expression of *Arabidopsis PIP2* aquaporins in lily pollen increases the plasma membrane water permeability of grain but not of tube protoplasts. (submitted to New Phytologist).